# NUTRITION, IMMUNITY AND VIRAL INFECTIONS

EDITED BY: Julio Villena, Maria Guadalupe Vizoso Pinto, Haruki Kitazawa and Takeshi Shimosato

PUBLISHED IN: Frontiers in Nutrition and Frontiers in Immunology

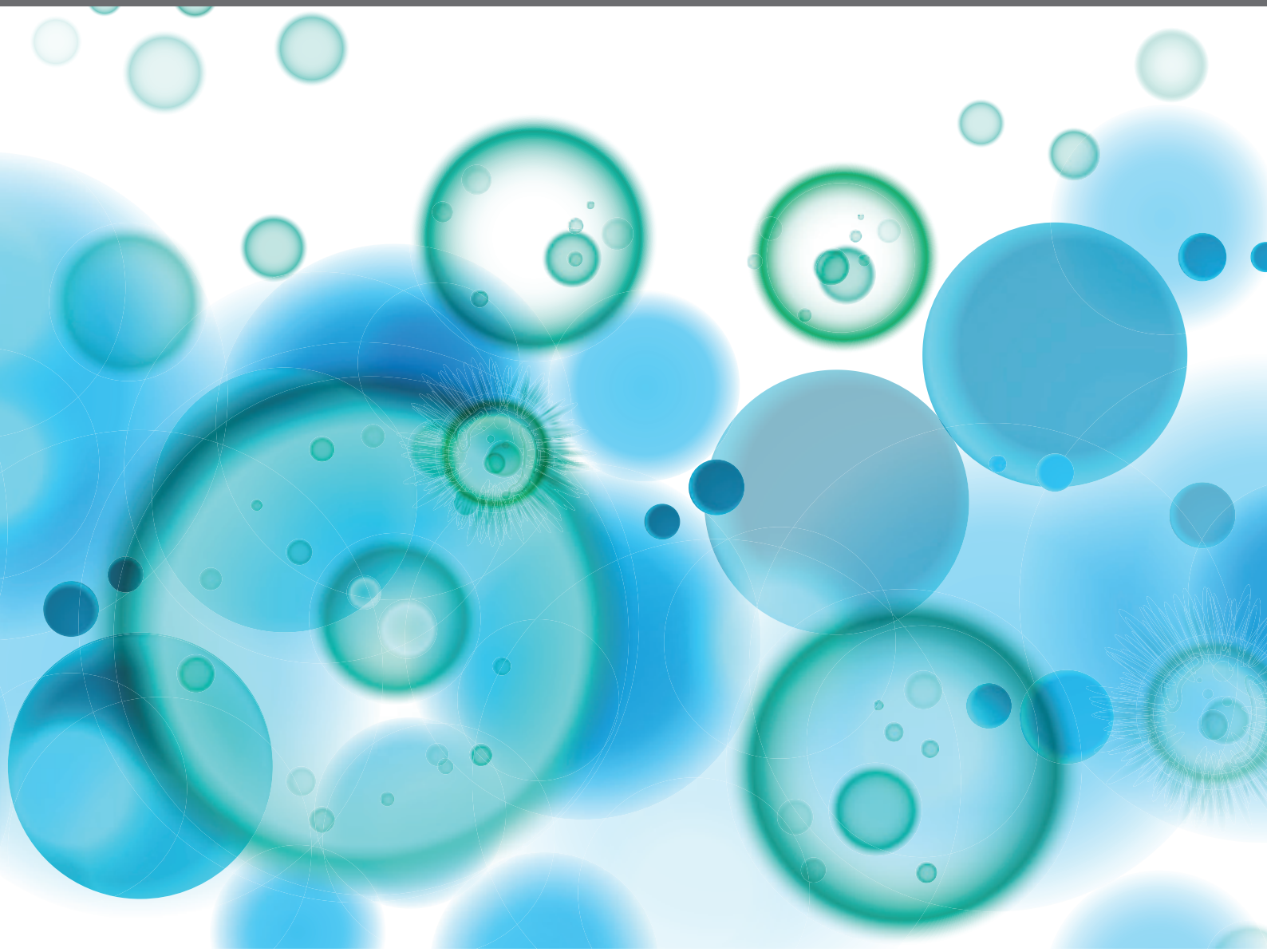

frontiers Research Topics

# frontiers



ISSN 1664-8714
ISBN 978-2-88966-129-9
DOI 10.3389/978-2-88966-129-9

## About Frontiers

Frontiers is more than just an open-access publisher of scholarly articles: it is a pioneering approach to the world of academia, radically improving the way scholarly research is managed. The grand vision of Frontiers is a world where all people have an equal opportunity to seek, share and generate knowledge. Frontiers provides immediate and permanent online open access to all its publications, but this alone is not enough to realize our grand goals.

## Frontiers Journal Series

The Frontiers Journal Series is a multi-tier and interdisciplinary set of open-access, online journals, promising a paradigm shift from the current review, selection and dissemination processes in academic publishing. All Frontiers journals are driven by researchers for researchers; therefore, they constitute a service to the scholarly community. At the same time, the Frontiers Journal Series operates on a revolutionary invention, the tiered publishing system, initially addressing specific communities of scholars, and gradually climbing up to broader public understanding, thus serving the interests of the lay society, too.

## Dedication to Quality

Each Frontiers article is a landmark of the highest quality, thanks to genuinely collaborative interactions between authors and review editors, who include some of the world's best academicians. Research must be certified by peers before entering a stream of knowledge that may eventually reach the public - and shape society; therefore, Frontiers only applies the most rigorous and unbiased reviews.
Frontiers revolutionizes research publishing by freely delivering the most outstanding research, evaluated with no bias from both the academic and social point of view. By applying the most advanced information technologies, Frontiers is catapulting scholarly publishing into a new generation.

## What are Frontiers Research Topics?

Frontiers Research Topics are very popular trademarks of the Frontiers Journals Series: they are collections of at least ten articles, all centered on a particular subject. With their unique mix of varied contributions from Original Research to Review Articles, Frontiers Research Topics unify the most influential researchers, the latest key findings and historical advances in a hot research area! Find out more on how to host your own Frontiers Research Topic or contribute to one as an author by contacting the Frontiers Editorial Office: researchtopics@frontiersin.org

# NUTRITION, IMMUNITY AND VIRAL INFECTIONS

Topic Editors:
**Julio Villena,** CONICET Centro de Referencia para Lactobacilos (CERELA), Argentina
**Maria Guadalupe Vizoso Pinto,** Consejo Nacional de Investigaciones Científicas y Técnicas (CONICET), Argentina
**Haruki Kitazawa,** Tohoku University, Japan
**Takeshi Shimosato,** Shinshu University, Japan

**Citation:** Villena, J., Pinto, M. G. V., Kitazawa, H., Shimosato, T., eds. (2020). Nutrition, Immunity and Viral Infections. Lausanne: Frontiers Media SA.
doi: 10.3389/978-2-88966-129-9

# Table of Contents

frontiers in Nutrition

EDITORIAL
published: 08 September 2020
doi: 10.3389/fnut.2020.00125

# Editorial: Nutrition, Immunity and Viral Infections

*Julio Villena*[1,2]*, *Takeshi Shimosato*[3], *María Guadalupe Vizoso-Pinto*[4,5] and *Haruki Kitazawa*[2,6]*

[1] Laboratory of Immunobiotechnology, Reference Centre for Lactobacilli, National Council of Scientific and Technological Research, San Miguel de Tucumán, Argentina, [2] Food and Feed Immunology Group, Laboratory of Animal Products Chemistry, Graduate School of Agricultural Science, Tohoku University, Sendai, Japan, [3] Department of Biomolecular Innovation, Institute for Biomedical Sciences, Shinshu University, Nagano, Japan, [4] Infection Biology Lab, Instituto Superior de Investigaciones Biológicas, National Council of Scientific and Technological Research - National University of Tucuman, San Miguel de Tucumán, Argentina, [5] Laboratorio de Ciencias Básicas (Genética), Facultad de Medicina, Universidad Nacional de Tucumán, San Miguel de Tucumán, Argentina, [6] Livestock Immunology Unit, International Education and Research Centre for Food and Agricultural Immunology, Graduate School of Agricultural Science, Tohoku University, Sendai, Japan

**Keywords: virus infection, immunity, immunobiotics, nutritional immunology, mucosal immmunity**

## Editorial on the Research Topic

## Nutrition, Immunity and Viral Infections

OPEN ACCESS

***Edited and reviewed by:***
*Willem Van Eden,*
*Utrecht University, Netherlands*

***Correspondence:**
*Julio Villena*
*jcvillena@cerela.org.ar*
*Haruki Kitazawa*
*haruki.kitazawa.c7@tohoku.ac.jp*

***Specialty section:***
*This article was submitted to Nutritional Immunology, a section of the journal Frontiers in Nutrition*

***Received:*** *21 June 2020*
***Accepted:*** *30 June 2020*
***Published:*** *08 September 2020*

***Citation:***
*Villena J, Shimosato T, Vizoso-Pinto MG and Kitazawa H (2020) Editorial: Nutrition, Immunity and Viral Infections. Front. Nutr. 7:125. doi: 10.3389/fnut.2020.00125*

Viral infectious diseases have a great impact on humankind. Pandemic, epidemic, and endemic viral diseases produce considerable morbidity and mortality, negatively affecting not only health and well-being but also local and global economies by increasing school and work absenteeism as well as the healthcare system expenses. Probably the best example of this global threat is the infectious disease caused by the novel Severe Acute Respiratory Syndrome Coronavirus 2 (SARS-CoV-2), which has infected millions of people globally during the 2019-2020 pandemic [WHO, coronavirus pandemic; (1)]. Viral infections not only affect the economy in terms of human life, they also induce losses in livestock and crops (2), and can break down the barriers between animals and people, creating new potential dangers to human health (3). The SARS-CoV-2 pandemic pushed healthcare systems around the world to the limit and put pressure on the scientific community to provide solutions that help to prevent or alleviate its harmful effects. In consequence, in the past few months, there has been a reevaluation of the work of scientists actively investigating the biological features of viral infections, as well as potential preventive and therapeutic tools to combat them.

As a discipline, Nutritional Immunology is working actively, contributing to the prevention of viral infections (4–7). One of the most important fields of Nutritional Immunology is the study of the relationship between nutrition, immunity, and infections. During recent decades, incredible advances have been made in understanding how nutrients (or the lack of them) influence the microbiota and the immune system and affect resistance to viral infections. Scientists have gained insight into the cellular and molecular interactions of nutrients and microorganisms with the immune system, and this information has allowed the development of practical applications and biotechnological tools for improving the immune system and ameliorating the negative consequences of viral infections in humans and animals. The manuscripts gathered in this Research Topic are examples of the mechanistic and applied investigations into the effects of nutritional and immunological interventions on viral diseases.

The interaction and stimulation of intestinal epithelial cells (IECs) and antigen presenting cells (APCs) in the gastrointestinal mucosa by beneficial immunomodulatory microorganisms have been suggested as one of the most important mechanisms involved in the improvement of the resistance against viral infections induced by nutritional and immunological interventions with probiotic foods and feeds (1, 4, 8). Therefore, there is great interest in elucidating the mechanisms involved in the interaction between beneficial microorganisms with IECs and APCs, which are the first to meet the microbes and their molecules reaching the intestinal mucosa. In this Research Topic, Garcia-Castillo et al., Kanmani and Kim, and Albarracin et al., provide some clues of the cellular and molecular mechanisms involved in the beneficial interactions of probiotic lactobacilli strains with IECs and APCs. Interestingly, Albarracin et al., have demonstrated that the interaction of probiotic lactobacilli such as *Lactobacillus rhamnosus* CRL1505 or *L. plantarum* MPL16 with IECs not only influences the antiviral immune response in the gastrointestinal tract but, in addition, may contribute to the beneficial modulation of the innate antiviral responses in distant mucosal tissues such as the respiratory tract.

In addition to studying the probiotic-induced immune changes in the host, it is also necessary to find out which bacterial molecules are responsible for their beneficial effects. In this regard, Mizuno et al. developed a D-alanyl-lipoteichoic acid biosynthesis protein knockout-mutant strain, to demonstrate the key role of lipoteichoic acid in the anti-inflammatory effect induced by the probiotic *L. plantarum* CRL1506 strain in the context of Toll-like receptor (TLR)-3-mediated intestinal inflammation. The characterization of the immunomodulatory effects of beneficial microorganisms and their effector molecules on the mucosal immune system provides a scientific basis to apply them for modulating both the innate immunity and the adaptive immunity targeting specific antigens. Thus, microorganisms and immunomodulatory molecules have been proposed as adjuvants for the generation of mucosal vaccines. Raya Tonetti et al. demonstrated that bacterium-like particles (BLPs) obtained from different immunomodulatory lactobacilli strains differed in their abilities to regulate intestinal and systemic adaptive immune responses induced by the oral administration of a rotavirus vaccine. The work proposed that BLPs derived from highly immunomodulatory lactobacilli strain as an excellent alternative for the development of mucosal antiviral vaccines, indicating that it is necessary to appropriately select BLPs to find those with the most efficient adjuvant properties. In addition, Nigar and Shimosato have reviewed how unmethylated cytosine–guanine dinucleotide (CpG) motifs and single-stranded synthetic oligodeoxynucleotides, acting through TLR9 activation, are potent stimulators of the host immune response making them an interesting alternative as mucosal adjuvants for antiviral and antitumor vaccines.

Nutrients such as micronutrients and flavonoids also have been shown to influence the immune responses against viral infections. In this regard, zinc has been shown to regulate diverse physiological functions and to play crucial, and sometimes divergent roles in viral infections. Kar et al. demonstrated that zinc depletion inhibited Dengue Virus and Japanese Encephalitis Virus infections in IECs but had no effect on rotavirus infection. These results pointed out that modulation of zinc homeostasis during virus infection could be a component of the host antiviral response. Thus, the modulation of zinc homeostasis could be used as a potent antiviral strategy against flaviviruses. On the other hand, Wu et al. reported that puerarin, an isoflavonoid isolated from the traditional Chinese herb Gegen, differentially modulates the innate immune response against the Porcine Epidemic Diarrhea Virus. The proteomic study performed in this work both in cell cultures and in neonatal pigs demonstrated the ability of puerarin to inhibit the virus-induced nuclear factor (NF)-κB activation and inflammatory damage as well as to increase the expression of several interferon (IFN)-stimulated genes. These two original research articles are examples of how Nutritional Immunology applied to viral infections can offer the scientific basis for the development of new antiviral foods and feeds.

On the other hand, it is well-known that the adipose tissue plays key roles in immunometabolism in health and disease conditions such as viral infections. Therefore, investigating the ability of cells in the adipose tissue to respond to microbial ligands may contribute to a better understanding of the role of this physiological system in resistance to infections. It was reported that human and mouse adipocytes are capable of responding to TLR3 activation by producing tumor necrosis factor (TNF)-α, interleukin (IL)-6, IL-8, and chemokine C-C motif ligand (CCL)-2 as well as IFN-α/β and multiple antiviral proteins (9, 10), indicating that adipose cells are able to trigger innate antiviral responses. In this Research Topic, Igata et al. performed a global transcriptomic study in porcine intramuscular mature adipocytes following the stimulation with TLR2, TLR3, and TLR4 ligands. Interestingly, the work demonstrated that porcine adipocytes, similar to human and mouse cells, can respond to TLR3 activation by increasing the expression of several genes (*CCL2, CCL8, CCL5, CCL3L1, IL1β,* and *IL12*) that participate in antiviral inflammatory responses. This work opens the doors for future research on the response of adipocytes in the defense of viral infections in the porcine host, as well as its potential use as a human model.

Interestingly, zebrafish has become a well-recognized animal model to study host-microbe-immune interactions because of the diverse set of laboratory tools available for these cyprinids, including the possibility of generating germ-free individuals or the *in vivo* imaging of specific immune cell populations in whole transgenic organisms. López Nadal et al. revised the practical advantages of zebrafish and discussed how this model sheds light on the mechanisms by which feed influences host-microbe-immune interactions and ultimately fish health and resistance to infections. As an interesting example of the use of the zebrafish model for the study of immunomodulatory feeds Ikeda-Ohtsubo et al., reported the capacity of a fucose-rich sulfated polysaccharide called fucoidan, extracted from edible seaweed *Cladosiphon okamuranus*, to modulate microbiota and immune responses.

The collection of reviews and original research articles presented under this Research Topic provide a comprehensive set of information on the potential of nutritional interventions to beneficially modulate antiviral immune responses in both humans and animals. The editors hope that this topic will act as a

potent stimulus for further research in this growing and exciting area of the Nutritional Immunology.

## AUTHOR CONTRIBUTIONS

All authors listed have made a substantial, direct and intellectual contribution to the work, and approved it for publication.

## FUNDING

This work was supported by the Core-to-Core Program (Advanced Research Networks) of the Japan Society for the Promotion of Science titled Establishment of an International Agricultural Immunology Research-core for a Quantum Improvement in Food Safety.

## REFERENCES

1. Villena J, Kitazawa H. The modulation of mucosal antiviral immunity by immunobiotics: could they offer any benefit in the SARS-CoV-2 pandemic? *Front Physiol.* (2020) 11:699. doi: 10.3389/fphys.2020.00699
2. Villena J, Kitazawa H, Van Wees SCM, Pieterse CMJ, Takahashi H. Receptors and signaling pathways for recognition of bacteria in livestock and crops: prospects for beneficial microbes in healthy growth strategies. *Front Immunol.* (2018) 9:2223. doi: 10.3389/fimmu.2018.02223
3. Cui J, Li F, Shi ZL. Origin and evolution of pathogenic coronaviruses. *Nat Rev Microbiol.* (2019) 17:181–92. doi: 10.1038/s41579-018-0118-9
4. Villena J, Vizoso-Pinto MG, Kitazawa H. Intestinal innate antiviral immunity and immunobiotics: beneficial effects against rotavirus infection. *Front Immunol.* (2016) 7:563. doi: 10.3389/fimmu.2016.00563
5. Zelaya H, Alvarez S, Kitazawa H, Villena J. Respiratory antiviral immunity and immunobiotics: beneficial effects on inflammation-coagulation interaction during influenza virus infection. *Front Immunol.* (2016) 7:633. doi: 10.3389/fimmu.2016.00633
6. Honce R, Schultz-Cherry S. Impact of obesity on influenza a virus pathogenesis, immune response, and evolution. *Front Immunol.* (2019) 10:1071. doi: 10.3389/fimmu.2019.01071
7. Zhang L, Liu Y. Potential interventions for novel coronavirus in China: a systematic review. *J Med Virol.* (2020) 92:479–90. doi: 10.1002/jmv.25707
8. Uyeno Y, Shigemori S, Shimosato T. Effect of probiotics/prebiotics on cattle health and productivity. *Microbes Environ.* (2015) 30:126–32. doi: 10.1264/jsme2.ME14176
9. Ballak DB, van Asseldonk EJP, van Diepen JA, Jansen H, Hijmans A, Joosten LAB. TLR-3 is present in human adipocytes, but its signalling is not required for obesity-induced inflammation in adipose tissue *in vivo*. *PLoS ONE.* (2015) 10:e0123152. doi: 10.1371/journal.pone.0123152
10. Yu L, Yan K, Liu P, Li N, Liu Z, Zhu W, et al. Pattern recognition receptor-initiated innate antiviral response in mouse adipose cells. *Immunol Cell Biol.* (2014) 92:105–15. doi: 10.1038/icb.2013.66

**Conflict of Interest:** The authors declare that the research was conducted in the absence of any commercial or financial relationships that could be construed as a potential conflict of interest.

frontiers in Immunology

ORIGINAL RESEARCH
published: 29 May 2019
doi: 10.3389/fimmu.2019.01180

# Transcriptome Modifications in Porcine Adipocytes via Toll-Like Receptors Activation

*Manami Igata[1,2†], Md. Aminul Islam[1,2,3†‡], Asuka Tada[1,2], Michihiro Takagi[1,2], A. K. M. Humayun Kober[1,2,4‡], Leonardo Albarracin[1,5,6], Hisashi Aso[2,7], Wakako Ikeda-Ohtsubo[1,2], Kenji Miyazawa[8], Kazutoyo Yoda[8], Fang He[8], Hideki Takahashi[9,10], Julio Villena[1,5*] and Haruki Kitazawa[1,2*]*

[1] Food and Feed Immunology Group, Laboratory of Animal Products Chemistry, Graduate School of Agricultural Science, Tohoku University, Sendai, Japan, [2] Livestock Immunology Unit, International Education and Research Centre for Food and Agricultural Immunology (CFAI), Graduate School of Agricultural Science, Tohoku University, Sendai, Japan, [3] Department of Medicine, Faculty of Veterinary Science, Bangladesh Agricultural University, Mymensingh, Bangladesh, [4] Department of Dairy and Poultry Science, Chittagong Veterinary and Animal Sciences University, Chittangong, Bangladesh, [5] Laboratory of Immunobiotechnology, Reference Centre for Lactobacilli (CERELA-CONICET), San Miguel de Tucumán, Argentina, [6] Scientific Computing Laboratory, Computer Science Department, Faculty of Exact Science and Technology, National University of Tucuman, San Miguel de Tucumán, Argentina, [7] Cell Biology Laboratory, Graduate School of Agricultural Science, Tohoku University, Sendai, Japan, [8] Technical Research Laboratory, Takanashi Milk Products Co., Ltd., Yokohama, Japan, [9] Laboratory of Plant Pathology, Graduate School of Agricultural Science, Tohoku University, Sendai, Japan, [10] Plant Immunology Unit, International Education and Research Centre for Food and Agricultural Immunology, Graduate School of Agricultural Science, Tohoku University, Sendai, Japan

OPEN ACCESS

**Edited by:**
Pinyi Lu,
Biotechnology HPC Software Applications Institute (BHSAI), United States

**Reviewed by:**
Harry D. Dawson, United States Department of Agriculture, United States
Kate J. Claycombe, United States Department of Agriculture, United States
Yuanqing Liu, Sanofi Pasteur, France

***Correspondence:**
Julio Villena
jcvillena@cerela.org.ar
Haruki Kitazawa
haruki.kitazawa.c7@tohoku.ac.jp

[†] These authors have contributed equally to this work

[‡] JSPS Postdoctoral Fellow

**Specialty section:**
This article was submitted to Nutritional Immunology, a section of the journal Frontiers in Immunology

**Received:** 26 February 2019
**Accepted:** 09 May 2019
**Published:** 29 May 2019

**Citation:**
Igata M, Islam MA, Tada A, Takagi M, Kober AKMH, Albarracin L, Aso H, Ikeda-Ohtsubo W, Miyazawa K, Yoda K, He F, Takahashi H, Villena J and Kitazawa H (2019) Transcriptome Modifications in Porcine Adipocytes via Toll-Like Receptors Activation. Front. Immunol. 10:1180. doi: 10.3389/fimmu.2019.01180

Adipocytes are the most important cell type in adipose tissue playing key roles in immunometabolism. We previously reported that nine members of the Toll-like receptor (TLR) family are expressed in an originally established porcine intramuscular pre-adipocyte (PPI) cell line. However, the ability of TLR ligands to modulate immunometabolic transcriptome modifications in porcine adipocytes has not been elucidated. Herein, we characterized the global transcriptome modifications in porcine intramuscular mature adipocytes (pMA), differentiated from PPI, following stimulation with Pam3csk4, Poly(I:C) or LPS which are ligands for TLR2, TLR3, and TLR4, respectively. Analysis of microarray data identified 530 (218 up, 312 down), 520 (245 up, 275 down), and 525 (239 up, 286 down) differentially expressed genes (DEGs) in pMA following the stimulation with Pam3csk4, Poly(I:C), and LPS, respectively. Gene ontology classification revealed that DEGs are involved in several biological processes including those belonging to immune response and lipid metabolism pathways. Functionally annotated genes were organized into two groups for downstream analysis: immune response related genes (cytokines, chemokines, complement factors, adhesion molecules, and signal transduction), and genes involved with metabolic and endocrine functions (hormones and receptors, growth factors, and lipid biosynthesis). Differential expression analysis revealed that *EGR1, NOTCH1, NOS2, TNFAIP3, TRAF3IP1, INSR, CXCR4, PPARA, MAPK10,* and *C3* are the top 10 commonly altered genes of TLRs induced transcriptional modification of pMA. However, the protein-protein interaction network of DEGs identified *EPOR, C3, STAR, CCL2,* and *SAA2* as the major hub genes, which were also exhibited higher centrality estimates in the Gene-Transcription factor interaction network. Our results provide new insights of transcriptome

modifications associated with TLRs activation in porcine adipocytes and identified key regulatory genes that could be used as biomarkers for the evaluation of treatments having immunomodularoty and/or metabolic functional beneficial effects in porcine adipocytes.

**Keywords: transcriptome, adipocytes, microarray, TLRs (Toll-like receptors), immunometabolism, pig**

## INTRODUCTION

The innate immune system recognizes infectious microbial pathogens through germ line-encoded patterns recognition receptors (PRRs), such as Toll-like receptors (TLRs), and nucleotide-binding oligomerization domain (NOD)-like receptors (1). These receptors interact with the evolutionarily conserved microbial structures known as microbial associated molecular patterns (MAMPs), including lipopolysaccharides (LPS), lipoteichoic acids (LTA), peptidoglycan (PGN), and double stranded viral RNA, which are essential for the survival of microorganisms (2). In addition, PRRs also recognize endogenous damage-associated molecular patterns (DAMPs) derived from dead cells or injury (3), such as free fatty acids, cholesterol, high glucose concentration, ceramides, and urate crystals (4). Although low levels of DAMPs are beneficial during tissue repair, excessive amounts induce chronic low-grade inflammation in various tissue including adipose tissues. Deregulated inflammation in the adipose tissue is involved in the development metabolic disorders like obesity, atherosclerosis, and type-2 diabetes mellitus (5). Therefore, elucidation of the cellular transcriptome modifications in adipocytes associated with the activation of their PRRs is of great importance to understand in more depth the physiopathological mechanisms involved in the metabolic diseases with an inflammatory component and to propose alternatives to prevent them.

TLRs are an important family of PRRs with capacity to sense several types of MAMPs and thereby trigger inflammatory responses (6). Depending on the cellular localization TLRs can be categorized into two subgroups: trans-membrane (such as TLR1, TLR2, TLR4, TLR5, TLR6, and TLR11) and intracellular (such as TLR3, TLR7, TLR8, and TLR9) receptors (6, 7). Early in the immune response TLR ligation induces gene transcription leading to inflammation, tissue repair and initiation of adaptive immunity (6, 8, 9). Previous studies reported that Pam3csk4 is recognized at the cell membrane by TLR1/2 as a mimic of bacterial lipopeptides (10). Poly(I:C), a synthetic double-stranded RNA is recognized in the endosome by TLR3 (11), while LPS is recognized by TLR4 sequentially at the cell membrane and endosome (8, 12). Upon binding to respective ligands, TLRs recruit a set of specific adapter molecules such as myeloid differentiation primary response gene 88 (MyD88), Toll/interleukin-1 receptor (TIR) domain-containing adapter protein (TIRAP), TIR-domain-containing adapter-inducing interferon-β (TRIF), or TRIF-related adapter molecule (TRAM) to initiate the downstream signal transductions that lead to the activation of different transcriptional factor such as nuclear factor-kappa B (NF-kB), activator protein-1 (AP-1), and interferon regulatory factor (IRF) (2, 6). The transcription factors specifically signal the cells to secrete proinflammatory cytokines and chemokines, type-I interferon, and antimicrobial peptides (6), which coordinately induce inflammatory responses.

The adipose tissue is a highly active organ capable of integrating metabolic, endocrine, and immune functions into a single entity that plays a crucial part on systemic homeostasis (4, 13). In addition to its role as an endocrine gland with pleotropic function in the metabolism (14), adipose tissue is increasingly becoming recognized as part of the innate immune system (15, 16). Adipose tissue contains several distinct groups of cells including mature adipocytes, pre-adipocytes, fibroblasts, M1/M2 macrophages; neutrophils, dendritic cells, eosinophils, and endothelial cells (17). Pre-adipocytes have the ability to differentiate into mature adipocyte according to the energy balance (17, 18). Morphologically, adipocytes are spherical cells with a single large lipid droplet formed by triglycerides that account >90% of the cell's volume (19). Mature adipocytes are functionally the most important cell type in adipose tissue and play roles in storing triglycerides and systemic energy balance (20), as well as in antigen presentation (21). Upon stimulation by MAMPs and/or DAMPs, mature adipocytes secret a wide variety of cytokines and other mediators, which are able to contribute to the generation of both local and systemic immune responses (13, 22).

Different transcriptomic analytic approaches have been employed to identify key regulatory genes in response to multi-TLR activation in white blood cells (23) and macrophages (24). Transcriptomic studies aimed to elucidate the gene expression changes after *in vitro* stimulation with different MAMPs have been also performed in human adipocytes (15, 25). However, there is no detailed information on immunotranscriptomic responses following TLRs activation in the porcine adipocytes. Pigs are considered as one of the closest approximate animal models for studying human diseases because of their anatomical, physiological and immunological similarities with humans (26). By using a porcine intramuscular pre-adipocyte (PIP) cell line originally established by our group (27), we recently demonstrated that nine TLRs (TLR 1-9) are expressed in PIP and differentiated porcine mature adipocytes (pMA) (28). Importantly, TLR2 and TLR4 showed significantly higher expression in pMA as compared to PIP while TLR3 showed higher expression in PIP than that of pMA (28). We therefore, aimed herein to characterize the global transcriptome modifications downstream of TLR2, TLR3, and TLR4 activation in pMA. We obtained a global overview of the modulation of the transcriptomic response in pMA and its association with immune, metabolic and endocrine responses. Results of the present study indicated that several immune genes including *EGR1, NOTCH1, NOS2, TNFAIP3, TRAF3IP1, INSR, CXCR4, PPARA, MAPK10,* and *C3* were differentially modulated in pMA cells after TLR ligation. Our results provide new insights of

transcriptome modifications associated with TLRs activation in porcine adipocytes and indicate that pMA cells are an interesting tool to study *in vitro* the immune responses triggered by TLR2, TLR3, or TLR4 in this cell population.

# MATERIALS AND METHODS

## Cell Line, Culture Condition, and Differentiation

Porcine intramuscular pre-adipocyte (PIP) cell line was previously established by our group (27), which was derived from marbling muscle tissue of the musculus longissimus thoracis from female Duroc pig. Culture conditions for inducing adipogenesis were performed according to our previous work (28), In brief, PIP cells (between the 26th and 35th passages) were maintained in Dulbecco's modified Eagle medium (DMEM; Gibco™, Paisley, Scotland, UK) supplemented with 10% (v/v) fetal calf serum (FCS; Sigma-Aldrich, Tokyo, Japan), 100 U/ml penicillin and 100 μg/ml streptomycin (Gibco™ 15140122, Life Technologies) as a growth medium. The PIP cells were plated at density of $2.5 \times 10^4/cm^2$ in 6-well cell culture plates (BD Falcon, Tokyo, Japan), and incubated at 37°C in a humidified atmosphere of 5% $CO_2$. The 4-day post-confluent PIP cells were fed with differentiation medium for another 4 days to yield the differentiated adipocyte. The differentiation medium composed with DMEM containing 10% FCS and 50 ng/ml insulin (swine, Sigma-Aldrich, Tokyo, Japan), 0.25 μM dexamethasone (Sigma-Aldrich), 2 mM octanoate (Wako, Osaka, Japan), 200 μM oleate (Ardorich, Milwaukee, WI, USA), 100 U/ml penicillin, and 100 μg/ml streptomycin. The medium was changed every day. The differentiation of PIP into functionally matured porcine mature adipocyte (pMA) was confirmed by detecting the presence of intracellular lipid droplets with Oil red O staining according to our previous publication (28). Briefly, cells were rinsed three times in Dulbecco's Phosphate-Buffered Saline and then fixed in 10% (v/v) formaldehyde for 30 min. Subsequently, the fixed cells were rapidly rinsed with MiliQ water. Finally, 0.5% Oil red O (Sigma-Aldrich, Tokyo, Japan) in isopropanol was added to the cells for 5 min to visualize lipid droplets stained red. The cytosolic triglyceride content was analyzed using LabAssay™ triglyceride kit (FUJIFILM Wako Chemicals USA, Corp.) according to the manufacturer's protocol. In addition, qRT-PCR-based (method followed as described later in this section) expression of specific marker genes were also evaluated for adipocyte maturation.

## Stimulation to Porcine Mature Adipocyte (pMA) by TLR Ligands

Synthetic analogs for three Toll-like receptors: TLR2, TLR4 and TLR3; were used to mimic the inflammatory response induced by gram positive bacteria, gram negative bacteria, and by virus infection, respectively. Pam3csk4, Poly(I:C), and LPS were used as ligands for TLR2, TLR3, and TLR4, respectively. For optimizing the dose of ligands, we first stimulated pMA cells ($2.5 \times 10^4/cm^2$) with serial dilutions of each ligand and evaluated CCL2 expression. The optimal doses were selected according to their ability to increase CCL2 expression at least five-folds as compared to that of control (data not shown). The pMA cells were seeded at density of $2.5 \times 10^4/cm^2$ in 6 well or 12 well plates (BD Falcon, Tokyo, Japan). The 4-day post-confluent pMA cells were stimulated either with Pam3csk4 (10 ng/ml), Poly(I:C) (0.1 μg/ml), or LPS (0.1 μg/ml) at 37°C with 5% $CO_2$ for 12 h.

## RNA Isolation and Quality Control

Total RNA was isolated from the ligand-treated and control pMA cells using PureLink RNA Mini Kit (Life Technology Inc., USA) along with on-column DNase treatment. RNA integrity, quality and quantity were evaluated with microcapillary electrophoresis (2100 Bioanalyzer, Agilent Technologies, Santa Clara, CA, USA) using the Agilent RNA 6000 Nano kit (Agilent Technologies, Santa Clara, CA, USA). Only samples with RNA integrity number (RIN) of >8 were used for this gene expression study.

## Microarray Hybridization

The microarray hybridization was performed with Porcine Gene Expression Microarray 4 × 44 K oligonucleotide slide (v2.0, Agilent Technologies, Santa Clara, CA, USA) containing 43,803 probes for the identification of known genes of the porcine transcriptome. The microarray experiment was conducted at Hokkaido System Science Co., according to the one-color Microarray-based Gene Expression Analysis protocol v6.7 (Agilent Technologies, Santa Clara, CA, USA). For each samples, 200 ng of total RNA was converted into cDNA by reverse transcription. The cDNA was subsequently transcribed into cRNA and labeled with cyanine 3 (Cy3). About 1.65 μg of labeled cRNA was mixed with hybridization buffer and hybridized on microarray slide (4 samples in each slide) for 17 h at 65°C with constant rotation. After hybridization, microarrays were cleaned with Gene Expression wash buffer and scanned with High-Resolution Microarray Scanner (Agilent Technologies, Santa Clara, CA, USA). The Feature Extraction software (v10.7.3.1, Agilent Technologies, Santa Clara, CA, USA) was used for detailed analysis of scanned images including filtering the outlier spots, background subtraction from features and dye normalization. The spot intensity data for individual sample were extracted for statistical analysis.

## Statistical Analysis of Microarray Data

The normalization and differential expression analysis of microarray data were performed with GeneSpring GX software (v13.1, Agilent Technologies, USA). The $\log_2$ transformed expression values of probes were normalized based on 75 percentile shifts. In order to determine the TLR-ligand induced differential expression of genes, an unpaired *t*-test was performed between untreated control and TLR-ligand stimulated samples. The pairwise comparisons were performed between control and each of the three TLR-ligand stimulations to detect the differentially expressed genes. Benjamini and Hochberg (B-H) adjustment method was applied for multiple test correction. Significant differentially expressed genes were selected on the basis of two criteria: an adjusted *p*-value (FDR, false discover rate) of <0.05, and a cutoff in fold change of at least 1.5. The human orthologs gene symbols of DEGs were determined using dbOrtho

panel of the bioDBnet tool (29) which were used for downstream functional analyses.

## Gene Ontology (GO) and Pathway Analyses

For biological interpretation of differential gene expressions, GO enrichment and pathway analysis was performed using the Database for Annotation, Visualization, and Integrated Discovery (DAVID, v6.8) (30). Human orthologous symbols of DEGs were uploaded to the DAVID web portal and the official gene symbol was chosen as identifier. Then enriched biological themes, particularly GO terms and KEGG pathways were extracted. In the analysis, GO terms and KEGG pathways with an FDR-adjusted $p < 0.05$ were retained.

## Network Enrichment Analyses

In order to visualize TLR ligands-induced transcriptional network as well as to identify the regulatory genes, the sub-network enrichment analysis was performed using NetworkAnalyst online tool (31). This tool uses the InnateDB protein-protein interaction datasets comprised of 14,755 proteins and 145,955 literature-curated interactions for human (32). Human orthologous gene symbols of the common DEGs from all three stimulation were uploaded into the NetworkAnalyst to construct the interaction network based on Walktrap algorithm taking only direct interaction of seed genes. The network was depicted as nodes (circles representing genes) connected by edges (lines representing direct molecular interactions). Two topological measures such as degree (number of connections to the other nodes) and betweenness (number of shortest paths going through the nodes) centrality were taken into account for detecting highly interconnected genes (Hubs) of the network. Nodes having higher degree and betweenness were considered as potentially important hubs in the cellular signal trafficking. In addition, a gene regulatory network focusing the adipose tissue specific gene-transcription factor (Gene-TF) interaction network was also constructed using the NetworkAnalyst tool (31). For constructing the Gene-TF network, transcription factor and gene target data derived from the ENCODE ChIP-seq data were used. Only peak intensity signal <500 and the predicted regulatory potential score <1 were included based on BETA Minus algorithm (33).

## Validation of Microarray Expression by qRT-PCR

Two-step real-time PCR (qRT-PCR) was performed to confirm the microarray results by quantifying expression of selected mRNAs in pMA. Primer sequences are presented in **Table 1**. Total RNA was isolated from each sample using TRIzol reagent (Invitrogen, Carlsbad, CA, USA) followed by treated with gDNA Wipeout Buffer (Qiagen, Tokyo, Japan). All cDNAs were synthesized using the Quantitect reverse transcription Kit (Qiagen, Tokyo, Japan) according to the manufacturer's recommendations. The qRT-PCR was performed using 7300 real-time PCR system (Applied Biosystems, Warrington, UK) using the TaqMan® gene expression assay kit (Life Technologies) and TaqMan® Universal Master Mix II, with UNG (Applied Biosystems, Warrington, UK). The PCR cycling conditions were 2 min at 50°C, followed by 10 min at 95°C, and then 40 cycles of 15 s at 95°C, 1 min at 60°C. The reaction mixtures contained 2.5 μl of sample cDNA, 1 μl gene expression assay and 10 μl TaqMan® Universal Master mix II, with UNG, and 6.5 μl distilled water. According to the minimum information for publication of quantitative real-time PCR experiments guidelines, Beta actin (ACTB) was used as a house-keeping gene because of its high stability across various porcine tissues (34, 35). Relative index was calculated as the ratio of target mRNA expression to ACTB. Then, raw data were transferred from the mean Ct values of replicated samples to copy number of the established standard curve.

## Statistical Analysis of qRT-PCR Data

The raw data were log-transformed followed by checking the normality by Kolmogorov-Smirnov test. Comparisons between mean values were carried out using one-way ANOVA and Fisher's least significant difference test. For every cases, $p < 0.05$ was considered significant. The Pearson's correlation coefficient between the expression values obtained microarray and qRT-PCR were calculated to explore the linear relationship between the microarray and qRT-PCR results.

# RESULTS

## Differentiation of Adipocytes From PIP

Differentiation of functionally matured adipocytes from pre-adipocytes is an essential biological process. In order to obtain porcine mature adipocytes (pMA), we cultured the porcine intramuscular pre-adipocyte (PIP) cells (25) supplemented with differentiation medium for 4 days. The maturation of adipocytes was confirmed by the detection of lipid droplets in cell cytoplasm under microscopy using Oil red O staining as well as triglyceride assay. The PIP cells at the day of seedling showed no lipid droplets (**Figure 1A**). Following 1 day of culture, some cells started to exhibit flattened cellular morphology (**Figure 1B**). Finally, after 4 days of culture more than 95% of the PIP cells exhibited more lipid droplets indicated their differentiation into fully mature adipocytes (**Figure 1C**). A significant ($p < 0.05$) increased lipid accumulation within the cells indicated their maturation into adipocytes (**Figure 1D**).

In order to further confirm the adipocyte maturation, we quantified the expressions of some differentiation marker genes using qRT-PCR (**Figure 2**). The expression of peroxisome proliferator-activated receptor γ (PPARγ) and insulin receptor (INSR) were significantly increased in PIP after 4 days of culture with differentiation medium while cytochrome P540 receptor 3A (CYP3A46) and free fatty acid receptor 2 (FFAR2) were down regulated. The glutamine fructose-6-phosphate transaminase 1 (GFPT1) showed a decreasing trend but activin receptor type 1B (ACVR1B) and PPARα showed an increasing trend of expression (**Figure 2**).

## Differentially Expressed Transcripts in pMA After TLRs Activation

Stimulation of pMA with TLRs induced changes in a total of 1,575 genes. Among them, 702 (44.57%) and 873 (55.43%) genes were up- and down-regulated, respectively (**Table 2**). The

**TABLE 1 |** Sequences of the primers used for qRT-PCR study.

| Gene symbol | Primer sequence (3′-5′) | Size (bp) | Accession no |
|---|---|---|---|
| ACTB | F: CAT CAC CAT CGG CAA CGA | 144 | XM_003124280.5 |
| | R: GCG TAG AGG TCC TTC CTG ATG T | | |
| INSR | F: AGA GCG GAT CGA GTT TCT CA | 245 | XM_021083943.1 |
| | R: CCA TCC CAT CAG CAA TCT CT | | |
| PPARγ | F: ACA CCG AGA TGC CGT T | 56 | XM_005669788.3 |
| | R: CGA CAG GTC CAC AGA G | | |
| PPARA | F: CGA CCT GGA AAG CCC GTT AT | 148 | NM_001044526.1 |
| | R: GGA TCC ATC TGA TCC CGG AC | | |
| ACVR1B | F: CAT CGA GGG GAT GAT CAA GT | 211 | NM_001195322.1 |
| | R: GGC AAT GTC AAT GGT GTC AG | | |
| CYP3A46 | F: ACA GCA TTT GGA GTG AAC GTC | 250 | NM_001134824.1 |
| | R: CCA CTC GGT GCT TTT GTG TAT | | |
| GFPT1 | F: ATG CTC TTC AGC AGG TGG TT | 232 | XM_005662490.3 |
| | R: TCT ACG GTT ACC GAT TTG GC | | |
| FFAR2 | F: TCA TGG GTT TCG GCT TCT AC | 191 | XM_021093196.1 |
| | R: AAC GAT GAA CAC GAC AGT GC | | |
| TLR2 | F: ACA TGA AGA TGA TGT GGG CC | 109 | XM_005653577.3 |
| | R: TAG GAG TCC TGC TCA CTG TA | | |
| TLR3 | F: TAG AGA CAT GGA TTG CTC CC | 435 | NM_001097444.1 |
| | R: AAC TTC TGG AAT GCA GGT CC | | |
| TLR4 | F: CTC TGC CTT CAC TAC AGA GA | 322 | NM_001293316.1 |
| | R: CTG AGT CGT CTC CAG AAG AT | | |
| EPCAM | F: GCG ATA GCG ATT GTT GCT GG | 106 | NM_214419.1 |
| | R: CCC TAT GCA TCT CGC CCA TC | | |
| SELL | F: GTG ATG CAG GGT ACT ACG GG | 108 | NM_001112678.1 |
| | R: AGA ACT TGC CCA AAG GGT GA | | |
| SAA2 | F: AGA GCC TAC TCG GAC ATG AGA GA | 65 | NM_001044552.1 |
| | R: CCC CGG GCA TGG AAG TAC | | |
| CCL5 | F: CCA GCA GCA AGT GCT CCA T | 60 | NM_001129946.1 |
| | R: ACA CCT GGC GGT TCT TTC TG | | |
| CXCL2 | F: CCG GGA CCC CAC TGT GA | 62 | NM_001001861.2 |
| | R: CAAACTTCCTGACCATTCTTGAGA | | |
| CFB | F: CCT CGG GCT CCA TGA ATA TC | 56 | NM_001101824.1 |
| | R: TGC CCC AAT GCT GTC TGA T | | |
| C3 | F: CCA ACA GGG AGT GCA ACG A | 70 | NM_214009.1 |
| | R: TGA CTC CGT GTC TGG GAC TTG | | |
| CSF1 | F: CCA ACA GGG AGT GCA ACG A | 147 | NM_001244523.1 |
| | R: TGA CTC CGT GTC TGG GAC TTG | | |
| TGFB3 | F: TTG CTA AAT GCT CCA GCC AG | 90 | NM_214198.1 |
| | R: GCC TCC GCC TGT AGA ACA AG | | |
| TNFAIP3 | F: CCC TGG GGC ATT ATG GGT TT | 60 | NM_001267890.1 |
| | R: CCT CAC ACG TTG TAG CAC CT | | |
| CCL2 | F: CCT CCC TGG AAA GCC AGA A | 58 | NM_214214.1 |
| | R: GTG CCA CAA GCT TCC TCA CTT | | |
| TNFα | F: CGA CTC AGT GCC GAG ATC AA | 58 | JF831365.1 |
| | R: CCT GCC CAG ATT CAA AG | | |
| IL8 | F: GCT CTC TGT GAG GCT GCA GTT | 62 | NM_213867.1 |
| | R: TTT ATG CAC TGG CAT CGA AGT T | | |
| IL6 | F: TGG ATA AGC TGC AGT CAC AG | 109 | NM_214399.1 |
| | R: ATT ATC CGA ATG GCC CTC AG | | |
| IL1α | F: AGA ATC TCA GAA ACC CGA CTG TTT | 62 | NM_214029.1 |
| | R: TTC AGC AAC ACG GGT TCG T | | |
| IL1β | F: GCC CTG TAC CCC AAC TGG TA | 61 | NM_001302388.2 |
| | R: CCA GGA AGA CGG GCT TTT G | | |

*F, Forward; R, Reverse; bp, base pair.*

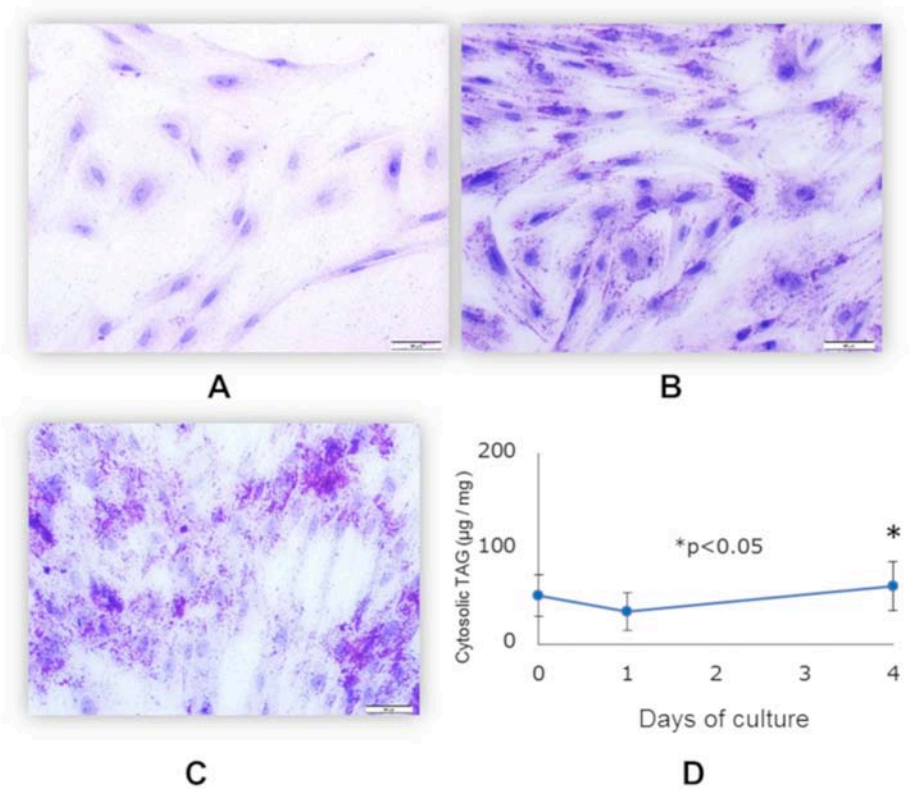


**FIGURE 1 |** Differentiation of mature porcine adipocytes (pMA) from porcine intramuscular pre-adipocyte (PIP). Oil-red O stained images display the cellular morphology at day 0 **(A)**, day 1 **(B),** and day 4 **(C)** of culture of PIP cells with differentiation media. Fat accumulation was determined by triglyceride assay **(D)**. Data (Mean ± SD) presented are the average of 3 independent experiments performed in triplicates.

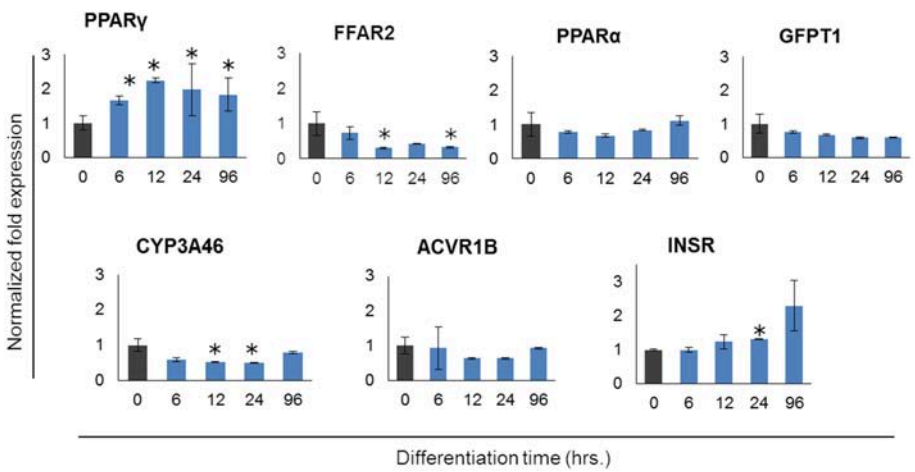


**FIGURE 2 |** Expression profiles of marker genes for adipocyte differentiation in porcine intramuscular pre-adipocyte (PIP) and porcine mature adipocytes (pMA). The asterisk (*) indicates Statistical differences with significant levels of $P < 0.05$. Data (Mean ± SD) presented are the average of 3 independent experiments performed in triplicates.

TLR2 ligand Pam3csk4 differentially regulated 530 transcripts in pMA, being 218 and 312 transcripts up- and down-regulated, respectively. After TLR3 stimulation 245 transcripts were up-regulated while 275 transcripts were down-regulated in pMA. In addition, stimulation of pMA with LPS up-regulated 239 transcripts and down-regulated 286 transcripts (**Table 2**). The list of significantly (adjusted $p<0.05$) up-regulated and down-regulated genes are presented in **Supplementary Tables S1–S3**.

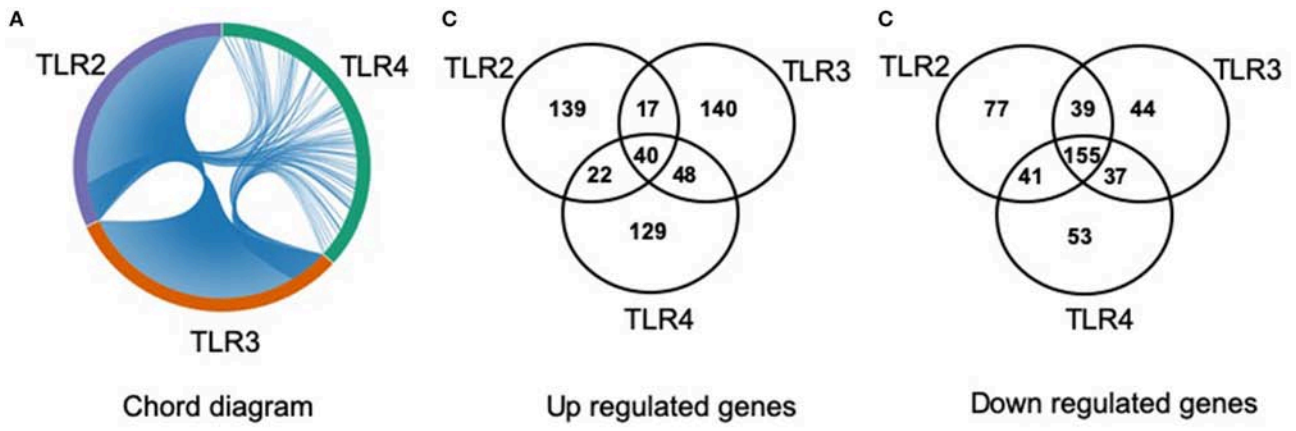


**FIGURE 3 |** Distribution of number of differentially regulated genes in mature porcine adipocytes (pMA) among intersections of three contrast pairs of ligand stimulation. **(A)** Chord diagram showing the proportion of transcripts shared among stimulants. **(B)** The number of up regulated transcripts after each stimulant and their intersections. **(C)** The number of down regulated transcripts after each stimulant and their intersections.

**TABLE 2 |** Number of differentially regulated genes in the porcine intramuscular adipocytes after Pam3csk4, Poly(I:C) and LPS stimulation.

| | Pam3csk4 vs. control | Poly(I:C) vs. control | LPS vs. control |
|---|---|---|---|
| Up | 218 | 245 | 239 |
| Down | 312 | 275 | 286 |
| Total | 530 | 520 | 525 |

## Intersections of TLR Ligand-Induced Differentially Regulated Transcripts

The lists of differentially regulated transcripts obtained from three pairwise contrasts were overlapped to assess the cross-talk among the three TLR ligands. We observed that there were 195 differentially expressed transcripts shared by the three stimulations. Among them, 40 were up- and 155 were down-regulated transcripts (**Figure 3**). A total of 251 differentially expressed transcripts were common between TLR2 and TLR3 stimulation, 57 and 194 were up- and down-regulated, respectively. In addition, 280 differentially expressed transcripts were common between TLR3 and TLR4 stimulation. A total of 258 transcripts were shared by pMA stimulated with TLR2 or TLR4. Among them, 62 were up- and 196 were down-regulated transcripts (**Figure 3**).

## Gene Ontology Classification

In order to characterize the biological implications of the differentially expressed genes in pMA after TLRs stimulations, we performed the GO and pathway enrichment analysis using DAVID online tool. Based on the ascending order of adjusted *p*-value, the top 15 GO biological process significantly enriched with the differentially expressed genes following Pam3csk4, Poly(I:C), and LPS stimulation are presented in **Figure 4**. There were some common GO terms enriched following each of the three TLR treatments including immune response (GO: 0006955), inflammatory responses (GO: 0006954), oxidation-reduction process (GO: 0055114), chemokine-mediated signaling (GO: 0070098), and positive regulation of ERK1 and ERK2 cascade (GO: 0070374). Cell adhesion (GO: 0007155), chemotaxis (GO: 0006935), and insulin secretion (GO: 0030073) were commonly enriched GO biological process between Poly(I:C) and LPS stimulation, while enrichment of calcium ion transport (GO: 0006816) was shared between Pam3csk4 and Poly(I:C) stimulation. The full list of enriched GO and pathways are presented in **Supplementary Table S4**.

## Transcript Abundances Associated With Immune Response Function

The expression patterns of differentially modulated immune related genes in pMA following TLR activation are presented in **Figure 5**. The mRNAs of cytokine and cytokine receptors including *IL1β, IL1α, IL13RA2, IL1RAPL1, IL9, IL10, IL15, IL6R, IL12B, IL18A, IL20RB, IL23R, IFNB1,* and *IFN-omega5* showed differential expression. The expression of chemokine and chemokine receptors including *CCL2, CCL20, CCL8, IL8, CX3CR1, CXCL9, CSF3, CXCL12, CXCR4, CCL5, CCL3L1, CCR1, CCR7, CXCR6, CCR9,* and *CXCL1* were differentially regulated. The expression of complement factors including *C3, CFB, CFH, F9,* and *THBD*; and adhesion molecules including *EPCAM, ITGA2, SELE, SELL,* and *MCAM* were differentially modulated following TLR activation in pMA. The signal transduction molecules including *TNFAIP3, TNFSF4, TRAF3IP1, MAPK, NOTCH1, NF-kB, NKAPL, MALL,* and *CRABP1* showed differential expression in pMA after 12 h of TLR activation (**Figure 5**).

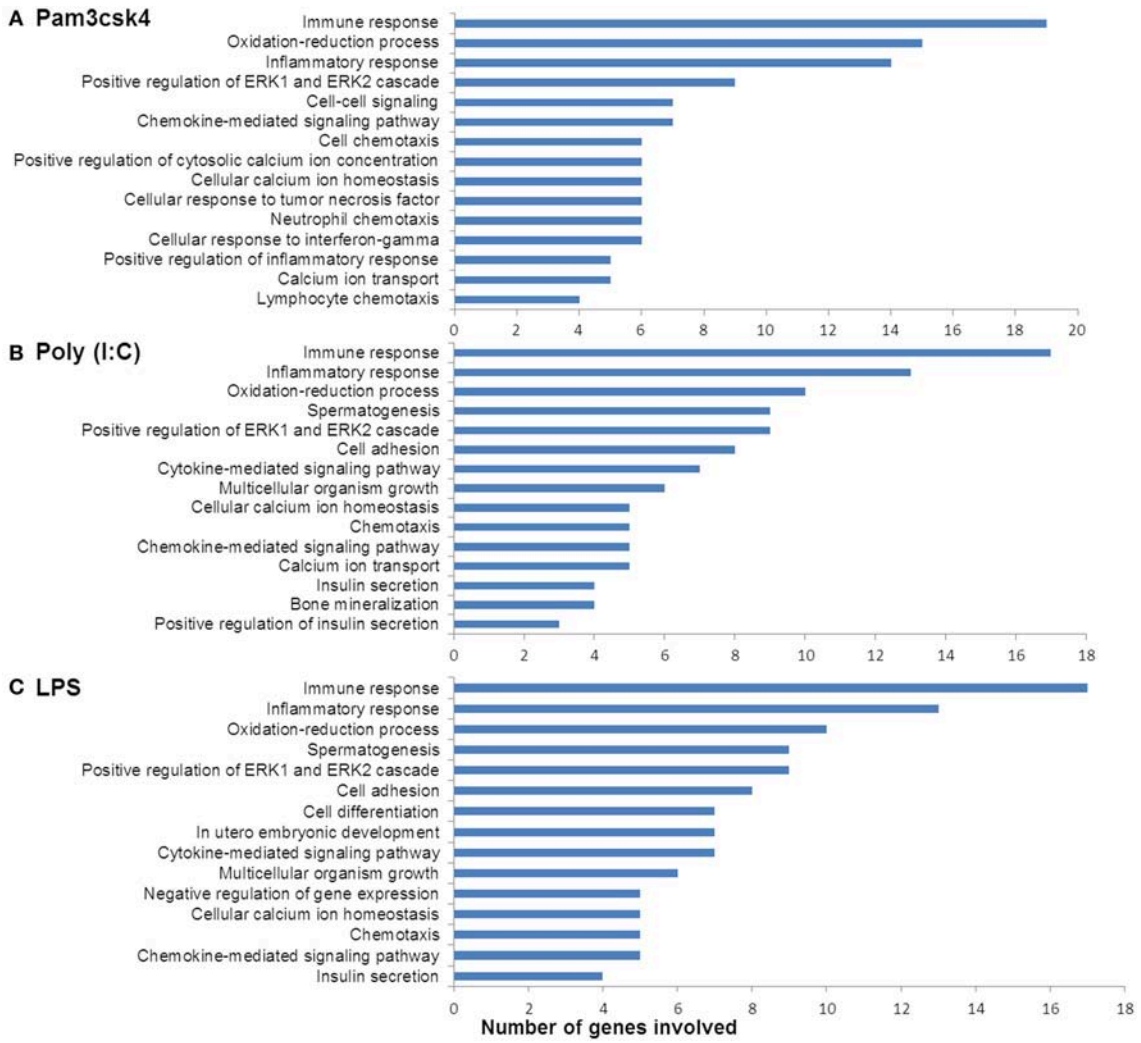


**FIGURE 4 |** Enrichment of GO terms by differentially expressed genes in porcine mature adipocyes (pMA) after stimulation with **(A)** Pam3csk4, **(B)** Poly(I:C), and **(C)** LPS. GO terms shown were passed the statistical significance threshold ($p < 0.05$).

## Transcripts Abundance Associated With Metabolic and Endocrine Functions

Differentially regulated transcripts encoded for proteins involved in metabolism and endocrine functions are summarized in **Figure 6**. Among them, genes involved in lipid metabolism included *FFAR2, APOB, APOM, ADIPOQ, CYP8B1, CYP2C49, CYP2025, STAR, CYP21A2, ACACB, AKR1C1, CYP4A24, CYP2B22, FFAR1, PPARA, CYP27B1, CYP3A46, CYP2A19, CYP4F2,* and *CYP19A3*. The mRNAs for hormones and receptor including *ADRA1B, ADRA2B, ADRA1D, CCK, CHRM2, CHRNB2, DRD1, EPOR, ESRRB, GHRH, HTR1F, HTR2C, INSR, IRS1, P2RY1, P2Y12R, PC2, PRLR,* and *PTH1R* showed differential expressions in pMA after TLR activation. In addition, TLR activation resulted in a differential expression of some growth factors including *EGF, EGR1, EGR3, EGFR4, EGF17, EGF23, KLF1, SCG5, RETN, ITLN2,* and *GHSR* in the porcine adipocytes (**Figure 6**).

## Gene Expression Measured by qRT-PCR

In order to confirm the microarray expression results, we quantified mRNAs of several differentially expressed genes as well as some other genes which are known to be involved in immune and metabolic functions by using qRT-PCR. The Pearson's correlation coefficient ($r = 0.9064$, $p < 0.001$) indicated that microarray expression results were strongly correlated with that obtained from qRT-PCR (**Figure 7A**). Among the genes quantified by qRT-PCR, *SAA2* was significantly up regulated and *EPCAM* was down regulated after all the ligand stimulation (**Figure 7B**). The expression of *SELL, PPARA, INSR,* and *ADIPOQ* were up regulated after both Pam3csk4 and Poly(I:C) stimulation but down regulated after LPS stimulation. *GLP2R* expression was increased after Pam3csk4 and LPS stimulation but *CCL5* was increased only after Poly(I:C) stimulation (**Figure 7B**). Among the immune response related genes, up regulation of *CXCL2, C3, CSF1, TNFAIP3, CCL2, TNFα, IFNβ, IL8, IL6,*

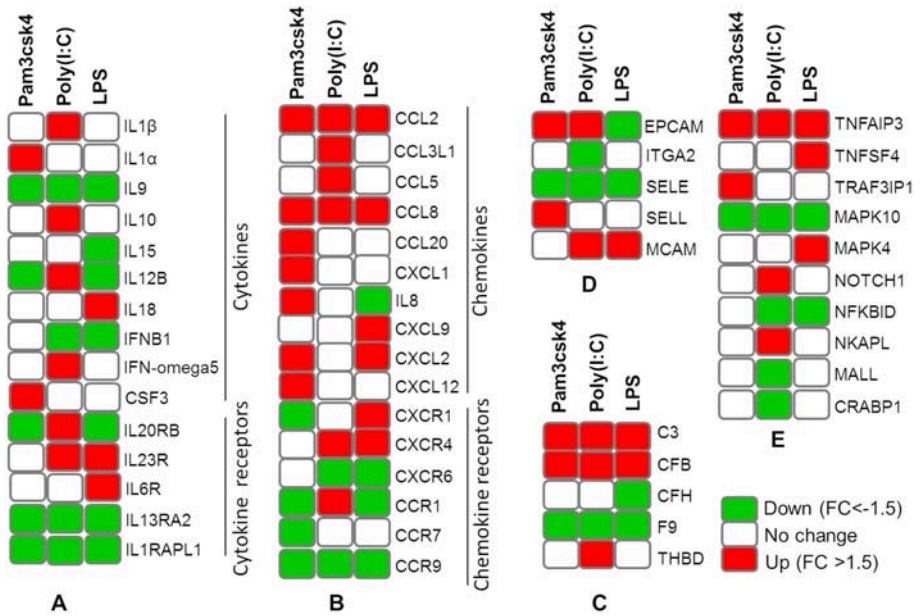


**FIGURE 5 |** Heatmap showing the expression patterns of different groups of immune related genes measured by microarray in mature porcine adipocytes (pMA) stimulated with different TLRs ligands. Groups of genes include cytokines and cytokine receptors **(A)**, chemokines and chemokine receptors **(B)**, complement factors **(C)**, adhesion molecules **(D)**, and signal transduction molecules **(E)**.

and *IL1α* were noticed relatively more in case of Pam3csk4 and LPS stimulation than Poly(I:C) stimulation (**Figure 7C**). The expression of CFB was increased after Pam3csk and Poly(I:C) stimulation but decreased after LPS stimulation. *IL1β* was increased after Poly(I:C) stimulation, but decreased after Pam3csk4 and LPS stimulation. Expression of *TGFB3* was remained stable following all three stimulation (**Figure 7C**).

## Protein-Protein Interaction (PPI) Network

The PPI network is a hierarchical structure, where the hubs play a central role in directing cellular response to a given stimulus. To identify the hub genes involved in the regulation of transcriptome modification of pMA following TLRs ligation, we have constructed and visualized the PPI network of differentially expressed transcripts (**Figure 8**). The hub nodes of the network were selected based on the values of two centrality measures interpreted serially, first "degree" then "betweenness." Accordingly, *RELA, HNF4A, SP1, EPOR, C3, STAR, CCL2,* and *SAA2* were identified as major hub genes of the TLRs induced transcriptional network in the pMA (**Figure 8**). Though *RELA, HNF4A,* and *SP1* were not differentially expressed in the TLR ligand-treated pMA but predicted to be involved in the regulation of PPI-network. The centrality measures of the network nodes/interactome are presented in **Supplementary Table S5**.

## Gene-Centered Transcription Factor Network

Transcription factors (TF) are potential regulators of differential gene expression. We constructed a gene-TF interaction network in order to explore the involvement of transcription factors in TLR ligand-induced differential gene expression in porcine adipocytes using NetworkAnalyst. Gene-TF network illustrated that potential hub genes of PPI network also exhibited higher centrality estimates in the Gene-TF interaction network indicating their possible regulation by transcription factors. The transcriptional factor binding site (TFBS) analysis revealed that promoter regions of C*3, TNFAIP3, CFB, CXCL2, STAR, ADIPOQ, CYP8B1, SOD2, EPCAM, EPOR, SAA2,* and *CCR9* genes have DNA-binding sites of transcription factors, which are likely contributing pMA transcriptional modification (**Figure 9**). In particular, *TNFAIP3, CXCL2, STAR,* and *ADIPOQ* are regulated by *NF-kB* transcription factor. The network centrality measures of potential genes are presented in **Supplementary Table S6**.

# DISCUSSION

In recent years, it became clearer that along with the metabolic and endocrine functions, the adipose tissue exerts multiple roles in the generation and regulation of immune responses (4, 13). In this work, we performed a microarray-based global transcriptome profiling of pMA after *in vitro* stimulation with TLR ligands in order to evaluate the immune and metabolic responses of porcine adipocytes triggered by the activation of these PRRs.

The differentiation and maturation of adipocytes is crucial for their proper physiological functions and for the prevention of metabolic disorders (36, 37). Apart from those in the main subcutaneous and visceral fat depots, adipogenic differentiation has also been described in other locations, including skin, bone marrow, and skeletal muscle (36). A recent microarray

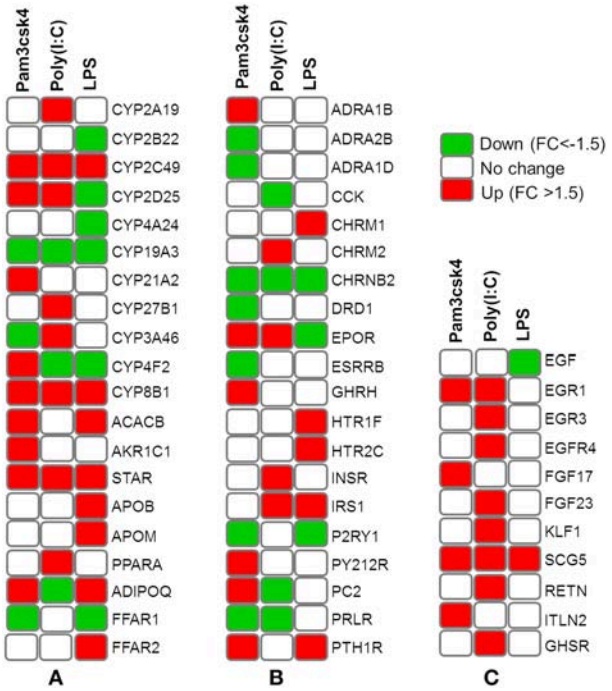


**FIGURE 6 |** Heatmap showing the expressions of genes associated with metabolism and endocrine functions measured by microarray in mature porcine adipocytes (pMA) stimulated with different TLRs ligands. Groups of genes include those related to lipid metabolism **(A)**, hormones and receptors **(B)**, and growth factors **(C)**.

study based on primary cells of intramuscular preadipocytes obtained from Landrace pigs has reported gene expression changes associated with adipocyte differentiation (38). Among other genes, pattern recognition receptors were differentially expressed when preadipocytes were compared with pMA (38), which was in line with our previous findings (28). Then, we focused our attention in pMA. Here, we confirmed the differentiation of intramuscular preadipocytes cell line obtained from Duroc pigs by the evaluation of fat accumulation, and expression of several marker genes. Thus, adipocytes used for this transcriptome analysis were functionally mature. In addition, in our previous study we demonstrated that members of the TLR family including TLR2, TLR3, and TLR4 focused in the present study are expressed in pMA (28).

The TLR2 is activated by the lipopeptides/peptidoglycan present in the cell wall of bacteria. It has been reported that human and murine adipocytes express TLR2 (15, 25, 39). Stimulation of adipocytes from humans and mice with the TLR1/2 ligand Pam3Csy or the TLR2/6 ligand MALP-2 differentially modulated the release of the proinflammatory factors including *IL6*, *IL8*, and *CCL2* in those cells (15, 39), whereas resistin was either not affected or even down regulated by both ligands (15). The role of the adipose tissue in the innate immune response induced by local or systemic infection with *Staphylococcus aureus* has been studied *in vivo* in a rodent model (40). The work reported that systemic bacterial infection resulted in a shift from anti- to pro-inflammatory cytokines in the adipose tissues transcriptome profile clearly demonstrating the role of adipocytes in the development of immune response (40). To the best of our knowledge, no transcriptional analysis has been performed in porcine adipocytes in response to TLR2 activation. Similar to human and murine adipocytes, we observed that pMA stimulated with Pam3csk showed a major transcriptome alteration, and that the differentially regulated transcripts were known to be involved in the positive regulation of inflammatory responses, including cytokines (*IL1α, IL12B*), chemokines (*CXCL1, CXCL2, CCL20, CSF3*), and adhesion molecules (*SELL*) (**Figure 10**). This result indicates the ability of porcine adipocytes in participating in immune responses triggered by TLR2 activation.

On the other hand, the LPS from gram-negative bacteria is a well-known innate immune stimulant of TLR4 activation (6). The responsiveness of human adipocytes to LPS stimulation has been widely documented (15, 25); therefore, we speculated that porcine adipocytes would also have the ability to response to LPS in a similar way. LPS/TLR4 interaction induces signaling pathways through the adaptor molecule MyD88, which results in the activation of transcription factor such as NF-kB and AP-1 (6, 9, 41). MyD88 recruits different interleukin-1 receptor associated kinase (IRAK) family proteins and TNF receptor-associated factors 6 (TRAF6) (42). This complex activates TGF-activated kinase 1 (TAK1), leading to activation of NF-kB and mitogen activated protein kinases (MAPKs) (43), which in turn induce the expression of factors participating in inflammatory responses. In agreement, we observed that several signal transduction molecules including members of TNF, MAPK, and NF-kB pathways were found to be differentially expressed in pMA following the activation of TLR4. Of note, pMA stimulated with LPS showed an up-regulation of *CXCL2* and *CXCL9* that are strongly chemotactic for lymphocytes. Similar to our results, LPS up-regulated the expression of *CCL2* and *CCL8* in human adipocytes (44), and *CCL2* in mouse adipocytes (15). Of note, although microarray results showed down-regulation of *IL8* and no effect on *IL6* expression after LPS stimulation (**Figure 5**), we checked the expression of both cytokines by qRT-PCR because of their up-regulation is well-reported in LPS responses of human (44), mouse (15), and pig (45) adipocytes. Although it was statistically insignificant, but both *IL6* and *IL8* expression showed an upward trend after LPS stimulation (**Figure 7C**). In addition, an increase in the expression of *IL18*, which is a cytokine belongs to the *IL1* superfamily and has the ability to stimulate the cellular immune response through the activation of natural killer cells (NK) cells and T cells, was observed after TLR4 activation in pMA (**Figure 10**). These results are in line with study of Vielma et al. (46) who used fibroblast-derived adipocytes and spleen lymphocytes in order to evaluate whether adipose cells were able to modulate the function of immune cells. The work demonstrated that adipocyte-conditioned medium was able to activate spleen lymphocytes and stimulate their production of the inflammatory cytokines IL6, IL9, IFNγ, and TNFα.

Interestingly, TLR3 activation in pMA also led to the development of a complex transcriptomic response. TLR3 ligation lead to the activation of NF-kB and MAPKs to induce

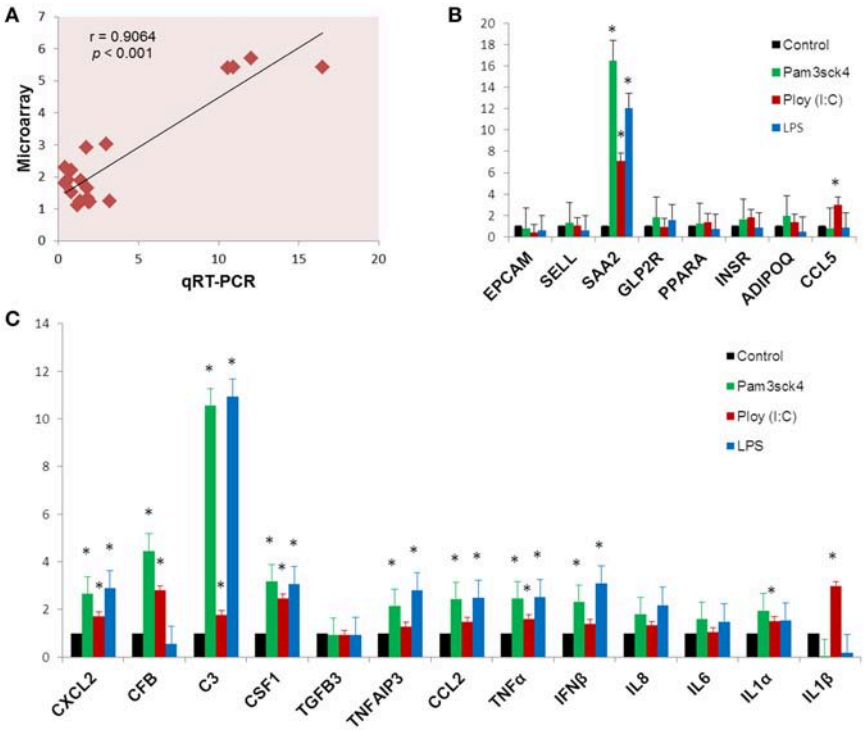


**FIGURE 7 |** Gene expression results obtained from qRT-PCR. The Pearson's correlation coefficient between expression results obtained from microarray and qRT-PCR **(A)**. The expression profiles of metabolism **(B)** and immune response **(C)** related genes measured by qRT-PCR. Y-axis represents the fold expressions. The asterisk (*) indicates Statistical differences with significant levels of $p < 0.05$. Data (Mean ± SE) presented are the average of 3 independent experiments performed in triplicates.

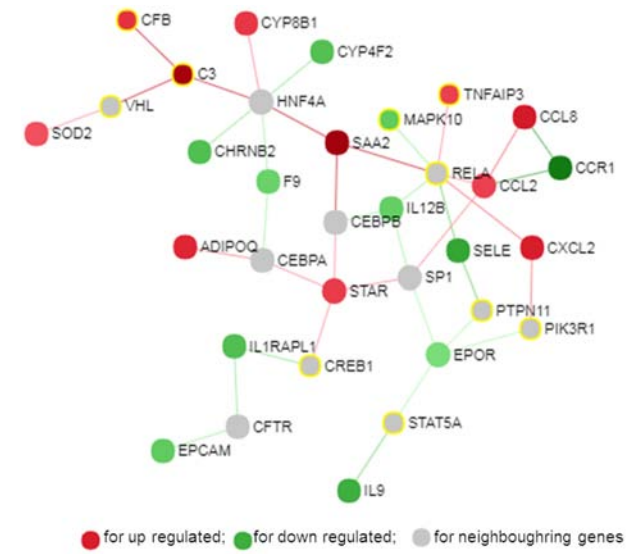


**FIGURE 8 |** Protein-protein interaction network of the common genes in mature porcine adipocytes (pMA) stimulated with different TLRs ligands obtained from NetworkAnalyst.

pro-inflammatory cytokines (43), and the phosphorylation and activation of IRF3, leading to IFNγ (42) and type I interferons (47) production. It was described that TLR3 is highly expressed and functionally active in human (48) and mouse (49) adipocytes. Stimulation of human and mouse adipocytes with Poly(I:C) is able to induce the expression of pro-inflammatory factors such as *TNFα*, *IL6*, *IL8*, and *CCL2* as well as IFN-α/β and multiple anti-viral proteins including $2'5'$-oligoadenylate synthetase and Mx GTPase 1 (48, 49), indicating that adipose cells are able to trigger innate antiviral responses. Here, we observed that TLR3 activation in pMA increased the expression of several inflammatory genes (*CCL2, CCL8, CCL5, CCL3L1, IL1β, IL12B,* and *MCAM*) that participate in the antiviral inflammatory responses resembling human and mice adipocytes (**Figure 10**). However, our transcriptomic analysis was no able to detect increases in the expression of IFN-α/β or IFN-induced antiviral genes. Deeper kinetic and dose-response studies are necessary to establish whether this difference between porcine and human/mice adipocytes are due to differences related to the species or are an effect of the experimental conditions.

Activation of human adipocytes by multiple TLRs ligands was reported to induce pro-inflammatory and pro-diabetic responses through the phosphorylation of extracellular signal-induced kinase and c-Jun N-terminal kinase pathways (25). Human adipocytes have shown the ability to synthesize and secrete complement factors, C1q/TNF-related proteins (CTRPs) (15, 16), cytokines, chemokines, and pro- and anti-inflammatory adipokines including resistin, visfatin, leptin, and adiponectin; as well as antibacterial peptides such as lipocalin-2 and cathelicidin in response to multiple TLRs ligands (25, 50). In addition,

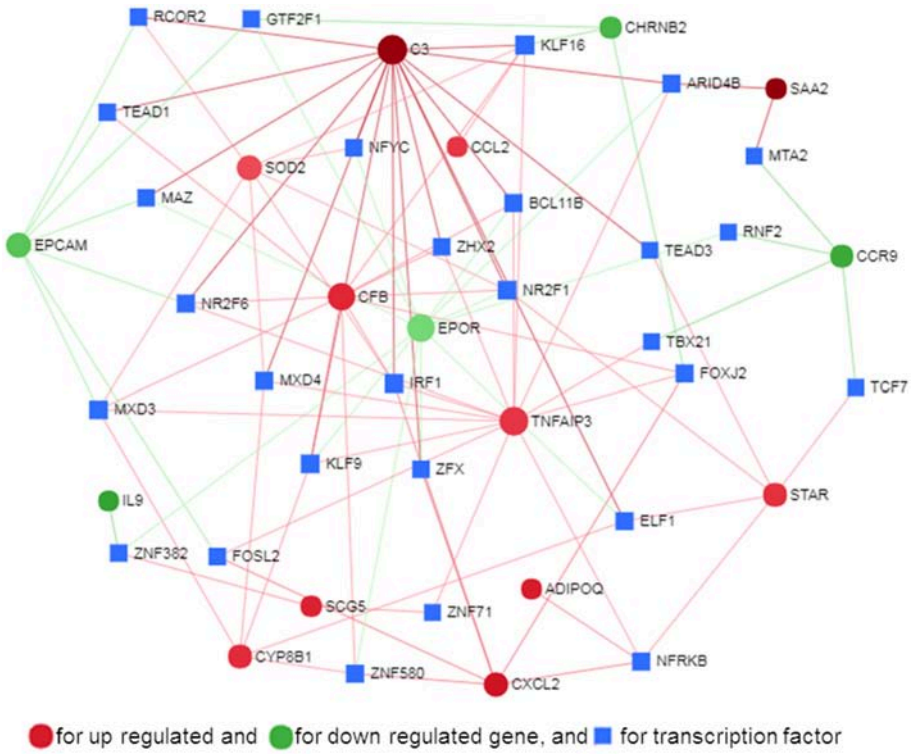


**FIGURE 9 |** Gene-transcription factor regulatory network for the common genes in mature porcine adipocytes (pMA) stimulated with different TLRs ligands obtained from NetworkAnalyst.

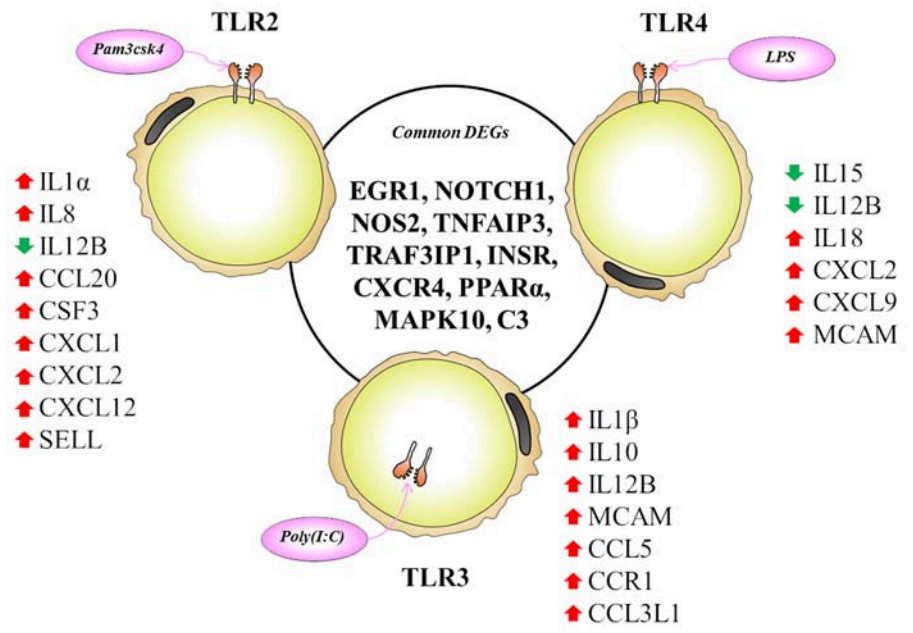


**FIGURE 10 |** Most significantly altered genes after TLR2, 3 and 4 activation in porcine adipocytes. Genes presented in central circle are the common DEGs for all three TLR activation while individual list close to each TLR are the unique DEGs for them. Red arrow indicates upregulation while green arrow indicates the downregulation of corresponding genes.

taking into consideration that in most cases microorganisms carry more than one TLR-ligand and that infections with multiple pathogens, such as virus-bacteria superinfections, have become a common disease scenario; we focused in the transcripts showing differential expression after the activation with the three TLRs in pMA. These commonly differentially regulated genes (**Figure 10**) are involved in two major biological functions: inflammatory response and insulin mediated metabolism, in agreement with previous reports that evaluated TLRs activation in human adipocytes (15, 16, 25, 48). In fact, immune response, cytokine-mediated signaling, inflammatory responses, oxidation-reduction process, positive regulation of ERK1/ERK2 and lipid metabolisms are commonly enriched GO terms in pMA following TLR2, TLR3, or TLR4 activation.

Here we report that *EGR1, NOTCH1, NOS2, TNFAIP3, TRAF3IP1, INSR, CXCR4, PPARA, MAPK10,* and *C3* are the top 10 (based on fold expression) commonly altered genes of TLRs induced transcriptional modification in pMA (**Figure 10**). It is well-known that *TNFAIP3, CXCR4, MAPK4, MAPK10,* and *IL8* among others are involved in the generation of innate immune responses (2, 6, 8, 9). Other common DEGs like *EGR1* and *INSR* are known to be involved in insulin and glucose metabolism (35). *PPARA* and *NOS2* participate in adipocyte maturation (35, 37). However, the immune response and the lipid metabolism are complex traits, not regulated only by a particular gene but rather by networks of complex molecular interactions (51). Therefore, network analysis based on larger immune-specific and metabolic-specific gene databases is considered to be more effective strategy for identification of regulatory genes (31). The PPI network predicted *RELA, HNF4A, SP1, EPOR, C3, STAR, CCL2,* and *SAA2* as the major regulatory hub genes of TLRs-induced transcriptional network in porcine adipocytes. Interestingly, *C3* is the hub gene that overlapped with top 10 common DEGs. The *C3* is the central component of complement system and plays a vital role in the innate immune response, which was up-regulated in pMA stimulated with TLRs ligands. It was reported that the agonists for TLR2, TLR4, and TLR9 are able to activate the complement-TLR crosstalk, which signals through MyD88 pathway and mediated inflammatory responses (52). We also observed that the hub genes of PPI network also exhibited higher centrality estimates in the gene-centered transcription factor interaction network indicating their potential to regulate the TLR-induced transcriptional modifications in the porcine adipocytes. A long-term goal of our laboratory is to establish an adipocyte-based *in vitro* evaluation system for the selection of beneficial microbes able to differentially modulate immune responses in the adipose tissue for their application in the prevention of immunometabolic diseases in human and animals. We have been successful in a similar approach before by establishing a porcine intestinal epithelial (PIE) cells model for the efficient selection of anti-diarrheal immunomodulatory probiotic bacteria (53).

The physiological roles including metabolic and secretory function of adipocytes are distinguished by their tissue origin, appearance and location of the body (54, 55). The intramuscular adipocytes play pivotal role in the control of systemic energy balance (56) and immuno-metabolic homeostasis (57). However, due to their particular location in close vicinity with muscle fibers, the biology of intramuscular adipocytes may differ from those originated from other location. Among the hub genes identified in this study, *EPOR*, *STAR,* and *SAA2* are known to be involved in lipid metabolism. Serum amyloid A (SAA) including *SAA2,* have been reported to function in metabolic homeostasis and healthy adipose development through accompanying with retinoic acid, a potential regulator of lipid metabolism (58). In addition, though the lipolysis pathway was not induced after TLRs ligation in intramuscular derived pMA, the intracellular calcium homeostasis and positive regulation of insulin secretion pathways were significantly enriched, which indicates that the TLR-induced transcriptional modification is linked to metabolic changes. These are in line with finding of Gardan et al. (55) who reported that porcine intramuscular adipocytes display a relatively lower lipogenic activity compared with adipocytes isolated from subcutaneous or visceral adipose tissue. Besides the subcutaneous and visceral fat depots, adipogenic differentiation appears to be beneficial in the skin; however, adipogenesis in the skeletal muscle is associated with pathology (36). Therefore, the results obtained in this work indicate that pMA are a useful tool for the *in vitro* study of the transcriptomic changes associated not only with the innate immune response, but also with inflammatory disorders linked to lipid metabolism and hormones resulting from TLRs ligation in porcine adipocytes.

## CONCLUSION

This study reported for the first time the global transcriptome modifications in porcine adipocytes following activation of TLR2, TLR3, or TLR4. We demonstrated that the activation of TLRs in porcine mature adipocytes induced modifications of transcripts involved not only in the immune response, but also in cellular lipid metabolism. Sub-network enrichment analysis suggested that *EPOR, C3, STAR, CCL2,* and *SAA2* are the major hub genes of TLRs-mediated transcriptional network responses of porcine adipocytes. In addition, gene-transcription factor interaction network analysis revealed the potentials of hub genes to regulate the TLRs-induced transcriptional modification. Therefore, we identified key regulatory genes that could be used as candidates for the evaluation of immune-modulators (e.g., immunomodulatory probiotic bacteria) having functional beneficial effects (e.g., anti-inflammatory capacity) in porcine adipocytes.

## DATA AVAILABILITY

The MIMAE (minimum information about a microarray experiment) standard raw microarray dataset have been submitted to the NCBI-GEO database under the access number GSE124171.

## AUTHOR CONTRIBUTIONS

MI, MAI, JV, and HK designed the study. MI, AT, and MT did the cell culture and qRT-PCR experiments, and prepared the microarray samples. KM, KY, and FH arranged the kit, chemicals, and reagents. MAI analyzed the expression data and

wrote the manuscript. LA contributed to data analysis and results interpretation. AK, WI-O, HA, and HT reviewed the manuscript. HK and JV approved the final version of the manuscript.

## FUNDING

This study was supported by a Grant-in-Aid for Scientific Research (A) (19H00965), (B) (16H05019), Challenging Exploratory Research (26660216, 16K15028), Open Partnership Joint Projects of JSPS Bilateral Joint Research Projects from the Japan Society for the Promotion of Science (JSPS) to HK, and the Research Project on Development of Agricultural Products and Foods with Health-promoting benefits (NARO), and the Science and Technology Research Promotion Program for Agriculture, Forestry, Fisheries and Food Industry, Japan to HA, and the grants for Scientific Research on Innovative Areas from the Ministry of Education, Culture, Science, Sports and Technology (MEXT) of Japan (Grant numbers: 16H06429, 16K21723, and 16H06435) to HT. MAI and AK were supported by JSPS (Postdoctoral Fellowship for Foreign Researchers, Program No. 18F18081 and 15F15401, respectively). This work was also supported by JSPS Core-to-Core Program, A. Advanced Research Networks entitled Establishment of international agricultural immunology research-core for a quantum improvement in food safety.

## SUPPLEMENTARY MATERIAL

The Supplementary Material for this article can be found online at: https://www.frontiersin.org/articles/10.3389/fimmu.2019.01180/full#supplementary-material

**Supplementary Table S1 |** Top 40 significantly (adjusted $p < 0.05$) differentially expressed genes in pMA after Pam3csk stimulation (.xlxs).

**Supplementary Table S2 |** Top 40 significantly (adjusted $p < 0.05$) differentially expressed genes in pMA after Poly(I:C) stimulation (.xlxs).

**Supplementary Table S3 |** Top 40 significantly (adjusted $p < 0.05$) differentially expressed genes in pMA after LPS stimulation (.xlxs).

**Supplementary Table S4 |** GO terms and pathways enriched by TLR ligand-induced DEGs in adipocytes obtained from DAVID analysis (.xlxs).

**Supplementary Table S5 |** Centrality estimates of protein interaction network of TLR ligand-induced DEGs in adipocytes obtained from NetworkAnalyst (.xlxs).

**Supplementary Table S6 |** Centrality estimates of Gene-transcription factor interaction network of TLR ligand-induced DEGs in adipocytes obtained from NetworkAnalyst (.xlxs).

## REFERENCES

1. Akira S, Uematsu S, Takeuchi O. Pathogen recognition and innate immunity. *Cell*. (2006) 124:783–801. doi: 10.1016/j.cell.2006.02.015
2. Kawai T, Akira S. Toll-like receptors and their crosstalk with other innate receptors in infection and immunity. *Immunity*. (2011) 34:637–50. doi: 10.1016/j.immuni.2011.05.006
3. Chen GY, Nunez G. Sterile inflammation: sensing and reacting to damage. *Nat Rev Immunol. (*2010) 10:826–37. doi: 10.1038/nri2873
4. Grant RW, Dixit VD. Adipose tissue as an immunological organ. *Obesity*. (2015) 23:512–8. doi: 10.1002/oby.21003
5. Piccinini AM, Midwood KS. DAMPening inflammation by modulating TLR signalling. *Mediat Inflamm*. (2010) 2010:672395. doi: 10.1155/2010/672395
6. Kawai T, Akira S. The role of pattern-recognition receptors in innate immunity: update on Toll-like receptors. *Nat Immunol*. (2010) 11:373–84. doi: 10.1038/ni.1863
7. Jin MS, Lee J-O. Structures of the toll-like receptor family and its ligand complexes. *Immunity*. (2008) 29:182–91. doi: 10.1016/j.immuni.2008.07.007
8. Takeuchi O, Akira S. Pattern recognition receptors and inflammation. *Cell*. (2010) 140:805–20. doi: 10.1016/j.cell.2010.01.022
9. Medzhitov R, Horng T. Transcriptional control of the inflammatory response. *Nat Rev Immunol*. (2009) 9:692–703. doi: 10.1038/nri2634
10. Takeuchi O, Kawai T, Muhlradt PF, Morr M, Radolf JD, Zychlinsky A, et al. Discrimination of bacterial lipoproteins by Toll-like receptor 6. *Int Immunol*. (2001) 13:933–40. doi: 10.1093/intimm/13.7.933
11. Alexopoulou L, Holt AC, Medzhitov R, Flavell RA. Recognition of double-stranded RNA and activation of NF-kappaB by Toll-like receptor 3. *Nature*. (2001) 413:732–8. doi: 10.1038/35099560
12. Kagan JC, Su T, Horng T, Chow A, Akira S, Medzhitov R. TRAM couples endocytosis of Toll-like receptor 4 to the induction of interferon-beta. *Nat Immunol*. (2008) 9:361–8. doi: 10.1038/ni1569
13. Maurizi G, Della Guardia L, Maurizi A, Poloni A. Adipocytes properties and crosstalk with immune system in obesity-related inflammation. *J Cell Physiol*. (2018) 233:88–97. doi: 10.1002/jcp.25855
14. Kershaw EE, Flier JS. Adipose tissue as an endocrine organ. *J Clin Endocrinol Metab*. (2004) 89:2548–56. doi: 10.1210/jc.2004-0395
15. Kopp A, Buechler C, Neumeier M, Weigert J, Aslanidis C, Scholmerich J, et al. Innate immunity and adipocyte function: ligand-specific activation of multiple Toll-like receptors modulates cytokine, adipokine, and chemokine secretion in adipocytes. *Obesity*. (2009) 17:648–56. doi: 10.1038/oby.2008.607
16. Schaffler A, Scholmerich J, Salzberger B. Adipose tissue as an immunological organ: Toll-like receptors, C1q/TNFs and CTRPs. *Trends Immunol*. (2007) 28:393–9. doi: 10.1016/j.it.2007.07.003
17. Zhu H-J, Ding H-H, Deng J-Y, Pan H, Wang L-J, Li N-S, et al. Inhibition of preadipocyte differentiation and adipogenesis by zinc-alpha2-glycoprotein treatment in 3T3-L1 cells. *J Diabetes Investig*. (2013) 4:252–60. doi: 10.1111/jdi.12046
18. Charriere G, Cousin B, Arnaud E, Andre M, Bacou F, Penicaud L, et al. Preadipocyte conversion to macrophage. Evidence of plasticity. *J Biol Chem*. (2003) 278:9850–5. doi: 10.1074/jbc.M210811200
19. Cinti S. Transdifferentiation properties of adipocytes in the adipose organ. *Am J Physiol Endocrinol Metab*. (2009) 297:E977–86. doi: 10.1152/ajpendo.00183.2009
20. Gimble J, Guilak F. Adipose-derived adult stem cells: isolation, characterization, and differentiation potential. *Cytotherapy*. (2003) 5:362–9. doi: 10.1080/14653240310003026
21. Deng T, Lyon CJ, Minze LJ, Lin J, Zou J, Liu JZ, et al. Class II major histocompatibility complex plays an essential role in obesity-induced adipose inflammation. *Cell Metab*. (2013) 17:411–22. doi: 10.1016/j.cmet.2013.02.009
22. Desruisseaux MS, Nagajyothi, Trujillo ME, Tanowitz HB, Scherer PE. Adipocyte, adipose tissue, and infectious disease. *Infect Immun*. (2007) 75:1066–78. doi: 10.1128/IAI.01455-06
23. Blankley S, Graham CM, Howes A, Bloom CI, Berry MP, Chaussabel D, et al. Identification of the key differential transcriptional responses of human whole blood following TLR2 or TLR4 ligation *in-vitro*. *PLoS ONE*. (2014) 9:e97702. doi: 10.1371/journal.pone.0097702
24. Lin B, Dutta B, Fraser ID. Systematic investigation of multi-TLR sensing identifies regulators of sustained gene activation in macrophages. *Cell Syst*. (2017) 5:25–37.e3. doi: 10.1016/j.cels.2017.06.014
25. Kopp A, Buechler C, Bala M, Neumeier M, Scholmerich J, Schaffler A. Toll-like receptor ligands cause proinflammatory and prodiabetic activation of adipocytes via phosphorylation of extracellular signal-regilated kinase and c-jun N-terminal kinase but not interferon regulatory factor-3. *Endocrinology*. (2010) 151:1097–108. doi: 10.1210/en.2009-1140

26. Ziegler A, Gonzalez L, Blikslager A. Large animal models: the key to translational discovery in digestive disease research. *Cell Mol Gastroenterol Hepatol.* (2016) 2:716–24. doi: 10.1016/j.jcmgh.2016.09.003
27. Sanosaka M, Minashima T, Suzuki K, Watanabe K, Ohwada S, Hagino A, et al. A combination of octanoate and oleate promotes in vitro differentiation of porcine intramuscular adipocytes. *Comp Biochem Physiol B Biochem Mol Biol.* (2008) 149:285–92. doi: 10.1016/j.cbpb.2007.09.019
28. Suzuki M, Tada A, Kanmani P, Watanabe H, Aso H, Suda Y, et al. Advanced application of porcine intramuscular adipocytes for evaluating anti-adipogenic and anti-inflammatory activities of immunobiotics. *PLoS ONE*. (2015) 10:e0119644. doi: 10.1371/journal.pone.0119644
29. Mudunuri U, Che A, Yi M, Stephens RM. bioDBnet: the biological database network. *Bioinformatics*. (2009) 25:555–6. doi: 10.1093/bioinformatics/btn654
30. Huang DW, Sherman BT, Lempicki RA. Bioinformatics enrichment tools: paths toward the comprehensive functional analysis of large gene lists. *Nucleic Acids Res*. (2009) 37:1–13. doi: 10.1093/nar/gkn923
31. Xia J, Benner MJ, Hancock RE. NetworkAnalyst–integrative approaches for protein-protein interaction network analysis and visual exploration. *Nucleic Acids Res*. (2014) 42:W167–74. doi: 10.1093/nar/gku443
32. Breuer K, Foroushani AK, Laird MR, Chen C, Sribnaia A, Lo R, et al. InnateDB: systems biology of innate immunity and beyond–recent updates and continuing curation. *Nucleic Acids Res*. (2013) 41:D1228–33. doi: 10.1093/nar/gks1147
33. Wang S, Sun H, Ma J, Zang C, Wang C, Wang J, et al. Target analysis by integration of transcriptome and ChIP-seq data with BETA. *Nat Protoc*. (2013) 8:2502–15. doi: 10.1038/nprot.2013.150
34. Bustin SA, Benes V, Garson JA, Hellemans J, Huggett J, Kubista M, et al. The MIQE guidelines: minimum information for publication of quantitative real-time PCR experiments. *Clin Chem*. (2009) 55:611–22. doi: 10.1373/clinchem.2008.112797
35. Nygard A-B, Jorgensen CB, Cirera S, Fredholm M. Selection of reference genes for gene expression studies in pig tissues using SYBR green qPCR. *BMC Mol Biol*. (2007) 8:67. doi: 10.1186/1471-2199-8-67
36. Ghaben AL, Scherer PE. Adipogenesis and metabolic health. *Nat Rev Mol Cell Biol.* (2009) 20:242–58. doi: 10. 10.1038/s41580-018-0093-z
37. Cipolletta D, Feuerer M, Li A, Kamei N, Lee J, Shoelson SE, et al. PPAR-gamma is a major driver of the accumulation and phenotype of adipose tissue Treg cells. *Nature.* (2012) 486:549–53. doi: 10.1038/nature11132
38. Mo D, Yu K, Chen H, Liu X, He Z, Cong P, et al. Transcriptome landscape of porcine intramuscular adipocyte during differentiation. *J. Agric. Food Chem.* (2017) 65:6317–28. doi: 10.1021/acs.jafc.7b02039
39. Ajuwon KM, Banz W, Winters TA. Stimulation with Peptidoglycan induces interleukin 6 and TLR2 expression and a concomitant downregulation of expression of adiponectin receptors 1 and 2 in 3T3-L1 adipocytes. *J Inflamm.* (2009) 6:8. doi: 10.1186/1476-9255-6-8
40. Schmid A, Karrasch T, Thomalla M, Schlegel J, Salzberger B, Schaffler A, et al. Innate immunity of adipose tissue in rodent models of local and systemic staphylococcus aureus infection. *Mediat Inflamm*. (2017) 2017:5315602. doi: 10.1155/2017/5315602
41. Moresco EM, LaVine D, Beutler B. Toll-like receptors. *Curr Biol*. (2011) 21: R488–93. doi: 10.1016/j.cub.2011.05.039
42. Uematsu S, Akira S. Toll-like receptors and type I interferons. *J Biol Chem*. (2007) 282:15319–23. doi: 10.1074/jbc.R700009200
43. Uematsu S, Akira S. Toll-like receptors and innate immunity. *J Mol Med*. (2006) 84:712–25. doi: 10.1007/s00109-006-0084-y
44. Meijer K, de Vries M, Al-Lahham S, Bruinenberg M, Weening D, Dijkstra M, et al. Human primary adipocytes exhibit immune cell function: adipocytes prime inflammation independent of macrophages. *PLoS ONE.* (2011) 6:e17154. doi: 10.1371/journal.pone.0017154
45. Wang L, Li X, Wang Y. GSK3β inhibition attenuates LPS-induced IL-6 expression in porcine adipocytes. *Sci. Rep.* (2018) 8:15967. doi: 10.1038/s41598-018-34186-0.
46. Vielma SA, Klein RL, Levingston CA, Young MR. Adipocytes as immune regulatory cells. *Int Immunopharmacol.* (2013) 16:224–31. doi: 10.1016/j.intimp.2013.04.002
47. Honda K, Taniguchi T. IRFs: master regulators of signalling by Toll-like receptors and cytosolic pattern-recognition receptors. *Nat Rev Immunol*. (2006) 6:644–58. doi: 10.1038/nri1900
48. Ballak DB, van Asseldonk EJP, van Diepen JA, Jansen H, Hijmans A, Joosten LAB. TLR-3 is present in human adipocytes, but its signalling is not required for obesity-induced inflammation in adipose tissue *in vivo*. *PLoS ONE*. (2015) 10: e0123152. doi: 10.1371/journal.pone.0123152
49. Yu L, Yan K, Liu P, Li N, Liu Z, Zhu W, et al. Pattern recognition receptor-initiated innate antiviral response in mouse adipose cells. *Immunol Cell Biol*. (2014) 92:105–15. doi: 10.1038/icb.2013.66
50. Zhang L-J, Guerrero-Juarez CF, Hata T, Bapat SP, Ramos R, Plikus MV, et al. Innate immunity. Dermal adipocytes protect against invasive Staphylococcus aureus skin infection. *Science*. (2015) 347:67–71. doi: 10.1126/science.1260972
51. Gardy JL, Lynn DJ, Brinkman FS, Hancock RE. Enabling a systems biology approach to immunology: focus on innate immunity. *Trends Immunol*. (2009) 30:249–62. doi: 10.1016/j.it.2009.03.009
52. Zhang X, Kimura Y, Fang C, Zhou L, Sfyroera G, Lambris JD, et al. Regulation of Toll-like receptor-mediated inflammatory response by complement *in vivo*. *Blood*. (2007) 110:228–36. doi: 10.1182/blood-2006-12-063636
53. Moue M, Tohno M, Shimazu T, Kido T, Aso H, Saito T, et al. Toll-like receptor 4 and cytokine expression involved in functional immune response in an originally established porcine intestinal epitheliocyte cell line. *Biochim Biophys Acta.* (2008) 1780:134–44. doi: 10.1016/j.bbagen.2007.11.006
54. Roca-Rivada A, Bravo SB, Pérez-Sotelo D, Alonso J, Castro AI, Baamonde I, et al. CILAIR-based secretome analysis of obese visceral and subcutaneous adipose tissues reveals distinctive ECM remodeling and inflammation mediators. *Sci. Rep*. (2015) 5:12214. doi: 10.1038/srep12214.
55. Gardan D, Gondret F, Louveau I. Lipid metabolism and secretory function of porcine intramuscular adipocytes compared with subcutaneous and perirenal adipocytes. *Am J Physiol Endocrine Metab*. (2006) 291:E372–80. doi: 10.1152/ajpendo.00482.2005
56. Rosen ED, Spiegelman BM. Adipocytes as regulators of energy balance and glucose homeostasis. *Nature*. (2006) 444:847–53. doi: 10.1038/nature05483
57. Hegde V, Dhurandhar NV. Microbes and obesity-interrelationship between infection, adipose tissue and the immune system. *Clin Microbiol Infect*. (2013) 19:314–20. doi: 10.1111/1469-0691.1215
58. Wang B, Fu X, Liang X, Deavila JM, Wang Z, Zhao L, et al. Retinoic acid induces white adipose tissue browning by increasing adipose vascularity and inducing beige adipogenesis of PDGFRalpha+ adipose progenitors. *Cell Discov*. (2017) 3:17036. doi: 10.1038/celldisc.2017.36


**Conflict of Interest Statement:** KM, KY, and FH are employed by Takanashi Milk Products Co., Ltd.

The remaining authors declare that the research was conducted in the absence of any commercial or financial relationships that could be construed as a potential conflict of interest.

frontiers in Immunology

ORIGINAL RESEARCH
published: 13 June 2019
doi: 10.3389/fimmu.2019.01376

# Evaluation of the Immunomodulatory Activities of the Probiotic Strain *Lactobacillus fermentum* UCO-979C

*Valeria Garcia-Castillo[1,2,3], Ryoya Komatsu[3,4], Patricia Clua[2], Yuhki Indo[3,4], Michihiro Takagi[3,4], Susana Salva[2], Md. Aminul Islam[3,4,5†], Susana Alvarez[2], Hideki Takahashi[6,7], Apolinaria Garcia-Cancino[1]*, Haruki Kitazawa[3,4]* and Julio Villena[2,4]**

[1] Laboratory of Bacterial Pathogenicity, Faculty of Biological Sciences, University of Concepcion, Concepcion, Chile, [2] Laboratory of Immunobiotechnology, Reference Centre for Lactobacilli (CERELA-CONICET), Tucuman, Argentina, [3] Food and Feed Immunology Group, Laboratory of Animal Products Chemistry, Graduate School of Agricultural Science, Tohoku University, Sendai, Japan, [4] Livestock Immunology Unit, International Education and Research Center for Food Agricultural Immunology (CFAI), Graduate School of Agricultural Science, Tohoku University, Sendai, Japan, [5] Department of Medicine, Faculty of Veterinary Science, Bangladesh Agricultural University, Mymensingh, Bangladesh, [6] Laboratory of Plant Pathology, Graduate School of Agricultural Science, Tohoku University, Sendai, Japan, [7] Plant Immunology Unit, International Education and Research Center for Food Agricultural Immunology, Graduate School of Agricultural Science, Tohoku University, Sendai, Japan

*Lactobacillus fermentum* UCO-979C, a strain isolated from a human stomach, was previously characterized by its potential probiotic properties. The UCO-979C strain displayed the ability to beneficially regulate the innate immune response triggered by *Helicobacter pylori* infection in human gastric epithelial cells. In this work, we conducted further *in vitro* studies in intestinal epithelial cells (IECs) and *in vivo* experiments in mice in order to characterize the potential immunomodulatory effects of *L. fermentum* UCO-979C on the intestinal mucosa. Results demonstrated that the UCO-979C strain is capable to differentially modulate the immune response of IECs triggered by Toll-like receptor 4 (TLR4) activation through the modulation of TLR negative regulators' expression. In addition, we demonstrated for the first time that *L. fermentum* UCO-979C is able to exert its immunomodulatory effect in the intestinal mucosa *in vivo*. The feeding of mice with *L. fermentum* UCO-979C significantly increased the production of intestinal IFN-γ, stimulated intestinal and peritoneal macrophages and increased the number of Peyer's patches $CD4^+$ T cells. In addition, *L. fermentum* UCO-979C augmented intestinal IL-6, reduced the number of immature $B220^+CD24^{high}$ B cells from Peyer's patches, enhanced the number of mature B $B220^+CD24^{low}$ cells, and significantly increased intestinal IgA content. The results of this work revealed that *L. fermentum* UCO-979C has several characteristics making it an excellent candidate for the development of immunobiotic functional foods aimed to differentially regulate immune responses against gastric and intestinal pathogens.

**Keywords: *Lactobacillus fermentum* UCO-979C, intestinal immunity, macrophages, PIE cells, immunobiotics**

OPEN ACCESS

***Edited by:***
*Wilson Savino, Oswaldo Cruz Foundation (Fiocruz), Brazil*

***Reviewed by:***
*Margarida Castell, University of Barcelona, Spain*
*Yaqing Qie, Mayo Clinic Florida, United States*

***Correspondence:**
*Apolinaria Garcia-Cancino*
*apgarcia@udec.cl*
*Haruki Kitazawa*
*haruki.kitazawa.c7@tohoku.ac.jp*
*Julio Villena*
*jcvillena@cerela.org.ar*

*†JSPS Postdoctoral Fellow*

***Specialty section:***
*This article was submitted to Nutritional Immunology, a section of the journal Frontiers in Immunology*

***Received:*** *27 February 2019*
***Accepted:*** *30 May 2019*
***Published:*** *13 June 2019*

***Citation:***
*Garcia-Castillo V, Komatsu R, Clua P, Indo Y, Takagi M, Salva S, Islam MA, Alvarez S, Takahashi H, Garcia-Cancino A, Kitazawa H and Villena J (2019) Evaluation of the Immunomodulatory Activities of the Probiotic Strain Lactobacillus fermentum UCO-979C. Front. Immunol. 10:1376. doi: 10.3389/fimmu.2019.01376*

## INTRODUCTION

It is widely recognized that commensal microorganisms are relevant for human and animals health, participating in several important biological functions including nutrients digestion, vitamins synthesis, and pathogens inhibition (1, 2). The importance of beneficial microorganisms of the microbiota in the maintenance of immune health was also demonstrated in a convincing way (3, 4). Several effective tools have already been developed in order to study and manipulate the microbiota, improve their beneficial properties for the host, and protect against immune-related diseases (5, 6). In this regard, the development of immunomodulatory probiotic (immunobiotic) interventions offers opportunities for the modulation of the mucosal immune system toward long lasting health (7).

The beneficial role of immunobiotic lactic acid bacteria (LAB) has been extensively reported, supporting their implementation to improve some immunological functions in the host (8–10). The beneficial effect of immunobiotics on the immune system occurs through direct and indirect interactions of bacteria with immune and non-immune cells (11–14), leading to cells' activation and proliferation, cytokines production, IgA secretion, antimicrobial peptides synthesis, and tight junctions improvement (2, 11–14). Several research works including recent transcriptomic analysis revealed that the immunomodulatory effect of immunobiotics is a strain-specific characteristic (2, 12, 15), and therefore, each individual strain has to be studied in detail in order to explore its immunomodulatory potential.

Immunobiotics has been proposed as an alternative to prevent bacterial and viral infections in gastrointestinal tract (10). Experimental models have demonstrated that immunobiotics can attenuate the severity of infections caused by several gastrointestinal pathogens including *Helicobacter pylori, Citrobacter rodentium, Listeria monocytogenes,* and *Salmonella typhimurium* (16). In this regard, it was reported that some *Lactobacillus* strains are able to increase the resistance against the gastric pathogen *H. pylori*. Among the mechanisms proposed to explain the beneficial effects of probiotic lactobacilli are the production of antimicrobial compounds, the inhibition of pathogen's adhesion and the modulation of the immune system (17–19). We previously isolated *Lactobacillus fermentum* UCO-979C from a human stomach sample and characterized its potential probiotic properties (20, 21). We observed that this strain is able to efficiently adhere to the gastric mucosa as demonstrated by *in vitro* experiments in human gastric adenocarcinoma cell-line (AGS cells) and *in vivo* studies in Mongolian gerbils (21). *L. fermentum* UCO-979C also showed the ability to strongly inhibit the adhesion, growth and urease activity of *H. pylori* (21, 22). Moreover, we recently reported that the UCO-979C strain beneficially modulates the innate immune response triggered by *H. pylori* infection in human gastric epithelial cells and macrophages (23). Our data showed reduced levels of the pro-inflammatory factors IL-8, TNF-α, IL-1β, IL-6, and MCP-1 expressions in *L. fermentum* UCO-979C-treated AGS cells when compared to untreated infected controls. In addition, improved production of the regulatory cytokine TGF-β in response to *H. pylori* infection was detected in *L. fermentum* UCO-979C-treated AGS cells (23). Interestingly, *L. fermentum* UCO-979C was also capable of reducing the production of TNF-α and improving IFN-γ and IL-10 levels in macrophages challenged with *H. pylori* (23).

Taking into consideration the effect of *L. fermentum* UCO-979C on the gastric immune response against *H. pylori* infection, we wonder whether this probiotic *Lactobacillus* strain is also able to modulate immune responses in the intestinal tract. Therefore, we conducted *in vitro* studies in intestinal epithelial cells (IECs) and *in vivo* experiments in mice in order to characterize the immunomodulatory effects of *L. fermentum* UCO-979C on the intestinal mucosa.

## MATERIALS AND METHODS

### Microorganisms

*Lactobacillus fermentum* UCO-979C was obtained from the Bacterial Pathogenicity Laboratory culture collection at University of Concepción (Concepcion, Chile) (20, 21). *L. fermentum* CRL973 was obtained from the CERELA culture collection (Tucuman, Argentina). Lactobacilli strains were activated from frozen stock and cultured in Mann-Rogosa Sharpe Agar (MRS Difco) at 37°C. After 24 h incubation, a single colony was transferred to MRS broth (MRS Difco) and cultured at 37°C for 24 h. Then, bacterial cells were washed three times with phosphate buffered saline (PBS) and adjusted to appropriate concentrations for the *in vitro* and *in vivo* experiments.

Enterotoxigenic *Escherichia coli* (ETEC) strain 987P (O9: H-: 987 pilus+: heat stable toxin+) was obtained from the National Institute of Animal Health (Tsukuba, Japan) (24–26). ETEC cells were grown in blood agar (5% sheep blood) for 24 h at 37°C and transferred to tryptic soy broth (TSB; Becton, Dickinson and Company, USA) and cultured 20 h at 37°C with shaking. After incubation, the subcultures of bacteria were centrifuged at 5,000 × g for 10 min at 4°C and washed with PBS (pH 7.2). Finally, ETEC cells were heat killed at 100°C for 15 min and then washed with PBS. Heat-stable ETEC pathogen associated molecular patterns (PAMPs) were suspended in DMEM for the experimental challenge.

*Sacharomyces boulardi* was obtained from commercial lyophilized preparation (Floratil—Argentina). The yeast suspensions were prepared in PBS and heat inactivated during 15 min in 100°C water bath and adjusted to $10^7$ cells/ml for *ex vivo* phagocytosis assay.

### Porcine Intestinal Epitheliocytes

Porcine intestinal epitheliocytes (PIE cells) are non-transformed intestinal cultured cells derived from intestinal epithelia isolated from an unsuckled neonatal swine. When PIE cells are cultured, they assumed a monolayer, cobblestone, and epithelial-like morphology, with close contact between cells (24). PIE cells were maintained in Dulbecco's modified Eagle's medium (DMEM) (Invitrogen Corporation, Carlsbad, CA, USA) supplemented with 10% fetal calf serum FCS (Hyclone, Logan, USA), 100 mg/ml penicillin, and 100 U/ml streptomycin at 37°C in an atmosphere of 5% $CO_2$. PIE cells grow rapidly and are well adapted to culture conditions even without transformation or immortalization.

However, the proliferative ability of PIE cells diminishes after 50 passages in culture. Therefore, we used PIE cells only between the 20th and 40th passages in these experiments (25, 26). Briefly, PIE cells were cultured in 250 ml flasks ($1.0 \times 10^6$ cells) for 5 days after reaching 80–90% confluence, changing culture media every 1–2 days, followed by subculturing in 24 well flasks for immunostimulation assays as described below.

## Immunomodulatory Assay in PIE Cells

Lactobacilli were re-suspended in DMEM (10% FCS), enumerated in a microscope using a Petroff-Hausser counting chamber, and stored at −80°C until use. PIE cells were plated at $3 \times 10^4$ cells/well of a 12-well type I collagen-coated plates (Iwaki, Tokyo, Japan), and cultured for 3 days. After changing medium, lactobacilli ($5 \times 10^8$ cells/ml) were added followed by stirring in microplate mixer and co- cultured for 48 h at 37°C 5% $CO_2$ atmosphere. Then, each well was washed vigorously with medium at least 3 times to eliminate bacteria. Gene expression of cytokines, chemokines, complement, and coagulation factors as well as negative regulators of TLR signaling were studied without any inflammatory challenge (basal levels) or after heat-stable ETEC PAMPs challenge ($5 \times 10^7$ cells/ml) for 12 h (25) by using RT-PCR as described below.

## Quantitative Expression Analysis by RT-PCR

Two-step real-time qPCR was performed to characterize the expression of selected genes in PIE cells. Total RNA was isolated from each PIE cell sample using TRIzol reagent (Invitrogen). RNA purity and concentration were assessed using NanoDrop™ 1,000 Spectophotometer. All cDNAs were synthesized using the PrimeScript RT Reagent kit with the treatment of gDNA eraser (Takara—Bio, Japan) according to the manufacturer's recommendations. Real-time quantitative PCR (qRT-PCR) was carried out using a 7,300 real-time PCR system (Applied Biosystems, Warrington, UK) and the Platinum SYBR green qPCR SuperMix uracil-DNA glycosylase (UDG) with 6-carboxyl-X-rhodamine (ROX) (Invitrogen). The primers used in this study were described previously (25–27). The PCR cycling conditions were 2 min at 50°C, followed by 5 min at 95°C, and then 40 cycles of 15 s at 95°C, 30 s at 60°C, and 30 s at 72°C, followed by a dissociation stage of 15 s at 95°C, 1 min at 60°C, 15 s at 95°C and 15 s at 60°C. The reaction mixtures contained 2.5 μl of cDNA and 7.5 μl of master mix, which included the sense and antisense primers. According to the guidelines for minimum information for publication of qRT-PCR experiments, β-actin was used as a housekeeping gene, to normalize cDNA levels for differences in total cDNA levels in the samples, because of its high stability across porcine various tissues (28). The relative index of a cytokine mRNA in PIE cells stimulated with lactobacilli was calculated as follows: first, the average cytokine expression levels from at least three samples challenged with ETEC without prestimulation with lactobacilli were set to 100. Then, relative expressions of cytokines were calculated in the samples prestimulated with lactobacilli followed by ETEC challenge (25).

## Animals and Feeding Procedures

Female 6–8 weeks old Balb/c mice were obtained from the closed colony kept at CERELA (Tucuman, Argentina). They were housed in plastic cages with controlled room temperature (22 ± 2°C temperature, 55 ± 2% humidity) and were fed *ad libitum* conventional balanced diet. Animal welfare was ensured by researchers and special trained staff in animal care and handling at CERELA. Animal health and behavior were monitored twice a day. This study was carried out in strict accordance with the recommendations in the Guide for the Care and Use of Laboratory Animals of the Guidelines for Animal Experimentation of CERELA. The CERELA Institutional Animal Care and Use Committee prospectively approved this research under the protocol BIOT-CRL-17.

Mice were housed individually during the experiments and the assays for each parameter studied were performed in 5–6 mice per group. *L. fermentum* UCO-979C or CRL973 were administered to different groups of mice for 2 consecutive days at a dose of $10^8$ cells/mouse/day in the drinking water (4 ml per mice per day). Bacteria were prepared as described above, suspended in 5 ml of 10% skimmed milk and added to the drinking water.

In some experiments, 1 day after at the end of the lactobacilli treatments, mice were challenged with lipopolysaccharide (LPS) to induce inflammation. Mice received 8 mg/kg of LPS from *E. coli* O55:B5 by intraperitoneal injection.

## *Ex vivo* Phagocytosis Assay

Peritoneal macrophages were collected aseptically from mice as described previously (29, 30). Briefly, after exposing inner skin, cold PBS containing 10% fetal bovine serum was carefully injected into peritoneal cavity. The fluid was collected and macrophages were washed twice with PBS containing bovine serum albumin (BSA) and adjusted to a concentration of $1 \times 10^6$ cells/ml. Phagocytosis was performed using a heat-killed *S. boulardi*. Mixtures of opsonized yeasts in mouse autologous serum (10%) were added to 0.2 ml of macrophage suspension. The mixture was incubated for 30 min at 37°C. The percentage of phagocytosis was expressed as the percentage of phagocytizing macrophages in 200 cells counted using an optical microscope (30, 31).

## Nitro Blue Tetrazolium Test (NBT)

The bactericidal activity (oxidative burst) of peritoneal macrophages was measured using the NBT reduction test (Sigma-Aldrich, St. Louis, MO, USA) as previously described (30). Briefly, 200 μl of peritoneal macrophages obtained as described above were incubated with 120 μl of NBT reagent and incubated first at 37°C for 10 min and then 10 min at room temperature. NBT was added to each sample and incubated at 37°C for 20 min. In the presence of oxidative metabolites, NBT (yellow) is reduced to formazan, which forms a blue precipitate. Smears were prepared and, after staining, the samples were examined under a light microscope for blue precipitates. Randomly, 100 cells were counted and the percentage of NBT positive (+) cells were determined (30, 31).

## Cytokine Concentrations

The concentration of cytokines was determined in blood and intestinal samples of UCO-979C-tretated and control mice. Blood samples were obtained through cardiac puncture at the end of each treatment and collected in heparinized tubes. Intestinal fluid samples were obtained as the method described previously (31). Briefly, the small intestine was flushed with 5 ml of PBS and the fluid was centrifuged (10,000 × g, 4°C for 10 min) to separate particulate material. The supernatant was kept frozen until use. Tumor necrosis factor α (TNF-α), interferon γ (IFN-γ), and interleukin 10 (IL-10) concentrations in serum and intestinal fluid, were measured with commercially available enzyme-linked immunosorbent assay (ELISA) kits following the manufacturer's recommendations (R&D Systems, MN, USA).

## Flow Cytometry

Peritoneal macrophages were collected as described above. Peyer's patches were collected and mechanically disaggregated. A single-cell suspension from the Peyer's patches of each mouse was obtained by gently passing the collected tissue through a tissue strainer with PBS with 2% FCS (FACS buffer). Cell suspensions were subjected to red blood cells lysis (Tris-ammonium chloride, BD PharMingen) flowed by counting on a hemacytometer. Viability of cells was assessed by trypan blue exclusion. Cell suspensions were pre-incubated with anti-mouse CD32/CD16 monoclonal antibody (Fc block) for 30 min at 4°C. Cells were incubated with the antibody mixes for 30 min at 4°C and washed with FACS buffer. The following antibodies from BD Biosciences were used: FITC-labeled anti-mouse MHC-II, FITC-labeled anti-mouse CD86, PE-labeled anti-mouse CD11b, PE-labeled anti-mouse F4/80, PE-labeled anti-mouse Ly6C, PE-labeled anti-mouse CD24, biotinylated anti-mouse B220, FITC-labeled anti-mouse CD3, PE-labeled anti-mouse CD8, and biotinylated anti-mouse CD4 antibodies. Streptavidin-PerCP was used as a second-step reagent. Flow cytometry was performed using a BD FACSCaliburTM flow cytometer (BD Biosciences) and data were analyzed using FlowJo software (TreeStar).

## Statistical Analysis

Experiments were performed in triplicate and results expressed as the mean ± SD. For the comparison of two groups, the Student's *t*-test was used. For the comparison of more than two groups, a one-way analysis of variance (ANOVA) was performed followed by and Tukey's test. In all cases, a level of significance of $p < 0.05$ was considered.

# RESULTS

## *L. fermentum* UCO-979C Modifies Cytokine Profile in PIE Cells

We first evaluated whether *L. fermentum* UCO-979C was able to modify the cytokine expression profile of PIE cells by evaluating the mRNA levels of IL-6, CXCL8 (IL-8), CXCL5 (AMCF-II), CXCL9, CXCL10 (IP-10), CXCL11, and CCL8 (MCP1) as shown in **Figure 1**. Then, in order to evaluate whether the immunomodulatory effects of *L. fermentum* UCO-979C were a strain specific property, we performed comparative experiments with the strain of the same species *L. fermentum* CRL973. Stimulation of PIE cells with the UCO-979C or CRL973 strains increased the expression of IL-6 and CXCL9, respectively, while no differences were found between controls and lactobacilli-treated PIE cells when the other chemokines were analyzed. The modulation of cytokines and chemokines was also studied in the context of inflammation. For this purpose, PIE cells were treated with lactobacilli and then challenged with heat-stable ETEC PAMPs that are able to trigger Toll-like receptor 4 (TLR4) activation in this cell line (25, 26). Untreated PIE cells challenged with ETEC were used as controls. Heat-stable ETEC PAMPs significantly increased the expression of all the inflammatory cytokines and chemokines in all the experimental groups (**Figure 1**). However, the mRNA expression levels of IL-6 and CCL8 were significantly higher in lactobacilli-treated cells. In addition, expression of CXCL8, CXCL10, and CXCL11 were lower in lactobacilli-treated PIE cells than in controls. Interestingly, only *L. fermentum* CRL973 was able to reduce CXCL5 expression (**Figure 1**). *L. fermentum* CRL973 increased CXCL9 expression after ETEC challenge while the UCO-979C strain reduced the expression of this chemokine (**Figure 1**). Our previous immunotranscriptomics studies in PIE cells revealed that in addition to cytokines and chemokines, immunomodulatory probiotic strains are able also to modulate factors from the complement and coagulation systems (27). Therefore, we evaluated the expressions of C1S, C1R, C3, CFB, and F3 in PIE cells under inflammatory and non-inflammatory conditions (**Figure 2**). No significant expression differences were observed for these factors when control and lactobacilli-treated PIE cells were compared. Challenge with heat-stable ETEC PAMPs increased C1S, C1R, C3, CFB, and F3 expressions in all the experimental groups. *L. fermentum* UCO-979C-treated PIE cells had significantly lower levels of C1S and C3, and higher levels of C1R and CFB expression as compared to controls. While *L. fermentum* CRL973-treated PIE cells exhibited significantly lower levels of C1S, C1R, and CFB than controls (**Figure 2**). No significant differences were observed in F3 expression when control and lactobacilli-treated PIE cells were compared.

## *L. fermentum* UCO-979C Modifies Negative Regulators of TLR4 Signaling in PIE Cells

We next evaluated whether *L. fermentum* UCO-979C was able to modify the expression of negative regulators of TLR4 signaling in PIE cells (**Figure 3**). No significant differences were observed in the expression of A20, Bcl3, MKP-1, and SIGIRR when untreated control, and lactobacilli-treated PIE cells were compared. Both, UCO-979C and CRL973 strains were able to reduce the expression of Tollip in PIE cells, while *L. fermentum* CRL973 increased IRAK-M expression. Challenge with heat-stable ETEC PAMPs increased A20, Bcl3, MKP-1, IRAK-M, and SIGIRR in all the experimental groups. *L. fermentum* UCO-979C-treated PIE cells had significantly lower levels of MKP-1 and Tollip, and higher levels of Bcl3 than controls, while *L. fermentum* CRL973 showed significantly lower levels of A20 and IRAK-M expressions than controls (**Figure 3**). Both lactobacilli improved the expression of SIGIRR.

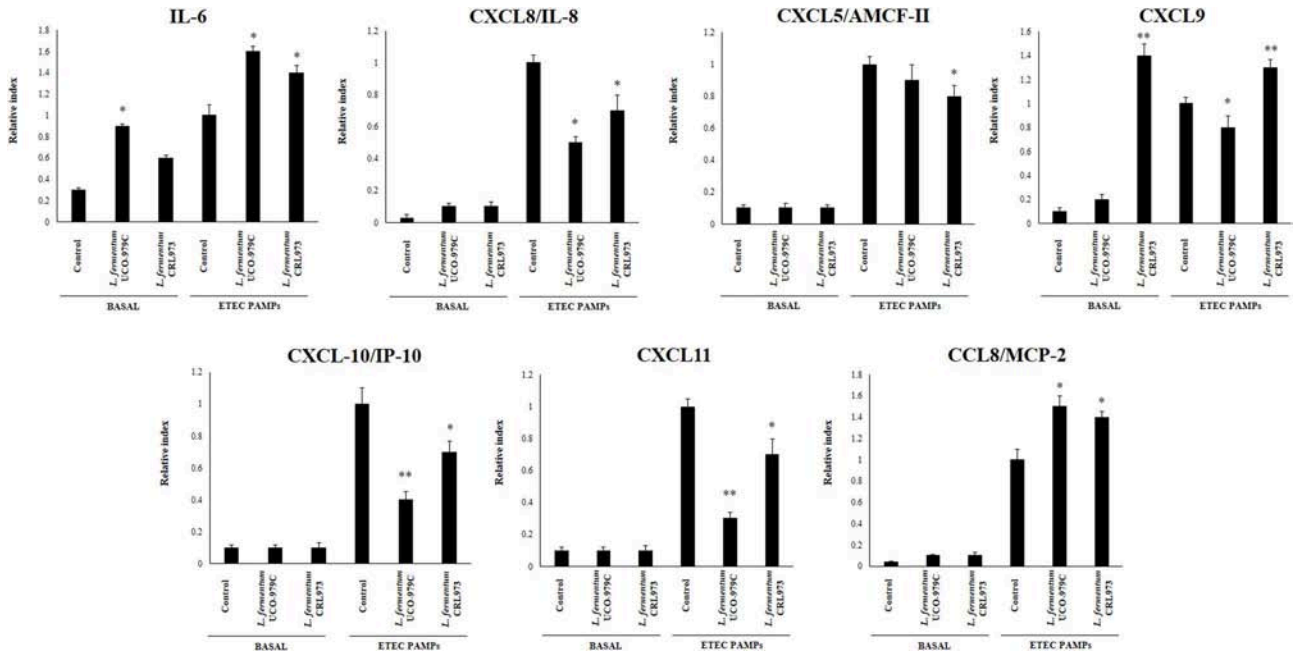


**FIGURE 1 |** Effect of *Lactobacillus fermentum* UCO-979C and *L. fermentum* CRL973 on the expression of cytokines and chemokines in porcine intestinal epithelial (PIE) cells. PIE cells were pre-treated with UCO-979C or CRL973 strains for 48 h and then stimulated with heat-stable Enterotoxigenic *Escherichia coli* (ETEC) pathogen-associated molecular patterns (PAMPs). The expression of cytokines (IL-6) and chemokines (CXCL5, CXCL8, CXCL9, CXCL10, CXCL11, and CCL8) were studied at 48 h after lactobacilli stimulation (basal) or at 12 h after heat-stable ETEC PAMPs challenge. The results represent three independent experiments. Results are expressed as mean ± SD. Significantly different from control PIE cells at the same time point *($P < 0.05$), **($P < 0.01$).

## *L. fermentum* UCO-979C Modulates Intestinal Immunity *in vivo*

Taking into consideration that the capacity of increasing IgA production in the gut, and stimulating macrophages and dendritic cells are amongst the beneficial effects of lactobacilli on the immune system (30, 32), we next aimed to evaluate *in vivo* the ability of *L. fermentum* UCO-979C to modulate those parameters. As shown in **Figure 4**, administration of the UCO-979C strain significantly increased the phagocytic activity of peritoneal macrophages while this effect was absent in the case of CRL973 strain. In order to study the activation of respiratory burst in peritoneal macrophages, we used the NBT method as described previously (30). Both, UCO-979C and CRL973 treatments were equally effective for increasing the percentage of $NBT^+$ cells in the population of macrophages obtained from the peritoneal cavity (**Figure 4**). In addition, mice orally treated with the UCO-979C strain had significantly higher levels of intestinal IgA antibodies than control animals while *L. fermentum* CRL973 did not induce significant changes (**Figure 4**). It has established that the *in vivo* immunomodulatory abilities of probiotic bacteria are in part attributable to altered production of cytokines that play pivotal roles in coordinating the immune function. Then, we analyzed the concentrations of cytokines in intestinal fluid and serum obtained from lactobacilli-treated mice, to determine the local and systemic effects induced by both *L. fermentum* strains (**Figure 5**). No significant differences were observed between lactobacilli-treated and control mice when intestinal and serum TNF-α concentrations were analyzed. Intestinal IFN-γ protein level was augmented by both *L. fermentum* UCO-979C and CRL973 while no differences were observed for serum IFN-γ between the groups. In addition, *L. fermentum* UCO-979C significantly increased intestinal and serum IL-10 levels, an effect that was not observed for the CRL973 strain (**Figure 5**). We also evaluated the levels of these three cytokines: TNF-α, IFN-γ, and IL-10, in mice after the intraperitoneal challenge with LPS (**Figure 6**). The inflammatory stimulus increased the concentration of intestinal and serum TNF-α, and IFN-γ in all experimental groups. However, TNF-α level was significantly lower in *L. fermentum* UCO-979C-treated mice when compared with those receiving the CRL973 strain or controls. In addition, both lactobacilli augmented the production of intestinal IFN-γ after the challenge with LPS while only UCO-979C strain increased the levels of this cytokine in serum (**Figure 6**). LPS challenge also increased IL-10 both in intestinal fluid and serum of mice; however, the levels of this immunoregulatory cytokine were significantly higher in *L. fermentum* UCO-979C-treated mice when compared with those receiving the CRL973 strain or controls (**Figure 6**).

## *L. fermentum* UCO-979C Modulates Intestinal Immune Cell Populations *in vivo*

We aimed to evaluate the effect of *L. fermentum* UCO-979C on peritoneal and intestinal immune cell populations in order to further characterize the immunomodulatory activity

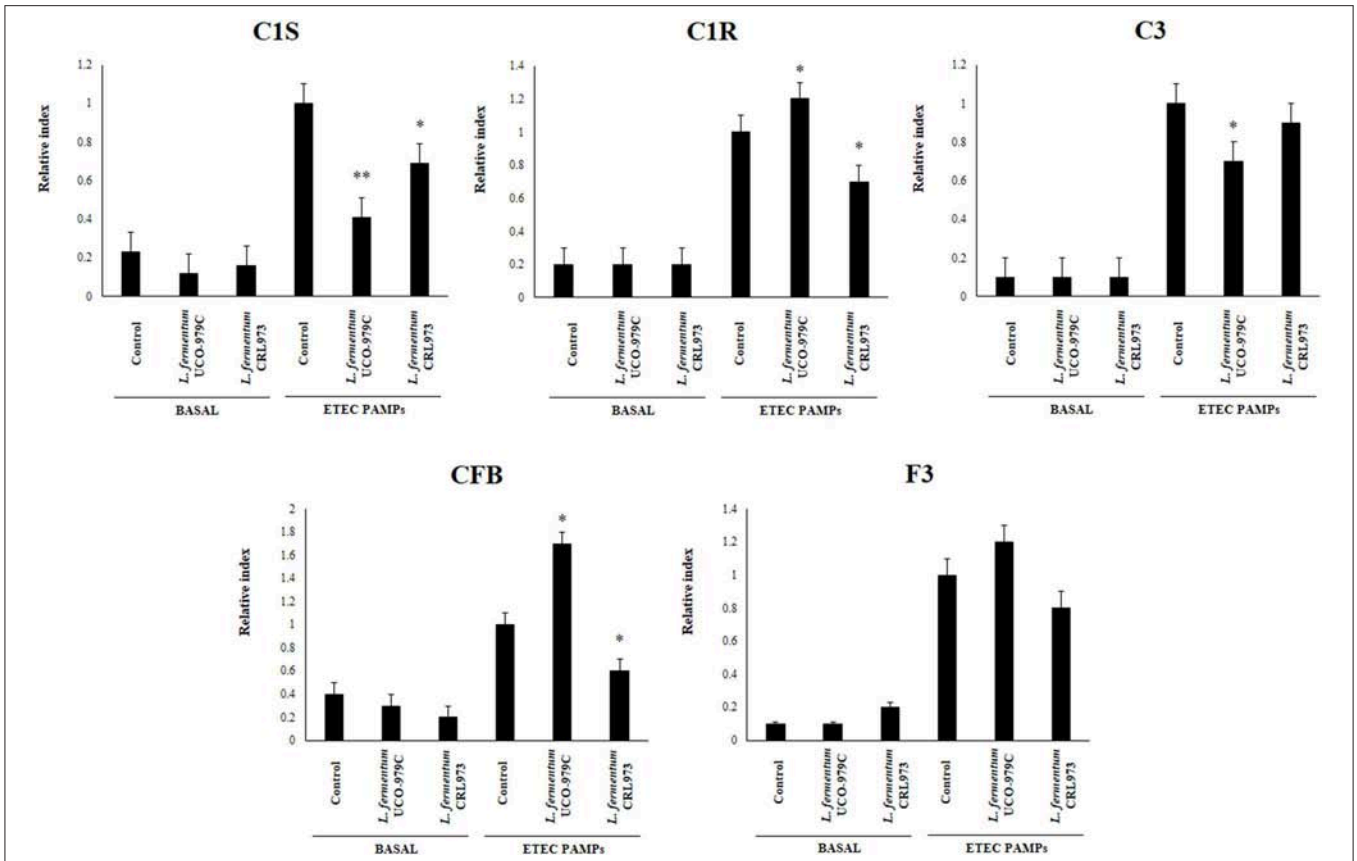


**FIGURE 2 |** Effect of *Lactobacillus fermentum* UCO-979C and *L. fermentum* CRL973 on the expression of factors from the complement and coagulation systems in porcine intestinal epithelial (PIE) cells. PIE cells were pre-treated with UCO-979C or CRL973 strains for 48 h and then stimulated with heat-stable Enterotoxigenic *Escherichia coli* (ETEC) pathogen-associated molecular patterns (PAMPs). The expression of factors from the complement (C1S, C1R, C3, and CFB) and coagulation (F3) systems were studied at 48 h after lactobacilli stimulation (basal) or at 12 h after heat-stable ETEC PAMPs challenge. The results represent three independent experiments. Results are expressed as mean ± SD. Significantly different from control PIE cells at the same time point *($P < 0.05$), **($P < 0.01$).

of this strain. In the peritoneal fluid, resident macrophages ($F4/80^+$ cells) as well as inflammatory monocyte and neutrophils ($Ly6C/Gr1^+$ cells) were studied by flow cytometry. As shown in **Figure 7**, the percentage of peritoneal $F4/80^+$ macrophages as well as activated macrophages ($F4/80^+MCH\text{-}II^+$ cells) was increased in UCO-979C-treated mice when compared to controls, while no significant differences between the groups were observed when $Ly6C/Gr1^+$ and $Ly6C/Gr1^+MHC\text{-}II^+$ cells were studied. Antigen presenting cells were also analyzed in Peyer's patches of mice (**Figure 8**). No significant differences were observed between UCO-979C-tretaed and control mice when $CD11b^+$ (dendritic cells) or $F4/80^+$ (macrophages) cells from Peyer's patches were evaluated. In addition, there were no differences between the groups in activated $CD11b^+CD86^+$ dendritic cells; however, the percentage of activated $F4/80^+CD86^+$ macrophages were significantly higher in *L. fermentum* UCO-979C-treated mice when compared with controls (**Figure 8**). Finally, B and T cells populations in Peyer's patches were studied (**Figure 9**). *L. fermentum* UCO-979C treatment improved the proportions of both $CD3^+CD4^+$ and $CD3^+CD8^+$ T cells when compared to controls. No differences between the groups were detected in the population of $B220^{high}$ cells; however, the proportion of $B220^{low}$ and $B220^+CD24^{high}$ cells (immature B cells) from Peyer's patches were significantly reduced in *L. fermentum* UCO-979C-treated mice when compared with controls (**Figure 9**). In addition, $B220^+CD24^{low}$ population (mature B cells) from Peyer's patches were higher in *L. fermentum* UCO-979C-treated mice than that of controls.

## DISCUSSION

We previously reported that *L. fermentum* UCO-979C modulates the innate immune response in human gastric epithelial cells and macrophages, and improves protection against *H. pylori* infection (23). Here, we demonstrated for the first time that the UCO-979C strain is also capable of modulating the intestinal immune system.

The recent scientific advances in the biology of IECs have dramatically expanded our appreciation of their immunological functions. IECs establish an interconnected network with underlying immune cells and with the microbiota on their surface, and these complex interactions between intestinal cells

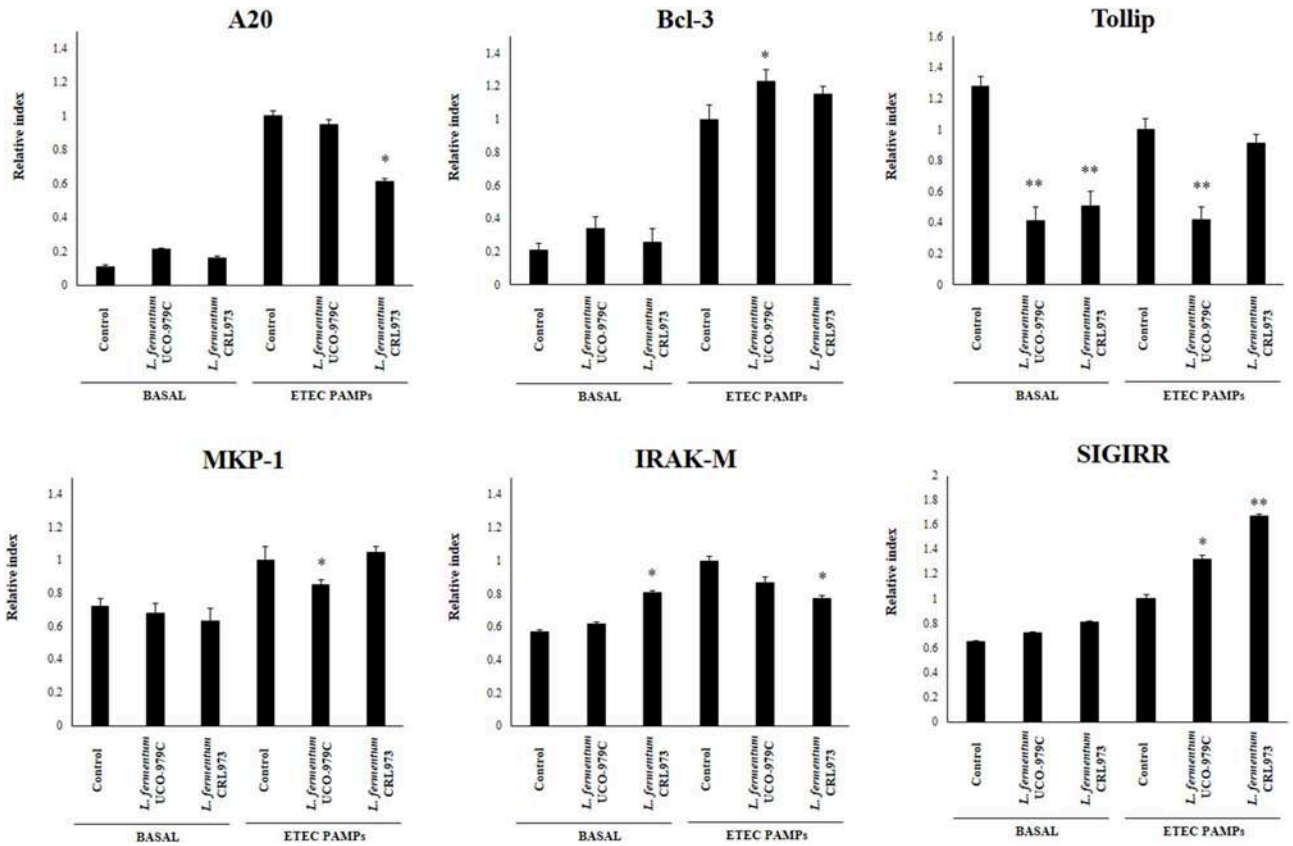


**FIGURE 3 |** Effect of *Lactobacillus fermentum* UCO-979C and *L. fermentum* CRL973 on the expression of negative regulators of the Toll-like receptor (TLR) signaling pathway in porcine intestinal epithelial (PIE) cells. PIE cells were pre-treated with UCO-979C or CRL973 strains for 48 h and then stimulated with heat-stable Enterotoxigenic *Escherichia coli* (ETEC) pathogen-associated molecular patterns (PAMPs). The expression of negative regulators of the TLR signaling pathway were studied at 48 h after lactobacilli stimulation (basal) or at 12 h after heat-stable ETEC PAMPs challenge. The results represent three independent experiments. Results are expressed as mean ± SD. Significantly different from control PIE cells at the same time point *($P < 0.05$), **($P < 0.01$).

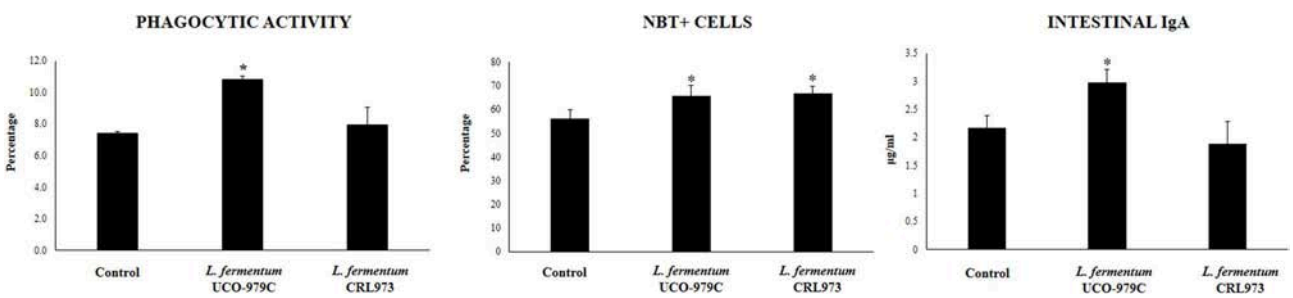


**FIGURE 4 |** Effect of *Lactobacillus fermentum* UCO-979C and *L. fermentum* CRL973 on peritoneal macrophages activities and intestinal IgA production in adult immunocompetent mice. *L. fermentum* UCO-979C or CRL973 were administered to different groups of mice for 2 consecutive days at a dose of $10^8$ cells/mouse/day. Untreated mice were used as controls. One day after the last lactobacilli administration, phagocytic and bactericidal (oxidative burst) activities of peritoneal macrophages, and intestinal IgA concentrations were determined. The results represent three independent experiments. Results are expressed as mean ± SD. Significantly different from control mice *($P < 0.05$).

and microorganisms significantly influence the host defense against threats from the intestinal lumen (33, 34). IECs play crucial roles in the recognition of microorganisms in both homeostatic and pathologic conditions through the expression of innate receptors including the TLRs. Signaling through TLR by pathogens in IECs initiates signaling cascades that culminates in the expression and secretion of various cytokines, chemokines, and other inflammatory factors which signal and

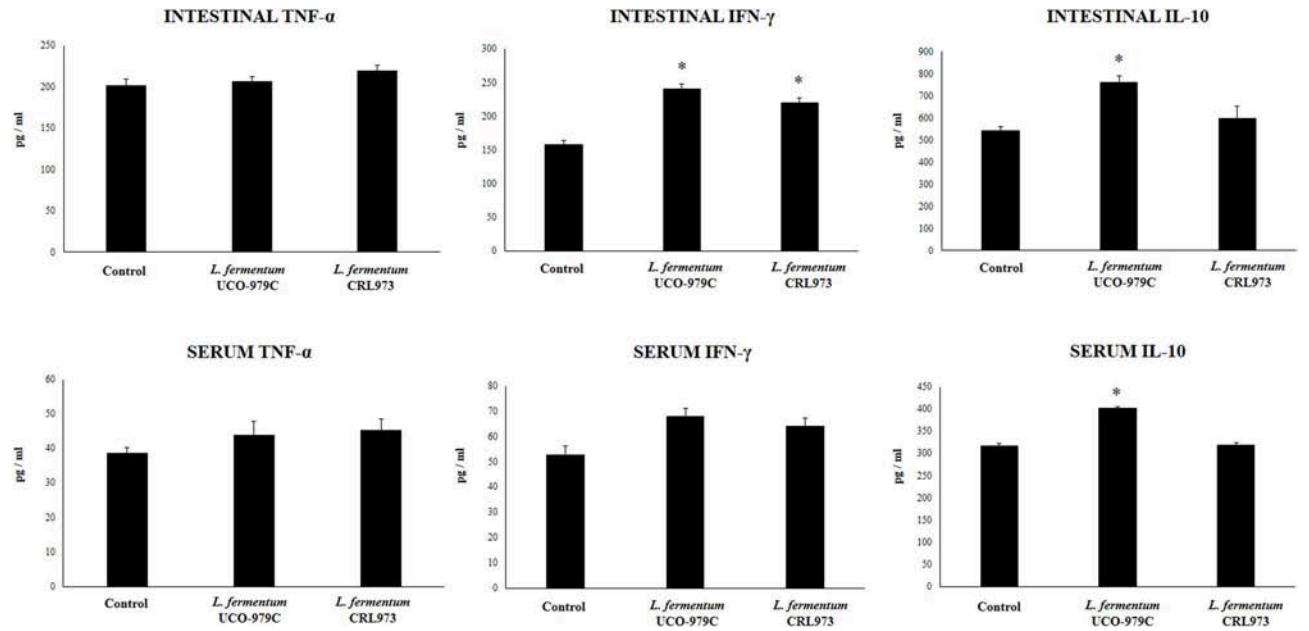


**FIGURE 5 |** Effect of *Lactobacillus fermentum* UCO-979C and *L. fermentum* CRL973 on intestinal and serum cytokines of adult immunocompetent mice. *L. fermentum* UCO-979C or CRL973 were administered to different groups of mice for 2 consecutive days at a dose of $10^8$ cells/mouse/day. Untreated mice were used as controls. One day after the last lactobacilli administration, the concentrations of TNF-α, IFN-γ, and IL-10 in intestinal fluid and serum were determined. The results represent three independent experiments. Results are expressed as mean ± SD. Significantly different from control mice *($P < 0.05$).

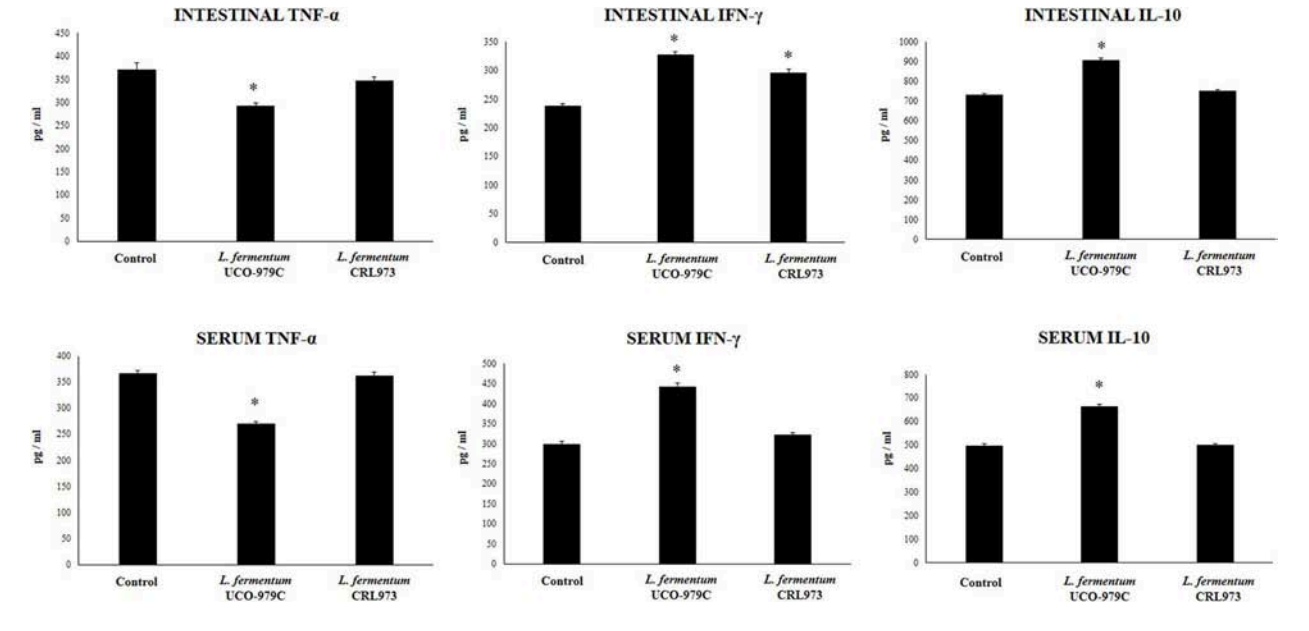


**FIGURE 6 |** Effect of *Lactobacillus fermentum* UCO-979C and *L. fermentum* CRL973 on intestinal and serum cytokines of adult immunocompetent mice after lipopolysaccharide (LPS) challenge. *L. fermentum* UCO-979C or CRL973 were administered to different groups of mice for 2 consecutive days at a dose of $10^8$ cells/mouse/day. Untreated mice were used as controls. Lactobacilli-treated and control mice were challenged with LPS by intraperitoneal injection. One day after the challenge, the concentrations of TNF-α, IFN-γ, and IL-10 in intestinal fluid and serum were determined by ELISA. The results represent three independent experiments. Results are expressed as mean ± SD. Significantly different from control mice *($P < 0.05$).

prime underlying immune cells (33, 34). It was also reported that commensal and probiotic bacteria are recognized by IECs through innate receptors (13). Moreover, immunobiotic bacteria are able to influence TLR signaling induced by pathogens in IECs and therefore, to differentially modulate immune responses (13).

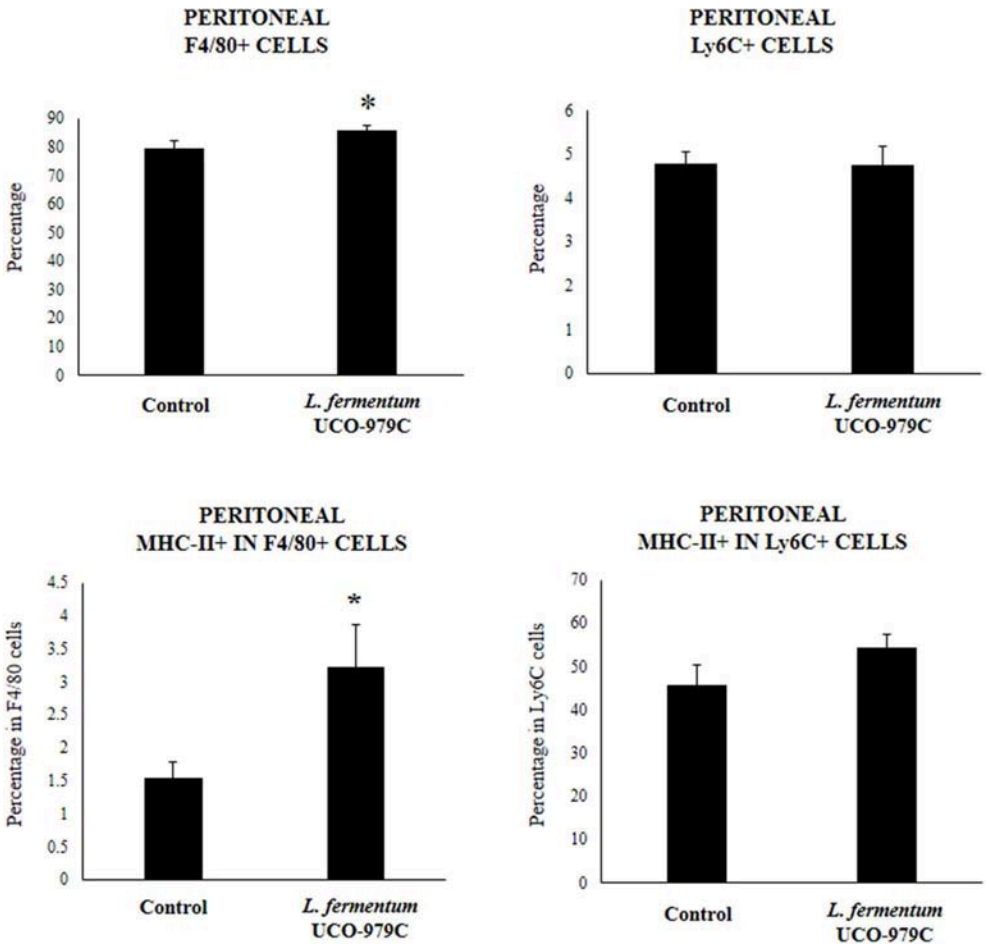


**FIGURE 7 |** Effect of *Lactobacillus fermentum* UCO-979C on peritoneal phagocytic cells of adult immunocompetent mice. *L. fermentum* UCO-979C was administered to mice for 2 consecutive days at a dose of $10^8$ cells/mouse/day. Untreated mice were used as controls. One day after the last lactobacilli administration, peritoneal phagocytes were evaluated by flow cytometry. The results represent three independent experiments. Results are expressed as mean ± SD. Significantly different from control mice *($P < 0.05$).

We have previously used PIE cells to evaluate the effect of immunobiotic bacteria on TLR signaling induced by PAMPs. We demonstrated that stimulation of PIE cells with heat-stable ETEC PAMPs activates NF-kB and induces the phosphorylation of MAPK-ERK, MAPK-p38, and MAPK-JNK leading to the production of inflammatory cytokines (25). Later, by performing transcriptomic studies we corroborated these findings by demonstrating that activation of NF-kB and MAPK pathways in PIE cells results in an increased expression of several chemokines including CCL4, CCL5, CCL8, CCL20, CXCL2, CXCL5, CXCL9, CXCL10, CXCL11, CSF2, as well as complement and coagulation factors (27). Interestingly, we have also demonstrated that prestimulation of PIE cells with the immunobiotic strain *Lactobacillus jensenii* TL2937 differentially modulated the expression of inflammatory factors produced in response to heat-stable ETEC PAMPs challenge (25, 27) (**Figure 10A**). The upregulation of the negative regulators MKP-1, A20, and Bcl-3 induced by the TL2937 strain in PIE cells was found to be related to the different immunotrascriptomic response after heat-stable ETEC PAMPs challenge (25, 27). Here, we performed similar experiments in order to evaluate the immunomodulatory effects of *L. fermentum* UCO-979C in IECs. Our results showed that the prestimulation of PIE cells with the UCO-979C strain differentially modulated the expression of inflammatory factors induced by the heat-stable ETEC PAMPs challenge (**Figure 10A**). The changes induced by *L. fermentum* UCO-979C were distinct from those previously observed for the immunobiotic strain TL2937. While *L. jensenii* TL2937 induced a clear and remarkable anti-inflammatory effect (25, 27), *L. fermentum* UCO-979C produced a stimulant/anti-inflammatory mixed effect (**Figure 10A**). Though some inflammatory factors such as CXCL8, CXCL9, CXCL10, CXCL11, C1S, and C3 were significantly reduced in UCO-979C-treated PIE cells; others like IL-6, CCL8, C1R, and CFB were upregulated.

The up- and down-regulation of inflammatory factors correlated with the changes induced by *L. fermentum* UCO-979C on the expression of negative regulators of TLR4 signaling as evidenced by the augmented expression of SIGIRR and Bcl3,

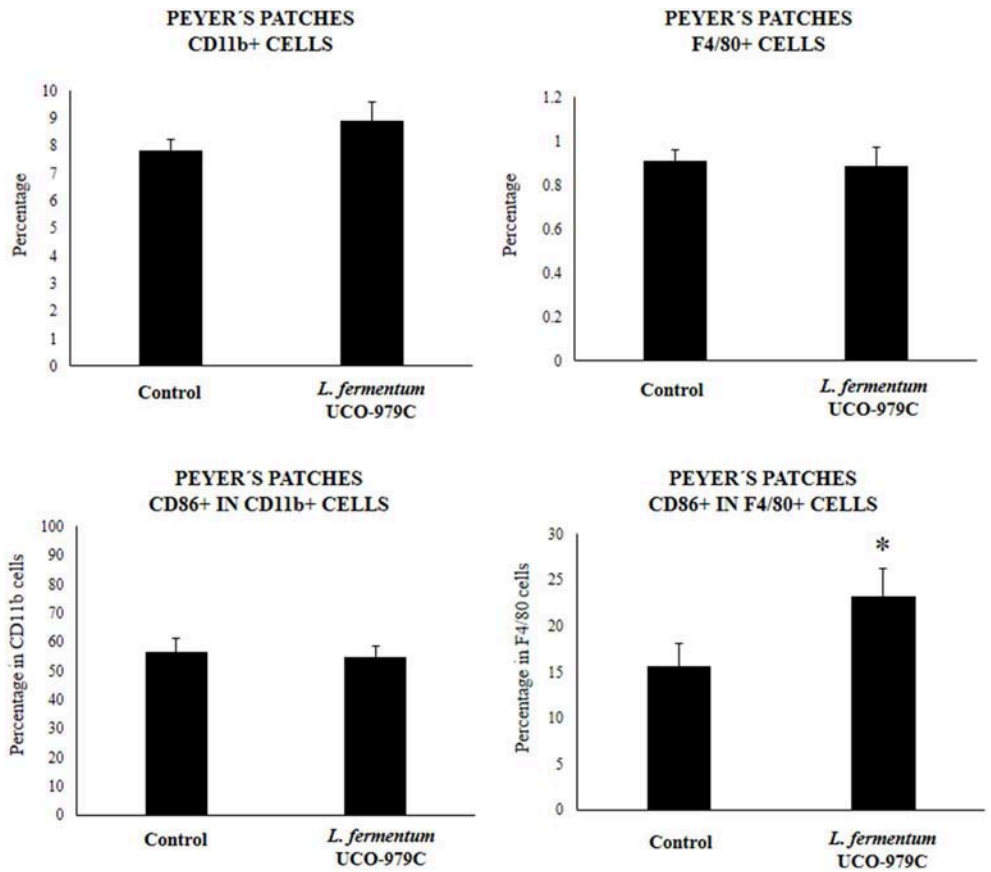


**FIGURE 8 |** Effect of *Lactobacillus fermentum* UCO-979C on Peyer's patches phagocytic cells of adult immunocompetent mice. *L. fermentum* UCO-979C was administered to mice for 2 consecutive days at a dose of $10^8$ cells/mouse/day. Untreated mice were used as controls. One day after the last lactobacilli administration, Peyer's patches phagocytes were evaluated by flow cytometry. The results represent three independent experiments. Results are expressed as mean ± SD. Significantly different from control mice *($P < 0.05$).

and the reduced expression of Tollip and MKP-1 (**Figure 10A**). The intestinal innate immune system needs to keep a balance in TLR activation to confer protection and avoid exaggerated inflammatory responses. Several levels of negative regulation have been described for TLR activation including the expression of membrane bound suppressors and intracellular inhibitors (13, 35). In this regard, some probiotic strains have shown to reduce TLR negative regulators and control the inflammation (36). *Lactobacillus amylovorus* DSM 16698 was reported to diminish IL-1β and IL-8 levels in IECs infected with ETEC K88 through the modulation of the negative regulators Tollip and IRAK-M (37). ETEC K88-challenged pigs exhibited a reduced inflammatory response after *L. acidophilus* administration and this effect was associated with an increased expression of splenic Tollip, IRAK-M, A20, and Bcl-3 (38). In addition, *L. plantarum* CGMCC1258 increased SIGIRR, Bcl3, and MKP-1 gene expressions in porcine IECs challenged with ETEC K88 ameliorating the production of IL-8 and TNF-α (39).

The stimulating/anti-inflammatory mixed effect of *L. fermentum* UCO-979C in PIE cells contrast with our previous findings in AGS cells (23). We demonstrated that *L. fermentum* UCO-979C significantly diminished the production of IL-8, TNF-α, IL-1β, IL-6, and MCP-1 in AGS cells challenged with *H. pylori*. Of interest, in addition to its capacity to reduce the production of pro-inflammatory factors we observed that *L. fermentum* UCO-979C was also capable to improve the production of TGF-β in *H. pylori*-infected AGS cells. These findings indicate that it is of great importance to characterize the immunomodulatory properties of the probiotic strains in different cellular models since it is not possible to extrapolate their effect in one mucosal tissue to another.

Several studies have reported the beneficial effects of immunobiotics on intestinal health and those studies have shown that the most remarkable effect of immunobiotics on intestinal cytokine dynamics is the increase of TNF-α, IFN-γ, and the regulatory cytokine IL-10 (30, 40). We have shown consistently that the oral administration of immunobiotic strains including *L. casei* CRL431, *L. plantarum* CRL1506, and *L. rhamnosus* CRL1505 improves the production of TNF-α, IFN-γ, and IL-10 in the gut (30, 31, 41). Moreover, we demonstrated that oral administration of the immunostimulatory strain *L. rhamnosus* CRL1505 to mice improved the activation of intestinal and

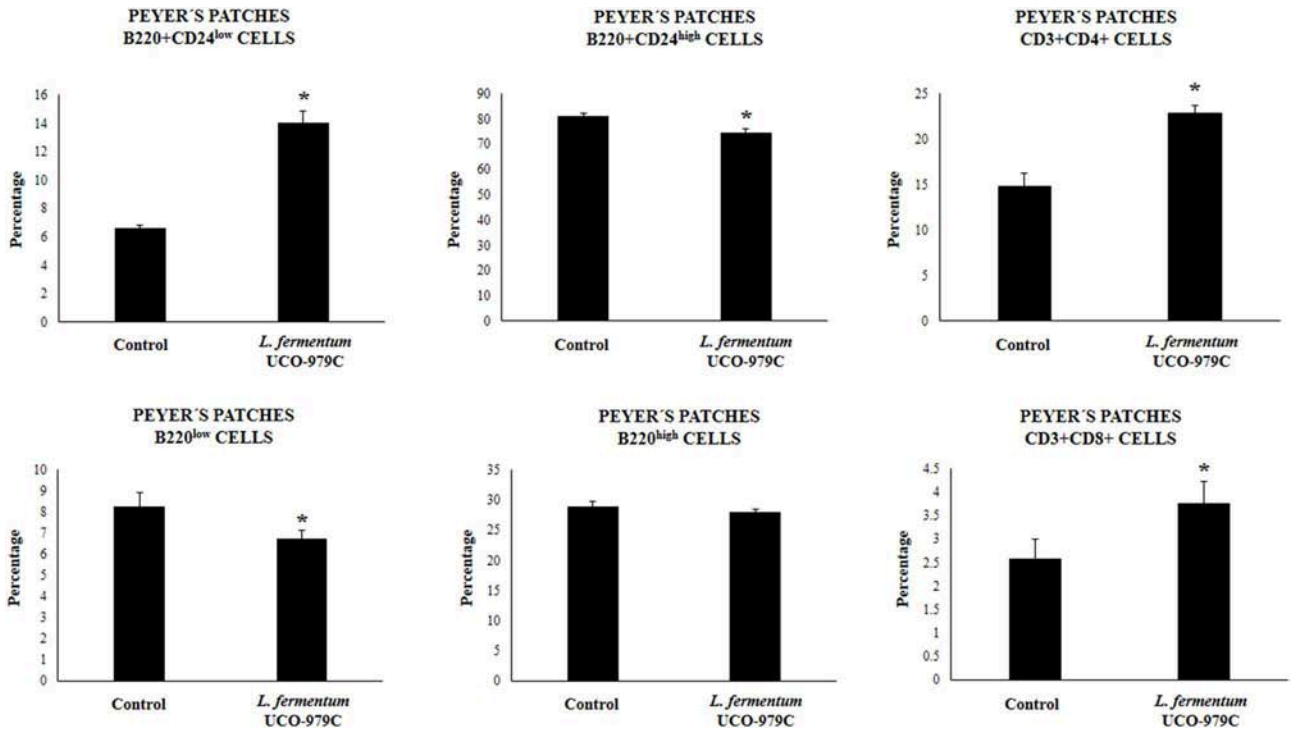


**FIGURE 9 |** Effect of *Lactobacillus fermentum* UCO-979C on Peyer's patches lymphocytes of adult immunocompetent mice. *L. fermentum* UCO-979C was administered to mice for 2 consecutive days at a dose of $10^8$ cells/mouse/day. Untreated mice were used as controls. One day after the last lactobacilli administration, Peyer's patches T and B cells were evaluated by flow cytometry. The results represent three independent experiments. Results are expressed as mean ± SD. Significantly different from control mice *($P < 0.05$).

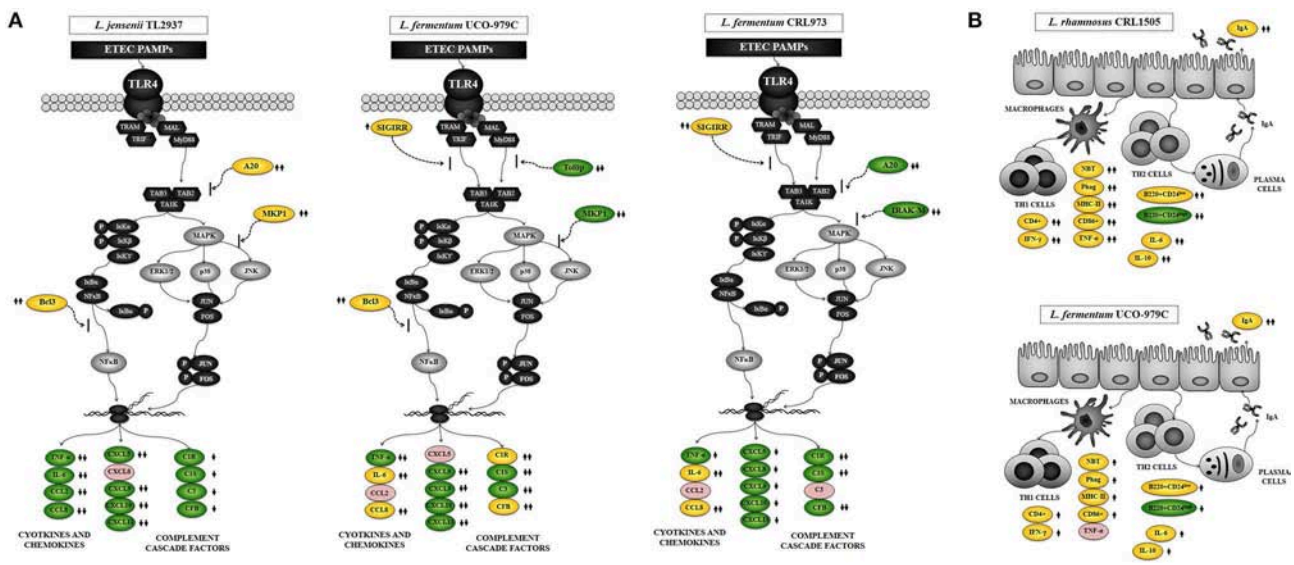


**FIGURE 10 |** Proposed mechanisms for the immunomodulatory activity of *Lactobacillus fermentum* UCO-979C on intestinal mucosa. **(A)** Effect of *L. fermentum* UCO-979C on intestinal epithelial cells and modulation of the inflammatory response triggered by heat-stable Enterotoxigenic *Escherichia coli* (ETEC) pathogen-associated molecular patterns (PAMPs). The immunomodulatory activity of the UCO-979C strain is compared with the activity of the probiotic strain *Lactobacillus jensenii* TL2937 and with *L. fermentum* CRL973. **(B)** Effect of *L. fermentum* UCO-979C on intestinal immune cells. The immunomodulatory activity of the UCO-979C strain is compared with the activity of the probiotic strain *Lactobacillus rhamnosus* CRL1505.

peritoneal macrophages as well as Peyer's patches $CD4^+IFN\text{-}\gamma^+$ T cells (30, 31, 41). In the present study, the oral administration of *L. fermentum* UCO-979C significantly improved the production of IFN-γ, and IL-10 but not the TNF-α. The UCO-979C strain stimulated intestinal and peritoneal macrophages and improved Peyer's patches $CD4^+$ T cells, although the effects were less pronounced than those previously observed for the CRL1505 strain (**Figure 10B**). These results indicate that *L. fermentum* UCO-979C would be capable of stimulating $CD4^+$ T cells in the gut, increasing IFN-γ production and consequently stimulating the macrophages. In fact, peritoneal macrophages of UCO-979C-treated mice had improved levels of parameters that are involved in several fundamental steps of the phagocytic process including attachment to surface and internalization of *S. boulardii* as well as their microbicidal activity through oxidative burst. We previously reported that *L. fermentum* UCO-979C modulated cytokine production in THP-1 macrophages challenged either with *H. pylori* or LPS (23). The UCO-979C strain was able to reduce the production of TNF-α, and to improve IFN-γ levels in challenged THP-1 macrophages. In addition, we demonstrated that *L. fermentum* UCO-979C increased the production of IL-10 in THP-1 macrophages challenged with *H. pylori* (23). Our previous results and those obtained in this work therefore suggest that the UCO-979C strain could exert an immunomodulatory effect on macrophages acting directly on them or indirectly through the cytokines produced by IECs or other immune cells.

Another effect that has been consistently described for probiotics on the intestinal immune system is their ability to improve secretory IgA production, which is supported in most cases by an improved production of factors released by IECs. Cytokines produced by IECs such as IL-6 are capable of promoting the switch from IgM to IgA expression in B cells (31, 40). It is considered that approximately 80% of antibody-secreting plasma cells in the human body are located in the gut. Intestinal antibody-secreting plasma cells produce secretory IgA that plays an important protective role against pathogens and toxins through a variety of non-inflammatory activities that increase their clearance, and prevent their access to the intestinal epithelium (42). Dimeric IgA also neutralize endocytosed LPS in intestinal epithelium, preventing NF-κB activation (43). IgA-producing B cells can be generated by both T cell-dependent and -independent processes (44). T cell-dependent responses usually occur in germinal centers in lymphoid tissues such as the Peyer's patches and mesenteric lymph nodes. In such structures, B cells undergo several rounds of activation and maturation that are supported by follicular T cells that express co-stimulatory molecules and cytokines. In T-independent responses, which occur outside germinal centers, B cells are activated by IECs and innate immune cells to produce polyreactive IgA (45). The T-independent IgA production is induced by and influences the composition of indigenous members of the microbiota (42). In addition, improvement of T-independent IgA induction supported by TGF-β, IL-4, IL-2, IL-6, and IL-10 was also demonstrated for immunobiotic strains including *L. casei* CRL431 (40), *L. rhamnosus* GG (46), and *L. rhamnosus* CRL1505 (31). In this work, we have observed that the oral administration of the *L. fermentum* UCO-979C improves intestinal IL-6, reduces immature $B220^+CD24^{high}$ B cells from Peyer's patches, enhances mature B $B220^+CD24^{low}$ cells and significantly increases intestinal IgA, although these effects were less pronounced than those observed for the CRL1505 strain (**Figure 10B**).

Interestingly, *L. fermentum* CRL973 showed a modest immunomodulatory effect *in vitro* (**Figure 10A**). The CRL973 strain increased the expression of SIGIRR and reduced the expression of the negative regulators A20 and IRAK-M in PIE cells after heat-stable ETEC PAMPs challenge. However, the *in vivo* studies in mice demonstrated that the CRL973 strain was not able to exert an immunomodulatory effect since no improvement of intestinal cytokines, IgA production, or activation of peritoneal macrophages was observed in the CRL973-treated mice. These findings are of importance since they confirm the general knowledge that the immunobiotic properties are dependent on each specific strain. Moreover, results of this study open up an interesting possibility for future research since cellular, molecular, and genomic comparative studies between both UCO-979C and CRL973 strains could help to understand the immunological mechanisms involved in the beneficial effects of *L. fermentum* UCO-979.

We have demonstrated that *L. fermentum* UCO-979C is able to differentially modulate the cytokine response of human gastric epithelial cells and macrophages, and to improve protection against *H. pylori* infection *in vitro* (23). The UCO-979C strain is also capable to modulate the immune response of IECs triggered by heat-stable ETEC PAMPs challenge. Notably, we demonstrated here for the first time that *L. fermentum* UCO-979C is able to exert its immunomodulatory effect in the intestinal mucosa *in vivo*. Therefore, *L. fermentum* UCO-979C has several characteristics for making it an excellent candidate for the development of immunobiotic functional foods to prevent infections by gastric and intestinal pathogens. The *in vivo* evaluation of the ability of the UCO-979C strain to beneficially influence the immune response and improve protection against *H. pylori* and other intestinal pathogenic Gram-negative bacteria is an interesting point for further research.

## DATA AVAILABILITY

The raw data supporting the conclusions of this manuscript will be made available by the authors, without undue reservation, to any qualified researcher.

## ETHICS STATEMENT

This study was carried out in strict accordance with the recommendations in the Guide for the Care and Use of Laboratory Animals of the Guidelines for Animal Experimentation of CERELA. The CERELA Institutional Animal Care and Use Committee prospectively approved this research under the protocol BIOT-CRL-17.

## AUTHOR CONTRIBUTIONS

JV and HK designed the study. VG-C, RK, YI, MT, and MI did the *in vitro* experiments. VG-C, PC, and SS did the *in vivo* experiments. VG-C, JV, HK, and HT provided financial support. VG-C, JV, HK, AG-C, and SA contributed to data analysis and results interpretation. VG-C, JV, HK, and MI wrote the manuscript. HK, JV, and AG-C approved the final version of manuscript.

## FUNDING

This study was supported by ANPCyT–FONCyT Grants PICT-2013-3219 and PICT-201-0410 to JV, CONICYT National Doctorate Grant 21150603 to VG-C, and a Grant-in-Aid for Scientific Research (B) (2) (16H05019), Challenging Exploratory Research (26660216, 16K15028), Open Partnership Joint Projects of JSPS Bilateral Joint Research Projects from the Japan Society for the Promotion of Science (JSPS) to HK, and the grants for Scientific Research on Innovative Areas from the Ministry of Education, Culture, Science, Sports and Technology (MEXT) of Japan (Grant numbers: 16H06429, 16K21723, and 16H06435) to HT. MI was supported by JSPS (Postdoctoral Fellowship for Foreign Researchers, Program No. 18F18081). This work was also supported by the JSPS Core-to-Core Program Advanced Research Networks Establishment of international agricultural immunology research-core for a quantum improvement in food safety.

## REFERENCES

1. Dicks LMT, Geldenhuys J, Mikkelsen LS, Brandsborg E, Marcotte H. Our gut microbiota: a long walk to homeostasis. *Benef Microbes*. (2018) 9:3–20. doi: 10.3920/BM2017.0066
2. Sánchez B, Delgado S, Blanco-Míguez A, Lourenço A, Gueimonde M, Margolles A. Probiotics, gut microbiota, and their influence on host health and disease. *Mol Nutr Food Res*. (2017) 6:1–15. doi: 10.1002/mnfr.201600240
3. Hooper LV, Littman DR, Macpherson AJ. Interactions between the microbiota and the immune system. *Science*. (2012) 336:1268–73. doi: 10.1126/science.1223490
4. Hevia A, Delgado S, Sánchez B, Margolles A. Molecular players involved in the interaction between beneficial bacteria and the immune system. *Front Microbiol*. (2015) 6:1285 doi: 10.3389/fmicb.2015.01285
5. Neville BA, Forster SC, Lawley TD. Commensal Koch's postulates: establishing causation in human microbiota research. *Curr Opin Microbiol*. (2018) 42:47–52. doi: 10.1016/j.mib.2017.10.001
6. Highlander SK. High throughput sequencing methods for microbiome profiling: application to food animal systems. *Anim Health Res Rev*. (2012) 13:40–53. doi: 10.1017/S1466252312000126
7. Wang B, Yao M, Lv L, Ling Z, Li L. The human microbiota in health and disease. *Engineering*. (2017) 3:71–82. doi: 10.1016/J.ENG.2017.01.008
8. Perdigón G, Fuller R, Raya R. Lactic acid bacteria and their effect on the immune system further reading. *Curr Issues Intest Microbiol*. (2001) 2:27–42.
9. Clancy R. Immunobiotics and the probiotic evolution. *FEMS Immunol Med Microbiol*. (2003) 38:9–12. doi: 10.1016/S0928-8244(03)00147-0
10. Kitazawa H, Villena J, Alvarez S. *Probiotics: Immunobiotics and Immunogenics*. CRC Press. (2013). Available online at: https://books.google.com/books?id=FJ3NBQAAQBAJ&pgis=1
11. Wu R, Jeffrey M, Johnson-Henry K, Green-Johnson J, Sherman P. Impact of prebiotics, probiotics and gut derived metabolites on host immunity. *LymphoSign J*. (2016) 4:1–24. doi: 10.14785/lymphosign-2016-0012
12. Lebeer S, Bron PA, Marco ML, Van Pijkeren JP, O'Connell Motherway M, Hill C, et al. Identification of probiotic effector molecules: present state and future perspectives. *Curr Opin Biotechnol*. (2018) 49:217–23. doi: 10.1016/j.copbio.2017.10.007
13. Villena J, Kitazawa H. Modulation of intestinal TLR4-inflammatory signaling pathways by probiotic microorganisms: lessons learned from *Lactobacillus jensenii* TL2937. *Front Immunol*. (2014) 4:512 doi: 10.3389/fimmu.2013.00512
14. Ren C, Zhang Q, De Haan BJ, Zhang H, Faas MM, De Vos P. Identification of TLR2/TLR6 signalling lactic acid bacteria for supporting immune regulation. *Sci Rep*. (2016) 6:34561 doi: 10.1038/srep34561
15. Barberi C, Campana S, De Pasquale C, Rabbani Khorasgani M, Ferlazzo G, Bonaccorsi I. T cell polarizing properties of probiotic bacteria. *Immunol Lett*. (2015) 168:337–42. doi: 10.1016/j.imlet.2015.11.005
16. Bron PA, Kleerebezem M, Brummer RJ, Cani PD, Mercenier A, MacDonald TT, et al. Can probiotics modulate human disease by impacting intestinal barrier function? *Br J Nutr*. (2017) 117:93–107. doi: 10.1017/S0007114516004037
17. Lesbros-Pantoflickova D, Corthésy-Theulaz I, Blum AL. *Helicobacter pylori* and probiotics. *J Nutr*. (2007) 137:812S—8S. doi: 10.1093/jn/137.3.812S
18. Goderska K, Agudo Pena S, Alarcon T. *Helicobacter pylori* treatment: antibiotics or probiotics. *Appl Microbiol Biotechnol*. (2017) 102:1–7. doi: 10.1007/s00253-017-8535-7
19. Homan M, Orel R. Are probiotics useful in *Helicobacter pylori* eradication? *World J Gastroenterol*. (2015) 21:10644–53. doi: 10.3748/wjg.v21.i37.10644
20. Garcia CA, Henriquez AP, Retamal RC, Pineda CS, Delgado Sch C, Gonzalez CC. Probiotic properties of *Lactobacillus* spp isolated from gastric biopsies of *Helicobacter pylori* infected and non-infected individuals. *Rev Med Chil*. (2009) 137:369–76. doi: 10.4067/S0034-98872009000300007
21. García A, Navarro K, Sanhueza E, Pineda S, Pastene E, Quezada M, et al. Characterization of *Lactobacillus fermentum* UCO-979C, a probiotic strain with a potent anti-*Helicobacter pylori* activity. *Electron J Biotechnol*. (2017) 25:75–83. doi: 10.1016/j.ejbt.2016.11.008
22. Merino JS, García A, Pastene E, Salas A, Saez K, González CL. *Lactobacillus fermentum* UCO-979C strongly inhibited *Helicobacter pylori* SS1 in *Meriones unguiculatus*. *Benef Microbes*. (2018) 9:625–7. doi: 10.3920/BM2017.0160
23. Garcia-Castillo V, Zelaya H, Ilabaca A, Espinoza-Monje M, Komatsu R, Albarracin L, et al. *Lactobacillus fermentum* UCO-979C beneficially modulates the innate immune response triggered by *Helicobacter pylori* infection *in vitro*. *Benef Microbes*. (2018) 9:829–41. doi: 10.3920/BM2018.0019
24. Moue M, Tohno M, Shimazu T, Kido T, Aso H, Saito T, et al. Toll-like receptor 4 and cytokine expression involved in functional immune response in an originally established porcine intestinal epitheliocyte cell line. *Biochim Biophys Acta Gen Subj*. (2008) 1780:134–44. doi: 10.1016/j.bbagen.2007.11.006
25. Shimazu T, Villena J, Tohno M, Fujie H, Hosoya S, Shimosato T, et al. Immunobiotic *Lactobacillus jensenii* elicits anti-inflammatory activity in porcine intestinal epithelial cells by modulating negative regulators of the toll-like receptor signaling pathway. *Infect Immun*. (2012) 80:276–88. doi: 10.1128/IAI.05729-11
26. Tomosada Y, Villena J, Murata K, Chiba E, Shimazu T, Aso H, et al. Immunoregulatory effect of bifidobacteria strains in porcine intestinal epithelial cells through modulation of ubiquitin-editing enzyme A20 expression. *PLoS ONE*. (2013) 8:e59259 doi: 10.1371/journal.pone.0059259
27. Kobayashi H, Albarracin L, Sato N, Kanmani P, Kober AKMH, Ikeda-Ohtsubo W, et al. Modulation of porcine intestinal epitheliocytes immunetranscriptome response by *Lactobacillus jensenii* TL2937. *Benef Microbes*. (2016) 7:769–82. doi: 10.3920/BM2016.0095
28. Nygard AB, Jorgensen CB, Cirera S, Fredholm M. Selection of reference genes for gene expression studies in pig tissues using SYBR green qPCR. *BMC Mol Biol*. (2007) 8:67. doi: 10.1186/1471-2199-8-67
29. Ray A, Dittel BN. Isolation of mouse peritoneal cavity cells. *J Vis Exp*. (2010) 35:1488. doi: 10.3791/1488

30. Marranzino G, Villena J, Salva S, Alvarez S. Stimulation of macrophages by immunobiotic *Lactobacillus* strains: influence beyond the intestinal tract. *Microbiol Immunol*. (2012) 56:771–81. doi: 10.1111/j.1348-0421.2012.00495.x
31. Salva S, Villena J, Alvarez S. Immunomodulatory activity of *Lactobacillus rhamnosus* strains isolated from goat milk: impact on intestinal and respiratory infections. *Int J Food Microbiol*. (2010) 141:82–9. doi: 10.1016/j.ijfoodmicro.2010.03.013
32. Tsukida K, Takahashi T, Iida H, Kanmani P, Suda Y, Nochi T, et al. Immunoregulatory effects triggered by immunobiotic *Lactobacillus jensenii* TL2937 strain involve efficient phagocytosis in porcine antigen presenting cells. *BMC Immunol*. (2016) 17:1–12. doi: 10.1186/s12865-016-0160-1
33. Abreu MT. Toll-like receptor signalling in the intestinal epithelium: how bacterial recognition shapes intestinal function. *Nat Rev Immunol*. (2010) 10:131–44. doi: 10.1038/nri2707
34. Allaire JM, Crowley SM, Law HT, Chang SY, Ko HJ, Vallance BA. The intestinal epithelium: central coordinator of mucosal immunity. *Trends Immunol*. (2018) 39:677–96. doi: 10.1016/j.it.2018.04.002
35. Liew FY, Xu D, Brint EK, O'Neill LAJ. Negative regulation of toll-like receptor-mediated immune responses. *Nat Rev Immunol*. (2005) 5:446–58. doi: 10.1038/nri1630
36. Llewellyn A, Foey A. Probiotic modulation of innate cell pathogen sensing and signaling events. *Nutrients*. (2017) 9:1–21. doi: 10.3390/nu9101156
37. Finamore A, Roselli M, Imbinto A, Seeboth J, Oswald IP, Mengheri E. *Lactobacillus amylovorus* inhibits the TLR4 inflammatory signaling triggered by enterotoxigenic *Escherichia coli* via modulation of the negative regulators and involvement of TLR2 in intestinal caco-2 cells and pig explants. *PLoS ONE*. (2014) 9:e94891. doi: 10.1371/journal.pone.0094891
38. Li H, Zhang L, Chen L, Zhu Q, Wang W, Qiao J. *Lactobacillus acidophilus* alleviates the inflammatory response to enterotoxigenic *Escherichia coli* K88 via inhibition of the NF-κB and p38 mitogen-activated protein kinase signaling pathways in piglets. *BMC Microbiol*. (2016) 16:273. doi: 10.1186/s12866-016-0862-9
39. Wu Y, Zhu C, Chen Z, Chen Z, Zhang W, Ma X, et al. Protective effects of *Lactobacillus plantarum* on epithelial barrier disruption causedby enterotoxigenic *Escherichia coli* in intestinal porcine epithelial cells. *Vet Immunol Immunopathol*. (2016) 172:55–63. doi: 10.1016/j.vetimm.2016.03.005
40. Maldonado C, De Moreno De Leblanc A, Vinderola G, Bibas Bonet ME, Perdigón G. Proposed model: mechanisms of immunomodulation induced by probiotic bacteria. *Clin Vaccine Immunol*. (2007) 14:485–92. doi: 10.1128/CVI.00406-06
41. Villena J, Chiba E, Tomosada Y, Salva S, Marranzino G, Kitazawa H, et al. Orally administered L*actobacillus rhamnosus* modulates the respiratory immune response triggered by the viral pathogen-associated molecular pattern poly(I:C). *BMC Immunol*. (2012) 13:53. doi: 10.1186/1471-2172-13-53
42. Jahnsen FL, Bækkevold ES, Hov JR, Landsverk OJ. Do long-lived plasma cells maintain a healthy microbiota in the gut? *Trends Immunol*. (2018) 39:196–208. doi: 10.1016/j.it.2017.10.006
43. Cario E, Podolsky DK. Intestinal epithelial tollerance versus intollerance of commensals. *Mol Immunol*. (2005) 42:887–93. doi: 10.1016/j.molimm.2004.12.002
44. Pabst O. New concepts in the generation and functions of IgA. *Nat Rev Immunol*. (2012) 12:821–32. doi: 10.1038/nri3322
45. Stephens WZ, Round JL. IgA targets the troublemakers. *Cell Host Microbe*. (2014) 16:265–7. doi: 10.1016/j.chom.2014.08.012
46. Wang Y, Liu L, Moore DJ, Shen X, Peek RM, Acra SA, et al. An LGG-derived protein promotes IgA production through upregulation of APRIL expression in intestinal epithelial cells. *Mucosal Immunol*. (2017) 10:373–84. doi: 10.1038/mi.2016.57

**Conflict of Interest Statement:** The authors declare that the research was conducted in the absence of any commercial or financial relationships that could be construed as a potential conflict of interest.

frontiers in Immunology

ORIGINAL RESEARCH
published: 03 July 2019
doi: 10.3389/fimmu.2019.01536

# Immunobiotic Strains Modulate Toll-Like Receptor 3 Agonist Induced Innate Antiviral Immune Response in Human Intestinal Epithelial Cells by Modulating IFN Regulatory Factor 3 and NF-κB Signaling

*Paulraj Kanmani and Hojun Kim**

*Department of Rehabilitation Medicine of Korean Medicine, Dongguk University Ilsan Hospital, Gyeongj-si, South Korea*

OPEN ACCESS

***Edited by:***
*Julio Villena,*
*CONICET Centro de Referencia para Lactobacilos (CERELA), Argentina*

***Reviewed by:***
*Leonardo Albarracin,*
*CONICET Centro de Referencia para Lactobacilos (CERELA), Argentina*
*Imad Omar Al Kassaa,*
*Lebanese University, Lebanon*

****Correspondence:***
*Hojun Kim*
*kimklar@dongguk.ac.kr*

***Specialty section:***
*This article was submitted to Nutritional Immunology, a section of the journal Frontiers in Immunology*

***Received:*** *30 March 2019*
***Accepted:*** *19 June 2019*
***Published:*** *03 July 2019*

***Citation:***
*Kanmani P and Kim H (2019) Immunobiotic Strains Modulate Toll-Like Receptor 3 Agonist Induced Innate Antiviral Immune Response in Human Intestinal Epithelial Cells by Modulating IFN Regulatory Factor 3 and NF-κB Signaling. Front. Immunol. 10:1536. doi: 10.3389/fimmu.2019.01536*

Many studies have demonstrated that immunobiotics with immunoregulatory functions improve the outcomes of several bacterial and viral infections by modulating the mucosal immune system. However, the precise mechanisms underlying the immunoregulatory and antiviral activities of immunobiotics have not yet been elucidated in detail. The present study was conducted to determine whether selected lactic acid bacteria (LAB) modulate toll-like receptor 3 (TLR3) agonist polyinosinic:polycytidylic acid (PolyI:C) induced viral response in human intestinal epithelial cells (IECs). PolyI:C increased the expression of interferon-β (IFN-β), interleukin-6 (IL-6), interleukin-8 (IL-8), monocyte chemoattractant protein (MCP-1), and interleukin-1β (IL-1β) in HCT116 cells, and these up-regulations were significantly altered when cells were pre-stimulated with LAB isolated from Korean fermented foods. LAB strains were capable to up-regulate IFN-β but down-regulated IL-6, IL-8, MCP-1, and IL-1β mRNA levels as compared with PolyI: C. HCT-116 cell treatment with LABs beneficially modulated the mRNA levels of C-X-C motif chemokine 10 (CXCL-10), 2-5A oligoadenylate synthetase 1 (OSA1), myxovirus resistance protein (MxA), TLR3, and retinoic acid inducible gene-I (RIG-I), and TLR negative regulators. In addition, LABs increased IFN-β, IFN-α, and interleukin-10 (IL-10) and decreased tumor necrosis factor-α (TNF-α) and IL-1β protein/mRNA levels in THP-1 cells. LABs also protected the cells by maintaining tight-junction proteins (zonula occludens-1 and occludin). The beneficial effects of these LABs were mediated via modulation of the interferon regulatory factor 3 (IRF3) and nuclear factor-kappa B (NF-κB) pathways. Overall, the results of this study indicate that immunobiotics have potent antiviral and anti-inflammatory activities that may use as antiviral substitutes for human and animal applications.

**Keywords: probiotics, PolyI:C, inflammatory response, antiviral immune response, immunoregulatory activity, intestinal epithelial cells**

## INTRODUCTION

The gastrointestinal tracts (GITs) of humans and animals contain innate and adaptive immune cells that permit colonization by trillions of commensal microorganisms, which enhance digestion, and host mucosal immunity. Of the immune cells, intestinal epithelial cells (IECs) are the potent innate immune cells lined as a monolayer in the lumen of the GIT (1). These cells also act as a first line of defense against invading pathogens, including viruses such as rotaviruses (2, 3). IECs are able to sense and respond to various microbial stimuli from foreign and commensal microbiota via specialized surface membrane receptors such as toll-like receptors (TLRs) (1, 4). TLRs are a type of pattern recognition receptor (PRR), which have the ability to induce innate and adaptive immunity against invading pathogens by recognizing their molecular patterns (4). Among the TLRs, toll-like receptor 3 (TLR3) is able to recognize double stranded RNA (dsRNA) and to triggers intracellular signal transduction pathways in response to dsRNA viruses (5). After being ligated, TLR3 activates the transcription factors nuclear factor-kappa B (NF-κB) and interferon regulatory factor (IRF) via TLR adaptors molecules such as MyD88, Toll/interleukin-1 (IL-1) domain containing adaptor inducing IFN (TRIF), and TIRF-related adaptor molecule (TRAM), to produce inflammatory cytokines and interferons (IFNs) (6, 7). dsRNA is also recognized by cytosolic receptors such as retinoic acid inducible gene-I (RIG-1) and melanoma differentiation associated antigen 5 (MAD-5) (8, 9), which interact with IFN-β promoter stimulator-1 (IPS-1)/mitochondrial antiviral-signaling protein (MAVS) adaptor proteins and thus activate NF-κB and interferon regulatory factor 3 and 7 (IRF3, 7) to augment the expressions of inflammatory mediators and type I IFNs (7, 8). Collectively, previous reports suggest that IECs possess more than one receptor to sense dsRNA and its analog, and that they respond via two separate signaling pathways (7).

Polyinosinic:polycytidylic acid (PolyI:C) is a synthetic dsRNA analog that is often used to induce inflammatory responses that mimic response induced by dsRNA viruses (5). TLR3 and RIG-I/MDA-5 receptors have been reported to be able to recognize PolyI:C and to activate transcription factors responsible for the expressions of inflammatory cytokines/chemokines and type I IFNs (7, 10). The production of IFNs, especially of type I IFNs, plays a crucial role in protecting host immune system from viral invasion. In particular, IFN-β has the ability to inhibit viral replication (7). The absence of IFN-β in mice was highly infected by viruses (11). In addition, the activation of type I IFN signaling induces the expression of several antiviral genes, such as myxovirus resistance protein (MxA), and 2′-5′ oligoadenuylate dependent endoribonuclease (RNase-L), that helps maintain antiviral states induced by IFNs in hosts via several mechanisms (12, 13).

Lactic acid bacteria (LAB), a group of commensal bacteria that are able to exert probiotic effects by mutually interacting with host IECs (14). Lactobacilli and bifidobacteria are the members of LAB, which are dominantly colonizing in the GIT and boost the host immune system to combat viral infections (15). Several studies evaluated the beneficial actions of these strains against viral and PolyI:C-mediated inflammatory responses (3, 16–18). In addition, the extracellular polysaccharides (EPS) of these probiotic strains have also been reported to promote host defense mechanism and to attenuate inflammatory responses induced by pathogens or PolyI:C (3, 19, 20). Most studies used IECs (Human and Porcine IECs) as an *in vitro* model to study innate anti-viral immune response of LAB strains against rotavirus (RV) and PolyI:C (21–23). Human intestinal epithelial (HT-29) cells potently respond to PolyI:C by up-regulating immune gene proteins related to the TLR signaling pathway (10), and a study using porcine jejunal cells (IPEC-J2) showed treatment with *L. rhamnosus* GG reduced inflammatory response and RV infection *in vitro* (22). Also, PolyI:C increased the mRNA level of inflammatory cytokines (IL-6, IL-8, MCP-1) and interferon (IFN-α and IFN-β) in porcine IECs (PIE cells) (17, 23), whereas PIE cells treated with immunobiotic *L. casei* MEP221106 up-regulated IFN-α and IFN-β and down-regulated IL-6 and MCP-1 in response to the TLR3 agonist PolyI:C (16). These studies also suggest that IECs are the *in vitro* useful model to select and study of probiotic bacteria against viral or PolyI:C induced immune response *in vitro*. In addition, IECs would helpful to study molecular insight into mechanisms involved in the viral and anti-viral response of PolyI:C and probiotic strains via analysis of TLRs expression, activation, and modulation of innate immune signaling pathways and negative regulatory proteins. In the present study, we used human colon cell line (HCT116) to investigate the antiviral effects of probiotic bacteria isolated from Korean foods. To induce viral response, HCT116 cells were treated with PolyI:C and then examined for changes in the expressions of inflammatory cytokines, IFNs, anti-viral proteins, and TLR negative regulators. In addition, modulations of tight-junction proteins (ZO-1 and occludin) and signaling molecules (IRF-3 and IκB-α,) were also examined by western blotting after treating cells with *Lactobacillus plantarum*, *Weissella cibaria*, or *Lactobacillus sakei*.

## MATERIALS AND METHODS

### Bacterial Strains

The strains *L. plantarum* DU1, *W. cibaria* DU1, and *L. sakei* DU2 used in this study were previously isolated from Korean fermented foods and maintained in MRS (deMan-Rogosa-Sharp) medium at −70°C. LABs were grown at 37°C for 19 h, centrifuged, washed with distilled phosphate buffered saline (PBS), and re-suspended in Roswell Park Memorial Institute 1640 medium (RPMI 1640, Gyeongsagbuk-do, South Korea) at desired concentrations, then stored at −4°C until required. The cytotoxicity of these strains on human cell line was determined previously using a cell viability assay kit (EZ-CYTOX, DOGEN Bio Co. Ltd) (24).

### Cell Culture

The human colon and monocytic cells (HCT116 cells and THP-1) were used in this study that were obtained from the Korean Cell Line Bank (Seoul). HCT116 cells were cultured in RPMI medium supplemented with 10% fetal bovine serum (FBS), and 1% penicillin/streptomycin (P/S) at 37°C, under 5% $CO_2$. The

medium was changed at 1-day interval for 5–6 days. Cells from passages 20–40 were used in the present study. In addition, THP-1 cells were also cultured in RPMI-1640 medium containing FBS (1%), P/S (1%), and mercaptoethanol (0.05 mM) at 37°C, under 5% $CO_2$ for 5–6 days. To induce differentiation, cells were incubated with PMA (phorbol-12-myristate-13-acetate) medium for 48 h and then in fresh RPMI medium for 24 h. PMA medium was prepared by adding PMA (50 ng/ml) to RPMI medium.

## Analysis of Antiviral Activity of LABs in HCT116 Cells

HCT116 cells ($3 \times 10^4$ cells/ml) were placed in collagen coated plates (SPL Life Sciences Co. Ltd, Gyeonggi-do, Korea), and incubated at 37°C, under 5% $CO_2$ for 5–6 days. Cultured cells were then incubated with LAB strains ($5 \times 10^7$ cells/ml) for 48 h and post-incubated with PolyI:C (10 μg/ml) for 3 or 12 h. HCT116 cells stimulated with PolyI:C and medium alone were used as positive and negative controls, respectively. The RNA was extracted from treated cells and the expressions of type I interferon (IFN-α, IFN-β), antiviral proteins [(MxA, OAS1, C-X-C motif chemokine 10 (CXCL-10)], signaling receptors (RIG-I, TLR3), inflammatory cytokines/chemokine (IL-6, IL-8, MCP1, IL-1β), and TLR negative regulators such as A20, toll-interacting protein (Tollip), single Ig interleukin 1 –related receptor (SIGIRR) and IL-1 receptor-associated kinase-M (IRAK-M) were analyzed by qRT-PCR.

## RNA Extraction and Quantitative Polymerase Chain Reaction (qPCR)

Total RNA was isolated from cells by adding TRIzol reagent (Invitrogen), and used to synthesize cDNA using a Thermal cycler (BioRad, Hercules, CA, USA). qPCR was performed with a 7300 real-time PCR system (Roche Applied Science, Indianapolis, IN, USA) using SYBR green and targeted primers (24). PCR reaction mixtures (20 μl) contained 1 μl of cDNA and 19 μl of master mix, which included SYBR green and forward and reverse primers (1 pmol/μl). Amplifications were performed using the following procedure; 95°C for 5 min, followed by 40 cycles of 95°C for 15 s, 60°-63°C for 30 s, and 72°C for 30 s. β-actin was used as the internal control to normalize cDNA levels.

## Co-culture Study

HCT116 cells ($3.5 \times 10^4$ cells/well) were cultured in apical transwell culture inserts (transparent PTFE membrane coated collagen (0.4 μm pore size); Transwell-COL, Corning Inc., NY, USA) at 37°C under 5% $CO_2$ for 5–6 days. Then, HCT116 cells were co-cultured with THP-1 cells ($1 \times 10^5$ cells/well) taken in a basolateral culture chamber. To examine the anti-viral immune response of LABs, HCT116 cells monolayer [Transepithelial electric resistance (TEER value ~541 $\Omega$ cm2)] was stimulated with LABs for 48 h, after which 10 μg/ml of PolyI:C was added to the THP-1 cells cultured chamber and incubated for an additional 12 h at 37°C. Cell free supernatants from the basolateral chamber was collected and stored at −4°C to estimate the protein level of tumor necrosis factor-α (TNF-α). In addition, RNA from THP-1 was used to analyze the expression of IFN-α, IFN-β, IL-10, and IL-1β by qRT-PCR.

## Enzyme-Linked Immunosorbent Assay (ELISA)

To determine whether LABs reduced TNF-α production in the co-culture model, TNF-α levels in THP-1 cell free supernatants from basolateral sides were quantified using a commercially available ELISA kit (Human TNF-α Quantikine ELISA kit, R & D system, MN, USA).

## Proteins Extraction and Western Blot Analysis

HCT116 cells ($1.8 \times 10^5$ cells/dish) were seeded in dishes (60 mm) and incubated at 37°C under 5% $CO_2$ for 5–6 days. Fully confluent cells were then stimulated as follows; cells stimulated with LAB strains alone (48 h), cells stimulated with PolyI:C alone (2 h), cells pre-stimulated with LAB strains and combined with PolyI:C for last 2 h (PolyI:C combined 2 h), cells pre-stimulated with LAB strains and post-stimulated with PolyI:C for 2 h (2 h, PolyI:C post-treatment separately), and cells co-stimulated with LAB strains +PolyI:C (48 h both combined). Treated cells were washed three times with distilled PBS and lysed with 200 μl of CellLytic M cell lysis reagent (Sigma-Aldrich, St. Louis, MO) containing phosphatase and protease inhibitors. Lysed cells were scraped and transferred to fresh Eppendorf tubes (1.5 ml), sonicated at 50% for 3–5 s, and stored at −70°C until required. Total protein in collected samples was estimated using bicinchoninic acid (BCA) assay kits (Thermo Scientific, Pierce, Rockford, IL, USA) after heating samples at 95°C for 5 min.

For western blotting, lysed samples were loaded in 10% SDS-polyacrylamide gels, and separated proteins were transferred to nitrocellulose membranes (Trans-Blot Turbo™, BioRad) that were incubated with blocking buffer for 1–2 h and then incubated with targeted proteins specific primary and secondary antibodies. Tight junction proteins (zonula occludens-1, occludin), phosphorylation of interferon regulatory factor 3 (p-IRF3) and nuclear factor kappa B (p-IκB-α) levels were evaluated by incubating membranes overnight with ZO-1 (D7D12) antibody (ZO-1, Cat. #8193), phosphor-IRF3 (Ser396) antibody (p-IRF3, Cat. #29047), phospho-IκB-α antibody (p-IκB-α, Cat. #2859) (Cell Signaling Technology, Beverly, MA, USA), occludin antibody (E-5: Cat.#SC-133256), and β-actin antibody (C4, Cat. #SC-47778) (Santa Cruz Biotechnology Inc., Dallas, Texas) at dilutions of 1,000:1. Membranes were then washed with TBS-T buffer and incubated with Goat anti-rabbit IgG-HRP polyclonal antibody (AbFrontier, Cat. #LFSA8002, Seoul). After 1–2 h of incubation, membranes were washed with TBS-T buffer, and treated with western blot detection solution (Dyne ECL Star, Korea). The optical protein bands were detected and the densitogram peaks were estimated using the Image J software (National Institute of Health, Bethesda, MD, USA).

## Statistical Analysis

The data were expressed as the average (mean ± SD) value of three repeated experiments. Significant differences among the groups were determined by one-way analysis of variance (ANOVA) with Tukey multiple range test using SPSS ver.

12.0 (SPSS Inc., Chicago, IL, USA). Statistical significance was accepted for $p$ values of $< 0.05$.

# RESULTS

## LABs Modified PolyI:C Induced IFN-β Expression in HCT116 Cells

We first evaluated whether the three LAB strains (*L. plantarum* DU1, *Weissella cibaria* DU1, and *L. sakei*) induced IFN-β production in response to PolyI:C in HCT116 cells. Cells were pre-incubated with LABs and then post-stimulated with PolyI:C for different hours. The results of RT-PCR showed that the expression of IFN-β varied depending on the stimulation hours. Stimulation of cells with PolyI:C alone increased the expression of IFN-β at both 3 and 12 h (**Figure 1**). The PolyI:C induced IFN-β expression was further up-regulated when cells were pre-incubated with LABs. *W. cibaria* and *L. sakei* were significantly ($p$ <0.05) increased the level of IFN-β in 3 h, whereas *L. plantarum* showed level was not significantly higher than PolyI:C. But at 12 h, all LAB strains significantly ($p$ <0.05) increased the mRNA level of IFN-β in response to PolyI:C in HCT116 cells, indicating that LABs showed strong antiviral activity against PolyI:C at late stage of stimulation.

## Effect of LABs on Inflammatory Cytokine/Chemokine Expressions in HCT116 Cells

To investigate whether LABs inhibit PolyI:C-induced inflammatory cytokine/chemokine expressions, HCT116 cells were pretreated with LABs and then with PolyI:C, as described above. As shown in **Figure 2**, PolyI:C treatment tended to increase the mRNA levels of IL-6, IL-8, MCP-1 and IL-1β, but LABs pretreatment altered these expressions in a time-dependent manner. At 3 h, cells pre-stimulated with LABs altered the expression of all cytokines, however they were relatively similar to the levels of PolyI:C (**Figure 2**). In contrary, all LAB strains had profound effects on the reduction of IL-6, IL-8, MCP-1, and IL-1β at 12 h, and these reductions were significantly ($p$ <0.05) lower than PolyI:C.

## LABs Altered TJ Proteins in HCT116 Cells

To analyze the effect of LABs on alternation of TJ, we examined the level of ZO-1 and occludin proteins in HCT116 cells that were pre or co-stimulated with LAB strains and PolyI:C or PolyI:C alone. HCT116 cells treated with PolyI:C decreased the level of ZO-1, and this decrease was attenuated by pre or co-treated with LAB strains (**Figure 3**). As compared to PolyI:C, all LABs except *L. plantarum* and *W. cibaria* showed significantly higher level of ZO-1 in HCT116 cells post-treated with PolyI:C for 2 h. In addition, higher level of ZO-1 was observed in HCT116 cells co-stimulated with LABs and PolyI:C for 48 h. Relatively, similar pattern of results were observed in the protein level of occludin (**Figure 4**). LABs treatment increased occludin protein in HCT116 cells that were post-stimulated with PolyI:C for 2 h. In addition, the occludin was found to be higher in cells that were co-stimulated with LABs and PolyI:C for 2 and 48 h. These results indicates that LABs protect the cells against PolyI:C by maintaining the tight-junction proteins.

## LABs Modulated PolyI:C-Induced Cytokine and Antiviral Protein Expressions in HCT116 Cells

HCT116 cells were treated with LABs and followed by post-stimulation with PolyI:C for 3 or 12 h. Relative mRNA levels of cytokines, antiviral proteins, and signaling receptors were determined by RT-PCR. CXCL-10 levels were significantly increased in HCT116 cells treated with PolyI:C for 3 or 12 h (**Figure 5**). Pre-stimulation of cells with LABs modulated PolyI:C induced cytokine mRNA levels. *L. plantarum* or *W. cibaria* pretreatment increased CXCL-10 level after 3 h of PolyI:C post-treatment, whereas *L. sakei* pretreatment had no effect. However, pretreatment with all three LABs up-regulated mRNA levels of the antiviral proteins (OAS1 and MxA) as compared with PolyI:C. The expression of RIG-I and TLR3 weren't significantly increased by LAB strains as compared with PolyI:C. In contrary, the expression of CXCL-10 was significantly ($p < 0.05$) decreased when cells were pre-stimulated with LABs except *L. sakei* for 12 h, whereas the expressions of OAS1 and MxA were increased by LABs (except *W. cibaria* for MxA) in HCT116 cells (**Figure 5**). In addition, *L. plantarum* and *L. sakei* were significantly increased the level of RIG-I in HCT116 cells. The mRNA level of TLR3 was significantly increased when cells were pre-treated with *W. cibarai* as compared with PolyI:C.

## Effect of LABs on TNF-α Production in THP-1 Cells

To investigate the effect of LABs on TNF-α production, we used a co-culture model mimicking intestinal conditions by allowing cell crosstalk via the secretions of soluble factors into the surrounding medium. HCT116 cells were co-cultured with THP-1 cells and stimulated with LABs and followed by PolyI:C for 12 h. TNF-α levels in medium were determined by ELISA. Results are shown in **Figure 6**A. PolyI:C treatment tended to increase the production of TNF-α in THP-1 cells; however, LABs pre-stimulation suppressed THP-1 cells to produce lower level of TNF-α as compared to PolyI:C treatment alone.

## LABs Modulated PolyI:C-Induced IFNs and Inflammatory and Anti-inflammatory Cytokines in THP-1 Cells

To investigate whether LABs indirectly modulate PolyI:C induced type 1 IFNs and cytokines in THP-1 cells via HCT116 cells, we extracted RNA from THP-1 cells that were stimulated with LABs and PolyI:C. The expression of interleukin-10 (IL-10), interleukin 1β (IL-1β), IFN-α, and IFN-β was analyzed by qRT-PCR. The mRNA level of IL-10 was significantly increased by all three LABs in THP-1 cells post-stimulated with PolyI:C for 12 h. On the other hand, *W. cibaria* exhibited significant reduction in the level of IL-1β in THP-1 cells (**Figures 6**B,C). *L. plantarum* and *L. sakei* did not significantly diminish IL-1β expression as compared to PolyI:C. Stimulation of THP-1

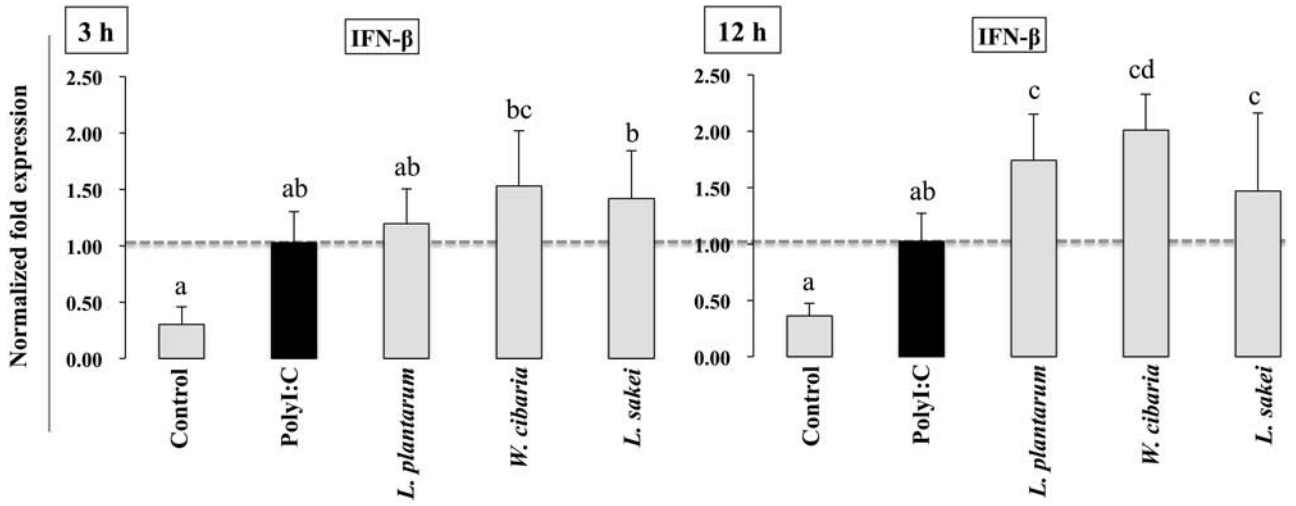


**FIGURE 1 |** LAB strains up-regulate PolyI:C induced IFN-β in IECs. After HCT116 were treated with LAB strains and PolyI:C, the expression of IFN-β was determined by RT-PCR. Cells treated with either PolyI:C or medium alone were used as positive and negative controls, respectively. The positive control was used for comparison of LAB strains treated groups. The mean differences among the different superscript letters (a, b, ab, cd) were significant at 0.05 level. LABs were able to up-regulate IFN-β level in response to PolyI:C.

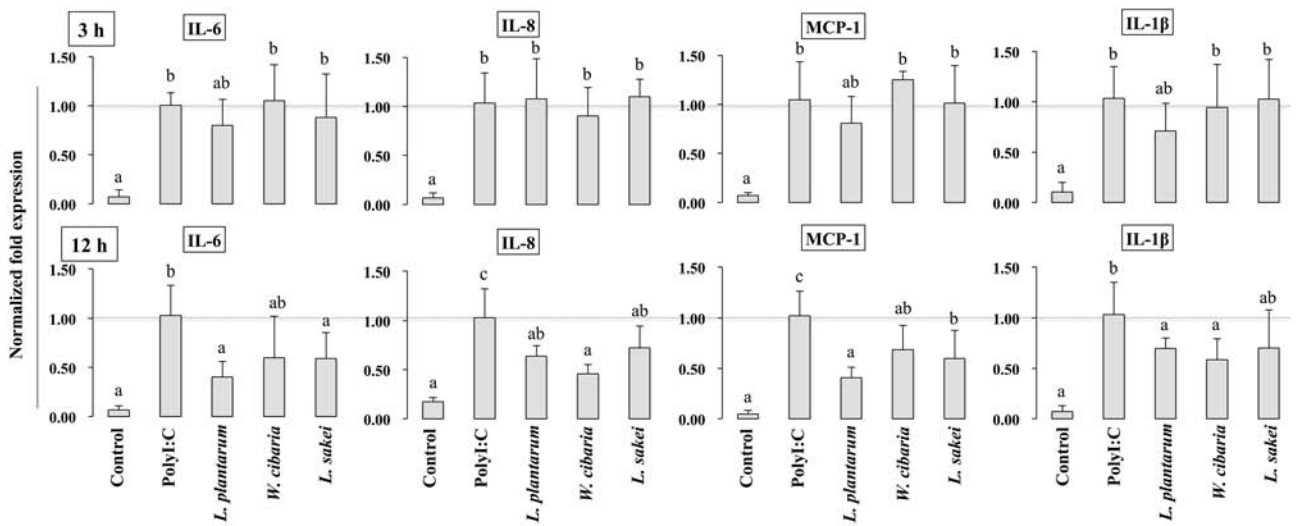


**FIGURE 2 |** LAB strains attenuate the inflammatory response triggered by TLR3 in IECs. After HCT116 cells were treated with LAB strains and PolyI:C, the expression of IL-6, IL-8, MCP-1, and IL-1β were analyzed by RT-PCR. Cells treated with either PolyI:C or medium alone were used as positive and negative controls, respectively. The positive control was used for comparison of LAB strains treated groups. The mean differences among the different superscript letters (a, b, ab) were significant at 0.05 level. LABs decreased the expression of PolyI:C induced inflammatory cytokines in HCT116 cells.

cells with PolyI:C increased the expressions of IFN-α and IFN-β and these expressions were further increased by LABs post-stimulation (**Figure 7**).

## LABs Modulated the Expressions of TLR Negative Regulators in HCT116 Cells

To gain more insight into the mechanisms of LABs on modulation of innate antiviral immune responses of TLR signaling, we examined the expression of genes that negatively regulate TLR signaling in HCT116 that were treated with LABs and PolyI:C. The expression of A20, Tollip, SIGIRR, and IRAKM was analyzed by qRT-PCR. Stimulation of cells with PolyI:C increased the mRNA levels of A20, while it didn't up-regulate the levels of Tollip, SIGIRR, and IRAKM (**Figure 8**). The PolyI:C mediated expressions levels were able to modulate by LAB strains in a time dependent manner. At 3 h, *L. plantarum* and *L. sakei* treated HCT116 cells showed increase in level of A20, whereas the level of Tollip was only increased by *L. sakei,* and this increase was significantly higher ($p < 0.05$) than that induced by PolyI:C and other strains. But, all LABs weren't significantly increased

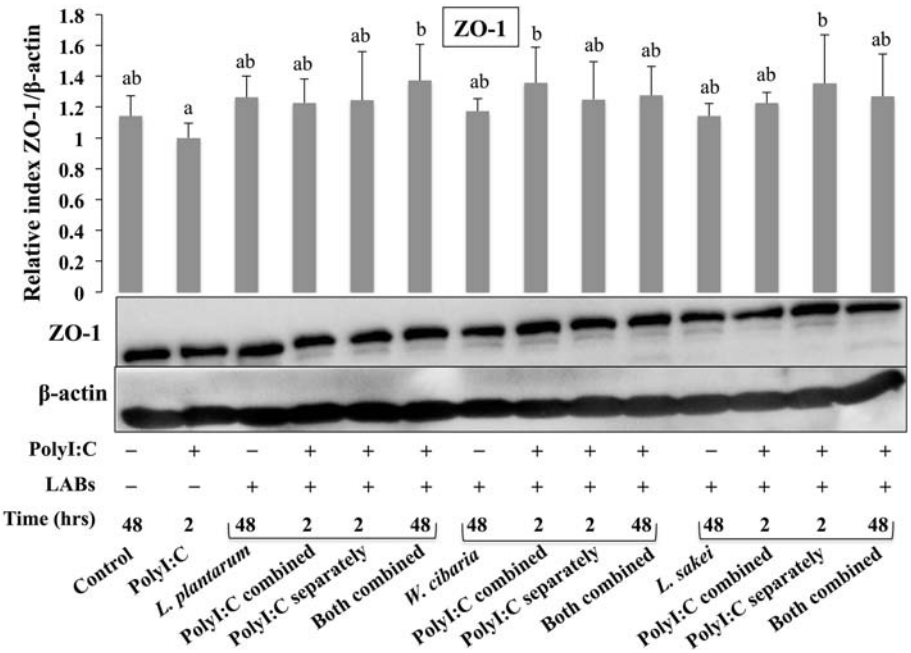


**FIGURE 3 |** LAB strains modulate TJ protein (ZO-1) in HCT116 cells. Cells were stimulated as follows: control, PolyI:C alone, LABs alone (48 h), LABs+PolyI:C (2 h, Poly:C combined treatment), LABs+PolyI:C (2 h, PolyI:C post-treatment separately), and or LABs+PolyI:C (48 h both combined). The level of tight-junction protein (ZO-1) was analyzed by western blot. The loading control beta-actin was reused for illustrative purposes. The bar graphs represent the results of three independent experiments. The mean differences among the different superscript letters (a, b, ab) were significant at 0.05 level. LABs stimulation modulated ZO-1 level in response PolyI:C.

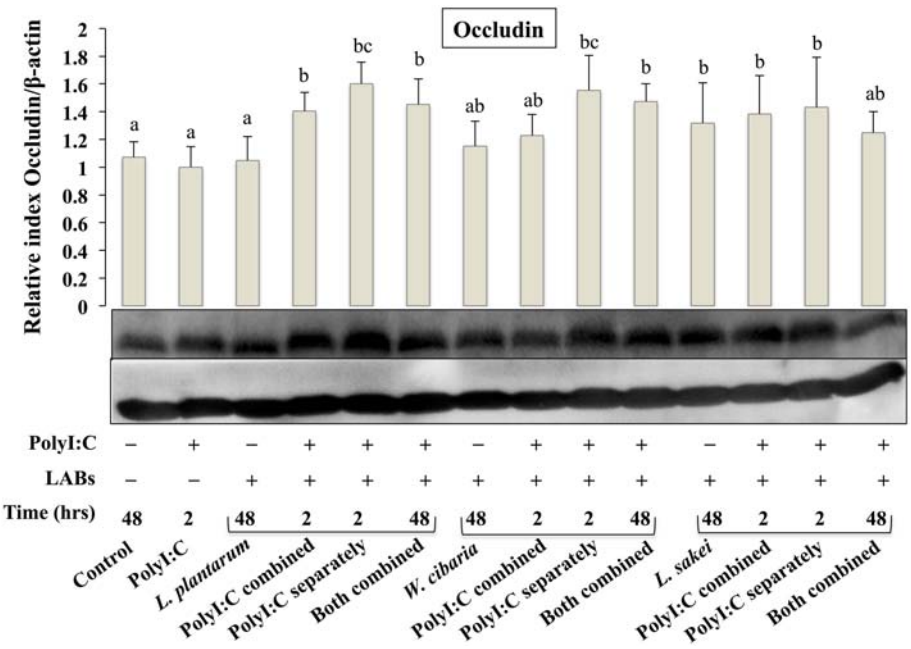


**FIGURE 4 |** LAB strains modulate TJ protein (Occludin) in HCT116 cells. Cells were stimulated as follows: control, PolyI:C alone, LABs alone (48 h), LABs+PolyI:C (2 h, Poly:C combined treatment), LABs+PolyI:C (2 h, PolyI:C post-treatment separately), and or LABs+PolyI:C (48 h both combined). The level of TJ protein (ZO-1) was analyzed by western blot. The loading control beta-actin was reused for illustrative purposes. The bar graphs represent the results of three independent experiments. The mean differences among the different superscript letters (a, b, ab, c, bc) were significant at 0.05 level. LABs alone or co-treated with PolyI:C increased the level of occludin in HCT116 cells.

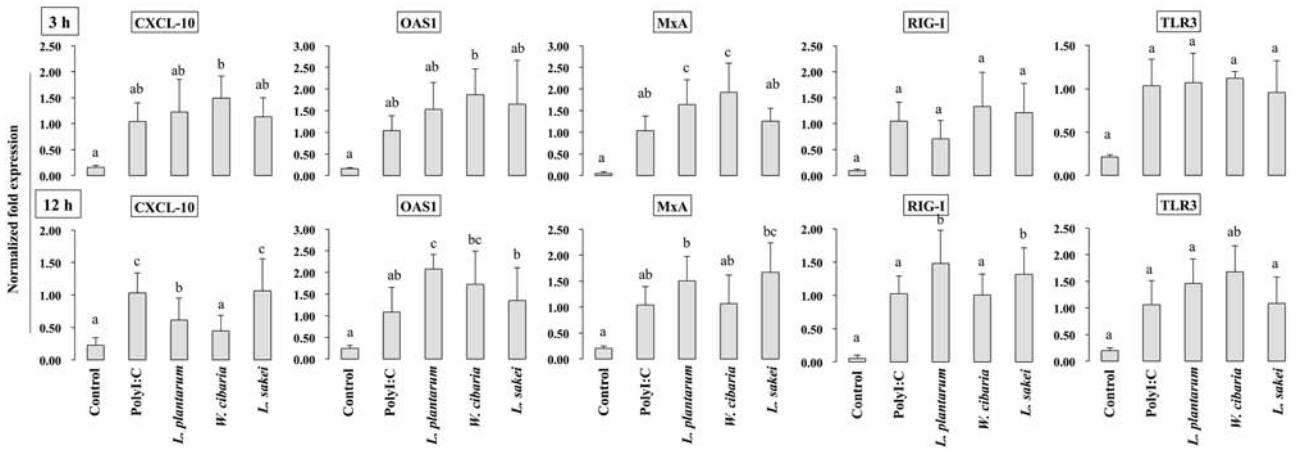


**FIGURE 5 |** LABs modulate expressions of antiviral proteins and receptors in HCT116 cells. After HCT116 cells stimulated with LABs and PolyI:C for 3 and 12 h, the mRNA level of CXCL-10, OAS1, MxA, RIG-I, and TLR3 was evaluated by RT-PCR. Cells treated with either PolyI:C or medium alone were used as positive and negative controls, respectively. The positive control was used for comparison of LAB strains treated groups. The mean differences among the different superscript letters (a, b, ab, c, bc) were significant at 0.05 level. LABs stimulation decreased the level of CXCL-10, while increased level of other anti-viral proteins at 12 h in HCT116 cells, post-treated with PolyI:C.

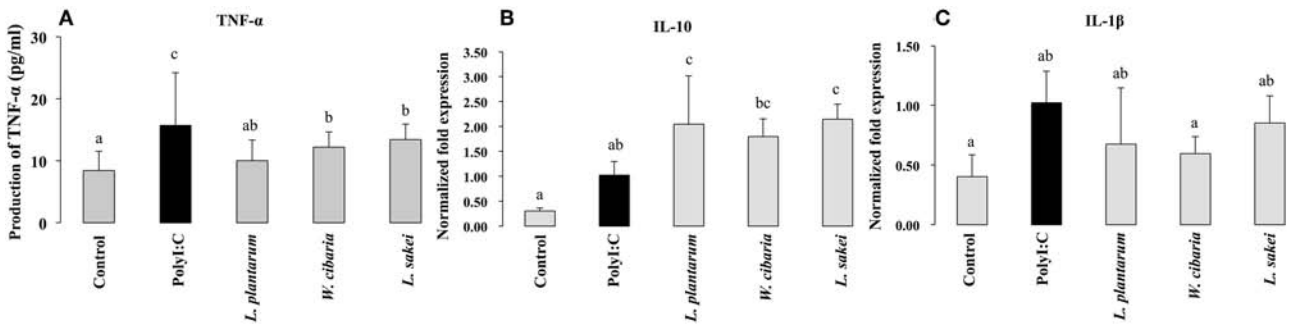


**FIGURE 6 |** Effect of LABs on modulation of inflammatory and anti-inflammatory cytokines expression in THP-1 cells cultured with HCT116 cells. After HCT116 cells were stimulated with LABs, and followed by THP-1 cells with PolyI:C for 12 h, the production of TNF-α in the basolateral medium and mRNA level of IL-10 and IL-1β in THP-1 cells was analyzed by ELISA and RT-PCR. Cells treated with either PolyI:C or medium alone were used as positive and negative controls respectively The positive control was used for comparison of LAB strains treated groups. The mean differences among the different superscript letters (a, b, ab, c, bc) were significant at 0.05 level. LABs stimulation decreased the level of TNF-α, IL-1β, while increased level of IL-10 in THP-1 cells, post-treated with PolyI:C.

the level of SIGIRR as compared to PolyI:C. In addition, there was no significant alternation observed in the level of IRAKM. In contrary, *L. plantarum* and *W. cibaria* reduced the level of A20 on 12 h, whereas all LABs showed significantly ($p < 0.05$) increase in levels of Tollip and SIGIRR as compared to PolyI:C (**Figure 8**). Furthermore, IRAKM mRNA expression was significantly increased by *L. plantarum* and *L. sakei*

## LABs Modulated the Phosphorylations of IRF3 and IκB-α in HCT116 Cells

Activation of TLR3 by PolyI:C recruits several intracellular signaling molecules (TRAF3, IRF3, and NF-κB) to induce expressions of type 1 IFNs and inflammatory cytokines. Therefore, we examined whether LABs were able to modulate phosphorylation of IRF3 and IκB-α in HCT116 cells stimulated with PolyI:C. The level of p-IRF3 was increased when cells were treated with LABs in the presence of PolyI:C for 2 or 48 h (**Figure 9**). As compared to PolyI:C, LABs were able to increase the level of p-IRF3 in HCT116 cells post-treated with PolyI:C for 2 h. In contrary, PolyI:C alone significantly increased the phosphorylation of IκB-α in HCT116 cells, but cells treated with LABs alone or co-treated with LABs and PolyI:C for 48 h significantly decreased the level of IκB-α (**Figure 10**). In addition, stimulation of cells with LABs in the presence of PolyI:C for 2 h or post-stimulation with PolyI:C for 2 h diminished phosphorylation of IκB-α in HCT 116 cells as compared with PolyI:C alone. These results suggest LABs exhibits innate antiviral immune response by modulating the IRF3 and NF-κB pathways.

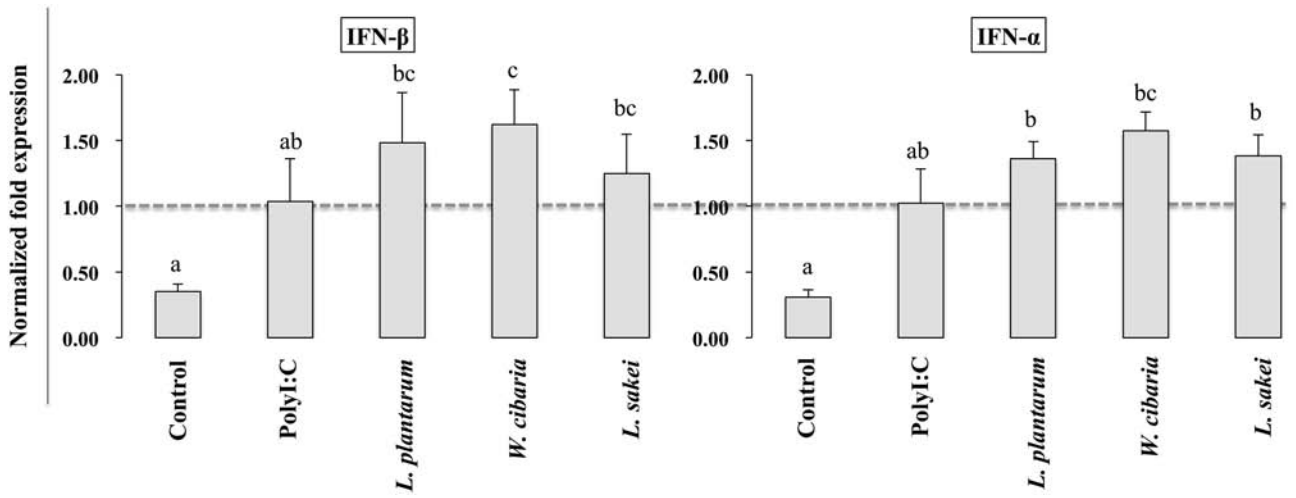


**FIGURE 7 |** Effect of LABs on up-regulation of antiviral IFNs in THP-1 cells cultured with HCT116 cells. The expression of IFN-α and IFN-β were analyzed by RT-PCR. Cells treated with either PolyI:C or medium alone were used as positive and negative controls, respectively. The positive control was used for comparison of LAB strains treated groups The mean differences among the different superscript letters (a, b, ab, c, bc) were significant at 0.05 level. LABs stimulation increased the level of IL-1β and IFN-α in response to PolyI:C THP-1 cells.

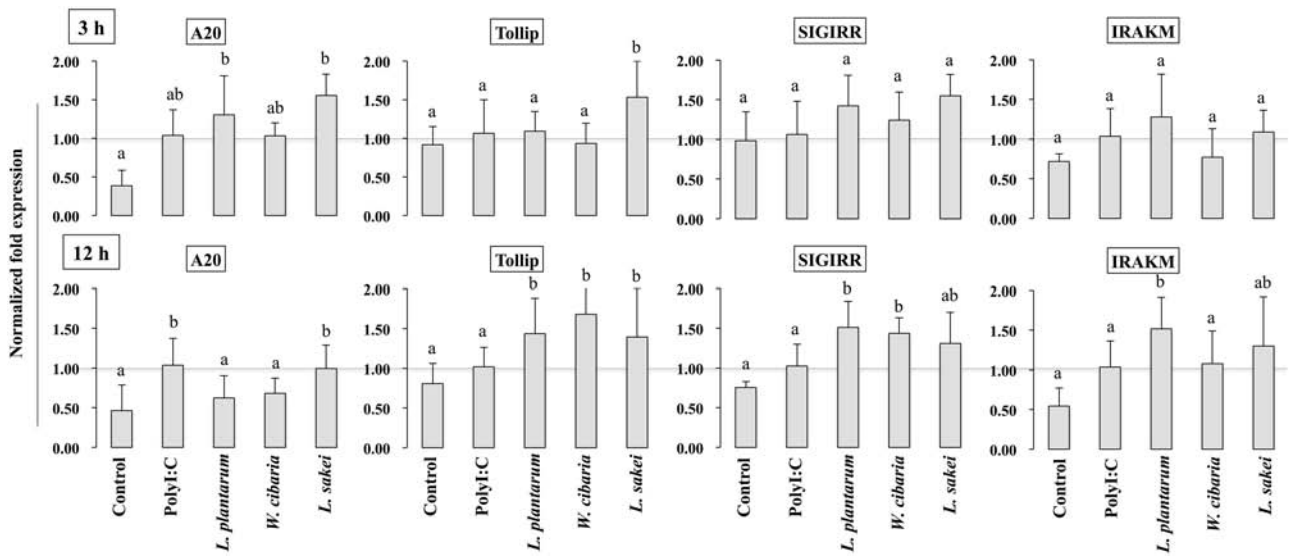


**FIGURE 8 |** Analysis of TLRs negative regulators expression in HCT116 cells. After HCT116 cells treated LAB strains and PolyI:C for 3 and 12 h. The expression of A20, Tollip, SIGIRR, and IRAK-M were evaluated by RT-PCR. Cells treated with either PolyI:C or medium alone were used as positive and negative controls, respectively. The positive control was used for comparison of LAB strains treated groups The mean differences among the different superscript letters (a, b, ab) were significant at 0.05 level. LABs were able to modulate expression of negative regulators of TLR signaling in HCT116 cells, stimulated with PolyI:C.

## DISCUSSION

Intestinal epithelium contains IECs, which play important roles in maintenance of the intestinal immune system. Upon meeting pathogens, IECs capable to induce mucosal immune responses by expressing soluble factors such as cytokines/chemokines to recruit and activate immune cells including leukocytes and neutrophil granulocytes to the infected area, and by producing type I IFNs, antiviral proteins, and effector molecules to limit pathogens replications (25, 26). The expressions of TLRs in IECs play an important role on induction of mucosal immune responses in the intestine by sensing antigens derived from pathogens during their infection. Several studies have reported TLRs expressions and their vital roles on induction of host defense system against infectious diseases (4, 27). Activation of TLR3 by dsRNA induces production of several antiviral proteins such as IFN regulatory factors, type I IFNs, and cytokines/chemokines to establish antiviral state against viruses (28–30). Among the IFNs, IFN-β is a key cytokine that positively contributes to host innate immunity and defense against several

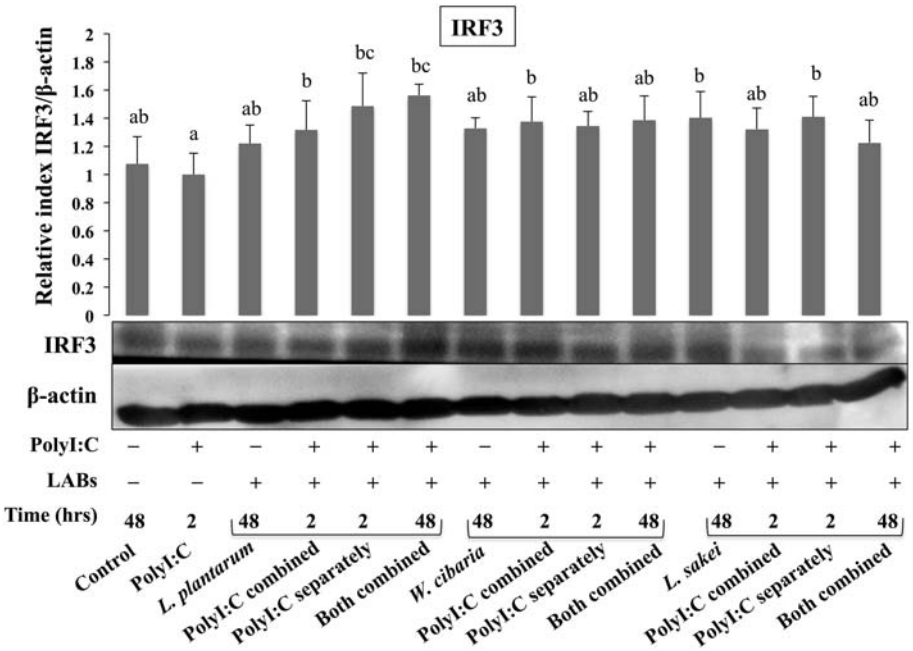


**FIGURE 9 |** The ability of LABs to increase PolyI;C induced regulatory factor *in vitro*. HCT116 cells were stimulated as follows: control, PolyI:C alone, LABs alone (48 h), PolyI:C alone (2 h), LABs+PolyI:C (2 h, Poly:C combined treatment), LABs+PolyI:C (2 h, PolyI:C post-treatment separately), and or LABs+PolyI:C (48 h both combined). The phosphorylation of interferon regulatory factor 3 (IRF3) was analyzed by western blot. The loading control beta-actin was reused for illustrative purposes. The bar graphs are representative of three independent experiments. The mean differences among the different superscript letters (a, b, ab, bc) were significant at 0.05 level. LABs alone or co-treated with PolyI:C increased the phosphorylation of IRF3 in HCT116 cells.

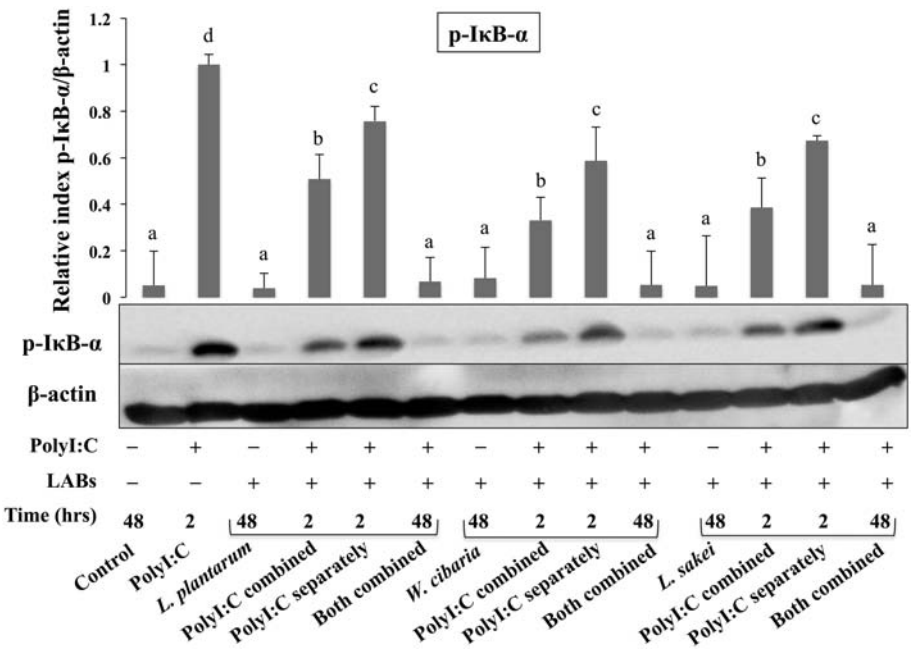


**FIGURE 10 |** LABs inhibited PolyI;C induced activation of the NF-κB pathway *in vitro*. HCT116 cells were stimulated as follows: control, PolyI:C alone, LABs alone (48 h), PolyI:C alone (2 h), LABs+PolyI:C (2 h, Poly:C combined treatment), LABs+PolyI:C (2 h, PolyI:C post-treatment separately), and or LABs+PolyI:C (48 h both combined). The phosphorylation of IκB-α was analyzed by western blot. The loading control beta-actin was reused for illustrative purposes. The bar graphs are representative of three independent experiments. The mean differences among the different superscript letters (a, b, c, d) were significant at 0.05 level. LABs alone or co-treated with PolyI:C decreased the phosphorylation of IκB-α in HCT116 cells.

viruses including rotavirus (31). In addition, the up-regulation of IFN-β induces transcription of other viral response genes involved in viral protection. IFN-β deficient mice have been shown to be more susceptible to influenza virus infection (32). Broquet et al. (33) reported that IFN-β showed protection against RVs by reducing their replication in IECs. Therefore, IFN-β is considered a potent antiviral chemokine, and thus, is used to screen or study the antiviral effects of immunobiotic strains and their related compounds. In this regard, we have evaluated whether LAB strains induce the expression of IFN-β in HCT116 cells. We found that LABs stimulation increased the expression of IFN-β in response to PolyI:C. Our findings are in good agreement with the results of others studies obtained for *Bifidobacterium infantis* MCC12 and *B. breve* MCC1274 (3), *Lactobacillus casei* MEP221106 (16), *Lactobacillus delbrueckii* TUA4408L (29), and *L. casei* Zhang (34). Probiotic *L. acidophilus* NCFM was able to increase the expression of IFN-β in bone marrow derived dendritic cells *in vitro* (35). Treatment of porcine IECs with *L. rhamnosus* CRL1505 induced expression of higher level of IFN-β, in response to PolyI:C (17). Moreover, probiotic *B. longum* SPM1206 and *L. ruminis* SPM0211 induced IFN-β expression in mice and Caco2 cells infected with RV (36).

In addition to the production of anti-viral cytokines, immunobiotics have been shown to improve protection against inflammatory condition or viral infection by regulating the expression of pro-inflammatory cytokines/chemokines (3, 16). We also found that LABs were able to reduce expression of pro-inflammatory cytokines (IL-6, IL-8, MCP-1, and IL-1β) in HCCT116 cells stimulated with PolyI:C. Production of these cytokines has also been reported to play crucial roles in host innate response against virus infections. The expression of pro-inflammatory cytokines (IL-6 and IL-8) was up-regulated in epithelial cells infected with RVs (37, 38), and infection of HT-29 cells with RVs increased the IL-8 level, which is dependent on protein kinase activity and NF-κB activation (37, 38). Clemente et al. (39) found that the infection of epithelial cells with RVs induced production of IL-6 and IL-8 via activation of the MAPK pathway. Porcine IECs cells treated with *L. acidophilus* and *L. rhamnosus* GG reduced the level of IL-6 and mucin, and increased TLR2 level in response to RV (22).

During the host infected with virus, the activation of TLR signaling increases expression of type I IFNs, which induces transcription of several IFN-stimulated genes (ISGs) that encode proteins with potent antiviral effector functions to block viral replication (40). MxA and RNase-L proteins are promising IFN-induced proteins with broad anti-viral activity against several different DNA and RNA viruses (13, 41). Myxovirus resistance protein (MxA) mainly targets viral nucleoproteins for its attachment, and reduces replication and intracellular proliferation of viruses. RNase L (2′-5′ oligoadenylate dependent endoribonuclease) is believed to contribute role in the anti-viral activity of IFNs and the stability of IFN-induced genes such as ISG (13). 2-5A oligoadenylate synthetase (OSA), especially OSA1, activates the latent form of RNase L, and thus, causes the cleavage of viral RNA and inhibits viral replication and proliferation. Furthermore, viral protein (VP3) derived from RVs has been shown to inhibit RNase L activity by cleaving 2-5A (42). Previous studies reported that immunobiotics have the ability to improve expression of these IFN stimulated antiviral proteins (MxA and OAS) along with higher level of IFN-β (3, 43). We also found that cells stimulated with LABs increased MxA and OAS1 levels in response to PolyI:C. Similarly, *L. delbrueckii* TUA4408L and *B. infantis* MCC12 increased the expression of these antiviral proteins in bovine and porcine IECs (29, 43). Viruses have evolved mechanisms to eradicate host immune system by interacting with PRR receptors that mediate signaling cascades to develop antiviral immunity (41). RIG-1 and TLR3 are RRR receptors that can initiate signaling cascades for IFN-β up-regulation (44) The pre-exposure of cells to LABs increased the expressions of RIG-1 and TLR3, which confirmed the antiviral effects of LAB strains *in vitro* (3).

The intestinal barrier is a tight structure that provides protection against harmful environments, but it has been reported to be dysfunctional that associated with paracellular permeability in several diseases. Tight-Junction (TJ) proteins are the responsible components that connect IECs with neighbor cells and control paracellular gut permeability (45). Administration of PolyI:C has been shown to induce severe mucosal damage in the mouse small intestine of mice, which is probably due to the activation of TLR3 signaling by PolyI:C (46). Our study showed that the presence of LAB strains increased the level of TJ proteins (ZO-1 and occluding), indicating that LABs have the ability to maintain gut-barrier integrity and reduce gut dysfunction. Intestinal epithelium acts as a mucosal barrier that mediates signaling to underlying immune cells by sensing antigens and intestinal changes (47). Cross-talk between these two cells is an important feature that helps maintain the mucosal barrier and provides protection against infectious diseases and harmful environments. In a Transwell experiment, basolateral treatment of RAW264.7 cells with lipopolysaccharide increased the productions of TNF-α and IL-8 in Caco2 cells that were taken in apical side (48). Another *in vitro* study, it was reported that in response to commensals, IECs were able to stimulate underlying dendritic cells (DCs) by secreting several inflammatory proteins (49). TNF-α is a pleiotropic pro-inflammatory cytokine, which has been shown to play critical roles in the pathogeneses of several diseases, including viral infections. In response to PolyI:C, bone marrow derived macrophages, Raw264.7, and THP-1 cells increased TNF-α production *in vitro* (50, 51). IL-10 is a prime anti-inflammatory cytokine that plays key roles in the maintenance of gut hemostasis and innate immunity and in the pathogenesis of IBD (52). Through co-culture study, we found that LAB strains improved the cross-talk between IECs and THP-1 cells, which resulted in decreased levels of pro-inflammatory cytokines (TNF-α, IL-1β) and increased levels of anti-inflammatory cytokine (IL-10) and INFs. These results were consistent with those of other study (53), in which HT-29 cells stimulated with three probiotics strains (*L. helveticus* R0052, *B. longum* subsp. *infantis* R0033, *B. bifidum* R0071) decreased the level of TNF-α and IL-8 in response to PolyI:C.

TLR activation is an important process that could be involved in the development of infectious diseases. Once it activated, several intracellular proteins actively participate in control

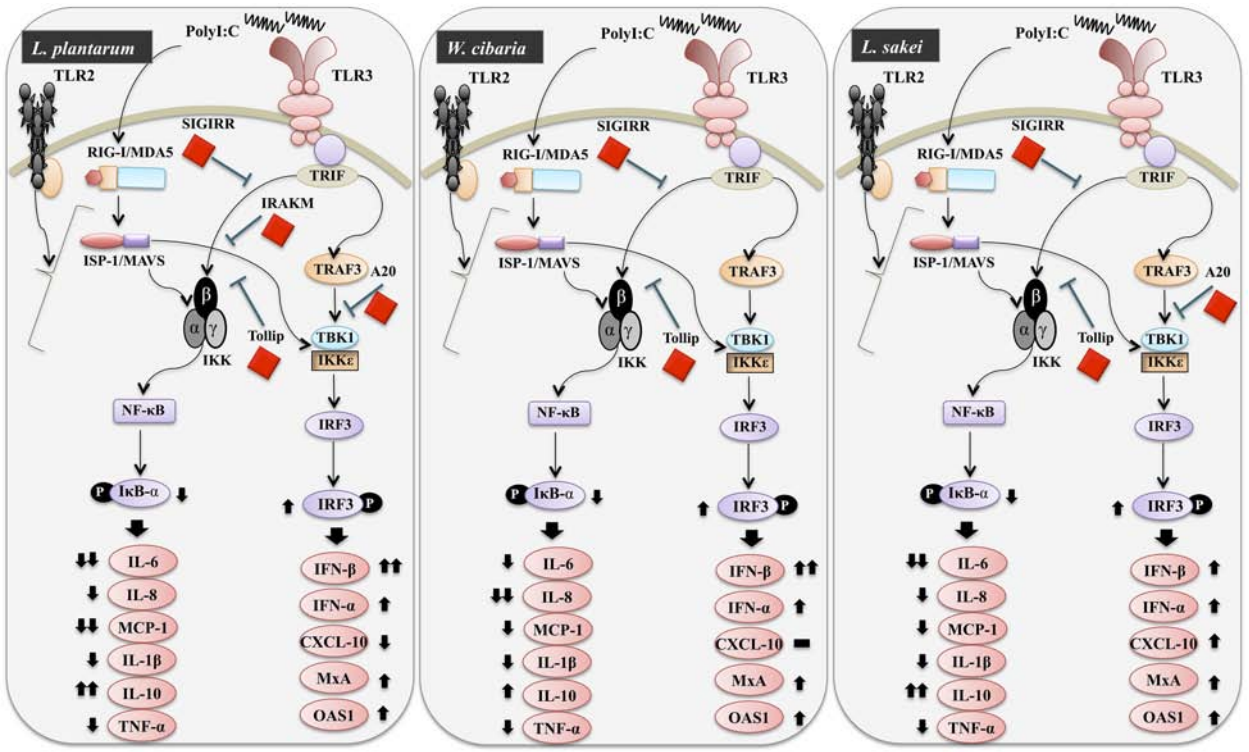


**FIGURE 11 |** Schematic model for the mechanisms involved in the antiviral activity of *L. plantarum*, *W. cibaria*, and *L. sakei in vitro*.

of hyper-activation of TLR signaling pathways by negatively regulating the transcription of TLR genes. Tollip, SIGIRR, A20, and IRAK-M are the potent negative regulators that have been shown to attenuate over activation of TLR signaling in IECs (54). High levels of Tollip may prevent inflammatory cytokine production by commensal bacteria in the gut (55), and the knockdown of Tollip increased the expression of inflammatory cytokines and activation of NF-κB in Caco-2 cells (56). SIGIRR is a transmembrane receptor that may be expressed by IECs and immature DCs derived from gut. Polentarutti et al. (57) reported that SIGIRR overexpression could inhibit IL-1 and IL-18 mediated NF-κB activation in DCs, and thus, it playing a role in the regulation of intestinal inflammatory response. In another study, the expression of SIGIRR in IECs attenuated exaggerated inflammatory response and promoted commensal bacteria colonization against intestinal pathogens, indicating a close relationship exists between commensal bacteria, and IECs (4). A20 is a zinc-finger protein and its knockdown in mouse macrophage increased the inflammatory cytokine expressions in response to TLR2 and TLR3 ligands (4). In addition, the presence of A20 has been reported to suppress TLR3-mediated activation of IRF3 in transfected cells (58). In view of these observations, we evaluated the expressions of TLR negative regulators in HCT116 cells stimulated with PolyI:C. Exposure of cells to LABs were able to modulate expression of negative regulators of TLR signaling in HCT116 cells, which indicate LAB mediated attenuation of inflammatory response *in vitro*. Similar results were observed in other studies for *B. infantis* MCC12 and *B. breve* MCC1274 (3), *L. delbrueckii* OLL1073R-1 (18), and *L. delbrueckii* TUA4408L (29). During viral infections, PRRs of host cells activate IFN regulatory factors (IRFs) that regulate the production of IFN-β (44). In particular, NSP-1 (a non-structural protein of RVs) has been reported to have high affinity for IRF3, which results in proteasome-dependent degradation of transcription factors (59). In the present study, as we expected, challenging of HCT116 cells with LABs increased the phosphorylation of IRF3 in response to TLR3 agonist. Furthermore, NF-κB pathway is an important TLR signaling pathway and its activation increases the production of inflammatory cytokines *in vitro* and *in vivo* (60). Therefore, we also analyzed activation of the NF-κB pathway in HCT116 cells. We found that LAB strains down-regulated p-IκB-α, indicating that LABs were able to attenuate PolyI:C induced viral and inflammatory response by modulating IRF3 and NF-κB pathways (**Figure 11**). Similar results were obtained by Kim et al. (30), who reported that lipoteichoic acid of *L. plantarum* attenuated PolyI:C mediated NF-κB activation in porcine IPEC-J2 cells.

In conclusion, our study demonstrated that *in vitro* exposure of different LAB strains beneficially modulates innate antiviral immune responses induced by PolyI:C in HCT116 cells. LABs significantly up-regulated the mRNA level of IFN-β and down-regulated IL-6, IL-8, MCP-1, and IL-1β levels by modulating the expressions of negative regulators of TLRs and the activations of IFR3 and NF-κB pathways. Our results also show that cells co-treated with LABs and PolyI:C improved the gut barrier integrity by maintaining of TJ proteins *in vitro*, suggesting LABs might

protect IECs from harmful environments *in vivo*. Furthermore, our co-culture study showed that LABs indirectly modulated TLR3 triggered innate antiviral response in monocyte-derived macrophages. Overall, LABs protected cells from PolyI:C *in vitro,* and an additional study will be performed to determine whether these findings are duplicated *in vivo*.

## DATA AVAILABILITY

All datasets generated for this study are included in the manuscript and/or the **Supplementary Files**.

## AUTHOR CONTRIBUTIONS

PK and HK designed the study and assisted with the experiments and interpretation of results. PK performed the assays and wrote the manuscript. All authors read and approved the final manuscript.

## FUNDING

This work was supported by a grants from the National Research Foundation of Korea (NRF) funded by the Korean Government (#NRF-2019R1A2B5B01070365), and by the Korean Research Fellowship (KRF) program of the NRF (#NRF-2016H1D3A1937971).

## SUPPLEMENTARY MATERIAL

The Supplementary Material for this article can be found online at: https://www.frontiersin.org/articles/10.3389/fimmu.2019.01536/full#supplementary-material

## REFERENCES

1. Peterson LW, Artis D. Intestinal epithelial cells: regulators of barrier function and immune homeostasis. *Nat Rev Immunol*. (2014) 14:141–53. doi: 10.1038/nri3608
2. Goto Y, Lamichhane A, Kamioka M, Sato S, Honda K, Kunisawa J, et al. IL-10 producing $CD4^+$ T cells negatively regulate fucosylation of epithelial cells in the gut. *Sci Rep*. (2015) 5:1–11. doi: 10.1038/srep15918
3. Ishizuka T, Kanmani P, Kobayashi K, Miyazaki A, Soma, J, Suda Y, et al. Immunobiotic Bifidobacteria strains protect against rotavirus infection in porcine intestinal epitheliocytes via regulation of antiviral pattern recognition receptor signaling. *PLoS ONE*. (2015) 11:e0152416. doi: 10.1371/journal.pone.0152416
4. Liew FY, Xu D, Brint EK, O'Neill LAJ. Negative regulation of toll-like receptor-mediated immune responses. *Nat Rev Immunol*. (2005) 5:446–58. doi: 10.1038/nri1630
5. Alexopoulou L, Holt AC, Medzhitov R, Flavell RA. Recognition of double-stranded RNA and activation of NF-κB by Toll-like receptor 3. *Nature*. (2001) 413:732–38. doi: 10.1038/35099560
6. O'Neill LA, Bowie AG. The family of five: TIR-domain-containing adaptors in Toll-like receptor signaling. *Nat Rev Immunol*. (2007) 7:353–64. doi: 10.1038/nri2079
7. Matsumoto M, Seya T. TLR3: interferon induction by double- stranded RNA including poly(I:C). *Adv Drug Deliv Rev*. (2008) 60:805 12. doi: 10.1016/j.addr.2007.11.005
8. Arnold MM, Sen A, Greenberg HB, Patton JH. The battle between rotavirus and its host for control of the interferon signaling pathway. *PLoS Pathog*. (2013) 9:e1003064. doi: 10.1371/journal.ppat.1003064
9. Ge Y, Mansell A, Ussher JE. Rotavirus NPS4 triggers secretion of proinflammatory cytokines from macrophage via toll-like receptors 2. *J Virol*. (2013) 87:11160–67. doi: 10.1128/JVI.03099-12
10. MacPherson C, Audy J, Mathieu O, Tompkins TA. Multistrain probiotic modulation of intestinal epithelial cells' immune response to a double-stranded RNA ligand, Poly(I·C). *Appl Envir Microbiol*. (2014) 80:1692. doi: 10.1128/AEM.03411-13
11. Deonarain R, Alcami A, Alexiou M, Dallman MJ, Gewert DR, Porter CG. Impaired antiviral response and alpha/beta interferon induction in mice lacking beta interferon. *J Virol*. (2000) 74:3404–09. doi: 10.1128/JVI.74.7.3404-3409.2000
12. Mitchell PS, Patzina C, Emerman M, Haller O, Malik, HS, Kochs G. Evolution-guided identification of antiviral specificity determinants in the broadly acting interferon-induced innate immunity factor MxA. *Cell Host Microbe*. (2012) 12:598–04. doi: 10.1016/j.chom.2012.09.005
13. Liang SL, Quirk D, Zhou A. RNase L: its biological roles and regulation. *IUBMB Life*. (2006) 58:508–14. doi: 10.1080/15216540600838232
14. Siciliano RA, Mazzeo, MF. Molecular mechanisms of probiotic action: a proteomic perspective. *Cur Opin Microbiol*. (2012) 15:390–96. doi: 10.1016/j.mib.2012.03.006
15. Kaila M, Isolauri E, Saxelin M, Arvilommi H, Vesikari, T. Viable versus inactivated *Lactobacillus strain* GG in acute rotavirus diarrhoea. *Arc Dis Child*. (1995) 72:51–3. doi: 10.1136/adc.72.1.51
16. Hosoya S, Villena J, Shimazu T, Tohno M, Fujie H, Chiba E, et al. Immunobiotic lactic acid bacteria beneficially regulate immune response triggered by poly(I:C) in porcine intestinal epithelial cells. *Vet Res*. (2011) 42:111. doi: 10.1186/1297-9716-42-111
17. Villena J, Chiba E, Vizoso-Pinto MG, Tomosada Y, Takahashi T, Ishizuka T, et al. Immunobiotic *Lactobacillus rhamnosus* strains differentially modulate antiviral immune response in porcine intestinal epithelial and antigen presenting cells. *BMC Microbiol*. (2014) 14:126. doi: 10.1186/1471-2180-14-126
18. Kanmani P, Albarracin L, Kobayashi H, Iida H, Komatsu R, Humayun Kober AKM, et al. Exopolysaccharides from *Lactobacillus delbrueckii* OLL1073R-1 modulate innate antiviral immune response in porcine intestinal epithelial cells. *Mol Immunol*. (2018) 93:253–65. doi: 10.1016/j.molimm.2017.07.009
19. Wachi S, Kanmani P, Tomosada Y, Kobayashi H, Yuri T, Egusa S, et al. *Lactobacillus delbrueckii* TUA4408L and its extracellular polysaccharides attenuate enterotoxigenic Escherichia coli-induced inflammatory response in porcine intestinal epitheliocytes via Toll-like receptor-2 and 4. *Mol Nutr Food Res*. (2014) 58:2080–93. doi: 10.1002/mnfr.201400218
20. Murofushi Y, Villena J, Morie K, Kanmani P, Tohno M, Shimazu T, et al. The toll-like receptor family protein RP105/MD1 complex is involved in the immunoregulatory effect of exopolysaccharides from *Lactobacillus plantarum* N14. *Molecul Immunol*. (2014) 64:63–75. doi: 10.1016/j.molimm.2014.10.027
21. Kumar A, Zhang J, Yu FSX. Toll-like receptor 3 agonist poly(I:C)-induced antiviral response in human corneal epithelial cells. *Immunology*. (2005) 117:11–21. doi: 10.1111/j.1365-2567.2005.02258.x
22. Liu F, Li G, Wen K, Bui T, Cao D, Zhang Y, et al. Porcine small intestinal epithelial cell line (IPEC-J2) of rotavirus infection as a new model for the study of innate immune responses to rotaviruses and probiotics. *Viral Immunol*. (2010) 23:135–49. doi: 10.1089/vim.2009.0088
23. Hosoya S, Villena J, Chiba E, Shimazu T, Suda Y, Aso H, et al. Advanced application of porcine intestinal epithelial cells for the selection of immunobiotics modulating toll-like receptor 3-mediated inflammation. *J Microbiol Immunol Infect*. (2013) 46:474–78. doi: 10.1016/j.jmii.2012.04.005

24. Kanmani P, Kim, JH. Protective effects of lactic acid bacteria against TLR4 induced inflammatory response in hepatoma HepG2 cells through modulation of toll-like receptor negative regulators of mitogen-activated protein kinase and NF-kB signaling. *Front Immunol*. (2018) 9:1537. doi: 10.3389/fimmu.2018.01537
25. Miller MD, Krangel MS. Biology and biochemistry of the chemokines: a family of chemotactic and inflammatory cytokines. *Crit Rev Immunol*. (1992) 12:17–46.
26. Fraser-Pitt DJ, Cameron P, McNeilly TN, Boyd A, Manson ED, Smith DG. Phosphorylation of the epidermal growth factor receptor (EGFR) is essential for interleukin-8 release from intestinal epithelial cells in response to challenge with *Escherichia coli* O157: H7 flagellin. *Microbiology*. (2011) 157:2339–47. doi: 10.1099/mic.0.047670-0
27. Lee JD, Mo JH, Shen C, Rucker AN, Raz E. Toll-like receptor signaling in intestinal epithelial cells contributes to colonic homoeostasis. *Curr Opin Gastroenterol*. (2007) 23:27–31. doi: 10.1097/MOG.0b013e3280118272
28. Villena J, Vizoso-Pinto MG, Kitazawa H. Intestinal innate antiviral immunity and immunobiotics: beneficial effects against rotavirus infection. *Front Immunol*. (2016) 7:563. doi: 10.3389/fimmu.2016.00563
29. Kanmani P, Albarracin L, Kobayashi H, Hebert EM, Saavedra L, Komatsu R, et al. Genomic characterization of *Lactobacillus delbrueckii* TUA4408L and evaluation of the antiviral activities of its extracellular polysaccharides in porcine intestinal epithelial cells. *Front Immunol*. (2018) 9:2178. doi: 10.3389/fimmu.2018.02178
30. Kim KW, Kang SS, Woo SJ, Park OJ, Ahn KB, Song KD, et al. Lipoteichoic ccid of probiotic *Lactobacillus plantarum* attenuates Poly I:C-induced IL-8 production in porcine intestinal epithelial cells. *Front Microbiol*. (2017) 8:1827. doi: 10.3389/fmicb.2017.01827
31. Taniguchi T, Takaoka A. The interferon-α/β system in antiviral responses: a multimodal machinery of gene regulation by the IRF family of transcription factors. *Curr Opin Immunol*. (2002) 14:111–16. doi: 10.1016/S0952-7915(01)00305-3
32. Koerner I, Kochs G, Kalinke U, Weiss S, Staeheli, P. Protective role of beta interferon in host defense against influenza A virus. *J Virol*. (2007) 81:2025–30. doi: 10.1128/JVI.01718-06
33. Broquet AH, Hirata Y, McAllister CS, Kagnoff MF. RIG-I/MDA5/ MAVS are required to signal a protective IFN response in rotavirus-infected intestinal epithelium. *J Immunol*. (2011) 186:1618–26. doi: 10.4049/jimmunol.1002862
34. Wang Y, Xie J, Wang N, Li Y, Sun X, Zhang Y, et al. *Lactobacillus casei* Zhang modulate cytokine and Toll-like receptor expression and beneficially regulate poly I:C-induced immune responses in RAW264.7 macrophages. *Microbiol Immunol*. (2013) 57:54–62. doi: 10.1111/j.1348-0421.516.x
35. Weiss G, Rasmussen S, Zeuthen LH, Nielsen BH, Jarmer H, Jespersen L, et al. *Lactobacillus acidophilus* induces virus immune defence genes in murine dendritic cells by a Toll-like receptor-2-dependent mechanism. *Immunology*. (2010) 131:268–81. doi: 10.1111/j.1365-2567.2010.03301.x
36. Kang JY, Lee DK, Ha NJ, Shin HS. Antiviral effects of *Lactobacillus ruminis* SPM0211 and *Bifidobacterium longum* SPM1205 and SPM1206 on rotavirus-infected Caco-2 cells and a neonatal mouse model. *J Microbiol*. (2015) 53:796–03. doi: 10.1007/s12275-015-5302-2
37. Sheth R, Anderson J, Sato, T, Oh B, Hempson SJ, Rollo E, et al. Rotavirus stimulates IL-8 secretion from cultured epithelial cells. *Virology*. (1996) 221:251–9. doi: 10.1006/viro.1996.0374
38. Rollo EE, Kumar KP, Reich NC, Cohen J, Angel J, Greenberg HB, et al. 1999. The epithelial cell response to rotavirus infection. *J Immunol*. (1999) 163:4442–52.
39. Clemente MG, Patton JT, Anders RA, Yolken RH, Schwarz KB. Rotavirus infects human biliary epithelial cells and stimulates secretion of cytokines IL-6 and IL-8 via MAPK pathway. *BioMed Res Int*. (2015) 2015:697238. doi: 10.1155/2015/697238
40. Schoggins JW, Rice CM. Rice interferon-stimulated genes and their antiviral effector functions. *Curr Opin Virol*. (2011) 1:519–25. doi: 10.1016/j.coviro.2011.10.008
41. Mitchell PS, Emerman M, Malik HS. An evolutionary perspective on the broad antiviral specificity of MxA. *Cur Opin Microbiol*. (2013) 16:493–99. doi: 10.1016/j.mib.2013.04.005
42. Zhang R, Jha BK, Ogden KM, Dong B, Zhao L, Elliott R, et al. Homologous 2′,5′-phosphodiesterases from disparate RNA viruses antagonize antiviral innate immunity. *Proc Natl Acad Sci USA*. (2013) 110:13114–19. doi: 10.1073/pnas.1306917110
43. Kobayasi H, Kanmani P, Ishizuka T, Miyazaki A, Soma J, Albarracin L, et al. Development of an *in vitro* immunobiotic evaluation system against rotavirus infection in bovine intestinal epitheliocytes. *Beneficial Microb*. (2017) 8:309–21. doi: 10.3920/BM2016.0155
44. Arnold MA, Patton JT. Rotavirus antagonism of the innate immune response. *Viruses*. (2009) 1:1035–56. doi: 10.3390/v1031035
45. Konig J, Wells J, DCani P, Garcia-Rodenas CL, MacDonald T, Mercenier A, et al. Human intestinal barrier function in health and disease. *Clin Transl Gastroenterol*. (2016) 7:e196. doi: 10.1038/ctg.2016.54
46. Zhou R, Wei H, Sun R, Tian Z. Recognition of double-stranded RNA by TLR3 induces severe small intestinal injury in mice. *J Immunol*. (2007) 178:4548–56. doi: 10.4049/jimmunol.178.7.4548
47. Bermudez-Brito M, Muñoz-Quezada S, Gómez-Llorente C, Matencio E, Romero F, Gil A. *Lactobacillus paracasei* CNCM I-4034 and its culture supernatant modulate Salmonella-induced inflammation in a novel transwell co-culture of human intestinal-like dendritic and Caco-2 cells. *BMC Microbiol*. (2015) 15:79. doi: 10.1186/s12866-015-0408-6
48. Kure I, Nishiumi S, Nishitani Y, Tanoue T, Ishida T, Mizuno M, et al. Lipoxin A(4) reduces lipopolysaccharide-induced inflammation in macrophages and intestinal epithelial cells through inhibition of nuclear factor-B activation. *J Pharmacol Exp Therapeut*. (2010) 332:541–48. doi: 10.1124/jpet.109.159046
49. Rimoldi M, Chieppa M, Larghi P, Vulcano M, Allavena P, Rescigno M. Monocyte-derived dendritic cells activated by bacteria or by bacteria-stimulated epithelial cells are functionally different. *Blood*. (2005) 106:2818–26. doi: 10.1182/blood-2004-11-4321
50. Hasan M, Ruksznis C, Wang Y, Anne Leifer C. Antimicrobial peptide inhibits poly(I:C) induced immune responses. *J Immunol*. (2011) 187:5653–59. doi: 10.4049/jimmunol.1102144
51. Lyons C, Fernandes P, Fanning LJ, Houston A, Brint E. Engagement of Fas on macrophages modulates PolyI:C induced cytokine production with specific enhancement of IP-10. *PLoS ONE*. (2015) 10:e0123635. doi: 10.1371/journal.pone.0123635
52. Schreiber S, Heinig T, Thiele HG, Raedler, A. Immunoregulatory role of IL-10 in patients with inflammatory bowel disease. *Gastroenterology*. (1995) 108:1434–44. doi: 10.1016/0016-5085(95)90692-4
53. MacPherson CW, Shastri P, Mathieu O, Tompkins TA, Burguière P. Genome-wide immune modulation of TLR3-mediated inflammation in intestinal epithelial cells differs between single and multi-Strain probiotic combination. *PLoS ONE*. (2017) 12:e0169847. doi: 10.1371/journal.pone.0169847
54. Yan F, Polk DB. Commensal bacteria in the gut: learning who our friends are. *Curr Opin Gastroenterol*. (2004) 20:565–71. doi: 10.1097/00001574-200411000-00011
55. Melmed G, Thomas LS, Lee N, Tesfay SY, Lukasek K, Michelsen KS, et al. Human intestinal epithelial cells are broadly unresponsive to Toll-like receptor 2-dependent bacterial ligands: implications for host-microbial interactions in the gut. *J Immunol*. (2003) 170:1406–15. doi: 10.4049/jimmunol.170.3.1406
56. Maillard MH, Bega H, Uhlig HH, Barnich N, Grandjean T, Chamaillard M, et al. Toll-interacting protein modulates colitis susceptibility in mice. *Inflamm Bowel Dis*. (2014) 20:660–70. doi: 10.1097/MIB.0000000000000006
57. Polentarutti N, Rol GP, Muzio M, Bosisio D, Camnasio M, Riva F, et al. Unique pattern of expression and inhibition of IL-1 signaling by the IL-1 receptor family member TIR8/SIGIRR. *Eur Cytokine Netw*. (2003) 14:211–18.
58. Saitoh T, Yamamoto M, Miyagishi M, Taira K, Nakanishi M, Fujita T, et al. A20 is a negative regulator of IFN regulatory factor 3 signaling. *J Immunol*. (2005) 174:1507–12. doi: 10.4049/jimmunol.174.3.1507

59. Graff JW, Ewen J, Ettayebi K, Hardy ME. Zinc-binding domain of rotavirus NSP1 is required for proteasome-dependent degradation of IRF3 and autoregulatory NSP1 stability. *J Gen Virol*. (2007) 88:613–20. doi: 10.1099/vir.0.82255-0
60. Kim YG, Ohta T, Takahashi T, Kushiro A, Nomoto K, Yokokura T, et al. Probiotic *Lactobacillus casei* activates innate immunity via NF-κB and p38 MAP kinase signaling pathways. *Microbes Infect*. (2006) 8:994–05. doi: 10.1016/j.micinf.2005.10.019

**Conflict of Interest Statement:** The authors declare that the research was conducted in the absence of any commercial or financial relationships that could be construed as a potential conflict of interest.

frontiers in Immunology

ORIGINAL RESEARCH
published: 17 July 2019
doi: 10.3389/fimmu.2019.01674

# Cathelicidin-WA Facilitated Intestinal Fatty Acid Absorption Through Enhancing PPAR-γ Dependent Barrier Function

*Xin Zong†, Xiaoxuan Cao†, Hong Wang, Xiao Xiao, Yizhen Wang* and Zeqing Lu**

*Key Laboratory of Animal Nutrition and Feed Science in Eastern China, Ministry of Agriculture, College of Animal Sciences, Zhejiang University, Hangzhou, China*

The molecular mechanisms underlying the cellular uptake of long-chain fatty acids and the regulation of this process have been debated in recent decades. Here, we established an intestinal barrier dysfunction model in mice and Caco2 cell line by Lipopolysaccharide (LPS), and evaluated the fatty acid uptake capacity of the intestine. We found that LPS stimulation restricted the absorption of long chain fatty acid (LCFA), while Cathelicidin-WA (CWA) pretreatment facilitated this physiological process. At the molecular level, our results demonstrated that the stimulatory effects of CWA on intestinal lipid absorption were dependent on cluster determinant 36 and fatty acid transport protein 4, but not fatty acid–binding protein. Further, an enhanced intestinal barrier was observed *in vivo* and *in vitro* when CWA alleviated the fatty acid absorption disorder induced by LPS stimulation. Mechanistically, peroxisome proliferator-activated receptor (PPAR-γ) signaling was considered as a key pathway for CWA to enhance LCFA absorption and barrier function. Treatment with a PPAR-γ inhibitor led to impaired intestinal barrier function and suppressed LCFA uptake. Moreover, once PPAR-γ signaling was blocked, CWA pretreatment could not maintain the stability of the intestinal epithelial cell barrier or LCFA uptake after LPS stimulation. Collectively, these findings suggested that PPAR-γ may serve as a target for specific therapies aimed at alleviating fatty acid uptake disorder, and CWA showed considerable potential as a new PPAR-γ agonist to strengthen intestinal barrier function against fatty acid malabsorption.

**Keywords: cathelicidin-WA, fatty acids, intestinal barrier, PPAR-γ, lipopolysaccharides**

OPEN ACCESS

***Edited by:***
*Julio Villena, CONICET Centro de Referencia para Lactobacilos (CERELA), Argentina*

***Reviewed by:***
*Roxana Beatriz Medina, CONICET Centro de Referencia para Lactobacilos (CERELA), Argentina*
*Paulraj Kanmani, Tohoku University, Japan*

***Correspondence:**
*Yizhen Wang*
*yzwang321@zju.edu.cn*
*Zeqing Lu*
*zqlu2012@zju.edu.cn*

*†These authors have contributed equally to this work as share first authorship*

***Specialty section:***
*This article was submitted to Nutritional Immunology, a section of the journal Frontiers in Immunology*

***Received:*** *03 June 2019*
***Accepted:*** *04 July 2019*
***Published:*** *17 July 2019*

***Citation:***
*Zong X, Cao X, Wang H, Xiao X, Wang Y and Lu Z (2019) Cathelicidin-WA Facilitated Intestinal Fatty Acid Absorption Through Enhancing PPAR-γ Dependent Barrier Function. Front. Immunol. 10:1674. doi: 10.3389/fimmu.2019.01674*

## INTRODUCTION

Long-chain fatty acids (LCFAs, FAs with 12–18 carbons and varying degrees of unsaturation), stored as triglycerides in the body, serve several important functions in the human body (1). First, LCFAs are one of the most important sources of energy, and could provide twice as much energy as carbohydrates and proteins on a per weight basis (2). Second, dietary LCFAs are the only source of essential fatty acids that serve as substrates for lipid biosynthesis, and protein modification (1). Intestinal fatty acid absorption is a multistep process, that is associated with fatty acid transporters on the apical membrane of enterocytes, including cluster determinant 36 (CD36), plasma membrane–associated fatty acid–binding proteins (FABP), and a family of fatty acid

transport proteins (FATP) 1–6 (3–5). Because of the metabolic syndrome is related to cardiovascular disease, obesity, diabetes, and cancer, many studies have focused mainly on identifying cellular, physical/chemical, and genetic determinants of intestinal fatty acid absorption in humans and laboratory animals (6).

It is generally known that before cholesterol and fatty acid molecules can interact with their corresponding transporters for uptake and absorption, they must pass through a diffusion barrier (7, 8). Intestinal mucosa is a diffusion-limiting barrier, that simultaneously promotes nutrient and water transport while serving as a protective barrier, and neither property is absolute (9). Wang et al. (7) found that epithelial mucin1 was necessary for normal intestinal uptake and absorption of cholesterol in mice, as evidenced by a 50% reduction in cholesterol absorption efficiency in mucin1 knockout mice.

Cathelicidin peptides, a family of antimicrobial peptides, not only exhibit antimicrobial activities (10), but also function as immune regulators (11). Recently, cathelicidin peptides have been found to protect intestinal epithelial barrier function in infected mice (12, 13). Our previous study showed that cathelicidin peptide (CWA) from snake attenuated EHEC-induced inflammation and microbiota disruption in the intestine of mice (14). Nevertheless, the effects of CWA on fatty acid absorption and the underlying mechanisms remain unknown.

In this study, we characterized the effect of cathelicidin peptide CWA on intestinal LCFA absorption during Lipopolysaccharide (LPS) induced intestinal barrier dysfunction in mice and Caco-2 cells. We present new evidence implicating CWA as a potent stimulator of LCFA absorption in the intestine and explore potential mechanisms through enhancing peroxisome proliferator activated receptor (PPAR) γ- dependent barrier function.

# MATERIALS AND METHODS

## Peptide Synthesis

Cathelicidin-WA (CWA) was chemically synthesized by a standard solid-phase method using Automatic Peptide Synthesizer (Aapptec, Louisville, KY, USA) from C-terminus to N-terminus according to the sequence designed by our laboratory (14). The synthetic CWA was purified by semi-preparative HPLC, achieving 96% purity of the peptide and characterized by analytical HPLC (Agilent 121 Technologies, CA, USA). The peptide was dissolved in PBS and stored at −80°C until use.

## Reagents

Ultrapure LPS from *E.coli* strain O55:B5, FD4 and 4,4-difluoro-5,7-dimethyl-4-bora-3a, and 4a-diaza-s-indacene-3-hexadecanoic acid (BODIPY-C16) were purchased from Sigma-Aldrich (St. Louis. MO, USA). Olive oil and palmitic acid were purchased from Aladdin (Shanghai, China). Tyloxapol was purchased from Sigma Aldrich (St. Louis, USA). GW9662 and Rosiglitazone were obtained from Target Molecule (Shanghai, China).The rabbit antibodies for β-actin, ZO-1, CD36, FATP4, I-FABP, PPAR-γ were purchased from Proteintech (Wuhan, China). The rabbit antibodies for occludin and claudin-1 were obtained from Abcam (Cambridge, MA, USA). The secondary antibody (goat-anti-rabbit IgG) was purchased from HuaAn (Hangzhou, China).

## Animals and Treatments

Forty C57BL/6 male mice (5∼6 weeks of age) were obtained from the Laboratory Animal Center of Zhejiang University. All the mice were housed in plastic cages on a layer of wood shavings with chow diet and water ad libitum under standard conditions. The animals were allowed to acclimatize to the environment for 1 week before the experiment. The animal experimental protocol was approved by the Animal Care and Use Committee of Zhejiang University.

As shown in **Table 1**, the mice were randomly divided into four groups of 10 each: control, LPS treatment (10 mg/kg), CWA pretreatment (5 mg/kg), and CWA+LPS (5 mg/kg CWA pretreatment followed by 10 mg/kg LPS treatment). CWA was injected intraperitoneally once daily for 6 days, whereas the control and LPS groups were intraperitoneally injected with an

**TABLE 1 |** Experimental design and scheme of the animal treatments.

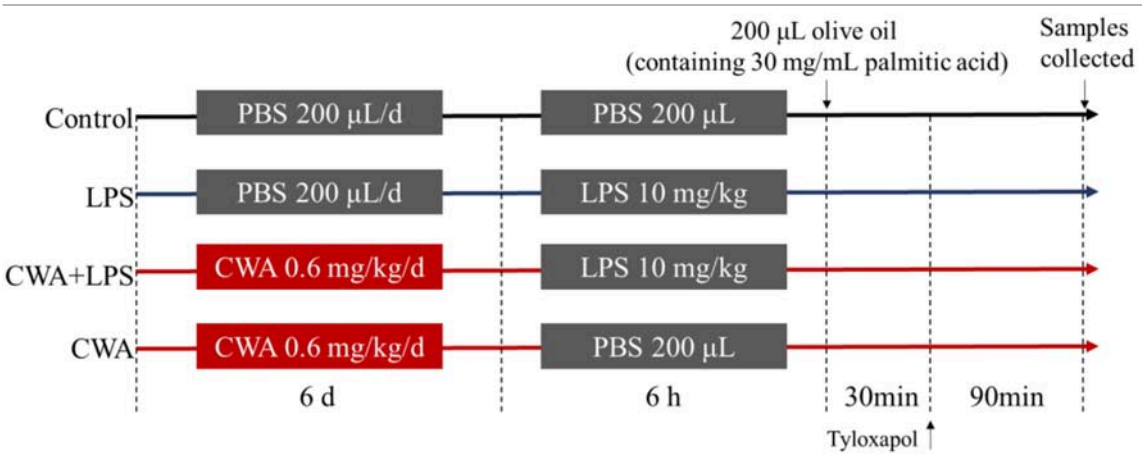

**TABLE 2 |** Primer sequences for q-PCR.

| Gene | | Sequence (5′→ 3′) | Genebank No. |
|---|---|---|---|
| IL-6 | Forward: | TCCTACCCCAATTTCCAATGCT | NM_031168.2 |
| | Reverse: | TGGTCTTGGTCCTTAGCCAC | |
| TNF-α | Forward: | GCTCTTCTGTCTACTGAACTTCGG | NM_013693.3 |
| | Reverse: | ATGATCTGAGTGTGAGGGTCTGG | |
| Occludin | Forward: | CAGGTGAATGGGTCACCGAG | NM_008756.2 |
| | Reverse: | CAGGCTCCCAAGATAAGCGA | |
| ZO-1 | Forward: | GGGAAGTTACGTGCGGGAG | NM_009386.2 |
| | Reverse: | AGTGGGACAAAAGTCCGGG | |
| Claudin-1 | Forward: | GGCCTTGGCTGTACCTTACC | NM_016674.4 |
| | Reverse: | GGAGCACCTTATCCCCGTTT | |
| ApoA-IV | Forward: | GCGTGCAGGAGAAACTCAAC | NM_007468.2 |
| | Reverse: | GCTGGTCGATTTTTGCGGAG | |
| CD36 | Forward: | GGCAACCAACCACAAATTAGCA | NM_007643.4 |
| | Reverse: | AAGGCTAGGAAACCATCCACC | |
| FATP4 | Forward: | GACTTCTCCAGCCGTTTCCA | NM_011989.5 |
| | Reverse: | AGGACAGGATGCGGCTATTG | |
| I-FABP | Forward: | ATGCCCACATGCTGTAGTTGA | NM_007980.3 |
| | Reverse: | AACCTAACCGCCTCACATGC | |
| DGAT-1 | Forward: | TTTCCGTCCAGGGTGGTAGT | NM_010046.3 |
| | Reverse: | ATCTTGCAGACGATGGCACC | |
| DGAT-2 | Forward: | GGCTACGTTGGCTGGTAACT | NM_026384.3 |
| | Reverse: | TCTTCAGGGTGACTGCGTTC | |
| β-actin | Forward: | TGAGCTGCGTTTTACACCCT | NM_007393.5 |
| | Reverse: | GCCTTCACCGTTCCAGTTTTT | |

equal volume of sterile saline. On day 6, mice in the LPS and CWA+LPS groups were intraperitoneally injected with LPS (10 mg/kg, 200 μL per mouse) 1 h after CWA or saline treatment, and the other groups were injected with an equal volume of saline. The lipid absorption assessment was performed 6 h after LPS or saline injection, and the mice were administered 200 μL olive oil (containing 30 mg/mL palmitic acid) by gavage and then received an intraperitoneal injection of tyloxapol (15% in saline, 0.5 g/kg) 30 min later. The mice were killed and blood samples were collected by cardiac puncture 2 h after an oral fat bolus.

## Cell Culture

The human colorectal cancer cell line Caco-2 cells (a generous gift from Dr. Fengjie, College of Animal Science, Zhejiang University) were obtained from Cell Bank of the Chinese Academy of Sciences (Shanghai, China) and cultured in DMEM-F12 medium supplemented with 10% (V/V) fetal bovine serum and antibiotics (100 U/ml penicillin and 100 μg/mL streptomycin sulfate) at 37°C in humidified incubator under 5% $CO_2$ in air.

## Intestinal Morphology

The proximal jejunum of the mice was fixed in 4% paraformaldehyde and embedded by paraffin, followed by slicing and staining with hematoxylin and eosin (H&E) or oil red O staining solution. Images of the slices were obtained using the Leica DM3000 Microsystem, then the villi height and crypt depth were measured by Leica Application Suite Version 3.7.0 (Leica, Wetzlar, Germany).

## Transmission Electron Microscopy

The tight junction structure was observed by TEM as previously described (10). A jejunum specimen of ∼1 cm in length was excised with a sharp scalpel and fixed in 2.5% glutaraldehyde for 4 h at 4°C, followed by fixation in osmic acid and embedding in epon. Ultrathin sections were obtained using a diamond knife and stained with uranyl acetate and lead citrate before examination by TEM (JEM-1011; JEOL USA). Digital electron micrographs were acquired with a 1,024 × 1,024 pixel CCD camera system (AMT Corp., Denver, MA).

## Serum Lipids and Inflammatory Cytokines

To determine the concentration of TNF-α and IL-6 in the serum, ELISA kits (Raybiotech, Guangzhou, China) were used. The assays were carried out according to the manufacturer's instructions.

## Determination of Fatty Acid Uptake *in vitro*

Caco2 cells were seeded in BIOCOAT Collagen I 96-well plates (black wells, clear bottom) for 1 week because of the differentiation process. The fatty acid uptake was evaluated by intracellular BODIPY-labeled fatty acid as previously described (15). Briefly, the cells starved for 1 h in MEM medium (without phenol red), which was and replaced with 100 μL of a BODIPY-C16 reaction mixture prepared in D-Hanks (5 μM C1-BODIPY-C16, 5 μM fatty-free BSA and 3.9 mM trypan blue, 50 μL MEM medium). The plates were maintained in the dark and incubated for 10 min at 37°C in 5% $CO_2$. Then the intracellular fluorescence was measured by a Molecular Devices SpectraMax M5 plate reader following excitation at 485 nm and emission at 528 nm. Fatty acid uptake differences were compared by the relative fluorescence.

## Measurement of Transepithelial Electrical Resistance (TEER)

Caco-2 cells were grown on 12-mm Transwell filters (Corning, NY, USA). When the TEER of cell monolayers became stable (∼3 weeks later), they are ready to be studied. Then the TEER of polarized Caco-2 cells were measured using Millicell-ERS voltohmmeter (Millipore, USA) at 1, 3, 6, 12 h after LPS stimulation. Changes were calculated as a percentage of baseline TEER (0 h).

## *In vitro* Intestinal Paracellular Permeability Assay

Immediately after the last determination of TEER value, 100 μL of 4 kDa fluorescein isothiocyanate-labeled dextran (FD4, 1 mg/mL) was added to apical chamber. The transwell plates were cultured at 37°C for 30 min, and then the concentrations of FD4 in the basolateral chamber were determined at an excitation wavelength of 480 nm and an emission wavelength of 520 nm according to the standard curve, which was established from the fluorescence of FD4 at concentration of 100, 200, 500, 1,000, 2,000, 3,000, 4,000, 5,000 pmol/L.

## RNA Extraction and Quantitative Real Time PCR (q-PCR)

Total RNA was isolated using TRIzol reagent (Invitrogen, USA). The concentration and purity of the RNA were evaluated using NanoDrop2000 (Thermo Fisher Scientific, Waltham, USA). Then 2 μg RNA was subjected to reverse transcription reaction with random primers. q-PCR was performed with SYBR Green master mix (Roche, Mannheim, Germany) using a StepOnePlus Real Time PCR systems (Applied Biosystems, Foster City, USA). The gene-specific primers for the q-PCR are listed in **Table 2** and the relative mRNA expression of the target gene was determined using the 2-ΔΔCt method.

## Western Blot Analysis

Total protein extracts of scraped jejunal mucosa or cells were harvested by Total Protein Extraction Kit (KeyGen BioTECH, Nanjing, China). Equivalent amounts of protein were separated by SDS-PAGE and electroblotted onto PVDF membranes (Millipore, Bedford, MA, USA) followed by blocking with 5% fat-free milk. Then membranes were incubated overnight at 4°C with primary antibodies including ZO-1, occludin, claudin-1, CD36, FATP4, I-FABP, PPARγ, and β-actin. After washing with TBST, membranes were incubated with secondary antibodies for 1 h at room temperature. The protein bands were visualized with an ECL assay kit (Servicebio, Wuhan,

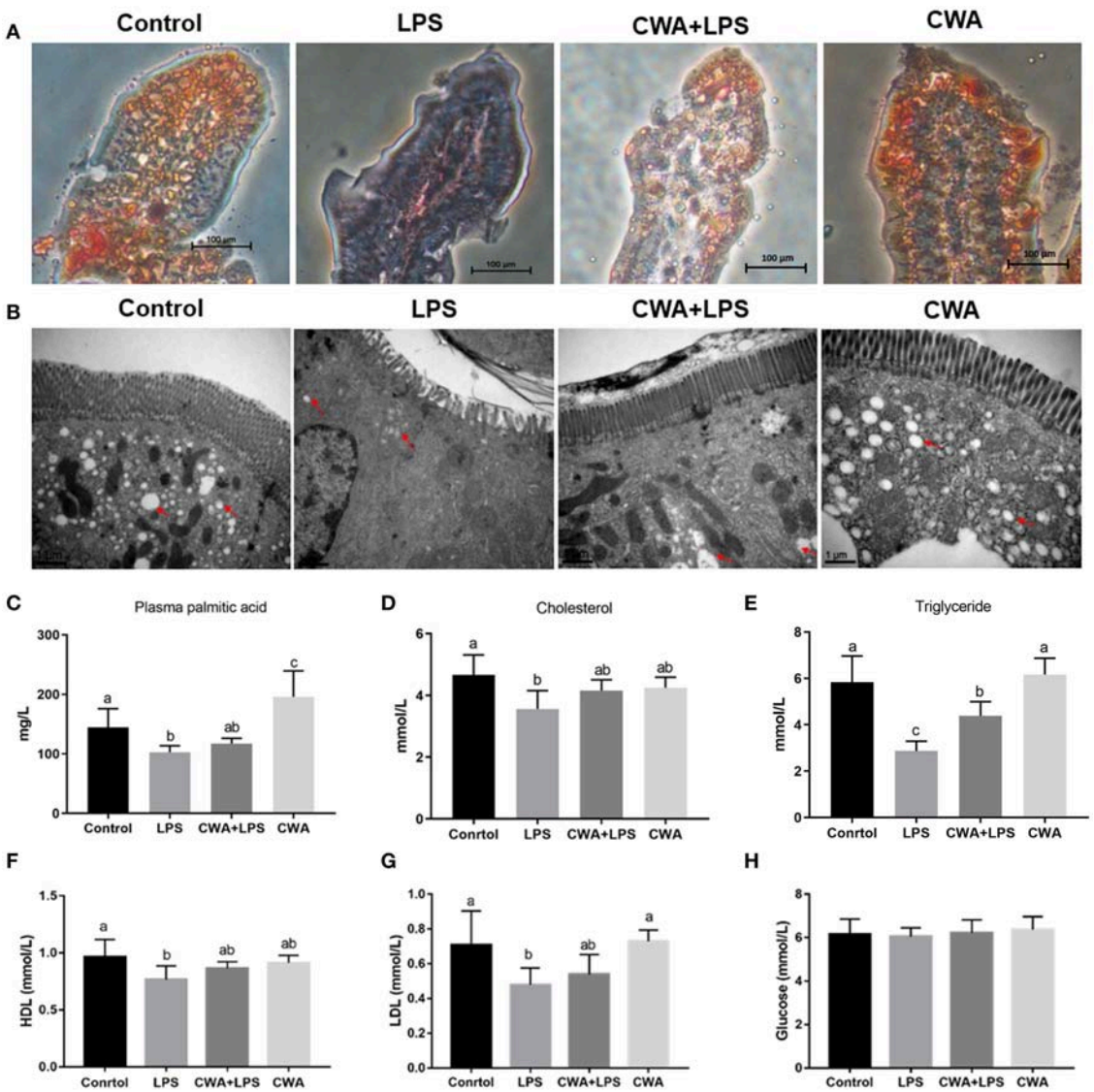


**FIGURE 1 |** Stimulatory effects of CWA on intestinal lipid absorption. The samples were collected 6 h after LPS withdrawal and 2 h after continuous intraduodenal fat infusion in mice treated with tyloxapol. **(A)** Lipid droplets were stained with Oil red O in jejunum sections, bar = 100 μm. **(B)** Electron microscopy images showing lipid droplets in jejunum, bar = 1 μm, red arrows indicate the positions of lipid droplets. **(C)** The concentration of palmitic acid in serum was analyzed by Gas chromatography, $n = 9$, biological replicates. **(D–H)** The concentration of cholesterol **(D)**, triglyceride **(E)**, high density lipoprotein **(F)**, low density lipoprotein **(G)**, and glucose **(H)** in serum were determined by commercial kit, $n = 9$, biological replicates. The data are expressed as the mean ± SEM; bars with different small capital letters are statistically different from one another.

China) and the band intensity was quantified by Image J software.

## Statistical Analysis

All statistical calculations were performed in GraphPad Prism 7 (San Diego, USA) and expressed as the mean ± SD. Data were subjected to one-way ANOVA with Duncan's multiple range test. $P < 0.05$ was considered as statistically significant.

# RESULTS

## CWA Prevented the LCFA Absorption Disorder in LPS-Treated Mice

To directly examine whether CWA facilitates the utilization of LCFA, we measured intracellular triglyceride levels in the intestine of mice that received palmitic acid orally. As shown in the oil red O staining results (**Figure 1A**), some vacuolized enterocytes on the remaining villus tops in mice treated with LPS only contained a few fat droplets, while fat droplets were completely absent in the villus interstitium, which was significantly different from the control group. In contrast, in CWA-pretreated mice, most enterocytes contained no fat droplets while many small fat droplets were present in the villus interstitium. As an independent validation, a similar phenomenon was found by TEM observation (**Figure 1B**).

To substantiate this finding further, we found that the level of palmitic acid was not different in LPS-treated mice with or without CWA stimulation, but it increased significantly in CWA only-treated mice compared to control mice (**Figure 1C**). Although the levels of serum cholesterol were not changed between treatments, the level of triglycerides, the main storage form of fatty acids, in LPS-treated mice decreased markedly in comparison with control mice, and CWA pretreatment effectively alleviated the symptoms (**Figures 1D,E**). Moreover, we analyzed glucose and lipid metabolites in the serum. As shown in **Figures 1F,G**, compared with the control group, LPS stimulation decreased high-density lipoproteins (HDL) and low-density lipoproteins (LDL) levels, and CWA treatment prevented this decrease. However, it was likely that glucose metabolism was not sensitive to LPS and CWA stimulation (**Figure 1H**). These results indicated that LPS restricted LCFA absorption in the intestine, while CWA pretreatment restored the absorptive process during LPS stimulation.

## CWA Enhanced the Expression of Fatty Acid Absorption-Related Genes in LPS-Treated Mice

To investigate the genetic basis of the effect of CWA on the absorption of LCFA, the expression of specific protein transporters implicated in intestinal fatty acid absorption was examined by q-PCR. We found that the expression of CD36 and FATP4 decreased markedly after LPS stimulation, while CWA pretreatment blocked the decrease in their expression induced by LPS (**Figures 2A,B**). Conversely,

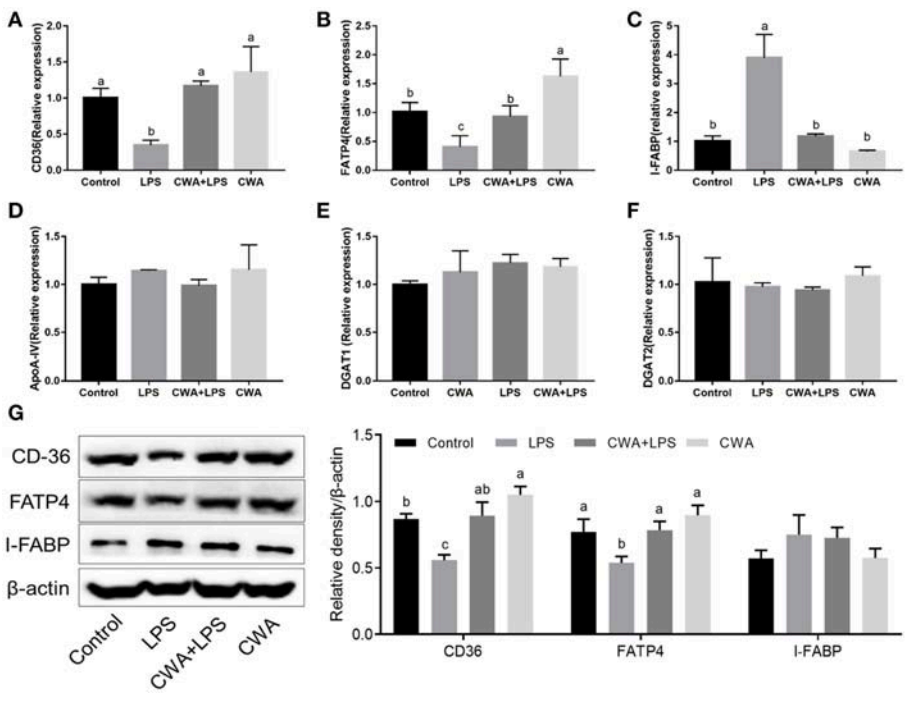


**FIGURE 2 |** CWA enhanced the expression of fatty acid absorption related genes in LPS stimulated mice. **(A–F)** q-PCR to quantify fatty acid absorption related mRNA levels and results are presented relative to those of gapdh. **(G)** Immunoblot to determine the levels of CD36, FATP4, and I-FABP. The right panel shows the relative levels quantified by densitometry and normalized to β-actin. The data are expressed as the mean ± SEM, $n = 9$, biological replicates; bars with different small capital letters are statistically different from one another.

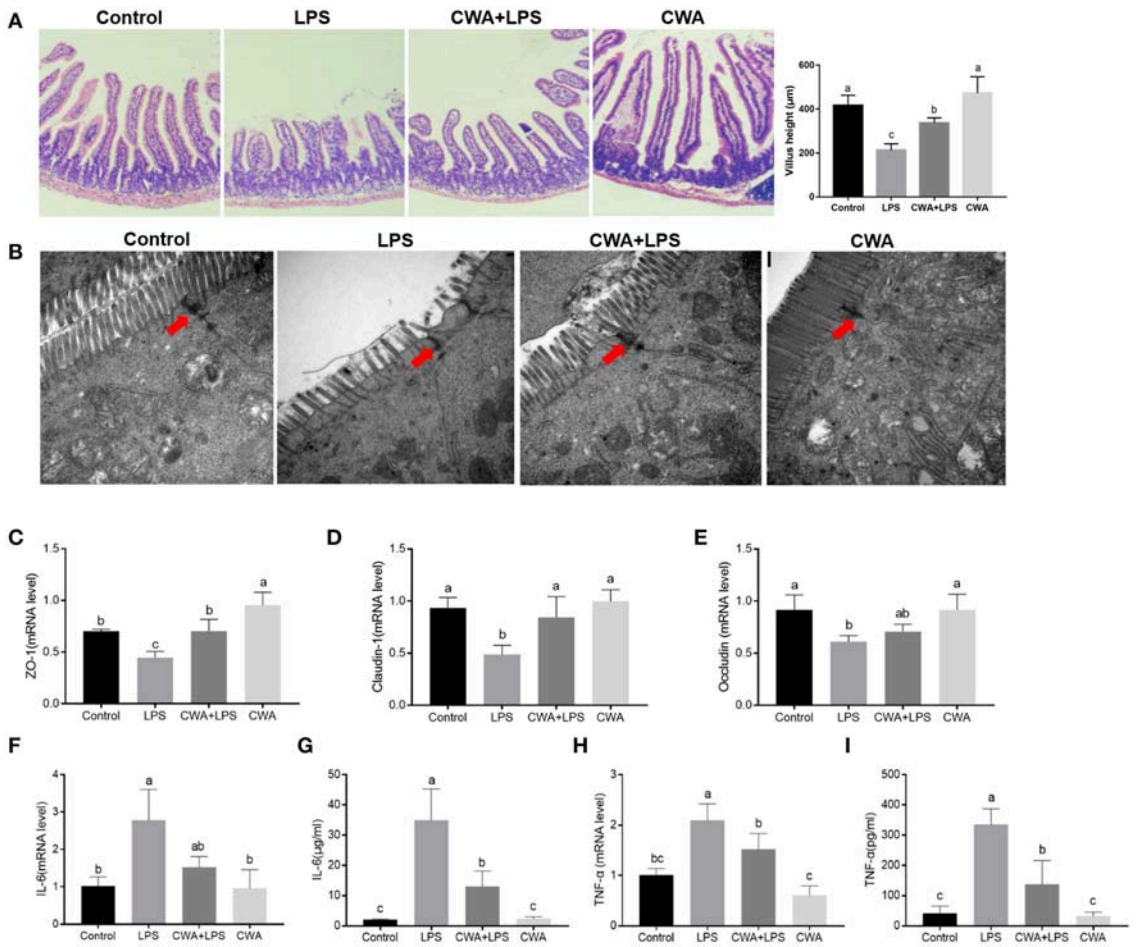


**FIGURE 3 |** CWA prevented LPS-induced impairment of jejunum epithelium tissues. **(A)** Representative H&E-stained section from jejunum (Magnification, 100×), Villus heights of the jejunum (left; $n = 45$ for each group of mice). **(B)** Electron microscopy images showing desmosomes in intestinal epithelium (Magnification, 25000×). **(C–E)** q-PCR quantified ZO-1 **(C)**, Claudin-1 **(D)**, and Occludin **(E)** mRNA abundance in jejunum and results are presented relative to those of gapdh, $n = 9$, biological replicates. **(F–I)** q-PCR quantified mRNA abundance of IL-6 **(F)** and TNF-α **(H)** in jejunum, and Elisa determined serum concentration of IL-6 **(G)** and TNF-α **(I)**, $n = 9$, biological replicates. The data are expressed as the mean ± SEM; bars with different small capital letters are statistically different from one another.

and interestingly, compared with the control group, the expression of intestinal fatty acid binding protein (I-FABP) increased notably with LPS treatment, but no difference was noted in CWA-pretreated mice (**Figure 2C**). However, the expression of intestinal ApoA-IV, DGAT1, and DGAT2 upon LPS stimulation did not change among any of the treatment groups (**Figures 2D–F**).

Furthermore, Western blot analyses showed that exogenous CWA increased CD36 and FATP4 protein levels in mice treated with LPS, which was consistent with the qPCR results (**Figure 2G**). Curiously, there was no difference in the IFABP protein levels between each treatment (**Figure 2G**). These experiments demonstrated that the stimulatory effects of CWA on intestinal lipid absorption were dependent on the fatty acid transporters CD36 and FATP4.

## Effects of CWA on LPS-Induced Mouse Intestinal Barrier Injury

Cathelicidin peptides improve the intestinal barrier function. We investigated whether the improved fatty acid absorption by CWA was related to its role in regulating intestinal barrier function. As shown in **Figure 3A**, compared with the control mice, increased villous height and decreased crypt depth were observed in the jejunum after LPS challenge, whereas CWA pretreatment attenuated the LPS-induced villous atrophy and crypt hyperplasia.

Tight junction proteins (TJs) exert a primary role in maintaining intestinal barrier function (9). To further evaluate the protective effect of CWA on the barrier function, transmission electron microscopy was used to observe TJ structure. We found that LPS destroyed the TJ structure in the jejunum, which was clearly prevented by CWA pretreatment

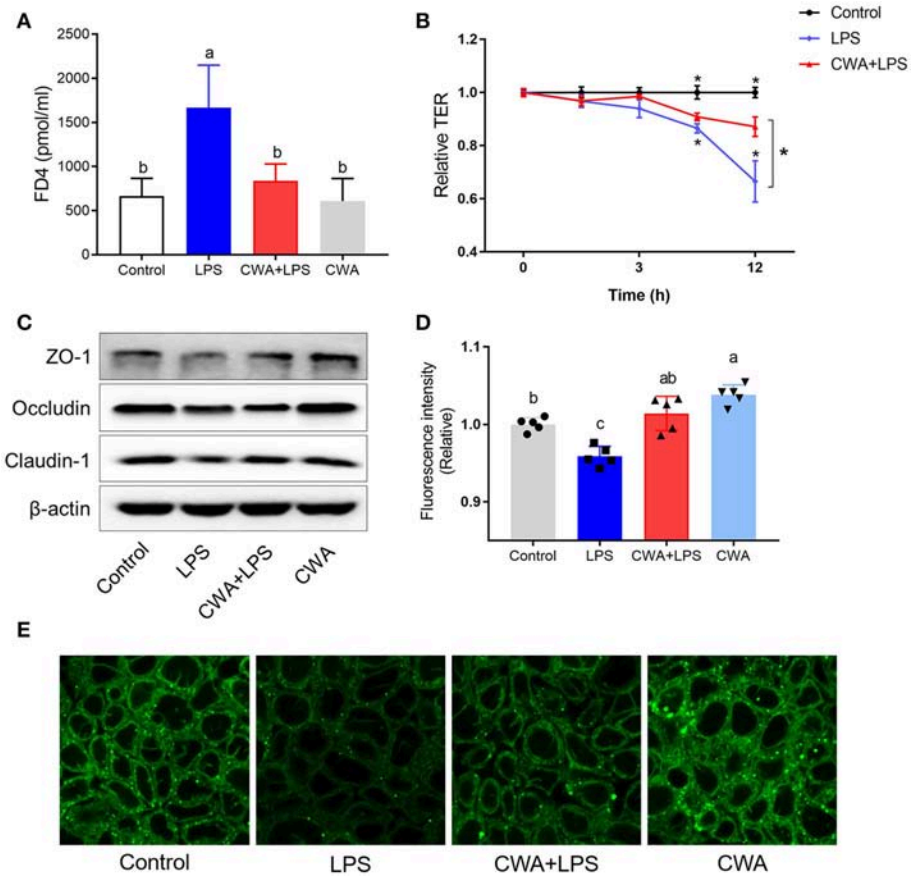


**FIGURE 4 |** CWA (20 μg/ml) accelerated absorption of Bodipy FA in LPS injured Caco-2 cell. **(A)** Effect of CWA on cellular permeability to FD4. **(B)** Effect of CWA on TEER of a Caco-2 cell monolayer. **(C)** Western blot analysis of tight junction proteins in Caco-2 cell. **(D,E)** Effect of CWA on fatty acids uptake in Caco-2 cell. Caco-2 cells treated with medium in the presence of the Bodipy-C16 (8 μM) for 5 min. **(D)** The absorption level of Bodipy C16 was observed by confocal microscope. **(E)** General level of Bodipy FA absorption was measured by Microplate reader. The data are expressed as the mean ± SEM, $n = 3$, biological replicates; bars with different small capital letters are statistically different from one another.

(**Figure 3B**). Moreover, the expression of TJ markers, zonula occludens (ZO)−1, occludin, and Claudin-1 were detected by qPCR. All genes were downregulated in mice treated with LPS alone compared with normal animals. Administration of CWA increased the expression of all genes bringing it close to the level of the control group (**Figures 3C–E**). Additionally, we found that CWA attenuated the inflammatory response caused by LPS stimulation. Compared with the control group, the LPS-treated mice exhibited highly elevated expression of TNF-α and IL-6. The administration of CWA to LPS-treated mice significantly decreased these inflammatory mediators (**Figures 3F–I**). These results further strengthen the evidence linking CWA and intestinal barrier injury.

## CWA Prevented LCFA Malabsorption in LPS-Injured Caco-2 Cells

To understand the mechanism by which CWA promoted LCFA absorption, a barrier-injured intestinal epithelial cell model was established with Caco-2 cells cultured in Transwell plates. Consistent with the *in vivo* findings, the results in **Figure 4A** show only a 20% drop in TEER values compared to the baseline values under LPS treatment conditions in the cells pretreated with CWA, whereas an ∼40% decline was found in the cells treated with LPS alone (**Figure 4B**). The effect of CWA was further confirmed with a FD4 permeability assay (**Figure 4A**). At the molecular level, we verified that CWA pretreatment prevented the decreased expression of TJ markers ZO-1, occludin, and Claudin-1 induced by LPS challenge (**Figure 4C**). These results illustrated the protective effects of CWA on LPS-induced intestinal barrier dysfunction *in vitro*.

4,4-Difluoro-5,7-dimethyl-4-bora-3a,4a-diaza-s-indacene-3-hexadecanoic acid (Bodipy-C16) is a fatty acid analog used to study fatty acid uptake in cells (16). The incorporation of this analog into cellular lipids is similar to that of native LCFA. We used the fluorescent fatty acid analog Bodipy-C16 to measure the ability of the Caco-2 cells to take up fatty acids. Notably, upon LPS stimulation, LCFA uptake was limited, while CWA pretreatment dramatically increased the amount of fatty acid uptake when compared to the LPS-challenged group (**Figure 4D**). Similarly, the promotion of fatty acid uptake by

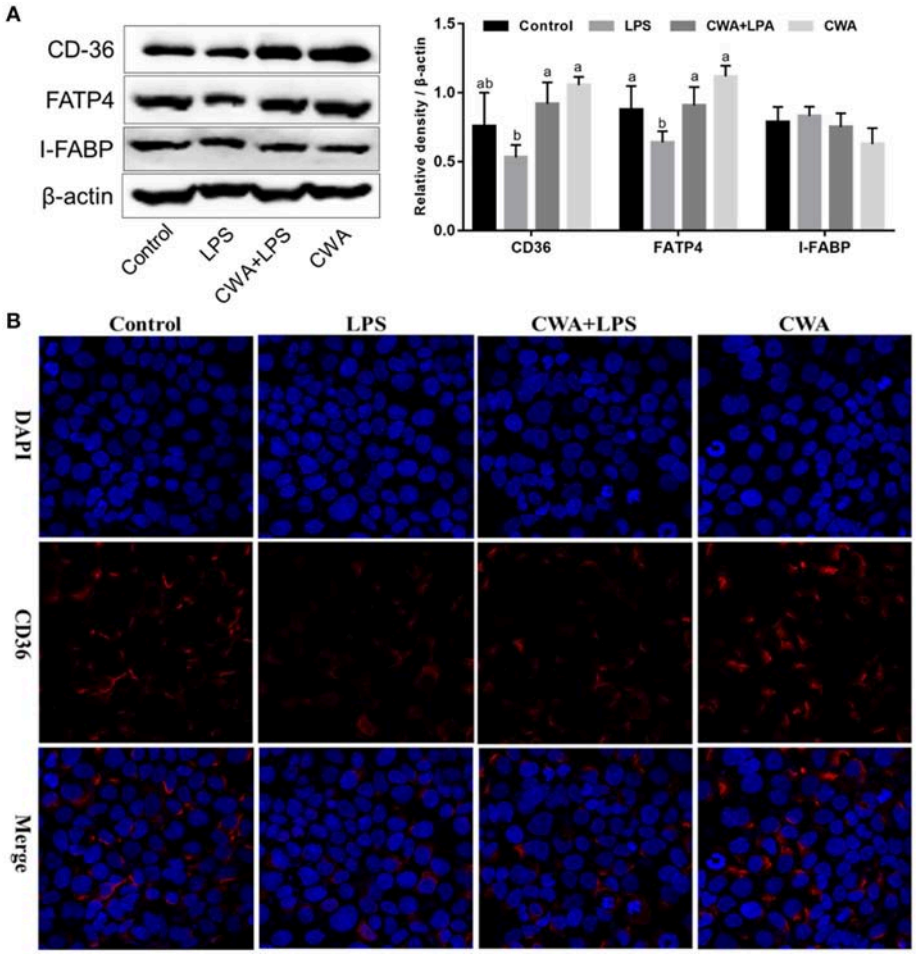


**FIGURE 5 |** Effect of CWA on the expression and distribution of fatty acid transport proteins. **(A)** Western blot analysis of the expression of fatty acid transport protein. The right panel shows the relative levels quantified by densitometry and normalized to β-actin. **(B)** Immunofluorescence analysis of the expression and distribution of CD36. The data are expressed as the mean ± SEM, $n = 3$, biological replicates; bars with different small capital letters are statistically different from one another.

CWA in cells treated with LPS was further confirmed by confocal microscopy with Bodipy-C16 (**Figure 4E**).

## CWA Strengthened LCFA Absorption Dependent on FATP4 and CD36

In humans and mice, CD36 is detected in epithelial cells of the small intestine along the gastrocolic and crypt-to-villus axes in a pattern paralleling that of other proteins implicated in LCFA uptake (5, 17). First, the expression of specific protein transporters implicated in intestinal fatty acid absorption was examined by Western blot analyses. Consistent with previous findings, no difference was noted in the protein levels of IFABP (**Figure 5A**). Moreover, we found that CWA significantly increased the expression of CD36 and FATP4, whose expression was suppressed by LPS stimulation (**Figure 5A**).

Immunofluorescence visualization of CD36 suggested that this protein is expressed on the membrane, poised for fatty acid uptake (**Figure 5B**). LPS stimulation visibly decreased the expression of CD36, which was prevented by CWA pretreatment (**Figure 5B**). Thus, a potential mechanism by which CWA promotes LCFA absorption is through increasing the expression of CD36 on the membrane by means of enhanced barrier function.

## CWA Facilitated LCFA Absorption and Barrier Function Through PPAR-γ Activation

PPAR-γ signaling is required for both intestinal barrier function and nutrient transport (18, 19). We hypothesized that CWA enhanced barrier function and that LCFA absorption was dependent on PPAR-γ. We first analyzed the expression of PPAR-γ, and as shown in **Figure 6A**, CWA treatment activated PPAR-γ in the presence or absence of LPS stimulation. To test the hypothesis further, an inhibitor and agonist of PPAR-γ were used. As expected, the inhibitor GW9662 inhibited and the agonist rosiglitazone activated the expression of PPAR-γ (**Figure 6B**). Furthermore, we found that CWA pretreatment failed to maintain the stability of the intestinal epithelial cell

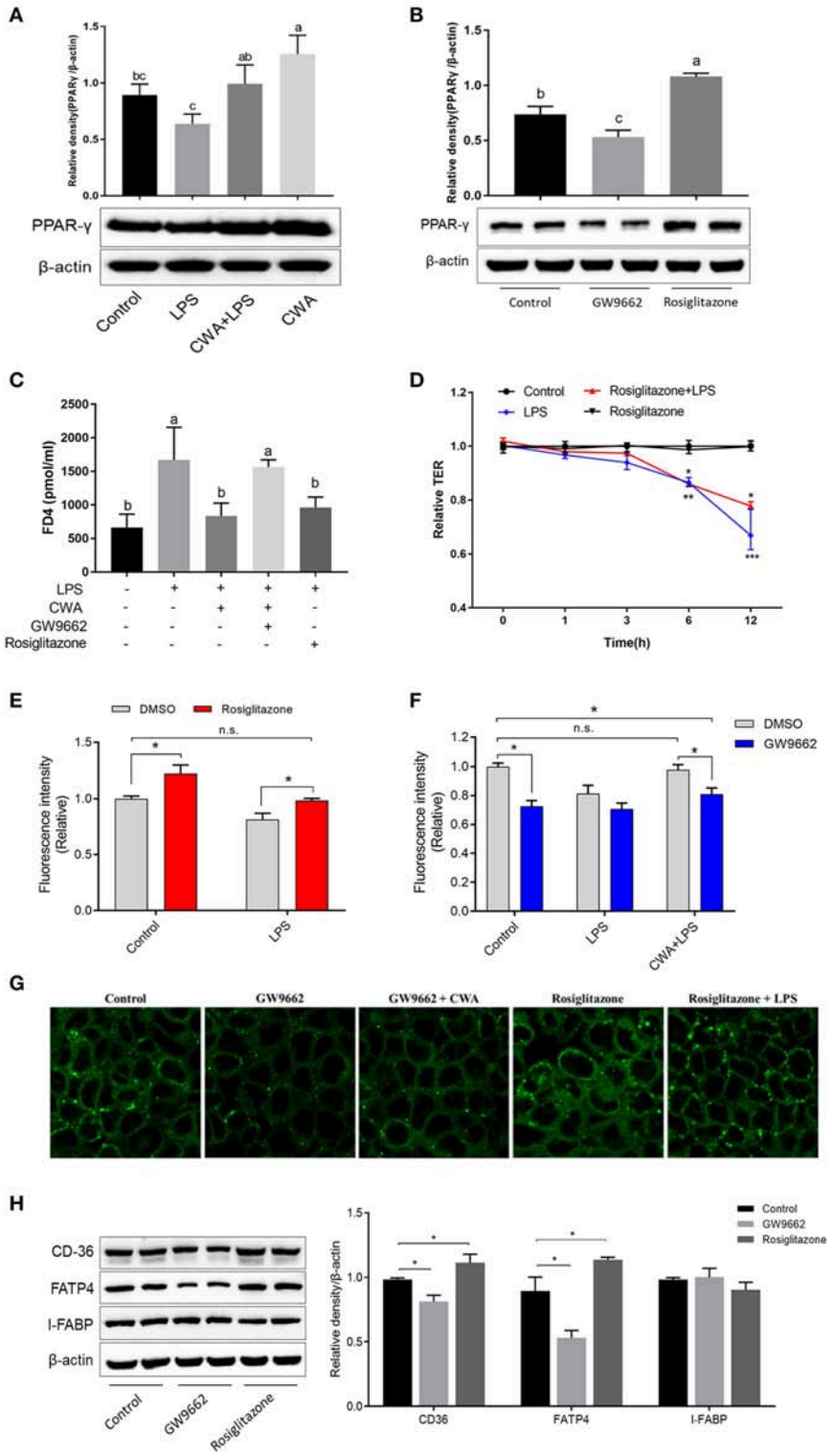


**FIGURE 6 |** CWA facilitated intestinal fatty acid absorption and barrier function through PPAR-γ activation. **(A)** Effect of CWA on PPAR-γ activation. **(B)** Effects of GW9662 and Rosiglitazone on PPAR-γ. The top panel shows the relative levels quantified by densitometry and normalized to β-actin. **(C)** PPAR-γ is essential to the protection effects of CWA on FD4 permeation. **(D)** PPAR-γ activation ameliorates the LPS-induced TEER decrease. **(E)** PPAR-γ activation enhances intestinal fatty acid absorption. **(F)** CWA facilitated intestinal fatty acid absorption dependent on PPAR-γ activation. Fatty acid uptake was assessed by intracellular fluorescence intensity of Bodioy-C16. **(G)** CWA enhanced intestinal fatty acid absorption through activating PPAR-γ. Fatty acid uptake was assessed through intracellular

*(Continued)*

**FIGURE 6 |** fluorescence intensity of BODIPY C16 by fluorescence microscope. **(H)** Western blot analysis of the expression of fatty acid transport proteins after agonist or inhibitor of PPAR-γ treatment. The right panel shows the relative levels quantified by densitometry and normalized to β-actin. The data are expressed as the mean ± SEM, $n = 3$, biological replicates; bars with different small capital letters are statistically different from one another. $^*P < 0.05$, n.s. represented not significant.

barrier after LPS administration when PPAR-γ signaling was inhibited (**Figure 6C**). Comparisons showed that the effect of CWA was similar to that of rosiglitazone (**Figure 6C**). These results indicated that CWA was a potential agonist of PPAR-γ. Moreover, the effect of rosiglitazone on TEER was in line with the effect of CWA, which further confirmed the conclusion that PPAR-γ is a key factor in the effect of CWA on the intestinal barrier (**Figure 6D**).

We further investigated the role of PPAR-γ in the process of fatty acid uptake, which is closely related to barrier function. Based on the result of fatty acid uptake ability, we found that PPAR-γ activation resulted in enhanced fatty acid uptake, regardless of LPS stimulation (**Figure 6E**). These findings were validated with the PPAR-γ inhibitor (**Figure 6F**). Next, we assessed the effects of CWA on fatty acid uptake upon LPS challenge when the expression of PPAR-γ was suppressed. As shown in **Figure 6F**, once the activity of PPAR-γ was inhibited, CWA was not able to maintain the absorption of fatty acids in the cells treated with LPS. In addition, the above conclusions were ascertained visually (**Figure 6G**). At the gene level, consistent with our hypothesis, when the activity of PPAR-γ was inhibited, the expression of FATP4 and CD36 were suppressed. Moreover, the opposite effect was observed with PPAR-γ agonists, which further verified the result (**Figure 6H**).

## DISCUSSION

In our work, sufficient evidence has demonstrated that, in addition to its protective effects on the intestinal barrier, exogenous CWA may act as a PPAR-γ agonist controlling intestinal LCFA absorption. More concretely, we established LPS-induced intestinal barrier dysfunction models in mice and the Caco2 cell line and evaluated the fatty acid uptake capacity of the intestine, which still requires further investigation. Then, we discovered that CWA, a cathelicidin peptide identified in snakes, enhanced LCFA uptake, especially under the pathological state of the intestine. Finally, the molecular mechanism was elucidated, showing that CWA facilitated intestinal fatty acid absorption by enhancing PPAR-γ-dependent barrier function.

LCFAs are well-recognized as fundamental and essential nutrients for human physiology. Most LCFAs are present as esters in phospholipids and triglycerides, forms in which they perform the vital functions of membrane maintenance and energy storage. Our data suggested that CWA enhanced intestinal LCFA uptake *in vivo* and *in vitro*, which was further confirmed by the cellular triglycerides. However, CWA had no effect on the glucose balance. These results indicated that there were different absorption mechanisms between fatty acids and glucose, which was dependent on glucose transporters, such as GLUT family (20). There is debate about the overall fatty acid uptake process and whether one or more membrane-associated proteins could regulate cellular fatty acid uptake (21–23). The theory that transfer to the cytosolic leaflet of the membrane is carried out by a membrane-bound protein is the proposed pathway for the movement of LCFA into cells through the plasma membrane (24, 25). Numerous proteins have been identified for the movement of LCFA across the membrane, such as CD36, FATP, FABP, and caveolin-1 (26–28). Our data suggested that CD36 and FATP4, but not IFABP, were involved in the process of CWA regulating LCFA uptake. To our surprise, unlike the protein level, LPS stimulation significantly increased the mRNA level of IFABP. We speculated that CWA may be involved in the translation of IFABP, which still needs further study. Diacylglycerol O-acyltransferase (DGAT1) 1/2, the key enzymes in triglyceride synthesis (29), were not sensitive to CWA or LPS stimulation. The results indicated that the beneficial effects of CWA were limited to LCFA uptake.

A poorly understood feature of metabolic syndrome is that it is associated with intestinal barrier dysfunction (8, 30). The intestinal barrier is mainly composed of the mucus layer, the epithelial layer, and the underlying lamina propria. Tight junction (TJ) proteins are apical intercellular structures that connect the intestinal epithelial cells and regulate paracellular permeability (31, 32). The core TJ complex, consists of occludin, ZOs, and members of the claudin family. TJ plays a critical role in paracellular permeability by conferring selectivity to the flow of ions, small molecules and solutes between cells, which is important for the responsiveness of cells to directional stimuli and transport functions (33). Therefore, we hypothesized that CWA enhanced fatty acid absorption by strengthening barrier function. As expected, from the results of H&E, TJ structure, and the expression of a TJ marker, we found that CWA effectively attenuated LPS-induced intestinal barrier dysfunction in the jejunum. Furthermore, the results were confirmed in polarized Caco-2 cells cultured in Transwell *in vitro*. Consistent with this finding, previous studies have shown that the cathelicidin peptide cathelicidin-BF attenuates the DSS-induced disruption of mucin expression in the mouse intestine (34). Moreover, LL-37 can enhance epithelial barrier function by regulating Rac1 activation (35). This evidence indicated that the promotion of LCFA uptake by CWA was closely related to its barrier regulation function. However, the direct interaction needs to be further identified by TJ marker gene knockdown.

PPAR-γ is a member of the nuclear hormone receptor superfamily and a ligand-activated transcription factor (36, 37). It plays a critical role in the control of not only adipocyte differentiation, lipid metabolism and immunity but also the barrier functions of epithelial and endothelial cells (37–40). In the present study, in addition to CWA treatment enhancing the

expression of PPAR-γ, similar effects on LCFA uptake and barrier function were also found in cells treated with CWA and the PPAR-γ agonist rosiglitazone. These results suggested that CWA may be a potential agonist of PPAR-γ. More interestingly, once PPAR-γ signaling was inhibited, CWA pretreatment could no longer maintain LCFA uptake and the barrier function after LPS stimulation. Therefore, PPAR-γ was indispensable for CWA to regulate LCFA uptake through enhancing barrier function. Taken together, our results demonstrate that exogenous CWA may thus provide a possible strategy for fatty acid absorption disorder in pathologic conditions.

## DATA AVAILABILITY

The datasets generated for this study are available on request to the corresponding author.

## ETHICS STATEMENT

The animal study was reviewed and approved by Animal Care and Use Committee of Zhejiang University. Written informed consent was obtained from the owners for the participation of their animals in this study.

## AUTHOR CONTRIBUTIONS

XZ, XC, and YW designed the research. XC and HW performed experiments and collected data. XC analyzed the data. XZ wrote the manuscript. XX, YW, and ZL reviewed the manuscript.

## FUNDING

This work was supported by the National Natural Science Foundation of China (Grants 31630075, 31601947).

## ACKNOWLEDGMENTS

The authors thank the Electronic Microscopy Center and Agricultural, Biological, and Environmental Test Center of Zhejiang University for assistance with confocal microscopy and TEM studies.

## REFERENCES

1. Makrides M, Collins CT, Gibson RA. Impact of fatty acid status on growth and neurobehavioural development in humans. *Matern Child Nutr.* (2011) 7 (Suppl. 2):80–8. doi: 10.1111/j.1740-8709.2011.00304.x
2. Wang DQ. Regulation of intestinal cholesterol absorption. *Annu Rev Physiol.* (2007) 69:221–48. doi: 10.1146/annurev.physiol.69.031905.160725
3. Abumrad N, Harmon C, Ibrahimi A. Membrane transport of long-chain fatty acids: evidence for a facilitated process. *J Lipid Res*. (1998) 39:2309–18.
4. Stahl A, Hirsch DJ, Gimeno RE, Punreddy S, Ge P, Watson N, et al. Identification of the major intestinal fatty acid transport protein. *Mol Cell.* (1999) 4:299–308. doi: 10.1016/S1097-2765(00)80332-9
5. Poirier H, Degrace P, Niot I, Bernard A, Besnard P. Localization and regulation of the putative membrane fatty-acid transporter (FAT) in the small intestine. Comparison with fatty acid-binding proteins (FABP). *Eur J Biochem.* (1996) 238:368–73. doi: 10.1111/j.1432-1033.1996.0368z.x
6. Wang TY, Liu M, Portincasa P, Wang DQH. New insights into the molecular mechanism of intestinal fatty acid absorption. *Eur J Clin Invest*. (2013) 43:1203–23. doi: 10.1111/eci.12161
7. Wang HH, Afdhal NH, Gendler SJ, Wang DQ. Lack of the intestinal Muc1 mucin impairs cholesterol uptake and absorption but not fatty acid uptake in Muc1-/- mice. *Am J Physiol Gastrointest Liver Physiol.* (2004) 287:G547–54. doi: 10.1152/ajpgi.00097.2004
8. Thaiss CA, Levy M, Grosheva I, Zheng D, Soffer E, Blacher E, et al. Hyperglycemia drives intestinal barrier dysfunction and risk for enteric infection. *Science*. (2018) 359:1376–83. doi: 10.1126/science.aar3318
9. Odenwald MA, Turner JR. The intestinal epithelial barrier: a therapeutic target? *Nat Rev Gastroenterol Hepatol.* (2017) 14:9–21. doi: 10.1038/nrgastro.2016.169
10. Zong X, Hu WY, Song DG, Li Z, Du HH, Lu ZQ, et al. Porcine lactoferrin-derived peptide LFP-20 protects intestinal barrier by maintaining tight junction complex and modulating inflammatory response. *Biochem Pharmacol*. (2016) 104:74–82. doi: 10.1016/j.bcp.2016.01.009
11. Brogden KA, Ackermann M, McCray PB Jr, Tack BF. Antimicrobial peptides in animals and their role in host defences. *Int J Antimicrob Agents.* (2003) 22:465–78. doi: 10.1016/S0924-8579(03)00180-8
12. Tai EK, Wu WK, Wang XJ, Wong HP, Yu L, Li ZJ, et al. Intrarectal administration of mCRAMP-encoding plasmid reverses exacerbated colitis in Cnlp(-/-) mice. *Gene Ther*. (2013) 20:187–93. doi: 10.1038/gt.2012.22
13. Otte JM, Zdebik AE, Brand S, Chromik AM, Strauss S, Schmitz F, et al. Effects of the cathelicidin LL-37 on intestinal epithelial barrier integrity. *Regul Pept*. (2009) 156:104–17. doi: 10.1016/j.regpep.2009.03.009
14. Yi H, Hu W, Chen S, Lu Z, Wang Y. Cathelicidin-WA improves intestinal epithelial barrier function and enhances host defense against enterohemorrhagic *Escherichia coli* O157:H7 infection. *J Immunol*. (2017) 198:1696–705. doi: 10.4049/jimmunol.1601221
15. Arias-Barrau E, Dirusso CC, Black PN. Methods to monitor fatty acid transport proceeding through vectorial acylation. *Methods Mol Biol.* (2009) 580:233–49. doi: 10.1007/978-1-60761-325-1_13
16. Jang C, Oh SF, Wada S, Rowe GC, Liu L, Chan MC, et al. A branched-chain amino acid metabolite drives vascular fatty acid transport and causes insulin resistance. *Nat Med*. (2016) 22:421–6. doi: 10.1038/nm.4057
17. Chen M, Yang Y, Braunstein E, Georgeson KE, Harmon CM. Gut expression and regulation of FAT/CD36: possible role in fatty acid transport in rat enterocytes. *Am J Physiol Endocrinol Metab.* (2001) 281:E916–23. doi: 10.1152/ajpendo.2001.281.5.E916
18. Ogasawara N, Kojima T, Go M, Ohkuni T, Koizumi J, Kamekura R, et al. PPAR gamma agonists upregulate the barrier function of tight junctions via a PKC pathway in human nasal epithelial cells. *Pharmacol Res*. (2010) 61:489–98. doi: 10.1016/j.phrs.2010.03.002
19. Flores JJ, Klebe D, Rolland WB, Lekic T, Krafft PR, Zhang JH. PPARgamma-induced upregulation of CD36 enhances hematoma resolution and attenuates long-term neurological deficits after germinal matrix hemorrhage in neonatal rats. *Neurobiol Dis*. (2016) 87:124–33. doi: 10.1016/j.nbd.2015.12.015
20. Hebert DN, Carruthers A. Glucose transporter oligomeric structure determines transporter function. Reversible redox-dependent interconversions of tetrameric and dimeric GLUT1. *J Biol Chem.* (1992) 267:23829–38.
21. Su X, Abumrad NA. Cellular fatty acid uptake: a pathway under construction. *Trends Endocrin Met*. (2009) 20:72–7. doi: 10.1016/j.tem.2008.11.001
22. Hamilton JA. New insights into the roles of proteins and lipids in membrane transport of fatty acids. *Prostag Leukotr Ess.* (2007) 77:355–61. doi: 10.1016/j.plefa.2007.10.020
23. Jay AG, Hamilton JA. The enigmatic membrane fatty acid transporter CD36: new insights into fatty acid binding and their effects on uptake of oxidized LDL. *Prostag Leukotr Ess.* (2018) 138:64–70. doi: 10.1016/j.plefa.2016.05.005
24. Abumrad N, Harmon C, Ibrahimi A. Membrane transport of long-chain fatty acids: evidence for a facilitated process. *J Lipid Res.* (1998) 39:2309–18.

25. McArthur MJ, Atshaves BP, Frolov A, Foxworth WD, Kier AB, Schroeder F. Cellular uptake and intracellular trafficking of long chain fatty acids. *J Lipid Res*. (1999) 40:1371–83.
26. Glatz JF, Luiken JJ, Bonen A. Involvement of membrane-associated proteins in the acute regulation of cellular fatty acid uptake. *J Mol Neurosci*. (2001) 16:123–32; discussion 151–7. doi: 10.1385/JMN:16:2-3:123
27. Lobo S, Wiczer BM, Smith AJ, Hall AM, Bernlohr DA. Fatty acid metabolism in adipocytes: functional analysis of fatty acid transport proteins 1 and 4. *J Lipid Res*. (2007) 48:609–20. doi: 10.1194/jlr.M600441-JLR200
28. Trigatti BL, Anderson RGW, Gerber GE. Identification of caveolin-1 as a fatty acid binding protein. *Biochem Bioph Res Co*. (1999) 255:34–9. doi: 10.1006/bbrc.1998.0123
29. Yen CLE, Stone SJ, Koliwad S, Harris C, Farese RV. DGAT enzymes and triacylglycerol biosynthesis. *J Lipid Res*. (2008) 49:2283–301. doi: 10.1194/jlr.R800018-JLR200
30. Winer DA, Luck H, Tsai S, Winer S. The intestinal immune system in obesity and insulin resistance. *Cell Metab*. (2016) 23:413–26. doi: 10.1016/j.cmet.2016.01.003
31. Konig J, Wells J, Cani PD, Garcia-Rodenas CL, MacDonald T, Mercenier A, et al. Human intestinal barrier function in health and disease. *Clin Transl Gastroenterol*. (2016) 7:e196. doi: 10.1038/ctg.2016.54
32. Han F, Zhang H, Xia X, Xiong H, Song D, Zong X, et al. Porcine beta-defensin 2 attenuates inflammation and mucosal lesions in dextran sodium sulfate-induced colitis. *J Immunol*. (2015) 194:1882–93. doi: 10.4049/jimmunol.1402300
33. Bischoff SC, Barbara G, Buurman W, Ockhuizen T, Schulzke JD, Serino M, ewt al. Intestinal permeability–a new target for disease prevention and therapy. *BMC Gastroenterol*. (2014) 14:189. doi: 10.1186/s12876-014-0189-7
34. Zhang H, Xia X, Han F, Jiang Q, Rong Y, Song D, et al. A novel antimicrobial peptide from bungarus fasciatus, attenuates disease in a dextran sulfate sodium model of colitis. *Mol Pharm*. (2015) 12:1648–61. doi: 10.1021/acs.molpharmaceut.5b00069
35. Akiyama T, Niyonsaba F, Kiatsurayanon C, Nguyen TT, Ushio H, Fujimura T, et al. The human cathelicidin LL-37 host defense peptide upregulates tight junction-related proteins and increases human epidermal keratinocyte barrier function. *J Innate Immun*. (2014) 6:739–53. doi: 10.1159/000362789
36. Desvergne B, Wahli W. Peroxisome proliferator-activated receptors: nuclear control of metabolism. *Endocr Rev*. (1999) 20:649–88. doi: 10.1210/edrv.20.5.0380
37. Bensinger SJ, Tontonoz P. Integration of metabolism and inflammation by lipid-activated nuclear receptors. *Nature*. (2008) 454:470–7. doi: 10.1038/nature07202
38. Straus DS, Glass CK. Anti-inflammatory actions of PPAR ligands: new insights on cellular and molecular mechanisms. *Trends Immunol*. (2007) 28:551–8. doi: 10.1016/j.it.2007.09.003
39. Ponferrada, Caso JR, Alou L, Colon A, Sevillano D, Moro MA, et al. The role of PPAR gamma on restoration of colonic homeostasis after experimental stress-induced inflammation and dysfunction. *Gastroenterology*. (2007) 132:1791–803. doi: 10.1053/j.gastro.2007.02.032
40. Huang W, Eum SY, Andras IE, Hennig B, Toborek M. PPAR alpha and PPAR gamma attenuate HIV-induced dysregulation of tight junction proteins by modulations of matrix metalloproteinase and proteasome activities. *Faseb J*. (2009) 23:1596–606. doi: 10.1096/fj.08-121624


**Conflict of Interest Statement:** The authors declare that the research was conducted in the absence of any commercial or financial relationships that could be construed as a potential conflict of interest.

frontiers in Nutrition

REVIEW
published: 27 August 2019
doi: 10.3389/fnut.2019.00140

# Cooperation of Oligodeoxynucleotides and Synthetic Molecules as Enhanced Immune Modulators

*Shireen Nigar*[1] *and Takeshi Shimosato*[2*†]

[1] Department of Nutrition and Food Technology, Jashore University of Science and Technology, Jashore, Bangladesh,
[2] Department of Biomolecular Innovation, Institute for Biomedical Sciences, Shinshu University, Nagano, Japan

Unmethylated cytosine–guanine dinucleotide (CpG) motifs are potent stimulators of the host immune response. Cellular recognition of CpG motifs occurs via Toll-like receptor 9 (TLR9), which normally activates immune responses to pathogen-associated molecular patterns (PAMPs) indicative of infection. Oligodeoxynucleotides (ODNs) containing unmethylated CpGs mimic the immunostimulatory activity of viral/microbial DNA. Synthetic ODNs harboring CpG motifs resembling those identified in viral/microbial DNA trigger an identical response, such that these immunomodulatory ODNs have therapeutic potential. CpG DNA has been investigated as an agent for the management of malignancy, asthma, allergy, and contagious diseases, and as an adjuvant in immunotherapy. In this review, we discuss the potential synergy between synthetic ODNs and other synthetic molecules and their immunomodulatory effects. We also summarize the different synthetic molecules that function as immune modulators and outline the phenomenon of TLR-mediated immune responses. We previously reported a novel synthetic ODN that acts synergistically with other synthetic molecules (including CpG ODNs, the synthetic triacylated lipopeptide $Pam_3CSK_4$, lipopolysaccharide, and zymosan) that could serve as an immune therapy. Additionally, several clinical trials have evaluated the use of CpG ODNs with other immune factors such as granulocyte-macrophage colony-stimulating factor, cytokines, and both endosomal and cell-surface TLR ligands as adjuvants for the augmentation of vaccine activity. Furthermore, we discuss the structural recognition of ODNs by TLRs and the mechanism of functional modulation of TLRs in the context of the potential application of ODNs as wide-spectrum therapeutic agents.

**Keywords: ligands, molecule, ODN, synergy, TLR**

OPEN ACCESS

***Edited by:***
*Pinyi Lu,*
*Biotechnology HPC Software Applications Institute (BHSAI), United States*

***Reviewed by:***
*Margaret J. Lange, University of Missouri, United States*
*Bisheng Zhou, University of Illinois at Chicago, United States*

***Correspondence:**
*Takeshi Shimosato*
*shimot@shinshu-u.ac.jp*

**†ORCID:**
*Takeshi Shimosato*
*orcid.org/0000-0001-8132-1911*

***Specialty section:***
*This article was submitted to Nutritional Immunology, a section of the journal Frontiers in Nutrition*

***Received:*** *17 May 2019*
***Accepted:*** *13 August 2019*
***Published:*** *27 August 2019*

***Citation:***
*Nigar S and Shimosato T (2019) Cooperation of Oligodeoxynucleotides and Synthetic Molecules as Enhanced Immune Modulators. Front. Nutr. 6:140. doi: 10.3389/fnut.2019.00140*

## INTRODUCTION

The immune system provides biosecurity against aggression by pathogens. The human body maintains impediments to prohibit entrance by microbes. Innate and adaptive components are part of the immune system. Innate immune responses provide a prompt response by the body. Innate immune reactions are mediated by Toll-like receptors (TLRs), a representative, evolutionarily conserved group of proteins that are able to induce innate immune reactions,

particularly against bacterial infections, through the recognition of pathogen-associated molecular patterns (PAMPs) (1, 2), to recognize and eradicate invading organisms (3). The germline-encoded pattern recognition receptors (PRRs) recognize conserved molecular patterns that activate the innate immune system. This response is coordinated by specialized cells such as basophils, dendritic cells (DCs), eosinophils, macrophages, monocytes, natural killer (NK) cells, neutrophils, and NKT cells (4). PRRs bind to molecular identification molecules, fundamental structural molecules, or historical segments that are preserved among microbes. This provides the innate immune system with the ability to rapidly counter a comprehensive scope of contagious agents that contact the dermis and mucous membranes.

TLRs are an important family of PRRs that are activated by PAMPs expressed by bacteria, viruses, fungi, and protozoa (5, 6). PAMPs are the key molecules that mediate microbial destruction by processes such as mobilization of phagocytes to infected tissues and microbial killing. TLR family members are classified into two types: cell membrane receptors and endosome-associated receptors. Here, lipoprotein is derived from gram-positive bacteria and induces signaling pathways through TLR2 and other receptors (7, 8). Lipopolysaccharide is a cell wall component of gram-negative bacteria that induces signaling through TLR4 (9). Flagellin (a TLR5 agonist) is derived from the cell wall of *Saccharomyces cerevisiae*. Zymosan, an extract from *S. cerevisiae*, is recognized by another heterodimer, TLR2/6. These TLR agonists act as potent immune stimulators that activate adaptive immune responses as well as recognize microbial components such as lipids, lipoproteins, and flagella. Different types of TLR have different recognition sites. TLR3 recognizes double-stranded RNA, and TLR7/8 recognizes single-stranded RNA. On the other hand, the recognition site of TLR9 is single-stranded synthetic oligodeoxynucleotides (ODNs) or viral/microbial DNA. TLR9 also recognizes unmethylated cytosine-guanine dinucleotide (CpG) motifs (10–13) expressed in the intracellular vesicles of prokaryotic cells (e.g., endoplasmic reticulum, endosomes, and lysosomes).

TLRs are part of a universal group of molecules that consists of extracellular leucine-rich repeats and a cytoplasmic Toll interleukin-1 receptor domain (14). TLRs recognize PAMPs and have specific immune functions. TLR activation initiates and maintains innate and adaptive immune pathways in association with memory function (15). Adapters induce signaling cascades that terminate in the stimulation of nuclear factor kappa B, mitogen-activated protein kinase, and interferon (IFN) regulatory factors 1, 3, 5, and 7 (16). Collectively, these transcription factors induce a variety of cytokines, and chemokines, some of which regulate cellular proliferation, growth, and maintenance. Thus, TLRs are an important group of receptors through which the innate immune system recognizes invasive microorganisms. Here, we discuss the synergistic activities of TLR1/2, TLR4, TLR2/6 with synthetic ODNs in the immune system. Furthermore, we discuss the immune synergistic phenomenon of TLRs in the context of the potential application of ODNs as therapeutic agents.

# OLIGODEOXYNUCLEOTIDES AS IMMUNE MODULATORS

## CpG ODNs

ODNs containing CpG motifs trigger host defense mechanisms that involve both innate and adaptive immune responses. TLR9 recognizes viral/microbial DNA containing CpG motifs, triggering alterations in the cellular redox balance and the induction of cell signaling pathways, including mitogen-activated protein kinase and nuclear factor kappa B (17). Bacterial DNA serves as a PAMP, which is recognized by the vertebrate immune system for coordination of immune responses correlated with immunity (18). CpGs are extremely prevalent in prokaryotic DNA, but rare in eukaryotic DNA (19, 20). Overall, CpG hexamer motifs contain one or more CpG-deoxynucleotides, and the number, position, spacing, and surrounding bases of these motifs mediate their immunostimulatory activities (21–23). These CpG-hexamer motifs also have species-specific activity, which is determined by their structural features and length (18, 24, 25). Another research group explored whether bacterial DNA combines with other bacterial products to trigger the secretion of interleukin (IL)-6, IL-12, IFN-γ, and IgM (26). CpG motifs of synthetic ODNs stimulate B cells (18, 27), NK cells (28, 29), and specialized antigen-presenting cells (APCs) to multiply and/or secrete a variety of cytokines, chemokines, and immunoglobulins (30–32). CpG class A (CpG-A) is particularly effective at stimulating NK cells and inducing production of IFN-α by plasmacytoid dendritic cells (pDCs), whereas CpG class B (CpG-B) is an especially potent B-cell activator. CpG-driven immune activation aggravates inflammatory tissue deterioration, stimulates the advancement of autoimmune disorders, and enhances lethal shock (33–37).

CpG DNA has been sought after as a therapeutic agent and adjuvant immunotherapy for the treatment of cancer, asthma, allergies, and infectious diseases, but this agent frequently involves phosphorothioate or chemical modification. Such modification may lead to imperfections owing to integral toxicity combined with an ephemeral anticoagulant effect, induction of the complement cascade, or inhibition of a primary fibroblast growth component attached to surface receptors due to non-specific protein binding (38). Therefore, CpG DNA can activate Th1 cytokine production, which stimulates a cytotoxic T-cell response with increasing Ig production; this has been observed in the therapy of a wide spectrum of infections, including viral infections and inflammatory disorders (21, 39–41).

Several classes of CpG ODNs exist and are based on structural attributes and immunomodulatory actions. Examples include CpG-A (also known as type D) (42), which induces secretion of IFN-α and stimulates pDC maturation, and monomeric CpG-B (or type K) (42), which induces production of tumor necrosis factor (TNF)- α, promotes pDC maturation, and fully stimulates B cells. Lastly, the dimeric CpG class C (CpG-C) incorporates elements of both CpG-A and CpG-B, albeit with intermediate strength. Different CpG ODNs are assembled CpG-A or CpG-B/C with a phosphorothioate backbone to avoid degradation by serum nucleases and to augment *in vitro* and *in vivo* activity. Apart from CpG-A, CpG-B, and CpG-C,

some researchers have suggested another unique class, P-class CpG ODN (CpG-P) (41), which can induce IFN-α production more than class C ODNs due to inclusion of two palindromic sequences. Therefore, synthetic CpG ODNs are considered to be promising immunomodulators (40).

## Novel Synergistic ODNs

The immunosynergistic effects of ODNs have been established in ODN research. Initially, research was conducted on the immunomodulatory (43), immunosuppressive (44, 45), and immunostimulatory (46) effects of ODNs. In 2017, Nigar et al. explored a novel ODN (named "iSN34") incorporated into *Lactobacillus rhamnosus*, GGATCC53108, that has synergistic effects on the immune response in CpG-induced immune activation (47). The iSN34 sequence is TTCCTAAGCTTGAGGCCT (48). Originally, we evaluated inhibitory or suppressive ODN (iODNs) with a TTAGGG motif. In 2013, Ito et al. successfully designed an effective iODN (designated "iSG3") and revealed that iSG3 has strong immunosuppressive activity (49). As a synergistic ODN, iSN34 could be incorporated with CpG to trigger the production of IL-6 and IL-6-secreting $CD19^+$ B cells. Thus, iSN34 may be an extraordinarily impressive adjuvant-mediated vaccine via Th1 that defends against intracellular pathogens, or iSN34 may provide antibody-mediated immunity compared to extracellular pathogens (47). We also conducted further investigations into the synergistic induction of IL-6 by the consolidation of iSN34 with the cell wall components of bacteria (TLR1/TLR2, TLR4) and fungi (TLR2/TLR6) (48). This review focuses on the synergistic immune effects of combining CpG ODNs with synthetic molecules associated with TLR ligands targeting inflammation and autoimmune diseases.

# IMMUNOTHERAPEUTIC APPLICATION OF ODNS AND OTHER SYNTHETIC MOLECULES

## Prevention and Treatment of Innate and Adaptive Immunity Dysfunction

Innate and adaptive immune responses are two key components of the immune system. Innate immune feedback is recognized as the body's primary defense by which non-specific cells engulf foreign organisms and molecules. Many cells of the immune system (monocytes, macrophages, DCs, neutrophils, eosinophils, basophils) along with NK cells and NKT cells (50) harmonize this response. These specialized cells bind to molecular signatures and are triggered by germline-encoded PRRs, which are fundamental receptors that recognize molecules that are conserved among microbes. This allows the innate immune system to react expeditiously to an extensive spectrum of organisms and protects the dermis and mucous membranes. In the innate immune system, TLRs are recognized as pattern recognition molecules. Alternatively, in the adaptive immune system, APCs are frequently triggered by activation of TLRs, are limited in mobilization, but maintain a remarkably antigen-specific response. This is attained through T-cell and B-cell receptors following somatic recombination. The innate immune system effectively defends humans from an immense spectrum of contaminants by relying on antecedent molecules. Moreover, the innate immune system eliminates the infectious microorganisms that trigger PRRs. Therefore, an equity between stimulation and inhibition must be maintained to provide a secure and potent immune response. Further investigation of the activity and response of the innate immune system will support the design of reliable and efficient therapeutic interventions.

In the vertebrate immune system, viral/microbial DNA that acts as PAMPs coordinates immune responses involving both innate and adaptive immunity. This stimulates the proliferation of B cells and the production of cytokines such as IL-12, IFN-γ, IL-6, and TNF-α, and of co-stimulatory molecules by monocytes/macrophages, B cells, and DCs (51). In this context, the ability of bacterial DNA to induce IL-6 is of particular concern. Immunomodulatory CpG ODNs are currently being assessed to establish the optimum induction of specific cytokine profiles and the activation of individual and mouse immune cells. In 2017, Nigar et al. demonstrated the immune synergistic effects of a combination of a non-CpG ODN (iSN34) and a CpG ODN (CpG-B). The activity of iSN34 was combined with different types of CpG-ODNs. The synergistic effects of iSN34 and CpG-B to stimulate the production of IL-6 would be an immensely effective adjuvant for Th1-mediated vaccines. The combined activity may be advantageous for the avoidance or treatment of inflammatory disorders such as rheumatoid arthritis, inflammatory bowel disease, multiple sclerosis, systemic-onset juvenile chronic arthritis, osteoporosis, and psoriasis (52–54). The synergistic effects of iSN34 and CpG ODN may have the unique ability to target the treatment of systemic inflammatory diseases.

## Use of ODNs as Immunotherapeutics Against Inflammatory Diseases

Inflammation is a vital process in response to injury or infection that occurs through a sequence of events to produce wound healing and maintenance of normal tissue homeostasis. It is a complicated process involving molecular mechanisms that recognize specific molecular patterns associated with infection or tissue injury. The inflammatory response is mediated by key regulators that are proinflammatory molecules. Inflammation involves the contribution of many enzymes and the infiltration of heterogeneous cells that modify chemokine gradients as well as the inflammatory response (55, 56).

Unwanted inflammation occurs regardless of whether consolidation of TLR3/TLR9 agonists leads to IFN-α or B-cell activation or the potentially immunoregulatory function of IL-10 (57). In a model of measles virus pathogenesis, B-cell proliferation and antibody secretion are suppressed not only by maternal antibodies (58, 59), but also by T-cell responses (60–64). The main mechanism of B-cell responses includes the neutralization of live-attenuated vaccines, which reduces epitope masking and interferes with the recognition of antigens by B cells. Then, neutralizing antibodies can only produce a B-cell response when the antibody can attach to the Fcγ IIB receptor

(CD32) on the B-cell surface (65). In 2018, Nigar et al. reported that association of iSN34 with TLR1/2, TLR4, and TLR2/6 induces IL-6, leading to a potent immune response (**Figure 1A**). They also revealed that the effects highlight the potential of TLRs, especially $CD19^+$ cells, as managers of B-cell activation, which performs a vital role in antigen-autonomous evolution and immunology-induced activation of B cells. These results suggest that inflammatory diseases can perhaps be treated by targeting upstream progression in innate immune cells.

## Vaccination

### T-Cell Vaccination

T-cell lymphomas are infrequent, but antagonistic malignancies can occur due to resistance to chemotherapy and chemotoxicity. The combination of melanoma with recurrent spontaneous $CD8^+$ T-cell responses is of clinical concern. In all enrolled patients, T-cell numbers improved following vaccination with Montanite (incomplete Freund's adjuvant, IFA) as an adjuvant treatment, and marked T-cell responses, which are associated with predominant generation of effector-memory-phenotype cells, were observed. Consequently, imiquimod induced a significant increase in the number of key-memory-phenotype cells and larger percentages of $CD127^+$ (IL-7R) T cells in lymphoma, whereas imiquimod and CpG-ODN synergistically induced the growth of effector $CD8^+$ T cells. Another investigation explored the T-cell induction properties associated with various adjuvants (IFA, imiquimod 5%) administered by unusual routes, such as subcutaneous, intradermal, and intranasal. That study did not report any autoimmune-related reactions after introducing immunotherapy with anti-cytotoxic T-lymphocyte-associated protein 4 antibody (ipilimumab) (66). By contrast, our data emphasize that significant proportions of central memory (CM)-phenotype cells ($CD45RA^-CCR7^+$) with enhanced expression of CD127 were induced by imiquimod. Therefore, in triggering the TLR7 agonist, imiquimod may elevate memory differentiation and potential T-cell responses (67–69). Despite the interest in memory cells, insufficient synthetic vaccines have been developed for the treatment of lymphoma. The generation of memory cells may depend on the canonical Wnt pathway with β-catenin/T-cell factor-1, the mammalian target of rapamycin, and AMP-activated protein kinase signaling pathways (67–69). Here, we indicate that the combination of imiquimod and IFA synergistically leads to the enhancement of memory-phenotype cells. This article documented that the synergistic effect of imiquimod and IFA may enhance vaccine efficacy (70), which supports the idea that innate immunity may be triggered via multiple microbe-associated molecular patterns.

### Measles Vaccines

CpG ODNs, which are generally recognized as present in viral/microbial DNA, but are unusual in mammalian DNA, enhance the innate immune response. ODNs and TLR ligands synergistically induce an immune response by triggering different signaling pathways and may affect antigen-dependent T-cell immune memory. Viruses induce type-I IFN through TLR3, TLR7, and TLR9. A combination of TLR3 and TLR9 agonists, which enhance the induction of type I IFN, was tested and found to fully activate the B-cell response after vaccination when assigned to inhibitory MeV-specific IgG. This mechanism suggests that TLR3 and TLR9 signal via the TIR-domain-containing adapter-inducing IFN-α (TRIF)/interferon regulatory factor (IRF)-3 and MyD88/IRF-7 pathways, respectively, as well as IFN-α and IFN-β, respectively. The principal tenet is that an amalgam of these agonists would result in greater induction of type-I IFN because of the synergistic effects mediated through the IFN receptor. This review suggests that the measles vaccine may lead to an optimum antibody response, even though it is reassembled with TLR3 and TLR9 agonists, which may have enormous potential for clinical control. An essential issue that remains unresolved in vaccinology is the inhibition of vaccination against transmittable diseases in humans (71–77) and animals (78–86) by maternal antibodies. In a recent review of measles vaccines in both patients and cotton rats (61), a research group discovered a relevant model of measles virus pathogenesis and affirmed that the proliferation of B cells and secretion of antibodies are suppressed by maternal antibodies (62). In addition, T-cell responses are often noticeable (60, 63, 64, 66, 69). However, the suppressive mechanisms of B-cell responses by maternal antibodies comprise the neutralization of live attenuated vaccines. The neutralization of live attenuated vaccines is not reasonable because the immune response against protein vaccines is further inhibited by maternal antibodies, and B-cell responses can also be suppressed by non-neutralizing antibodies (69) and attach to the Fcγ IIB receptor (CD32) on the surface of B cells (87).

### DNA Vaccine in a Mouse Model of B-Cell Lymphoma

B-cell lymphoma, also known as B-cell non-Hodgkin's lymphoma (NHL), comprises 90% of NHLs, which develop from different stages of B-cell growth and development. NHL is a diverse group of disorders that have divergent ancestral, histologic, and clinical backgrounds. Patients with NHL initially receive treatment with rituximab, a monoclonal anti-CD20 antibody, as well as cyclophosphamide, hydroxydaunorubicin, oncovin, and prednisone. Looking only at lymphoma targets, anti-CD20 contributes to B-cell deficiency through the following three essential mechanisms: (i) initiation of apoptosis, in which anti-CD20 inhibits intracellular signaling pathways; (ii) initiation of complement-dependent cytotoxicity; and (iii) approach to anti-CD20 targeted B cells (generally NK cells or macrophages), thereby stimulating antibody-dependent cytotoxicity (88).

The efficacy of cancer vaccines usually depends on the essential strength of Th1 and Th2 responses prompted by APCs and DCs, respectively. Th1-driven cytotoxic T-cell responses are effective for eradicating tumor cells. However, CpG ODNs, which are universally investigated TLR9 agonists, enhance the Th1 response and likewise result in substantial levels of the anti-inflammatory Th2-promoting cytokine IL-10, which could counteract the increasing Th1 response. Furthermore, concurrent immunotherapy with CpG ODNs

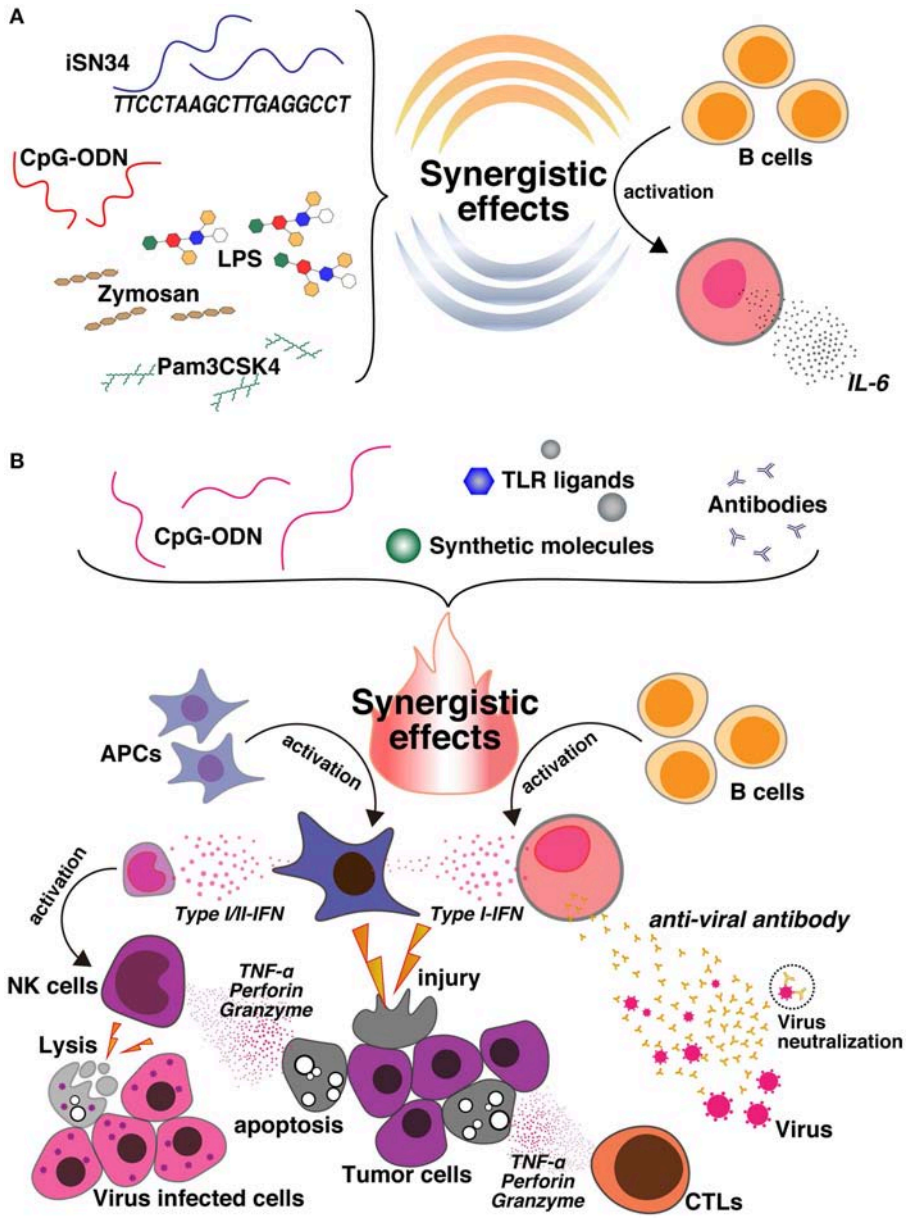


**FIGURE 1 | (A)** CpG ODNs are synergistically activated with a novel ODN, iSN34, and other TLR ligands, such as $Pam_3CSK_4$ (TLR1/2), LPS (TLR4), and Zymosan (TLR2/6). This synergy enhances IL-6 induction and activates B cells. **(B)** Co-delivery of CpG ODNs and different TLR ligands, synthetic molecules, and antibodies produces an immunosynergistic response, which promotes the secretion of Type I/II-IFN cytokines and also the production of B cells. This leads to the generation of tumor-specific antibodies, which may be useful for enhancing antitumor agents, cancer vaccines, and the immunoregulatory effects against inflammatory disorders, as well as enhancing antiviral action and facilitating apoptosis. In contrast, the synergy of CpG and the synthetic molecule also activates NK cells, leads to cell lysis, and is useful for preparing vaccines against virally infected cells.

and IL-10 siRNAs synergistically increases immune protection through a DNA vaccine against B-cell lymphoma in a prophylactic murine model. These outcomes suggest that PAMPs can be administered to modulate TLR ligand-mediated immune stimulation precisely in DCs through the co-delivery of cytokine-silencing siRNAs, thereby boosting antitumor immunity through an idiotype DNA vaccine in a mouse model of B-cell lymphoma.

## Cancer Immunotherapy

### Immunotherapeutics Against Lewis Lung Carcinoma

The TLR9 agonist CpG ODN has shown promise as an effective treatment for infectious disease, allergic disease and to have encouraging antitumor activity mediated by the stimulation of antitumor immunity in numerous animal models. Increasing evidence has shown significant advances in cancer immunotherapy, and numerous strategies have been developed

to deliver a tumor-specific immune response (89). Here, the synergistic effect of a TLR2-neutralizing antibody and a TLR9 agonist CpG ODN was observed to advance coherent immunotherapy against tumor metastasis. The mechanism of action for this combination regimen has been investigated (90). Metastasis treatment with CpG ODNs plus an anti-TLR2 antibody synergistically suppressed and subsequently improved infiltration of NK and cytotoxic T cells, reduced the recruitment of type-2 macrophages and regulatory T cells, and reduced the expression of immunosuppressive factors together with transforming growth factor-β1, cyclooxygenase-2, and indoleamine 2,3-dioxygenase. However, in a metastatic Lewis lung carcinoma mouse model, CpG ODNs and an anti-TLR2 antibody regimen eradicated synergistic immunosuppressive tissues from the tumor environment.

Immunosuppression by the TLR2 and TLR9 combination regimen on host immune and tumor cells for controlling metastatic behavior was associated with a nominal effect on initial subcutaneously embedded tumor growth (91–94). In 2007, Krieg demonstrated that CpG ODNs have a promising anticancer immunotherapeutic ability to trigger Th1 antibodies in the innate and adaptive immune system. On the other hand, TLR2 is an inimitable member of the TLR family because it activates an immunosuppressive response *in vivo* (95). The administration of CpG ODNs also improved the frequency of NK and cytotoxic T lymphocyte (CTL) infiltration, secretion of IFN-γ, and differentiation of M1 cells, but did not reduce the number of regulatory T cells in the spleen (89). These findings show that the synergistic effects of both CpG ODNs and the TLR2-neutralizing antibody are the result of enhanced immune cytotoxicity against tumor cells and show an anti-metastatic effect.

### Evaluation of Tumor Immunization

In this review, we discuss the synergistic activity of CpG ODNs and stimulator of interferon gene (STING)-ligand cyclic guanosine monophosphate-adenosine monophosphate (cGAMP). The STING-cGAMP interaction and CpG ODNs terminate NK cells, lead to production of IFN-γ, have similar effects as IL-12 and type-I IFNs, and are differentially controlled by IRF3/7, STING, and MyD88. The aggregation of CpG ODNs and cGAMP is an effective type-1 adjuvant that leads to robust Th1-type and cytotoxic $CD8^+$ T-cell responses. In murine tumor models, researchers administered intratumorally vaccinated CpG ODNs and cGAMP synergistically, which resulted in a significantly decreased tumor size. This treatment thus functioned as an antigen-free anticancer agent. Moreover, Th1 cells play vital roles in the generation of antitumor immunity, which resulted in suitable activation and effector functions of CTLs, including IFN-γ production (96, 97). Thus, Th1 cells are the key inducers of type-1 immunity and are preeminent in phagocytic activity (98, 99). An important feature of CpG ODNs, mainly D-type CpG ODNs, is that they strongly induce both type-I and type-II IFNs, and are also rather incapable of inducing B-cell activation (42, 46). Taken together, these findings indicate that the synergistic effects induced by K3 CpG and cGAMP may lead to potent activation of NKs and induction of IFN-γ. However, these mechanisms partially rely on IL-12 and type-I IFNs. This review also illustrates that the synergistic effects of CpG ODNs and cGAMP result in a strong antitumor agent, suggesting that synergy may be advantageous for immunotherapeutic applications (100).

### Treatment of B-Cell Chronic Lymphocytic Leukemia

B-cell chronic lymphocytic leukemia (B-CLL) is the most prevalent adult leukemia, targeting mainly older individuals in the U.S., Europe, and Australia (101). Its clinical progression involves stroma-dependent B-CLL growth within lymphoid tissue. Mongini et al. reported that high proliferator status *in vitro* was linked to diminished patient survival with immunohistochemical evidence of apoptotic cells and IL-15-producing cells proximal to B-CLL pseudo-follicles in patients' spleens. They also suggested that ODNs and IL-15 signaling may synergistically promote *in vivo* B-CLL growth. B-CLL depends on TLR9 signals, which led some researchers to investigate whether *in vitro* exposure to CpG ODNs triggers the proliferation of blood-derived B-CLL (102–104), and whether co-stimuli may make TLR9 signals uniformly stimulatory for B cells. IL-15, an inflammatory cytokine produced by endothelial cells (105, 106), is a plausible candidate for promoting the TLR9-triggered growth of B-CLL. However, this cytokine is best known for its major effects on the growth or survival of NK cells, $CD8^+$ T cells, and intra-epithelial γ/σ cells (107, 108). This suggests that the cooperation of CpG ODNs and recombinant human IL-15 may boost the response of B-CLL through TLR9 signaling and the survival of carboxyfluorescein diacetate succinimidyl ester-labeled B-CLL cells with approaches that have yielded important insights concerning clonal growth and the activation-induced death of normal human B cells (109–111).

## CONCLUSION AND FUTURE PERSPECTIVES

This review emphasized the immune activity of CpG ODNs with synthetic molecules to produce an innate and adaptive immune system response. Overall, the results show that the incorporation of CpG ODNs and various synthetic molecules improves humoral and cellular immune responses. Thus, the synergistic effects of CpG ODNs enhance both Th1 and Th2 responses and advances maturation of APCs. This review demonstrated the widespread immune response involving CpG and different synthetic molecules such as granulocyte-macrophage colony-stimulating factor (112), IL-15 (113), the STING ligand (114), Gardiquimod (115), IL-10 siRNA (116), poly (I:C) (57, 117, 118), encapsulated poly(γ-PGA-Phe) (119), imiquimod (120, 121), TLR2-neutralizing antibody (95), and iSN34 (47, 48) (**Table 1**). Furthermore, the application of CpG ODNs and synthetic molecules as adjuvant treatment was demonstrated to improve immunity even in cases with weakened immune systems. Most of the representative studies showed that CpG ODNs and other synthetic molecules induced the immunogenicity of B-cell and effector T-cell responses,

**TABLE 1 |** Synergistic effects of oligodeoxynucleotides combined with synthetic compounds on immunotherapy.

| Synergistic compounds | Activated immune response | Stimulated cells | Regulation of cytokine expression | Immunotherapy | References |
|---|---|---|---|---|---|
| CpG-ODN +GMCSF | Enhanced Th1 response | CD80 and CD86 stimulation | Induced IL-6 and IL-12 | Evaluation in tumor immunization | (112) |
| CpG-ODN +IL-15 | Significant rise in iCa+ followed by rapid apoptosis | $CD38^+$ progeny | IL-2, IL-10 | Treatment of B-CLL | (113) |
| CpG-ODN +STING ligand | Th1 response and suppressed Th2 | Induced $CD8^+$ T cells | IFN-γ, IL-12 | Promising antitumor agent | (114) |
| CpG-ODN +TLR2 neutralizing antibody | Enhanced infiltration of NK cells and CTLs. Reduced type-2 macrophages and Tregs | Production of CD8/CD4 | Suppression of TGF-β1, cyclooxygenase-2, and indoleamine 2,3-dioxygenase | Immunotherapeutic against Lewis lung carcinoma | (95) |
| CpG-ODN (1826) +IL-10 siRNA | Enhanced Th1 response, also induced Th2 | CD86, CD80, and CD40 were expressed at a significantly higher percentage on BMDCs | Upregulated IL-12 p35 and IL-12 p40 in BMDCs | DNA vaccine in a mouse model of B-cell lymphoma | (116) |
| CpG-ODN (2216) +poly I:C (TLR3 ligand) | Enhanced Th1 response | Induced B-cell response | Induced type I-IFN, IL-6, and IL-10 | Use as vaccine Potential immunoregulatory function controlling unwanted inflammation | (57, 118) |
| CpG-ODN +poly I:C (TLR3 ligand) +antigen | Maturation of mAPCs in human immune cells | CD80 and CD86 stimulation | Induced IL-6, type I/II-IFN, IL-12, and TNF-α | Cancer prevention vaccine | (117) |
| CpG-ODN +γ-PGA-Phe (TLR4 stimulator) | Synergistically activated macrophages and induced Th1 response | Antigen-specific IFN-γ-producing T cells | Induced TNF-α | Vaccine delivery and adjuvant system | (119) |
| CpG-A +imiquimod (TLR7 ligand) | Promoted memory cell activation linked to DC activation | Induced effector $CD8^+$ T-cell responses | Upregulation of IFN-α | T-cell vaccination against infections and malignant diseases | (120, 121) |
| CpG-ODN (1826) +gardiquimod (TLR7 ligand) | Induced macrophage tolerance | Negative regulation of SOCS1 | Reduced TNF-α and IL-6 expression | Impaired response in chronic viral infection | (115) |
| CpG-ODN (MsST) +iSN34 | Enhanced Th1 response | Production of $CD19^+IL\text{-}6^+$ cells | Induced IL-6 expression | Prevention or treatment of dysfunction of innate and adaptive immunity | (47) |
| iSN34 +$Pam_3CSK_4$ (TLR1/2 ligand), LPS (TLR4 ligand), and zymosan (TLR2/6) ligands | Enhanced Th1 response | Production of $CD19^+IL\text{-}6^+$ cells | Induced IL-6 expression | Use as agonists and novel therapeutics for inflammatory diseases driven by TLR-mediated immune activation | (48) |

*This table lists representative examples of the synergistic activity of ODNs with other molecules and the immunomodulatory activity of the abovementioned immunosynergistic effects. GMCSF, granulocyte macrophage colony-stimulating factor; B-CLL, B-cell chronic lymphocytic leukemia; TGF, transforming growth factor; CTL, cytotoxic T lymphocyte; Treg, regulatory T cell; STING, stimulator of interferon genes; LPS, lipopolysaccharide; poly (I:C), polyinosinic-polycytidylic acid; DC, dendritic cell; IFN, interferon; SOCS1, suppressor of cytokine signaling 1; TNF, tumor necrosis factor; $Pam_3CSK_4$, synthetic triacylated lipopeptide; Th1, T helper type 1.*

macrophage stimulation, and antigen-specific IFN-γ-producing T cells. Therefore, the synergistic activity of CpG DNA and the abovementioned synthetic molecules can induce Th1 cytokine production, thereby stimulating CTLs with increasing Ig production. These activities play a role in the treatment of an extensive spectrum of diseases, comprising cancer, viral and bacterial infections, allergic diseases, and inflammatory disorders (21, 35, 122, 123). Interestingly, these studies also confirmed the clear synergistic activity of TLR9 agonist CpG ODNs and different synthetic molecules (**Figure 1B**), which may be effective for enhancing immunoregulation in inflammatory disorders, or for heat-killed *Brucella abortus* (HKBa) treatment, antitumor agents, DNA vaccines for B-CLL, measles vaccines, T-cell vaccines, cancer vaccines, and treatment of Lewis lung carcinoma, as well as antiviral action. Patients administered adjuvanted vaccines produced stronger antigen-specific serum antibodies and $CD8^+$ and $CD4^+$ T-cell responses. Anticancer immunity was produced more quickly

in cases immunized with CpG-adjuvanted vaccines (124). However, the immune effects varied, and the effects of CpG ODNs and other immune factors, such as the frequency of NK cells or DCs, were seldom reproducible (100, 125–128). Certainly, demonstrating that the vaccine/adjuvant formulations (synergistic CpG ODNs and synthetic molecules) examined reproducibly change the advancement of tumors is essential. Of greater importance, the immune responses observed barely corresponded to clinical assumptions.

Based on the results outlined above, we considered the immunological aspects and ability of vaccine adjuvants to be suitable for use in antitumor immunotherapy, because the mechanisms of activity have been observed *in vitro* and *in vivo*. Additionally, this combination should be evaluated *in vivo* by estimating the initiation of antigen-specific T-cell and B-cell responses after combination immunization in an immunization model. Therefore, our results provide insight into the processes of the associated response of TLR9 and specific synthetic molecules, which potentially encourage the immunotherapeutic and adjuvant equities of their combination.

## AUTHOR CONTRIBUTIONS

SN and TS conceived, designed, and wrote the manuscript.

## FUNDING

The review was funded by a Grant-in-Aid for Scientific Research (B) (No. 17H03907) from the Japan Society for the Promotion of Science (JSPS) to TS.

## ACKNOWLEDGMENTS

The iSN34 study mentioned in this review is based on the doctorate thesis by SN from Shinshu University, Japan. The new knowledge from the iSN34 study was described in this review and may be a therapeutic advancement in immunology research.

## REFERENCES

1. Akira S, Takeda K, Kaisho T. Toll-like receptors: critical proteins linking innate and acquired immunity. *Nat Immunol*. (2001) 2:675–80. doi: 10.1038/90609
2. Takeda K, Akira S. Roles of Toll-like receptors in innate immune responses. *Genes Cells*. (2001) 6:733–42. doi: 10.1046/j.1365-2443.2001.00458.x
3. Akira S, Hemmi H. Recognition of pathogen-associated molecular patterns by TLR family. *Immunol Lett*. (2003) 85:85–95. doi: 10.1016/S0165-2478(02)00228-6
4. Medzhitov R, Janeway CA Jr. Innate immunity: impact on the adaptive immune response. *Curr Opin Immunol*. (1997) 9:4–9. doi: 10.1016/S0952-7915(97)80152-5
5. Kumagai Y, Takeuchi O, Akira S. Pathogen recognition by innate receptors. *J Infect Chemother*. (2008) 14:86–92. doi: 10.1007/s10156-008-0596-1
6. Takeda K, Kaisho T, Akira S. Toll-like receptors. *Annu Rev Immunol*. (2003) 21:335–76. doi: 10.1146/annurev.immunol.21.120601.141126
7. Kaisho T, Akira S. Toll-like receptors and their signaling mechanism in innate immunity. *Acta Odontol Scand*. (2001) 59:124–30. doi: 10.1080/000163501750266701
8. Patel M, Xu D, Kewin P, Choo-Kang B, McSharry C, Thomson NC, et al. TLR2 agonist ameliorates established allergic airway inflammation by promoting Th1 response and not via regulatory T cells. *J Immunol*. (2005) 174:7558–63. doi: 10.4049/jimmunol.174.12.7558
9. Akashi S, Shimazu R, Ogata H, Nagai Y, Takeda K, Kimoto M, et al. Cutting edge: cell surface expression and lipopolysaccharide signaling via the toll-like receptor 4-MD-2 complex on mouse peritoneal macrophages. *J Immunol*. (2000) 164:3471–5. doi: 10.4049/jimmunol.164.7.3471
10. Alexopoulou L, Holt AC, Medzhitov R, Flavell RA. Recognition of double-stranded RNA and activation of NF-kappaB by Toll-like receptor 3. *Nature*. (2001) 413:732–8. doi: 10.1038/35099560
11. Heil F, Hemmi H, Hochrein H, Ampenberger F, Kirschning C, Akira S, et al. Species-specific recognition of single-stranded RNA via toll-like receptor 7 and 8. *Science*. (2004) 303:1526–9. doi: 10.1126/science.1093620
12. Kawai T, Akira S. The role of pattern-recognition receptors in innate immunity: update on Toll-like receptors. *Nat Immunol*. (2010) 11:373–84. doi: 10.1038/ni.1863
13. Takeshita F, Leifer CA, Gursel I, Ishii KJ, Takeshita S, Gursel M, et al. Cutting edge: role of Toll-like receptor 9 in CpG DNA-induced activation of human cells. *J Immunol*. (2001) 167:3555–8. doi: 10.4049/jimmunol.167.7.3555
14. Matsushima N, Tanaka T, Enkhbayar P, Mikami T, Taga M, Yamada K, et al. Comparative sequence analysis of leucine-rich repeats (LRRs) within vertebrate toll-like receptors. *BMC Genomics*. (2007) 8:124. doi: 10.1186/1471-2164-8-124
15. Schmidlin H, Diehl SA, Blom B. New insights into the regulation of human B-cell differentiation. *Trends Immunol*. (2009) 30:277–85. doi: 10.1016/j.it.2009.03.008
16. Fitzgerald KA, Rowe DC, Barnes BJ, Caffrey DR, Visintin A, Latz E, et al. LPS-TLR4 signaling to IRF-3/7 and NF-kappaB involves the toll adapters TRAM and TRIF. *J Exp Med*. (2003) 198:1043–55. doi: 10.1084/jem.20031023
17. Krieg AM. CpG motifs in bacterial DNA and their immune effects. *Annu Rev Immunol*. (2002) 20:709–60. doi: 10.1146/annurev.immunol.20.100301.064842
18. Krieg AM, Yi AK, Matson S, Waldschmidt TJ, Bishop GA, Teasdale R, et al. CpG motifs in bacterial DNA trigger direct B-cell activation. *Nature*. (1995) 374:546–9. doi: 10.1038/374546a0
19. Cardon LR, Burge C, Clayton DA, Karlin S. Pervasive CpG suppression in animal mitochondrial genomes. *Proc Natl Acad Sci USA*. (1994) 91:3799–803. doi: 10.1073/pnas.91.9.3799
20. Razin A, Friedman J. DNA methylation and its possible biological roles. *Prog Nucleic Acid Res Mol Biol*. (1981) 25:33–52. doi: 10.1016/S0079-6603(08)60482-1
21. Klinman DM, Yi AK, Beaucage SL, Conover J, Krieg AM. CpG motifs present in bacteria DNA rapidly induce lymphocytes to secrete interleukin 6, interleukin 12, and interferon gamma. *Proc Natl Acad Sci USA*. (1996) 93:2879–83. doi: 10.1073/pnas.93.7.2879
22. Pisetsky DS. Immune responses to DNA in normal and aberrant immunity. *Immunol Res*. (2000) 22:119–26. doi: 10.1385/IR:22:2-3:119
23. Yamamoto M, Yoshizaki K, Kishimoto T, Ito H. IL-6 is required for the development of Th1 cell-mediated murine colitis. *J Immunol*. (2000) 164:4878–82. doi: 10.4049/jimmunol.164.9.4878
24. Bauer M, Redecke V, Ellwart JW, Scherer B, Kremer JP, Wagner H, et al. Bacterial CpG-DNA triggers activation and maturation of human CD11c-, CD123+ dendritic cells. *J Immunol*. (2001) 166:5000–7. doi: 10.4049/jimmunol.166.8.5000
25. Chuang TH, Lee J, Kline L, Mathison JC, Ulevitch RJ. Toll-like receptor 9 mediates CpG-DNA signaling. *J Leukoc Biol*. (2002) 71:538–44.
26. Yi AK, Klinman DM, Martin TL, Matson S, Krieg AM. Rapid immune activation by CpG motifs in bacterial DNA. Systemic induction of IL-6 transcription through an antioxidant-sensitive pathway. *J Immunol*. (1996) 157:5394–402.
27. Ballas ZK, Rasmussen WL, Krieg AM. Induction of NK activity in murine and human cells by CpG motifs in oligodeoxynucleotides and bacterial DNA. *J Immunol*. (1996) 157:1840–5.

28. Sparwasser T, Miethke T, Lipford G, Erdmann A, Hacker H, Heeg K, et al. Macrophages sense pathogens via DNA motifs: induction of tumor necrosis factor-alpha-mediated shock. *Eur J Immunol*. (1997) 27:1671–9. doi: 10.1002/eji.1830270712
29. Verthelyi D, Ishii KJ, Gursel M, Takeshita F, Klinman DM. Human peripheral blood cells differentially recognize and respond to two distinct CPG motifs. *J Immunol*. (2001) 166:2372–7. doi: 10.4049/jimmunol.166.4.2372
30. Behboudi S, Chao D, Klenerman P, Austyn J. The effects of DNA containing CpG motif on dendritic cells. *Immunology*. (2000) 99:361–6. doi: 10.1046/j.1365-2567.2000.00979.x
31. Sparwasser T, Koch ES, Vabulas RM, Heeg K, Lipford GB, Ellwart JW, et al. Bacterial DNA and immunostimulatory CpG oligonucleotides trigger maturation and activation of murine dendritic cells. *Eur J Immunol*. (1998) 28:2045–54.
32. Stacey KJ, Sweet MJ, Hume DA. Macrophages ingest and are activated by bacterial DNA. *J Immunol*. (1996) 157:2116–22.
33. Cowdery JS, Chace JH, Yi AK, Krieg AM. Bacterial DNA induces NK cells to produce IFN-gamma *in vivo* and increases the toxicity of lipopolysaccharides. *J Immunol*. (1996) 156:4570–5.
34. Deng GM, Nilsson IM, Verdrengh M, Collins LV, Tarkowski A. Intra-articularly localized bacterial DNA containing CpG motifs induces arthritis. *Nat Med*. (1999) 5:702–5. doi: 10.1038/9554
35. Heikenwalder M, Polymenidou M, Junt T, Sigurdson C, Wagner H, Akira S, et al. Lymphoid follicle destruction and immunosuppression after repeated CpG oligodeoxynucleotide administration. *Nat Med*. (2004) 10:187–92. doi: 10.1038/nm987
36. Sparwasser T, Miethke T, Lipford G, Borschert K, Hacker H, Heeg K, et al. Bacterial DNA causes septic shock. *Nature*. (1997) 386:336–7. doi: 10.1038/386336a0
37. Zeuner RA, Verthelyi D, Gursel M, Ishii KJ, Klinman DM. Influence of stimulatory and suppressive DNA motifs on host susceptibility to inflammatory arthritis. *Arthritis Rheum*. (2003) 48:1701–7. doi: 10.1002/art.11035
38. Henry AJ, Cook JP, McDonnell JM, Mackay GA, Shi J, Sutton BJ, et al. Participation of the N-terminal region of Cepsilon3 in the binding of human IgE to its high-affinity receptor FcepsilonRI. *Biochemistry*. (1997) 36:15568–78. doi: 10.1021/bi971299+
39. Kandimalla ER, Yu D, Agrawal S. Towards optimal design of second-generation immunomodulatory oligonucleotides. *Curr Opin Mol Ther*. (2002) 4:122–9.
40. Krieg AM. Therapeutic potential of Toll-like receptor 9 activation. *Nat Rev Drug Discov*. (2006) 5:471–84. doi: 10.1038/nrd2059
41. Samulowitz U, Weber M, Weeratna R, Uhlmann E, Noll B, Krieg AM, et al. A novel class of immune-stimulatory CpG oligodeoxynucleotides unifies high potency in type I interferon induction with preferred structural properties. *Oligonucleotides*. (2010) 20:93–101. doi: 10.1089/oli.2009.0210
42. Klinman DM. Immunotherapeutic uses of CpG oligodeoxynucleotides. *Nat Rev Immunol*. (2004) 4:249–58. doi: 10.1038/nri1329
43. Wang Y, Yamamoto Y, Shigemori S, Watanabe T, Oshiro K, Wang X, et al. Inhibitory/suppressive oligodeoxynucleotide nanocapsules as simple oral delivery devices for preventing atopic dermatitis in mice. *Mol Ther*. (2015) 23:297–309. doi: 10.1038/mt.2014.239
44. Sato T, Yamamoto M, Shimosato T, Klinman DM. Accelerated wound healing mediated by activation of Toll-like receptor 9. *Wound Repair Regen*. (2010) 18:586–93. doi: 10.1111/j.1524-475X.2010.00632.x
45. Shirota H, Gursel I, Gursel M, Klinman DM. Suppressive oligodeoxynucleotides protect mice from lethal endotoxic shock. *J Immunol*. (2005) 174:4579–83. doi: 10.4049/jimmunol.174.8.4579
46. Wooldridge JE, Ballas Z, Krieg AM, Weiner GJ. Immunostimulatory oligodeoxynucleotides containing CpG motifs enhance the efficacy of monoclonal antibody therapy of lymphoma. *Blood*. (1997) 89:2994–8.
47. Nigar S, Yamamoto Y, Okajima T, Shigemori S, Sato T, Ogita T, et al. Synergistic oligodeoxynucleotide strongly promotes CpG-induced interleukin-6 production. *BMC Immunol*. (2017) 18:44. doi: 10.1186/s12865-017-0227-7
48. Nigar S, Yamamoto Y, Okajima T, Sato T, Ogita T, Shimosato T. Immune synergistic oligodeoxynucleotide from *Lactobacillus rhamnosus* GG enhances the immune response upon co-stimulation by bacterial and fungal cell wall components. *Anim Sci J*. (2018) 89:1504–11. doi: 10.1111/asj.13082
49. Ito Y, Shigemori S, Sato T, Shimazu T, Hatano K, Otani H, et al. Class I/II hybrid inhibitory oligodeoxynucleotide exerts Th1 and Th2 double immunosuppression. *FEBS Open Bio*. (2013) 3:41–5. doi: 10.1016/j.fob.2012.11.002
50. Megjugorac NJ, Young HA, Amrute SB, Olshalsky SL, Fitzgerald-Bocarsly P. Virally stimulated plasmacytoid dendritic cells produce chemokines and induce migration of T and NK cells. *J Leukoc Biol*. (2004) 75:504–14. doi: 10.1189/jlb.0603291
51. Zhao Q, Temsamani J, Zhou RZ, Agrawal S. Pattern and kinetics of cytokine production following administration of phosphorothioate oligonucleotides in mice. *Antisense Nucleic Acid Drug Dev*. (1997) 7:495–502. doi: 10.1089/oli.1.1997.7.495
52. Atreya R, Mudter J, Finotto S, Mullberg J, Jostock T, Wirtz S, et al. Blockade of interleukin 6 trans signaling suppresses T-cell resistance against apoptosis in chronic intestinal inflammation: evidence in crohn disease and experimental colitis *in vivo*. *Nat Med*. (2000) 6:583–8. doi: 10.1038/75068
53. Collins LE, DeCourcey J, Rochfort KD, Kristek M, Loscher CE. A role for syntaxin 3 in the secretion of IL-6 from dendritic cells following activation of toll-like receptors. *Front Immunol*. (2014) 5:691. doi: 10.3389/fimmu.2014.00691
54. Ulevitch RJ, Tobias PS. Receptor-dependent mechanisms of cell stimulation by bacterial endotoxin. *Annu Rev Immunol*. (1995) 13:437–57. doi: 10.1146/annurev.iy.13.040195.002253
55. Nahrendorf M, Swirski FK, Aikawa E, Stangenberg L, Wurdinger T, Figueiredo JL, et al. The healing myocardium sequentially mobilizes two monocyte subsets with divergent and complementary functions. *J Exp Med*. (2007) 204:3037–47. doi: 10.1084/jem.20070885
56. Swirski FK, Nahrendorf M. Leukocyte behavior in atherosclerosis, myocardial infarction, and heart failure. *Science*. (2013) 339:161–6. doi: 10.1126/science.1230719
57. Kim D, Niewiesk S. Synergistic induction of interferon alpha through TLR-3 and TLR-9 agonists identifies CD21 as interferon alpha receptor for the B cell response. *PLoS Pathog*. (2013) 9:e1003233. doi: 10.1371/journal.ppat.1003233
58. Gans HA, Arvin AM, Galinus J, Logan L, DeHovitz R, Maldonado Y. Deficiency of the humoral immune response to measles vaccine in infants immunized at age 6 months. *JAMA*. (1998) 280:527–32. doi: 10.1001/jama.280.6.527
59. Naniche D. Human immunology of measles virus infection. *Curr Top Microbiol Immunol*. (2009) 330:151–71. doi: 10.1007/978-3-540-70617-5_8
60. Gans H, DeHovitz R, Forghani B, Beeler J, Maldonado Y, Arvin AM. Measles and mumps vaccination as a model to investigate the developing immune system: passive and active immunity during the first year of life. *Vaccine*. (2003) 21:3398–405. doi: 10.1016/S0264-410X(03)00341-4
61. Gans H, Yasukawa L, Rinki M, DeHovitz R, Forghani B, Beeler J, et al. Immune responses to measles and mumps vaccination of infants at 6, 9, and 12 months. *J Infect Dis*. (2001) 184:817–26. doi: 10.1086/323346
62. Gans HA, Maldonado Y, Yasukawa LL, Beeler J, Audet S, Rinki MM, et al. IL-12, IFN-gamma, and T cell proliferation to measles in immunized infants. *J Immunol*. (1999) 162:5569–75.
63. Pueschel K, Tietz A, Carsillo M, Steward M, Niewiesk S. Measles virus-specific CD4 T-cell activity does not correlate with protection against lung infection or viral clearance. *J Virol*. (2007) 81:8571–8. doi: 10.1128/JVI.00160-07
64. Siegrist CA, Barrios C, Martinez X, Brandt C, Berney M, Cordova M, et al. Influence of maternal antibodies on vaccine responses: inhibition of antibody but not T cell responses allows successful early prime-boost strategies in mice. *Eur J Immunol*. (1998) 28:4138–48.
65. Kim D, Huey D, Oglesbee M, Niewiesk S. Insights into the regulatory mechanism controlling the inhibition of vaccine-induced seroconversion by maternal antibodies. *Blood*. (2011) 117:6143–51. doi: 10.1182/blood-2010-11-320317
66. Bouwhuis MG, Ten Hagen TL, Suciu S, Eggermont AM. Autoimmunity and treatment outcome in melanoma. *Curr Opin Oncol*. (2011) 23:170–6. doi: 10.1097/CCO.0b013e328341edff

67. Araki K, Youngblood B, Ahmed R. The role of mTOR in memory CD8 T-cell differentiation. *Immunol Rev*. (2010) 235:234–43. doi: 10.1111/j.0105-2896.2010.00898.x
68. Finlay D, Cantrell DA. Metabolism, migration and memory in cytotoxic T cells. *Nat Rev Immunol*. (2011) 11:109–17. doi: 10.1038/nri2888
69. Gattinoni L, Zhong XS, Palmer DC, Ji Y, Hinrichs CS, Yu Z, et al. Wnt signaling arrests effector T cell differentiation and generates CD8+ memory stem cells. *Nat Med*. (2009) 15:808–13. doi: 10.1038/nm.1982
70. Kasturi SP, Skountzou I, Albrecht RA, Koutsonanos D, Hua T, Nakaya HI, et al. Programming the magnitude and persistence of antibody responses with innate immunity. *Nature*. (2011) 470:543–7. doi: 10.1038/nature09737
71. Bjorkholm B, Granstrom M, Taranger J, Wahl M, Hagberg L. Influence of high titers of maternal antibody on the serologic response of infants to diphtheria vaccination at three, five and twelve months of age. *Pediatr Infect Dis J*. (1995) 14:846–50. doi: 10.1097/00006454-199510000-00005
72. Dagan R, Amir J, Mijalovsky A, Kalmanovitch I, Bar-Yochai A, Thoelen S, et al. Immunization against hepatitis A in the first year of life: priming despite the presence of maternal antibody. *Pediatr Infect Dis J*. (2000) 19:1045–52. doi: 10.1097/00006454-200011000-00004
73. del Canho R, Grosheide PM, Mazel JA, Heijtink RA, Hop WC, Gerards LJ, et al. Ten-year neonatal hepatitis B vaccination program, The Netherlands, 1982–1992: protective efficacy and long-term immunogenicity. *Vaccine*. (1997) 15:1624–30. doi: 10.1016/S0264-410X(97)00080-7
74. Englund JA, Anderson EL, Reed GF, Decker MD, Edwards KM, Pichichero ME, et al. The effect of maternal antibody on the serologic response and the incidence of adverse reactions after primary immunization with acellular and whole-cell pertussis vaccines combined with diphtheria and tetanus toxoids. *Pediatrics*. (1995) 96(Pt 2):580–4.
75. Letson GW, Shapiro CN, Kuehn D, Gardea C, Welty TK, Krause DS, et al. Effect of maternal antibody on immunogenicity of hepatitis A vaccine in infants. *J Pediatr*. (2004) 144:327–32. doi: 10.1016/j.jpeds.2003.11.030
76. Sormunen H, Stenvik M, Eskola J, Hovi T. Age- and dose-interval-dependent antibody responses to inactivated poliovirus vaccine. *J Med Virol*. (2001) 63:305–10.
77. Trollfors B. Factors influencing antibody responses to acellular pertussis vaccines. *Dev Biol Stand*. (1997) 89:279–82.
78. Bradshaw BJ, Edwards S. Antibody isotype responses to experimental infection with bovine herpesvirus 1 in calves with colostrally derived antibody. *Vet Microbiol*. (1996) 53:143–51. doi: 10.1016/S0378-1135(96)01242-4
79. Ellis JA, Gow SP, Goji N. Response to experimentally induced infection with bovine respiratory syncytial virus following intranasal vaccination of seropositive and seronegative calves. *J Am Vet Med Assoc*. (2010) 236:991–9. doi: 10.2460/javma.236.9.991
80. Fulton RW, Briggs RE, Payton ME, Confer AW, Saliki JT, Ridpath JF, et al. Maternally derived humoral immunity to bovine viral diarrhea virus (BVDV) 1a, BVDV1b, BVDV2, bovine herpesvirus-1, parainfluenza-3 virus bovine respiratory syncytial virus, Mannheimia haemolytica and *Pasteurella multocida* in beef calves, antibody decline by half-life studies and effect on response to vaccination. *Vaccine*. (2004) 22:643–9. doi: 10.1016/j.vaccine.2003.08.033
81. Klinkenberg D, Moormann RJ, de Smit AJ, Bouma A, de Jong MC. Influence of maternal antibodies on efficacy of a subunit vaccine: transmission of classical swine fever virus between pigs vaccinated at 2 weeks of age. *Vaccine*. (2002) 20:3005–13. doi: 10.1016/S0042-207X(02)00283-X
82. Mondal SP, Naqi SA. Maternal antibody to infectious bronchitis virus: its role in protection against infection and development of active immunity to vaccine. *Vet Immunol Immunopathol*. (2001) 79:31–40. doi: 10.1016/S0165-2427(01)00248-3
83. van der Sluijs MT, Kuhn EM, Makoschey B. A single vaccination with an inactivated bovine respiratory syncytial virus vaccine primes the cellular immune response in calves with maternal antibody. *BMC Vet Res*. (2010) 6:2. doi: 10.1186/1746-6148-6-2
84. van Maanen C, Bruin G, de Boer-Luijtze E, Smolders G, de Boer GF. Interference of maternal antibodies with the immune response of foals after vaccination against equine influenza. *Vet Q*. (1992) 14:13–7. doi: 10.1080/01652176.1992.9694319
85. Waner T, Naveh A, Ben Meir NS, Babichev Z, Carmichael LE. Assessment of immunization response to canine distemper virus vaccination in puppies using a clinic-based enzyme-linked immunosorbant assay. *Vet J*. (1998) 155:171–5. doi: 10.1016/S1090-0233(98)80013-0
86. Waner T, Naveh A, Wudovsky I, Carmichael LE. Assessment of maternal antibody decay and response to canine parvovirus vaccination using a clinic-based enzyme-linked immunosorbent assay. *J Vet Diagn Invest*. (1996) 8:427–32. doi: 10.1177/104063879600800404
87. Eidson CS, Thayer SG, Villegas P, Kleven SH. Vaccination of broiler chicks from breeder flocks immunized with a live or inactivated oil emulsion Newcastle disease vaccine. *Poult Sci*. (1982) 61:1621–9. doi: 10.3382/ps.0611621
88. Huang H, Hao S, Li F, Ye Z, Yang J, Xiang J. CD4+ Th1 cells promote CD8+ Tc1 cell survival, memory response, tumor localization and therapy by targeted delivery of interleukin 2 via acquired pMHC I complexes. *Immunology*. (2007) 120:148–59. doi: 10.1111/j.1365-2567.2006.02452.x
89. King J, Waxman J, Stauss H. Advances in tumour immunotherapy. *QJM*. (2008) 101:675–83. doi: 10.1093/qjmed/hcn050
90. Yang HZ, Cui B, Liu HZ, Mi S, Yan J, Yan HM, et al. Blocking TLR2 activity attenuates pulmonary metastases of tumor. *PLoS ONE*. (2009) 4:e6520. doi: 10.1371/journal.pone.0006520
91. Kim S, Takahashi H, Lin WW, Descargues P, Grivennikov S, Kim Y, et al. Carcinoma-produced factors activate myeloid cells through TLR2 to stimulate metastasis. *Nature*. (2009) 457:102–6. doi: 10.1038/nature07623
92. Netea MG, Van der Meer JW, Kullberg BJ. Toll-like receptors as an escape mechanism from the host defense. *Trends Microbiol*. (2004) 12:484–8. doi: 10.1016/j.tim.2004.09.004
93. Wang C, Cao S, Yan Y, Ying Q, Jiang T, Xu K, et al. TLR9 expression in glioma tissues correlated to glioma progression and the prognosis of GBM patients. *BMC Cancer*. (2010) 10:415. doi: 10.1186/1471-2407-10-415
94. Xie W, Wang Y, Huang Y, Yang H, Wang J, Hu Z. Toll-like receptor 2 mediates invasion via activating NF-kappaB in MDA-MB-231 breast cancer cells. *Biochem Biophys Res Commun*. (2009) 379:1027–32. doi: 10.1016/j.bbrc.2009.01.009
95. Yan J, Hua F, Liu HZ, Yang HZ, Hu ZW. Simultaneous TLR2 inhibition and TLR9 activation synergistically suppress tumor metastasis in mice. *Acta Pharmacol Sin*. (2012) 33:503–12. doi: 10.1038/aps.2011.193
96. Mantovani A, Sica A. Macrophages, innate immunity and cancer: balance, tolerance, and diversity. *Curr Opin Immunol*. (2010) 22:231–7. doi: 10.1016/j.coi.2010.01.009
97. Spellberg B, Edwards JE Jr. Type 1/Type 2 immunity in infectious diseases. *Clin Infect Dis*. (2001) 32:76–102. doi: 10.1086/317537
98. Hung K, Hayashi R, Lafond-Walker A, Lowenstein C, Pardoll D, Levitsky H. The central role of CD4(+) T cells in the antitumor immune response. *J Exp Med*. (1998) 188:2357–68. doi: 10.1084/jem.188.12.2357
99. Vesely MD, Kershaw MH, Schreiber RD, Smyth MJ. Natural innate and adaptive immunity to cancer. *Annu Rev Immunol*. (2011) 29:235–71. doi: 10.1146/annurev-immunol-031210-101324
100. Nigar S. A study on the immune effects of synergistic oligodeoxynucleotide from probiotics (Dissertation/Doctor's thesis). Shinshu University, Minamiminowa, Japan (2018).
101. van Gent R, Kater AP, Otto SA, Jaspers A, Borghans JA, Vrisekoop N, et al. *In vivo* dynamics of stable chronic lymphocytic leukemia inversely correlate with somatic hypermutation levels and suggest no major leukemic turnover in bone marrow. *Cancer Res*. (2008) 68:10137–44. doi: 10.1158/0008-5472.CAN-08-2325
102. Decker T, Schneller F, Sparwasser T, Tretter T, Lipford GB, Wagner H, et al. Immunostimulatory CpG-oligonucleotides cause proliferation, cytokine production, and an immunogenic phenotype in chronic lymphocytic leukemia B cells. *Blood*. (2000) 95:999–1006.
103. Jahrsdorfer B, Wooldridge JE, Blackwell SE, Taylor CM, Griffith TS, Link BK, et al. Immunostimulatory oligodeoxynucleotides induce apoptosis of B cell chronic lymphocytic leukemia cells. *J Leukoc Biol*. (2005) 77:378–87. doi: 10.1189/jlb.0604373
104. Longo PG, Laurenti L, Gobessi S, Petlickovski A, Pelosi M, Chiusolo P, et al. The Akt signaling pathway determines the different proliferative capacity of chronic lymphocytic leukemia B-cells from patients with progressive

and stable disease. *Leukemia*. (2007) 21:110–20. doi: 10.1038/sj.leu.2404417
105. Oppenheimer-Marks N, Brezinschek RI, Mohamadzadeh M, Vita R, Lipsky PE. Interleukin 15 is produced by endothelial cells and increases the transendothelial migration of T cells *in vitro* and in the SCID mouse-human rheumatoid arthritis model *in vivo*. *J Clin Invest*. (1998) 101:1261–72. doi: 10.1172/JCI1986
106. Park CS, Yoon SO, Armitage RJ, Choi YS. Follicular dendritic cells produce IL-15 that enhances germinal center B cell proliferation in membrane-bound form. *J Immunol*. (2004) 173:6676–83. doi: 10.4049/jimmunol.173.11.6676
107. Fehniger TA, Caligiuri MA. Interleukin 15: biology and relevance to human disease. *Blood*. (2001) 97:14–32. doi: 10.1182/blood.V97.1.14
108. Malamut G, El Machhour R, Montcuquet N, Martin-Lanneree S, Dusanter-Fourt I, Verkarre V, et al. IL-15 triggers an antiapoptotic pathway in human intraepithelial lymphocytes that is a potential new target in celiac disease-associated inflammation and lymphomagenesis. *J Clin Invest*. (2010) 120:2131–43. doi: 10.1172/JCI41344
109. Lee H, Haque S, Nieto J, Trott J, Inman JK, McCormick S, et al. A p53 axis regulates B cell receptor-triggered, innate immune system-driven B cell clonal expansion. *J Immunol*. (2012) 188:6093–108. doi: 10.4049/jimmunol.1103037
110. Mongini PK, Inman JK, Han H, Fattah RJ, Abramson SB, Attur M. APRIL and BAFF promote increased viability of replicating human B2 cells via mechanism involving cyclooxygenase 2. *J Immunol*. (2006) 176:6736–51. doi: 10.4049/jimmunol.176.11.6736
111. Mongini PK, Inman JK, Han H, Kalled SL, Fattah RJ, McCormick S. Innate immunity and human B cell clonal expansion: effects on the recirculating B2 subpopulation. *J Immunol*. (2005) 175:6143–54. doi: 10.4049/jimmunol.175.9.6143
112. Liu HM, Newbrough SE, Bhatia SK, Dahle CE, Krieg AM, Weiner GJ. Immunostimulatory CpG oligodeoxynucleotides enhance the immune response to vaccine strategies involving granulocyte-macrophage colony-stimulating factor. *Blood*. (1998) 92:3730–6.
113. Mongini PK, Gupta R, Boyle E, Nieto J, Lee H, Stein J, et al. TLR-9 and IL-15 synergy promotes the *in vitro* clonal expansion of chronic lymphocytic leukemia B cells. *J Immunol*. (2015) 195:901–23. doi: 10.4049/jimmunol.1403189
114. Temizoz B, Kuroda E, Ohata K, Jounai N, Ozasa K, Kobiyama K, et al. TLR9 and STING agonists synergistically induce innate and adaptive type-II IFN. *Eur J Immunol*. (2015) 45:1159–69. doi: 10.1002/eji.201445132
115. Lee HJ, Kim KC, Han JA, Choi SS, Jung YJ. The early induction of suppressor of cytokine signaling 1 and the downregulation of toll-like receptors 7 and 9 induce tolerance in costimulated macrophages. *Mol Cells*. (2015) 38:26–32. doi: 10.14348/molcells.2015.2136
116. Pradhan P, Qin H, Leleux JA, Gwak D, Sakamaki I, Kwak LW, et al. The effect of combined IL10 siRNA and CpG ODN as pathogen-mimicking microparticles on Th1/Th2 cytokine balance in dendritic cells and protective immunity against B cell lymphoma. *Biomaterials*. (2014) 35:5491–504. doi: 10.1016/j.biomaterials.2014.03.039
117. Bayyurt B, Tincer G, Almacioglu K, Alpdundar E, Gursel M, Gursel I. Encapsulation of two different TLR ligands into liposomes confer protective immunity and prevent tumor development. *J Control Release*. (2017) 247:134–44. doi: 10.1016/j.jconrel.2017.01.004
118. Kim D, Niewiesk S. Synergistic induction of interferon alpha through TLR-3 and TLR-9 agonists stimulates immune responses against measles virus in neonatal cotton rats. *Vaccine*. (2014) 32:265–70. doi: 10.1016/j.vaccine.2013.11.013
119. Shima F, Uto T, Akagi T, Akashi M. Synergistic stimulation of antigen presenting cells via TLR by combining CpG ODN and poly(gamma-glutamic acid)-based nanoparticles as vaccine adjuvants. *Bioconjug Chem*. (2013) 24:926–33. doi: 10.1021/bc300611b
120. Goldinger SM, Dummer R, Baumgaertner P, Mihic-Probst D, Schwarz K, Hammann-Haenni A, et al. Nano-particle vaccination combined with TLR-7 and−9 ligands triggers memory and effector CD8(+) T-cell responses in melanoma patients. *Eur J Immunol*. (2012) 42:3049–61. doi: 10.1002/eji.201142361
121. Sacre K, Criswell LA, McCune JM. Hydroxychloroquine is associated with impaired interferon-alpha and tumor necrosis factor-alpha production by plasmacytoid dendritic cells in systemic lupus erythematosus. *Arthritis Res Ther*. (2012) 14:R155. doi: 10.1186/ar3895
122. Dalpke A, Zimmermann S, Heeg K. CpG DNA in the prevention and treatment of infections. *BioDrugs*. (2002) 16:419–31. doi: 10.2165/00063030-200216060-00003
123. Sato Y, Roman M, Tighe H, Lee D, Corr M, Nguyen MD, et al. Immunostimulatory DNA sequences necessary for effective intradermal gene immunization. *Science*. (1996) 273:352–4. doi: 10.1126/science.273.5273.352
124. Scheiermann J, Klinman DM. Clinical evaluation of CpG oligonucleotides as adjuvants for vaccines targeting infectious diseases and cancer. *Vaccine*. (2014) 32:6377–89. doi: 10.1016/j.vaccine.2014.06.065
125. Fujiki F, Oka Y, Kawakatsu M, Tsuboi A, Tanaka-Harada Y, Hosen N, et al. A clear correlation between WT1-specific Th response and clinical response in WT1 CTL epitope vaccination. *Anticancer Res*. (2010) 30:2247–54.
126. Hara I, Takechi Y, Houghton AN. Implicating a role for immune recognition of self in tumor rejection: passive immunization against the brown locus protein. *J Exp Med*. (1995) 182:1609–14. doi: 10.1084/jem.182.5.1609
127. Klebanoff CA, Gattinoni L, Restifo NP. CD8+ T-cell memory in tumor immunology and immunotherapy. *Immunol Rev*. (2006) 211:214–24. doi: 10.1111/j.0105-2896.2006.00391.x
128. Ohno S, Okuyama R, Aruga A, Sugiyama H, Yamamoto M. Phase I trial of Wilms' Tumor 1 (WT1) peptide vaccine with GM-CSF or CpG in patients with solid malignancy. *Anticancer Res*. (2012) 32:2263–9.

**Conflict of Interest Statement:** The authors declare that the research was conducted in the absence of any commercial or financial relationships that could be construed as a potential conflict of interest.

frontiers in Immunology

ORIGINAL RESEARCH
published: 01 October 2019
doi: 10.3389/fimmu.2019.02347

# Zinc Chelation Specifically Inhibits Early Stages of Dengue Virus Replication by Activation of NF-κB and Induction of Antiviral Response in Epithelial Cells

*Meenakshi Kar[1†], Naseem Ahmed Khan[1†], Aleksha Panwar[1†], Sachendra S. Bais[2], Soumen Basak[2], Renu Goel[3], Shailaja Sopory[4] and Guruprasad R. Medigeshi[1*]*

[1] Clinical and Cellular Virology Lab, Translational Health Science and Technology Institute, Faridabad, India, [2] Systems Immunology Laboratory, National Institute of Immunology, New Delhi, India, [3] Drug Discovery Research Centre, Translational Health Science and Technology Institute, Faridabad, India, [4] Pediatric Biology Centre, Translational Health Science and Technology Institute, Faridabad, India

OPEN ACCESS

**Edited by:**
Haruki Kitazawa,
Tohoku University, Japan

**Reviewed by:**
Lei Shi,
Georgia State University,
United States
Xiaofei Sun,
University of California, San Francisco,
United States

***Correspondence:**
Guruprasad R. Medigeshi
gmedigeshi@thsti.res.in

[†]These authors have contributed equally to this work

**Specialty section:**
This article was submitted to Nutritional Immunology, a section of the journal Frontiers in Immunology

**Received:** 13 August 2019
**Accepted:** 17 September 2019
**Published:** 01 October 2019

**Citation:**
Kar M, Khan NA, Panwar A, Bais SS, Basak S, Goel R, Sopory S and Medigeshi GR (2019) Zinc Chelation Specifically Inhibits Early Stages of Dengue Virus Replication by Activation of NF-κB and Induction of Antiviral Response in Epithelial Cells. Front. Immunol. 10:2347. doi: 10.3389/fimmu.2019.02347

Zinc is an essential micronutrient which regulates diverse physiological functions and has been shown to play a crucial role in viral infections. Zinc has a necessary role in the replication of many viruses, however, antiviral action of zinc has also been demonstrated in *in vitro* infection models most likely through induction of host antiviral responses. Therefore, depending on the host machinery that the virus employs at different stages of infection, zinc may either facilitate, or inhibit virus infection. In this study, we show that zinc plays divergent roles in rotavirus and dengue virus infections in epithelial cells. Dengue virus infection did not perturb the epithelial barrier functions despite the release of virus from the basolateral surface whereas rotavirus infection led to disruption of epithelial junctions. In rotavirus infection, zinc supplementation post-infection did not block barrier disruption suggesting that zinc does not affect rotavirus life-cycle or protects epithelial barriers post-infection suggesting the involvement of cellular pathways in the beneficial effect of zinc supplementation in enteric infections. Zinc depletion by N,N,N',N'-tetrakis(2-pyridinylmethyl)-1,2-ethanediamine (TPEN) inhibited dengue virus and Japanese encephalitis virus (JEV) infection but had no effect on rotavirus. Time-of-addition experiments suggested that zinc chelation affected both early and late stages of dengue virus infectious cycle and zinc chelation abrogated dengue virus RNA replication. We show that transient zinc chelation induces ER stress and antiviral response by activating NF-kappaB leading to induction of interferon signaling. These results suggest that modulation of zinc homeostasis during virus infection could be a component of host antiviral response and altering zinc homeostasis may act as a potent antiviral strategy against flaviviruses.

**Keywords: dengue virus, zinc, rotavirus, epithelial cells, NF-kappaB**

## INTRODUCTION

Zinc is the most abundant micronutrient after iron and zinc deficiency rates in developing countries range from 20 to 30%. Zinc is known to regulate the functions of about 10% of the human proteome and a large number of physiological processes that are zinc dependent have been identified and characterized under conditions of zinc deficiency and supplementation. Some of the predominant zinc-dependent functions such as immune response, metabolism, nucleic acid synthesis and repair, apoptosis and redox homeostasis act as important determinants of host-pathogen interactions. As zinc homeostasis is closely linked to the normal functioning of both prokaryotic and eukaryotic cells, many pathogens are directly, or indirectly affected by perturbations in zinc homeostasis. Zinc finger proteins have been shown to play both proviral and antiviral roles in a number of studies with different viruses (1–3). Previous reports have also shown divergent effects of $Zn^{2+}$ on virus replication. Zinc inhibited RNA polymerase activity of a number of viruses including coronavirus, arterivirus, rhinovirus, and hepatitis C virus (4–9). Dengue virus (DENV), a mosquito-borne, positive-strand RNA virus from the family *Flaviviridae*, has emerged as one of the major public health concerns in India and recent estimates suggest that over 60 million people globally get infected with DENV every year (10). The crystal structures of NS5 protein of DENV and West Nile virus have identified zinc binding site in RdRp domain and propose an important structural role for zinc ions in polymerase activity (11, 12). Therefore, zinc is likely to play a prominent role in the polymerase activity of DENV. One of the prominent physiological functions of zinc is in the regulation of permeability barrier functions in epithelial and endothelial cells. Although many previous reports have focused on the pathogenesis of dengue using vascular endothelial cells, the effect of dengue virus infection on epithelial barrier functions has not been characterized. Epithelial cells play a major role in dengue transmission by mosquitos and animal studies indicate that epithelial cells are active sites of virus infection and contribute to pathogenesis (13, 14). Considering the important role of zinc in epithelial barrier functions, we were interested in investigating the effect of virus infection on epithelial barrier functions and to test whether zinc has a functional role in epithelial cells infected with dengue virus. We show that, similar to mid gut epithelial cells in mosquitos, dengue virus infected human intestinal epithelial cells, and was capable of exiting infected cells from both apical and basolateral surface without disrupting cellular junctions or affecting barrier functions unlike rotavirus infection which disrupted the epithelial barrier. Addition of $ZnSO_4$ in the culture medium after virus adsorption had no effect on viral titres or barrier functions. We utilized N,N,N',N'-tetrakis(2-pyridinylmethyl)-1,2-ethanediamine (TPEN), a zinc-specific chelator, to mimic acute zinc-deficiency in cell culture models of infection and investigated the effect of zinc depletion on DENV, Japanese encephalitis virus (JEV), and rotavirus (RV) infections. In this study, zinc chelation showed an inhibitory effect on DENV and JEV replication but had no effect on RV infection. We further probed the mechanism of action of TPEN and showed zinc chelation affect early stages of dengue life-cycle by inhibiting DENV RNA replication. By RNA seq analysis we observed that zinc chelation leads to induction of ER stress and heat shock proteins, activation of NF-κB leading to upregulation of a subset of type I interferon-dependent antiviral response which specifically blocks DENV replication. Thus, our study provides information on the role of zinc in flavivirus infection and demonstrates that alteration of zinc homeostasis leads to induction of an antiviral response involving ER stress and NF-κB that specifically affects flaviviruses.

## MATERIALS AND METHODS

### Cells and Viruses

Caco-2, A549, Huh-7, BHK-21, C6/36, HEp-2, PS, and MA104 cells were cultured as described previously (15–17). Virus strains used in the study and infection procedures has been described before (15–17). DENV-2 New Guinea C strain was a kind gift from Dr. Navin Khanna. Rotavirus was activated using 10 μg/mL trypsin (Worthington Biochemical Corporation) for 1 h at 37°C. Caco-2 cells were infected with activated virus at 0.5 MOI for 1 h in serum-free medium. After adsorption cells were washed twice with PBS and cells were grown in serum-free medium containing trypsin at 0.5 μg/mL. Throughout this study, we have used two epithelial cell lines, Caco-2 and A549 cells as both these cells support DENV infection. In all the experiments, Caco-2 cells were infected with DENV at 10 MOI and A549 at 5 MOI. Most of the experiments have been performed in both the cell lines and we have obtained similar results. Plaque assay for DENV, JEV, and RV was set up in BHK-21, PS, and MA 104 cells respectively as described previously (15–17).

### Treatment of Cells

Cells were treated with 0.5 μM *N*, *N*, *N*′, *N*′-tetrakis(2-pyridinylmethyl)-1,2-ethanediamine (TPEN) (Sigma) in serum-free media for chelation of intracellular zinc. Zinc levels were measured by flow cytometry as described in the labile zinc measurement section below. To study the effect of TPEN on virus infection, 0.5 μM TPEN was added in serum-free media after infection. At indicated time points, supernatant was collected for estimating virus titer by plaque assay and cells were collected for western blotting or quantitative real-time PCR (qRT-PCR) as described in the following sections. For time-of-addition experiments, Caco-2 cells infected with DENV were treated with TPEN at 8, 16, and 24 h pi. Supernatants were collected at 16 h post-addition of TPEN for measuring viral titers. Cells were used for RNA isolation and RT-PCR as described in the later sections. For rescue experiments, cells were treated with DMSO or TPEN for 4 h and medium containing TPEN was supplemented with 10 μM of $ZnSO_4$/$MnCl_2$/$MgCl_2$/$CuCl_2$/$FeSO_4$. For pre-treatment experiments, cells were treated with DMSO or 0.5 μM TPEN for 4 h. Cells were washed with PBS and infected with 10 MOI of DENV-2 and cultured for 24 h in DMEM containing 2% FBS without TPEN. For labile zinc recovery experiments, cells were treated with TPEN for 4 h, washed twice with PBS and cultured in serum-free medium for indicated periods and labile zinc pools were measured by confocal microscopy or flow

cytometry. For Salubrinal treatment, cells were infected with DENV and, 1 h pi, culture medium was supplemented with 50 μM Salubriinal along with DMSO or TPEN. Viral titres were estimated at 24 h pi.

## Labile Zinc Measurement by Flow Cytometry

Cells were washed once with PBS after treatment or infection following which they were detached using trypsin (80–120 μL) (Gibco) and collected by adding defined trypsin inhibitor (Gibco). Cells were resuspended in DMEM without phenol red (Gibco) supplemented with 2 mM L-glutamine (Gibco) (staining media). Cells were stained using either 5 μM Fluozin-3-AM (Molecular Probes) or 2.5 μM ZinPyr-1 (ZP-1) (Santa Cruz) in the staining media. For ZP-1 staining, medium containing 1 mM EDTA was added to chelate any extracellular zinc during staining. Cells were incubated for 30 min at 37°C in $CO_2$ incubator and mixed every 10 min. For assessing cell viability, fixable viability stain eFluor780 (Becton Dickinson Biosciences) was added to the cells at 1:500 dilution prepared in the staining medium and incubated for further 10 min at 37°C in the $CO_2$ incubator. Cells were washed using FACS buffer (PBS containing 0.25% FBS) and acquired in FACS Canto II (Becton Dickinson). The amount of labile zinc present in live cells was presented as the mean fluorescence intensity of Fluozin-3-AM and ZP-1. Images were quantitated using cellSens Software (Olympus).

## Quantitative RT-PCR Assay

Caco-2 cells were infected with DENV-2 at a MOI of 10 for 1 h. Similarly, A549 cells were infected with DENV-2 at a MOI of 5. After 1 h of virus adsorption cells were washed twice with PBS and serum-free DMEM supplemented with 0.5 μM TPEN was added. At indicated time points, supernatant was collected for estimating viral titres by plaque assay and cells were harvested for positive and negative strand detection PCR as described previously (18). Briefly, RNA was isolated using RNAiso Plus (Takara) as per manufacturer's instructions and reverse transcribed using forward or reverse primer. RT product was further amplified using primer and probe mix using TaqMan RNA-to-Ct one step kit (Applied Biosystems) as described previously (19). GAPDH primer probe mix (Applied Biosystems) was used as housekeeping control and used for normalizing dengue genome levels. Data was analyzed using ΔΔCt method. Viral entry experiments were performed by infecting Caco-2 cells with 10 MOI of DENV-2. One hour after virus adsorption, cells were collected by trypsinization and trypsin was inactivated by resuspending cells in complete medium. Cells were washed twice with PBS and total RNA was isolated and internalized DENV genome levels were determined as described above. For interferon pathway, RNA was isolated from cells at 4 and 8 h post-TPEN treatment and the indicated genes were quantitated by SyBR green chemistry using GAPDH as housekeeping control gene for normalization. The list of primers used is provided in Supplementary Information (**Supplementary Table 1**). Rotavirus genome levels were quantitated as described previously (20).

## Confocal Microscopy and Barrier Studies

Caco-2 and A549 cells were seeded at 30,000 cells per well in 3 μm pore size polycarbonate membranes for 4 days. Media was changed every alternate day and trans-electrical epithelial resistance (TEER) was monitored using a chopstick electrode. At day four, cells were washed with cold PBS and fixed in ice-cold methanol for 20 min at −20°C. Cells were washed twice using PBS followed by blocking using 0.2% BSA in IMF buffer for 5–10 min at room temperature (RT). Cells were incubated with antibodies against β-catenin (Sigma) and occludin (Invitrogen) in IMF buffer (20 mM HEPES pH 7.5, 0.1% Triton X-100, 150 mM NaCl, 5 mM EDTA, 0.02 % sodium azide) for 1 h at RT followed by washing and incubation with Alexa flour 568 tagged secondary antibodies (Molecular probes) for 30 min at RT in dark. Cells were washed with IMF buffer three times and stained with 4′,6-diamidino-2-phenylindole (DAPI) (Molecular probes) at 1:10,000 dilution for 10 min. Cells were washed with PBS, mounted using antifade solution (Molecular probes) and imaged using FV1000 fluorescence microscope (Olympus).

To assess the effect of zinc on epithelial barrier, Caco-2 and A549 cells were grown for 4 days in transwells. Cells were washed with PBS and 2% medium containing $ZnSO_4$ was added apically, basolaterally, or both sides of the transwells. TEER was monitored and cells were used for measuring zinc uptake and viability by flow cytometry as explained in labile zinc measurement section.

To assess effect of DENV and RV infection on epithelial cells barrier, Caco-2 cells were grown in transwells for 4 days and infected with DENV-2 and RV at 10 and 0.5 MOI, respectively as mentioned above. TEER was monitored till 72 h pi for DENV infection and 16 h pi for RV infection. Supernatants were collected from both apical and basolateral surface for measuring viral titres by plaque assay. Effect of zinc in rescuing RV induced barrier damage was assessed by adding 50 μM $ZnSO_4$ in the media of infected cells and measuring TEER and viral titres.

## Cytotoxicity and Cell Proliferation Assays

Cytotoxicity was assessed by CytoTox 96 Non-Radioactive Cytotoxicity Assay kit (Promega) which measures lactate dehydrogenase (LDH) activity in the culture supernatants. As a positive control for cytotoxicity, cells were lysed in 0.1% Triton-X-100 and the cell lysate was used for LDH measurement. The amount of LDH activity in the detergent-treated sample was considered as 100% and the sample's cytotoxicity was measured relative to the detergent control. Cell proliferation was measured using CellTiter 96® $AQ_{ueous}$ One Solution Cell Proliferation Assay (Promega) as per the manufacturer's instructions.

## Electrophoresis Mobility Shift Assays (EMSA)

Caco-2 cells were treated with DMSO or TPEN as described above for 4 and 8 h. Nuclear extracts were prepared and processed for EMSA as described previously (21). Briefly, nuclear extracts (NE) were prepared after treating Caco-2 cells with 0.5 μM TPEN for indicated periods and normalized for protein concentration. Thereafter, NE were incubated with NF-κB or Oct1 specific probes and then were resolved on native PAGE gel. The gel

images were acquired using PhosphorImager (GE, Amersham, UK) and quantified in ImageQuant 5.2.

## RNA Seq Analysis

### Sample Preparation

Caco-2 cells were seeded in a 24-well plate at the cell density of 100,000 cells per well. On day 2 post-seeding, cells were washed twice with PBS and serum-free DMEM containing DMSO and TPEN (0.5 μM) were added to respective wells and cultured for 4 h. After 4 h of treatment, media was removed and cells were washed twice with PBS. Cells were collected in 300 μl RNA lysis buffer (RNA prep kit-Zymo-R1051). RNA was prepared according to the manufacturer's instructions and eluted in 20 μl nuclease-free water. One microgram of total RNA was used for the construction of sequencing libraries using Illumina TruSeq RNA Sample Prep Kit (Cat#FC-122-1001).

For library construction, total RNA is extracted from a sample. After performing quality control (QC), passed sample is proceeded with the library construction. The extracted RNA with an RNA integrity number (RIN) of 7.0 was used for mRNA purification. mRNA was purified using oligo-dT beads (TruSeq RNA Sample Preparation Kit, Illumina) taking 1 μg of intact total RNA. The purified mRNA was fragmented at 90°C in the presence of divalent cations. The fragments were reverse transcribed using random hexamers and Superscript II Reverse Transcriptase (Life Technologies). Second strand cDNA was synthesized on the first strand template using RNaseH and DNA polymerase I. The cDNAs so obtained were cleaned using Beckman Coulter Agencourt Ampure XP SPRI beads.

### Library Construction

The sequencing library is prepared by random fragmentation of the cDNA sample, followed by 5′ and 3′ adapter ligation, after end-repair and the addition of an "A" base and SPRI cleanup. The prepared cDNA library was amplified using PCR for the enrichment of the adapter-ligated fragments. Alternatively, "tagmentation" combines the fragmentation and ligation reactions into a single step that greatly increases the efficiency of the library preparation process. The individual libraries were quantified using a NanoDrop spectrophotometer (Thermo Scientific) and validated for quality with a Bioanalyzer (Agilent Technologies). Adapter-ligated fragments are then PCR amplified and gel purified.

### Sequencing

For cluster generation, the library is loaded into a flow cell where fragments are captured on a lawn of surface-bound oligos complementary to the library adapters. Each fragment is then amplified into distinct, clonal clusters through bridge amplification. When cluster generation is complete, the templates are ready for sequencing. Illumina SBS technology utilizes a proprietary reversible terminator-based method that detects single bases as they are incorporated into DNA template strands. As all 4 reversible, terminator-bound dNTPs are present during each sequencing cycle, natural competition minimizes incorporation bias and greatly reduces raw error rates compared to other technologies. The result is highly accurate base-by-base sequencing that virtually eliminates sequence-context-specific errors, even within repetitive sequence regions and homopolymers.

### RNA Seq Data Analysis

Stringent quality control of Paired End sequence reads of all the samples was done using NGSQCTool kit (22). Paired end sequence reads with Phred score >Q30 was taken for further analysis. NCBI *Homosapien* Hg38 genome file was used for read alignment and identification of transcripts. TopHat pipeline (23) was used for alignment and Cufflink and Cuffdiff pipeline (24) was used for identification of transcript coding regions followed by quantitation and annotation using default parameters. Unsupervised hierarchical clustering of differentially expressed genes was done using Cluster 3.0 (25) and visualized using Java Tree View (26). Gene ontologies and pathways that harbor expressed transcripts were identified using DAVID Functional Annotation Tool [DAVID Bioinformatics Resources 6.8, NIAID/NIH]. Differentially expressed transcripts between Control and Treated samples were identified by CuffDiff data analysis pipeline using a fold-change threshold of absolute fold-change ≥1.5 and a statistically significant Student's *t*-test *P* value threshold adjusted for false discovery rate of <0.001. Statistically significantly enriched functional classes with a *P* value adjusted for false discovery rate of <0.05 derived using the hypergeometric distribution test corresponding to differentially expressed genes were determined using Student's *t*-test with Benjamini Hocheberg FDR test. The heat map for display expression pattern were obtained using Cluster 3.0 for normalizing and hierarchical clustering with average linkage based on Pearson coefficients, followed by Java Tree-View 1.1 program for visualizing the analyzing datasets (25, 26).

Furthermore, analysis was performed to identify the significant pathways, functions, and networks associated with significantly differentially expressed gene transcripts by using ingenuity pathway analysis (IPA) software (Ingenuity Systems, Redwood City, CA, www.qiagen.com/ingenuity). Differentially expressed (upregulated or downregulated) gene transcripts that showed a minimum of 2 fold change in DMSO samples as compared to that of TPEN treatment was imported to IPA for the core analysis. These differentially regulated genes are known as focus genes in IPA. A *p*-value was calculated using right-tailed Fisher's exact test to explain the significance of the pathways related to our genes list and it was set at <0.05 (or score > 1.3 score = –lop *P*). Additionally, all dysregulated transcripts were analyzed for the prediction of activation or inhibition of canonical pathway based on z-score. IPA automatically calculates the z-score in the range of $\sim -2 < z > 2$ based on differentially expressed genes from our dataset with the information stored in IPA knowledge database. Positive and negative z-score suggests the activation and inhibition of the pathway, respectively. The pathways are displayed graphically as a collection of nodes i.e., gene transcripts and edges-the biological relationships between the nodes. Different shades of red and green nodes reflect the relative fold change of gene transcripts. IPA algorithm has given white nodes to the genes not present in our list of differentially expressed genes. Solid and dotted lines indicate direct and

indirect interaction or regulation, respectively. Each line is has at least one reference from the literature.

## Data Analysis

Data was analyzed and charts were prepared using GraphPad Prism software. All experiments were performed with two or more replicates and graphs have been prepared representing data from at least two independent experiments with $n \geq 6$. Error bars represent mean ± SD. Statistical significance was estimated by *t*-test (unpaired, non-parametric) using Mann-Whitney test.

# RESULTS

## Epithelial Barrier Functions Are Regulated by Zinc Homeostasis

The role of Zinc on epithelial and endothelial permeability barrier functions has been demonstrated by a number of *in vitro* and *in vivo* studies. We were interested to test the effect of zinc supplementation in the context of permeability barrier functions in cells infected with viruses. We first examined the barrier properties of two epithelial cell lines Caco-2 (colon) and A549 (lung) by growing these cells on transwell inserts for 4 days and measuring the trans-epithelial electrical resistance (TEER) every day. Caco-2 cells have been reported to have higher expression of tight junction proteins and undergo differentiation whereas A549 cells have lower TEER values and do not undergo differentiation (27–30). As expected, the basal levels of TEER was about 200-fold lower in A549 cells as compared to Caco-2 on day 2, however, both cell lines showed an increase in the TEER values with time in culture and started to plateau by day 4 (**Supplementary Figures 1A,B**). We stained these transwells for occludin and β-catenin, a marker for tight junction and adherens junction, respectively. A549 cells showed a diffused and weak occludin staining while β-catenin staining showed a typical adherens junction pattern. In Caco-2 cells, both occludin and β-catenin showed a clear and intense tight and adherens junctional staining, respectively (**Supplementary Figure 1C**). To further determine the capacity to uptake Zn by these cells, we added $ZnSO_4$ in the apical medium and measured labile zinc levels after 24 h in both the cells by flow cytometry by zinc fluorophore, fluozin-3AM. Caco-2 cells showed a 3-fold increase in labile zinc levels under these conditions whereas labile zinc levels was unchanged in A549 cells (**Figure 1A**). These results suggest that A549 cells have very poor zinc uptake capacity as compared to Caco-2 cells. Therefore, all further experiments were performed in Caco-2 cells. We next measured the effect of zinc supplementation on barrier integrity in Caco-2 cells. Cells were grown for 4 days and Zn was added either to the apical medium or in the basolateral medium or in both the apical and basolateral chambers for 24 h. Zn supplementation had no effect in Caco-2 when added only in the apical or basolateral medium. However, when both apical and basolateral medium was supplemented with Zn, TEER values decreased significantly (**Figure 1B**). We next verified Zn uptake under these conditions by measuring labile Zn levels using fluozin-3AM, a cell permeable zinc fluorophore, by flow cytometry and observed about 2.5-fold

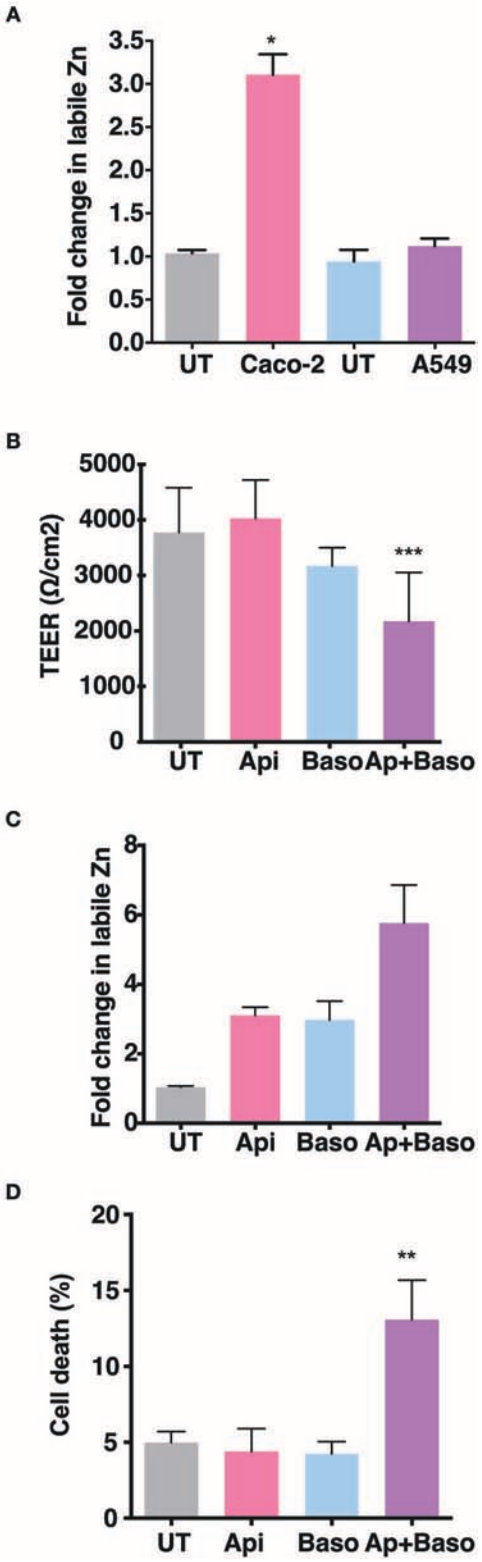


**FIGURE 1 |** Role of Zn in barrier functions in Caco-2 and A549 cells. Caco-2 and A549 cells were seeded at 30,000 cells per well and cultured in 3.0 μm transwell inserts for 4 days. **(A)** Comparison of zinc uptake in Caco-2 and

*(Continued)*

**FIGURE 1 |** A549 cells treated apically with 100 μM $ZnSO_4$ in 2% media for 24 h. **(B)** TEER of Caco-2 cells grown for 7 days treated with $ZnSO_4$ at 100 μM by apical, basolateral or apical + basolateral regions in 2% DMEM for 24 h. **(C)** Corresponding fold change in zinc levels in Caco-2 cells measured by FLZ-3AM staining at 24 h post treatment. **(D)** Percentage of dead cells in apical, basolateral, and apical + basolateral $ZnSO_4$ treated Caco-2 cells at 24 h measured by live dead stain using flow cytometry. Data are from at least two independent experiments and represent mean ± SD. $^{*}p < 0.05$, $^{**}p < 0.01$, $^{***}p < 0.001$.

uptake when Zn was added either on the apical or basolateral side and 5.5-fold increase in labile Zn levels when Zn was added in both apical and basolateral media (**Figure 1C**). To test if this increase in intracellular zinc leads to compromise in cell viability, we assessed cell viability by live-dead stain using flow cytometry and observed around 15% cell death when Zn was added in both apical and basolateral media suggesting that enhanced zinc uptake may compromise cell viability (**Figure 1D**).

## Dengue Virus and Rotavirus Differentially Affect Permeability Barrier Functions

Gastrointestinal bleeding is a hallmark of severe dengue disease and previous reports implicate inflammatory cytokines such as TNF-α as a major player in this event (31). However, primate models of dengue infection have shown gastrointestinal tract to be one of the sites of virus replication but there have been no investigations to assess the direct effect of dengue infection on gut barrier functions (14). We examined the effect of dengue infection on barrier integrity in Caco-2 cells grown on trans-wells. Cells were infected with DENV-2 serotype at 10 MOI and cultured for 3 days with TEER readings recorded every 24 hrs and supernatants collected from apical and basolateral chambers for estimating viral titers. We observed no effect on TEER in cells infected with DENV up to 72 h pi. Surprisingly, dengue infected cells showed a significantly higher TEER values at later stages infection (**Figure 2A**). Despite lack of any negative effect on barrier functions, dengue virus was detected both in the apical and basolateral chamber of infected cells as early as 24 h pi and the virus titers steadily increased up to 72 h pi (**Figure 2B**). These results suggest that dengue virus does not directly disrupt epithelial barrier functions and is capable of exiting infected cells from the basolateral membranes. We used rotavirus (RV), which has been showed to infect Caco-2 cells and disrupt barrier functions by previous studies (32), as a positive control and observed that TEER was disrupted by RV infection at 16 h pi (**Figures 2C,D**) further confirming that these cells were not resistant to barrier disruption. We measured cell viability in rotavirus infection at 16 h pi by live-dead staining using flow cytometry and did not find any difference between mock and RV infection suggesting that factors other than cytotoxicity are responsible for disruption in the TEER (**Figure 2E**). Many Zn supplementation trials suggest that Zn therapy is beneficial in reducing the duration and severity in children infected with RV (33). Since Zn addition alone did not impact permeability barrier functions under our experimental conditions, we were interested in assessing the function of zinc on barrier functions in the context of RV infection. We next tested if addition of zinc into the medium 1 h after virus adsorption would prevent barrier disruption induced by RV. Cells were infected with 0.5 MOI of RV followed by apical treatment with 50 μM $ZnSO_4$ till 16 h pi. TEER dropped by about 60% in RV-infected cells at 16 h pi but infected cells treated with Zn did not show any improvement in the TEER suggesting Zn did not rescue damaged barrier in cells post- infection in RV infected cells (**Figure 2F**).

## Zinc Chelation Specifically Inhibits Flavivirus Infection

The essential role of Zn in cellular functions has been demonstrated by many studies by using TPEN, a cell-permeable Zn chelator (34–36). We sought to mimic zinc deficiency *in vitro* using TPEN and determine the effect of Zn depletion on DENV infection. Many previous studies have shown around 70–80% depletion in labile Zn levels using high concentrations of TPEN for short duration (37, 38). We first measured the effect of increasing concentrations of TPEN on cell proliferation. Cells were treated with 0.25, 0.5, 0.75, and 1 μM TPEN for 24 h and cell proliferation was assessed. We observed that TPEN concentration above 0.5 μM affected cell proliferation (**Figure 3A**). Similarly, TPEN treatment above 0.5 μM showed cytotoxic effect and hence all further experiments were performed with 0.5 μM TPEN (**Figure 3B**). We estimated zinc depletion by FACS by staining with zinc fluorophore, ZP-1, after treatment with 0.125, 0.25, and 0.5 μM of TPEN for 4 h and found around 20 and 40% reduction in the mean fluorescence intensity of ZP-1 with 0.25 and 0.5 μM TPEN, respectively (**Figure 3C**). Next, Caco-2 cells were infected with DENV (10 MOI) or JEV (3 MOI) or RV (0.5 MOI) and after 1 h of virus adsorption, cells were cultured in serum-free medium containing DMSO (vehicle control) or 0.5 μM TPEN. Viral titers in the supernatant were measured by plaque assay at 24 h pi (for DENV and JEV) or 16 h pi (for RV). Zinc depletion by TPEN led to a substantial reduction in viral titers for both flaviviruses, DENV and JEV, but had no effect on RV titers in Caco-2 cells (**Figures 3D–H**). These results indicate that zinc chelation by TPEN, which results in moderate depletion in the labile zinc levels under our experimental conditions, has a drastic negative effect on flaviviruses but not on rotavirus suggesting that the cellular zinc levels have a differential effect on the life-cycle of positive (DENV and JEV) and double-stranded (RV) RNA viruses. TPEN binding has been shown to be highly specific to zinc; however, it has also been reported to bind to other metal ions albeit with far lower affinities (39). To further verify the specific role of zinc chelation by TPEN in DENV replication, we performed supplementation experiments after TPEN treatment. We assessed whether the effect of TPEN can be blocked by addition of salts of Zn or other divalent cations such as magnesium (Mg), manganese (Mn), copper (Cu), or iron (Fe). Caco-2 cells were treated with TPEN for 4 h after infection with DENV-2. After 4 h treatment, the culture medium was supplemented with 10 μM

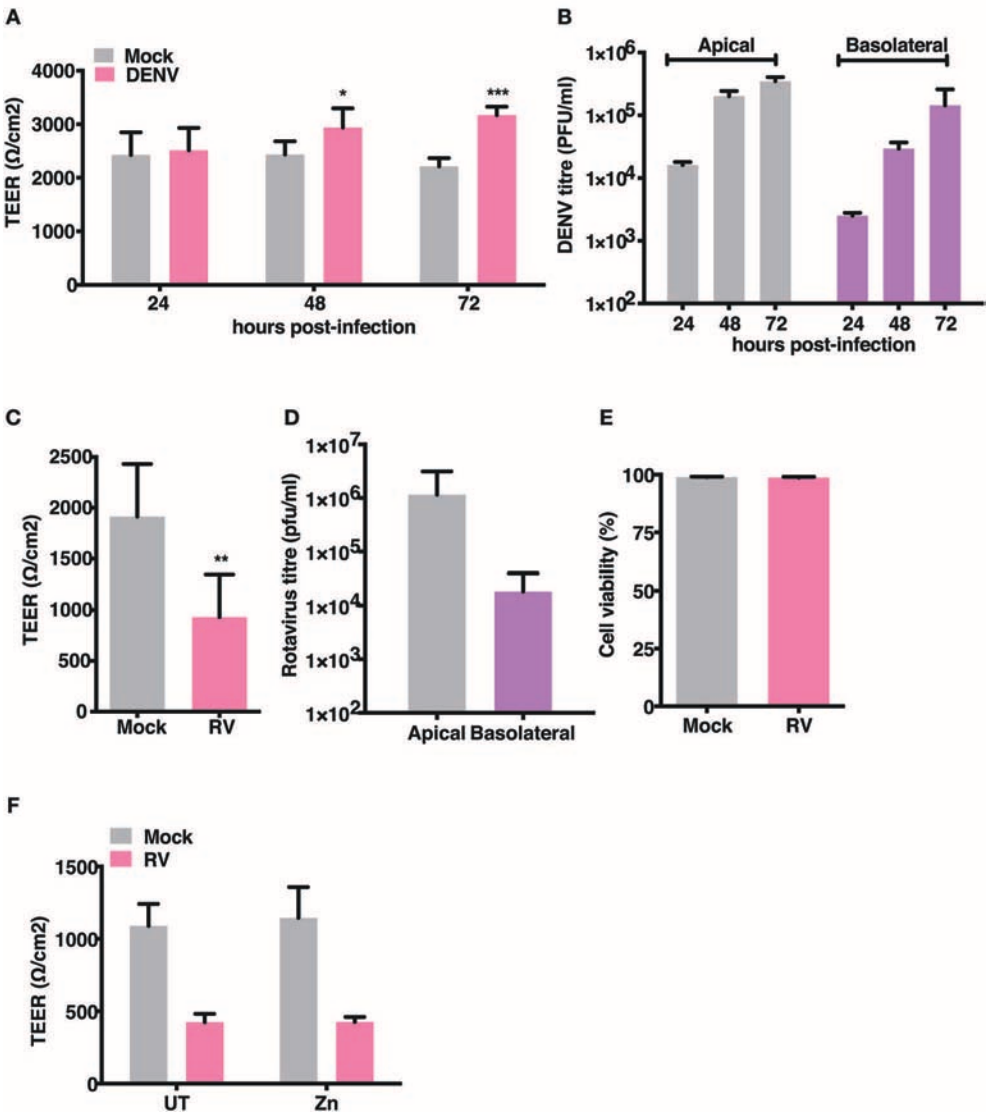


**FIGURE 2 |** Effect of RV and DENV infection on epithelial barrier functions. Caco-2 cells were grown on transwell inserts for 4 days. Cells were infected with RV and DENV-2 at 0.5 and 10 MOI, respectively and TEER was measured. **(A)** TEER of DENV infected Caco-2 cells compared to mock measured till 72 h pi **(B)** Representative DENV titres determined by plaque assay and represented as pfu/ml at indicated time points. **(C)** TEER of RV infected Caco-2 cells compared to mock at 16 h pi **(D)** Representative RV titres determined by plaque assay and represented as pfu/ml at 16 h pi. **(E)** Viability of Caco-2 cells infected with RV as compared to mock measured by live dead staining using flow cytometry **(F)** TEER at 16 h pi of Caco-2 cells grown in transwells and infected with RV followed by addition of 50 μM $ZnSO_4$. Data are from at least two independent experiments and represent mean ± SD. $^*p < 0.05$, $^{**}p < 0.01$, $^{***}p < 0.001$.

of $ZnSO_4$/$MnCl_2$/$MgCl_2$/$CuCl_2$/$FeSO_4$ and viral titers in the supernatant was measured by plaque assay at 24 h pi. We observed that only $ZnSO_4$ blocked the inhibitory effect of zinc chelation (**Figure 3I**). These results confirm that the inhibitory effect of TPEN is specifically due to zinc chelation.

## Zinc Chelation Affects DENV RNA Replication

To further demonstrate the mechanism of action of TPEN treatment in DENV infection, we performed time-of-addition experiments. We added TPEN at 8, 16, and 24 h pi and viral titers were measured after 16 h treatment at each time point. We observed a significant reduction in viral titers when TPEN was added at any of the time-points indicated above, however, the reduction in viral titers was more drastic at early stages of viral infection (**Figure 4A**). DENV is a positive strand RNA virus which replicates via negative strand RNA intermediates. Therefore, estimating the quantity of negative strand RNA is a direct measure of virus replication. We next measured the positive and negative strand viral RNA in total RNA isolated from cells from the time-of-addition experiments by RT-PCR. The amount of positive and negative strand RNA increased

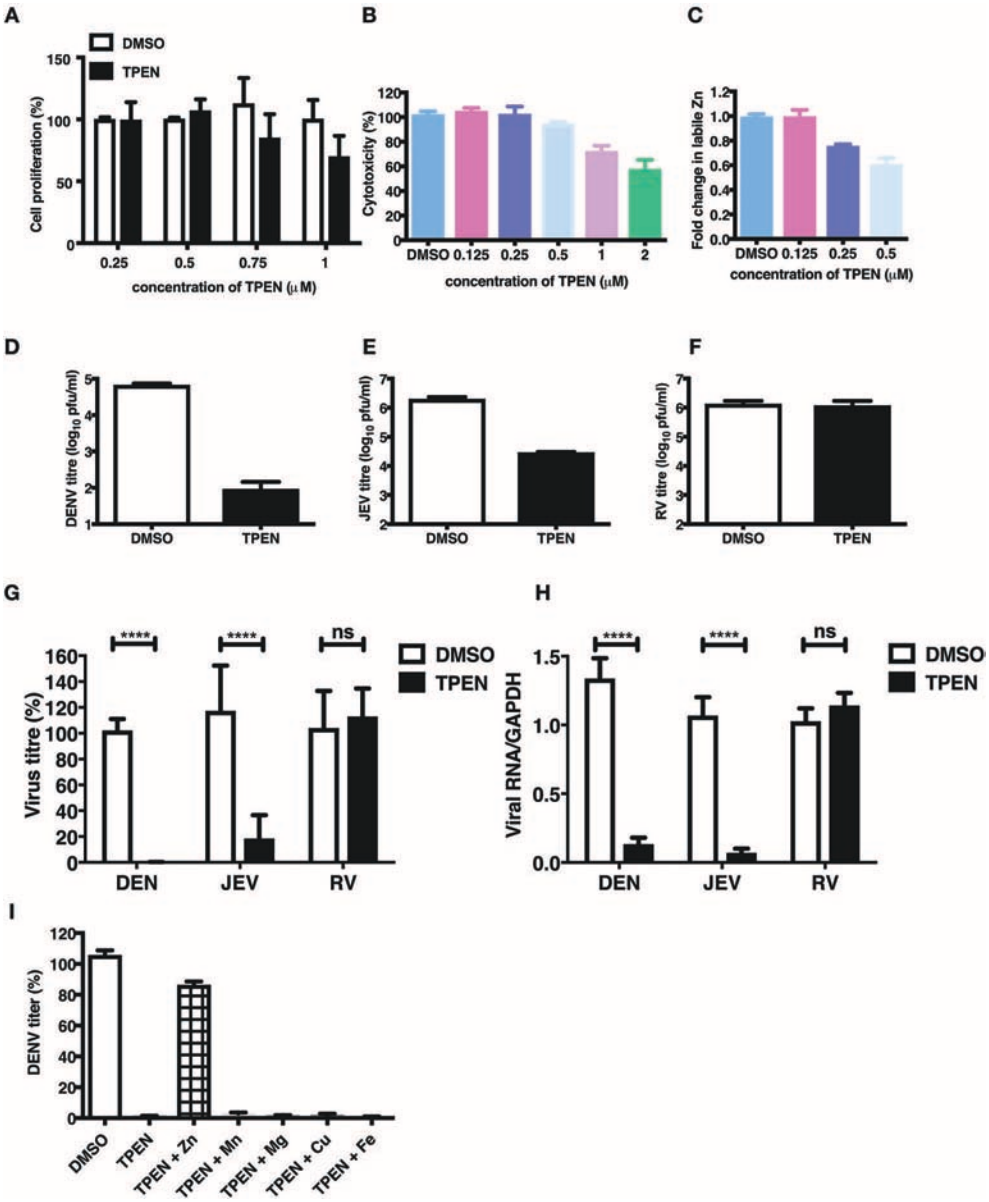


**FIGURE 3 |** Zinc depletion specifically inhibits flavivirus infection. Caco-2 cells were treated with indicated concentrations of TPEN and incubated for 24 h. Cell proliferation **(A)** and cytotoxicity **(B)** was measured as described in the methods section. **(C)** Caco-2 cells were treated with indicated concentrations of TPEN and incubated for 4 h and amount of zinc depletion was measured by FACS using ZP-1. **(D)** Caco-2 cells were infected with DENV (10 MOI) or **(E)** JEV (3 MOI) or **(F)** RV (0.5 MOI) followed by treatment with TPEN at 0.5 μM. Viral titers in the culture supernatants were determined by plaque assay at 24 h pi for DENV and JEV; at 16 h pi for RV. Representative experiments are shown in D-F. Compilation of data from two or more experiments is shown for viral titers **(G)** and RT-PCR **(H)**. **(I)** Caco-2 cells infected with DENV were treated with TPEN after virus adsorption for 4 h followed by addition of 10 μM of $ZnSO_4$/$MnCl_2$/$MgCl_2$/$CuCl_2$/$FeSO_4$ into the media. Viral titres were determined at 24 h post-addition of salts. All the data are from at least two independent experiments and presented as mean ± SD. ****$p < 0.0001$. ns, not significant.

to over hundred-fold in DMSO treated samples after 16 h of treatment relative to the time of treatment initiation, however, there was very minimal increase in viral RNA in TPEN-treated samples suggesting that zinc chelation affected viral replication (**Figures 4B,C**).

We further confirmed the effect of zinc chelation at early stages of viral replication by treating cells for short duration (2 and 4 h) after virus adsorption. Cells were further cultured in the absence of the inhibitor for 24 h pi. Total RNA was isolated and positive and negative strand RNA was measured. We observed a significant decrease in the amount of plus and minus strand RNA in TPEN treated cells in a time-dependent fashion where >80% reduction in RNA was observed in cells treated with TPEN for 4 h (**Figures 4D,E**). This data clearly

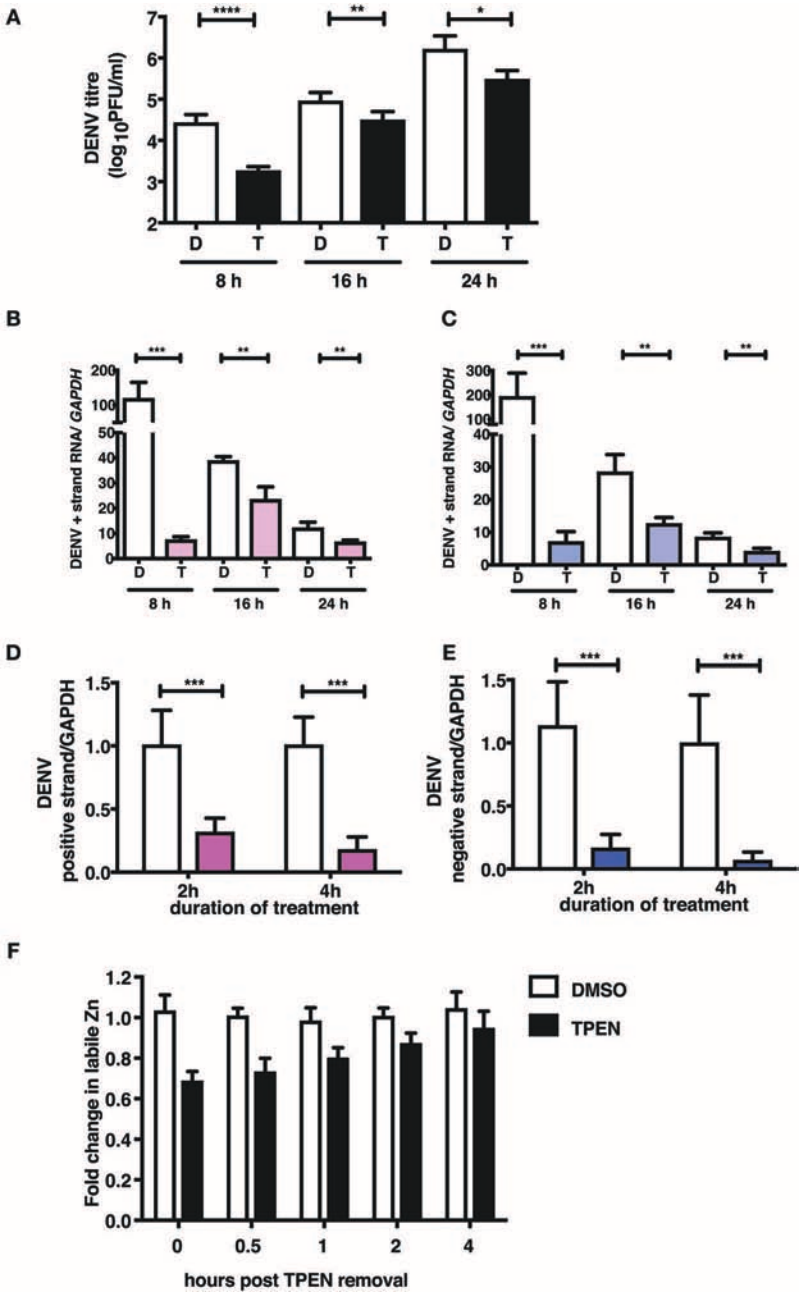


**FIGURE 4 |** Zinc chelation perturbs DENV replication. **(A)** Caco-2 cells were infected with DENV and TPEN was added at 8, 16 and 24 h pi. Viral titers in the culture supernatants were determined after 16 h of treatment. **(B)** DENV positive and **(C)** negative strand levels were quantitated by qRT-PCR. Data are presented as fold increase is relative to the samples collected at the time-of-addition of TPEN. Caco-2 cells were treated with DMSO or TPEN (0.5 μM) for 2 and 4 h pi. After treatment media was replaced with serum-free medium and cells were collected at 24 h pi for estimation of **(D)** positive and **(E)** negative strand RNA by qRT-PCR. Data are presented as relative fold change in positive or negative strand RNA between DMSO and TPEN treatment. GAPDH mRNA levels were used for normalization. **(F)** Caco-2 cells were treated with DMSO or TPEN (0.5 μM) for 4 h pi. After treatment, media was replaced with serum-free medium and recovery in labile zinc levels were estimated by FACS at indicated time points after media addition by ZP-1 staining. Data are from at least two independent experiments performed with two or more replicates. Data are presented as mean ± SD. $^{*}p < 0.05$, $^{**}p < 0.01$, $^{***}p < 0.001$, $^{****}p < 0.0001$.

demonstrates the requirement of cellular zinc or zinc-dependent processes for DENV RNA replication post-entry. We further estimated the time required for recovery of labile zinc pools after removal of TPEN in the medium. We observed that the labile zinc levels recovered to about 90% of DMSO controls within 2 h of replacing the medium suggesting that transient zinc chelation may activate pathways that counter dengue replication (**Figure 4F**).

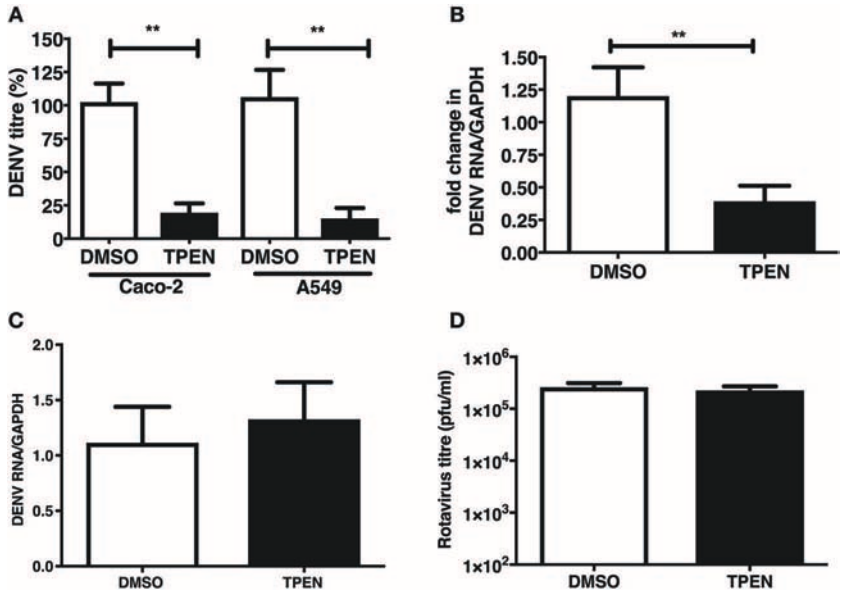


**FIGURE 5 |** Zinc chelation prior to DENV infection inhibits DENV infection. **(A)** Caco-2 or A549 cells were treated with DMSO or TPEN (0.5 μM) for 4 h prior to DENV infection. Infected cells were cultured for 24 h in the absence of TPEN and viral titers in the supernatant was measured by plaque assay and **(B)** DENV RNA was quantitated by qRT-PCR. **(C)** Cells pre-treated with TPEN and infected with DENV were collected by trypsinization 1 h pi and total RNA was isolated to measure internalized viral RNA by qRT-PCR. **(D)** Caco-2 cells were treated with DMSO or TPEN (0.5 μM) for 4 h prior to RV infection. Infected cells were cultured for 16 h in the absence of TPEN and viral titers in the supernatant was measured by plaque assay. All the data are from at least two independent experiments with triplicate samples. Data are presented as mean ± SD. $^{**}p < 0.01$.

## TPEN Pre-treatment Blocks DENV Infection

We were next interested in determining whether zinc chelation prior to dengue infection has any effect on virus infection. Caco-2 and A549 cells were pre-treated with TPEN for 4 h prior to DENV infection. Cells were infected as above and cultured for 24 h in the absence of TPEN. Virus titers in the supernatant was measured by plaque assays at 24 h pi. We observed a significant reduction in DENV titers in both the cell lines and DENV RNA levels were also reduced upon TPEN pre-treatment in Caco-2 cells suggesting that perturbing zinc homeostasis prior to infection also affects DENV infection (**Figures 5A,B**). This effect was not due to defect in cellular entry of the virus as the amount of internalized viral RNA after 1 h of virus adsorption was not different between mock-treated and zinc-depleted cells (**Figure 5C**). Pre-treating cells with TPEN had no effect on rotavirus infection (**Figure 5D**). These data suggest that zinc chelation specifically affects dengue virus infection.

## Zinc Chelation Activates Stress Response Pathways

Our results showed that a transient and reversible zinc chelation was sufficient to perturb DENV replication suggesting that chelating free zinc may modulate cellular pathways that negatively affect DENV replication. To gain further insights into the molecular mechanism behind zinc depletion-induced inhibition of DENV replication, we treated cells with TPEN for 4 h and processed total RNA for RNA seq analysis. One eighty three genes (99 genes were downregulated and 84 genes were upregulated) showed differential expression upon treatment (**Supplementary Table 2** and **Supplementary Figure 2**). The differential gene expression data obtained from RNA-seq was further analyzed by Ingenuity Pathway Analysis (IPA) for identifying interaction networks, molecular and cellular functions and pathways that are modulated upon zinc chelation. As expected from the diverse physiological functions regulated by zinc, the list of genes whose expression was altered due to zinc chelation was clustered around physiological functions such as post-translational modification, protein folding and signal transduction pathways (**Supplementary Table 3**). Network analysis of differentially expressed genes by IPA analysis further confirmed enrichment of genes involved in post-translational modification and protein folding which has 35 nodes includes 24 focus genes (**Figure 6**). Interestingly, induction of heat shock proteins and NF-κB activation emerged as one of the major nodes in the network analysis (**Figure 6**) suggesting that zinc chelation may lead to activation of ER stress and NF-κB pathway in addition of stress response involving heat shock proteins.

## Zinc Chelation Induces Antiviral Response Due to ER Stress and NF-κB Activation

RNA seq analysis suggested that zinc chelation may activate ER stress response and NF-κB and its downstream targets which may block dengue virus replication. We next tested if blocking unfolded protein response would rescue the inhibitory effect of zinc chelation. Cells were infected with DENV and cultured

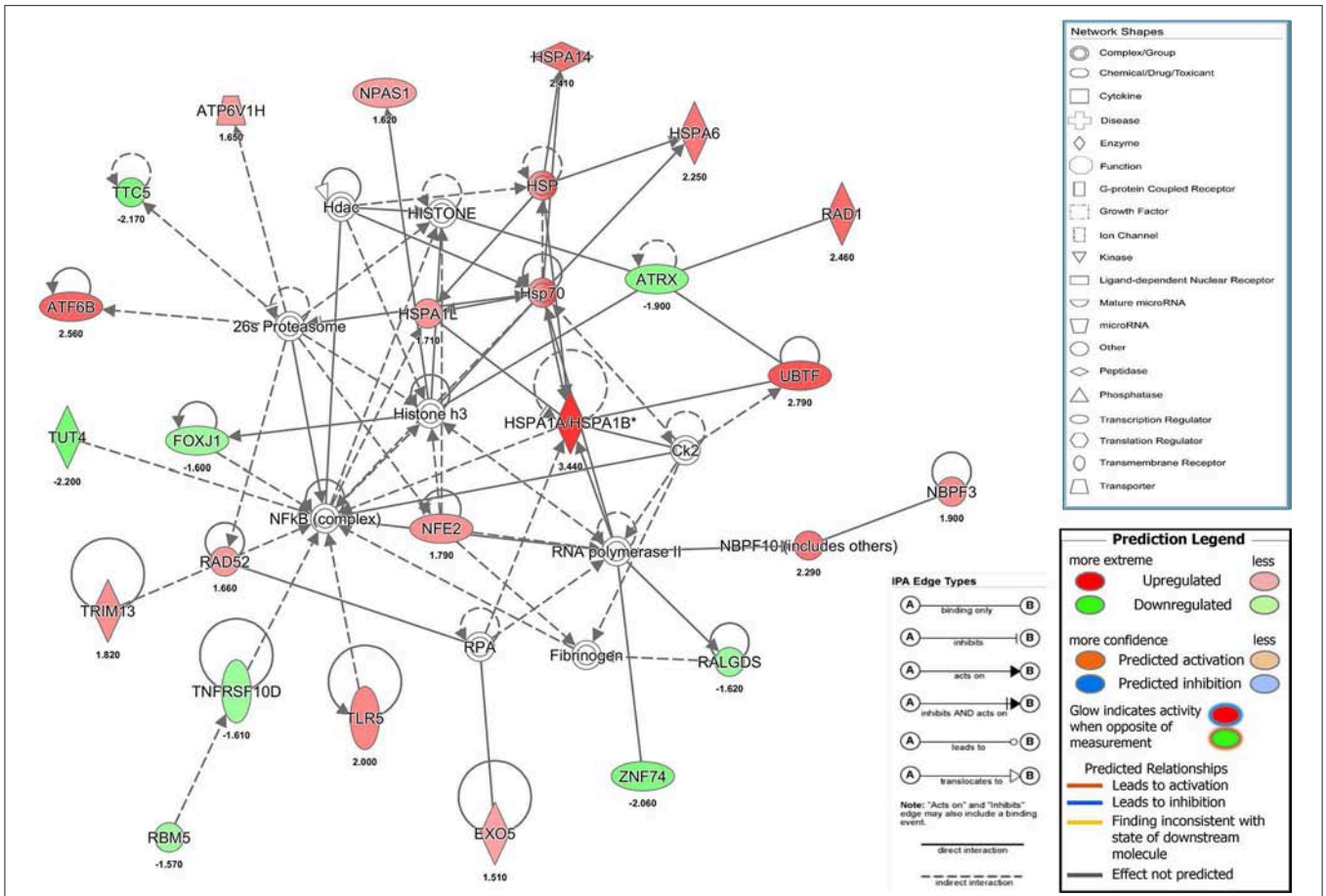


**FIGURE 6 |** Network analysis from RNA seq. Figure shows one of the functional networks (post-translational modification and protein folding) identified from the list of differentially expressed genes obtained from DMSO and TPEN treatment conditions by RNA seq analysis using ingenuity pathway analysis tool. Please see materials and methods section for further details.

in medium containing DMSO or TPEN in the presence of Salubrinal, an inhibitor of unfolded protein response (UPR) (40). Blocking UPR by Salubrinal rescued from the inhibition observed with zinc chelation suggesting a connection between zinc homeostasis, UPR and antiviral response (**Figure 7A**). To further confirm the induction of antiviral response due to zinc chelation, cells were treated with TPEN for 4 and 8 h and nuclear extracts were prepared to measure NF-κB activity by electrophoretic mobility shift assays (EMSA). We observed a time-dependent increase in NF-κB activity in TPEN-treated cells (**Figure 7A**). To further confirm the functional relevance of NF-κB activation, cells were treated with TPEN for 4 and 8 h and relative transcript levels of interferon-β and some of its downstream effectors were measured by RT-PCR. Zinc chelation by TPEN led to induction in IFN-β mRNA as early as 4 h post-treatment which further increased at 8 h post-treatment (**Figure 7B**). We further measured the mRNA levels of interferon-responsive genes namely, interferon-induced transmembrane protein 1 (IFITM1), interferon-stimulated gene 15 (ISG15), interferon-induced protein with tetratricopeptide repeats 2, 3, and 5 (IFIT2, IFIT3, and IFIT5) (**Figures 7C–H**). Of all these genes, only IFIT2, IFIT3, and IFIT5 showed induction, however, IFIT5 showed maximum induction as compared to IFIT2 and IFIT3 (**Figures 7F–H**). Interestingly, IFIT5 was one of the genes upregulated upon TPEN treatment in the RNA seq data (**Supplementary Table 2**). Our results suggest that zinc chelation activates NF-κB and generates an antiviral state by inducing a specific subset of interferon-mediated antiviral signaling that renders cells resistant to DENV infection.

## DISCUSSION

In this study, we focused on the effect of rotavirus and dengue virus infection on epithelial junctions and the importance of zinc in maintaining the barrier functions in Caco-2 cells in the context of virus infection. Zinc supplementation trials have shown that oral zinc as a supplement in diarrhea is beneficial in children over 6 months of age in regions where zinc deficiency is prevalent (33) indicating that chronic zinc deficiency could be corrected by zinc supplementation. However, whether zinc would be beneficial in enteric infections under normal conditions has been inconclusive. Furthermore, the effect of zinc supplementation in rotavirus diarrhea has been inconsistent (41–43). In our *in vitro* study, we show that zinc supplementation post-infection

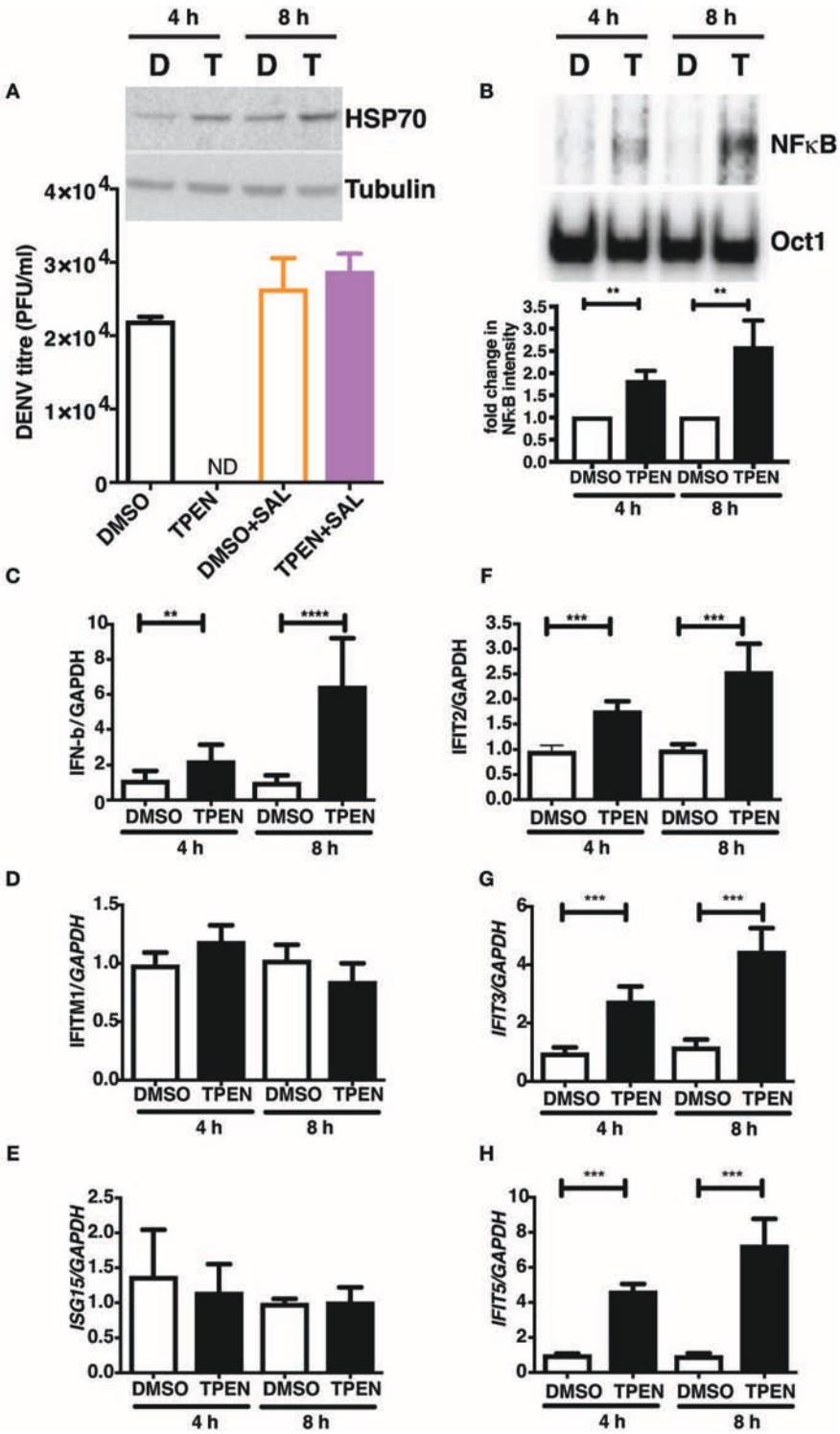


**FIGURE 7 |** Zinc chelation induces antiviral response. **(A)** Inset: Caco-2 cells were treated with 0.5 μM TPEN and DMSO for 4 and 8 h and used for western blot analysis of HSP70. Caco-2 cells were treated with DMSO or TPEN (0.5 μM) in the presence of 50 μM Salubrinal after infection and virus titers were determined at 24 h pi. **(B)** Caco-2 cells were treated with DMSO or TPEN (0.5 μM) for 4 or 8 h. Nuclear extracts were prepared and NF-κB DNA binding activity was assessed by EMSA. Oct1 served as a control for normalization. **(C–G)** Caco-2 cells were treated with DMSO or TPEN (0.5 μM) for 4 or 8 h. Total RNA was isolated and transcript levels of indicated genes were quantitated by RT-PCR. All the data are from at least two independent experiments with triplicate samples. Data are presented as mean ± SD. $^{**}p < 0.01$, $^{***}p < 0.001$, $^{****}p < 0.0001$.

had no effect on viral titres or barrier disruption in rotavirus-infected cells suggesting that the effect of zinc *in vivo* may involve its effect on immune response or other antiviral functions. Gastrointestinal manifestations are commonly observed in severe cases of dengue (44, 45) and the immunopathological nature of severe dengue disease suggests that these manifestations are a result of cytokine storm. However, replication of dengue virus in the midgut epithelial cells of mosquitos and isolation of viable virus from the intestine of experimentally-infected rhesus monkeys suggest that gut epithelial cells may be one of the active sites of DENV replication and virus dissemination (13, 14). We show that Caco-2 cells were not only permissive to dengue infection, but the virus was released from both the apical and basolateral surfaces without disruption of cellular junctions. Based on these observations we propose a crucial role for epithelial cells in dengue pathogenesis which needs to be further verified in relevant and immunocompetent animal models.

Zinc salts have been shown to inhibit some of the RNA viruses using *in vitro* assays or infection systems (4–9). Zinc has been shown to alter various stages of viral infection as in the case of poliovirus and other picornaviruses and hepatitis C virus where zinc salts were shown to inhibit viral protease activity (46, 47). Contrary to many of the aforesaid reports, zinc chelation was shown to inhibit the alfalfa mosaic virus RNA-dependent-RNA polymerase (RdRp) activity (48). The reverse transcriptase of RNA tumor viruses is a zinc metalloenzyme and zinc chelation was shown to inhibit the enzyme (49, 50). Similarly, zinc chelation also affected the RdRp activity of influenza viruses and the 2A proteinase of human rhinovirus (51, 52). Therefore, the role of zinc appears to be as diverse as the strategies of replication adopted by the RNA viruses from different families. We took the approach of mimicking moderate zinc deficiency conditions by zinc chelation using TPEN to identify the effect of zinc-dependent viral and cellular functions on RNA virus infections. We observed that zinc depletion by TPEN inhibited DENV and JEV infection but not RV infection. Time-of-addition experiments indicated that zinc plays an essential role at early stages of viral RNA replication, post-entry and post-uncoating, as observed by a drastic reduction in the synthesis of negative and positive strand RNA in TPEN-treated cells. Additionally, zinc chelation for only first 4 h of infection led to near-complete inhibition of virus replication. The inhibitory effect of TPEN was specific to Zn chelation because only Zn supplementation could reverse the effect and other divalent cations failed to do so.

Our RNA seq analysis provided insights into the molecular functions perturbed due to transient and moderate zinc depletion. Other than post-translational modification and protein folding, many zinc-finger proteins, which function as transcription factors, were dysregulated suggesting a global effect on host transcription and translation. Therefore, it is not surprising that addition of TPEN even at 24 h post-infection was able to significantly inhibit virus titers. However, these changes specifically affected flavivirus infection and had no effect on rotavirus suggesting that zinc homeostasis may regulate few viruses depending on the requirement of cellular zinc for completion of virus life-cycle. We further discovered that transient zinc chelation led to induction of an antiviral state in cells via induction of heat shock proteins and activation of NF-κB and upregulation of downstream effectors which inhibit DENV replication. Interferon-stimulated genes (ISGs) are a large group of genes which have diverse effects on viral infections and mostly act at early stages of virus life-cycle (53). The IFIT proteins are a family of antiviral proteins that form complexes to target viral RNA and inhibit translation (54–56). Although DENV has been shown to evade interferon responses, induction of ISGs at very early stages before the accumulation of viral proteins that target some of the innate immune components may tip the balance in favor of innate immune responses and block viral RNA replication. Surprisingly, labile zinc pool was restored within 2 h of removing the zinc chelator suggesting that transient zinc depletion activates the stress response involving heat shock proteins from the Hsp70 family and an antiviral state due to NF-κB activation. Interestingly, Hsp70 family members play a necessary role in dengue replication and Hsp70 has been proposed as an antiviral target (57, 58). The molecular mechanism linking zinc depletion to Hsp70 remains to be elucidated.

Zinc is an acute-phase reactant and zinc levels are redistributed during infections. It is plausible that this redistribution may create a transient state of zinc deficiency during acute viral infections which may indirectly protect cells by inducing an antiviral state. It has been suggested that pathogens may actively alter zinc levels and zinc chelation with TPEN was shown to improve survival of mice infected with *Aspergillus fumigatus* (59). In the case of HIV, zinc chelation by TPEN was shown to inhibit APOBEC3 degradation by HIV-1Vif and made the virus susceptible to the antiviral activity of APOBEC3 (60). These studies suggest that zinc chelation can be an attractive antimicrobial option. Considering that zinc ion was co-crystallized with dengue polymerase, the non-structural protein 5 (NS5) (11), we speculate that the DENV NS5 may utilize cellular zinc for viral RNA replication. It would be interesting to further investigate whether zinc homeostasis is altered during DENV replication. Therefore, cellular or tissue zinc homeostasis may also determine the efficiency with which pathogens replicate and disseminate *in vivo*. We speculate that in the case of acute viral infections, strategies to transiently block zinc redistribution during viremic stages may inhibit viruses that depend on cellular zinc pools for replication. This would provide a window for the immune system to gain an upper hand and control viral infection.

## DATA AVAILABILITY STATEMENT

The datasets generated for this study has been deposited in the Gene expression Omnibus (GEO) database with accession number GSE135873.

## AUTHOR CONTRIBUTIONS

MK, NK, AP, SSB, and RG performed experiments and analyzed data. SS and SB designed experiments and analyzed the data. GM conceived the study, designed experiments, performed experiments, analyzed data, and wrote the manuscript. All

the authors have reviewed and approved the final version of the manuscript.

## FUNDING

This work was supported by the Intermediate fellowship from Wellcome trust-DBT India alliance (IA/S/14/1/501291) to GM. MK received research fellowship from Department of Biotechnology, India (DBT-JRF/2012-12/324), NK received research fellowship from the University Grants Commission (ID:303673), AP received fellowship from the Council for Scientific and Industrial Research, India (09/1049/(0022)/2016). The funders had no role in study design, data collection and analysis, decision to publish or preparation of the manuscript.

## ACKNOWLEDGMENTS

We thank Amresh Kumar Singh and Richa Vaishnav for technical support and all members of CCV lab for their critical inputs.

## SUPPLEMENTARY MATERIAL

The Supplementary Material for this article can be found online at: https://www.frontiersin.org/articles/10.3389/fimmu.2019.02347/full#supplementary-material

## REFERENCES

1. Liu CH, Zhou L, Chen G, Krug RM. Battle between influenza A virus and a newly identified antiviral activity of the PARP-containing ZAPL protein. *Proc Natl Acad Sci USA*. (2015) 112:14048–53. doi: 10.1073/pnas.1509745112
2. Chen SC, Jeng KS, Lai MMC. Zinc finger-containing cellular transcription corepressor ZBTB25 promotes influenza virus RNA transcription and is a target for zinc ejector drugs. *J Virol*. (2017) 91:e00842–17. doi: 10.1128/JVI.00842-17
3. Read SA, Parnell G, Booth D, Douglas MW, George J, Ahlenstiel G. The antiviral role of zinc and metallothioneins in hepatitis C infection. *J Viral Hepat*. (2018) 25:491–501. doi: 10.1111/jvh.12845
4. Gaudernak E, Seipelt J, Triendl A, Grassauer A, Kuechler E. Antiviral effects of pyrrolidine dithiocarbamate on human rhinoviruses. *J Virol*. (2002) 76:6004–15. doi: 10.1128/JVI.76.12.6004-6015.2002
5. Merluzzi VJ, Cipriano D, McNeil D, Fuchs V, Supeau C, Rosenthal AS, et al. Evaluation of zinc complexes on the replication of rhinovirus 2 *in vitro*. *Res Commun Chem Pathol Pharmacol*. (1989) 66:425–40.
6. Si X, McManus BM, Zhang J, Yuan J, Cheung C, Esfandiarei M, et al. Pyrrolidine dithiocarbamate reduces coxsackievirus B3 replication through inhibition of the ubiquitin-proteasome pathway. *J Virol*. (2005) 79:8014–23. doi: 10.1128/JVI.79.13.8014-8023.2005
7. te Velthuis AJ, van den Worm SH, Sims AC, Baric RS, Snijder EJ, van Hemert MJ. Zn(2+) inhibits coronavirus and arterivirus RNA polymerase activity *in vitro* and zinc ionophores block the replication of these viruses in cell culture. *PLoS Pathog*. (2010) 6:e1001176. doi: 10.1371/journal.ppat.1001176
8. Yamasaki S, Sakata-Sogawa K, Hasegawa A, Suzuki T, Kabu K, Sato E, et al. Zinc is a novel intracellular second messenger. *J Cell Biol*. (2007) 177:637–45. doi: 10.1083/jcb.200702081
9. Kaushik N, Subramani C, Anang S, Muthumohan R, Shalimar, Nayak B, et al. Zinc salts block hepatitis E virus replication by inhibiting the activity of viral RNA-dependent RNA polymerase. *J Virol*. (2017) 91:e00754–17. doi: 10.1128/JVI.00754-17
10. Stanaway JD, Shepard DS, Undurraga EA, Halasa YA, Coffeng LE, Brady OJ, et al. The global burden of dengue: an analysis from the Global Burden of Disease Study 2013. *Lancet Infect Dis*. (2016) 16:712–23. doi: 10.1016/S1473-3099(16)00026-8
11. Yap TL, Xu T, Chen YL, Malet H, Egloff MP, Canard B, et al. Crystal structure of the dengue virus RNA-dependent RNA polymerase catalytic domain at 1.85-angstrom resolution. *J Virol*. (2007) 81:4753–65. doi: 10.1128/JVI.02283-06
12. El Sahili A, Lescar J. Dengue virus non-structural protein 5. *Viruses*. (2017) 9:E91. doi: 10.3390/v9040091
13. Salazar MI, Richardson JH, Sanchez-Vargas I, Olson KE, Beaty BJ. Dengue virus type 2: replication and tropisms in orally infected Aedes aegypti mosquitoes. *BMC Microbiol*. (2007) 7:9. doi: 10.1186/1471-2180-7-9
14. Marchette NJ, Halstead SB, Nash DR, Stenhouse AC. Recovery of dengue viruses from tissues of experimentally infected rhesus monkeys. *Appl Microbiol*. (1972) 24:328–33.
15. Agrawal T, Schu P, Medigeshi GR. Adaptor protein complexes-1 and 3 are involved at distinct stages of flavivirus life-cycle. *Sci Rep*. (2013) 3:1813. doi: 10.1038/srep01813
16. Agrawal T, Sharvani V, Nair D, Medigeshi GR. Japanese encephalitis virus disrupts cell-cell junctions and affects the epithelial permeability barrier functions. *PLoS ONE*. (2013) 8:e69465. doi: 10.1371/journal.pone.0069465
17. Medigeshi GR, Kumar R, Dhamija E, Agrawal T, Kar M. N-desmethylclozapine, fluoxetine, and salmeterol inhibit postentry stages of the dengue virus life cycle. *Antimicrob Agents Chemother*. (2016) 60:6709–18. doi: 10.1128/AAC.01367-16
18. Kar M, Singla M, Chandele A, Kabra SK, Lodha R, Medigeshi GR. Dengue virus entry and replication does not lead to productive infection in platelets. *Open Forum Infect Dis*. (2017) 4:ofx051. doi: 10.1093/ofid/ofx051
19. Gurukumar KR, Priyadarshini D, Patil JA, Bhagat A, Singh A, Shah PS, et al. Development of real time PCR for detection and quantitation of Dengue viruses. *Virol J*. (2009) 6:10. doi: 10.1186/1743-422X-6-10
20. Jothikumar N, Kang G, Hill VR. Broadly reactive TaqMan® assay for real-time RT-PCR detection of rotavirus in clinical and environmental samples. *J Virol Methods*. (2009) 155:126–31. doi: 10.1016/j.jviromet.2008.09.025
21. Mukherjee T, Chatterjee B, Dhar A, Bais SS, Chawla M, Roy P, et al. A TNF-p100 pathway subverts noncanonical NF-kappaB signaling in inflamed secondary lymphoid organs. *EMBO J*. (2017) 36:3501–16. doi: 10.15252/embj.201796919
22. Patel RK, Jain M. NGS QC Toolkit: a toolkit for quality control of next generation sequencing data. *PLoS ONE*. (2012) 7:e30619. doi: 10.1371/journal.pone.0030619
23. Trapnell C, Pachter L, Salzberg SL. TopHat: discovering splice junctions with RNA-Seq. *Bioinformatics*. (2009) 25:1105–11. doi: 10.1093/bioinformatics/btp120
24. Trapnell C, Roberts A, Goff L, Pertea G, Kim D, Kelley DR, et al. Differential gene and transcript expression analysis of RNA-seq experiments with TopHat and Cufflinks. *Nat Protoc*. (2012) 7:562–78. doi: 10.1038/nprot.2012.016
25. de Hoon MJ, Imoto S, Nolan J, Miyano S. Open source clustering software. *Bioinformatics*. (2004) 20:1453–4. doi: 10.1093/bioinformatics/bth078
26. Saldanha AJ. Java treeview–extensible visualization of microarray data. *Bioinformatics*. (2004) 20:3246–8. doi: 10.1093/bioinformatics/bth349
27. Wang Y, Mumm JB, Herbst R, Kolbeck R, Wang Y. IL-22 increases permeability of intestinal epithelial tight junctions by enhancing claudin-2 expression. *J Immunol*. (2017) 199:3316–25. doi: 10.4049/jimmunol.1700152
28. Ren H, Birch NP, Suresh V. An optimised human cell culture model for alveolar epithelial transport. *PLoS ONE*. (2016) 11:e0165225. doi: 10.1371/journal.pone.0165225
29. Heijink IH, Brandenburg SM, Noordhoek JA, Postma DS, Slebos DJ, van Oosterhout AJ. Characterisation of cell adhesion in airway epithelial cell types using electric cell-substrate impedance sensing. *Eur Respir J*. (2010) 35:894–903. doi: 10.1183/09031936.00065809

30. Verhoeckx K, Cotter P, López-Expósito I, Kleiveland C, Lea T, Mackie A, et al., editors. *The Impact of Food Bioactives on Health: in vitro and ex vivo Models*. Cham: Springer (2015). doi: 10.1007/978-3-319-16104-4
31. Watanabe S, Chan KW, Wang J, Rivino L, Lok SM, Vasudevan SG. Dengue virus infection with highly neutralizing levels of cross-reactive antibodies causes acute lethal small intestinal pathology without a high level of viremia in mice. *J Virol.* (2015) 89:5847–61. doi: 10.1128/JVI.00216-15
32. Dickman KG, Hempson SJ, Anderson J, Lippe S, Zhao L, Burakoff R, et al. Rotavirus alters paracellular permeability and energy metabolism in Caco-2 cells. *Am J Physiol Gastrointest Liver Physiol.* (2000) 279:G757–66. doi: 10.1152/ajpgi.2000.279.4.G757
33. Lazzerini M, Wanzira H. Oral zinc for treating diarrhoea in children. *Cochrane Database Syst Rev.* (2016) 12:Cd005436. doi: 10.1002/14651858.CD005436.pub5
34. Homma K, Fujisawa T, Tsuburaya N, Yamaguchi N, Kadowaki H, Takeda K, et al. SOD1 as a molecular switch for initiating the homeostatic ER stress response under zinc deficiency. *Mol Cell.* (2013) 52:75–86. doi: 10.1016/j.molcel.2013.08.038
35. Kawamata T, Horie T, Matsunami M, Sasaki M, Ohsumi Y. Zinc starvation induces autophagy in yeast. *J Biol Chem.* (2017) 292:8520–30. doi: 10.1074/jbc.M116.762948
36. Shumaker DK, Vann LR, Goldberg MW, Allen TD, Wilson KL. TPEN, a Zn2+/Fe2+ chelator with low affinity for Ca2+, inhibits lamin assembly, destabilizes nuclear architecture and may independently protect nuclei from apoptosis *in vitro*. *Cell Calcium.* (1998) 23:151–64. doi: 10.1016/S0143-4160(98)90114-2
37. Rahal ON, Fatfat M, Hankache C, Osman B, Khalife H, Machaca K, et al. Chk1 and DNA-PK mediate TPEN-induced DNA damage in a ROS dependent manner in human colon cancer cells. *Cancer Biol Ther.* (2016) 17:1139–48. doi: 10.1080/15384047.2016.1235658
38. Zhu B, Wang J, Zhou F, Liu Y, Lai Y, Wang J, et al. Zinc depletion by TPEN induces apoptosis in human acute promyelocytic nb4 cells. *Cell Physiol Biochem.* (2017) 42:1822–36. doi: 10.1159/000479539
39. Hyun HJ, Sohn JH, Ha DW, Ahn YH, Koh JY, Yoon YH. Depletion of intracellular zinc and copper with TPEN results in apoptosis of cultured human retinal pigment epithelial cells. *Invest Ophthalmol Visual Sci.* (2001) 42:460–5.
40. Boyce M, Bryant KF, Jousse C, Long K, Harding HP, Scheuner D, et al. A selective inhibitor of eIF2alpha dephosphorylation protects cells from ER stress. *Science.* (2005) 307:935–9. doi: 10.1126/science.1101902
41. Bhatnagar S, Bahl R, Sharma PK, Kumar GT, Saxena SK, Bhan MK. Zinc with oral rehydration therapy reduces stool output and duration of diarrhea in hospitalized children: a randomized controlled trial. *J Pediatr Gastroenterol Nutr.* (2004) 38:34–40. doi: 10.1097/00005176-200401000-00010
42. Dalgic N, Sancar M, Bayraktar B, Pullu M, Hasim O. Probiotic, zinc and lactose-free formula in children with rotavirus diarrhea: are they effective? *Pediatr Int.* (2011) 53:677–82. doi: 10.1111/j.1442-200X.2011.03325.x
43. Jiang CX, Xu CD, Yang CQ. [Therapeutic effects of zinc supplement as adjunctive therapy in infants and young children with rotavirus enteritis]. *Zhongguo Dang Dai Er Ke Za Zhi.* (2016) 18:826–30. doi: 10.7499/j.issn.1008-8830.2016.09.008
44. Ooi ET, Ganesananthan S, Anil R, Kwok FY, Sinniah M. Gastrointestinal manifestations of dengue infection in adults. *Med J Malaysia.* (2008) 63:401–5.
45. Vejchapipat P, Theamboonlers A, Chongsrisawat V, Poovorawan Y. An evidence of intestinal mucosal injury in dengue infection. *South Asian J Trop Med Public Health.* (2006) 37:79–82.
46. Nicklin MJH, Toyoda H, Murray MG, Wimmer E. Proteolytic processing in the replication of polio and related viruses. *Bio/Technology.* (1986) 4:33–42. doi: 10.1038/nbt0186-33
47. Tedbury PR, Harris M. Characterisation of the role of zinc in the hepatitis C virus NS2/3 auto-cleavage and NS3 protease activities. *J Mol Biol.* (2007) 366:1652–60. doi: 10.1016/j.jmb.2006.12.062
48. Quadt R, Jaspars EM. Effect of removal of zinc on alfalfa mosaic virus RNA-dependent RNA polymerase. *FEBS Lett.* (1991) 278:61–2. doi: 10.1016/0014-5793(91)80083-F
49. Poiesz BJ, Seal G, Loeb LA. Reverse transcriptase: correlation of zinc content with activity. *Proc Natl Acad Sci USA.* (1974) 71:4892–6. doi: 10.1073/pnas.71.12.4892
50. Auld DS, Kawaguchi H, Livingston DM, Vallee BL. RNA-dependent DNA polymerase (reverse transcriptase) from avian myeloblastosis virus: a zinc metalloenzyme. *Proc Natl Acad Sci USA.* (1974) 71:2091–5. doi: 10.1073/pnas.71.5.2091
51. Oxford JS, Perrin DD. Inhibition of the particle-associated RNA-dependent RNA polymerase activity of influenza viruses by chelating agents. *J General Virol.* (1974) 23:59–71. doi: 10.1099/0022-1317-23-1-59
52. Sommergruber W, Casari G, Fessl F, Seipelt J, Skern T. The 2A proteinase of human rhinovirus is a zinc containing enzyme. *Virology.* (1994) 204:815–8. doi: 10.1006/viro.1994.1599
53. Schoggins JW, Wilson SJ, Panis M, Murphy MY, Jones CT, Bieniasz P, et al. A diverse range of gene products are effectors of the type I interferon antiviral response. *Nature.* (2011) 472:481–5. doi: 10.1038/nature09907
54. Fleith RC, Mears HV, Leong XY, Sanford TJ, Emmott E, Graham SC, et al. IFIT3 and IFIT2/3 promote IFIT1-mediated translation inhibition by enhancing binding to non-self RNA. *Nucleic Acids Res.* (2018) 46:5269–85. doi: 10.1093/nar/gky191
55. Johnson B, VanBlargan LA, Xu W, White JP, Shan C, Shi PY, et al. Human IFIT3 modulates IFIT1 RNA binding specificity and protein stability. *Immunity.* (2018) 48:487–99.e5. doi: 10.1016/j.immuni.2018.01.014
56. Mears HV, Sweeney TR. Better together: the role of IFIT protein-protein interactions in the antiviral response. *J Gen Virol.* (2018) 99:1463–77. doi: 10.1099/jgv.0.001149
57. Taguwa S, Maringer K, Li X, Bernal-Rubio D, Rauch JN, Gestwicki JE, et al. Defining Hsp70 subnetworks in dengue virus replication reveals key vulnerability in flavivirus infection. *Cell.* (2015) 163:1108–23. doi: 10.1016/j.cell.2015.10.046
58. Howe MK, Speer BL, Hughes PF, Loiselle DR, Vasudevan S, Haystead TA. An inducible heat shock protein 70 small molecule inhibitor demonstrates anti-dengue virus activity, validating Hsp70 as a host antiviral target. *Antiviral Res.* (2016) 130:81–92. doi: 10.1016/j.antiviral.2016.03.017
59. Laskaris P, Atrouni A, Calera JA, d'Enfert C, Munier-Lehmann H, Cavaillon J-M, et al. Administration of zinc chelators improves survival of mice infected with named-content genus-species named-content- Aspergillus fumigatus both in Monotherapy and in Combination with Caspofungin. *Antimicrob Agents Chemother.* (2016) 60:5631–9. doi: 10.1128/AAC.00324-16
60. Xiao Z, Ehrlich E, Luo K, Xiong Y, Yu XF. Zinc chelation inhibits HIV Vif activity and liberates antiviral function of the cytidine deaminase APOBEC3G. *FASEB J.* (2007) 21:217–22. doi: 10.1096/fj.06-6773com


**Conflict of Interest:** The authors declare that the research was conducted in the absence of any commercial or financial relationships that could be construed as a potential conflict of interest.

frontiers in Immunology

ORIGINAL RESEARCH
published: 23 January 2020
doi: 10.3389/fimmu.2020.00015

# Immunomodulatory Properties of Bacterium-Like Particles Obtained From Immunobiotic Lactobacilli: Prospects for Their Use as Mucosal Adjuvants

*Fernanda Raya Tonetti*[1,2,3], *Lorena Arce*[1,2,3], *Susana Salva*[4], *Susana Alvarez*[4], *Hideki Takahashi*[5,6], *Haruki Kitazawa*[7,8], *Maria Guadalupe Vizoso-Pinto*[1,2,3*†] and *Julio Villena*[4,7*†]

[1] Infection Biology Lab, Instituto Superior de Investigaciones Biológicas (INSIBIO), CONICET-UNT, Tucumán, Argentina, [2] Facultad de Medicina, Universidad Nacional de Tucumán (UNT), Tucumán, Argentina, [3] Laboratorio de Ciencias Básicas & Or. Genética, Facultad de Medicina, Universidad Nacional de Tucumán, Tucumán, Argentina, [4] Laboratory of Immunobiotechnology, Reference Centre for Lactobacilli (CERELA-CONICET), Tucumán, Argentina, [5] Laboratory of Plant Pathology, Graduate School of Agricultural Science, Tohoku University, Sendai, Japan, [6] Plant Immunology Unit, International Education and Research Center for Food Agricultural Immunology, Graduate School of Agricultural Science, Tohoku University, Sendai, Japan, [7] Food and Feed Immunology Group, Laboratory of Animal Products Chemistry, Graduate School of Agricultural Science, Tohoku University, Sendai, Japan, [8] Livestock Immunology Unit, International Education and Research Center for Food Agricultural Immunology (CFAI), Graduate School of Agricultural Science, Tohoku University, Sendai, Japan

OPEN ACCESS

**Edited by:**
*Wilson Savino, Oswaldo Cruz Foundation (Fiocruz), Brazil*

**Reviewed by:**
*Yanfei Zhang, Geisinger Health System, United States*
*Jeff Xingdong Yang, National Institutes of Health (NIH), United States*

***Correspondence:**
*Maria Guadalupe Vizoso-Pinto*
*mgvizoso@fm.unt.edu.ar*
*Julio Villena*
*jcvillena@cerela.org.ar*

*†These authors have contributed equally to this work*

**Specialty section:**
*This article was submitted to Nutritional Immunology, a section of the journal Frontiers in Immunology*

**Received:** *06 June 2019*
**Accepted:** *06 January 2020*
**Published:** *23 January 2020*

**Citation:**
*Raya Tonetti F, Arce L, Salva S, Alvarez S, Takahashi H, Kitazawa H, Vizoso-Pinto MG and Villena J (2020) Immunomodulatory Properties of Bacterium-Like Particles Obtained From Immunobiotic Lactobacilli: Prospects for Their Use as Mucosal Adjuvants. Front. Immunol. 11:15. doi: 10.3389/fimmu.2020.00015*

Non-viable lactic acid bacteria (LAB) have been proposed as antigen delivery platforms called bacterium-like particles (BLPs). Most studies have been performed with *Lactococcus lactis*-derived BLPs where multiple antigens were attached to the peptidoglycan surface and used to successfully induce specific immune responses. It is well-established that the immunomodulatory properties of LAB are strain dependent and therefore, the BLPs derived from each individual strain could have different adjuvant capacities. In this work, we obtained BLPs from immunomodulatory (immunobiotics) and non-immunomodulatory *Lactobacillus rhamnosus* and *Lactobacillus plantarum* strains and comparatively evaluated their ability to improve the intestinal and systemic immune responses elicited by an attenuated rotavirus vaccine. Results demonstrated that orally administered BLPs from non-immunomodulatory strains did not induce significant changes in the immune response triggered by rotavirus vaccine in mice. On the contrary, BLPs derived from immunobiotic lactobacilli were able to improve the levels of anti-rotavirus intestinal IgA and serum IgG, the numbers of $CD24^+B220^+$ B and $CD4^+$ T cells in Peyer's patches and spleen as well as the production of IFN-γ by immune cells. Interestingly, among immunobiotics-derived BLPs, those obtained from *L. rhamnosus* CRL1505 and *L. rhamnosus* IBL027 enhanced more efficiently the intestinal and systemic humoral immune responses when compared to BLPs from other immunobiotic bacteria. The findings of this work indicate that it is necessary to perform an appropriate selection of BLPs in order to find those with the most efficient adjuvant properties. We propose the term Immunobiotic-like particles (IBLPs) for the BLPs derived from CRL1505 and IBL027 strains that are an excellent alternative for the development of mucosal vaccines.

**Keywords: lactobacilli, bacterium-like particles, mucosal vaccine, adjuvant, rotavirus**

## INTRODUCTION

Lactic acid bacteria (LAB) have been studied for several years as potential delivery systems and/or adjuvants for mucosal vaccine development. In this regard, recombinant LAB expressing pathogen's antigens in their cell-walls have been used as oral or nasal vaccines in animal models (1–4). The mucosal administration of recombinant LAB was shown to elicit specific systemic and mucosal immune responses against selected antigens. However, the administration of genetically modified organisms is associated with ethical concerns related to the possible dissemination of virulence factors or antibiotic resistant genes. Then, similar to other genetically modified organisms, recombinant LAB expressing antigens from pathogens and carrying antibiotic resistant genes cannot be applied in humans.

An original alternative to the use of genetically modified LAB was the development of bacterium-like particles (BLPs) derived from the acid and heat treatments of *Lactococcus lactis* (5–8). These *L. lactis*-derived BLPs, also known as Gram-positive enhancer matrix particles, do not contain DNA or cytoplasmic proteins but conserve the adjuvant capacities of the bacteria. The acid/heat treatment results in the bacterial death, which implies greater safety related to the maximum dose administered, and in addition to causing the loss of genetic material, exposes the peptidoglycan of the cell-wall increasing its capacity to bind proteins with lysine motifs (LysM) at least 10 times (5). The ability of BLPs to improve the protective immunity generated at the mucosal level by recombinant proteins from different pathogens fused to LysM has been widely evaluated. The microbial pathogens tested in those investigations included bacteria, parasites and viruses such as *Streptococcus pneumoniae* (5), *Plasmodium berghei* (7, 9), and Influenza virus (10). Those studies clearly demonstrated that *L. lactis*-derived BLPs are a promising adjuvant for mucosal immunization.

The immunomodulatory properties of LAB proved to depend on each individual strain. Previously, we evaluated the ability of immunomodulatory viable LAB strains, administered by the oral route in the same dose and during the same period, on intestinal immunity (11–13). We found that although both *Lactobacillus rhamnosus* CRL1505 and *Lactobacillus plantarum* CRL1506 improved the intestinal immunity and the protection against pathogens, the CRL1505 strain was more efficient than the CRL1506 to achieve those beneficial effects (11–13). Similarly, both *L. lactis* NZ9000 and *L. rhamnosus* CRL1505 administered by the nasal route were able to improve respiratory immunity and confer protection against *S. pneumoniae* infection. However, the protective effect induced by *L. lactis* NZ9000 was modest when compared to *L. rhamnosus* CRL1505 and it was necessary a longer administration period of lactococci than lactobacilli (14–16).

We hypothesized that BLPs obtained from different immunomodulatory LAB would have different adjuvant capacity when used in mucosal vaccine formulations. In this work, we obtained BLPs from immunomodulatory (immunobiotics), and non-immunomodulatory *L. rhamnosus* and *L. plantarum* strains and comparatively evaluated their ability to improve intestinal and systemic immune responses to an oral attenuated rotavirus vaccine.

## MATERIALS AND METHODS

### Microorganisms and Bacterium-Like Particles

*L. rhamnosus* CRL1505, *L. plantarum* CRL1506 and *L. plantarum* CRL1905 were obtained from the culture collection of CERELA (Tucumán, Argentina). *L. rhamnosus* IBL027 was obtained from the culture collection of the Infection Biology Laboratory of INSIBIO (Tucumán, Argentina). Lactobacilli ($10^{10}$ CFU stored at −70°C) were activated and cultured for 12 h at 37°C (final log phase) in Man-Rogosa-Sharpe (MRS) broth culture media. The bacteria were harvested by centrifugation and washed with sterile PBS (0.01 mol/L, pH 7.2). Chemical pre-treatment of lactobacilli to generate BLP and immunomodulatory bacterium-like particles (IBLP) was performed as follows. Bacteria from a fresh overnight culture (100 ml) were collected by centrifugation (10 min, 13,000 x g) and washed once with sterile distilled water. Afterwards, the pellet was suspended in 20 ml of 0.1 M HCl and boiled in a water bath for 45 min. Next, the cells were washed three times in 50 ml sterile phosphate buffer saline (PBS), pH 7.4, with vigorous vortexing. After the last washing step, cells were resuspended in 10 ml PBS and stored at −20°C. The number of IBLP particles per milliliter was adjusted according to the CFU/ml determined in the starting culture. Viability of BLPs and IBLPs was checked by plating the suspensions and several dilutions on to MRS agar plates, which were incubated overnight at 37°C in microaerophilia.

### Electron Microscopy

For transmission electron microscopy, samples were prepared according to the Centro de Investigaciones y Servicios de Microscopía Electronica (CISME–CONICET) standard procedure. Briefly, *L. rhamnosus* CRL1505 and IBLP1505 were fixed by adding Karnovsky fixative. After 24 h of fixation at 4°C, samples were washed three times with 0.1M sodium phosphate buffer (pH 7.4) and postfixed overnight in a solution containing 1% osmium tetroxide in sodium phosphate buffer. After dehydratation with a graded ethanol series, the samples were embedded in Spurr resin. Ultrathin sections were cut with an ultramicrotome and examined with a Zeiss Libra 120 transmission electron microscope.

### Animals and Ethical Statement

Four-week-old female BALB/c mice were obtained from the closed colony at CERELA (Tucumán, Argentina) in SPF conditions. Animals were housed in plastic cages and environmental conditions were kept constant, in agreement with the standards for animal housing. Animal welfare was in charge of researchers and special staff trained in animal care and handling at CERELA. Animal health and behavior were monitored twice a day.

This study was carried out in strict accordance with the recommendations in the Guide for the Care and Use of Laboratory Animals of the Guidelines for Animal

Experimentation of CERELA. The CERELA Institutional Animal Care and Use Committee prospectively approved this research under the protocol BIOT-CRL-18.

## Immunization Protocols

Mice were vaccinated with the commercial, oral, pentavalent, and live rotavirus vaccine RotaTeq® (Merck & Co., Inc.). Two sets of experiments with different immunization protocols were used. In the first set of experiments, mice were vaccinated with 30 μl of rotavirus vaccine and $10^8$ bacterial cells or particles (high vaccine/low adjuvant immunization protocol). Mice that received only 30 μl of rotavirus vaccine were used as controls. In a second set of experiments, mice were vaccinated with 7.5 μl of rotavirus vaccine and $10^9$ bacterial cells or particles (low vaccine/high adjuvant immunization protocol). Mice that received only 7.5 μl of rotavirus vaccine were used as controls. In both protocols, mice were immunized orally on days 0, 14 and 28. Seven days after the last immunization (day 35), the specific humoral and cellular immune responses were evaluated as described below.

## Serum and Intestinal Antibodies

Blood samples were obtained through cardiac puncture seven days after the last immunization (day 35) and collected in heparinized tubes. Intestinal fluid samples were obtained as described previously (11). Briefly, the small intestine was flushed with 5 ml of PBS and the fluid was centrifuged (10,000×g 4°C for 10 min) to separate particulate material. The supernatant was kept frozen until use. Specific anti-rotavirus antibodies (IgA and IgG) were determined by ELISA. Plates were coated with 1.5 μg of Rotateq per well overnight at 4°C and blocked with serum bovine albumin. Appropriate dilutions of the samples (serum 1:20; intestinal fluid 1:2) were incubated for 1 h at 37°C. Peroxidase conjugated anti-mouse IgG, or IgA antibodies (1:500) (Sigma-Aldrich) were added and incubated for 1 h at 37°C. The reaction was developed with TMB Substrate Reagent (Sigma-Aldrich) and measured at 450 nm in a microplate reader.

## Flow Cytometry

Ilium Payer's patches and spleens were collected and mechanically disaggregated. A single-cell suspension from the Peyer's patches or spleens of each mouse was obtained by gently passing the collected tissue through a tissue strainer with PBS supplemented with 2% FCS (FACS buffer). Cell suspensions were subjected to red blood cells lysis (Tris-ammonium chloride, BD PharMingen) and counted on a hemocytometer. Trypan blue exclusion method was used to assess viability of cells. Cell suspensions were pre-incubated with anti-mouse CD32/CD16 monoclonal antibody (Fc block) for 30 min at 4°C. Cells were incubated with the antibody mixes for 30 min at 4°C and washed with FACS buffer. The following antibodies from BD Biosciences were used: PE-labeled anti-mouse CD24, biotinylated anti-mouse B220, PE-labeled anti-mouse CD45, biotinylated anti-mouse CD45, FITC-labeled anti-mouse CD3, PE-labeled anti-mouse CD8, and biotinylated anti-mouse CD4 antibodies. Streptavidin-PerCP was used as a second-step reagent. Flow cytometry was performed using a BD FACSCaliburTM flow cytometer (BD Biosciences) and data were analyzed using FlowJo software (TreeStar).

## Cytokine Production by Immune Cells

Ilium Payer's patches and spleens were collected, and a single-cell suspension from each mouse was obtained as described above. After red blood cells lysis, isolated cells were suspended in complete DMEM (Invitrogen) supplemented with 10% FCS (Sigma), 50 μg/ml penicillin-streptomycin, and 50 μg/ml gentamicin (Invitrogen). Cells ($4 \times 10^6$ cells/well) were cultured in 24-well plates in the presence of 0.5 μl of the rotavirus vaccine. Cytokines were quantified in culture supernatants by ELISA after 24 h at 37°C. The concentrations of tumor necrosis factor (TNF)-α, interferon (IFN)-γ, and interleukin (IL)-4 were measured on the supernatants of the stimulated mononuclear cells isolated from Peyer's patches or spleen with commercially available enzyme-linked immunosorbent assay (ELISA) kits following the manufacturer's recommendations (R&D Systems, MN, USA).

## Statistical Analysis

Each experimental group consisted of 3 mice per group at each time point and experiments were performed in triplicate ($n = 9$ for each parameter studied). Results were expressed as mean ± standard deviation (SD). The differences between groups were analyzed using student *t*-test. Differences were considered significant at $p < 0.05$. ANOVA one-way was used for analysis of variance among multiple groups.

# RESULTS

## Development of IBLP From *L. rhamnosus* CRL1505

The heat-acid treatment of the lactobacilli results in non-living particles. This procedure most likely affected the protein and DNA content of the IBLPs. The intracellular contents of the IBLPs seemed to be partially released or degraded (**Figure 1**). IBLPs have the same size and shape than living lactobacilli. Peptidoglycan, the main component of the lactobacilli's cell wall, was exposed by the harsh acid treatment. This peptidoglycan matrix preserved the structural integrity of lactobacilli (**Figure 1**).

## IBLP From *L. rhamnosus* CRL1505 Enhance the Humoral Immune Response Against Rotavirus Vaccine

In order to evaluate the adjuvant capacity of IBLP1505, we selected an oral pentavalent vaccine that contains five live reassortant rotaviruses. Then, mice were immunized on days 0, 14, and 28 by the oral route with the rotavirus vaccine and IBLP1505 as described in detail in the materials and methods section. Mice orally immunized with the vaccine alone or added with viable *L. rhamnosus* CRL1505 were used for comparisons. The levels of rotavirus-specific intestinal IgA and serum IgG were determined seven days after the last immunization. In a first set of experiments, mice were vaccinated with 30 μl of vaccine and $10^8$ bacterial cells or particles (high vaccine/low adjuvant immunization protocol). As shown in **Figure 2A**, both

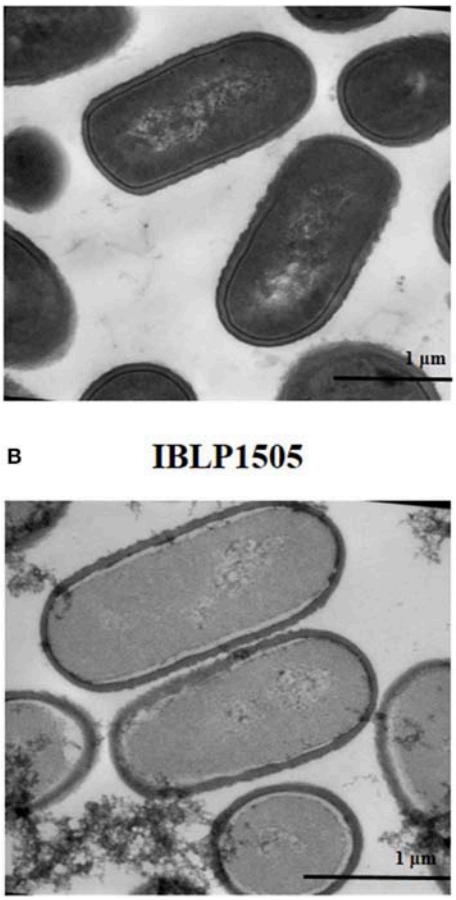


**FIGURE 1 |** Transmission electron microscopy analysis. **(A)** *Lactobacillus rhamnosus* CRL1505 untreated cells and **(B)** bacterium-like particles obtained from *L. rhamnosus* CRL1505 (IBLP1505) were fixed with Karnovsky fixative, postfixed with 1% osmium tetroxide in sodium phosphate buffer and embedded in Spurr resin. Ultrathin sections cuts were examined with a Zeiss libra 120 Transmission Electron Microscope.

intestinal and serum specific antibodies were detected in control mice indicating that the vaccine induced mucosal and systemic humoral immune responses in our model. The levels of rotavirus-specific intestinal IgA and serum IgG in mice immunized with the rotavirus vaccine and IBLP1505 were significantly higher when compared to controls (**Figure 2A**). In addition, intestinal IgA in mice immunized with the rotavirus vaccine and viable *L. rhamnosus* CRL1505 were significantly higher than controls. However, in this group of mice, the levels of serum specific IgG antibodies were not different from controls (**Figure 2A**).

In a second set of experiments, we evaluated whether the dose of rotavirus vaccine could be reduced by using a higher dose of IBLP1505 (low vaccine/high adjuvant immunization protocol). Then, mice were vaccinated with 7.5 µl of vaccine and $10^9$ bacterial cells or particles. As shown in **Figure 2B**, the levels of intestinal rotavirus-specific IgA did not change in comparison with the previous vaccination protocol. However, a significant reduction of serum specific IgG antibodies was detected. The levels of intestinal IgA and serum IgG antibodies in mice immunized with the rotavirus vaccine and IBLP1505 were significantly higher than controls (**Figure 2B**). We also observed that intestinal IgA levels were higher and that serum IgG levels were lower than the values obtained in the first immunization protocol (**Figure 2A**). Interestingly, the group of mice receiving the low vaccine dose together with viable *L. rhamnosus* CRL1505 had rotavirus-specific intestinal IgA and serum IgG antibodies that were not different from controls (**Figure 2B**).

## IBLP From *L. rhamnosus* CRL1505 Enhance the Mucosal Cellular Immune Response Against Rotavirus Vaccine

We next evaluated whether the two immunization protocols were able to modify the mucosal and systemic cellular immune elicited by rotavirus vaccine. First, we evaluated the proportion of $CD3^+CD4^+$ and $CD3^+CD8^+$ T cells as well as $CD24^+B220^+$ B cells in Peyer's patches of vaccinated mice. In the high vaccine/low IBLP1505 immunization protocol (**Figure 3A**), the vaccination of control mice did not induce significant changes in $CD3^+CD4^+$, $CD3^+CD8^+$, or $CD24^+B220^+$ cells percentages when compared with non-immunized mice (data not shown). In addition, no differences were observed in $CD3^+CD4^+$ and $CD3^+CD8^+$ T cells when mice immunized with rotavirus vaccine and IBLP1505 or viable *L. rhamnosus* CRL1505 were compared to controls. However, the vaccination protocols that included IBLP1505 or viable *L. rhamnosus* CRL1505 as adjuvants significantly increased the proportion of $CD24^+B220^+$ B cells in Peyer's patches when compared to controls (**Figure 3A**). In the low vaccine/high adjuvant immunization protocol (**Figure 3B**), the vaccination of mice with the rotavirus vaccine and IBLP1505 significantly increased $CD3^+CD4^+$ T cells as well as $CD24^+B220^+$ B cells in Peyer's patches. Mice, which received rotavirus vaccine and viable *L. rhamnosus* CRL1505 only had significantly higher $CD3^+CD4^+$ T cells than controls (**Figure 3B**). No significant differences between the groups were observed regarding $CD3^+CD8^+$ T cell counts.

We then assessed the ability of immune cells obtained from the Peyer's patches of vaccinated mice to induce cytokines in response to the *ex vivo* stimulation with the rotavirus vaccine. For this purpose, isolated immune cells were cultured and after challenging them with rotavirus the levels of TNF-α, IFN-γ and IL-4 were evaluated in the supernatants (**Figure 4**). As expected, the vaccination of control mice with the two protocols used in this work significantly increased the production of TNF-α, IFN-γ, and IL-4 by Peyer's patches immune cells in response to vaccine stimulation when compared with non-immunized mice (data not shown). In addition, both the high vaccine/low IBLP1505 and the low vaccine/high IBLP1505 immunization protocols significantly enhanced the production of TNF-α, IFN-γ, and IL-4 when compared to the control group (**Figure 4**). Similarly, the vaccination protocols

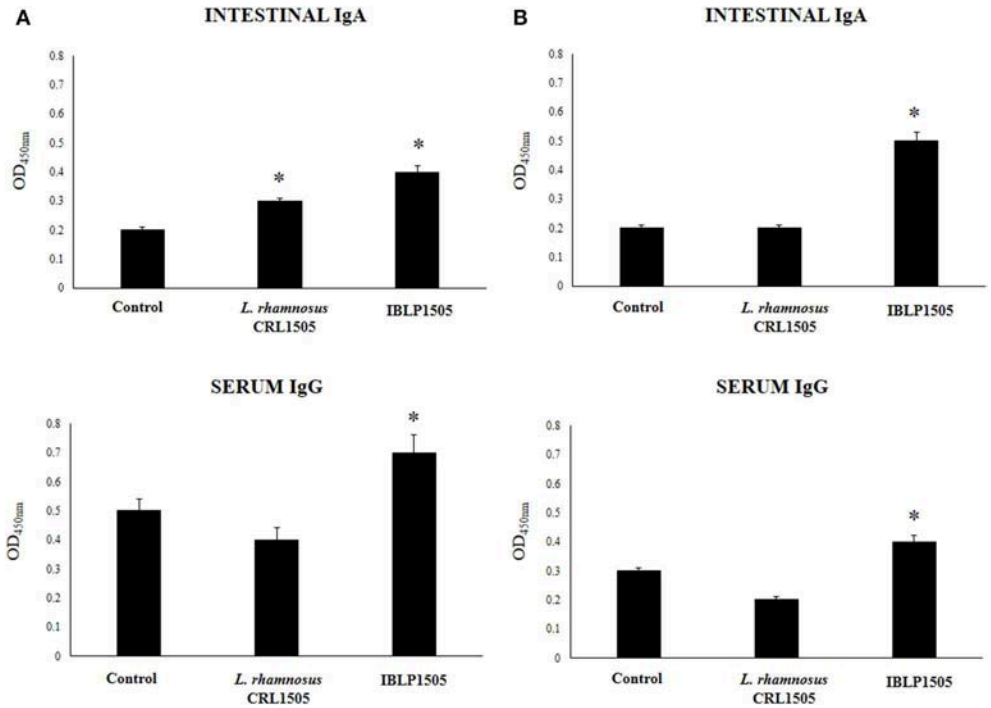


**FIGURE 2 |** Effect of immunobiotic bacterium-like particles obtained from *Lactobacillus rhamnosus* CRL1505 (IBLP1505) on the humoral immune response induced by the immunization of mice with an oral rotavirus vaccine. Mice (4-week-old) were immunized on days 0, 14, and 28 by the oral route with the rotavirus vaccine and IBLP1505 as adjuvant. Mice orally vaccinated with rotavirus vaccine only (controls) and mice receiving the vaccine with viable *L. rhamnosus* CRL1505 as adjuvant were used for comparisons. Two immunization protocols were used: **(A)** each mouse was vaccinated with 30 μl of vaccine and $10^8$ bacterial cells or particles; **(B)** each mouse was vaccinated with 7.5 μl of vaccine and $10^9$ bacterial cells or particles. Seven days after the last immunization, serum, and intestinal fluid samples were obtained for the determination of IgA and IgG specific antibodies. Each experimental group consisted of 3 mice per group and experiments were performed in triplicate ($n = 9$). Results were expressed as mean ± standard deviation. Differences were considered significant at $P < 0.05$ when compared with animals immunized with rotavirus vaccine only (*).

using viable *L. rhamnosus* CRL1505 as adjuvant increased the levels of these cytokines when compared to control mice (**Figure 4**).

## IBLP From *L. rhamnosus* CRL1505 Enhance the Systemic Cellular Immune Response Against Rotavirus Vaccine

The proportions of $CD3^+CD4^+$ and $CD3^+CD8^+$ T cells as well as $CD24^+B220^+$ B cells in spleen of vaccinated mice were also evaluated. No significant differences were observed between the groups when these immune cell populations were evaluated for both immunization protocols (data not shown). In addition, the levels of TNF-α, IFN-γ, and IL-4 were quantified in the supernatants of cultured isolated immune cells from spleens after the challenge with the rotavirus vaccine (**Figure 5**). In the high vaccine/low IBLP1505 or viable *L. rhamnosus* CRL1505 immunization protocols (**Figure 5A**), the vaccination with rotavirus vaccine and adjuvants significantly increased the production of TNF-α, IFN-γ, and IL-4 by splenocytes when compared to controls. Interestingly, the levels of TNF-α and IFN-γ were significantly higher in mice immunized with viable *L. rhamnosus* CRL1505 than in those receiving IBLP1505 (**Figure 5A**). On the other hand, in the low vaccine/high IBLP1505 or viable *L. rhamnosus* CRL1505 immunization protocols (**Figure 5B**), the vaccination of mice significantly enhanced the production of the three cytokines by splenocytes when compared to controls.

## The Adjuvant Capacities of BLP From Lactobacilli Are Strain-Dependent

Finally, we aimed to evaluate whether the adjuvant capacity of IBLP1505 was a strain characteristic or if it was shared by BLP derived from other immunomodulatory strains. Then, we obtained BLP from the immunomodulatory strains *L. rhamnosus* IBL027 and *L. plantarum* CRL1506 and from the non-immunomodulatory strain *L. plantarum* CRL1905. The particles were designated as IBLP027, IBLP1506, and BLP1905 and used to immunize mice with the low vaccine/high adjuvant immunization protocol. As shown in **Figure 6**, IBLP027 was as effective as IBLP1505 to improve the production of rotavirus-specific intestinal IgA and serum IgG antibodies. In addition, intestinal IgA in mice immunized with the rotavirus vaccine and IBLP1506 were significantly higher than controls. However, these antibodies were lower when compared to those in mice receiving IBLP027 or IBLP1505 (**Figure 6**). The immunization with BLP1905 was not able to significantly change the levels of rotavirus-specific intestinal IgA and serum IgG antibodies when compared to controls.

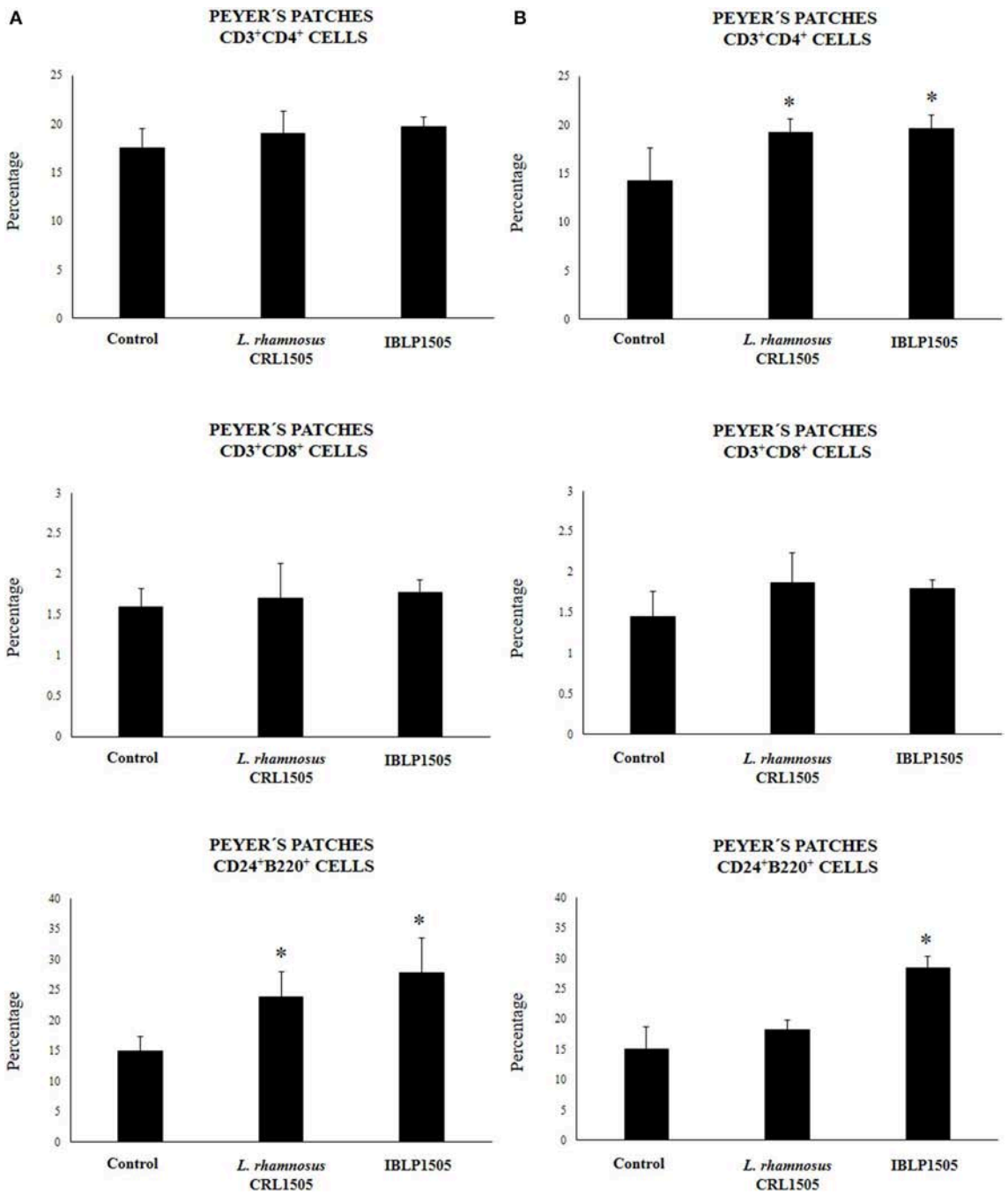


**FIGURE 3 |** Effect of immunobiotic bacterium-like particles obtained from *Lactobacillus rhamnosus* CRL1505 (IBLP1505) on the cellular immune response induced by the immunization of mice with an oral rotavirus vaccine. Mice (4-week-old) were immunized on days 0, 14, and 28 by the oral route with the rotavirus vaccine and IBLP1505 as adjuvant. Mice orally vaccinated with rotavirus vaccine only (controls) and mice receiving the vaccine with viable *L. rhamnosus* CRL1505 as adjuvant were used for comparisons. Two immunization protocols were used: **(A)** each mouse was vaccinated with 30 μl of vaccine and $10^8$ bacterial cells or particles; **(B)** each mouse was vaccinated with 7.5 μl of vaccine and $10^9$ bacterial cells or particles. Seven days after the last immunization, Peyer's patches samples were obtained for the study of $CD3^+CD4^+$, $CD3^+CD8^+$ T and $CD24^+B220^+$ B cells within the $CD45^+$ population by flow cytometry. Each experimental group consisted of 3 mice per group and experiments were performed in triplicate ($n = 9$). Results were expressed as mean ± standard deviation. Differences were considered significant at $P < 0.05$ when compared with animals immunized with rotavirus vaccine only (*).

In addition, we assessed the ability of immune cells obtained from the Peyer's patches and spleens of mice vaccinated with IBLP027, IBLP1506, or BLP1905 to induce TNF-α, IFN-γ and IL-4 in response to the *ex vivo* stimulation with rotavirus (**Figure 6**). IBLP027 was as effective as IBLP1505 to improve the production of TNF-α and IFN-γ by intestinal and spleen

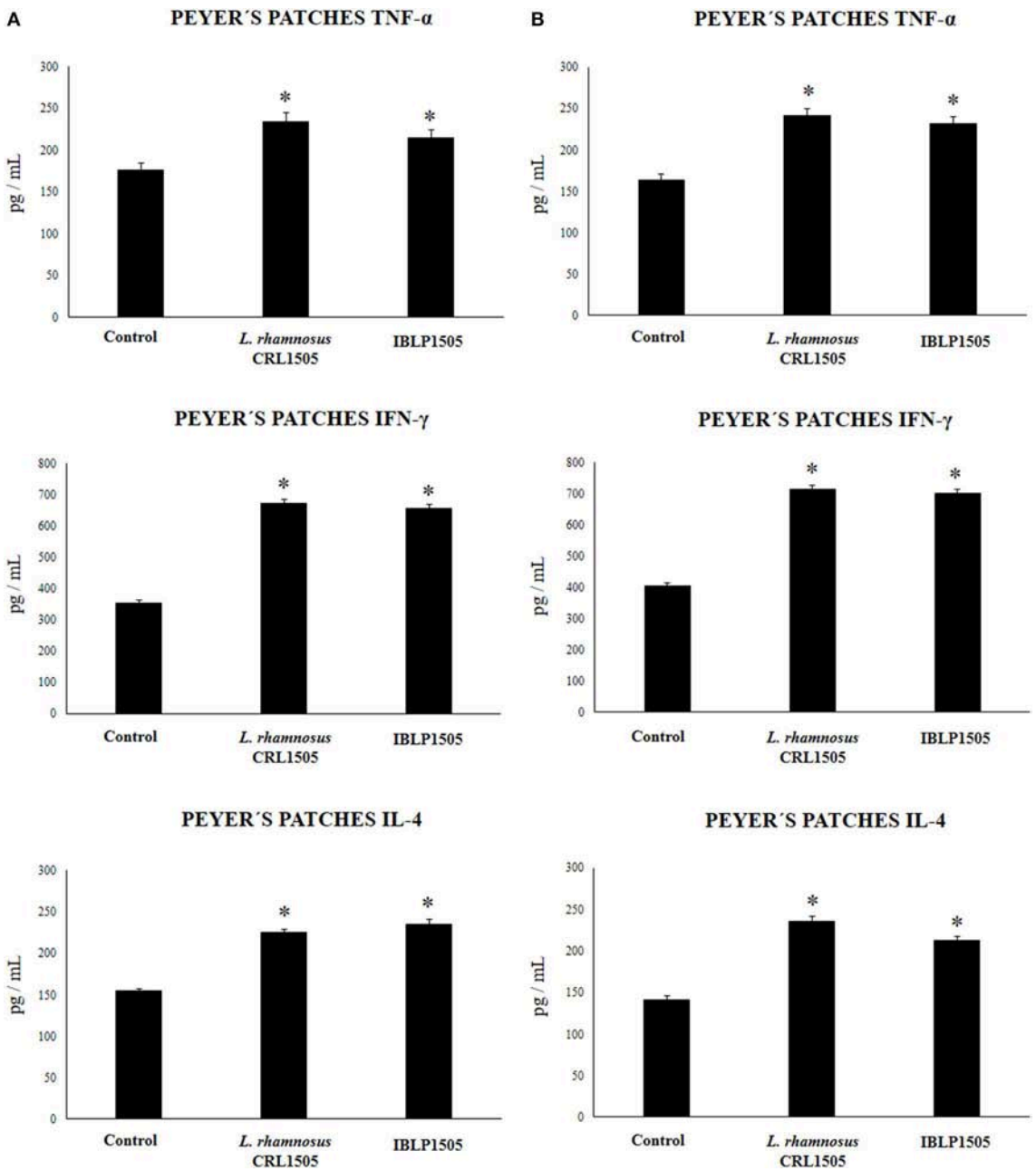


**FIGURE 4 |** Effect of immunobiotic bacterium-like particles obtained from *Lactobacillus rhamnosus* CRL1505 (IBLP1505) on the cellular immune response induced by the immunization of mice with an oral rotavirus vaccine. Mice (4-week-old) were immunized on days 0, 14, and 28 by the oral route with the rotavirus vaccine and IBLP1505 as adjuvant. Mice orally vaccinated with rotavirus vaccine only (controls) and mice receiving the vaccine with viable *L. rhamnosus* CRL1505 as adjuvant were used for comparisons. Two immunization protocols were used: **(A)** each mouse was vaccinated with 30 μl of vaccine and $10^8$ bacterial cells or particles; **(B)** each mouse was vaccinated with 7.5 μl of vaccine and $10^9$ bacterial cells or particles. Seven days after the last immunization, immune cells from Peyer's patches were isolated and *in vitro* stimulated with rotavirus vaccine. Tumor necrosis factor (TNF)-α, interferon (IFN)-γ and interleukin (IL)-4 were measured in culture supernatants. Each experimental group consisted of 3 mice per group and experiments were performed in triplicate ($n = 9$). Results were expressed as mean ± standard deviation. Differences were considered significant at $P < 0.05$ when compared with animals immunized with rotavirus vaccine only (*).

immune cells in response to rotavirus challenge. Vaccination with the rotavirus vaccine and IBLP1506 increased the levels of IFN-γ produced by Peyer's patches cells. However, this cytokine was significantly lower when compared to the observed in mice receiving IBLP027 or IBLP1505 (**Figure 6**). The immunization with BLP1905 was not able to significantly change the levels of TNF-α and IFN-γ produced by intestinal or spleen cells when compared to controls. Similar to IBLP1505 (**Figures 4**, **5**),

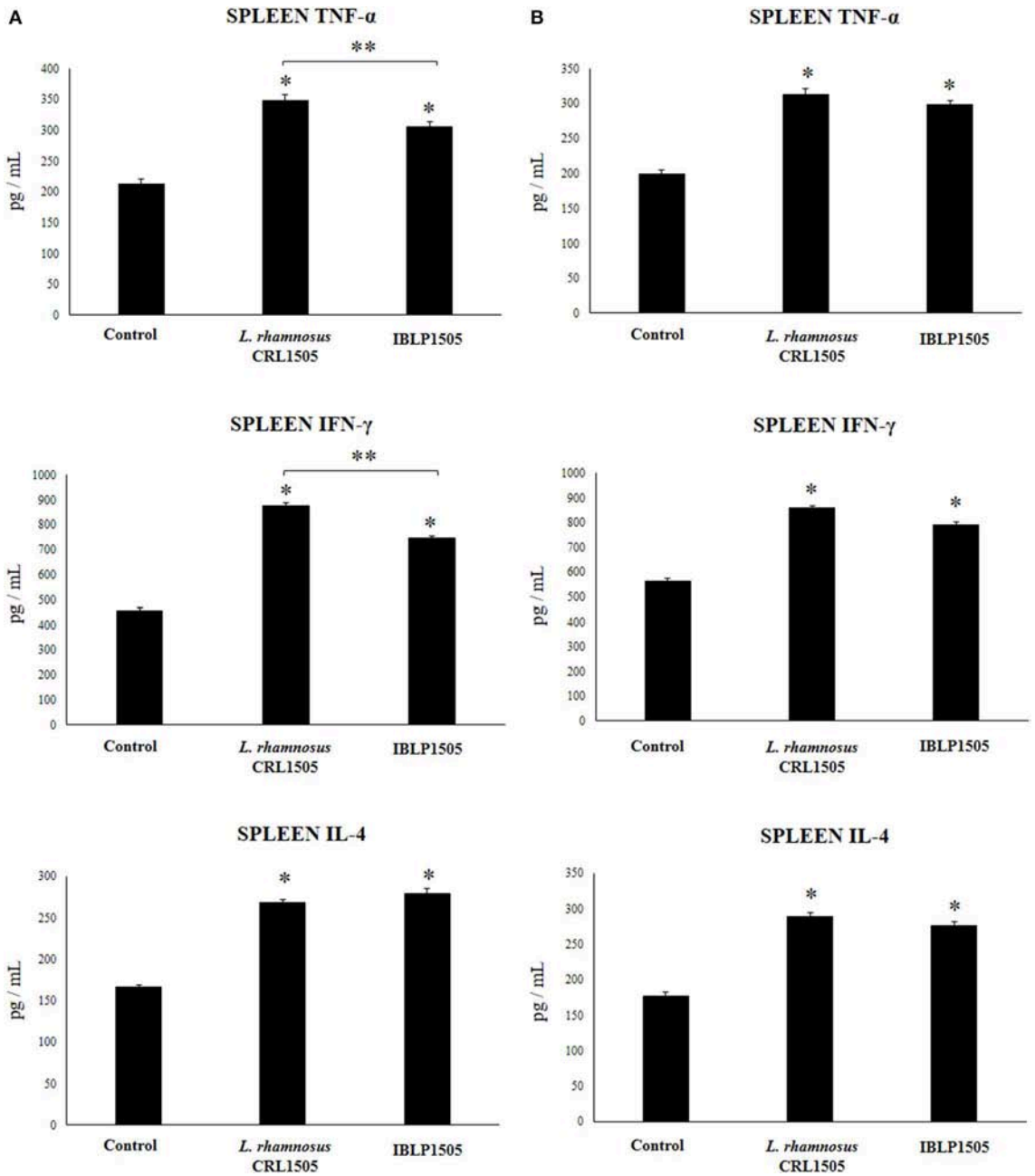


**FIGURE 5 |** Effect of immunobiotic bacterium-like particles obtained from *Lactobacillus rhamnosus* CRL1505 (IBLP1505) on the cellular immune response induced by the immunization of mice with an oral rotavirus vaccine. Mice (4-week-old) were immunized on days 0, 14, and 28 by the oral route with the rotavirus vaccine and IBLP1505 as adjuvant. Mice orally vaccinated with rotavirus vaccine only (controls) and mice receiving the vaccine with viable *L. rhamnosus* CRL1505 as adjuvant were used for comparisons. Two immunization protocols were used: **(A)** each mouse was vaccinated with 30 μl of vaccine and $10^8$ bacterial cells or particles; **(B)** each mouse was vaccinated with 7.5 μl of vaccine and $10^9$ bacterial cells or particles. Seven days after the last immunization, immune cells from spleens were isolated and *in vitro* stimulated with rotavirus vaccine. Tumor necrosis factor (TNF)-α, interferon (IFN)-γ and interleukin (IL)-4 were measured in culture supernatants. Each experimental group consisted of 3 mice per group and experiments were performed in triplicate ($n = 9$). Results were expressed as mean ± standard deviation. Differences were considered significant at $P < 0.05$ when compared with animals immunized with rotavirus vaccine only (*) or between the indicated groups (**).

IBLP027, IBLP1506, and BLP1905 improved the levels of IL-4 in immune cells obtained from the Payer's patches and spleens. There was no statistical differences among the groups (data not shown).

## DISCUSSION

There is an urgent need to develop effective vaccines to reduce the global burden of infectious disease in both humans

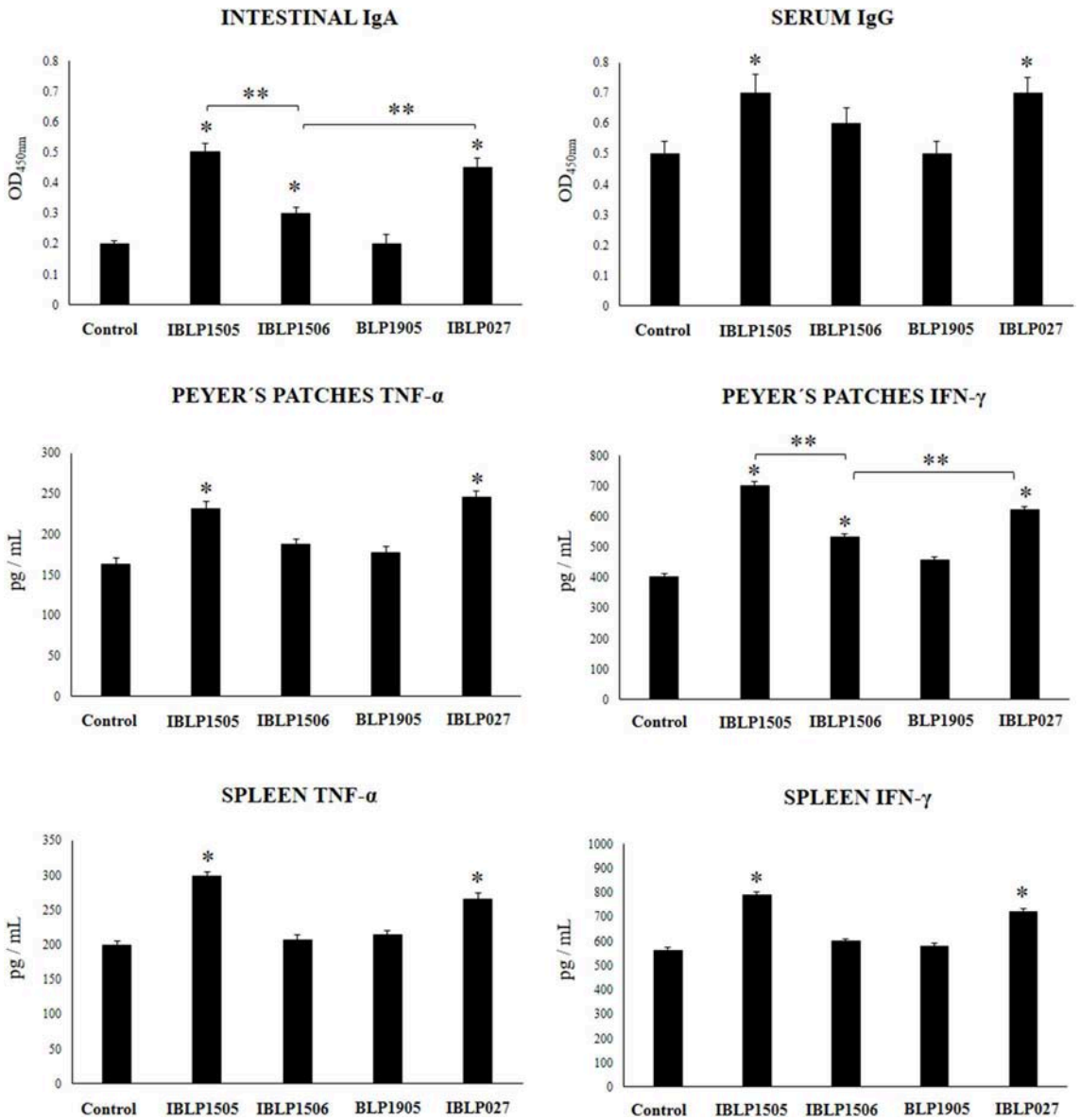


**FIGURE 6 |** Effect of bacterium-like particles obtained from different lactobacilli strains on the immune response triggered by the immunization of mice with an oral rotavirus vaccine. Mice (4-week-old) were immunized on days 0, 14, and 28 by the oral route with the rotavirus vaccine and bacterium-like particles from obtained from the immunomodulatory strains *L. rhamnosus* CRL1505 (IBLP1505), *L. rhamnosus* IBL027 (IBLP027), and *L. plantarum* CRL1506 (IBLP1506) and from the non-immunomodulatory strain *L. plantarum* CRL1905 (IBLP1905) as adjuvants. Mice orally vaccinated with rotavirus vaccine only (controls) were used for comparisons. Each mouse was vaccinated with 7.5 μl of vaccine and $10^9$ bacterial particles. Seven days after the last immunization, serum, and intestinal fluid samples were obtained for the determination of IgA and IgG specific antibodies. In addition, immune cells from Peyer's patches and spleen were isolated, cultured and stimulated with rotaviral vaccine. TNF-α, and IFN-γ concentrations were determined in the supernatants by ELISA. Each experimental group consisted of 3 mice per group and experiments were performed in triplicate ($n = 9$). Results were expressed as mean ± standard deviation. Differences were considered significant at $P < 0.05$ when compared with animals immunized with rotavirus vaccine only (*) or between the indicated groups (**).

and animals. The use of mucosal vaccines triggers local and systemic responses limiting the pathogens at the site of entry, reducing their replication in epithelial cells, the alteration of the epithelial barrier, and the action of toxins on the mucosa. In addition, mucosal vaccination helps preventing the spread of the pathogen to internal tissues and to the environment (17, 18). Despite the several advantages of mucosal vaccination, it faces many difficulties including poor immunogenicity at low concentrations, chemical and enzymatic degradation, potential toxicity, and the risk of generating tolerance rather than protective immunity (17, 19). In this work, we demonstrated that IBLP derived from highly efficient immunomodulatory lactobacilli are an interesting alternative as mucosal adjuvants.

It is well-documented that within the gastrointestinal tract, immunomodulatory LAB are capable to interact with the

host's epithelial and immune cells, and thereby beneficially influence epithelial barrier and immune functions (20). It has been proposed that the final outcome of a host cell response against beneficial immunomodulatory microorganisms depends on the combination of distinct microbial-associated molecular patterns (MAMPs) that can interact with various pattern recognition receptors (PRRs) and associated co-receptors to trigger different signaling pathways (20, 21). The unique combination of cellular and molecular interactions that are established between a certain microorganism with the host cells explains why the immunomodulatory properties of LAB are a strain dependent characteristic. The results of the present work strongly suggest that the same principle could be applied to IBLP derived from different LAB strains. In our hands, IBLP derived from immunomodulatory *L. rhamnosus* CRL1505, *L. rhamnosus* IBL027 and *L. plantarum* CRL1506 showed adjuvant capacities when used together with the rotavirus vaccine while the particles derived from the non-immunomodulatory *L. plantarum* CRL1905 strain were not able to induce modifications in the immune response triggered by the oral vaccination. Moreover, our experiments demonstrated that the particles derived from the immunomodulatory *Lactobacillus* strains had different adjuvant capacities in terms of their ability to improve the cellular and humoral immune responses triggered by rotavirus vaccination.

Our previous comparative *in vitro* studies evaluating the ability of *L. rhamnosus* CRL1505 and *L. plantarum* CRL1506 to modulate immune responses in intestinal epithelial cells and antigen presenting cells (APCs) found significant differences between the two lactobacilli strains (22, 23). It was demonstrated that intestinal epithelial cells were modulated by immunobiotic CRL1505 and CRL1506 in a strain-dependent fashion to enhance antiviral responses (23). Interestingly, *L. rhamnosus* CRL1505 was more efficient that *L. plantarum* CRL1506 to increase the expression of IFN-β and IL-6 in intestinal epithelial cells, both cytokines known to influence immune responses generated by immune cells located under the epithelium. In addition, both lactobacilli strains were reported to functionally modulate APCs from porcine Peyer's patches. However, *L. rhamnosus* CRL1505 was more efficient than *L. plantarum* CRL1506 to improve the expression of IL-1β, IL-6, and IFN-γ in porcine $CD172a^{+}CD11R1^{high}$ and $CD172a^{-}CD11R1^{low}$ dendritic cells (22). The improved Th1 response induced by *L. rhamnosus* CRL1505 in porcine APCs was triggered by TLR2 signaling and included augmented expression of MHC-II and co-stimulatory molecules. Then, our previous results would indicate that IBLP1505 is more efficient than IBLP1506 to modulate the response of intestinal epithelial cells and APCs to the challenge with attenuated rotavirus. Moreover, it is tempting to speculate that IBLP1505 and IBLP027 are able to interact more efficiently with intestinal APCs than IBLP1506, inducing an increase in their activation and antigenic presentation capacity, and generating effector immune responses. In fact, both humoral and cellular intestinal specific immune responses were significantly improved in mice immunized with rotavirus vaccine and IBLP1505 or IBLP027 than in animals treated with the vaccine and IBLP1506, indicating the different capacity of the particles to serve as effective mucosal adjuvants.

Recombinant LAB expressing rotavirus antigens have been evaluated as vaccine candidates (24–27). *L. casei* ATCC 393 (24) and *L. lactis* NZ9000 (25) expressing the major protective antigen VP4 from rotavirus efficiently induced the production of serum IgG and mucosal IgA anti-VP4 antibodies, which also demonstrated neutralizing effects on rotavirus infection. Rodríguez-Díaz et al. (26), evaluated the effect of the oral immunization of mice with *L. lactis* expressing the rotavirus VP8 protein intracellularly and extracellularly. Low mucosal IgA synthesis was found only when the secreting *L. lactis* strain was used. On the other hand, Esteban et al. (27), evaluated the immunogenicity of the rotavirus VP6 protein expressed on the surface of *L. lactis*. Authors described the ability of the recombinant *L. lactis* VP6 to significantly increase the levels of specific serum IgG antibodies although it should be mentioned that the researchers used the subcutaneous route for the immunization of mice. Despite the positive results obtained with the aforementioned recombinant bacteria, there is still general concern about the massive use of genetically modified microorganisms because of the possibility of the introduction of exogenous DNA in the intestinal microbiota, especially plasmids that confer antibiotic resistance. The IBLPs evaluated in this work can help to alleviate these concerns associated to recombinant bacteria because they are non-genetically modified and non-living.

By using a directed chromosomal integration approach, Yin et al. (28) were able to develop a stable *L. casei* strain expressing the porcine rotavirus VP4 antigen. The oral immunization of mice with recombinant *L. casei* VP4 induced both specific intestinal and systemic humoral immune responses. Although this improved chromosome recombination and gene expression system could represent an efficient method for safe vaccines production, it would be necessary to design a recombinant bacterium for each vaccine antigen (from the same virus or from different viruses), which would significantly increase the cost of these types of vaccines. On the other hand, IBLPs are able to incorporate efficiently one or more different antigens on their surfaces, which gives them an additional advantage over recombinant bacteria, even with those that could be considered safe for human use.

To the best of our knowledge, few reports have evaluated the ability of non-living LAB as mucosal adjuvants and/or delivery antigens for rotavirus vaccine development. Temprana et al. (29), offered an option to the use of genetically modified organisms in immunizations by obtaining cell wall-derived fragments by mechanical rupture of a recombinant *L. lactis* NZ9000 expressing a cell wall-anchored version of the rotavirus VP6 protein. Authors evaluated the ability of those cell wall-derived fragments containing the VP6 protein to induce specific

immunity in mice by using intragrastric immunizations. The report indicated that it was not possible to detect VP6-specific serum IgG or IgA in the mice immunized intragastrically, even when additional mucosal adjuvants were used. In addition, the humoral immune response induced by the experimental vaccine was evaluated while its impact on the specific cellular immune response was not studied. In this work, we offer a different alternative, which can be administered orally and efficiently potentiate the local and systemic immune responses against rotavirus. Furthermore, we demonstrate that our strategy not only stimulate the humoral immunity but in addition, a specific Th1 mucosal response can be also generated against the antigens administered with IBLP. Our results suggest that the adjuvant potential of IBLPs could also be exploited for subunit vaccines, as it was the case of the hepatitis E virus (HEV) capsid protein (ORF2) orally administered with IBLP1505 or IBLP027, which induced both antigen-specific humoral and cellular immune responses in mice (30). Then, the evaluation of the ability of rotavirus antigens co-administered with IBLP or fused to a LysM domain and expressed on the surface of IBLP to generate specific protective immune responses is an interesting topic of on-going research.

Some studies have demonstrated that the administration of viable immunobiotic lactobacilli with attenuated rotavirus vaccines significantly augment the ability of the vaccine to stimulate the specific humoral immune response. In this regard, by using a neonatal gnotobiotic pig model, Wen et al. (31) demonstrated that orally administered *L. rhamnosus* GG increase the levels of virus-specific intestinal IgA after vaccination with attenuated human rotavirus. Similarly, *L. acidophilus* NCFM improved rotavirus-specific antibody production as well as memory B-cell responses to attenuated rotavirus vaccine (32). In line with those studies, we showed here that orally administered viable *L. rhamnosus* CRL1505 improved the humoral immune response of rotavirus-vaccinated mice. Interestingly, mice immunized with rotavirus vaccine and viable *L. rhamnosus* CRL1505 showed lower intestinal IgA and serum IgG specific antibodies than mice vaccinated with IBLP1505 as mucosal adjuvant. This phenomenon could be related to the great ability of viable *L. rhamnosus* CRL1505 to stimulate the innate antiviral intestinal immune responses (11–13, 22). Transcriptomic studies revealed the capacity of *L. rhamnosus* CRL1505 to differentially modulate the innate antiviral immune response in porcine intestinal epithelial cells. Higher expression levels of type I IFNs as well as in several antiviral factors including *ifit1*, *nlpr3*, *mda5*, *msx1, rig1 ifit2,* and *mx2* were found in CRL1505-treated cells when compared to control cells (23). In addition, it was demonstrated *in vitro* that viable *L. rhamnosus* CRL1505 is able to efficiently stimulate the expression of IFN-γ in porcine intestinal $CD172a^{+}CD11R1^{-}$ macrophages (22). Then, we hypothesize that the administration of viable *L. rhamnosus* CRL1505 to mice would improve those antiviral mechanisms in the intestinal mucosa, allowing a rapid an efficient elimination of attenuated rotavirus included in the vaccine formulation. The effective elimination of the attenuated pathogens by the innate immune mechanisms would be responsible for the lower interaction of rotavirus with DCs and therefore for the lower stimulation of the adaptive immune response. These results indicate that IBLP1505 has an advantage with respect to viable bacteria to stimulate the intestinal and systemic specific adaptive immune responses to attenuated virus. However, it is important to investigate and compare the ability of viable *L. rhamnosus* CRL1505 and IBLP1505 to stimulate the adaptive immune responses when subunit vaccines are used instead of vaccines based on attenuated pathogens.

There is a growing need for the development of new and improved mucosal vaccines to diminish the morbidity and mortality associated to infectious diseases, particularly against those targeting the respiratory and gastrointestinal tracts (17, 18). The search and characterization of mucosal adjuvants to enhance the immunity against antigens is of fundamental importance to advance in this path. In this regard, BLPs obtained from immunomodulatory beneficial microorganisms are an interesting alternative. Our findings indicate that an appropriate selection of BLPs is necessary in order to find those with the most efficient adjuvant properties. We propose the term Immunobiotic-like particles (IBLPs) for the BLPs derived from highly immunomodulatory strains such as *L. rhamnosus* CRL1505 and *L. rhamnosus* IBL027 that are a promising alternative for the development of mucosal vaccines.

## DATA AVAILABILITY STATEMENT

The datasets generated for this study are available on request to the corresponding author.

## ETHICS STATEMENT

The animal study was reviewed and approved by the CERELA Institutional Animal Care and Use Committee under the protocol BIOT-CRL-18. This study was carried out in strict accordance with the recommendations in the Guide for the Care and Use of Laboratory Animals of the Guidelines for Animal Experimentation of CERELA.

## AUTHOR'S NOTE

FR and LA hold CONICET scholarships. SS, SA, MV-P, and JV are members of CONICET.

## AUTHOR CONTRIBUTIONS

JV and MV-P designed the study and wrote the manuscript. FR, LA, and SS did the experiments. MV-P, JV, HK, and HT provided financial support. JV, MV-P, HK, and SA contributed to data analysis and results interpretation.

## FUNDING

This study was supported by grants of the Agencia Nacional de Ciencia y Técnica (PICT-2016-0853 and 1314 PICT-2016-0410), CONICET (PIP057), and Fundación Allende to JV and MV-P.

This study was also supported by a Grant-in-Aid for Scientific Research (A) (19H00965), (B) (16H05019) and Open Partnership Joint Projects of JSPS Bilateral Joint Research Projects from the Japan Society for the Promotion of Science (JSPS), and by grants from the project of NARO Bio-oriented Technology Research Advancement Institution (Research Program on development of innovation technology, No. 01002A) to HK, and also the grants for Scientific Research on Innovative Areas from the Ministry of Education, Culture, Science, Sports, and Technology (MEXT) of Japan (Grant numbers: 16H06429, 16K21723, and 16H06435) to HT. This work was also supported by JSPS Core-to-Core Program, A. Advanced Research Networks entitled Establishment of international agricultural immunology research-core for a quantum improvement in food safety.

## REFERENCES

1. Bermudez-Humaran LG, Cortes-Perez NG, Le Loir Y, Alcocer-Gonzalez JM, Tamez-Guerra RS, de Oca-Luna RM, et al. An inducible surface presentation system improves cellular immunity against human papillomavirus type 16 E7 antigen in mice after nasal administration with recombinant lactococci. *J Med Microbiol*. (2004) 53:427–33. doi: 10.1099/jmm.0.05472-0
2. Bermudez-Humaran LG, Cortes-Perez NG, Le Loir Y, Gruss A, Rodriguez-Padilla C, Saucedo-Cardenas O, et al. Fusion to a carrier protein and a synthetic propeptide enhances E7 HPV-16 production and secretion in *Lactococcus lactis*. *Biotechnol Prog*. (2003) 19:1101–4. doi: 10.1021/bp0340077
3. Villena J, Medina M, Raya R, Alvarez S. Oral immunization with recombinant *Lactococcus lactis* confers protection against respiratory pneumococcal infection. *Can J Microbiol*. (2008) 54:845–53. doi: 10.1139/W08-077
4. Szatraj K, Szczepankowska AK, Chmielewska-Jeznach M. Lactic acid bacteria - promising vaccine vectors: possibilities, limitations, doubts. *J Appl Microbiol*. (2017) 123:325–39. doi: 10.1111/jam.13446
5. Audouy SA, van Roosmalen ML, Neef J, Kanninga R, Post E, van Deemter M, et al. *Lactococcus lactis* GEM particles displaying pneumococcal antigens induce local and systemic immune responses following intranasal immunization. *Vaccine*. (2006) 24:5434–41. doi: 10.1016/j.vaccine.2006.03.054
6. Bosma T, Kanninga R, Neef J, Audouy SA, van Roosmalen ML, Steen A, et al. Novel surface display system for proteins on non-genetically modified gram-positive bacteria. *Appl Environ Microbiol*. (2006) 72:880–9. doi: 10.1128/AEM.72.1.880-889.2006
7. Ramasamy R, Yasawardena S, Zomer A, Venema G, Kok J, Leenhouts K. Immunogenicity of a malaria parasite antigen displayed by *Lactococcus lactis* in oral immunisations. *Vaccine*. (2006) 24:3900–8. doi: 10.1016/j.vaccine.2006.02.040
8. van Roosmalen ML, Kanninga R, El Khattabi M, Neef J, Audouy S, Bosma T, et al. Mucosal vaccine delivery of antigens tightly bound to an adjuvant particle made from food-grade bacteria. *Methods*. (2006) 38:144–9. doi: 10.1016/j.ymeth.2005.09.015
9. Nganou-Makamdop K, van Roosmalen ML, Audouy SA, van Gemert GJ, Leenhouts K, Hermsen CC, et al. Bacterium-like particles as multi-epitope delivery platform for *Plasmodium berghei* circumsporozoite protein induce complete protection against malaria in mice. *Malaria J*. (2012) 11:50. doi: 10.1186/1475-2875-11-50
10. Saluja V, Amorij JP, van Roosmalen ML, Leenhouts K, Huckriede A, Hinrichs WL, et al. Intranasal delivery of influenza subunit vaccine formulated with GEM particles as an adjuvant. *AAPS J*. (2010) 12:109–16. doi: 10.1208/s12248-009-9168-2
11. Salva S, Villena J, Alvarez S. Immunomodulatory activity of *Lactobacillus rhamnosus* strains isolated from goat milk: impact on intestinal and respiratory infections. *Int J Food Microbiol*. (2010) 141:82–9. doi: 10.1016/j.ijfoodmicro.2010.03.013
12. Villena J, Chiba E, Tomosada Y, Salva S, Marranzino G, Kitazawa H, et al. Orally administered *Lactobacillus rhamnosus* modulates the respiratory immune response triggered by the viral pathogen-associated molecular pattern poly(I:C). *BMC Immunol*. (2012) 13:53. doi: 10.1186/1471-2172-13-53
13. Tada A, Zelaya H, Clua P, Salva S, Alvarez S, Kitazawa H, et al. Immunobiotic Lactobacillus strains reduce small intestinal injury induced by intraepithelial lymphocytes after Toll-like receptor 3 activation. *Inflamm Res*. (2016) 65:771–83. doi: 10.1007/s00011-016-0957-7
14. Medina M, Villena J, Salva S, Vintini E, Langella P, Alvarez S. Nasal administration of *Lactococcus lactis* improves local and systemic immune responses against *Streptococcus pneumoniae*. *Microbiol Immunol*. (2008) 52:399–409. doi: 10.1111/j.1348-0421.2008.00050.x
15. Barbieri N, Villena J, Herrera M, Salva S, Alvarez S. Nasally administered *Lactobacillus rhamnosus* accelerate the recovery of humoral immunity in B lymphocyte-deficient malnourished mice. *J Nutr*. (2013) 143:227–35. doi: 10.3945/jn.112.165811
16. Tomosada Y, Chiba E, Zelaya H, Takahashi T, Tsukida K, Kitazawa H, et al. Nasally administered *Lactobacillus rhamnosus* strains differentially modulate respiratory antiviral immune responses and induce protection against respiratory syncytial virus infection. *BMC Immunol*. (2013) 14:40. doi: 10.1186/1471-2172-14-40
17. Srivastava A, Gowda DV, Madhunapantula SV, Shinde CG, Iyer M. Mucosal vaccines: a paradigm shift in the development of mucosal adjuvants and delivery vehicles. *Acta Pathol Microbiol Immunol Scand*. (2015) 123:275–88. doi: 10.1111/apm.12351
18. Miquel-Clopes A, Bentley EG, Stewart JP, Carding SR. Mucosal vaccines and technology. *Clin Exp Immunol*. (2019) 196:205–14. doi: 10.1111/cei.13285
19. Woodrow KA, Bennett KM, Lo DD. Mucosal vaccine design and delivery. *Annu Rev Biomed Eng*. (2012) 14:17–46. doi: 10.1146/annurev-bioeng-071811-150054
20. Villena J, Vizoso-Pinto MG, Kitazawa H. Intestinal innate antiviral immunity and immunobiotics: beneficial effects against rotavirus infection. *Front Immunol*. (2016) 7:563. doi: 10.3389/fimmu.2016.00563
21. Lebeer S, Vanderleyden J, De Keersmaecker SC. Host interactions of probiotic bacterial surface molecules: comparison with commensals and pathogens. *Nat Rev Microbiol*. (2010) 8:171–84. doi: 10.1038/nrmicro2297
22. Villena J, Chiba E, Vizoso-Pinto MG, Tomosada Y, Takahashi T, Ishizuka T, et al. Immunobiotic *Lactobacillus rhamnosus* strains differentially modulate antiviral immune response in porcine intestinal epithelial and antigen presenting cells. *BMC Microbiol*. (2014) 14:126. doi: 10.1186/1471-2180-14-126
23. Albarracin L, Kobayashi H, Iida H, Sato N, Nochi T, Aso H, et al. Transcriptomic analysis of the innate antiviral immune response in porcine intestinal epithelial cells: influence of immunobiotic lactobacilli. *Front Immunol*. (2017) 8:57. doi: 10.3389/fimmu.2017.00057
24. Qiao X, Li G, Wang X, Li X, Liu M, Li Y. Recombinant porcine rotavirus VP4 and VP4-LTB expressed in Lactobacillus casei induced mucosal and systemic antibody responses in mice. *BMC Microbiol*. (2009) 9:249. doi: 10.1186/1471-2180-9-249
25. Li YJ, Ma GP, Li GW, Qiao XY, Ge JW, Tang LJ, et al. Oral vaccination with the porcine rotavirus VP4 outer capsid protein expressed by *Lactococcus lactis* induces specific antibody production. *J Biomed Biotechnol*. (2010) 2010:708460. doi: 10.1155/2010/708460
26. Rodríguez-Díaz J, Montava R, Viana R, Buesa J, Pérez-Martínez G, Monedero V. Oral immunization of mice with *Lactococcus lactis* expressing the rotavirus VP8 protein. *Biotechnol Lett*. (2011) 33:1169–75. doi: 10.1007/s10529-011-0551-6
27. Esteban LE, Temprana CF, Argüelles MH, Glikmann G, Castello AA. Antigenicity and immunogenicity of rotavirus VP6 protein

expressed on the surface of *Lactococcus lactis*. *Biomed Res Int.* (2013) 2013:298598. doi: 10.1155/2013/298598
28. Yin JY, Guo CQ, Wang Z, Yu ML, Gao S, Bukhari SM, et al. Directed chromosomal integration and expression of porcine rotavirus outer capsid protein VP4 in *Lactobacillus casei* ATCC393. *Appl Microbiol Biotechnol.* (2016) 100:9593–604. doi: 10.1007/s00253-016-7779-y
29. Temprana CF, Argüelles MH, Gutierrez NM, Barril PA, Esteban LE, Silvestre D, et al. Rotavirus VP6 protein mucosally delivered by cell wall-derived particles from *Lactococcus lactis* induces protection against infection in a murine model. *PLoS ONE.* (2018) 13:e0203700. doi: 10.1371/journal.pone.0203700
30. Arce LP, Raya Tonetti MF, Raimondo MP, Müller MF, Salva S, Alvarez S, et al. Oral vaccination with hepatitis E Virus capsid protein and immunobiotic bacterium-like particles induce intestinal and systemic immunity in mice. *Probiot Antimicrob Proteins.* (2019). doi: 10.1007/s12602-019-09598-7
31. Wen K, Liu F, Li G, Bai M, Kocher J, Yang X, et al. *Lactobacillus rhamnosus* GG dosage affects the adjuvanticity and protection against rotavirus diarrhea in gnotobiotic pigs. *J Pediatr Gastroenterol Nutr.* (2015) 60:834–43. doi: 10.1097/MPG.0000000000000694
32. Liu F, Wen K, Li G, Yang X, Kocher J, Bui T, et al. Dual functions of *Lactobacillus acidophilus* NCFM as protection against rotavirus diarrhea. *J Pediatr Gastroenterol Nutr.* (2014) 58:169–76. doi: 10.1097/MPG.0000000000000197

**Conflict of Interest:** The authors declare that the research was conducted in the absence of any commercial or financial relationships that could be construed as a potential conflict of interest.

frontiers in Immunology

REVIEW
published: 05 February 2020
doi: 10.3389/fimmu.2020.00114

# Feed, Microbiota, and Gut Immunity: Using the Zebrafish Model to Understand Fish Health

*Adrià López Nadal*[1,2], *Wakako Ikeda-Ohtsubo*[3], *Detmer Sipkema*[4], *David Peggs*[5], *Charles McGurk*[5], *Maria Forlenza*[1], *Geert F. Wiegertjes*[2] *and Sylvia Brugman*[1]*

[1] *Cell Biology and Immunology Group, Wageningen University and Research, Wageningen, Netherlands,* [2] *Aquaculture and Fisheries Group, Wageningen University and Research, Wageningen, Netherlands,* [3] *Laboratory of Animal Products Chemistry, Graduate School of Agricultural Science, Tohoku University, Sendai, Japan,* [4] *Microbiology, Wageningen University and Research, Wageningen, Netherlands,* [5] *Skretting Aquaculture Research Centre, Stavanger, Norway*

Aquafeed companies aim to provide solutions to the various challenges related to nutrition and health in aquaculture. Solutions to promote feed efficiency and growth, as well as improving the fish health or protect the fish gut from inflammation may include dietary additives such as prebiotics and probiotics. The general assumption is that feed additives can alter the fish microbiota which, in turn, interacts with the host immune system. However, the exact mechanisms by which feed influences host-microbe-immune interactions in fish still remain largely unexplored. Zebrafish rapidly have become a well-recognized animal model to study host-microbe-immune interactions because of the diverse set of research tools available for these small cyprinids. Genome editing technologies can create specific gene-deficient zebrafish that may contribute to our understanding of immune functions. Zebrafish larvae are optically transparent, which allows for *in vivo* imaging of specific (immune) cell populations in whole transgenic organisms. Germ-free individuals can be reared to study host-microbe interactions. Altogether, these unique zebrafish features may help shed light on the mechanisms by which feed influences host-microbe-immune interactions and ultimately fish health. In this review, we first describe the anatomy and function of the zebrafish gut: the main surface where feed influences host-microbe-immune interactions. Then, we further describe what is currently known about the molecular pathways that underlie this interaction in the zebrafish gut. Finally, we summarize and critically review most of the recent research on prebiotics and probiotics in relation to alterations of zebrafish microbiota and immune responses. We discuss the advantages and disadvantages of the zebrafish as an animal model for other fish species to study feed effects on host-microbe-immune interactions.

**Keywords: zebrafish, immunity, prebiotics, probiotics, microbiota, intestine, gut**

OPEN ACCESS

***Edited by:***
*Julio Villena,*
*CONICET Centro de Referencia para Lactobacilos (CERELA), Argentina*

***Reviewed by:***
*Zhigang Zhou,*
*Feed Research Institute (CAAS), China*
*Xiaofei Sun,*
*University of California, San Francisco, United States*

****Correspondence:***
*Sylvia Brugman*
*Sylvia.brugman@wur.nl*

***Specialty section:***
*This article was submitted to Nutritional Immunology, a section of the journal Frontiers in Immunology*

***Received:*** *15 November 2019*
***Accepted:*** *16 January 2020*
***Published:*** *05 February 2020*

***Citation:***
*López Nadal A, Ikeda-Ohtsubo W, Sipkema D, Peggs D, McGurk C, Forlenza M, Wiegertjes GF and Brugman S (2020) Feed, Microbiota, and Gut Immunity: Using the Zebrafish Model to Understand Fish Health. Front. Immunol. 11:114. doi: 10.3389/fimmu.2020.00114*

## ZEBRAFISH AS A MODEL FOR IMMUNITY

In late 1960s, the Hungarian molecular biologist George Streisinger obtained zebrafish (*Danio rerio*) to investigate molecular mechanisms applying forward genetics in a vertebrate model [reviewed in (1)]. Initially, researchers used zebrafish to study developmental biology followed by the employment of zebrafish in numerous other fields. Among these, zebrafish stood-out as a model

to study immunity due to the high presence (∼70%) of human orthologous genes in the zebrafish genome (2) and its intrinsic characteristics. Zebrafish are small (<5 cm), highly prolific (200–300 new progeny per week) and fast growing compared to mice. Zebrafish develop *ex-utero* which, combined with the embryos' transparency, enables investigation of ontogeny *in vivo* from an early time point in development [reviewed in (3)]. Moreover, the use of transgenic fish facilitates *in vivo* visualization of specific immune cell populations such as neutrophils (4) based on expression of the neutrophil-associated enzyme myeloperoxidase (5) using fluorescent microscopy. In addition, their well-annotated genome eased the generation of mutant zebrafish lines, some of which contributed to elucidate immune gene functions [reviewed in (3)]. In the last decade, genome editing techniques based on Zinc finger nuclease [reviwed in (6)], TALENs (7) and the highly successful CRISPR-Cas technique (8, 9) changed the speed at which single gene functions can be addressed in this model organism. Currently gene insertion still appears more challenging than gene knock-out, something that will undoubtedly change in the near future (10). Zebrafish characteristics combined with these unique research tools established these small cyprinids as an important animal model to study immune processes and underlying molecular mechanisms.

## ZEBRAFISH INTESTINE: STRUCTURE, FUNCTION, AND MICROBIOTA

Zebrafish do not have a stomach and their digestive tract is anatomically divided into separate sections: the mouth, the esophagus, three gut segments (anterior, middle, and posterior) and the anus. The zebrafish esophagus is connected with the anterior gut segment, where the nutrient absorption predominantly occurs due to a high presence of digestive enzymes. Nutrient uptake gradually diminishes from the anterior to the posterior gut segments. Ion transport, water reabsorption, fermentation processes as well as certain immune functions occur in the middle and posterior gut segment (11, 12). Wang et al. investigated the gene expression of the adult zebrafish gut and compared it to the gut of mice which is anatomically divided into: mouth, esophagus, stomach, three small intestine sections [duodenum, jejunum, and ileum), cecum, large intestine, rectum and anus (13)]. In this study the zebrafish gut was divided into equal-length segments (called S1–S7, from anterior to posterior) and, based on subsequent transcriptomic analysis, regrouped into three main segments: S1–S5, S6, and S7 corresponding to small and large murine gut (14). Subsequently, Lickwar et al. performed transcriptomics on adult intestinal epithelial cells (IECs) from zebrafish, stickleback, mouse and human (15). They specified that the segments S1-S4 of the zebrafish gut presented 493 highly expressed genes from which 70 were also upregulated in the mouse anterior gut (duodenum and ileum-like segments). Next to this, the authors found a core set of genes present in all vertebrate IECs as well as conservation in transcriptional start sites and regulatory regions, independent of sequence similarity (15).

Besides all the similarities described above, there are clear anatomical differences between zebrafish and the murine digestive tract. Zebrafish do not have a stomach, intestinal crypts, Peyer's patches nor Paneth cells [reviewed in (16)]. In addition, there are dissimilarities in feeding habits, environmental conditions, body sizes and/or specific metabolic requirements. The fact that for instance, lipid metabolism is regulated by similar gut segments between zebrafish and mouse does not imply homology since their metabolism differs greatly: i.e., zebrafish do not have brown fat (13). Still it remains striking that IECs of different species are more similar in gene expression and regulation (regardless of species intestinal anatomy or feeding habits) than different cell types of the same species (15). The evidence that gene expression and regulation of this expression in the gut is so highly conserved between species suggests the potential of zebrafish as a valid model for other fish species such as other cyprinids or salmonids when investigating intestinal function.

It has been shown in mice that colonization of the gut with specific microbes induces immune system function. For example, colonization of germ-free (GF) mice with segmented filamentous bacteria induced activation of CD4+ T cells as well as IgA production (17). Rawls et al. generated a GF zebrafish larval model to study the function of the gut microbiota (18). Using this model they examined the effect of colonization on the host transcriptional response (6 dpf - days post fertilization- larvae) by DNA microarray analysis. Similarly to mice or humans, microbiota-associated gene expressions clustered in several canonical pathways mainly related to four physiological functions: epithelial cell turn-over, nutrient metabolism, xenobiotic metabolism, and innate immune responses (18). In mammals, microbiome colonization may occur during birth (19) or prenatally in the womb (20). In zebrafish, microbiome colonization is thought to occur at hatching although vertical transmission of microbiome components during oviposition has also been suggested (21). Recently, the colonization cycle of microbial species into the gut of zebrafish larvae has been studied in more detail using several generations of GF zebrafish larvae mono-associated with *Aeromonas veronii* (22). The colonization cycle was found to be divided in four steps: (1) immigration of environmental microbes into the fish, (2) gut adaptation of such microbes, (3) microbe emigration from the host to the environment, and (4) environmental adaptation of the microbes. Both environmental and host gut microbial adaptation were assessed by microbial growth rate, abundance and persistence within the gut or the environment. When comparing four evolved isolates (undergone multiple cycles through the host) and the ancestral strain the authors observed that the evolved isolates were more abundantly present in the fish gut, emphasizing the role of immigration and further adaptation of species into the zebrafish gut.

Earlier colonization studies showed that immigration into the host and gut adaptation are found to be time-specific for each microbe: γ-Proteobacteria were highly abundant in environmental samples as well as in the gut of zebrafish larvae while β-Proteobacteria were mostly abundant in environmental samples and in the gut of juvenile zebrafish, indicating a

delayed colonization by certain species of β-Proteobacteria after initial exposure (23). Further research may clarify the specific species involved in the colonization process and whether the colonization delay is due to low microbe immigration to or adaptation to the host gut. During colonization, two major microbial shifts in colonization of zebrafish were described: a first shift at 10 dpf from embryo to larvae and a second shift between 35 and 75 dpf, from juvenile to early adult (23). During the first shift at 10 dpf some individuals had high taxa an richness samples (resembling embryos) while others showed low taxa richness and diversity (resembling juveniles). This distribution could be the result of different developing speed among the larvae. Since feeding generally commences at 6 dpf and zebrafish larvae actively hunt for the (live) feed some fish grow and develop faster than others. In support of the zebrafish observations, studies in other fish species also describe an age-dependent decrease in species density and diversity of the gut microbial community from larval to adult stages [reviewed in (24)]. The embryo-to-larva shift could be due to the consumption of exogenous feed (Paramecium) and the juvenile-to-early-adult shift could be due to physiological processes such as sexual maturation (23). Nonetheless, it cannot be excluded that microbiota may adapt and expand due to certain feed components or that the live feed itself brings along microbes and microbial analysis of feed samples could further clarify gut colonization dynamics. Most significantly, so far a putative contribution of a maturing immune system regarding microbiota composition has hardly been addressed in zebrafish.

Larval zebrafish have functional and well-developed organs but their immune system is not completely mature yet. Adaptive immune maturation in zebrafish is an active research topic within the scientific field. In a relatively small study, we showed that T cells control Proteobacteria *(Vibrio)* abundance in the zebrafish gut, providing evidence that like in mice the adaptive immune system plays a role in shaping the microbiota composition (25). T cells are present in the thymus by 4 dpf as shown by using CD4-1:mCherry transgenic zebrafish (26) and CD8a+ antibody staining (27). It was shown that T cells egress from the thymus as early as 10 dpf. This suggests that from that time point onwards systemic adaptive responses could be mounted in the zebrafish. However, more in depth studies on the exact timing (the variability thereof) and functionality of these thymic emigrants are warranted.

After the initial colonization period, important for both host and microbe development, the microbiota is believed to enter a stable state. Comparison of gut microbiota of wild-caught zebrafish and zebrafish raised in two separate laboratory facilities revealed that there is a shared so-called core gut microbiota (23, 28). High quality 16S rRNA gene analysis showed common and abundant bacterial groups represented by 21 operational taxonomic units (OTUs), dominated by members of the Proteobacteria phylum (genera *Aeromonas* and *Shewanella*) followed by Fusobacteria or Firmicutes (class Bacilli), Actinobacteria and Bacteroidetes phyla (28).

In conclusion, all organisms on earth are colonized with bacterial species from their environment. The host and colonizing microbes adapt to ensure fitness of both the host and microbiota. It is important to realize that only performing colonization studies using zebrafish larvae may not represent the complete picture. Especially the maturation of the host immune system can have a profound effects on shaping the intestinal microbiota and, therefore, extrapolation of larval results to juveniles or adults should be carefully examined. Nonetheless, the fact that zebrafish can be reared GF and are still optically transparent at 10 dpf together with the possibility of transgenesis of immune cell populations make zebrafish a very powerful organism to study the timing of microbial colonization and immune system maturation.

## SHAPING THE MICROBIOTA: ENVIRONMENTAL AND HOST FACTORS

Microbes can establish symbiotic relationships with their host by, for instance, facilitating nutrient digestion of diets. Host (biotic) and environmental (abiotic) factors play a role in the modulation of the (intestinal) microbiota. For example, zebrafish larvae exposed to naturally found concentrations of antibiotics together with an antinutritional factor (soy saponin) showed an increased neutrophil recruitment in the gut as well as dysbiosis in the overall microbiome composition (29). A meta-analysis of 16S rRNA gene sequence data from 25 individual fish gut communities (30) integrated five already published zebrafish data-sets (28, 31). Microbial intestinal communities from different species clustered together and separately from environmental samples. Within the intestinal microbial cluster different gut bacterial communities exist depending on trophic level (herbivores, carnivores, or omnivores), habitats (saltwater, freshwater, estuarine, or migratory fish), and sampling methods (30). Taking the observations together, the symbiotic process between host and bacteria is highly conserved and partly depends on diet and natural habitat.

So which host mechanisms influence the gut microbiota composition? In order to study to what extend the gut selects the microbial community, GF mice were colonized with gut microbiota of conventionally-raised (CONV) zebrafish and vice-versa, GF zebrafish were colonized with gut microbiota of CONV mice. The mouse microbiota generally contains a higher proportion of Firmicutes and Bacteroides compared to the zebrafish microbiota which is dominated by Proteobacteria. Interestingly, after transfer of the mouse microbiota into GF zebrafish, the relative abundance of the Proteobacteria increased toward a microbiota composition of zebrafish. Vice-versa, when zebrafish microbes (dominated by Proteobacteria) were transferred to mice recipient the Firmicutes from this zebrafish content flourished up to >50% compared to the Firmicutes abundance of 1% in original zebrafish microbiota (31). Therefore, it seems that the host gut environment shapes the microbiota.

The immune system is part of this host gut environment. For example, zebrafish gut macrophages can shape the microbiota via interferon regulatory factor *irf8*. Adult *irf8*-deficient zebrafish displayed a reduced number of macrophages (mpeg1.1 promoter), presented reduced *c1q* genes expression (*c1qa*, *c1qb*, *c1qc,* and *c1ql*) and severe dysbiosis (Fusobacteria, α-

and γ-Proteobacteria diminished in favor of δ-Proteobacteria) compared to controls. Downregulation of *c1q* genes may imply an ineffective complement system which could contribute to the observed dysregulation of commensal microbiota. Restauration of *irf8* expression reversed *c1q* genes expression and the levels of commensal microbes (32). However, a recent study showed that the mpeg1.1 promoter is not only marking macrophages but also phagocytic B lymphocytes in adult zebrafish (33). This might indicate that B cells might also play a role in shaping the microbiota.

In addition to the influence of the fish innate immune system on shaping the microbial communities, there is evidence that the adaptive immune system also plays a role in this process. Adult wild-type zebrafish displayed a decreased abundance of Proteobacteria (*Vibrio)* compared to zebrafish lacking adaptive immunity (rag1-/-), indicating that the innate immune system alone cannot fully regulate all members of the microbiota in the gut. Also, adoptive transfer of T and non-T cells (B and NK-like cells) from wild-types to rag1-/- fish showed that transfer of T cells, but not B/NK-like cells, in the rag1-/- fish diminished *Vibrio* spp. outgrowth 1 week after transfer, suggesting that T cells could regulate the abundance of certain intestinal microbial species. Furthermore, the lack of adaptive immune response together with altered microbiota induced an inflamed state in the gut of aged zebrafish (14 weeks post feralization): *il-1β* and *cxcl2-l2* were upregulated and *il10*, *ifnγ*, and *il17f2* downregulated compared to controls. These aged rag1-/- zebrafish developed dropsy (edema caused by bacterial infection) or became anorexic, confirming the physiological effects of an absence of adaptive immunity and possibly a dysregulated microbiota (25). Others also tested the contribution of the adaptive immune system to gut microbiota in adult zebrafish. In this study, rag1-/- or wild-type zebrafish were either housed separately or were co-housed. In segregated genotypes, rag1-/- microbial communities differed from that of wild-types, suggesting a selective pressure of the adaptive immune system. However, such effect was lost when rag1-/- and wild-type zebrafish were housed together (34). This study suggested that housing could have more influence on microbial diversity than (the absence of the) adaptive immunity. The observation seems to contradict an earlier meta-analysis where different rearing conditions did not result in phylogenetically divergent gut microbiota although cohousing of distinct genotypes was not included in their study (30). Even though the exact extent to which the host immune system affects the microbiota is not completely elucidated, the aforementioned studies (25, 31, 32, 34) suggest selective pressures of the innate and adaptive immune system on the composition of the host gut microbiota.

Contrary to the putative selective pressure of the gut immunity on the microbiota, chance and random distribution (neutral model) was also investigated as explanation for the initial/early assembly of the zebrafish gut microbial community (35). Non-neutral processes, such as immune system or feed could become more important for microbial modulation at older stages. Gut bacterial communities in zebrafish could be modulated mostly by ecological dynamics outside of the host, on a broader scale (35, 36). Although microbial ecology processes outside the host certainly play a role in the assembly of the host-gut microbiota, it seems unlikely that chance and random microbial dispersion could vastly explain the similarities of gut microbial compositions across species (30). The fact that gut microbial communities of mammals and fish cluster together suggests that specific pressures to the intestinal environment shape the intestinal microbiota. The earlier mentioned colonization cycle proposed by Robinson et al. (22) already takes into account a broader perspective of the environmental ecology including extra- and intra-host factors, such as gut adaptation of the microbes, but only non-fed larvae were analyzed. Taken together these observations, it is highly probable that the intestinal microbiota is, at least partly, modulated by the innate and adaptive host-immune system.

## MICROBE-HOST INTERACTION IN ZEBRAFISH INTESTINE: MOLECULAR IMMUNE MECHANISMS

The host gut exerts selective pressure on the microbiota (reviewed in the section above), which in turn influences host immune responses. In **Figure 1**, we summarized the host-microbe molecular pathways in the zebrafish gut cells. Commensal gram-negative microbes produce low quantities of lipopolysaccharide (LPS) which activate intestinal alkaline phosphatase (Iap) (44). Iap is an endogenous protein located in the apical intestinal epithelium and secretes surfactant-like particles to the intestinal lumen (45). Activated Iap counteracts LPS-associated intestinal inflammation, as quantified by neutrophil infiltration in the gut of zebrafish larvae (37). In mammals, after Toll like receptor (TLR)-microbial recognition and Myd88 adaptor protein activation, a downstream signaling cascade follows, including nuclear factor κ-light-chain-enhancer of activated B cells (NF-κB) signal transduction to the nucleus [reviewed in (46); and in (47)].

Recently, a TLR2-Myd88-dependent transcriptional feedback mechanism was described upon microbial colonization by using *myd88* deficient zebrafish larvae (38). The proposed mechanism involves microbial stimuli being recognized by TLR2 and partly suppress *myd88* but enabling enough *myd88* transcriptional activity to possibly induce protective mucin secretion in the apical intestinal epithelium. However, downstream TLR-*myd88* induction of mucin has only been demonstrated in *ex-vivo* mice experiments (48) and not yet in zebrafish. In GF zebrafish, TLR2 cannot suppress *myd88* expression and its elevated levels leads to stimulation of activator protein 1 (AP-1) transcription factors, which resulted in an overall increase in leukocytes (macrophages) in the gut (38). Nonetheless, GF zebrafish did not show enhanced inflammation as could be expected from AP-1 over-expression. Thus, other mechanisms perhaps absent in larval stages–i.e., adaptive immunity- must be involved in myd88 regulation. Knock-out myd88-/- juveniles or adult zebrafish could be used to further investigate the role of adaptive immunity in regulating microbe-host interaction.

In line with the observation that Myd88 is a key regulator of host-microbe interaction in the gut of larval zebrafish, microbiota determined secretory or absorptive differentiation of IECs via

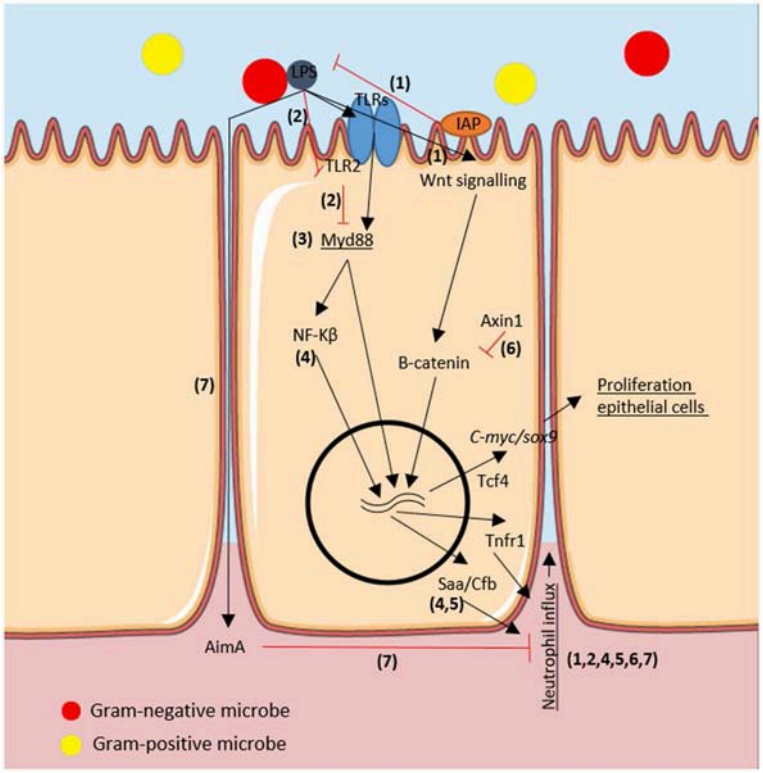


**FIGURE 1 |** Immuno-modulatory molecular pathways regarding the microbe-host interaction in the epithelium of the zebrafish intestine. We depicted the molecules involved in the proliferation of epithelial cells and in the neutrophil influx as a host-responses to microbiota in the zebrafish gut. In black arrows activation processes, in red inhibition processes. Genes are in italics and host-associated responses are underlined. Numbers correspond to articles proving such molecular interactions: 1: Bates et al. (37); 2: Koch et al. (38); 3: Troll et al. (39) 4: Kanther et al. (40), 5: Murdoch et al. (41), 6: Cheesman et al. (42), and 7: Rolig et al. (43).

inhibiting Myd88-Notch signaling (39). Notch signaling is a crucial mechanism for intestinal stem cell differentiation into secretory intestinal cells in zebrafish (49). The study focused more on the downstream Myd88 signaling rather than on the recognition of the microbes via TLRs. TLRs have been thoroughly studied in zebrafish [reviewed in (50)] yet to our knowledge there are no studies showing a direct link of feed components to subsequent TLR-myd88-Notch signaling and increased secretory fate of IECs (Goblet cell differentiation) via changes in the microbiota. In the future, several TLR knock-out zebrafish could be engineered to understand how specific feed components and/or the microbiota trigger relevant molecular pathways.

Single microbial species can also influence the zebrafish larval immune system. Gram-negative *Pseudomonas aeruginosa* stimulated NF-$\kappa$B-dependent expression of innate immune genes such as complement factor b (*cfb)* and serum amyloid a (*saa)* which enhanced neutrophil influx (40). In a recent article, *saa*-deficient zebrafish displayed aberrant neutrophil responses to wounding but increased clearance of pathogenic bacteria. Interestingly, *saa* function depended on microbial colonization of GF individuals. To prove that *saa* produced in the gut can systemically affect neutrophil recruitment, they created a transgenic zebrafish expressing *saa* specifically in IECs by using the *cldn15la* promoter fragment to drive mCherry fluorescence, located in the IECs. *Saa* produced in the gut in response to microbiota systemically prevented excessive inflammation (tested by tail amputations) as well as reduced bactericidal potential and neutrophil activation (41). Thus, besides the aforementioned functions (38, 39), Myd88 activation after TLR-microbial recognition orchestrates neutrophil migration to inflamed tissues as previously shown by Kanther et al. (40) and also pathogenic bacterial clearance in a *saa*-dependent manner (41) in zebrafish larvae in response to microbiota.

Further molecular pathways have been studied by generating specific gene mutations in zebrafish, such as a*xin1*. *Axin1* mutant zebrafish showed upregulated Wnt signaling and β-catenin protein levels (42). It was previously shown in mice that β-catenin accumulates in the cytoplasm and, at a threshold concentration, translocates to the nucleus where (with cofactors such as intestine-specific transcription factor Tcf4) it switches on expression of pro-proliferative genes like *c-myc* or *sox9* (51, 52). Induction of *c-myc* and *sox9* in turn increases IEC proliferation. Similarly, *axin1* mutant zebrafish showed increased cell proliferation in the intestine but not when *axin1* mutant zebrafish were reared GF, indicating that the microbiota triggers this increased cell proliferation, confirming earlier results showing increased epithelial turn-over upon microbial colonization (18). Interestingly, mono-association of resident

bacteria *Aeromonas veronii* was enough to increase intestinal cell proliferation in *axin1* mutant zebrafish by the same mechanisms: upregulating Wnt signaling and β-catenin protein expression. It can be concluded that the microbiota plays a role in the proliferation of epithelial cells in the zebrafish gut during microbial colonization via two mechanisms: TLR recognition with Myd88 downstream signaling and Wnt signaling with β-catenin protein accumulation and pro-proliferative gene activation (42). Increased intestinal cell turnover in the developing zebrafish larvae may be beneficial for the host to renew damaged epithelial cells and to shed potentially pathogenic bacteria attached to the epithelium.

To quantify host immune responses to multi-species rather than mono-association, a species quantitative model was created. Two variables were assessed in the zebrafish larvae model: the neutrophil response to individual strains and the absolute abundances of community members. Specific microbes, regardless of their relative abundances, played a major role in the neutrophil influx. GF zebrafish were colonized with different species (*Aeromonas*, *Vibrio,* and *Shewanella*) and neutrophil influx into the gut was investigated. *Shewanella* partly inhibited the *Vibrio* induction of neutrophil influx in the gut via cell-free supernatant (CFS). However, *Shewanella* CFS did not alter neutrophil influx in combination with *Aeromonas* mono-association (53). This study stresses the fact that mono-association experiments may be important to understand molecular mechanisms, however they may not reflect the *in vivo* situation where microbial species affect each other. Here, the authors used zebrafish larvae and neutrophil influx as the immune parameter, it would be interesting to see effects on other immune mediators, such as eosinophils which are abundantly present in the zebrafish gut. Although the knowledge of immunomodulatory factors produced by fish gut microbiota is limited, a recent study discovered a unique protein AimA ("Aeromonas immune modulator") secreted by *Aeromonas veronii*, which benefit both host and microbe. While AimA protects the host by preventing chemically and bacterially-induced intestinal inflammation, it protects *A. veronii* from host immune response and enhances colonization (43). Further studies are needed to understand how specific bacterial species and their associated secreted molecules are involved in overall immune modulation in the zebrafish intestine and systemically. For further reading on the modulation of innate immunity to commensal bacteria, we refer to a recently published review of Murdoch and Rawls (54) and for a more extensive review on hematopoiesis in the developing zebrafish to the review of Musad and coworkers (55).

## IMPACT OF PREBIOTICS AND PROBIOTICS ON THE ZEBRAFISH MICROBIOTA AND GUT IMMUNITY

In their natural environment, adult zebrafish eat zooplankton and insects. Analysis of the zebrafish gut content also revealed the presence of phytoplankton, spores and filamentous algae, among others [reviewed in (56)]. There is not a standard diet for zebrafish in captivity and feeding practices include feeding a mixture of live feeds such as rotifers, ciliates, *Artemia nauplii* and formulated dry feeds (57). Supplementary ingredients have been investigated in several commercially relevant fish species in order to increase growth and control aquaculture related diseases (58). More specifically, fish microbial communities may influence the immune system and decrease aquaculture-related diseases [reviewed in (24)]. An overall summary of key operational taxonomic units (OTUs) in various tissues (skin, gut, gills, and digesta) have been associated with fish diseases and infections compared to the wild-type individuals [reviewed in (59)]. The use of zebrafish as experimental model to develop novel feeds for farmed fish has gained interest, especially for the development of prebiotics and probiotics as immune and microbiome modulators [reviewed in (60)]. Although most of the prebiotics and probiotics assure benefits for the host, a careful assessment of their effects remains important, as shown for effects of human probiotics uncovering problematic research design, incomplete reporting, lack of transparency or under-reported safety were described [reviewed in (61)]. In the next section, we review the current literature on the effects of prebiotics and probiotics on the immune system and microbiota of zebrafish.

## PREBIOTICS

Prebiotics can be defined as non-digestible feed ingredients that have a beneficial effect toward the host by selectively stimulating the growth or the activity of commensal gut bacteria and thus improving host health [reviewed in (62)]. Prebiotics most often consist of small carbohydrate chains that are commercially available as oligosaccharides of glucose (like β-glucans), galactose, fructose, or mannose. The use of prebiotics as immuno-stimulants in farmed fish feed has been reviewed elsewhere (63), however the effect of prebiotics on zebrafish (gut) health and on microbiota composition needs further examination. We summarized such studies in **Table 1**. Most of the studies have been performed in larval zebrafish and only very few studies have been performed in adults. The most employed prebiotics in zebrafish research were fucoidans (sulphated polysaccharides mainly present in brown algae and brown seaweed), β-glucans (β-D-glucose polysaccharides extracted from cell walls of bacteria and fungi) and sometimes others, such as galactooligosaccharides. It is of note that not much is known about the modulation of the microbiota by prebiotics since most of the reviewed studies only investigated their immune stimulatory effects.

Fucoidans extracted from several brown algae; *Eklonia cava* (64), *Chnoospora minima* (66), and *Turbinaria ornata* (65) were administrated to zebrafish larvae in the water. In all three studies, larvae exposed to fucoidans displayed reduced levels of reactive oxygen species (ROS), inducible nitric oxygen synthase (iNOS) and improved cell viability in whole larvae after LPS challenge (64–66). However, in these studies the candidate prebiotics were diluted in the water when the embryos were 8 h post-fertilization. Since the mouth of the zebrafish embryo does not open until 3 dpf and the complete digestive tract is not fully

**TABLE 1 |** Summary of prebiotics, probiotics, and synbiont studies performed in zebrafish regarding immunity and microbiota.

| | Specie(s)/strain(s) | Zebrafish age | Microbiota composition | Immune-modulatory effects | Other relevant parameters | References |
|---|---|---|---|---|---|---|
| Prebiotic | Fucoidan from *Eklonia cava* | Embryos (not specified) | – | – Reduced the levels of ROS and NO after challenge with LPS and tail cutting | – | (64) |
| Prebiotic | Fucoidan from *Turbinaria ornata* | 3 dpf | – | – Reduced LPS-induced levels of *COX2*, *iNOS*, and ROS. | −Improved cell viability | (65) |
| Prebiotic | Fucoidan from *Chnoospora minima* | 3 dpf | – | – Reduced LPS-induced levels of *COX2*, *iNOS*, and ROS. | −Improved cell viability | (66) |
| Prebiotic | β-glucan from oats | 5 dpf | – | – Upregulation of *tnfa*, *il-1β, il10, il12, defb1, lyz, c-rel.* | −Increased survival after *E. tarda* challenge. | (67) |
| Prebiotic | β-glucan | 4 hpf−6dpf | – | – Upregulation of *tnfa, mpo, trf, lyz* | −Increased survival after *Vibrio anguillarum* challenge | (68) |
| Prebiotic | Fucoidan from *Cladosiphon okamuranus* | 6–9 dpf and adult zebrafish | –Decreased *E coli* and favored Rhizobiaceae and Burkholderiaceae in adults gut but not overall larvae. | – Reduction of *il-1β* but not *cxcl8, il10* nor *tnfb* in the zebrafish adult gut<br>−Increase of *il-1β, il10, tnfb* and *mmp9* in overall larvae. | – | Ikeda-Ohtsubo et al. (in this issue) |
| Prebiotic | Galactooligosaccharide supplemented in diet (0.5, 1, and 2%) | Adult zebrafish (8 weeks feeding) | – | –Upregulation of *tnfa* and *lyz*<br>−Increase in total immunoglobulin concentration. | – | (69) |
| Probiotic | 2 yeast species: *Debaryomyces* (Db) and *Pseudozyma* (Ps) | 2–3 dpf yeast exposure, gut sampling at 14 dpf | −Core microbiota differed from controls.<br>–Reduced Bacteroidetes abundance.<br>–Db increased species richness.<br>–Db increased abundance of *Pediococcus* and *Lactococcus*. | – | – | (70) |
| Probiotic | *Lactobacillus casei BL23* | From 3 to 25 dpf | – | –Upregulated expression of *il-1β*, *C3a* and *il-10* after 8 or 24 h post-challenge with *A. hydrophila*. | −Increased survival after *A. hydrophila* challenge | (71) |
| Probiotic | Yeasts*: Yarrowia lipolytica 242* (Yl242) and *Debaryomyces hansenii 97* (Dh97) | At 4 dpf, 2 h exposure | –Germ-free (GF) larvae and conventionally raised (CONV) larvae. | –Upregulation of *il-1β*, *c3, tnfa, mpx*, and *il10* in CONV larvae after *V. anguillarum* challenge<br>−Pre-treatment with Dh97 and Yl242 prevented gene upregulation in CONV and GF larvae. | –Increased survival of CONV and GF larvae due to yeast after challenge with *V. anguillarum* (GF higher mortality than CONV). | (72) |
| Probiotic | *Lactobacillus plantarum ST-III* (LAB) and bile salt hydrolase (BSH). Exposure to Triclosan (TCS) alone or with LAB (TL) or BSH (TB). | From 4 hpf to 90 dpf | −Gut microbiota clustered: LAB > Control > TL and BSH > TB > TCS.<br>–TCS shifted the microbiota and when LAB or BSH co-exposed microbiota resembled more to controls. | –LAB and TL reduced malonaldehyde in the gut.<br>–TCS upregulated *NF-kB* and *il-1β*, *tnfa* expression.<br>–TCS increased CD4+T cells in the lamina propria.<br>–TCS thinned intestinal mucosa, destructed epithelia and increased goblet cells. | –TCS induced fibrosis, increased lipid droplet, increased triglycerides, and total cholesterol concentrations in the liver compared to controls and LAB/TL treated fish. | (73) |
| Probiotic | 15 yeast strains | At 4 dpf, 2 h exposure | – | –Larvae after *V. anguillarum* displayed more neutrophils outside the caudal hematopoietic tissue | –All yeast except Mv15 and Csp9 increased survival after *V. anguillarum* challenge. | (74) |

*(Continued)*

**TABLE 1 |** Continued

| | Specie(s)/strain(s) | Zebrafish age | Microbiota composition | Immune-modulatory effects | Other relevant parameters | References |
|---|---|---|---|---|---|---|
| Probiotic | *L. plantarum* WCFS1 and *NA7* and *L. fermentum ATCC9338*, *NA4,* and *NA6*. | At 5 dpf, 24 h exposure | GF larvae | –NA4 exposure prior to TNBS challenge lowered levels *trfa* and *il-1β*<br>– *Il-10* expression was higher in larvae exposed to NA4 | – | (75) |
| Probiotic | 37 commensal or probiotic Gram-positive and Gram-negative bacteria | 6–9 dpf | – | – | –Increased survival by *V. parahaemolyticus, E. coli ED1a-sm* and *E. coli MG1655* F' upon *E. ictaluri* infection. | (76) |
| Probiotic | *Lactobacillus rhamnosus* | 96 hfp, 6 and 8 dpf | –Increased the rel. abundance of Firmicutes | –Enlarged enterocytes and microvilli on the apical surface of the epithelium. | –Increased total length and wet weight at 8 dpf. | (77) |
| Probiotic | B*. coagulans, L. plantarum, L. rhamnosus, Streptococcus thermophilus, Bifidobacterium infantis.* | Adult zebrafish (28 days feeding) | – | –*B. coagulans* and *L. plantarum* reduced the number of Masts cells in the gut after *A. hydrophila* challenge.<br>–*B. coagulans* and *L. plantarum* reduced expression of *tnfa* and *il10* and increased *il-1β* in the gut. | –*B. coagulans* and *L. plantarum* reduced mortality after *A. hydrophila* challenge. | (78) |
| Probiotic | *Lactobacillus plantarum* | Adult zebrafish (30 days feeing) | –*L. plantarum* clustered gut microbiota independently<br>–Reduced rel. abundance of Vibrionaceae, Pseudoalteromonadaceae, and Leuconostrocaceae and increased Lactobacillaceae, Stenotrophomonas, and Catenibacterium. | –Not clear effect of *L. plantarum* | –Upregulated canonical pathways related with energy metabolism and vitamin biosynthesis. | (79) |
| Probiotic | *Lactobacillus rhamnosus* | Adult fish (10 days feeding) | – | –Upregulated expression of *il1b*, *tnfa,* and *becn1* in the gut. | – | (80) |
| Probiotic | 8 probiotic strains were lyophilized and mixed with a commercial diet | Adult fish (30 days feeding) | – | –Downregulated *casp4* and *baxa* and upregulated *bcl2a* in the gut.<br>– Upregulated *il-1β*, *tnfa*, *myd88*, *il10*, *casp1, nos2a, tgfb1a, nfkb, tlr1, tlr2, tlr3,* and *tlr9* (also in protein level, expect for Tlr2). | –Upregulated *cnr1/2* and *abhd4* and downregulated *faah* and *mgll* in the gut compared to controls. | (81) |
| Probiotic | *Bacillus amyloliquefaciens* | Adult fish (30 days feeding) | – | –Upregulated expression of *il-1β*, *il6*, *il21, tnfa, lyspzyme*, *tlr1, tlr3, and tlr4.* | –Increased survival after *A. hydrophila* and *S. agalactiae* challenges. | (82) |
| Probiotic | *E. coli 40, E. coli Nissle,* and *E. coli MG 1655 ΔptsG.* | Adult zebrafish | | –*E. coli 40* and *E. coli Nissle* decreased mucin found in water after *V. cholerae O395* or *V. cholerae El Tor* strain *N16961* challenge. | – | (83) |
| Probiotic & prebiotic | *Lactobacillus casei BL23* and exopolysaccharide-protein complex (EPSP) | 3–12 dpf | –Microbiota did not change due to *L. casei BL23.* | –*L. casei* upregulated *tnfa, il-1β, il-10,* and *Saa* after 24 h infection with *A. veronii* but downregulated after 48 h.<br>ESPS increased *tlr1*, *tlr2*, *il10*, *tnfa* expression, and decreased *il-1β* exp. | –*L. casei BL23* and EPSP increased survival after *Aeromonas veronii* infection. | (84) |
| Probiotic & prebiotic | *Ecklonia cava* (EC)<br>Celluclast enzymatic EC (ECC)<br>100% ethanol extract EC (ECE). | Adult zebrafish (21 days feeding) | –E. cava induced *L. brevis, L. pentosus* and *L. plantarum* growth. | –EC combined with *L. plantarum* increased *iNOS* and *COX2* in the gut after *E. tarda* challenge. | –EC, ECC, and ECE diminished colony counts of *E. tarda, S. iniae,* and *V. harveyi.*<br>EC reduced mortality *after E. tarda* challenge | (85) |

developed until 6 dpf (12) such studies do not prove a prebiotic effect on gut immunity. Preferably, zebrafish larvae with a fully developed digestive tract (6 dpf or older) are employed to study such interactions. Furthermore, prebiotics should be tested at physiologically relevant concentrations. Testing a prebiotic in zebrafish larvae may uncover a prebiotic function but often the overall goal would be to formulate novel diets containing the optimal concentration of prebiotic. For this aim, juvenile or adult zebrafish would be more suitable. We investigated the effect of fucoidan derived from the brown alga *Cladosiphon okamuranus* on microbiota composition in whole larvae (water exposure) and in adult zebrafish gut (feeding with flakes). In the gut of adult zebrafish, gene expression of *il-1β* was reduced and the dominant *Escherichia coli* (Proteobacteria) decreased in favor of Rhizobiaceae and Burkholderiaceae after feeding with fucoidan, while in larvae *il-1β, il-10, tnfb,* and *mmp9* increased but no microbial changes were observed (Ikeda-Ohtsubo, this issue).

Differently from fucoidans, β-glucans can act as immunostimulators in zebrafish. Beta-glucans from oats, upregulated gene expression of *tnfa, il-1β, il-10, il-12, defb1, lyz,* and *c-rel* in a dose-dependent manner in 5 dpf whole zebrafish larvae (67). In a similar study, β-glucan exposure from 4 hpf until 6 dpf upregulated *tnfa, mpo, tlf,* and *lyz* gene expression (68). In both studies, β-glucan administration in the water hampers its uptake quantification by the fish and again the exposure of very young larvae probably does not lead to gut-related effects. Oligosaccharides such as galactooligosaccharides (GOS) and fructooligosaccharides (FOS) are frequently used as prebiotics in agriculture and human infant nutrition to boost health via increased production of suggested beneficial bacterial fermentation products (63). Adult zebrafish fed with GOS for 8 weeks at 0.5, 1, and 2% inclusion levels displayed upregulation of *tnfa* and *lyz* expression and an increase in total immunoglobulins in the whole zebrafish (69). However, no gut specific read-outs were assessed.

It is clear that prebiotics can act on the immune system in a specific manner depending on their source of origin. Fucoidans can decrease inflammation markers whereas β-glucans and GOS increase gene expression of pro-inflammatory cytokines. Despite the promising outcomes, the vast majority of studies exposed undeveloped larvae to prebiotics which are unable to ingest the additive via free feeding. Prebiotics research should carefully evaluate gut health because is the organ where feed can potentially modulate the microbiota and the host immune system. If such candidate prebiotics are included within dry pellets and administrated to fish slightly before satiation (ensuring fish eat all the pellets), it is feasible to estimate the prebiotic gut levels and assess effects on gut microbiota and immunity with more clarity.

Several methods not yet extensively employed in the previously mentioned prebiotic studies may also be suitable for prebiotics gut health research in zebrafish. Firstly, histology and immunohistochemistry staining is needed to understand the immuno-modulatory effects in the gut tissue (i.e., disruption of the normal gut architecture). Transgenic zebrafish could potentially help to clarify which subpopulations of immune cells infiltrate the gut using fluorescently-activated cell sorting (FACS) and imaging. Furthermore, cell sorting of these sub-populations together with transcriptomics would depict the real effect of the prebiotic. Omics technologies (genomics, transcriptomics, proteomics, etc.) play an increasing important role in understanding the immune effects of aqua-feeds [reviewed in (86)] and omics-based read-outs should become more popular as their costs decrease.

Comparing the limited number of studies performed on zebrafish with a much larger number of studies performed in aquaculture species confirms that supplementation of β-glucans to feed of Atlantic salmon, trout or sea bass increases immune activity [reviewed in (87)] and trained immunity (88). However, only a limited number of studies have been performed on GOS supplementation. Dietary supplementation to Atlantic salmon of GOS at 1 g/kg feed for 4 months did not show effects on reactive oxygen species (ROS) production or lysozyme activity. Research on the use of seaweed is increasing, for example testing 10% inclusion levels of *Laminaria digitata* in feed of Atlantic salmon (89). The dietary seaweed improved chemokine-mediated signaling but the study only assessed transcriptional responses after LPS challenge so further research into the health effects of elevated or reduced gene expression is warranted. This last example nicely supports the use of zebrafish model, not to replace testing in aquaculture target species, but to prescreen feed components and further dissect the mechanism of action by live imaging and assessment of health parameters for prolonged periods, something difficult to achieve in large and costly aquaculture species.

## PROBIOTICS

Already in 1907, Elie Metchnikoff related the use of probiotics to elongation of life expectancy. For the purpose of this review we define probiotics as a live or inactivated microorganism, such as bacterium or yeast, that when administrated via feed or water, confers a benefit to the host, such as improved disease resistance or enhanced immune responses [adapted from (90, 91)]. Probiotics can influence the health of the host in several ways: secreting secondary metabolites that inhibit growth of microbial pathogens and/or directly stimulating immune responses to downregulate gut inflammation (92). Here we focused on the probiotic studies in zebrafish concerning (gut) immune and microbiota modulation (summarized in **Table 1**).

To assess potential health benefits of live probiotics it is important to understand their optimal environment inside the host (oxygen levels, pH, etc.) and their colonization route. Probiotic-host interaction was addressed by a model of oro-intestinal pathogen colonization in GF zebrafish (76). Firstly, 6 dpf zebrafish were exposed by immersion to 25 potential enteric fish pathogens after which mortality was recorded during 3 days. *Edwardsiella ictaluri* caused the highest larvae mortality and was further selected to challenge the fish. Then, larvae were pre-colonized with single strains of 37 possible probiotics prior to *E. ictaluri* challenge. From this extensive screening, *Vibrio parahaemolyticus*, *E. coli* ED1a-sm and *E. coli* MG1655 F' provided a significant increase in survival upon *E. ictaluri*

infection. *V. parahaemolyticus* protected the host by inhibiting *E. ictaluri* growth whereas *E. coli* protected via specific adhesion factors, such as F pili involved in biofilm and conjugation formations offering niches to other probiotic bacteria in the host (76). It is of note that zebrafish gills, although they are active in gas exchange 2 weeks after fertilization (93), provide a potential portal of entry for pathogens. Regretfully, gills were not included in the aforementioned study. Interestingly, in the same study, *Vibrio parahaemolyticus* was assessed as a possible probiotic whereas *Vibrio ichthyoenteri* was considered as a possible pathogen. The majority of the microbiota studies associate immune responses to taxonomic levels such as genera or families (i.e., *Vibrio* spp.) rather than species or strains. As a consequence, there is a generalization of an entire genus to a functions that could be species or even strain-specific. Such widely used generalizations may come from the difficulty to generate amplicons that are long enough to discriminate between closely related organisms. Besides, transcriptomics and shot gun approaches are preferred over 16S rRNA gene analysis to depict the active microbiota because they more informative regarding the fish health status (21). Adult zebrafish were also used to test probiotics as a model for human probiotic consumption. Adult zebrafish were exposed to two *E. coli* strains (Nissle and MG 1655 ΔptsG*)* and challenged with species of *Vibrio choleae* (strain El Tor). *E. coli* spp. decreased the mucin content found in the tank water, indicator of diarrhea (83) although these mucins could perhaps also result from skin shedding. It might be interesting to assess whether these *E. coli* spp. increase secretory cell development and therefore mucus secretion via reduction of Myd88-Notch signaling as previously reviewed (39). In addition, while in humans administration of bacteria via a solutions orally ingested is an efficient way of ensuring ingestion, addition of probiotics to the water may not guarantee uptake by fish and may affect overall fish mucosa (skin, gills, gut) and not only uptake in the gut. Besides, the environment of the fish gut is more aerobic than the human gut environment (21) and lactic acid bacteria may be outcompeted by other bacteria in these aerobic conditions. This rationale may explain why human probiotics (*Lactobacillus* spp.) tested in zebrafish by immersion did not confer protection against *E. ictaluri* infection (76). Several studies reported Lactic Acid Bacteria (LAB) as good probiotic candidates due to their ability to withstand and adhere to the gut, their lactic acid production which inhibits the growth of pathogenic bacteria and their strengthening of the mucosal barrier (94). Zebrafish immersed with *Lactobacillus casei* BL23 from 3-25 dpf displayed an increased survival compared to controls after an immersion challenge with *Aeromonas hydrophila*. Gut gene expression of *il-1β*, *C3a,* and *il-10* was upregulated after 8 and 24 h after *A. hydrophila* challenge compared to controls (71). Interestingly, potential probiotics from the genera *Lactobacillus* modulated gene regulation in a strain-specific fashion. As a matter of fact, GF larvae immersed with *Lactobacillus fermentum* NA4 displayed an increased *il-10* expression and a decreased *il-1β* and *tnfa* expression after chemically-induced inflammation compared to controls. However, in the same study, larvae immersed with several strains of *Lactobacillus plantarum* (WCFS1 and NA7] or other *Lactobacillus fermentum* strains (ATCC9338 and NA6) did not show these differences in gene expression (75). Dissimilarities in gene expression among the aforementioned studies (71, 75) could be due to fish age (3–25 vs. 7 dpf), tissue analyzed (gut vs. whole larvae) challenge applied (live pathogen vs. chemical) and the specific *Lactobacillus* strain used as a probiotic candidate. *Bacillus amyloquefaciens* supplemented twice a day for 30 days in a commercial diet upregulated *il-1β, il-6, il-21 tnfa, lysozyme, tlr1, tlr3.* and *tlr4* expression in adult zebrafish whole body and increased survival during *A. hydrophila* and *S. agalactiae* challenge (82). Upregulation of gene expression appeared related to enhanced innate immunity although no other immune parameters were taken into account. In another study in adult zebrafish, a commercial diet was supplemented with multiple lyophilized probiotic strains for 30 days. The probiotic mix upregulated *il-1β, tnfa, myd88, il-10, casp1, nos2a, tgfb1a, nfkb, tlr1, tlr2, tlr3,* and *tlr9* expression in the gut. Furthermore, the probiotic mix increased the protein levels encoded by all the upregulated genes (except for Tlr2 protein) (81). On the one hand, certain bacteria of the probiotic mix may have inhibited Tlr2, which in turn could have partly suppressed *myd88* (38). On the other hand, other bacteria of the probiotic mix may have enhanced expression of other TLRs that upregulated *myd88* and the overall Myd88-balance orchestrated innate immune responses. As previously reviewed, microbial species can influence host immunity irrespective of their abundance (53) and when using mix of probiotics the effects of each individual species are harder to disentangle. Other studies using LAB as probiotics did not only examined gene expression but also microbiota (73, 77, 79) and histological changes (77, 78) in the zebrafish gut (**Table 1**). Some studies investigated the potential of yeast as a probiotic for zebrafish. GF and CONV zebrafish larvae were immersed from 2–3 dpf in solutions of two yeasts after which gut microbiota were sampled at 14 dpf (70). Although microbial changes were observed, immune-related outcomes where not measured so the probiotic effect of the yeasts in this study remains undefined. In another study, 4 dpf zebrafish were exposed to 15 fluorescently labeled yeast strains for 2 h prior to *Vibro anguillarum* challenge (74). Most of the yeast strains conferred increased survival after challenge. In a later experiment, the same group further studied two of the yeast strains in GF and CONV larvae using a similar set-up. Exposure to either yeast strain significantly increased survival in GF and CONV larvae after *V. anguillarum* challenge (72). CONV zebrafish challenged with *V. anguillarum* displayed an upregulation of *il-1β, c3, tnfa, mpx,* and *il-10* expression. Pre-treatment with either yeast strain prevented such gene upregulation in CONV and GF larvae, indicating that these yeast strains might prevent or reduce the effects of *V. anguillarum* (72).

Zebrafish have also been employed for synbiotic studies which typically combine the use of prebiotics and probiotics. *Lactobacillus casei* BL23 and an exopolysaccharide complex (ESPS) were studied in combination in GF and CONV larvae from 3 to 12 dpf. *L. casei* exposure upregulated *tnfa, il-1β, il-10,* and *saa* expression after 24 h in a challenge with *Aeromonas veronii* and downregulated expression of these genes after a 48 h challenge. It is of note that the ESPS alone upregulated *tlr1, tlr2, il-10,* and *tnfa* and downregulated *il-1β* after 24 h challenge.

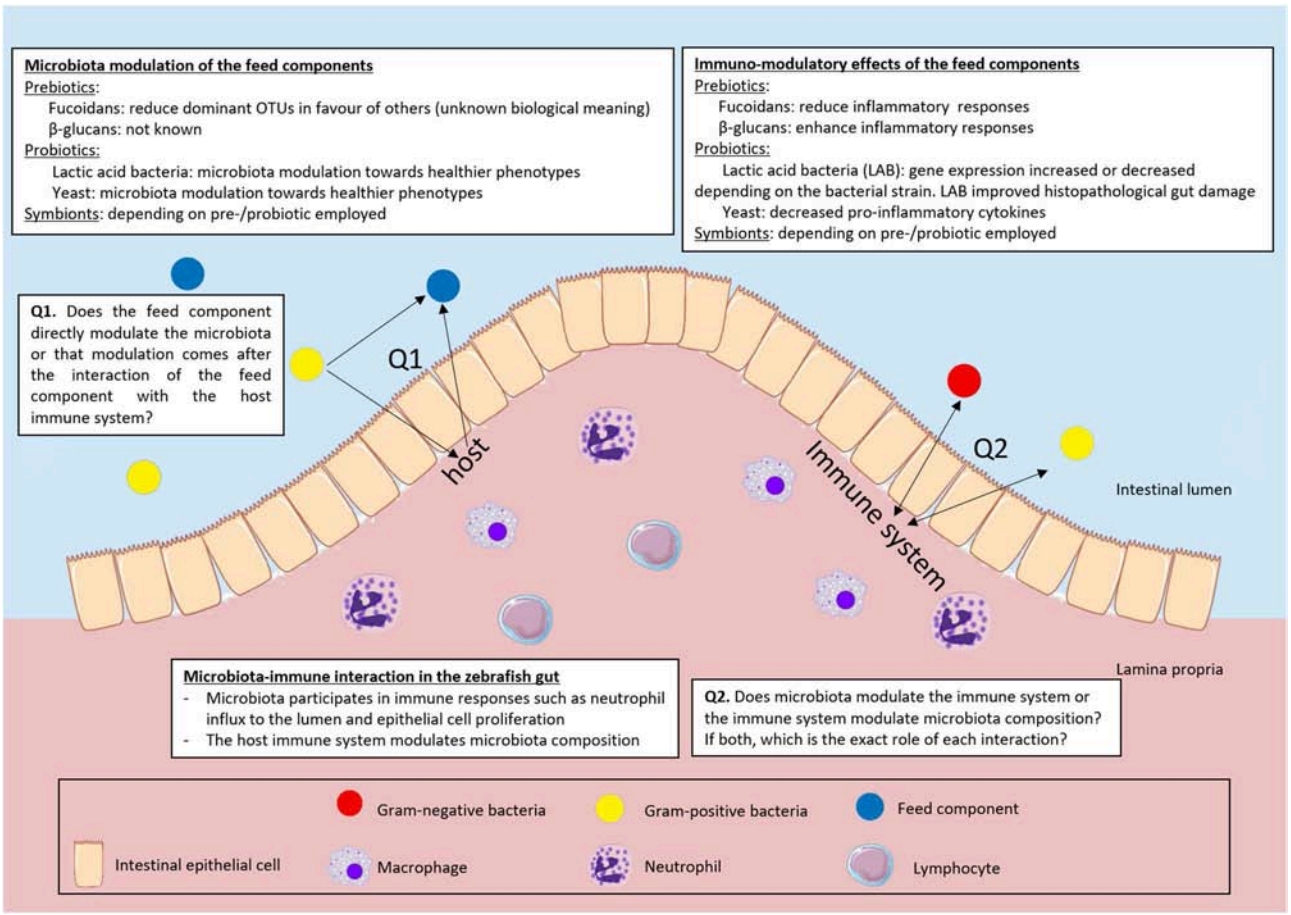


**FIGURE 2 |** Overview of the interaction of pre- and probiotics, immune system and microbiota in the zebrafish intestine. We summarized the interactions of microbiota and feed components, immune system and feed components and microbiota and immune system. We highlighted the questions that still remain unsolved in the field.

Synbiotically, *L. casei* BL23 and EPSP improved survival dose-dependently after *A. veronii* challenge (84). The combined supplementation of *E. cava* enzymatic digest, with enhanced biological activity, as prebiotic together with *L. plantarum* as a probiotic in adult zebrafish for 21 days reduced the level of *iNOS* and *cyclooxygenase 2* (*cox2*) in the gut. Moreover, when prebiotics and probiotics were administrated together, they increased survival compared to *L. plantarum*-treated fish alone after a challenge with *E. tarda* (85). Interestingly these studies suggest that certain extracts and/or biologically active compounds rather than the whole prebiotic may cause immune-modulation.

A large number of studies (co)exposed potential prebiotics and/or probiotics to zebrafish to improve their immune condition via microbial modulation (**Figure 2**). Remarkably, in most of these studies, gene expression was assumed a conclusive immunological read-out. Apart from the fact that gene expression does not always translate to protein functionality, often pro- and anti-inflammatory cytokines are upregulated or downregulated depending on the dynamics and the timing of the response. The gene expression may reflect the balance in the host during an immune response: specific and strong enough to fight potentially pathogenic bacteria but at the same time able to tolerate commensal host microbiota (95). This balance is also dependent on different cell types that work in concert to prevent excessive damage to the host when acting against an invading pathogen or ongoing inflammation. We need to understand the role and presence of different immune cell types that are involved in the different responses in much more detail before we can try to modulate the response to the benefit of the host. To this end, the zebrafish remains the ideal candidate model organism. To date, more studies could have made use of the unique tools in zebrafish such as live imaging of different transgenic reporter zebrafish (cytokines as well as immune cell populations) to get a much broader understanding of the complex dynamic interactions of host-feed-microbe interactions.

## CONCLUDING REMARKS

In this review we focused on the zebrafish as an animal model to study the effect of feed on host-microbe-immune interactions (summarized in **Figure 2**). Zebrafish are now widely used as models to study fundamental and evolutionary

processes that might uncover pathways relevant for both fish and mammals. The studies on microbial composition development summarized in this review reveal that although the gut microbial composition is dependent on salinity, trophic level and host phylogeny, mammalian, fish and insect gut microbiota still cluster together and separately from environmental samples. Thus, although mammals and fish live in distinct environments and clearly have different physiology, gene expression and regulation of gene expression in the gut is highly similar. IEC transcriptional profiles are more similar between species than responses of different cell types of the same species. Therefore, experimentation with zebrafish seems suitable to elucidate conserved molecular mechanisms.

Using zebrafish as a model for aquaculture species is of interest. Eighty percent of farmed fish are other cyprinids and therefore close relatives. We argue that using the zebrafish as a model for aquaculture species brings several advantages yet may never fully replace studies performed in the target species for validation. Nevertheless, using zebrafish as a pre-screen model to guide studies in aquaculture species might contribute to elucidate mechanisms underlying feed and host-microbe-immune interactions.

Recently, exiting new research using *in vivo* mice models has shown that the microbial community can influence the severity of viral infections (96, 97). Moreover, *in vitro* data using RAW264.7 cells showed antiviral activity of several *Lactobacillus* strains to murine norovirus (MNV) infection through IFN-β upregulation (98). Currently, it is unknown whether microbes can also alter fish-specific viral infectivity. This is an exciting new avenue of research that might lead to novel vaccination strategies, combining virus-targeting vaccines with prebiotic or probiotic treatment to change the microbiota as well as target the virus itself. A fundamental field in which zebrafish are most probably will contribute due to its unique advantages.

The studies published in the field using zebrafish will continue to increase and by combining existing technologies (omics, immunohistochemistry, FACS, *in vivo* imaging) or by emerging novel technology knowledge gaps will surely be filled. For future experiments it would greatly benefit our understanding if more holistic approaches would be taken. We need to combine read-out parameters such as gene expression, survival after challenges, gut architecture, immune cell recruitment, microbiota composition, metabolite production and behavioral data within each experiment to provide a broader picture of the consequences of certain treatments on the health of the fish. Only by carefully determining cause and effect by interrogating possible molecular pathways through gene editing we can provide a solid rationale for the design of novel immunomodulatory strategies.

## AUTHOR CONTRIBUTIONS

AL drafted the manuscript and the figures. WI-O, DS, DP, CM, MF, GW, and SB edited and contributed to writing the manuscript. SB, GW, and DS obtained the funding.

## FUNDING

Our work is generously funded by TTW-NWO (project number 15566). This work was partially supported by the Japan Society for the Promotion of Science (JSPS) through JSPS Core-to-Core Program (Advanced Research Networks) entitled "Establishment of international agricultural immunology research-core for a quantum improvement in food safety". WI-O was supported by a WIAS fellowship provided by the Graduate School of Animal Science of Wageningen University & Research.

## ACKNOWLEDGMENTS

The authors thank Ángel Chacón Orozco for editing the figures of this paper.

## REFERENCES

1. Grunwald DJ, Eisen JS. Hearwaters of the zebrafish - emergence of a new model vertebrate. *Nat Rev Genet.* (2002) 3:717–24. doi: 10.1038/nrg892
2. Howe K, Clark MD, Torroja CF, Torrance J, Berthelot C, Muffato M, et al. The zebrafish reference genome sequence and its relationship to the human genome. *Nature.* (2013) 496:498–503. doi: 10.1038/nature12111
3. Yoder JA, Nielsen ME, Amemiya CT, Litman GW. Zebrafish as an immunological model system. *Microbes Infect.* (2002) 4:1469–78. doi: 10.1016/S1286-4579(02)00029-1
4. Renshaw SA, Loynes CA, Trushell DMI, Elworthy S, Ingham PW, Whyte MKB. Plenary paper A transgenic zebrafish model of neutrophilic inflammation. *Blood J.* (2006) 108:3976–9. doi: 10.1182/blood-2006-05-024075
5. Buchan KD, Prajsnar TK, Ogryzko NV, De Jong NWM, Van Gent M, Kolata J, et al. A transgenic zebrafish line for *in vivo* visualisation of neutrophil myeloperoxidase. *PLoS ONE.* (2019) 14:e0215592. doi: 10.1371/journal.pone.0215592
6. Urnov FD, Rebar EJ, Holmes MC, Zhang HS, Gregory PD. Genome editing with engineered zinc finger nucleases. *Nat Rev Genet.* (2010) 11:636–46. doi: 10.1038/nrg2842
7. Bedell VM, Wang Y, Campbell JM, Poshusta TL, Starker CG, Krug RG, et al. *In vivo* genome editing using a high-efficiency TALEN system. *Nature.* (2012) 491:114–8. doi: 10.1038/nature11537
8. Hwang WY, Fu Y, Reyon D, Maeder ML, Tsai SQ, Sander JD, et al. Efficient genome editing in zebrafish using a CRISPR-Cas system. *Nat Biotechnol.* (2013) 31:227–9. doi: 10.1038/nbt.2501
9. Jao LE, Wente SR, Chen W. Efficient multiplex biallelic zebrafish genome editing using a CRISPR nuclease system. *Proc Natl Acad Sci USA.* (2013) 110:13904–9. doi: 10.1073/pnas.1308335110
10. Albadri S, Del Bene F, Revenu C. Genome editing using CRISPR/Cas9-based knock-in approaches in zebrafish. *Methods.* (2017) 121–2:77–85. doi: 10.1016/j.ymeth.2017.03.005
11. Wallace KN, Akhter S, Smith EM, Lorent K, Pack M. Intestinal growth and differentiation in zebrafish. *Mech Dev.* (2005) 122:157–73. doi: 10.1016/j.mod.2004.10.009
12. Wallace KN, Pack M. Unique and conserved aspects of gut development in zebrafish. *Dev Biol.* (2003) 255:12–29. doi: 10.1016/S0012-1606(02)00034-9
13. Nguyen TLA, Vieira-Silva S, Liston A, Raes J. How informative is the mouse for human gut microbiota research? *Dis Models Mech.* (2015) 8:1–16. doi: 10.1242/dmm.017400

14. Wang Z, Du J, Lam SH, Mathavan S, Matsudaira P, Gong Z. Morphological and molecular evidence for functional organization along the rostrocaudal axis of the adult zebrafish intestine. *BMC Genomics*. (2010) 11:392. doi: 10.1186/1471-2164-11-392
15. Lickwar CR, Camp JG, Weiser MLCJ, Kingsley DM, Furey TS, Sheikh SZ et al. Genomic dissection of conserved transcriptional regulation in intestinal epithelial cells. *PLOS Biol.* (2017) 15:e2002054. doi: 10.1371/journal.pbio.2002054
16. Brugman S. The zebrafish as a model to study intestinal inflammation. *Dev Comp Immunol.* (2016) 64:82–92. doi: 10.1016/j.dci.2016.02.020
17. Talham GL, Jiang HQ, Bos NA, Cebra JJ. Segmented filamentous bacteria are potent stimuli of a physiologically normal state of the murine gut mucosal immune system. *Infect Immun.* (1999) 67:1992–2000.
18. Rawls JF, Samuel BS, Gordon JI. Gnotobiotic zebrafish reveal evolutionarily conserved responses to the gut microbiota. *PNAS*. (2004) 101:4596–601. doi: 10.1073/pnas.0400706101
19. Perez-Muñoz ME, Arrieta MC, Ramer-Tait AE, Walter J. A critical assessment of the "sterile womb" and "*in utero* colonization" hypotheses: implications for research on the pioneer infant microbiome. *Microbiome.* (2017) 5:48. doi: 10.1186/s40168-017-0268-4
20. Walker RW, Clemente JC, Peter I, Loos RJF. The prenatal gut microbiome: are we colonized with bacteria *in utero*? *Pediatric Obes.* (2017) 12:3–17. doi: 10.1111/ijpo.12217
21. Llewellyn MS, Boutin S, Hoseinifar SH, Derome N. Teleost microbiomes: the state of the art in their characterization, manipulation and importance in aquaculture and fisheries. *Front Microbiol.* (2014) 5:207. doi: 10.3389/fmicb.2014.00207
22. Robinson CD, Klein HS, Murphy KD, Parthasarathy R, Guillemin K, Bohannan BJM. Experimental bacterial adaptation to the zebrafish gut reveals a primary role for immigration. *PLoS Biol.* (2018) 16:e2006893. doi: 10.1371/journal.pbio.2006893
23. Stephens WZ, Burns AR, Stagaman K, Wong S, Rawls JF, Guillemin K, et al. The composition of the zebrafish intestinal microbial community varies across development. *ISME J.* (2016) 10:644–54. doi: 10.1038/ismej.2015.140
24. de Bruijn I, Liu Y, Wiegertjes GF, Raaijmakers JM. Exploring fish microbial communities to mitigate emerging diseases in aquaculture. *FEMS Microbiol Ecol.* (2018) 94:fix161. doi: 10.1093/femsec/fix161
25. Brugman S, Schneeberger K, Witte M, Klein MR, van den Bogert B, Boekhorst J, et al. T lymphocytes control microbial composition by regulating the abundance of Vibrio in the zebrafish gut. *Gut Microbes*. (2014) 5:737–47. doi: 10.4161/19490976.2014.972228
26. Dee CT, Nagaraju RT, Athanasiadis EI, Gray C, Fernandez del Ama L, Johnston SA, et al. CD4-Transgenic zebrafish reveal tissue-resident Th2- and regulatory T cell–like populations and diverse mononuclear phagocytes. *J Immunol.* (2016) 197:3520–30. doi: 10.4049/jimmunol.1600959
27. Miyazawa R, Matsuura Y, Shibasaki Y, Imamura S, Nakanishi T. Cross-reactivity of monoclonal antibodies against CD4-1 and CD8α of ginbuna crucian carp with lymphocytes of zebrafish and other cyprinid species. *Dev Comp Immunol.* (2018) 80:15–23. doi: 10.1016/j.dci.2016.12.002
28. Roeselers G, Mittge EK, Stephens WZ, Parichy DM, Cavanaugh CM, Guillemin K, et al. Evidence for a core gut microbiota in the zebrafish. *ISME J.* (2011) 5:1595–608. doi: 10.1038/ismej.2011.38
29. López Nadal A, Peggs D, Wiegertjes GF, Brugman S. Exposure to Antibiotics affects saponin immersion-induced immune stimulation and shift in microbial composition in zebrafish larvae. *Front Microbiol.* (2018) 9:2588. doi: 10.3389/fmicb.2018.02588
30. Sullam KE, Essinger SD, Lozupone CA, Connor MPO, Rosen GL, Knight R, et al. Environmental and ecological factors that shape the gut 2 bacterial communities of fish: a meta-analysis - Supplementary. *Mol Ecol.* (2012) 21:3363–78. doi: 10.1111/j.1365-294X.2012.05552.x
31. Rawls JF, Mahowald MA, Ley RE, Gordon JI. Reciprocal gut microbiota transplants from zebrafish and mice to germ-free recipients reveal host habitat selection. *Cell.* (2006) 127:423–33. doi: 10.1016/j.cell.2006.08.043
32. Earley AM, Graves CL, Shiau CE. Critical role for a subset of intestinal macrophages in shaping gut microbiota in adult zebrafish. *Cell Rep.* (2018) 25:424–36. doi: 10.1016/j.celrep.2018.09.025
33. Ferrero G, Gomez E, Iyer S, Rovira M, Miserocchi M, Langenau DM, et al. The macrophage-expressed gene (mpeg) 1 identifies a subpopulation of B cells in the adult zebrafish. *bioRxiv.* (2019) 836098. doi: 10.1101/836098
34. Stagaman K, Burns AR, Guillemin K, Bohannan BJM. The role of adaptive immunity as an ecological filter on the gut microbiota in zebrafish. *ISME J.* (2017) 11:1630–9. doi: 10.1038/ismej.2017.28
35. Burns AR, Stephens WZ, Stagaman K, Wong S, Rawls JF, Guillemin K, et al. Contribution of neutral processes to the assembly of gut microbial communities in the zebrafish over host development. *ISME J.* (2016) 10:655–64. doi: 10.1038/ismej.2015.142
36. Burns AR, Guillemin K. The scales of the zebrafish: host–microbiota interactions from proteins to populations. *Curr Opin Microbiol.* (2017) 38:137–41. doi: 10.1016/j.mib.2017.05.011
37. Bates JM, Akerlund J, Mittge E, Guillemin K. Intestinal alkaline phosphatase detoxifies lipopolysaccharide and prevents inflammation in zebrafish in response to the gut microbiota. *Cell Host Microbe.* (2007) 2:371–82. doi: 10.1016/j.chom.2007.10.010
38. Koch BEV, Yang S, Lamers G, Stougaard J, Spaink HP. Intestinal microbiome adjusts the innate immune setpoint during colonization through negative regulation of MyD88. *Nat Commun.* (2018) 9:4099. doi: 10.1038/s41467-018-06658-4
39. Troll JV, Hamilton MK, Abel ML, Ganz J, Bates JM, Stephens WZ, et al. Microbiota promote secretory cell determination in the intestinal epithelium by modulating host Notch signaling. *Development.* (2018) 145:dev155317. doi: 10.1242/dev.155317
40. Kanther M, Sun X, Mhlbauer M, MacKey LC, Flynn EJ, Bagnat M, et al. Microbial colonization induces dynamic temporal and spatial patterns of NF-κB activation in the zebrafish digestive tract. *Gastroenterology.* (2011) 141:197–207. doi: 10.1053/j.gastro.2011.03.042
41. Murdoch CC, Espenschied ST, Matty MA, Mueller O, Tobin DM, Rawls JF. Intestinal serum amyloid a suppresses systemic neutrophil activation and bactericidal activity in response to microbiota colonization. *PLoS Pathog.* (2019) 15:e1007381. doi: 10.1371/journal.ppat.1007381
42. Cheesman SE, Neal JT, Mittge E, Seredick BM, Guillemin K. Epithelial cell proliferation in the developing zebrafish intestine is regulated by the Wnt pathway and microbial signaling via Myd88. *Proc Natl Acad Sci USA*. (2011) 108(Suppl_1):4570–7. doi: 10.1073/pnas.1000072107
43. Rolig AS, Sweeney EG, Kaye LE, DeSantis MD, Perkins A, Banse AV, et al. A bacterial immunomodulatory protein with lipocalin-like domains facilitates host–bacteria mutualism in larval zebrafish. *ELife.* (2018) 7:e37172. doi: 10.7554/eLife.37172
44. Bates JM, Mittge E, Kuhlman J, Baden KN, Cheesman SE, Guillemin K. Distinct signals from the microbiota promote different aspects of zebrafish gut differentiation. *Dev Biol.* (2006) 297:374–86. doi: 10.1016/j.ydbio.2006.05.006
45. Alpers DH, Zhang Y, Ahnen DJ. Synthesis and parallel secretion of rat intestinal alkaline phosphatase and a surfactant-like particle protein. *Am J Physiol Endocrinol Metab.* (1995) 268:E1205–14. doi: 10.1152/ajpendo.1995.268.6.E1205
46. Banerjee A, Gerondakis S. Coordinating TLR-activated signaling pathways in cells of the immune system. *Immunol Cell Biol.* (2007) 85:420–4. doi: 10.1038/sj.icb.7100098
47. Janssens S, Beyaert R. A universal role for MyD88 in TLR/IL-1R-mediated signaling. *Trends Biochem Sci.* (2002) 27:474–82. doi: 10.1016/S0968-0004(02)02145-X
48. Birchenough GMH, Nystrom EEL, Johansson MEV, Hansson GC. A sentinel goblet cell guards the colonic crypt by triggering Nlrp6-dependent Muc2 secretion. *Science.* (2016) 352:1535–42. doi: 10.1126/science.aaf7419
49. Crosnier C. Delta-Notch signalling controls commitment to a secretory fate in the zebrafish intestine. *Development.* (2005) 132:1093–104. doi: 10.1242/dev.01644
50. Kanwal Z, Wiegertjes GF, Veneman WJ, Meijer AH, Spaink HP. Comparative studies of Toll-like receptor signalling using zebrafish. *Dev Comp Immunol.* (2014) 46:35–52. doi: 10.1016/j.dci.2014.02.003
51. Blache P, Van De Wetering M, Duluc I, Domon C, Berta P, Freund JN, et al. SOX9 is an intestine crypt transcription factor, is regulated by the Wnt pathway, and represses the CDX2 and MUC2 genes. *J Cell Biol.* (2004) 166:37–47. doi: 10.1083/jcb.200311021
52. Wetering M, van de Sancho E, Verweij C, Lau W, de Oving I, Hurlstone A, et al. The beta-catenin/TCF-4 complex imposes a crypt

progenitor phenotype on colorectal cancer cells. *Cell.* (2002) 111:241–50. doi: 10.1016/S0092-8674(02)01014-0
53. Rolig AS, Parthasarathy R, Burns AR, Bohannan BJM, Guillemin K. Individual members of the microbiota disproportionately modulate host innate immune responses. *Cell Host Microbe.* (2015) 18:613–20. doi: 10.1016/j.chom.2015.10.009
54. Murdoch CC, Rawls JF. Commensal microbiota regulate vertebrate innate immunity-insights from the zebrafish. *Front Immunol.* (2019) 10:2100. doi: 10.3389/fimmu.2019.02100
55. Masud S, Torraca V, Meijer AH. Modeling infectious diseases in the context of a developing immune system. *Curr Top Dev Biol.* (2017) 124:277–329. doi: 10.1016/bs.ctdb.2016.10.006
56. Spence R, Gerlach G, Lawrence C, Smith C. The behaviour and ecology of the zebrafish, Danio rerio. *Biol Rev.* (2008) 83:13–34. doi: 10.1111/j.1469-185X.2007.00030.x
57. Westerfield M. *The Zebrafish Book. A Guide for the Laboratory Use of Zebrafish (Danio rerio).* 5th ed. Eugene: University of Oregon Press, Eugene (2007).
58. Hoseinifar SH, Sun YZ, Wang A, Zhou Z. Probiotics as means of diseases control in aquaculture, a review of current knowledge and future perspectives. *Front Microbiol.* (2018) 9:2429. doi: 10.3389/fmicb.2018.02429
59. Legrand TPRA, Wynne JW, Weyrich LS, Oxley APA. A microbial sea of possibilities: current knowledge and prospects for an improved understanding of the fish microbiome. *Rev Aquac.* (2019) raq.12375. doi: 10.1111/raq.12375
60. Ulloa PE, Medrano JF, Feijo CG. Zebrafish as animal model for aquaculture nutrition research. *Front Genet.* (2014) 5:313. doi: 10.3389/fgene.2014.00313
61. Lerner A, Shoenfeld Y, Matthias T. Probiotics: if it does not help it does not do any harm. Really? *Microorganisms.* (2019) 7:104. doi: 10.3390/microorganisms7040104
62. Gibson GR, Roberfroid MB. Dietary modulation of the human colonie microbiota: introducing the concept of prebiotics. *J Nutr.* (1995) 1401–12. doi: 10.1093/jn/125.6.1401
63. Song SK, Beck BR, Kim D, Park J, Kim J, Kim HD, et al. Prebiotics as immunostimulants in aquaculture: a review. *Fish Shellfish Immunol.* (2014) 40:40–8. doi: 10.1016/j.fsi.2014.06.016
64. Lee SH, Ko CI, Jee Y, Jeong Y, Kim M, Kim JS, et al. Anti-inflammatory effect of fucoidan extracted from Ecklonia cava in zebrafish model. *Carbohydr. Polym.* (2013) 92:84–9. doi: 10.1016/j.carbpol.2012.09.066
65. Jayawardena TU, Fernando IPS, Lee WW, Sanjeewa KKA, Kim HS, Lee DS, et al. Isolation and purification of fucoidan fraction in *Turbinaria ornata* from the Maldives; inflammation inhibitory potential under LPS stimulated conditions in *in-vitro* and *in-vivo* models. *Int J Biol Macromolecules.* (2019) 131:614–23. doi: 10.1016/j.ijbiomac.2019.03.105
66. Fernando IPS, Sanjeewa KKA, Samarakoon KW, Lee WW, Kim HS, Kang N, et al. A fucoidan fraction purified from Chnoospora minima; a potential inhibitor of LPS-induced inflammatory responses. *Int J Biol Macromolecules.* (2017) 104:1185–93. doi: 10.1016/j.ijbiomac.2017.07.031
67. Udayangani RMC, Dananjaya SHS, Fronte B, Kim CH, Lee J, De Zoysa M. Feeding of nano scale oats β-glucan enhances the host resistance against *Edwardsiella tarda* and protective immune modulation in zebrafish larvae. *Fish Shellfish Immunol.* (2017) 60:72–7. doi: 10.1016/j.fsi.2016.11.035
68. Oyarbide U, Rainieri S, Pardo MA. Zebrafish (*Danio rerio*) larvae as a system to test the efficacy of polysaccharides as immunostimulants. *Zebrafish.* (2012) 9:74–84. doi: 10.1089/zeb.2011.0724
69. Yousefi S, Hoseinifar SH, Paknejad H, Hajimoradloo A. The effects of dietary supplement of galactooligosaccharide on innate immunity, immune related genes expression and growth performance in zebrafish (*Danio rerio*). *Fish Shellfish Immunol.* (2018) 73:192–6. doi: 10.1016/j.fsi.2017.12.022
70. Siriyappagouder P, Galindo-Villegas J, Lokesh J, Mulero V, Fernandes JMO, Kiron V. Exposure to yeast shapes the intestinal bacterial community assembly in zebrafish larvae. *Front Microbiol.* (2018) 9:1868. doi: 10.3389/fmicb.2018.01868
71. Qin C, Xie Y, Wang Y, Li S, Ran C, He S, et al. Impact of *Lactobacillus casei* BL23 on the host transcriptome, growth and disease resistance in larval zebrafish. *Front Physiol.* (2018) 9:1245. doi: 10.3389/fphys.2018.01245
72. Caruffo M, Navarrete NC, Salgado OA, Faúndez NB, Gajardo MC, Feijóo CG, et al. Protective yeasts control *V. anguillarum* pathogenicity and modulate the innate immune response of challenged zebrafish (*Danio rerio*) larvae. *Front Cell Infect Microbiol.* (2016) 6:127. doi: 10.3389/fcimb.2016.00127
73. Zang L, Ma Y, Huang W, Ling Y, Sun L, Wang X, et al. Dietary *Lactobacillus plantarum* ST-III alleviates the toxic effects of triclosan on zebrafish (*Danio rerio*) via gut microbiota modulation. *Fish Shellfish Immunol.* (2019) 84:1157–69. doi: 10.1016/j.fsi.2018.11.007
74. Caruffo M, Navarrete N, Salgado O, Díaz A, López P, García K, et al. Potential probiotic yeasts isolated from the fish gut protect zebrafish (*Danio rerio*) from a *Vibrio anguillarum* challenge. *Front Microbiol.* (2015) 6:1093. doi: 10.3389/fmicb.2015.01093
75. Aoudia N, Rieu A, Briandet R, Deschamps J, Chluba J, Jego G, et al. Biofilms of *Lactobacillus plantarum* and *Lactobacillus fermentum*: effect on stress responses, antagonistic effects on pathogen growth and immunomodulatory properties. *Food Microbiol.* (2016) 53:51–9. doi: 10.1016/j.fm.2015.04.009
76. Rendueles O, Ferrières L, Frétaud M, Bégaud E, Herbomel P, Levraud JP, et al. A new zebrafish model of oro-intestinal pathogen colonization reveals a key role for adhesion in protection by probiotic bacteria. *PLoS Pathog.* (2012) 8:12. doi: 10.1371/journal.ppat.1002815
77. Falcinelli S, Picchietti S, Rodiles A, Cossignani L, Merrifield DL, Taddei AR, et al. *Lactobacillus rhamnosus* lowers zebrafish lipid content by changing gut microbiota and host transcription of genes involved in lipid metabolism. *Sci Rep.* (2015) 5:8–10. doi: 10.1038/srep09336
78. Wang Y, Ren Z, Fu L, Su X. Two highly adhesive lactic acid bacteria strains are protective in zebrafish infected with *Aeromonas hydrophila* by evocation of gut mucosal immunity. *J Appl Microbiol.* (2015) 120:441–51. doi: 10.1111/jam.13002
79. Davis DJ, Doerr HM, Grzelak AK, Busi SB, Jasarevic E, Ericsson AC, et al. *Lactobacillus plantarum* attenuates anxiety-related behavior and protects against stress-induced dysbiosis in adult zebrafish. *Sci Rep.* (2016) 6:33726. doi: 10.1038/srep33726
80. Gioacchini G, Giorgini E, Olivotto I, Maradonna F, Merrifield DL, Carnevali O. The influence of probiotics on zebrafish *Danio rerio* innate immunity and hepatic stress. *Zebrafish.* (2014) 11:98–106. doi: 10.1089/zeb.2013.0932
81. Gioacchini G, Rossi G, Carnevali O. Host-probiotic interaction: New insight into the role of the endocannabinoid system by *in vivo* and *ex vivo* approaches. *Sci Rep.* (2017) 7:1–12. doi: 10.1038/s41598-017-01322-1
82. Lin YS, Saputra F, Chen YC, Hu SY. Dietary administration of *Bacillus amyloliquefaciens* R8 reduces hepatic oxidative stress and enhances nutrient metabolism and immunity against *Aeromonas hydrophila* and *Streptococcus agalactiae* in zebrafish (*Danio rerio*). *Fish Shellfish Immunol.* (2019). 86:410–9. doi: 10.1016/j.fsi.2018.11.047
83. Nag D, Breen P, Raychaudhuri S, Withey JH. Glucose metabolism by *Escherichia coli* inhibits vibrio cholerae intestinal colonization of zebrafish. *Infect Immun.* (2018) 86:e00486-18. doi: 10.1128/IAI.00486-18
84. Qin C, Zhang Z, Wang Y, Li S, Ran C, Hu J, et al. EPSP of *L. casei* BL23 protected against the infection caused by *Aeromonas veronii* via enhancement of immune response in zebrafish. *Front Microbiol.* (2017) 8:2406. doi: 10.3389/fmicb.2017.02406
85. Lee WW, Oh JY, Kim EA, Kang N, Kim KN, Ahn G, et al. A prebiotic role of *Ecklonia cava* improves the mortality of *Edwardsiella tarda*-infected zebrafish models via regulating the growth of lactic acid bacteria and pathogen bacteria. *Fish Shellfish Immunol.* (2016) 54:620–8. doi: 10.1016/j.fsi.2016.05.018
86. Martin SAM, Król E. Nutrigenomics and immune function in fish: new insights from omics technologies. *Dev Comp Immunol.* (2017) 75:86–98. doi: 10.1016/j.dci.2017.02.024
87. Ringø E, Erik Olsen R, Gonzalez Vecino JL, Wadsworth S. Use of immunostimulants and nucleotides in aquaculture: a review. *J Mar Sci Res Dev.* (2012) 2:104. doi: 10.4172/2155-9910.1000104
88. Petit J, Wiegertjes GF. Long-lived effects of administering β-glucans: indications for trained immunity in fish. *Dev Comp Immunol.* (2016) 64:93–102. doi: 10.1016/j.dci.2016.03.003
89. Palstra AP, Kals J, Garcia AB, Dirks RP, Poelman M. Immunomodulatory effects of dietary seaweeds in LPS challenged Atlantic Salmon Salmo salar as determined by deep RNA sequencing of the head kidney transcriptome. *Front Physiol.* (2018) 9:625. doi: 10.3389/fphys.2018.00625
90. Brugman S, Ikeda-Ohtsubo W, Braber S, Folkerts G, Pieterse CMJ, Bakker PAHM. A comparative review on microbiota manipulation: lessons from fish, plants, livestock, and human research. *Front Nutr.* (2018) 5:80. doi: 10.3389/fnut.2018.00080

91. Merrifield DL, Dimitroglou A, Foey A, Davies SJ, Baker RTM, Bøgwald J, et al. The current status and future focus of probiotic and prebiotic applications for salmonids. *Aquaculture.* (2010) 302:1–18. doi: 10.1016/j.aquaculture.2010.02.007
92. Hai NV. The use of probiotics in aquaculture. *J Appl Microbiol.* (2015) 119:917–35. doi: 10.1111/jam.12886
93. Pelster B, Bagatto B. Respiration. In: Perry SF, Ekker M, Farrell AP, Brauner CJ. *Fish Physiology: Zebrafish*. Vol. 29. 1st ed. Burlington, MA: Elsevier Inc. (2010). p. 289–305.
94. Ringø E, Gatesoupe F-J. Lactic acid bacteria in fish: a review. *Aquaculture*. (1998) 160:177–203. doi: 10.1016/S0044-8486(97)00299-8
95. Kelly C, Salinas I. Under pressure: interactions between commensal microbiota and the teleost immune system. *Front Immunol.* (2017) 8:559. doi: 10.3389/fimmu.2017.00559
96. Kane M, Case LK, Kopaskie K, Kozlova A, MacDearmid C, Chervonsky AV, et al. Successful transmission of a retrovirus depends on the commensal microbiota. *Science.* (2011) 334:245–9. doi: 10.1126/science.1210718
97. Kuss SK, Best GT, Etheredge CA, Pruijssers AJ, Frierson JM, Hooper LV, et al. Intestinal microbiota promote enericvirus replication and systemic pathogenesis. *Science.* (2011) 334:249–52. doi: 10.1126/science.1211057
98. Lee H, Ko GP. Antiviral effect of Vitamin A on norovirus infection via modulation of the gut microbiome. *Sci Rep.* (2016) 6:1–9. doi: 10.1038/srep25835

**Conflict of Interest:** DP and CM are employed by Skretting Aquaculture Research Center.

The remaining authors declare that the research was conducted in the absence of any commercial or financial relationships that could be construed as a potential conflict of interest.

frontiers in Immunology

ORIGINAL RESEARCH
published: 26 February 2020
doi: 10.3389/fimmu.2020.00169

# Quantitative Proteomic Analysis Reveals Antiviral and Anti-inflammatory Effects of Puerarin in Piglets Infected With Porcine Epidemic Diarrhea Virus

*Mengjun Wu*[1†], *Qian Zhang*[1†], *Dan Yi*[1†], *Tao Wu*[1], *Hongbo Chen*[1], *Shuangshuang Guo*[1], *Siyuan Li*[1], *Changzheng Ji*[1], *Lei Wang*[1], *Di Zhao*[1], *Yongqing Hou*[1*] *and Guoyao Wu*[1,2]

[1] *Hubei Key Laboratory of Animal Nutrition and Feed Science, Wuhan Polytechnic University, Wuhan, China,* [2] *Department of Animal Science, Texas A&M University, College Station, TX, United States*

OPEN ACCESS

**Edited by:**
*Julio Villena, CONICET Centro de Referencia para Lactobacilos (CERELA), Argentina*

**Reviewed by:**
*Lester J. Perez, University of Illinois at Urbana–Champaign, United States*
*Leonardo Albarracin, CONICET Centro de Referencia para Lactobacilos (CERELA), Argentina*

***Correspondence:**
*Yongqing Hou*
*houyq@aliyun.com*

[†]*These authors have contributed equally to this work and share first authorship*

**Specialty section:**
*This article was submitted to Nutritional Immunology, a section of the journal Frontiers in Immunology*

**Received:** *01 November 2019*
**Accepted:** *22 January 2020*
**Published:** *26 February 2020*

**Citation:**
*Wu M, Zhang Q, Yi D, Wu T, Chen H, Guo S, Li S, Ji C, Wang L, Zhao D, Hou Y and Wu G (2020) Quantitative Proteomic Analysis Reveals Antiviral and Anti-inflammatory Effects of Puerarin in Piglets Infected With Porcine Epidemic Diarrhea Virus. Front. Immunol. 11:169. doi: 10.3389/fimmu.2020.00169*

Porcine epidemic diarrhea virus (PEDV) has caused enormous economic losses to the swine industry worldwide in recent years. Puerarin (PR), a major isoflavonoid isolated from the Chinese herb Gegen, possesses many pharmacological activities, including anti-inflammatory, and anti-viral activities. This study was conducted with both PEDV-infected African green monkey kidney cells (Vero) and neonatal pigs to determine the effect of PR on PEDV infection and to elucidate the underlying mechanisms by using proteomic analyses. Twenty-four piglets fed a milk replacer were randomly allocated into one of three groups (Control, PEDV, and PEDV + PR). After a 5-day period of adaption, piglets ($n$ = 8/group) in the PEDV + PR were orally administered with PR (0.5 mg/kg body weight) between days 5 and 9, whereas piglets in the other two groups received the same volume of liquid milk replacer. On day 9, piglets were orally administered with either sterile saline or PEDV (Yunnan province strain) at $10^{4.5}$ $TCID_{50}$ (50% tissue culture infectious dose) per pig. On day 12 of the trial, jugular vein blood and intestinal samples were collected. In addition, Vero cells were assigned randomly into three groups (Control, PEDV, PEDV + PR). Cells in the PEDV and PEDV + PR groups were infected with PEDV at a multiplicity of infection of 0.01, while cells in the control group were treated with the same volume of sterile saline. One hour later, cells in the Control and PEDV groups were cultured in serum-free DMEM, while cells in the PEDV + PR group were supplemented with PR. After 36 h of culture, cells were harvested. PR attenuated the reductions in cell proliferation *in vitro* and growth performance in PEDV-infected piglets, and inhibited PEDV replication and the expression of several cytokines (including IL-8) both *in vitro* and *in vivo*. Proteomic analyses identified that the abundances of 29 proteins in the ileum were altered by PEDV infection and restored to the control level by PR. Pathway analyses revealed that PR restored the expression of several interferon-stimulated genes and selectively upregulated the expression of guanylate-binding proteins. Western blot

analyses showed that PR supplementation inhibited the PEDV-induced NF-κB activation. Collectively, these results indicate that PR could exert antiviral and anti-inflammatory effects in piglets infected with PEDV and have the potential to be an effective antiviral feed additive.

**Keywords: puerarin, porcine epidemic diarrhea virus, piglets, antiviral, anti-inflammatory, proteomics**

## INTRODUCTION

Porcine epidemic diarrhea (PED), a devastating enteric disease characterized by vomiting, anorexia, acute severe watery diarrhea, and dehydration, results in extremely high rates of morbidity and mortality in newborn piglets (1). Since December 2010, massive outbreaks of PED have occurred in China, with 80–100% morbidity and 50–90% mortality in suckling piglets (2, 3). The recent research provides evidence for airborne transmission of PED virus (PEDV) (4), which has greater transmission potential than other seasonal diarrhea viruses (5, 6). The small intestine, especially the jejunum and ileum, is the target tissue of PEDV infection (7). The M Protein and the N protein, being the most abundant envelope component and a structural basis for the helical nucleocapsid of PEDV, respectively, are commonly used in the clinical diagnosis of PED (8–10). To date, no feed additive is available to effectively inhibit the replication of PEDV.

Owing to the concerns about the toxicity of synthetic antiviral drugs, natural products are considered to be an important source of new drug development against viral infections (11). Puerarin (PR) is an isoflavonoid isolated from Gegen, which is a traditional Chinese herb medicine (12). PR has anti-oxidant and anti-inflammatory effects (13–15) and has been proven to be an effective antimicrobial agent (16). PR significantly prevented human alveolar epithelial A549 cells from *Staphylococcus aureus*-induced injury and may be considered as a potential candidate for the development of anti-virulence drugs in the treatment of *S. aureus*-mediated infections (17). A recent study found that pre-treatment with PR protected porcine intestinal epithelial cells (IPEC-J2 cells) from enterotoxigenic *Escherichia coli* (ETEC) infection through inhibiting bacterial adhesion and inflammatory responses (18). Another study found that PR had a moderate ability to reduce hepatitis B virus production *in vitro* (19). Additionally, *Kudzu* root-extracted PR inhibited HIV-1 replication by blocking the initial attachment of the viral particle to the cell surface in primary human $CD4^+$ T lymphocytes and macrophages (20). Lin et al. found that the water extract of *Pueraria lobata* Ohwi has anti-viral activity against human respiratory syncytial virus in human respiratory tract cell lines (21). Therefore, these results suggest that PR could be a promising supplement for antiviral therapy. However, little is known about its effectiveness against PEDV infection.

Proteomic analysis is widely used in biomedical science for discovering novel molecular interactions and pathways (22). The label-free quantitative proteomic (LFQP) analysis is a very powerful tool to profile global protein expression (23). Bioinformatics analysis has been applied to explore the mechanisms of interaction among the host, pathogen, and drug. In recent years, the quantitative proteomic analysis has been used to investigate the pathogenic mechanism of PEDV infection (24, 25). However, most of these studies are performed *in vitro* with a label-based quantitative proteomic (LQP) approach. Previous studies have indicated that the label-free approach by far outperforms the LQP method for the proteome coverage, as up to threefold more proteins are reproducibly identified in replicate measurements (26). It is of great importance to study the interaction between PEDV and the host *in vivo*, which could provide more biologically relevant insights into the pathogenesis of PEDV.

In this study, the antiviral effect of PR was evaluated in PEDV-infected Vero cells and neonatal pigs. Furthermore, an LFQP analysis was used to identify differentially regulated proteins (DRPs) in the small intestine and the mechanisms underlying the effects of PR on PEDV infection. Our findings are expected to provide a basis for the use of PR to treat PEDV infection.

## MATERIALS AND METHODS

### PEDV, Vero Cells, and PR

PEDV (Yunnan province strain, GenBank accession No. KT021228) and African green monkey kidney cells (Vero) were provided by the State Key Laboratory of Agricultural Microbiology, College of Veterinary Medicine, Huazhong Agricultural University, Wuhan, China. PR (purity ≥ 98%) was purchased from Macklin Inc. (Macklin, Shanghai, China).

### Viral Infection in Vero Cells

All experiments using live virus *in vitro* were conducted under biosafety level 2 (BSL2) conditions and strictly followed safety procedures. Vero cells were randomly assigned into three groups (Control, PEDV, PEDV + PR) and cultured in Dulbecco's modified Eagle's medium (DMEM, Tanee Chemicals, Beijing, China) supplemented with 10% fetal bovine serum (FBS; Gibco; Thermo Fisher Scientific, Inc., Waltham, MA, USA), and 1% penicillin–streptomycin–amphotericin B (PSF; Solarbio, Beijing, China) in 75-$cm^2$ flasks under the condition of 5% $CO_2$ at 37°C. Upon reaching 80–90% confluency, the cells were washed twice gently with serum-free DMEM prior to infection. Then the cells were cultured with PEDV at a multiplicity of infection (MOI)

**Abbreviations:** GBPs, guanylate-binding proteins; HPRT1, hypoxanthine phosphoribosyltransferase 1; IFIT3, interferon-induced protein 3; IL-1β, interleukin−1β; IL-8, interleukin-8; ISGs, interferon-stimulated genes; MCP-1, monocyte chemotactic protein 1; NF-κB, nuclear factor kappa-B; OAS1, 2′-5′oligoadenylate synthetase 1; PEDV, porcine epidemic diarrhea virus; PEDV-M, membrane protein (porcine epidemic diarrhea virus); PEDV-N, nucleocapsid protein (Porcine epidemic diarrhea virus); RPL4, ribosomal protein L4; $TCID_{50}$, 50% tissue culture infectious dose; TNF-α, tumor necrosis factor α.

of 0.01 in serum-free DMEM containing 5 μg/ml of trypsin (Genom, Hangzhou, China). Cells without PEDV infection were used as the Control. One hour later, the Control and PEDV groups were replenished with 100 μl of serum-free DMEM, whereas the PEDV + PR group was supplemented with PR. After 36 h of incubation, the cells were washed twice with phosphate-buffered saline (PBS; Gibco, USA) and harvested for further analysis.

## Animals and Treatments

The animal use protocol for this research was approved by the Animal Care and Use Committee of Wuhan Polytechnic University (Index number: 011043145-029-2013-000009). Twenty-four 7-day-old crossbred (Duroc × Landrace × Large White) healthy piglets (half male and half female), initially weighing 3.17 ± 0.25 kg, were purchased from a PEDV-negative farm. They were randomly allocated into one of three treatment groups (Control, PEDV, PEDV + PR; eight replicates per group). The experimental basal diet (a liquid milk replacer), which was formulated to meet the requirements of all nutrients for suckling piglets, was purchased from Wuhan Anyou Feed Co., Ltd. (Wuhan, China). Piglets were housed in clean pens with strict control of cross-infection. The entire trial period was 12 days. During day 5 to 9 of the trial, the piglets in the PEDV + PR group were orally administered with PR (0.5 mg/kg body weight; dissolved in the liquid milk replacer), and the piglets in the other two groups received the same volume of the liquid milk replacer. On day 9 of the trial, PEDV at a dose of $10^{4.5}$ $TCID_{50}$ (50% tissue culture infectious dose) per pig was orally inoculated to pigs in the PEDV and the PEDV + PR groups, while the Control group was mock inoculated in parallel with the same volume of sterile saline. Pigs were observed daily to record the health status and diarrhea incidence. On day 12, all piglets were weighed and sacrificed to obtain the jejunum, ileum, colonic chyme, and mesenteric lymph nodes. All samples were rapidly frozen in liquid nitrogen and then stored at−80°C until analysis. The protocols of PEDV infection and sample collection were described previously (27). The intestinal pathomorphology was observed as described previously (28).

## Quantitative RT-PCR (qRT-PCR) and Droplet Digital PCR (dd PCR)

The total RNA was extracted by TRIzol reagent (Takara, Dalian, China) to ensure its purity (a 28 S/18 S rRNA ratio of >1.8 and an $OD_{260}/OD_{280}$ ratio of approximately 2.0) according to the manufacturer's instructions. The cDNA was synthesized by RT-PCR using the PrimeScript® RT reagent Kit with gDNA Eraser kit (Takara, Dalian, China). The qPCR was performed using the SYBR® Premix Ex TaqTM (Takara, Dalian, China) on an Applied Biosystems 7,500 Fast Real-Time PCR System (Foster City, CA, USA). The relative expression level of each gene was calculated with the $2^{-\Delta\Delta CT}$ method (29). Monkey hypoxanthine phosphoribosyltransferase 1 (HPRT1) was used as the reference gene in Vero cells (30). Porcine ribosomal protein L4 (RPL4) was used as the reference gene in the jejunum, ileum, and mesenteric lymph nodes (28). The genomic DNA of the colon chyme was extracted by using the QIAamp® Fast DNA Stool Mini Kit (Qiagen, Hilden, Germany). Then the viral gene expression was detected by using the droplet digital PCR (dd PCR) method as described previously (31). Primers used in the present study are listed in **Table 1** (32–35).

**TABLE 1 |** The primer sequences used in the present study.

| Species | Gene name | Sequences | References |
|---|---|---|---|
| Monkey | HPRT1 | F:5′-TGACACTGGCAAAACAATGCA-3′ | (30) |
| | | R:5′-GGTCCTTTTCACCAGCAAGCT-3′ | |
| | IL-1β | F:5′-GCGGCAACGAGGATGACTT-3′ | (32) |
| | | R:5′-TGGCTACAACAACTGACACGG-3′ | |
| | IL-8 | F:5′-GGAACCATCTCGCTCTGTGTAA-3′ | (32) |
| | | R:5′-GGTCCACTCTCAATCACTCTCAG-3′ | |
| | TNF-α | F:5′-CACCACGCTCTTCTGTCT-3′ | (32) |
| | | R:5′-AGATGATCTGACTGCCTGAG-3′ | |
| | MCP-1 | F:5′-CTTCTGTGCCTGCTGCTCATA-3′ | (32) |
| | | R:5′-ACTTGCTGCTGGTGATTCTTCT-3′ | |
| Pig | RPL4 | F:5′-GGAAACCGTCGCGAGA-3′ | (28) |
| | | R:5′-GCCCCAGAGACAGTT-3′ | |
| | GBP-2 | F:5′-ACCAGGAGGTTTTCGTCTCTCTATT-3′ | Present study |
| | | R:5′-TCCTCTGCCTGTATCCCCTTT-3′ | |
| | IFIT3 | F:5′-GCATTTTCCAGCCAGCATC-3′ | (33) |
| | | R:5′-TCTGTTCCTTTCCTTTCCTTCCT-3′ | |
| | OAS1 | F:5′-TGGTGGTGGAGACACACACA-3′ | (33) |
| | | R:5′-CCAACCAgAgACCCATCCA-3′ | |
| | IFN-α | F:5′-ACTCCATCCTGGCTGTGAGGAAAT-3′ | (33) |
| | | R:5′-ACTCCATCCTGGCTGTGAGGAAAT-3′ | |
| | IFN-β | F:5′-ATGTCAGAAGCTCCTGGGACAGTT-3′ | (34) |
| | | R:5′-AGGTCATCCATCTGCCCATCAAGT-3′ | |
| PEDV | PEDV-M | F:5′-TCCCGTTGATGAGGTGAT-3′ | Present study |
| | | R:5′-AGGATGCTGAAAGCGAAAA-3′ | |
| | PEDV-N | F:5′-CGCAAAGACTGAACCCACTAACTT-3′ | (35) |
| | | R:5′-TTGCCTCTGTTGTTACTCGGGGAT-3′ | |

*Abbreviations: HPRT1, hypoxanthine phosphoribosyltransferase 1; RPL4, ribosomal protein L4; IL-1β, interleukin-1β; IL-8, interleukin-8; TNF-α, tumor necrosis factor α; MCP-1, monocyte chemotactic protein 1; PEDV-M, membrane protein (porcine epidemic diarrhea virus); PEDV-N, nucleocapsid protein (porcine epidemic diarrhea virus); GBP-2, guanylate-binding proteins; IFIT3, interferon-induced protein 3; OAS1, 2′-5′oligoadenylatesynthetase 1; IFN-α, interferon-α; IFN-β, interferon-β.*

## Cytokine Assays by Enzyme-Linked Immunosorbent Assay (ELISA)

The concentrations of cytokines (IL-1β, IL-6, IL-8) in the ileum of piglets were measured by using ELISA kits (RD Systems Quantikine, USA), which are specific for porcine cytokines. All the assay procedures were performed according to the manufacturer's instructions.

## Protein Extraction and Digestion

Four biological replicates per group, i.e., a total of 12 ileal samples, were used to analyze the intestinal proteome. First, 150 mg of ileal tissue was homogenized with 1 ml of Tissue Protein Extraction Reagent (Thermo Scientific, USA) containing Protease Inhibitor (Roche, USA) and then vortexed for 10 min

at 4°C. The soluble protein was collected after the removal of tissue debris by centrifugation (12,000 × g, 20 min, 4°C). The protein concentration was quantified by the bicinchoninic acid (BCA) assay (25). Approximately 200 μg of proteins from each sample was subjected to filter-aided sample preparation (FASP) trypsin digestion to generate peptides. Briefly, protein samples were diluted to 100 μl with 50 mM ammonium bicarbonate, and disulfide bonds in protein were reduced by treating the sample with 2 μl of 500 mM DL-dithiothreitol (DTT) in 100 μl of 50 mM ammonium bicarbonate for 150 min at 37°C (the final concentration of DDT was 10 mM), and then alkylated with 14 μl of 500 mM iodoacetamide (IAA) at room temperature (25°C) for 40 min in the dark (the final concentration of IAA was 60 mM). The detergent, DTT, and other low-molecular-weight components were removed by repeated dilution in 100 mM Tris-HCl UA buffer (containing 8 M urea, pH 8.5), followed by filtration through 10-kDa ultrafiltration units (Pall Corporation, USA). The filters were washed three times with 100 μl of UA buffer, followed by twice washes with 100 μl of 50 mM ammonium bicarbonate. Proteins were then digested using mass spectrometry-grade trypsin (Thermo Fisher Scientific, USA) in 50 mM ammonium bicarbonate by incubation overnight at 37°C and 800 rpm. The enzyme:substrate ratio was 1:50. The effluent was collected after centrifugation at 10,000 × g for 15 min and filtered twice with 50 μl of 50 mM ammonium bicarbonate. The effluent was combined and then acidified with 10% trifluoroacetate (TFA) to stop the reaction (the final concentration of TFA was 0.4%). The resulting peptides were desalted using a Pierce C18 Tips (Thermo Fisher Scientific, USA) and vacuum-dried. Prior to LC-MS/MS analysis, peptide samples were re-suspended in 40 μl of 0.1% v/v formic acid (FA) and 5% v/v acetonitrile (ACN) solution.

## Nano-LC-MS/MS Analysis

The nano-LC-MS/MS analysis was performed in 125 min on a Q Exactive mass spectrometer (Thermo Fisher Scientific, USA), which was coupled to an Easy-Nano Ultimate 3,000 UPLC system (Dionex, Thermo Fisher Scientific, USA). The peptide mixture (1 μg) was loaded into a trap column (100 μm × 20 mm; Acclaim PepMap 100; Thermo Fisher Scientific, USA) at 5 μl/min for 3 min. Peptide separation was carried out in a C18 capillary column (75 μm × 150 mm; Acclaim PepMap RSLC, Thermo Fisher Scientific, USA) at 300 nl/min. The mobile phase consisted of two solvents: 0.1% formic acid (FA) in water (solvent A) and 0.08% FA in 80% acetonitrile (ACN, solvent B). The following gradients were used: 0–3% B in 8 min, 3–8% B in 2 min, 8–28% B in 76 min, 28–45% B in 17 min, 45–99% B in 2 min, 99% B in 5 min, 99–3% B in 1 min, 3% B in 14 min. Then the separated peptides were analyzed in the Q Exactive Orbitrap mass spectrometer operated in the positive ion mode (nanospray voltage was 2.0 kV and source temperature was 250°C). The MS data were acquired using the data-dependent acquisition (DDA) mode. The mass spectrometer was operated in the Top-20 data-dependent mode with automatic switching between MS/MS and the full-scan MS mode (350–2,000 m/z) that was operated at a resolution of 70,000 with automatic gain control (AGC) target of $3 \times 10^6$ ions and a maximum ion transfer (IT) of 20 ms. The precursor ions were fragmented by high-energy collisional dissociation (HCD) and subjected to MS/MS scans with the following parameters: resolution, 17,500; fixed first mass, 120 m/z; isolation width, 1.6 m/z; AGC, $1 \times 10^5$ ions; maximum IT, 50 ms; intensity threshold, $1.6 \times 10^5$; normalized collision energy, 27%; dynamic exclusion duration, 40.0 s. These data were acquired by the Xcalibur software (version 4.0.27.10, Thermo Fisher Scientific, USA).

## MS Data Analysis

The peak lists extracted from raw MS data were further processed with the MaxQuant software (version 1.6.1.0, Max Planck Institute of Biochemistry in Martinsried, Germany) by using the XIC (extracted ion chromatogram)-based label-free quantitation algorithm and the UniProtKB *Sus scrofa* database (22,191 total entries, downloaded 11/10/18). The M and N proteins were analyzed similarly on the basis of PEDV CV777 strain database (seven total entries, downloaded 11/10/18). The following parameters were applied for the search: enzyme, trypsin; missed cleavages, 2; minimum peptide length, 7; de-isotopic, TRUE; fixed modification, carbamidomethyl (C), variable modification, oxidation (M) and acetylation (protein N-terminus); decoy database pattern, reverse; label-free quantification (LFQ), TRUE; LFQ minimum ratio count, 2; iBAQ, TRUE; match between runs, 2 min; peptide false discovery rate (FDR) $\leq 0.01$; protein FDR $\leq 0.01$. MaxQuant output files were analyzed with standard settings in the Perseus software (v.1.6.2.3, http://www.perseus-framework.org) (36). LFQ intensity values were used as the quantitative measurement of protein abundance for subsequent analysis. The data matrix was first filtered for the removal of contaminants and reverse decoy data. Each of the confident protein identification involves at least two unique peptides. LFQ intensity values were log2 transformed (37), and each sample was assigned to its corresponding group (Control, PEDV, or PEDV + PR). Proteins were filtered based on valid values (Min. number of values: four, Mode: in total). A data-imputation step was conducted to replace missing values with those that simulate signals of low abundant proteins (38). The latter were chosen randomly from a distribution specified by a downshift of 1.8 times the standard deviation (SD) of all measured values and a width of 0.3 times the SD. Two sample *t*-tests were performed for all relevant comparisons using a cutoff of $P < 0.05$ on the post imputation datasets to identify statistically significant differentially regulated proteins (DRPs).

## Bioinformatics Analysis

Heat-map was used to show the trend of protein expression between different samples with the aid of Metaboanalyst (https://www.metaboanalyst.ca/faces/home.xhtml). All those proteins that exhibited a fold-change of at least 1.5 ($P < 0.05$) were considered differentially regulated. The protein names were obtained from UniProt gene ID using the UniProt "Retrieve/ID mapping" function (http://www.uniprot.org/uploadlists/). For functional analysis, Gene Ontology (GO) annotation was retrieved from the GO database (http://www.geneontology.org/) for each protein in search of the

database. Due to the poor annotations of the porcine genome database, the differentially expressed proteins were input into the human database for the Reactome pathway analysis (http://www.reactome.org). In this study, cell signaling pathways were selected with the threshold of significance being defined as $P < 0.05$, FDR $< 0.05$, and minimum counts $> 3$. The relationships among the DRPs of the three groups were depicted in Venn diagrams (http://bioinformatics.psb.ugent.be/webtools/Venn/). Furthermore, protein–protein interaction networks were constructed using the online software String (https://string-db.org/) in combination with Cytoscape (v.3.7.1, https://cytoscape.org/).

## Validation of the Proteomic Analysis Results by Western Blot

The Western blot assay was carried out as previously described (39) to validate the results of proteomic study. In brief, proteins were extracted, denatured, and quantified using the BCA assay kit (Thermo Fisher Scientific, USA). Equivalent quantities of proteins from the independent biological replicates were separated by 10% SDS-PAGE, and the separated proteins were then electrophoretically transferred onto polyvinylidene difluoride (PVDF) membranes, which were subsequently blocked with 5% w/v skim milk in Tris-buffered saline containing Tween 20 (TBST) for 1.5 h at 25°C. Thereafter, the membranes were incubated at 4°C overnight with one of the following primary antibodies: signal transducers and activators of transcription 1 (STAT1; 1:1,000; Nova Biologicals), IFN-stimulated genes 15 (ISG15; 1:1,000; Abcam), myxovirus resistance 1 (MX1; 1:1,000; Abcam), retinoic acid-inducible gene 1 (DDX58; 1:1,000; Cell Signaling Technology), nuclear factor kappa-B (NF-κB p65; 1:1,000; Cell Signaling Technology), and phosphorylated-nuclear factor kappa-B (pNF-κB p65; 1:1,000; Cell Signaling). After washing three times with TBST, the membranes were incubated with the anti-rabbit (mouse) immunoglobulin G horseradish peroxidase-conjugated secondary antibody (1:5,000 dilution; Beijing ZhongShan Golden Bridge Biological Technology Co. Ltd, Beijing, China). The abundance of β-actin (1:4,000; Invitrogen) in each sample was also determined as an internal reference in the present study, whereas the histone H3 protein was determined as an internal reference for nuclear proteins.

## Statistical Analysis

The data of ADG, morphology, qRT-PCR, and Western blot were analyzed by using the one-way ANOVA procedure in the SPSS 17.0 software (SPSS Inc. Chicago, USA) and expressed as mean ± SD. The differences between means among the treatment groups were determined by the Duncan's multiple range test. In addition, data of the diarrhea rate were analyzed by the Chi-square test and expressed as a percentage. A value of $P < 0.05$ was taken to indicate statistical significance.

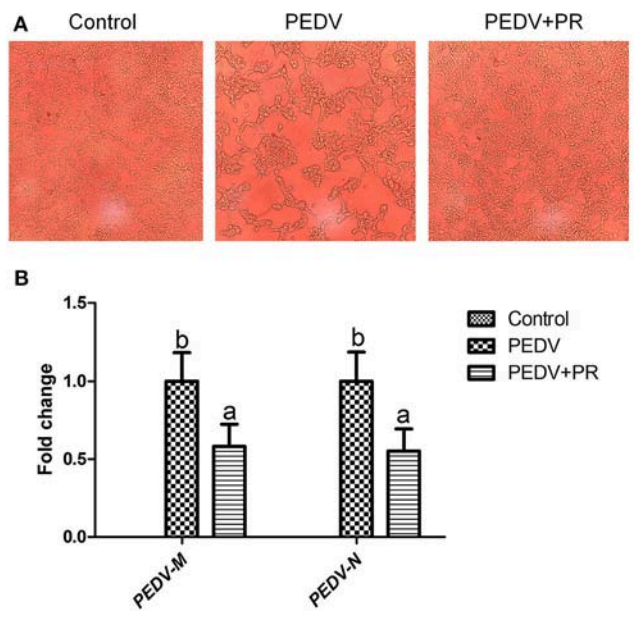


**FIGURE 1 |** Effects of puerarin on porcine epidemic diarrhea virus (PEDV) replication in Vero cells. **(A)** Microscopic morphology of Vero cells in culture (100×). Typical cytopathic effects (CPE) of PEDV in Vero cells were revealed by an optical microscope at 36 h post inoculation. Cell detachment appeared in the PEDV group compared to the Control group. However, the PEDV + PR group appeared to have fewer dead cells than the PEDV group. **(B)** Effects of puerarin on the expression of *M* and *N* genes of PEDV in Vero cells. Values are mean and pooled SEM, $n = 8$. [a,b]Values with different letters for the same gene are different ($P < 0.05$).

# RESULTS

## Effects of PR on PEDV Replication and PEDV-Induced Cytokine Expression in Vero Cells

To assess the role of PR on PEDV infection, an *in vitro* study was performed with Vero cells. Microscopic observation revealed that cells died and shed from the wall after PEDV infection (**Figure 1A**). However, cells in the PEDV + PR group exhibited a lower rate of deaths than the PEDV group ($P < 0.05$). qPCR

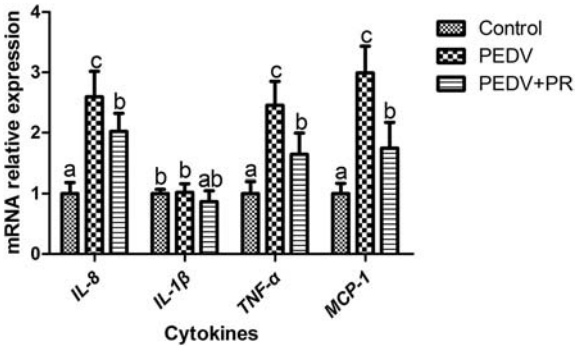


**FIGURE 2 |** Effects of puerarin on the expression of PEDV-induced cytokines in Vero cells. Values are mean and pooled SD, $n = 8$. [a,b,c]Values with different letters for the same gene are different ($P < 0.05$).

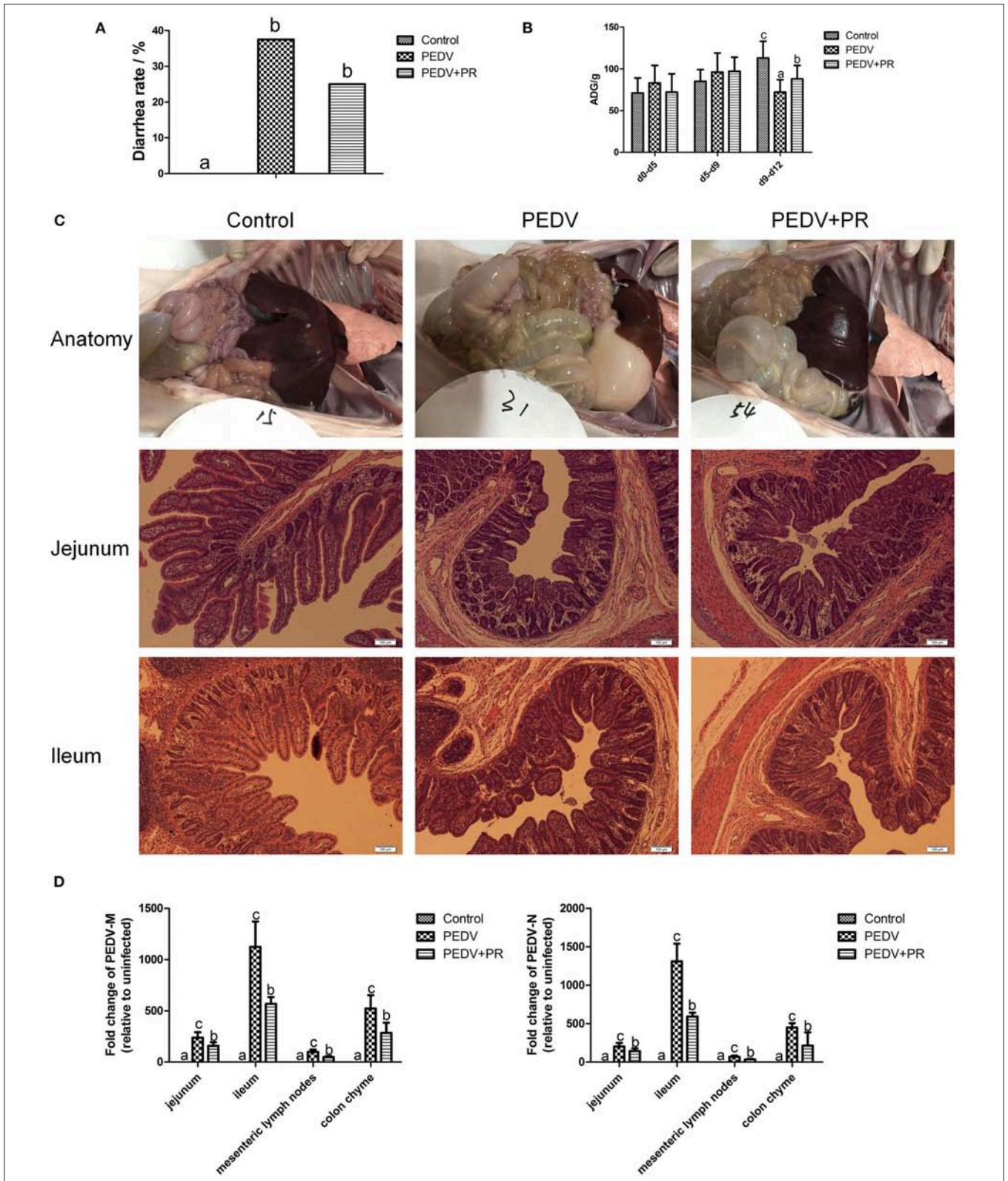


**FIGURE 3 |** Effects of puerarin on resistance in PEDV-infected piglets. **(A)** Effects of puerarin on the diarrhea incidence of piglets during PEDV infection. **(B)** Effects of puerarin on the average daily gain of piglets during PEDV infection. ADG, average daily weight gain. d0–d5: No treatment. d5–d9: Piglets in the PEDV + PR group

*(Continued)*

**FIGURE 3 |** were orally administered with puerarin (prepared in liquid milk replacer), and the other two groups of piglets received the same volume of liquid milk replacer. d9–d12: On day 9 of the experiment, 3.3 ml of PEDV were orally inoculated to the PEDV group and the PEDV + PR group, whereas the Control group received the same volume of saline. **(C)** Histopathological structures of piglet intestines in the Control, PEDV, and PEDV + PR groups. PEDV infection caused typical PED symptoms. Piglets in the PEDV group exhibited moderately thin and transparent intestinal walls with an accumulation of large amounts of fluid in the intestinal lumen. Pathological examination of the jejunum and ileum of piglets using the hematoxylin and eosin (H&E) staining revealed multifocal to diffuse villous atrophy. However, piglets in the PEDV + PR group exhibited less intestinal lesions than those in the PEDV group. **(D)** Effects of puerarin on the expression of *PEDV-M* and *-N* genes in different tissues of piglets. Values are mean and pooled SD, $n = 8$. $^{a,b,c}$Values with different letters for the same tissue are different ($P < 0.05$).

results showed that the mRNA levels of PEDV *N* and *M* genes were lower in the PEDV + PR group than those in the PEDV group (**Figure 1B**). Moreover, the expression of *IL-8*, *TNF-α*, and *MCP-1* genes were decreased ($P < 0.05$) in the PEDV + PR group compared with the PEDV group (**Figure 2**).

## Effects of PR on Resistance to PEDV Infection in Piglets

In this study, piglets in both PEDV and PEDV + PR groups exhibited watery diarrhea after PEDV infection. Diarrhea incidence in the PEDV + PR group tended to decrease in comparison with the PEDV group, but the difference did not reach statistical significance (**Figure 3A**). Moreover, other clinical symptoms, such as vomiting, anorexia, and reduced appetite, were mitigated in the PEDV + PR group in comparison with those in the PEDV group (data not shown). Prior to PEDV challenge (day 0–day 5 and day 5–day 9), average daily weight gain (ADG) did not differ among the three groups of piglets (**Figure 3B**). However, PEDV infection reduced ($P < 0.05$) the ADG of piglets (day 9–day 12), and oral administration of PR alleviated the reduction of ADG in PEDV-infected piglets ($P < 0.05$).

In the present study, the small intestine was typically distended by the accumulation of yellow fluid, and the small intestinal walls were thin and transparent in the PEDV and PEDV + PR groups. Histologic lesions were present in the jejunum and ileum of PEDV-infected groups, including the irregularity and desquamation of epithelial cells, as well as the defected and irregular striated border (**Figure 3C**). No pathological changes were observed in the small intestine of the control group (non-infected). Due to the severe villous atrophy in PEDV-infected piglets, villus height (VH), villus surface area, crypt depth (CD), and the ratio of VH/CD were further measured. Results showed that crypt depths were increased, whereas villus height, villus surface area, as well as the ratio (VH/CD) of jejunum and ileum were decreased ($P < 0.05$) in both PEDV and PEDV + PR groups. No statistical difference in the intestinal morphology was found between PEDV and PEDV + PR groups (**Table 2**).

To further determine the role of PR on PEDV infection *in vivo*, the mRNA levels for PEDV *M* and *N* genes were measured. The *M* and *N* genes were highly expressed in both PEDV and PEDV + PR groups, whereas no PEDV genes were detected in the Control group. These results indicated that the PEDV infection model was successfully established in this study. However, compared with the PEDV group, mRNA levels for the PEDV *M* and *N* genes were decreased ($P < 0.05$) in the jejunum, ileum, mesenteric lymph nodes, and the colon of PEDV + PR piglets (**Figure 3D**).

**TABLE 2 |** The intestinal morphology of piglets.

| Items | Control | PEDV | PEDV + PR |
|---|---|---|---|
| **Villus height (μm)** | | | |
| Jejunum | 309.63 ± 72.97$^{b}$ | 112.45 ± 17.07$^{a}$ | 114.13 ± 16.16$^{a}$ |
| Ileum | 251.27 ± 53.59$^{b}$ | 144.27 ± 24.78$^{a}$ | 116.04 ± 13.55$^{a}$ |
| **Crypt depth (μm)** | | | |
| Jejunum | 133.35 ± 14.08$^{a}$ | 172.04 ± 26.78$^{b}$ | 161.41 ± 21.94$^{b}$ |
| Ileum | 132.78 ± 14.82$^{a}$ | 161.16 ± 21.45$^{b}$ | 159.92 ± 29.25$^{b}$ |
| **Villus height/crypt depth** | | | |
| Jejunum | 2.37 ± 0.81$^{b}$ | 0.68 ± 0.10$^{a}$ | 0.76 ± 0.13$^{a}$ |
| Ileum | 1.96 ± 0.55$^{b}$ | 0.94 ± 0.16$^{a}$ | 0.81 ± 0.13$^{a}$ |
| **Villus surface area (μm$^2$)** | | | |
| Jejunum | 7372.09 ± 1901.61$^{b}$ | 2735.40 ± 570.41$^{a}$ | 2734.74 ± 454.43$^{a}$ |
| Ileum | 6751.92 ± 1895.39$^{b}$ | 3431.66 ± 695.99$^{a}$ | 2885.31 ± 173.09$^{a}$ |

*Values are mean and pooled SD, n = 8.*
*$^{a,b}$Values within a row not sharing a common superscript letter are different (P < 0.05).*

## Effects of PR on PEDV-Induced Cytokine Expression *in vivo*

As shown in **Figure 4A**, the mRNA expression levels of *IFN-α* and *IFN-β* were increased in the ileum of PEDV-infected piglets compared with the Control group. However, PR administration reduced ($P < 0.05$) the expression of *IFN-α* and *IFN-β* in PEDV-infected piglets. Similar patterns were also observed for the protein levels of IL-1β, IL-6, and IL-8 (**Figure 4B**).

## Identification and Comparison of DRPs

A total of 2,590, 2,574, and 2,642 proteins were identified and quantified in the control, PEDV, and PEDV + PR groups, respectively. Compared to the non-infected Control group, 52 proteins were upregulated and 112 proteins were downregulated in the PEDV group (FC > 1.5 or <0.67, $P < 0.05$). A total of 34 proteins were upregulated and 53 proteins were downregulated (FC > 1.5 or <0.67, $P < 0.05$) in the PEDV + PR group in comparison with the PEDV group. In addition, among these DRPs, 29 proteins were restored after PR intervention, including 13 downregulated and 16 upregulated proteins (**Figure 5**; **Table S1**).

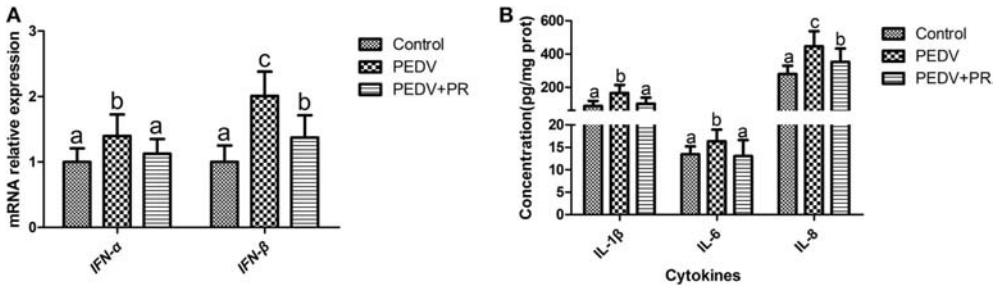


**FIGURE 4 |** Effects of puerarin on the expression of PEDV-induced cytokines in the ileum of piglets. **(A)** mRNA expression levels of *IFN-α and IFN-β* detected by qPCR in the ileum of piglets. **(B)** Protein expression levels of IL-1β, IL-6, and IL-8 detected by ELISA in the ileum of piglets. Values are mean and pooled SD, $n = 8$. $^{a,b,c}$Values with different letters for the same cytokine differ ($P < 0.05$).

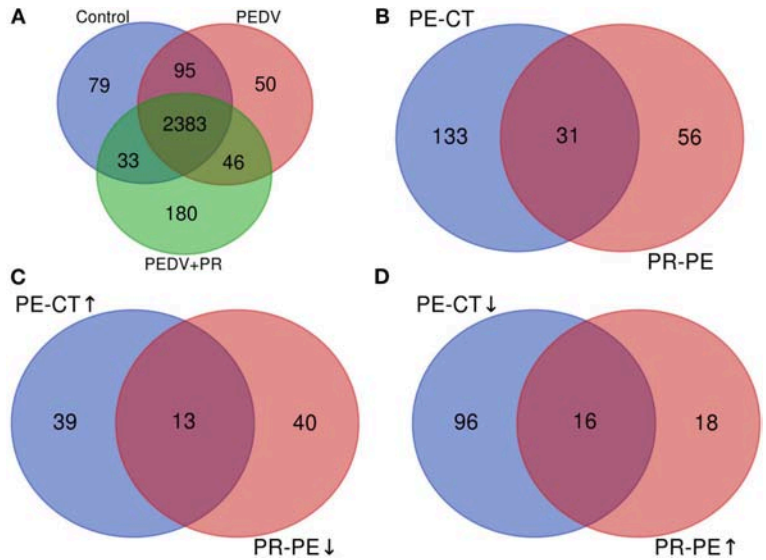


**FIGURE 5 |** Overview of the upregulated and downregulated proteins identified in the small intestine of PEDV-infected piglets. **(A)** The Venn diagram shows the total numbers of identified and quantified proteins. **(B)** The total numbers of differentially regulated proteins (DRPs) in the PE-CT and PR-PE groups. **(C)** The overlapped numbers of both upregulated proteins in the PE-CT groups and downregulated proteins in the PR-PE groups. **(D)** The overlapped numbers of both downregulated proteins in the PE-CT groups and upregulated proteins in the PR-PE groups. PE-CT, the PEDV group vs. the Control group; PR-PE, the PEDV + PR group vs. the PEDV group. $n = 4$; ↑, upregulated; ↓, downregulated.

## Bioinformatics Analysis of DRPs

In the present work, heat-maps were generated on all filtered proteins, and differences in protein expression were observed when the PEDV group was compared to the Control group or the PEDV + PR group (**Figures 6A,B**). Similar patterns of protein expression were found for the Control group and the PEDV + PR group (**Figure 6C**). To further identify the functional characterization, DRPs were analyzed on the basis of GO categories: cellular component (CCs), molecular function (MFs), and biological process (BPs) (40, 41). As shown in **Figure 7** and **Table S2**, BP analysis (FDR < 0.05) revealed that the DRPs associated with metabolic processes were enriched between the PEDV and Control groups. However, after PR intervention, the terms representing virus-related responses were most significant compared to the PEDV group. Meanwhile, the reactome pathway analysis identified that these DRPs were mainly involved in interferon signaling (**Figure 8**; **Table S3**). The protein–protein interaction networks also revealed that proteins related to interferon signaling interacted closely to fulfill their biological functions (**Figure 9**; **Table S4**).

## Validation of the Proteomic Analysis

To validate the results of the proteomic analyses, four proteins (STAT1, ISG15, MX1, DDX58) were analyzed using the Western blot technique. In accordance with the proteomic data, the expression of ISG15, MX1, and DDX58 was increased, but the expression of STAT1 was decreased post PEDV infection. PR intervention decreased ($P < 0.05$) the expression of ISG15, MX1, and DDX58, while it increased the expression of STAT1, compared to that of the PEDV group (**Figure 10A**). Owing to

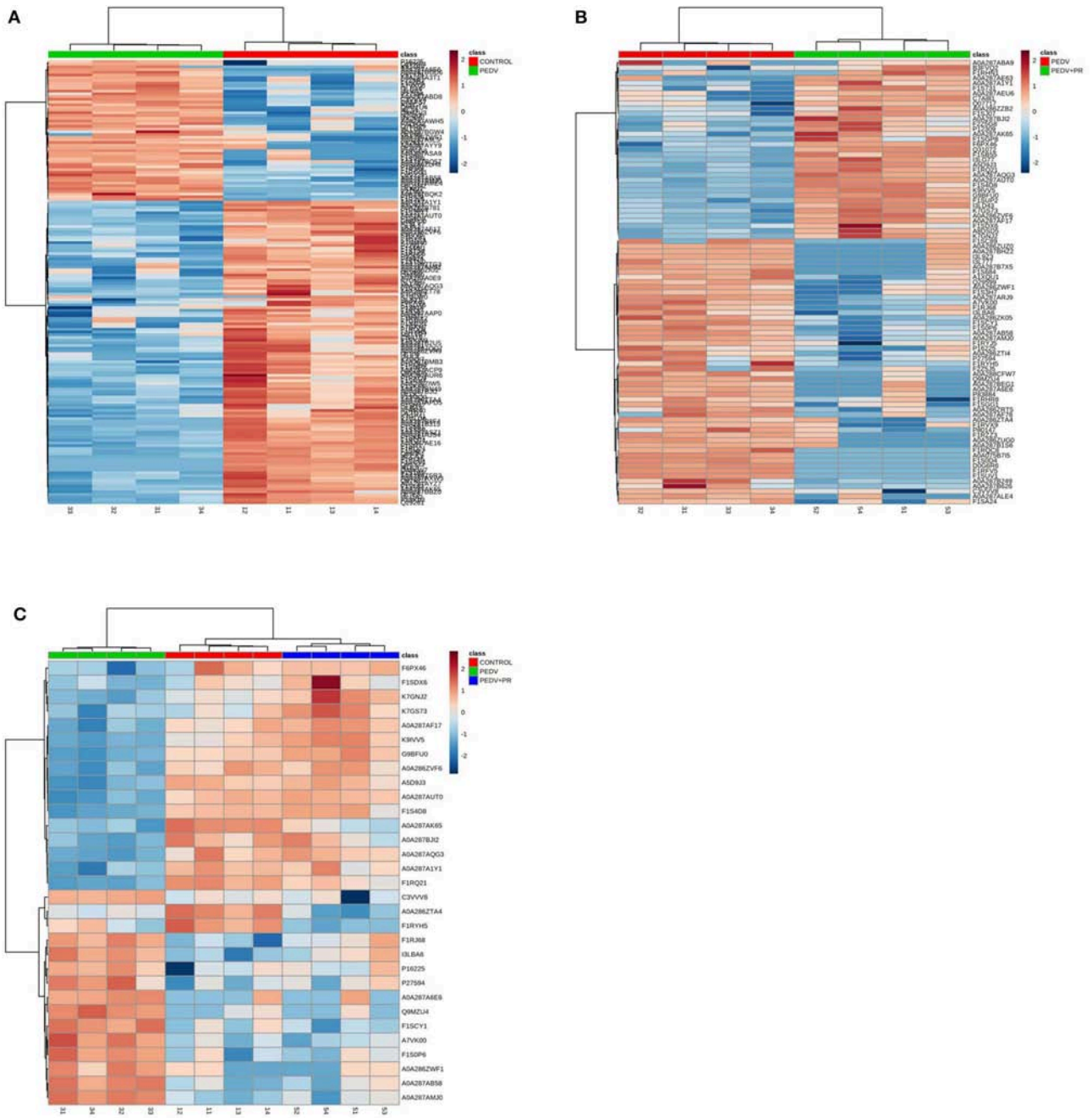


**FIGURE 6 |** Heat-maps of differentially regulated proteins (DRPs). **(A)** The PEDV group vs. the Control group. **(B)** The PEDV + PR group vs. the PEDV group. **(C)** DRPs among three groups. $n = 4$.

the lack of the appropriate antibodies for porcine tissues, qRT-PCR was alternatively used to validate the expression of *IFIT3*, *OAS1*, and *GBP2*. Likewise, a consistent trend of gene expression was observed among these groups of piglets (**Figure 10B**). The fold changes in the protein abundances among the three different groups of piglets, assessed by the LC-MS/MS analysis, are shown in **Figure 10**. These results indicated that the proteomics data are highly reliable.

## Regulation of Intestinal NF-κB Activation by PR in PEDV-Infected Piglets

NF-κB is a key transcriptional factor in cytokine production, which may facilitate PEDV pathogenesis (42, 43). As shown in **Figure 11**, PEDV infection increased ($P < 0.05$) the expression of NF-κB and pNF-κB, while both NF-κB, and pNF-κB expressions were almost fully restored to the control levels by PR

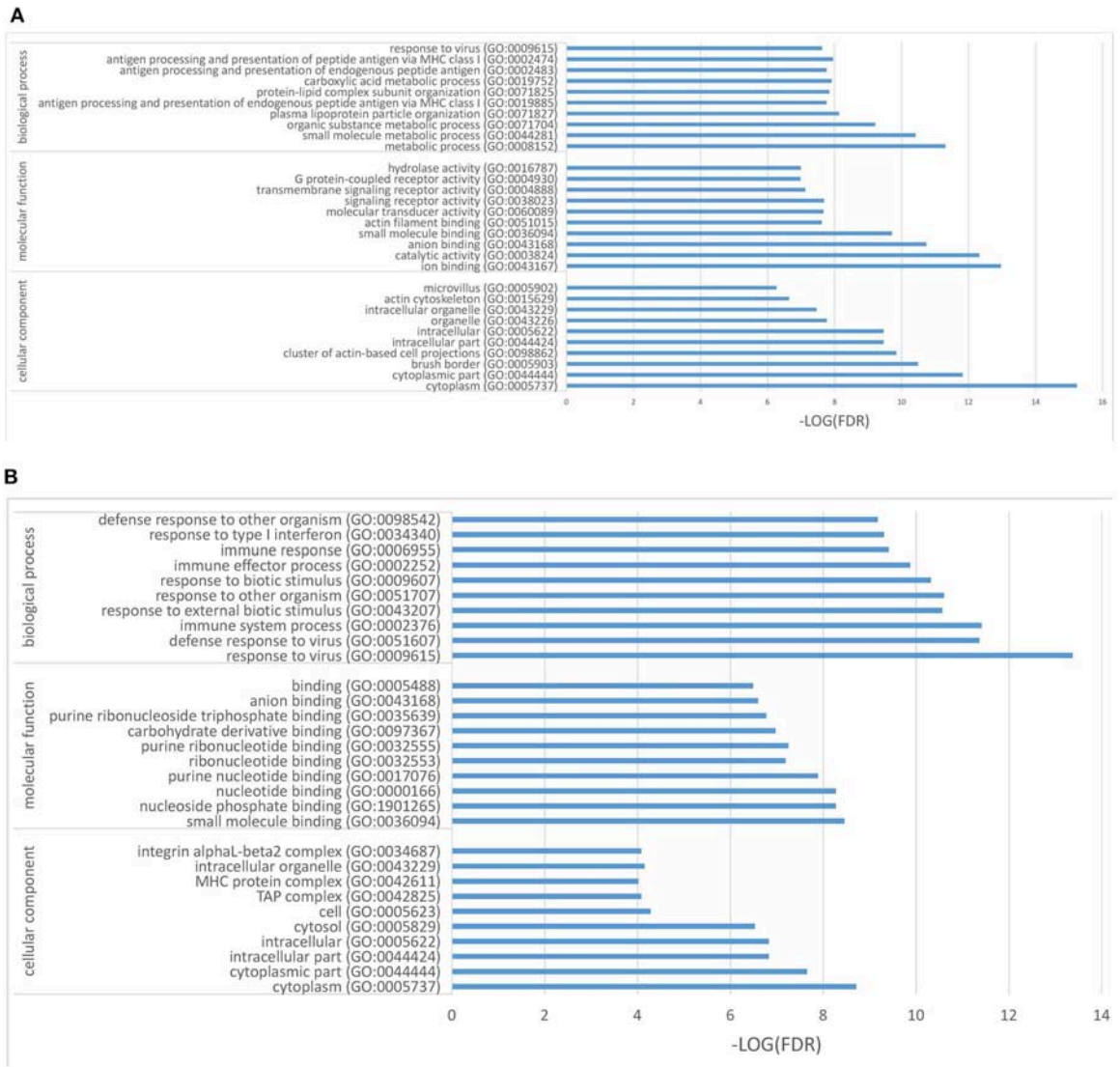


**FIGURE 7 |** Differentially regulated proteins (DRPs) were categorized into cellular component (CCs), molecular function (MFs), and biological process (BPs) based on the GO analysis. **(A)** The PEDV group vs. the Control group. **(B)** The PEDV + PR group vs. the PEDV group. $n = 4$.

administration, indicating that PR could inhibit PEDV-induced NF-κB activation *in vivo*.

## DISCUSSION

PEDV is the major etiological agent for the recent outbreaks of piglet diarrhea that has caused devastating economic losses to the swine industry worldwide. Traditional vaccine strategy cannot either provide a full protection for piglets or ensure a satisfying control of PEDV infection and spreading. Therefore, the development of safe, effective, and inexpensive antiviral drugs remains a great challenge to modern medicine. PR is a natural isoflavonoid extracted from Gegen in the traditional Chinese herb medicine. As a potential antiviral drug, effects of PR on PEDV infection are unknown. To date, although the proteomic technique has been widely applied to virus–host interaction studies, little information is available about the protein profiles of piglets infected with PEDV. In the current work, we determine the effect of PR on PEDV both *in vitro* and *in vivo* with the goal of elucidating the underlying mechanisms by a proteomic analysis.

PEDV can cause acute and watery diarrhea, vomiting, dehydration, and high mortality in neonatal piglets (43), and its adverse effect on growth performance of piglets was demonstrated by Curry et al. (44). Consistently, in the present study, PEDV infection resulted in a significant reduction in piglet ADG, but PR administration substantially alleviated the reduction of ADG, indicating that PR has a positive effect on the growth performance of PEDV-infected piglets. Although the reduction in diarrhea rate was not statistically significant due to the small sample size, the decreasing trend in diarrhea

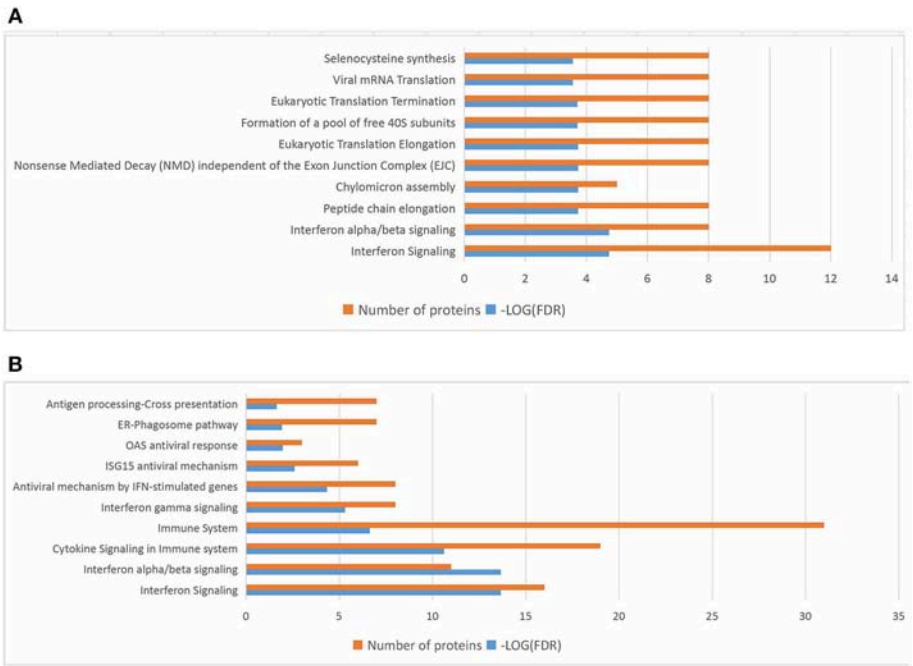


**FIGURE 8 |** Top 10 significant pathways in PEDV or PEDV + PR piglets based on the reactome pathway analysis of the differentially regulated proteins (DRPs). **(A)** The PEDV group vs. the Control group. **(B)** The PEDV + PR group vs. the PEDV group. $n = 4$.

rate and the weaker clinical symptoms indicated that the piglets in the PEDV + PR group were recovering better from illness. Similarly, dietary supplementation with soy isoflavone increased ADG and reduced the incidence of diarrhea in weaned piglets challenged with lipopolysaccharide (45). These results support the notion that isoflavonoid could be used to treat diarrhea (46). Our findings further demonstrated that PR could alleviate reduction in the growth performance of PEDV-infected piglets.

In the present study, the mRNA levels of genes that encoded for the *N* and *M* proteins of PEDV were decreased regardless of whether PR was administered after the entry of the virus into Vero cells *in vitro* or before PEDV infection in piglets. Similar results were found for the N and M protein levels, which were determined by the proteomic analysis (data not shown). These results indicated that PR could inhibit the replication of PEDV at different stages of its life cycle. Nevertheless, additional comprehensive studies are needed to verify this notion. In the current work, *in vitro* studies were performed with monkey cells and *in vivo* studies with piglets. Although they are different species, both of them are highly susceptible to PEDV, and PR could inhibit the replication of PEDV in both species. This suggests that PR was effective against PEDV *in vitro* and *in vivo*. Jejunal and ileal villus enterocytes are the main targets of PEDV replication (47), and PEDV also appears in feces and mesenteric lymph nodes (48). Consistently, we found that the piglet small intestine was the main target of PEDV. Intriguingly, the mRNA levels of *N* and *M* genes were extremely high in the ileum of piglets, even higher than those in the jejunum. Meanwhile, the mRNA levels of *N* and *M* genes were also high in colonic contents. Importantly, PR administration decreased the expression of the viral genes in the ileum, jejunal, colon, and mesenteric lymph nodes, indicating that PR plays an antiviral role in a large part of the gut. Previous studies showed that PR inhibited HIV-1 replication and human respiratory syncytial virus activities *in vitro* (20, 21). Some medicinal herbal extracts, such as oleanane triterpenes from the flowers of *Camellia japonica*, *Sophorae radix*, *Acanthopanacis cortex*, *Sanguisorbae radix*, and *Torilis fructus*, can inhibit PEDV replication (49, 50). To date, there is little information regarding an anti-PEDV effect of PR. To the best of our knowledge, this is the first study demonstrating that PR inhibited PEDV replication both *in vitro* and *in vivo*.

Inflammation and disease progression are initiated by pro-inflammatory cytokines and chemokines during viral infection (51). A previous study showed that the mRNA levels for pro-inflammatory cytokines (e.g., *IL-1β*, *IL-6*, *IL-8*, and *TNF-α*) were increased in Vero cells after PEDV infection (52). *MCP1/CCL2*, which is a chemokine, was also increased in response to PEDV infection (53). Likewise, we found that *IL-8*, *TNF-α*, and *MCP1* expressions were increased post PEDV infection in Vero cells and that the concentrations of IL-1β, IL-6, and IL-8 were increased in the ileum of PEDV-infected piglets, further substantiating the notion that PEDV could induce inflammatory response. Interestingly, inflammation appeared to be alleviated in the PEDV + PR group, as indicated by the decreased expression of the inflammatory cytokines. This result indicated that PR possessed an anti-inflammatory effect, which is

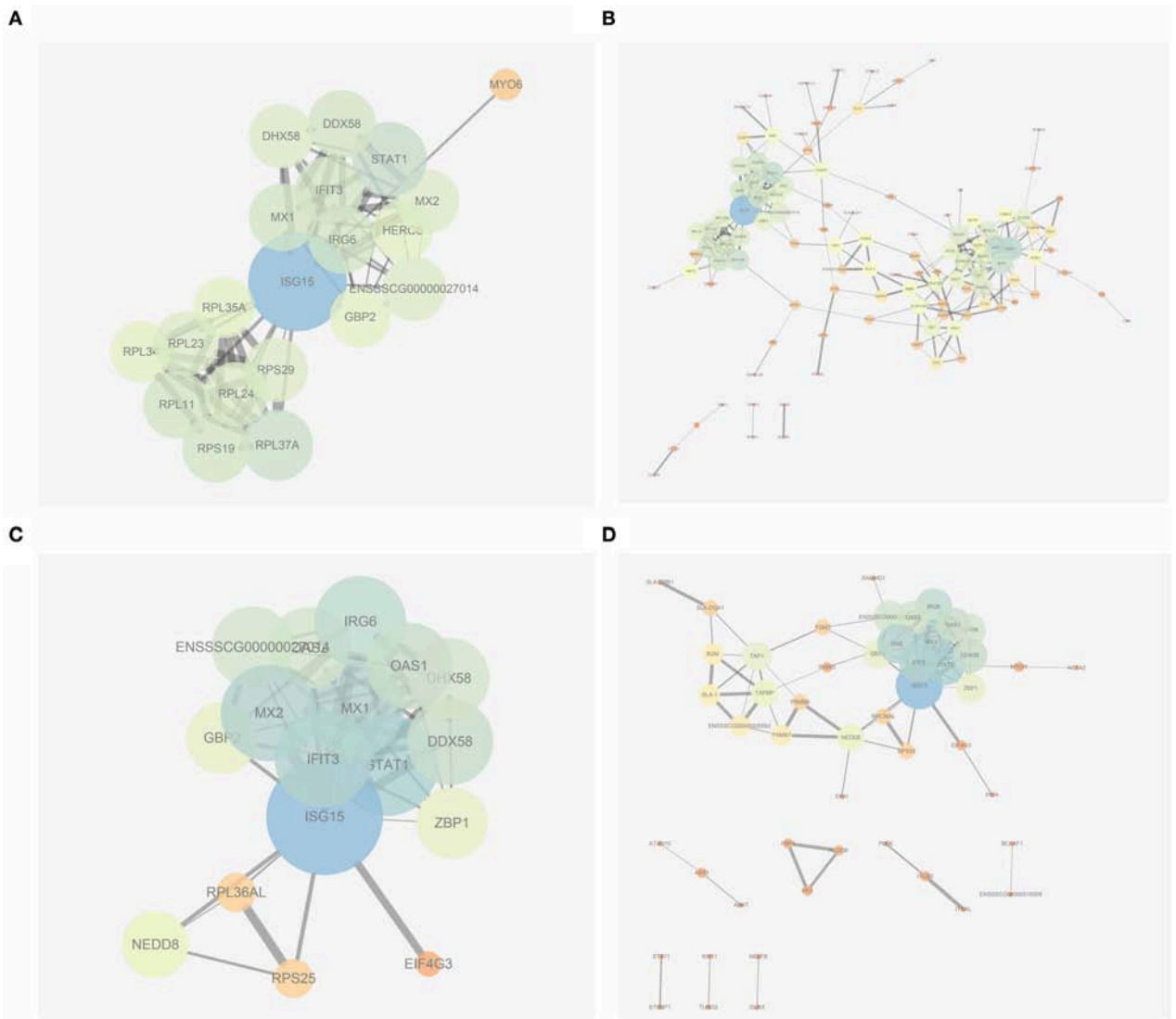


**FIGURE 9 |** Protein–protein interaction networks built by using the online software String and Cytoscape. **(A)** The most significant part of networks from the PEDV group vs. the Control group. **(B)** An overview of networks from the PEDV group vs. the Control group. **(C)** The most significant part of networks from the PEDV + PR group vs. the PEDV group. **(D)** An overview of networks from the PEDV + PR group vs. the PEDV group. $n = 4$.

consistent with the previous reports that the expression of genes for inflammatory mediators (e.g., *IL-1β*, *IL-6*, and *TNF-α*) were reduced by PR administration under inflammatory conditions (11, 54). Collectively, these findings support the view that PR can mitigate inflammation induced by PEDV infection *in vitro* and *in vivo*.

Cluster analyses are usually used to build groups of functionally related genes or proteins, thereby interpreting and identifying DRPs among different groups. In this study, nearly all of the overlapped DRPs (29/31) between the PEDV and Control groups or between the PEDV + PR and PEDV groups were reversely regulated by PR intervention, which could be clearly visualized by the heat-maps. Several functional enrichment analyses highlighted the importance of the interferon signaling pathway. Specifically, IFN-α/β and several ISGs were selectively upregulated at mRNA or protein levels in response to PEDV infection. This result is inconsistent with the previous report that PEDV antagonized interferon response (10, 55). Because almost all of the previous studies were conducted *in vitro*, the inconsistency may be attributed to the fact that results of *in vitro* experiments may not accurately reflect the situation *in vivo*. Moreover, an *in vivo* study performed by Annamalai et al. (56) demonstrated that serum IFN-α could be augmented at the early stage of PEDV infection. Of particular interest, PR administration appeared to regulate the interferon signaling pathway by maintaining the expression of IFN-α/β and ISGs at their normal physiological levels. It is noteworthy that

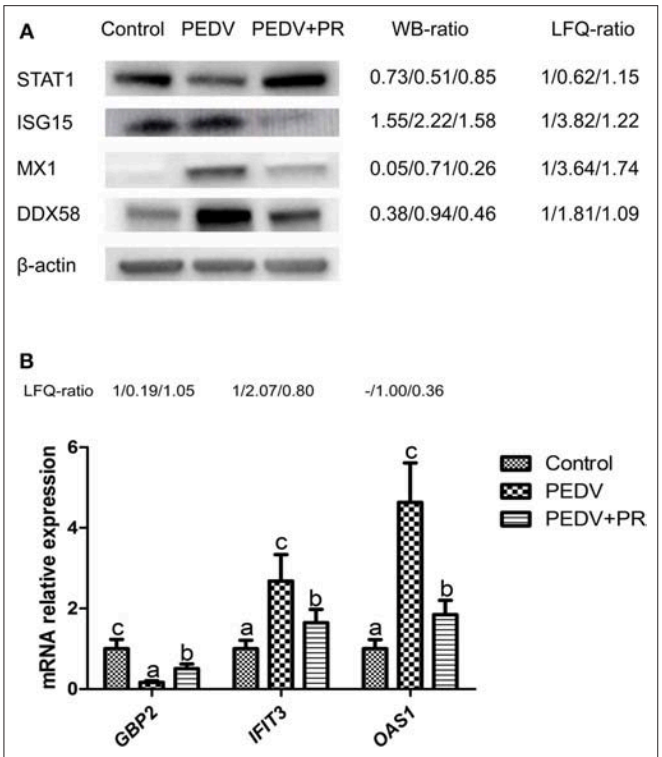


**FIGURE 10 |** Validation of differentially regulated proteins (DRPs) by Western blot and qRT-PCR analyses. **(A)** Western blot. **(B)** qRT-PCR. The WB ratio (Western blot ratio) was calculated based on the relative intensity. Beta-actin was used as the loading control. The LFQ ratios for PEDV/Control and PEDV + PR/Control obtained by MS analysis are shown on the right. Values are mean and SD, $n = 8$. $^{a,b,c}$Values with different letters for the same protein are different ($P < 0.05$). $n = 8$. -: This protein in the Control group was undetected in LFQ.

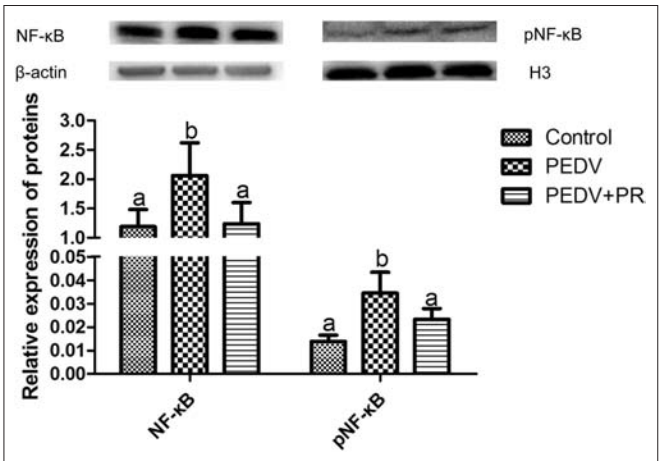


**FIGURE 11 |** Relative expression of NF-κB and pNF-κB in the ileum by the Western blot analysis. Values are mean and SD, $n = 8$. $^{a,b}$Values with different letters for the same protein are different ($P < 0.05$). $n = 8$.

GBP2, interferon-inducible guanylate-binding protein 2, was markedly upregulated in the PEDV + PR group. GBPs play an important role in antiviral infection (57). Further studies are warranted to determine whether PR exerts an antiviral effect by regulating GBP2 expression. Overall, these results indicated that PR regulated the interferon signaling pathway in PEDV-infected piglets.

The NF-κB pathway plays a central role in the regulation of immune responses. Such a function of NF-κB in PEDV infection is supported by several lines of evidence (32, 43, 58). Our results showed that PEDV induced NF-κB activation *in vivo* and that PR supplementation inhibited the NF-κB activation, which may contribute to the decrease in the expression of interferon-related genes and the production of cytokines. This is consistent with the previous findings that PR has an anti-inflammatory effect *in vitro* and *in vivo* (59, 60). Therefore, we suggest that PR is beneficial for restoring immune homeostasis after PEDV infection by inhibiting NF-κB activation.

## CONCLUSION

PR inhibited PEDV replication both *in vitro* and *in vivo* and alleviated the decrease of growth performance in piglets. Additionally, the quantitative proteomic analysis revealed that PR administration regulated the interferon signaling pathway in PEDV-infected piglets. Furthermore, PR attenuated NF-κB activation in the ileum. Taken together, these findings suggest that PR protected against PEDV infection via regulating the interferon and NF-κB signaling pathway. Our results are expected to aid in the development of effective antiviral feed additives and also have important implications for the production of veterinary drugs and human medicine.

## DATA AVAILABILITY STATEMENT

All datasets generated for this study are included in the article/**Supplementary Material**.

## ETHICS STATEMENT

The animal study was reviewed and approved by Animal Care and Use Committee at Wuhan Polytechnic University.

## AUTHOR CONTRIBUTIONS

MW, QZ, DY, YH, and GW were responsible for the study design, proteome, database search, data interpretation, drafting the paper, final approval, and agreement to be accountable. TW, HC, and SG were responsible for the study design, proteome, data interpretation, critical revision, final approval, and agreement to be accountable. SL, CJ, LW, and DZ were responsible of the animal experiments, data interpretation, critical revision, final approval, and agreement to be accountable.

## FUNDING

This work was supported by the National Key R&D Program (grant number 2016YFD0501210), the Program of National Agricultural Research Outstanding Talents of China (2015), Hubei Provincial Key R&D Program (2019ABA083), Texas A&M AgriLife Research (H-8200), and the Open Project of Hubei Key Laboratory of Animal Nutrition and Feed Science (grant number 201805).

## ACKNOWLEDGMENTS

We thank our students and technicians for their contributions to this research.

## SUPPLEMENTARY MATERIAL

The Supplementary Material for this article can be found online at: https://www.frontiersin.org/articles/10.3389/fimmu.2020.00169/full#supplementary-material

## REFERENCES

1. Song D, Park B. Porcine epidemic diarrhoea virus: a comprehensive review of molecular epidemiology, diagnosis, and vaccines. *Virus Genes.* (2012) 44:167–75. doi: 10.1007/s11262-012-0713-1
2. Bi J, Zeng S, Xiao S, Chen H, Fang L. Complete genome sequence of porcine epidemic diarrhea virus strain AJ1102 isolated from a suckling piglet with acute diarrhea in China. *J Virol.* (2012) 86:10910–1. doi: 10.1128/JVI.01919-12
3. Wang X, Niu B, Yan H, Gao D, Yang X, Chen L, et al. Genetic properties of endemic Chinese porcine epidemic diarrhea virus strains isolated since 2010. *Arch Virol.* (2013) 158:2487–94. doi: 10.1007/s00705-013-1767-7
4. Li Y, Wu Q, Huang L, Yuan C, Wang J, Yang Q. An alternative pathway of enteric PEDV dissemination from nasal cavity to intestinal mucosa in swine. *Nat Commun.* (2018) 9:3811. doi: 10.1038/s41467-018-06056-w
5. Choudhury B, Dastjerdi A, Doyle N, Frossard JP, Steinbach F. From the field to the lab-an European view on the global spread of PEDV. *Virus Res.* (2016) 226:40–9. doi: 10.1016/j.virusres.2016.09.003
6. Lee C. Porcine epidemic diarrhea virus: an emerging and re-emerging epizootic swine virus. *Virol J.* (2015) 12:193. doi: 10.1186/s12985-015-0421-2
7. Kim O, Chae C. In Situ hybridization for the detection and localization of porcine epidemic diarrhea virus in the intestinal tissues from naturally infected piglets. *Vet Pathol.* (2000) 37:62–7. doi: 10.1354/vp.37-1-62
8. Zhang Z, Chen J, Shi H, Chen X, Shi D, Feng L, et al. Identification of a conserved linear B-cell epitope in the M protein of porcine epidemic diarrhea virus. *Virol J.* (2012) 9:225. doi: 10.1186/1743-422X-9-225
9. Zhou M, Xu D, Li X, Li H, Shan M, Tang J, et al. Screening and identification of severe acute respiratory syndrome-associated coronavirus-specific CTL epitopes. *J Immunol.* (2014) 177:2138–45. doi: 10.4049/jimmunol.177.4.2138
10. Ding Z, Fang L, Jing H, Zeng S, Wang D, Liu L, et al. Porcine epidemic diarrhea virus nucleocapsid protein antagonizes beta interferon production by sequestering the interaction between IRF3 and TBK1. *J Virol.* (2014) 88:8936–45. doi: 10.1128/JVI.00700-14
11. Ullah MZ, Khan AU, Afridi R, Rasheed H, Khalid S, Naveed M, et al. Attenuation of inflammatory pain by puerarin in animal model of inflammation through inhibition of pro-inflammatory mediators. *Int Immunopharmacol.* (2018) 61:306–16. doi: 10.1016/j.intimp.2018.05.034
12. Wu L, Qiao H, Li Y, Li L. Protective roles of puerarin and danshensu on acute ischemic myocardial injury in rats. *Phytomedicine.* (2007) 14:652–8. doi: 10.1016/j.phymed.2007.07.060
13. Yao XJ, Yin JA, Xia YF, Wei ZF, Luo YB, Liu M, et al. Puerarin exerts antipyretic effect on lipopolysaccharide-induced fever in rats involving inhibition of pyrogen production from macrophages. *J Ethnopharmacol.* (2012) 141:322–30. doi: 10.1016/j.jep.2012.02.038
14. Yang X, Hu W, Zhang Q, Wang Y, Sun L. Puerarin inhibits c-reactive protein expression via suppression of nuclear factor κb activation in lipopolysaccharide-induced peripheral blood mononuclear cells of patients with stable angina pectoris. *Basic Clin Pharmacol Toxicol.* (2010) 107:637–42. doi: 10.1111/j.1742-7843.2010.00548.x
15. Xiao C, Li J, Dong X, He X, Niu X, Liu C, et al. Anti-oxidative and TNF-α suppressive activities of puerarin derivative (4AC) in RAW264.7 cells and collagen-induced arthritic rats. *Eur J Pharmacol.* (2011) 666:242–50. doi: 10.1016/j.ejphar.2011.05.061
16. Shin B, Park W. Zoonotic Diseases and phytochemical medicines for microbial infections in veterinary science: current state and future perspective. *Front Vet Sci.* (2018) 5:166. doi: 10.3389/fvets.2018.00166
17. Tang F, Li WH, Zhou X, Liu YH, Li Z, Tang YS, et al. Puerarin protects against staphylococcus aureus-induced injury of human alveolar epithelial A549 cells via downregulating alpha-hemolysin secretion. *Microb Drug Resist.* (2014) 20:357–63. doi: 10.1089/mdr.2013.0104
18. Liu X, Liu F, Ma Y, Li H, Ju X, Xu J. Effect of puerarin, baicalin and berberine hydrochloride on the regulation of IPEC-J2 cells infected with enterotoxigenic *Escherichia coli*. *Evid Based Complement Altern Med.* (2019) 2019:7438593. doi: 10.1155/2019/7438593
19. Romero MR, Efferth T, Serrano MA, Castaño B, MacIas RIR, Briz O, et al. Effect of artemisinin/artesunate as inhibitors of hepatitis B virus production in an "*in vitro*" replicative system. *Antiviral Res.* (2005) 68:75–83. doi: 10.1016/j.antiviral.2005.07.005
20. Mediouni S, Jablonski JA, Tsuda S, Richard A, Kessing C, Andrade MV, et al. Potent suppression of HIV-1 cell attachment by Kudzu root extract. *Retrovirology.* (2018) 15:64. doi: 10.1186/s12977-018-0446-x
21. Lin TJ, Yeh CF, Wang KC, Chiang LC, Tsai JJ, Chang JS. Water extract of pueraria lobata ohwi has anti-viral activity against human respiratory syncytial virus in human respiratory tract cell lines. *Kaohsiung J Med Sci.* (2013) 29:651–7. doi: 10.1016/j.kjms.2013.06.001
22. Jaleel A, Aneesh Kumar A, Ajith Kumar GS, Surendran A, Kartha CC. Label-free quantitative proteomics analysis reveals distinct molecular characteristics in endocardial endothelium. *Mol Cell Biochem.* (2019) 451:1–10. doi: 10.1007/s11010-018-3387-8
23. Wiener MC, Sachs JR, Deyanova EG, Yates NA. Differential mass spectrometry: a label-free LC-MS method for finding significant differences in complex peptide and protein mixtures. *Anal Chem.* (2004) 76:6085–96. doi: 10.1021/ac0493875
24. Lin H, Li B, Chen L, Ma Z, He K, Fan H. Differential protein analysis of IPEC-J2 cells infected with porcine epidemic diarrhea virus pandemic and classical strains elucidates the pathogenesis of infection. *J Proteome Res.* (2017) 16:2113–20. doi: 10.1021/acs.jproteome.6b00957
25. Sun D, Shi H, Guo D, Chen J, Shi D, Zhu Q, et al. Analysis of protein expression changes of the Vero E6 cells infected with classic PEDV strain CV777 by using quantitative proteomic technique. *J Virol Methods.* (2015) 218:27–39. doi: 10.1016/j.jviromet.2015.03.002
26. Megger DA, Pott LL, Ahrens M, Padden J, Bracht T, Kuhlmann K, et al. Comparison of label-free and label-based strategies for proteome analysis of hepatoma cell lines. *Biochim Biophys Acta.* (2014) 1844:967–76. doi: 10.1016/j.bbapap.2013.07.017
27. Wang L, Zhou J, Hou Y, Yi D, Ding B, Xie J, et al. N-Acetylcysteine supplementation alleviates intestinal injury in piglets infected by porcine epidemic diarrhea virus. *Amino Acids.* (2017) 49:1931–43. doi: 10.1007/s00726-017-2397-2
28. Hou Y, Wang L, Ding B, Liu Y, Zhu H, Liu J, et al. Dietary α-ketoglutarate supplementation ameliorates intestinal injury in lipopolysaccharide-challenged piglets. *Amino Acids.* (2010) 39:555–64. doi: 10.1007/s00726-010-0473-y
29. Song T, Wu T, Wei F, Li A, Wang F, Xie Y, et al. Construction of a cDNA library for miniature pig mandibular deciduous molars. *BMC Dev Biol.* (2014) 14:16. doi: 10.1186/1471-213X-14-16

30. Chey S, Claus C, Liebert UG. Validation and application of normalization factors for gene expression studies in rubella virus-infected cell lines with quantitative real-time PCR. *J Cell Biochem.* (2010) 110:118–28. doi: 10.1002/jcb.22518
31. Hindson BJ, Ness KD, Masquelier DA, Belgrader P, Heredia NJ, Makarewicz AJ, et al. High-throughput droplet digital PCR system for absolute quantitation of DNA copy number. *Anal Chem.* (2011) 83:8604–10. doi: 10.1021/ac202028g
32. Guo X, Zhang M, Zhang X, Tan X, Guo H, Zeng W, et al. Porcine epidemic diarrhea virus induces autophagy to benefit its replication. *Viruses.* (2017) 9:E53. doi: 10.3390/v9030053
33. Yi D, Hou Y, Wang L, Zhao D, Ding B, Wu T, et al. Gene expression profiles in the intestine of lipopolysaccharide-challenged piglets. *Front Biosci (Landmark Ed).* (2016) 21:487–01. doi: 10.2741/4404
34. Delgado-Ortega M, Melo S, Punyadarsaniya D, Ramé C, Olivier M, Soubieux D, et al. Innate immune response to a H3N2 subtype swine influenza virus in newborn porcine trachea cells, alveolar macrophages, and precision-cut lung slices. *Vet Res.* (2014) 45:42. doi: 10.1186/1297-9716-45-42
35. Fan B, Yu Z, Pang F, Xu X, Zhang B, Guo R, et al. Characterization of a pathogenic full-length cDNA clone of a virulent porcine epidemic diarrhea virus strain AH2012/12 in China. *Virology.* (2017) 500:50–61. doi: 10.1016/j.virol.2016.10.011
36. Tyanova S, Temu T, Sinitcyn P, Carlson A, Hein MY, Geiger T, et al. The perseus computational platform for comprehensive analysis of (prote)omics data. *Nat Methods.* (2016) 13:731–40. doi: 10.1038/nmeth.3901
37. Quackenbush J. Microarray data normalization and transformation. *Nat Genet.* (2002) 32:496–501. doi: 10.1038/ng1032
38. Deeb SJ, D'Souza RCJ, Cox J, Schmidt-Supprian M, Mann M. Super-SILAC allows classification of diffuse large B-cell lymphoma subtypes by their protein expression profiles. *Mol Cell Proteomics.* (2012) 11:77–89. doi: 10.1074/mcp.M111.015362
39. Hou Y, Wang L, Zhang W, Yang Z, Ding B, Zhu H, et al. Protective effects of N-acetylcysteine on intestinal functions of piglets challenged with lipopolysaccharide. *Amino Acids.* (2012) 43:1233–42. doi: 10.1007/s00726-011-1191-9
40. Thissen D, Steinberg L, Kuang D. Quick and easy implementation of the benjamini-hochberg procedure for controlling the false. *J Educ Behav Stat.* (2002) 27:77–83. doi: 10.3102/10769986027001077
41. Genovese CR, Lazar NA, Nichols T. Thresholding of statistical maps in functional neuroimaging using the false discovery rate. *Neuroimage.* (2002) 15:870–8. doi: 10.1006/nimg.2001.1037
42. Moynagh PN. The NF-κB pathway. *J Cell Sci.* (2005) 118:4589–92. doi: 10.1242/jcs.02579
43. Cao L, Ge X, Gao Y, Ren Y, Ren X, Li G. Porcine epidemic diarrhea virus infection induces NF-kB activation through the TLR2, TLR3 and TLR9 pathways in porcine intestinal epithelial cells. *J Gen Virol.* (2015) 96:1757–67. doi: 10.1099/vir.0.000133
44. Curry SM, Gibson KA, Burrough ER, Schwartz KJ, Yoon KJ, Gabler NK. Nursery pig growth performance and tissue accretion modulation due to porcine epidemic diarrhea virus or porcine deltacoronavirus challenge. *J Anim Sci.* (2017) 95:173–81. doi: 10.2527/jas.2016.1000
45. Zhu C, Wu Y, Jiang Z, Zheng C, Wang L, Yang X, et al. Dietary soy isoflavone attenuated growth performance and intestinal barrier functions in weaned piglets challenged with lipopolysaccharide. *Int Immunopharmacol.* (2015) 28:288–94. doi: 10.1016/j.intimp.2015.04.054
46. Wong KH, Li GQ, Li KM, Razmovski-Naumovski V, Chan K. Kudzu root: Traditional uses and potential medicinal benefits in diabetes and cardiovascular diseases. *J Ethnopharmacol.* (2011) 134:584–07. doi: 10.1016/j.jep.2011.02.001
47. Kim O, Choi C, Kim B, Chae C. Detection and differentiation of porcine epidemic diarrhoea virus and transmissible gastroenteritis virus in clinical samples by multiplex RT-PCR. *Vet Rec.* (2010) 146:637–40. doi: 10.1136/vr.146.22.637
48. Liu J, Li LM, Han JQ, Sun TR, Zhao X, Xu RT, et al. A TaqMan probe-based real-time PCR to differentiate porcine epidemic diarrhea virus virulent strains from attenuated vaccine strains. *Mol Cell Probes.* (2019) 45:37–42. doi: 10.1016/j.mcp.2019.04.003
49. Kim HY, Eo EY, Park H, Kim YC, Park S, Shin HJ, et al. Medicinal herbal extracts of sophorae radix, acanthopanacis cortex, sanguisorbae radix and torilis fructus inhibit coronavirus replication *in vitro*. *Antivir Ther.* (2010) 15:697–09. doi: 10.3851/IMP1615
50. Yang JL, Ha TKQ, Dhodary B, Pyo E, Nguyen NH, Cho H, et al. Oleanane triterpenes from the flowers of camellia japonica inhibit porcine epidemic diarrhea virus (PEDV) replication. *J Med Chem.* (2015) 58:1268–80. doi: 10.1021/jm501567f
51. Peterson KE, Robertson SJ, Portis JL, Chesebro B. Differences in cytokine and chemokine responses during neurological disease induced by polytropic murine retroviruses map to separate regions of the viral envelope gene. *J Virol.* (2001) 75:2848–56. doi: 10.1128/JVI.75.6.2848-2856.2001
52. Huan CC, Wang HX, Sheng XX, Wang R, Wang X, Mao X. Glycyrrhizin inhibits porcine epidemic diarrhea virus infection and attenuates the proinflammatory responses by inhibition of high mobility group box-1 protein. *Arch Virol.* (2017) 162:1467–76. doi: 10.1007/s00705-017-3259-7
53. Yu L, Dong J, Wang Y, Zhang P, Liu Y, Zhang L, et al. Porcine epidemic diarrhea virus nsp4 induces pro-inflammatory cytokine and chemokine expression inhibiting viral replication *in vitro*. *Arch Virol.* (2019) 164:1147–57. doi: 10.1007/s00705-019-04176-2
54. Deng HF, Wang S, Li L, Zhou Q, Guo WB, Wang XL, et al. Puerarin prevents vascular endothelial injury through suppression of NF-κB activation in LPS-challenged human umbilical vein endothelial cells. *Biomed Pharmacother.* (2018) 104:261–7. doi: 10.1016/j.biopha.2018.05.038
55. Guo L, Luo X, Li R, Xu Y, Zhang J, Ge J, et al. Porcine epidemic diarrhea virus infection inhibits interferon signaling by targeted degradation of STAT1. *J Virol.* (2016) 90:8281–92. doi: 10.1128/JVI.01091-16
56. Annamalai T, Saif LJ, Lu Z, Jung K. Age-dependent variation in innate immune responses to porcine epidemic diarrhea virus infection in suckling versus weaned pigs. *Vet Immunol Immunopathol.* (2015) 168:193–202. doi: 10.1016/j.vetimm.2015.09.006
57. Pan W, Zuo X, Feng T, Shi X, Dai J. Guanylate-binding protein 1 participates in cellular antiviral response to dengue virus. *Virol J.* (2012) 9:292. doi: 10.1186/1743-422X-9-292
58. Xu XG, Zhang H, Zhang Q, Dong J, Liang Y, Huang Y, et al. Porcine epidemic diarrhea virus E protein causes endoplasmic reticulum stress and up-regulates interleukin-8 expression. *Virol J.* (2013) 10:26. doi: 10.1186/1743-422X-10-26
59. Wang C, Wang W, Jin X, Shen J, Hu W, Jiang T. Puerarin attenuates inflammation and oxidation in mice with collagen antibody-induced arthritis via TLR4/NF-κB signaling. *Mol Med Rep.* (2016) 14:1365–70. doi: 10.3892/mmr.2016.5357
60. Lee JH, Jeon YD, Lee YM, Kim DK. The suppressive effect of puerarin on atopic dermatitis-like skin lesions through regulation of inflammatory mediators *in vitro* and *in vivo*. *Biochem Biophys Res Commun.* (2018) 498:707–14. doi: 10.1016/j.bbrc.2018.03.018


**Conflict of Interest:** The authors declare that the research was conducted in the absence of any commercial or financial relationships that could be construed as a potential conflict of interest.

frontiers in Immunology

ORIGINAL RESEARCH
published: 08 April 2020
doi: 10.3389/fimmu.2020.00543

# Efficient Selection of New Immunobiotic Strains With Antiviral Effects in Local and Distal Mucosal Sites by Using Porcine Intestinal Epitheliocytes

*Leonardo Albarracin[1,2†], Valeria Garcia-Castillo[1,3†], Yuki Masumizu[2], Yuhki Indo[2], Md Aminul Islam[2], Yoshihito Suda[4], Apolinaria Garcia-Cancino[3], Hisashi Aso[5,6], Hideki Takahashi[7,8], Haruki Kitazawa[2,6]* and Julio Villena[1,2]**

[1] Laboratory of Immunobiotechnology, Reference Centre for Lactobacilli (CERELA-CONICET), Tucuman, Argentina, [2] Food and Feed Immunology Group, Laboratory of Animal Products Chemistry, Graduate School of Agricultural Science, Tohoku University, Sendai, Japan, [3] Laboratory of Bacterial Pathogenicity, Faculty of Biological Sciences, University of Concepción, Concepción, Chile, [4] Department of Food, Agriculture and Environment, Miyagi University, Sendai, Japan, [5] Cell Biology Laboratory, Graduate School of Agricultural Science, Tohoku University, Sendai, Japan, [6] Livestock Immunology Unit, International Education and Research Center for Food Agricultural Immunology (CFAI), Graduate School of Agricultural Science, Tohoku University, Sendai, Japan, [7] Laboratory of Plant Pathology, Graduate School of Agricultural Science, Tohoku University, Sendai, Japan, [8] Plant Immunology Unit, International Education and Research Centre for Food and Agricultural Immunology (CFAI), Graduate School of Agricultural Science, Tohoku University, Sendai, Japan

OPEN ACCESS

**Edited by:**
*Lijuan Yuan,*
*Virginia Tech, United States*

**Reviewed by:**
*Francisco José Pérez-Cano,*
*University of Barcelona, Spain*
*Lei Shi,*
*Georgia State University, United States*

***Correspondence:**
*Haruki Kitazawa*
*haruki.kitazawa.c7@tohoku.ac.jp*
*Julio Villena*
*jcvillena@cerela.org.ar*

*† These authors have contributed equally to this work*

**Specialty section:**
*This article was submitted to Nutritional Immunology, a section of the journal Frontiers in Immunology*

**Received:** *30 November 2019*
**Accepted:** *10 March 2020*
**Published:** *08 April 2020*

**Citation:**
*Albarracin L, Garcia-Castillo V, Masumizu Y, Indo Y, Islam MA, Suda Y, Garcia-Cancino A, Aso H, Takahashi H, Kitazawa H and Villena J (2020) Efficient Selection of New Immunobiotic Strains With Antiviral Effects in Local and Distal Mucosal Sites by Using Porcine Intestinal Epitheliocytes. Front. Immunol. 11:543. doi: 10.3389/fimmu.2020.00543*

Previously, we evaluated the effect of the immunobiotic strain *Lactobacillus rhamnosus* CRL1505 on the transcriptomic response of porcine intestinal epithelial (PIE) cells triggered by the challenge with the Toll-like receptor 3 (TLR-3) agonist poly(I:C) and successfully identified a group of genes that can be used as prospective biomarkers for the screening of new antiviral immunobiotics. In this work, several strains of lactobacilli were evaluated according to their ability to modulate the expression of *IFN*α, *IFN*β, *RIG1*, *TLR3*, *OAS1*, *RNASEL*, *MX2*, *A20*, *CXCL5, CCL4*, *IL-15*, *SELL*, *SELE*, *EPCAM*, *PTGS2*, *PTEGES*, and *PTGER4* in PIE cells after the stimulation with poly(I:C). Comparative analysis of transcripts variations revealed that one of the studied bacteria, *Lactobacillus plantarum* MPL16, clustered together with the CRL1505 strain, indicating a similar immunomodulatory potential. Two sets of *in vivo* experiments in Balb/c mice were performed to evaluate *L. plantarum* MPL16 immunomodulatory activities. Orally administered MPL16 prior intraperitoneal injection of poly(I:C) significantly reduced the levels of the proinflammatory mediators tumor necrosis factor α (TNF-α), interleukin 6 (IL-6), and IL-15 in the intestinal mucosa. In addition, orally administered *L. plantarum* MPL16 prior nasal stimulation with poly(I:C) or respiratory syncytial virus infection significantly decreased the levels of the biochemical markers of lung tissue damage. In addition, reduced levels of the proinflammatory mediators TNF-α, IL-6, and IL-8 were found in MPL16-treated mice. Improved levels of IFN-β and IFN-γ in the respiratory mucosa were observed in mice treated with *L. plantarum* MPL16 when compared to control mice. The immunological changes induced by *L. plantarum* MPL16 were not

different from those previously reported for the CRL1505 strain in *in vitro* and *in vivo* studies. The results of this work confirm that new immunobiotic strains with the ability of stimulating both local and distal antiviral immune responses can be efficiently selected by evaluating the expression of biomarkers in PIE cells.

**Keywords: porcine intestinal epithelial cells, TLR3, *Lactobacillus rhamnosus* CRL1505, *Lactobacillus plantarum* MPL16, antiviral response, respiratory immunity**

## INTRODUCTION

More than a third of child deaths worldwide are attributed to malnutrition and its profound impact on the immune system and the host resistance to infections. In this sense, pneumonia and diarrhea remain the leading causes of death of children. Together, these two infectious diseases account for 29% of all deaths of children younger than 5 years and result in the loss of 2 million young lives annually (1). In 2009, the World Health Organization (WHO) separately published two strategies for the control of pneumonia and diarrhea. Since these strategies were implemented globally, it has been recognized that pneumonia and diarrhea could be treated more effectively in a coordinated manner. Thus, WHO-UNICEF published in 2013 an Integrated Global Action Plan for the Prevention and Control of Pneumonia and Diarrhea (GAPPD), which proposes a cohesive approach to ending deaths from preventable pneumonia and diarrhea in children (1). The GAPPD proposes interventions to create healthy environments, promotes practices to protect children from infectious diseases, and ensures that all children have access to appropriate preventive and treatment measures. The document emphasizes the importance of healthy nutrition to reduce the incidence and severity of pneumonia and diarrhea simultaneously.

Various clinical trials and studies in animal models have demonstrated the ability of probiotic lactic acid bacteria (LAB) with immunomodulatory activities, also known as immunobiotics, to improve the resistance to intestinal viral infections (2, 3). Although most of the research related to the beneficial effect of immunobiotics on the host's immune system has focused on the stimulation of intestinal immunity to protect against viral infections (4), it has also been shown that the oral administration of some immunobiotics strains can beneficially modulate not only the local intestinal immunity but also immune responses in distant mucosal sites such as the respiratory tract (5, 6). Then, it is believed that appropriate immunobiotic LAB strains can be effectively used as preventive therapies to improve antiviral defenses and reduce the complications from the deregulated inflammatory responses in both the intestine and the respiratory tract. Therefore, the efficient selection of immunobiotic strains that orally administered are capable of favorably modulating intestinal and respiratory antiviral immunity could contribute to reducing the risk of viral infections, having a simultaneous impact on resistance to pneumonia and diarrhea.

*Lactobacillus rhamnosus* CRL1505, orally administered to mice, is able to differentially modulate both intestinal (7, 8) and respiratory (9, 10) antiviral immunity. Moreover, in a randomized controlled trial conducted in children younger than 5 years, it was demonstrated that the immunobiotic CRL1505 strain is capable to enhance mucosal immunity and reduced the incidence and severity of intestinal and respiratory infections (2). Of note, our studies in mice models have clearly shown that the immunomodulatory capacities of *L. rhamnosus* CRL1505 are a strain-specific property because other immunobiotic strains such as *Lactobacillus plantarum* CRL1506 can stimulate only the intestinal immunity after their oral administration (7–10).

It is well known that intestinal epithelial cells (IECs) had a central role in determining the type of immune response triggered by antigens in the intestinal mucosa through their interactions with immune cells (11, 12). In this regard, studies have reported that immunomodulatory LAB modulate intestinal immune responses by regulating the functions of IECs (13). Therefore, we hypothesized that transcriptomic analysis evaluating the effect of *L. rhamnosus* CRL1505 and *L. plantarum* CRL1506 on IECs could bring valuable information about their capacity of modulating the intestinal innate antiviral immune response, as well as provide some clues about their differential ability to influence immunity in the respiratory tract. By using porcine intestinal epithelial (PIE) cells that express the pattern recognition receptor (PRR) Toll-like receptor 3 (TLR-3) and respond to poly(I:C) stimulation (14, 15); we studied the similarities and differences of *L. rhamnosus* CRL1505 and *L. plantarum* CRL1506 in terms of their ability to modulate the immunotranscriptomic response of epithelial cells (16). The transcriptional profiling performed in PIE cells allowed us to characterize the immune and immune-related genes involved in their response to TLR3 activation, which included type I interferons (IFNs), antiviral factors, cytokines, chemokines, adhesion molecules, enzymes involved in prostaglandin biosynthesis, PRRs, and negative regulators of the TLR signaling pathway. In addition, we were able to confirm that the CRL1505 and CRL1506 strains differently regulated the immunotranscriptomic response of poly(I:C)-challenged PIE cells (16). Quantitative and qualitative differences in the expression of immune and immune-related genes in PIE cells were found when *L. rhamnosus* CRL1505 and *L. plantarum* CRL1506 treatments were compared. Moreover, the comparative analysis of the effect of the two strains allowed us to identify a group of genes that could be used as potential biomarkers for the efficient selection of new antiviral immunobiotics in PIE cells, which could beneficially influence both the intestinal and the respiratory antiviral immunity.

In this work, we tested this hypothesis by evaluating the influence of several immunomodulatory and non-immunomodulatory lactobacilli strains in the expression of

*IFNα*, *IFNβ*, *RIG1*, *TLR3*, *OAS1*, *RNASEL*, *MX2*, *A20*, *CXCL5*, *CCL4*, *IL-15*, *SELL*, *SELE*, *EPCAM*, *PTGS2*, *PTEGES*, and *PTGER4* in poly(I:C)-challenged PIE cells and by studying *in vivo* the effect of orally administered lactobacilli on the intestinal and respiratory antiviral innate immune responses.

# MATERIALS AND METHODS

## PIE Cells

The PIE cell line was originally derived from intestinal epithelia isolated from an unsuckled neonatal swine (17). Porcine intestinal epithelial cells are intestinal non-transformed cultured cells that assume a monolayer with a cobblestone and epithelial-like morphology and with close contact between cells during culture (14, 17, 18). Porcine intestinal epithelial cells were maintained in Dulbecco modified eagle medium (DMEM) (Invitrogen Corporation, Carlsbad, CA, United States) supplemented with 10% fetal calf serum, 100 mg/mL streptomycin and 100 U/mL penicillin at 37°C in an atmosphere of 5% $CO_2$ (16, 18–20).

## Microorganisms

*Lactobacillus rhamnosus* CRL1505, *L. plantarum* CRL1506, *L. rhamnosus* CRL576, and *L. plantarum* CRL681 belong to CERELA Culture Collection; *L. rhamnosus* IBL07 belongs to the Infection Biology Laboratory of IMMCA-CONICET-UNT and was kindly given by Dr. Vizoso-Pinto. *Lactobacillus plantarum* MPL16 belongs to the Food and Feed Immunology Group Culture Collection, These strains were grown in Man–Rogosa–Sharpe broth at 37°C. For the *in vitro* immunomodulatory assays, overnight cultures were harvested by centrifugation, washed three times with sterile phosphate-buffered saline (PBS), counted in a Petroff–Hausser counting chamber, and resuspended in DMEM until use.

## Immunomodulatory Effect of Lactobacilli in PIE Cells

The study of the immunomodulatory capacity of lactobacilli was performed in PIE cells as described previously (15, 16, 18, 20). Porcine intestinal epithelial cells were seeded at $3 \times 10^4$ cells per well in 12-well type I collagen-coated plates (Sumitomo Bakelite Co., Tokyo, Japan) and cultured for 3 days. After changing medium, lactobacilli ($5 \times 10^8$ cells/mL) were added, and 48 h later, each well was washed vigorously with medium at least three times to eliminate all stimulants. Then cells were stimulated with poly(I:C) (60 μg/mL) for 12 h for reverse transcription–polymerase chain reaction (RT-PCR) studies.

## Quantitative Expression Analysis by Two-Step Real-Time Quantitative PCR

Two-step real-time quantitative PCR (qPCR) was performed to characterize the expression of selected genes in PIE cells as described previously (16). TRIzol reagent (Invitrogen) was used for total RNA isolation from each PIE cell sample, and Quantitect RT kit (Qiagen, Tokyo, Japan) was used for the synthesis of all cDNAs according to the manufacturer's recommendations. Real-time qPCR was carried out using a 7300 real-time PCR system (Applied Biosystems, Warrington, United Kingdom) and the Platinum SYBR green qPCR SuperMix uracil-DNA glycosylase with 6-carboxyl-X-rhodamine (ROX) (Invitrogen). The primers used for the study of *IFNα*, *IFNβ*, *RIG1*, *TLR3*, *OAS1*, *RNASEL*, *MX2*, *A20*, *CXCL5*, *CCL4*, *IL-15*, *SELL*, *SELE*, *EPCAM*, *PTGS2*, *PLA2G4A*, *PTEGES*, and *PTGER4* expressions in this study were described before (16, 20, 21). The PCR cycling conditions were 2 min at 50°C, followed by 2 min at 95°C, and then 40 cycles of 15 s at 95°C, 30 s at 60°C, and 30 s at 72°C. The reaction mixtures contained 5 μL of sample cDNA and 15 μL of master mix, which included the sense and antisense primers. According to the minimum information for publication of quantitative real-time PCR experiments guidelines, β-actin was used as a housekeeping gene because of its high stability across porcine various tissues (14, 15, 21). Expression of β-actin was used to normalize cDNA levels for differences in total cDNA levels in the samples.

## Animals, Feeding Procedures, and Poly(I:C) Challenge

Male 6-week-old BALB/c mice were obtained from the closed colony kept at CERELA-CONICET. Animals were housed in plastic cages in a controlled atmosphere (22°C ± 2°C temperature, 55% ±2% humidity) with a 12-h light/dark cycle. Lactobacilli were orally administered to different groups of mice for five consecutive days at a dose of $10^8$ cells/mouse per day in the drinking water (22, 23). The treated groups and the untreated control mice were fed a conventional balanced diet *ad libitum*.

Two sets of experiments were performed in treated and control mice. In the first set of experiments, mice were challenged by the intraperitoneal route with 100 μL of PBS containing 30 μg poly(I:C) according to our previous publication (8). Biochemical markers of injury as well as intestinal cytokines' concentrations were evaluated 2 days after poly(I:C) administration as described below. In the second set of experiments, mice were lightly anesthetized, and 100 μL of PBS, containing 250 μg poly(I:C) (equivalent to 10 mg/kg body weight), was administered via the nares according to our previous publication (7). Mice received three doses of poly(I:C) with 24-h rest period between each administration.

## Respiratory Syncytial Virus Infection

Infection with human respiratory syncytial virus (RSV) strain A2 was performed as described previously (9). Briefly, RSV was grown in Vero cells for 3 h at 37°C, 5% $CO_2$ at multiplicity of infection of 1 in 5 mL of DMEM. After cell lysis, virus supernatant was sucrose density gradient purified and stored in 30% sucrose at −80°C. For infection, mice were lightly anesthetized with isoflurane and intranasally challenged with $3.1 \times 10^6$ plaque forming units (PFU) of RSV (9).

For the evaluation of viral infection, the RSV immunoplaque assay was performed (9). In brief, lung tissue was removed from mice, homogenized using a pellet pestle, and centrifuged at 2,600 × *g* for 10 min at 4°C to clarify supernatant. Serial dilutions of lung tissue–clarified supernatants were added into fresh Vero

cells monolayers and incubated at 37°C, 5% $CO_2$ for 3 h. All samples were run in triplicate. After incubation and removal of supernatant, 1 mL of fresh DMEM medium containing 10% fetal bovine serum, 0.1% penicillin-streptomycin, and 0.001% ciprofloxacin was added to monolayers. When extensive syncytia developed, monolayers were fixed with 1 mL of ice-cold acetone:methanol (60:40). Then, wells were treated with primary RSV anti-F (clones 131-2A; Chemicon, Temecula, CA, United States) and anti-G{mouse monoclonal [8C5 (9B6)] to RSV glycoprotein; Abcam} antibodies for 2 h, followed by secondary horseradish peroxidase anti–mouse immunoglobulin antibody (anti–mouse immunoglobulin G, horseradish peroxidase–linked antibody #7076; Cell Signaling Technology, Danvers, MA, United States) for 1 h. Plates washed twice with PBS containing 0.5% Tween 20 (Sigma, St. Louis, MO, United States) after each antibody incubation step. Individual plaques were developed using a DAB substrate kit (ab64238; Abcam, Cambridge, United Kingdom) following the manufacturer's specifications. Results were expressed as log10 PFU/g of lung.

## Ethics Statement

Animals were housed in plastic cages and environmental conditions were kept constant, in agreement with the standards for animal housing. Animal welfare was in charge of researchers and special staff trained in animal care and handling at CERELA. The minimal number of animals required for an appropriate statistical analysis was calculated with the help of the Biostatistics Laboratory of CERELA.

Animals were housed individually during the experiments. All efforts were made to minimize the number of animals and their suffering. Animal health and behavior were monitored twice a day. Animals were euthanized immediately after the time point was reached by using xylazine and ketamine. No signs of discomfort or pain and no deaths were observed before mice reached the endpoints.

All experiments were carried out in compliance with the Guide for Care and Use of Laboratory Animals and approved by the Ethical Committee of Animal Care at CERELA, Argentina (protocol no. BIOT-CRL/14 and BIOT-CRL/11) (7, 8).

## Markers of Injury

Lactate dehydrogenase (LDH) and aspartate aminotransferase (AST) activities were determined in the serum to evaluate general toxicity of poly(I:C) in mice challenged by the intraperitoneal injection. Blood samples were obtained through cardiac puncture under anesthesia. LDH and AST activities, expressed as units per liter of serum, were determined by measuring the formation of the reduced form of nicotinamide adenine dinucleotide using the Wiener reagents and procedures (Wiener Lab, Buenos Aires, Argentina) (8).

Albumin content, a measure to quantitate increased permeability of the bronchoalveolar–capillarity barrier, and LDH activity, an indicator of general cytotoxicity, were determined in bronchoalveolar lavage (BAL) fluid. Bronchoalveolar lavage samples were obtained as described previously (7, 15). Briefly, the trachea was exposed and intubated with a catheter, and two sequential lavages were performed by injecting sterile PBS in each mouse lung. The recovered fluid was centrifuged for 10 min at 900 × *g*; the pellet was discarded, and the fluid was frozen at −70°C for subsequent analyses. Albumin content was determined colorimetrically based on albumin binding to bromocresol green using an albumin diagnostic kit (Wiener Lab). Lactate dehydrogenase activity, expressed as units per liter of BAL fluid, was determined by using the Wiener reagents and procedures (Wiener Lab) (7).

Lung wet-to-dry weight ratio was measured as previously described (7, 9). Wet-to-dry weight ratio was calculated as an index of intrapulmonary fluid accumulation, without correction for blood content.

## Cytokine Concentrations

Serum and BAL samples were obtained as described before (9). Briefly, blood samples were obtained by cardiac puncture under anesthesia. For BAL samples, the trachea was exposed surgically and intubated with a catheter. A small incision was made in the trachea, and two sequential lavages were performed in each mouse by injecting sterile PBS with 1% heparin. The recovered fluid was centrifuged for 10 min at 300 revolutions/min, and the supernatant was recovered. Intestinal fluid samples were obtained according to our previous publication (8). Briefly, the small intestine was flushed with 5 mL of PBS, and the fluid was centrifuged (10,000 × *g*, 4°C 10 min) to separate particulate material. The serum, BAL and intestinal supernatant samples were kept frozen at −80°C until use.

Tumor necrosis factor α (TNF-α), interleukin 6 (IL-6), IL-10, IL-15, IFN-β, and IFN-γ concentrations in serum, intestinal fluid, and BAL samples were measured with commercially available enzyme-linked immunosorbent assay technique kits following the manufacturer's recommendations (R&D Systems, Minneapolis, MN, United States).

## Statistical Analysis

Statistical analyses were performed using GLM and REG procedures available in the SAS computer program (SAS, 1994). Comparisons between mean values were carried out using one-way analysis of variance and Fisher least significant difference test. For these analyses, $P < 0.05$ and $P < 0.01$ were considered significant.

# RESULTS

## Modulation of TLR3-Induced Immunotranscriptome Changes in PIE Cells by Lactobacilli

Previously, we analyzed the effect of *L. rhamnosus* CRL1505 and *L. plantarum* CRL1506 on the innate immune response of PIE cells after the challenge with poly(I:C) by using a transcriptomic approach (16). From that study, we were able to select a set of potential biomarkers that would allow us to efficiently select new immunobiotic strains with antiviral capabilities including *IFNα*, *IFNβ*, *RIG1*, *TLR3*, *OAS1*, *RNASEL*, *MX2*, *A20*, *CXCL5*, *CCL4*, *IL-15*, *SELL*, *SELE*, *EPCAM*, *PTGS2*, *PLA2G4A*, *PTEGES*, and *PTGER4*. Then, in order to validate this assumption, PIE cells were stimulated with different lactobacilli including

immunomodulatory (*L. rhamnosus* CRL1505, *L. plantarum* CRL1506, *L. rhamnosus* IBL07, and *L. plantarum* MPL16) (8, 16, 24, 25) and non-immunomodulatory (*L. rhamnosus* CRL576 and *L. plantarum* CRL681) strains and then challenged with poly(I:C). The expression of the biomarkers was then evaluated. When the expressions of type I IFNs, antiviral factors, and the negative regulator A20 were analyzed, a strain-dependent effect was observed (**Figure 1**, **Supplementary Figure S1**). The CRL1505, CRL1506, and MPL16 strains were highly efficient for increasing *IFN*α, *MX2*, *OAS1*, and *TLR3* expression. In addition, *L. rhamnosus* CRL1505, and *L. plantarum* MPL16 were the lactobacilli with the highest capacity to increase the expression of *IFN*β and *RNASEL* (**Figure 1**). *Lactobacillus rhamnosus* IBL07 was capable of enhancing the mRNA levels of *IFN*α, *IFN*β, *OAS1*, *TLR3*, and *RNASEL*, but it was not as efficient as the CRL1505 and MPL16 strains. *RIG-1* was enhanced by all the immunomodulatory strains CRL1505, CRL1506, IBL027, and MPL16, whereas the non-immunomodulatory strains CRL681 and CRL576 were not able to induce changes in the expression of type I IFNs or antiviral factors (**Figure 1**, **Supplementary Figure S1**). *Lactobacillus rhamnosus* CRL1505, *L. plantarum* CRL1506, and *L. plantarum* MPL16 significantly reduced the expression of A20 in poly(I:C)-challenged PIE cells, whereas no effect was observed for the other studied strains (**Figure 1**).

The CRL1505 and MPL16 strains were highly efficient in enhancing the expression of *CCL4*, *CXCL5*, *EPCAM*, and *SELE* (**Figure 2**). The CRL1506 and IBL027 augmented the expression of *CCL4*, but the levels of this mRNA were significantly lower than in the CRL1505 or MPL16 groups (**Figure 2**). The four immunomodulatory strains increased *SELL* expression, being *L. plantarum* MPL16 the most efficient to achieve this effect. The non-immunomodulatory strains CRL681 and CRL576 were not able to induce changes in the expression of chemokines and adhesion molecules (**Figure 2**). *Lactobacillus rhamnosus* CRL1505, *L. plantarum* CRL1506, and *L. plantarum* MPL16 significantly reduced the expression of *IL-15* in poly(I:C)-challenged PIE cells, whereas no effect was observed for the other studied strains (**Figure 2**).

The expressions of *PTGS2*, *PLA2G4A*, and *PTEGES* were enhanced, and *PTGER4* was reduced by the four immunomodulatory strains (**Supplementary Figure S2**). However, *L. rhamnosus* CRL1505 and *L. plantarum* MPL16 were more efficient than *L. plantarum* CRL1506 and *L. rhamnosus* IBL027 to increase the expression of *PTGS2*, *PLA2G4A*, and *PTEGES* and reduce *PTGER4* in poly(I:C)-challenged PIE cells. The non-immunomodulatory strains CRL681 and CRL576 were not able to induce changes in the expression of the enzymes involved in prostaglandins biosynthesis (**Supplementary Figure S2**).

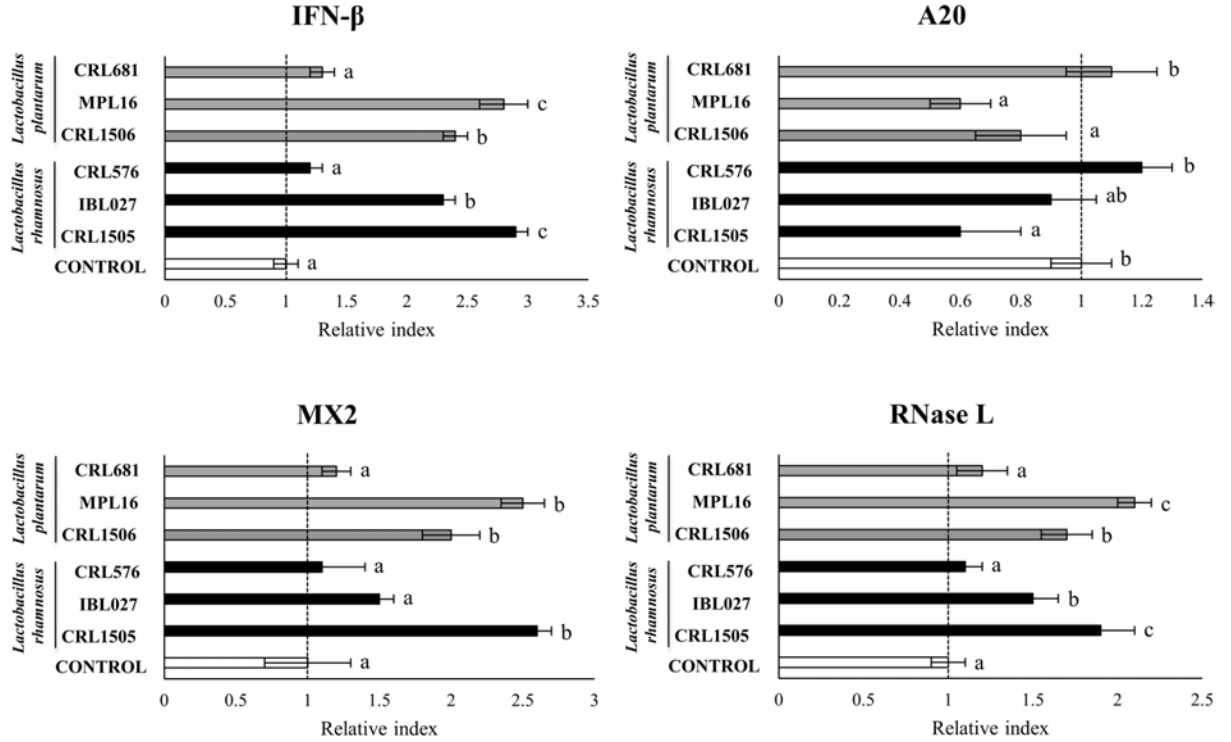


**FIGURE 1 |** Expression of interferon (*IFN*)-β, antiviral factors (*MX2* and *RNASEL*), and the negative regulator *A20* genes in porcine intestinal epithelial (PIE) cells treated with *Lactobacillus rhamnosus* CRL1505, *L. rhamnosus* IBL027, *L. rhamnosus* CRL576, *Lactobacillus plantarum* CRL1506, *L. plantarum* MPL16, or *L. plantarum* CRL681 and challenged with the viral molecular–associated pattern poly(I:C), analyzed by quantitative polymerase chain reaction. Porcine intestinal epithelial cells with no lactobacilli treatment and stimulated with poly(I:C) were used as controls. The results represent data from three independent experiments. Letters indicate significant differences ($P < 0.05$), a < b < c.

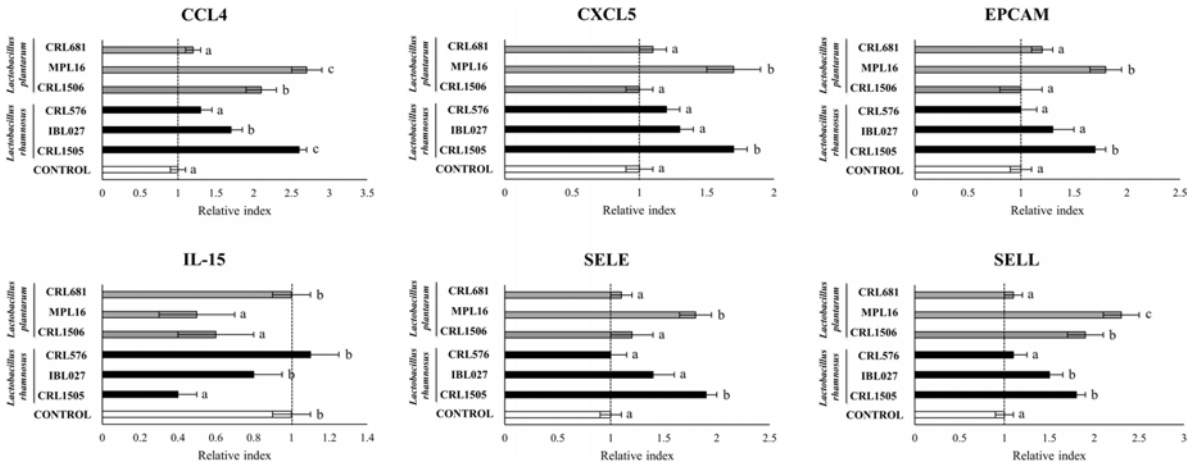


**FIGURE 2 |** Expression of chemokines [interleukin 15 (*IL-15*), *CCL4*, and *CXCL5*] and adhesion molecules (*EPCAM*, *SELE*, and *SELL*) genes in porcine intestinal epithelial (PIE) cells treated with *Lactobacillus rhamnosus* CRL1505, *L. rhamnosus* IBL027, *L. rhamnosus* CRL576, *Lactobacillus plantarum* CRL1506, *L. plantarum* MPL16, or *L. plantarum* CRL681 and challenged with the viral molecular–associated pattern poly(I:C), analyzed by quantitative polymerase chain reaction. Porcine intestinal epithelial cells with no lactobacilli treatment and stimulated with poly(I:C) were used as controls. The results represent data from three independent experiments. Letters indicate significant differences ($P < 0.05$), a < b < c.

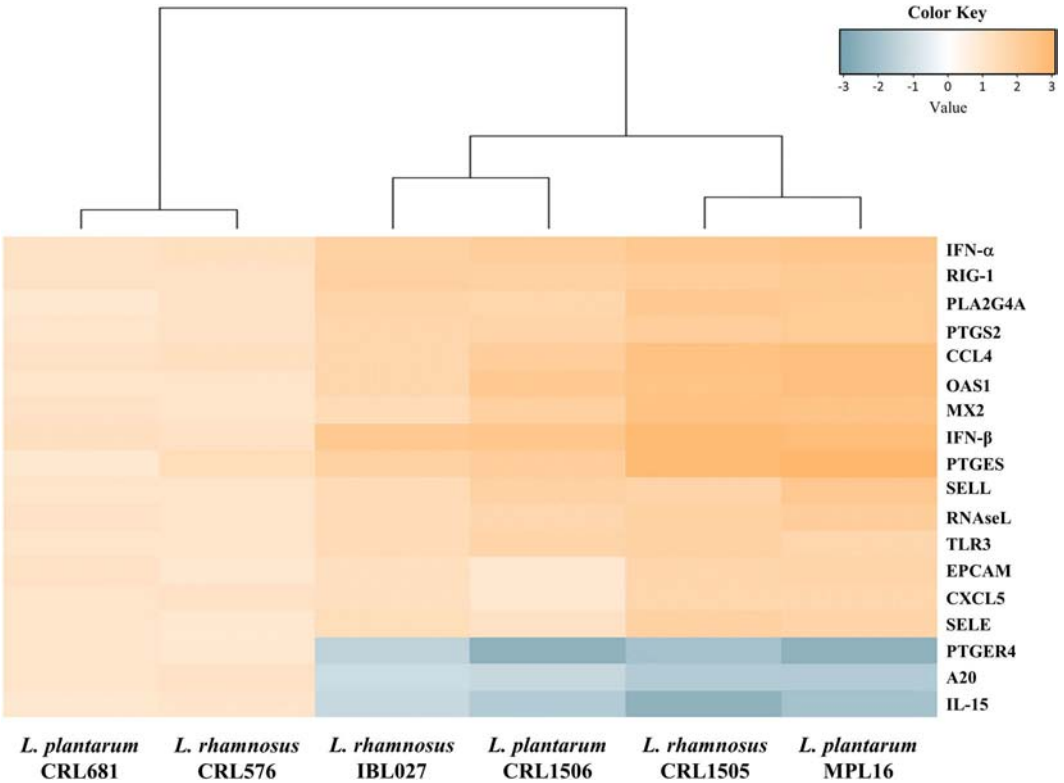


**FIGURE 3 |** Heat map analysis of the differentially regulated genes in porcine intestinal epithelial (PIE) cells treated with *Lactobacillus rhamnosus* CRL1505, *L. rhamnosus* IBL027, *L. rhamnosus* CRL576, *Lactobacillus plantarum* CRL1506, *L. plantarum* MPL16, or *L. plantarum* CRL681 and challenged with the viral molecular–associated pattern poly(I:C).

We performed a cluster analysis to depict the transcriptomic patterns of differentially modulated genes between lactobacilli-treated and control PIE cells, in order to find the strains with similar immunomodulatory properties in the context of TLR3 activation. As shown in **Figure 3**, the treatments with immunomodulatory lactobacilli plus poly(I:C) clustered

together and separated from the non-immunomodulatory strains. Moreover, *L. rhamnosus* CRL1505 and *L. plantarum* MPL16 were separated from *L. plantarum* CRL1506 and *L. rhamnosus* IBL027. These results indicate that *L. plantarum* MPL16 would have the ability to differentially regulate the immunotranscriptomic response in poy(I:C)-challenged PIE cells (**Supplementary Figure S3**) in a way comparable to that previously reported for *L. rhamnosus* CRL1505 (16, 20).

## Modulation of TLR3-Triggered Intestinal Immune Response in Mice by Lactobacilli

Next, we were interested in finding out whether the differences in the immunomodulatory activities of CRL1505, MPL16, CRL1506, and IBL027 observed in PIE cells could be also found in an *in vivo* model. Then, lactobacilli were given orally to different groups of mice, and the intestinal cytokine profile was evaluated before (basal levels) and after the intraperitoneal challenge with poly(I:C). As observed in **Supplementary Figure S4**, a strain-dependent ability in the modulation of the basal levels of intestinal cytokines was detected. The four immunomodulatory strains increased the intestinal levels of IFN-β, IFN-γ, and IL-10; however, *L. rhamnosus* CRL1505 and *L. plantarum* MPL16 were more efficient than the other strains to augment IFN-γ and IL-10. The non-immunomodulatory strains CRL681 and CRL576 did not modify the levels of intestinal IFN-β. Interestingly, *L. plantarum* CRL681 increased the levels of intestinal IFN-γ and IL-10 (**Supplementary Figure S4**). All the lactobacilli strains with the exception of *L. rhamnosus* CRL576 increased TNF-α, whereas the CRL1505, MPL16, IBL027, and CRL681 enhanced the intestinal levels of IL-6 (**Supplementary Figure S4**). The basal concentration of IL-15 was under the detection limits in all the experimental groups (data not shown).

We evaluated the biochemical markers LDH and AST in order to study the inflammatory damage after poly(I:C) administration (**Figure 4**). As we reported previously (8), the intraperitoneal challenge with poly(I:C) significantly increased LDH and AST activities in serum samples. The four immunomodulatory strains decreased serum LDH and AST, whereas the non-immunomodulatory strains CRL681 and CRL576 did not modify the levels of those markers (**Figure 4**).

In addition, the intraperitoneal administration of poly(I:C) significantly increased the levels of IFN-β; IFN-γ; the proinflammatory cytokines TNF-α, IL-6, and IL-15; and the regulatory cytokine IL-10 in the intestinal fluid (**Figure 5**). The four immunomodulatory strains were able to enhance the intestinal levels of IFN-β and IFN-γ after TLR3 activation. The CRL1505, MPL16, CRL1506, and IBL027 strain were also capable of significantly reducing the concentrations of TNF-α, IL-6, and IL-15 and increasing the levels of IL-10 in the intestine when compared to control mice (**Figure 5**). Of note, *L. rhamnosus* CRL1505 and *L. plantarum* MPL16 were more efficient than the other strains to reduce TNF-α and IL-15. The non-immunomodulatory strains CRL681 and CRL576 did not modify the levels of IFN-β, IFN-γ, TNF-α, IL-6, IL-15, or IL-10 when compared to controls (**Figure 5**).

Again, we performed a cluster analysis to depict the differentially modulated cytokines and injury markers between lactobacilli-treated and control mice, in order to find the strains with similar immunomodulatory properties in the *in vivo* mice model. As shown in **Figure 6**, a clear strain-dependent effect was observed in the ability of lactobacilli to modulate cytokines before and after poly(I:C) challenge. Interestingly, *L. rhamnosus* CRL1505 and *L. plantarum* MPL16 clustered together and separated from the other immunomodulatory strains *L. plantarum* CRL1506 and *L. rhamnosus* IBL027. These results allow us to speculate that *L. plantarum* MPL16 would have the ability to differentially regulate the intestinal innate immune response in poy(I:C)-challenged mice and protect against the inflammatory damage (**Supplementary Figure S5**) in a way comparable to that previously reported for *L. rhamnosus* CRL1505 (8).

## Modulation of TLR3-Triggered Respiratory Immune Response in Mice by Lactobacilli

We have previously reported that orally administered *L. rhamnosus* CRL1505 is able to beneficially modulate the respiratory immune response triggered by TLR3 activation (7) and improve the resistance against influenza virus (10) and RSV (9). We also showed that the capacity of orally administered CRL1505 strain to modulate immunity in distal mucosal sites is not sheared by the immunomodulatory strain *L. plantarum* CRL1506. Then, taking into considerations the similarities found in this work between the CRL1505 and MPL16 strains, we were interested in finding out whether orally administered *L. plantarum* MPL16 was able to influence respiratory tract immunity. For this purpose, lactobacilli were given orally to different groups of mice, and the serum and respiratory cytokine profile was evaluated before (basal levels) and after the nasal challenge with poly(I:C). The changes in the profile of cytokines induced in the BAL (**Supplementary Figure S6**) and serum (**Supplementary Figure S7**) by lactobacilli indicated a clear strain-dependent effect. When the levels of the different cytokines were analyzed in BAL, it was shown that only *L. rhamnosus* CRL1505 and *L. plantarum* MPL16 enhanced the concentrations of IFN-β. In addition, CRL1505, MPL16 and IBL027 increased the basal levels of IFN-γ and IL-10. However, *L. rhamnosus* IBL027 was less efficient than the CRL1505 and MPL16 to induce the up-regulation of those cytokines (**Supplementary Figure S6**). The basal levels of respiratory TNF-α were increased by *L. rhamnosus* CRL1505, *L. plantarum* MPL16, and *L. plantarum* CRL1506, whereas the CRL681 and CRL576 treatments induced no changes in any of the cytokines evaluated in the respiratory tract (**Supplementary Figure S6**).

All the immunomodulatory strains were capable of enhancing the concentrations of IFN-β, IFN-γ, TNF-α, and IL-10 in serum when compared to controls. However, *L. rhamnosus* CRL1505 and *L. plantarum* MPL16 were more efficient than the other immunomodulatory strains to increase the basal levels of serum IFN-γ, TNF-α, and IL-10. *Lactobacillus rhamnosus* CRL576 and *L. plantarum* CRL681 did not induce significant

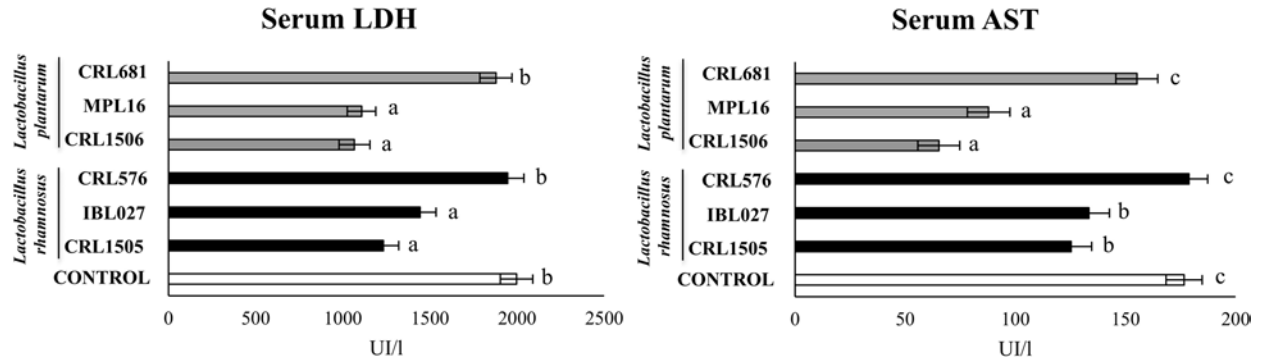


**FIGURE 4 |** Levels of serum injury markers [lactate dehydrogenase (LDH) and aspartate aminotransferase (AST)] in mice orally treated with *Lactobacillus rhamnosus* CRL1505, *L. rhamnosus* IBL027, *L. rhamnosus* CRL576, *Lactobacillus plantarum* CRL1506, *L. plantarum* MPL16, or *L. plantarum* CRL681 ($10^8$ cells/mouse per day for five consecutive days) and then challenged by the intraperitoneal route with 30 μg of the viral molecular–associated pattern poly(I:C). Mice with no lactobacilli treatment and challenged with poly(I:C) were used as controls. Serum injury markers were evaluated on day 2 after poly(:C) administration. The results represent data from three independent experiments ($n = 6$ per group). Letters indicate significant differences ($P < 0.05$), a < b < c.

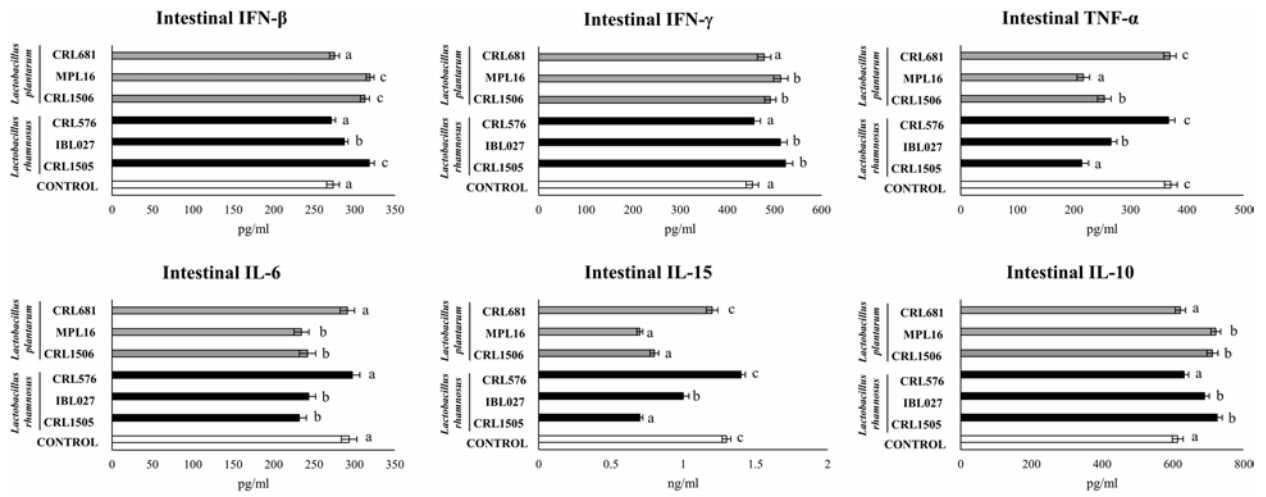


**FIGURE 5 |** Levels of intestinal interferons (IFN-β and IFN-γ), proinflammatory cytokines [TNF-α and interleukin 6 (IL-6)] and IL-10 in mice orally treated with *Lactobacillus rhamnosus* CRL1505, *L. rhamnosus* IBL027, *L. rhamnosus* CRL576, *Lactobacillus plantarum* CRL1506, *L. plantarum* MPL16, or *L. plantarum* CRL681 ($10^8$ cells/mouse per day for 5 consecutive days) and then challenged by the intraperitoneal route with 30 μg of the viral molecular–associated pattern poly(I:C). Mice with no lactobacilli treatment and challenged with poly(I:C) were used as controls. Immune factors were evaluated on day 2 after poly(:C) administration. The results represent data from three independent experiments ($n = 6$ per group). Letters indicate significant differences ($P < 0.05$), a < b < c.

changes in serum cytokines when compared to controls (**Supplementary Figure S7**).

We also evaluated the levels of the biochemical markers albumin and LDH in BAL as indicators of lung injury (7, 9, 10). The nasal challenge of mice with poly(I:C) significantly altered lungs function and induced lung injuries as demonstrated by the increased levels of BAL albumin and LDH (**Figure 7**), reflecting alteration of the alveolar–capillary barrier and local cellular damage. Only *L. rhamnosus* CRL1505 and *L. plantarum* MPL16 treatments were able to significantly reduce the levels of BAL LDH and albumin when compared to controls (**Figure 7**).

The nasal administration poly(I:C) significantly increased serum (**Supplementary Figure S8**) and respiratory (**Figure 8**) levels of IFN-β, IFN-γ, TNF-α, and IL-10. *Lactobacillus rhamnosus* CRL1505 and *L. plantarum* MPL16 enhanced the levels of IFN-β and IFN-γ in both serum and BAL, whereas *L. rhamnosus* IBL027 was capable of increasing only BAL IFN-γ. The four immunomodulatory strains were capable of reducing serum and BAL levels of TNF-α, however; the CRL1505 and MPL16 strains were more effective to down-regulate this inflammatory cytokine in the respiratory tract (**Figure 8**). In addition, the four immunomodulatory strains increased IL-10 in serum (**Supplementary Figure S8**), but only *L. rhamnosus* CRL1505 and *L. plantarum* MPL16 enhanced the levels of this immunoregulatory cytokine in the respiratory tract (**Figure 8**).

We performed a cluster analysis to depict the differentially modulated serum and BAL cytokines and lung injury markers

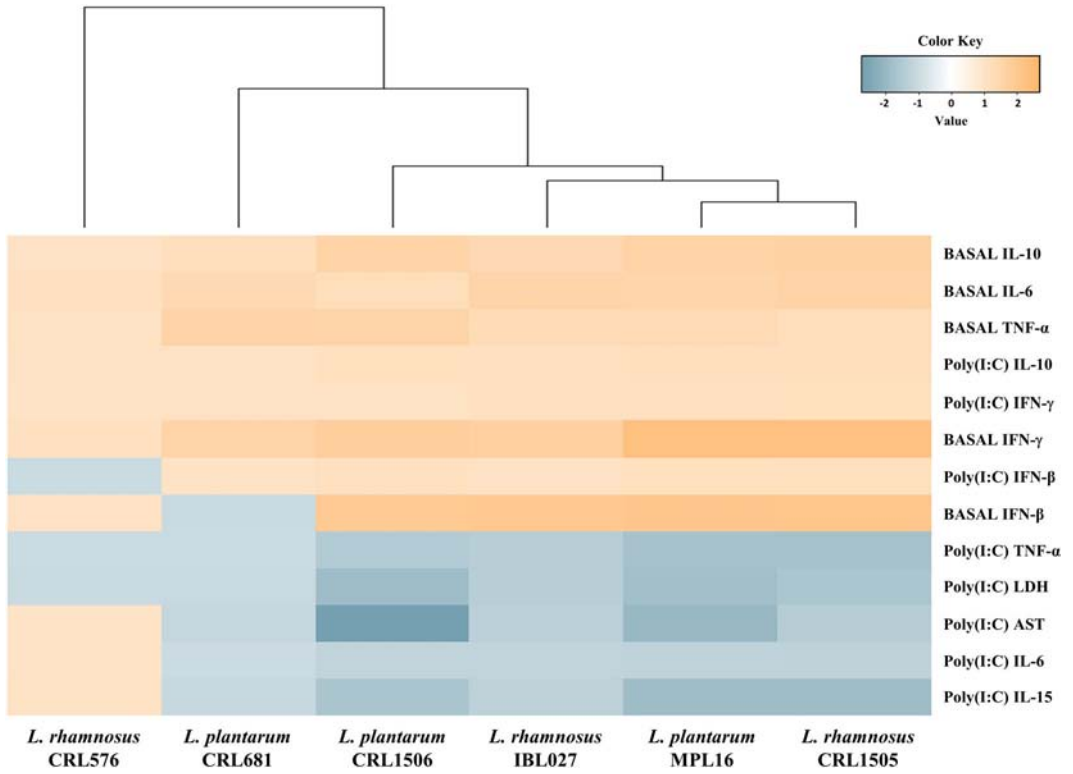


**FIGURE 6 |** Heat map analysis of the differentially regulated intestinal immune factors and serum injury markers before (basal) and after poly(I:C) challenge. Mice were orally treated with *Lactobacillus rhamnosus* CRL1505, *L. rhamnosus* IBL027, *L. rhamnosus* CRL576, *Lactobacillus plantarum* CRL1506, *L. plantarum* MPL16, or *L. plantarum* CRL681, and then challenged by the intraperitoneal route with the viral molecular–associated pattern poly(I:C).

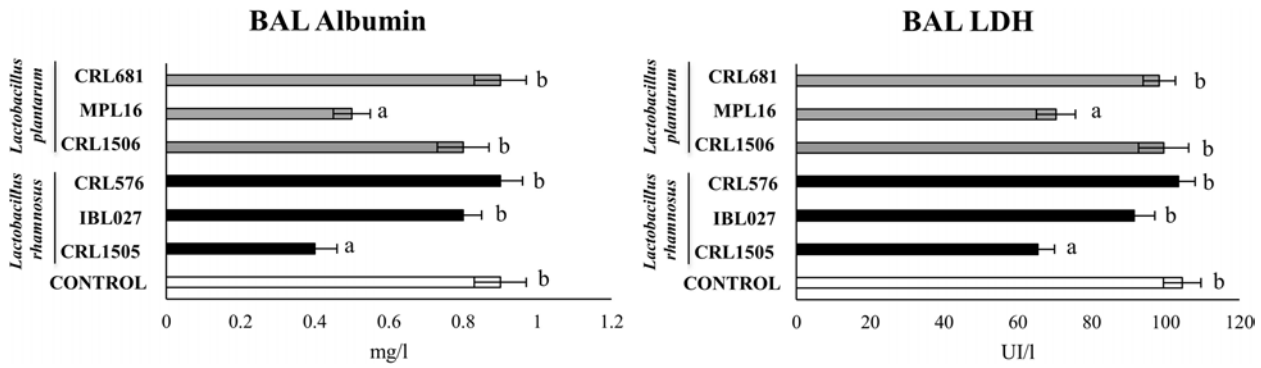


**FIGURE 7 |** Levels of bronchoalveolar lavage (BAL) injury markers [albumin and lactate dehydrogenase (LDH)] in mice orally treated with *Lactobacillus rhamnosus* CRL1505, *L. rhamnosus* IBL027, *L. rhamnosus* CRL576, *Lactobacillus plantarum* CRL1506, *L. plantarum* MPL16, or *L. plantarum* CRL681 ($10^8$ cells/mouse per day for five consecutive days) and then challenged by the nasal route with 250 μg of the viral molecular–associated pattern poly(I:C) for 3 consecutive days. Mice with no lactobacilli treatment and challenged with poly(I:C) were used as controls. Bronchoalveolar lavage injury markers were evaluated on day 2 after the last poly(:C) administration. The results represent data from three independent experiments ($n = 6$ per group). Letters indicate significant differences ($P < 0.05$), a < b < c.

between lactobacilli-treated and control mice. As shown in **Figure 9**, a clear strain-dependent effect was observed in the ability of lactobacilli to modulate immunity in the respiratory tract. Of note, *L. rhamnosus* CRL1505 and *L. plantarum* MPL16 clustered together and separated from the other immunomodulatory strains. These results allow us to speculate that *L. plantarum* MPL16 would have the ability to differentially regulate the systemic and respiratory innate immune response in poy(I:C)-challenged mice and protect against the lung inflammatory damage (**Supplementary Figure S9**) in a way comparable to that previously reported for *L. rhamnosus* CRL1505 (7).

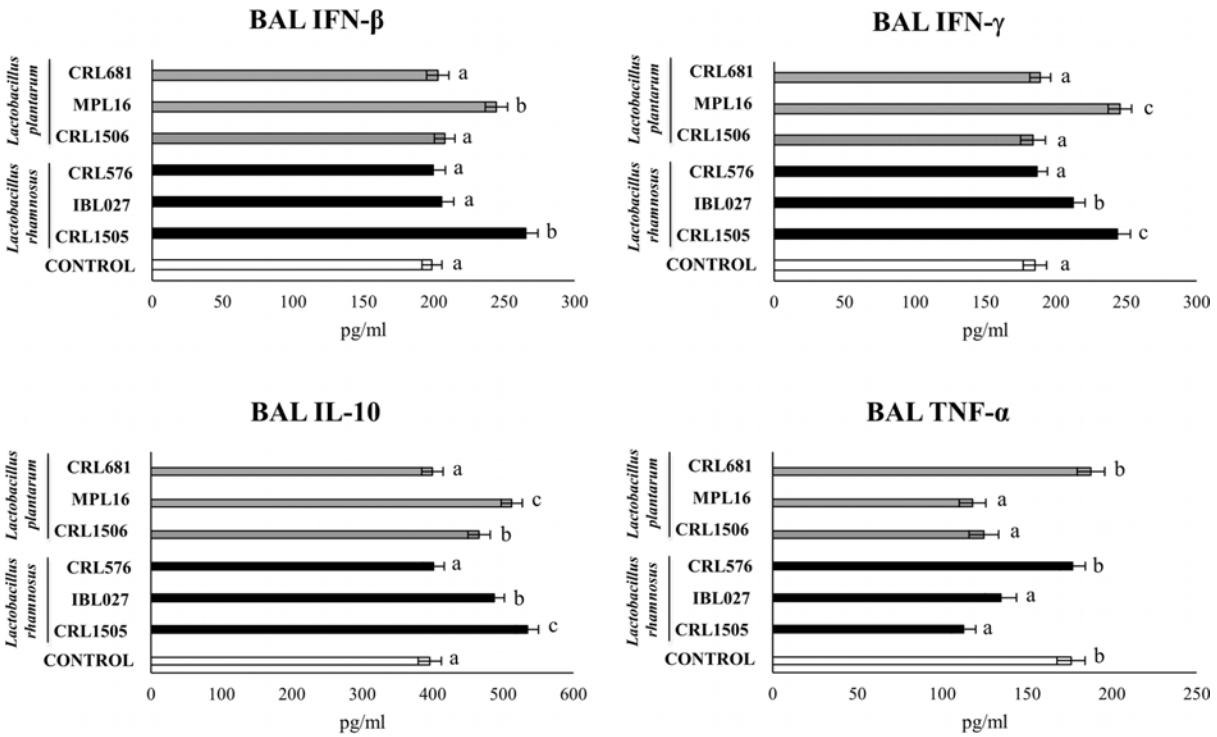


**FIGURE 8 |** Levels of bronchoalveolar lavage (BAL) interferons (IFN-β and IFN-γ), TNF-α, and interleukin 10 (IL-10) in mice orally treated with *Lactobacillus rhamnosus* CRL1505, *L. rhamnosus* IBL027, *L. rhamnosus* CRL576, *Lactobacillus plantarum* CRL1506, *L. plantarum* MPL16, or *L. plantarum* CRL681 ($10^8$ cells/mouse per day for 5 consecutive days) and then challenged by the nasal route with 250 μg of the viral molecular–associated pattern poly(I:C) for three consecutive days. Mice with no lactobacilli treatment and challenged with poly(I:C) were used as controls. Bronchoalveolar lavage immune factors were evaluated on day 2 after the last poly(:C) administration. The results represent data from three independent experiments ($n$ = 6 per group). Letters indicate significant differences ($P < 0.05$), a < b < c.

## Enhancement of the Resistance Against RSV Infection by *L. plantarum* MPL16

Finally, we aimed to test whether the oral administration of *L. plantarum* MPL16 was able to confer protection against a respiratory virus challenge. For this purpose, mice were fed the MPL16 strain and then nasally challenged with RSV. *Lactobacillus rhamnosus* CRL1505 and *L. plantarum* CRL1506 were used as positive and negative controls, respectively, according to our previous work demonstrating their different ability to protect against this viral pathogen (9). As shown in **Figure 10**, both *L. rhamnosus* CRL1505 and *L. plantarum* MPL16 were equally effective in reducing RSV lung titers, whereas the CRL1506 strain did not induce changes when compared to control mice. In addition, the MPL16 and CRL1505 strains significantly reduced the levels of the markers of lung damage, whereas *L. plantarum* CRL1506 was not able to achieve this effect (**Figure 10**). The levels of respiratory IFN-β, IFN-γ, TNF-α, and IL-10 were also evaluated after the challenge with RSV (**Figure 11**). Both *L. rhamnosus* CRL1505 and *L. plantarum* MPL16 enhanced the levels of IFN-β, IFN-γ, and IL-10 in BAL, whereas *L. plantarum* CRL1506 was not capable of increasing these cytokines when compared to controls. The CRL1506 strain did not induce changes in the levels of BAL TNF-α when compared to the control group. The MPL16 and CRL1505 strains significantly increased the respiratory levels of TNF-α, being *L. rhamnosus* CRL1505 more effective than *L. plantarum* MPL16 to achieve this effect (**Figure 11**).

## DISCUSSION

In middle- and low-income countries, intestinal and respiratory viral infections are the most common and deadly diseases in children (26–28). The use of functional foods such as those containing immunomodulatory probiotic lactobacilli has been proposed to stimulate the intestinal and the respiratory immune system, improving the outcome of viral diarrhea and pneumonia simultaneously. An example of the high probability of success of this strategy is the "Yogurito Nutritional Program" implemented in Argentina (2, 29). The program uses a probiotic yogurt containing the immunobiotic strain *L. rhamnosus* CRL1505 to prevent respiratory and gastrointestinal diseases by enhancing the immunological system of children attending public schools. Then, the selection of new immunobiotic strains that have different biotechnological properties but the same or better immunomodulatory capacities than *L. rhamnosus* CRL1505 could enhance the development of various types of functional foods that could be used

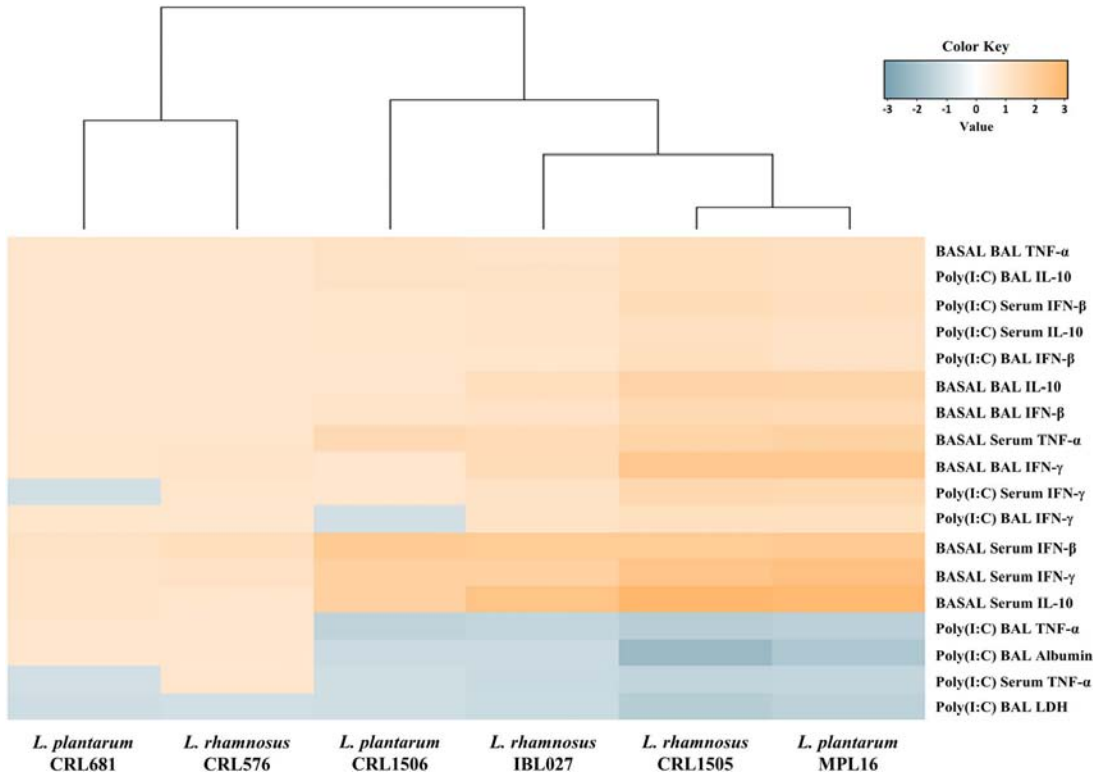


**FIGURE 9 |** Heat map analysis of the differentially regulated serum and bronchoalveolar lavage (BAL) immune factors and BAL injury markers before (basal) and after poly(I:C) challenge. Mice were orally treated with *Lactobacillus rhamnosus* CRL1505, *L. rhamnosus* IBL027, *L. rhamnosus* CRL576, *Lactobacillus plantarum* CRL1506, *L. plantarum* MPL16, or *L. plantarum* CRL681 and then challenged by the nasal route with the viral molecular–associated pattern poly(I:C) for three consecutive days.

around the world to reduce the incidence and severity of intestinal and pulmonary infections caused by viruses. Such selection, in addition to being efficient, should be performed using *in vitro* systems in order to minimize the use of experimental animals.

In this work, we demonstrated that the study of biomarkers expression in poly(I:C)-challenged PIE cells is a very effective tool for the selection of immunobiotics with the ability to modulate intestinal and respiratory antiviral immunity. The transcriptional profiling performed *in vitro* in poly(I:C)-challenged PIE cells in this work allowed us to select a new immunobiotic strain, *L. plantarum* MPL16, with the ability to stimulate *in vivo* the local (intestinal) and distal (respiratory) mucosal immune systems.

*Lactobacillus rhamnosus* CRL1505 and *L. plantarum* MPL16 similarly modulated gene expression in poly(I:C)-challenged PIE cells inducing significant increases of both *IFN*-α and *IFN*-β and in the antiviral factors *MX2*, *OAS1*, and *RNASEL*. Our previous studies in PIE cells showed that rotavirus can be detected by this cell line through TLR3, inducing the expression of *IFN*-β and up-regulating the antiviral genes *MxA* and *RNASEL* (15). Moreover, those studies demonstrated that immunobiotics strains with the ability to enhance *IFN*-β, *MxA*, and *RNASEL* were also capable of reducing rotavirus replication. We demonstrated that immunobiotic strains such as *L. rhamnosus* CRL1505 (16) and *Bifidobacterium infantis* MCC12 (15) increased the expression of IFN-β and antiviral factors by reducing the expression of *A20*. The down-regulation of *A20* gene expression in poly(I:C)-challenged PIE cells results in the improved activation of IRF3 and NF-κB signaling pathways, which increase the expression of not only *IFN*-α, *IFN*-β, *MX2*, *OAS1*, and *RNASEL* but in addition several other antiviral factors including *OASL*, *MX1*, *OAS2*, *RNASE4, IFIT1*, *IFIT3*, *IFIT2*, and *IFIT5* (**Supplementary Figure S3**) (16). The *in vivo* experiments in mice performed here also demonstrated that *L. plantarum* MPL16 is able to enhance the intestinal levels of IFN-β. Moreover, MPL16-treated mice also showed higher levels of intestinal IFN-γ as observed by *L. rhamnosus* CRL1505. It was reported that infection with rotavirus in suckling mice induces a significant up-regulation of different types of IFNs in the intestine including IFN-γ by T cells and type I IFNs by dendritic cells (DCs) and IECs (30). Interferons binding to their cognate cell surface receptors activate positive feedback loops that amplify the expression of IFNs as well as more than 300 different IFN-stimulated genes (31). This IFNs release then efficiently amplify the expression of antiviral proteins targeting a variety of viral replication steps in uninfected bystander cells. It was also shown in *in vitro* studies that the addition of purified exogenous IFNs after rotavirus infection of human IECs does not significantly hamper

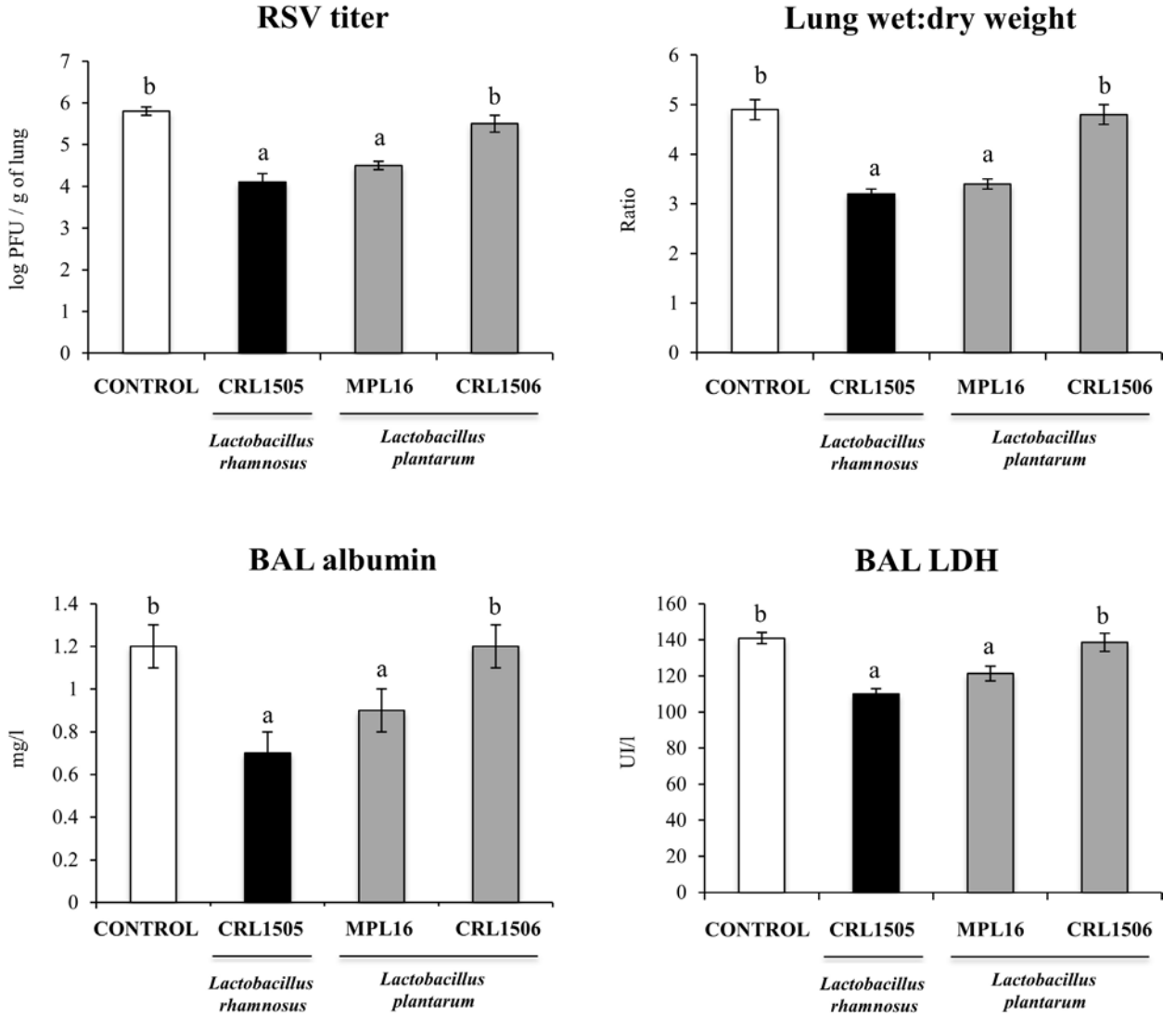


**FIGURE 10 |** Lung respiratory syncytial virus (RSV) titers, lung wet-to-dry ratio, and levels of bronchoalveolar lavage (BAL) injury markers [albumin and lactate dehydrogenase (LDH)] in mice orally treated with *Lactobacillus rhamnosus* CRL1505, *Lactobacillus plantarum* CRL1506, or *L. plantarum* MPL16 ($10^8$ cells/mouse per day for five consecutive days) and then challenged by the nasal route with RSV. Mice with no lactobacilli treatment and infected with RSV were used as controls. Respiratory syncytial virus titers and injury markers were evaluated on day 2 after viral infection. The results represent data from three independent experiments ($n = 6$ per group). Letters indicate significant differences ($P < 0.05$), a < b < c.

viral replication; however, IFN treatment of cells prior to viral challenge is required to achieve an efficient restriction of rotavirus replication (32).

The excessive activation of the inflammatory response or the failure in the mechanisms that control it significantly contributes to the injury of the infected tissue during viral infections. Intestinal epithelial cells produce a variety of cytokines and chemokines in response to the viral attack, including IL-6, IL-8, TNF-α, and granulocyte-macrophage colony-stimulating factor. The production of those inflammatory factors is important for the protection against the viral infection through their direct antiviral effects (33) or the recruitment and activation of phagocytes (34). However, infiltration of immune cells to the intestinal mucosa can contribute to the local damage mediated by the inflammatory and oxidative stress (35). In addition, it was reported that purified dsRNA from rotavirus is able to induce severe intestinal damage in mice through the activation of TLR3 signaling pathway (36). Moreover, it was also demonstrated that the intraperitoneal administration of the synthetic dsRNA poly(I:C) to mice mimics the inflammatory intestinal immune response elicited by rotavirus and induce mucosal erosion, villous atrophy, intestinal wall attenuation, and diarrhea (8, 36, 37). Interestingly, it was shown that the intestinal damage triggered by dsRNA-TRL3 interaction is mediated by the increased expression of IL-15 and retinoic acid early inducible 1 (RAE1) in IECs, which induce the activation of $CD3^+NK1.1^+CD8\alpha\alpha^+$ intraepithelial

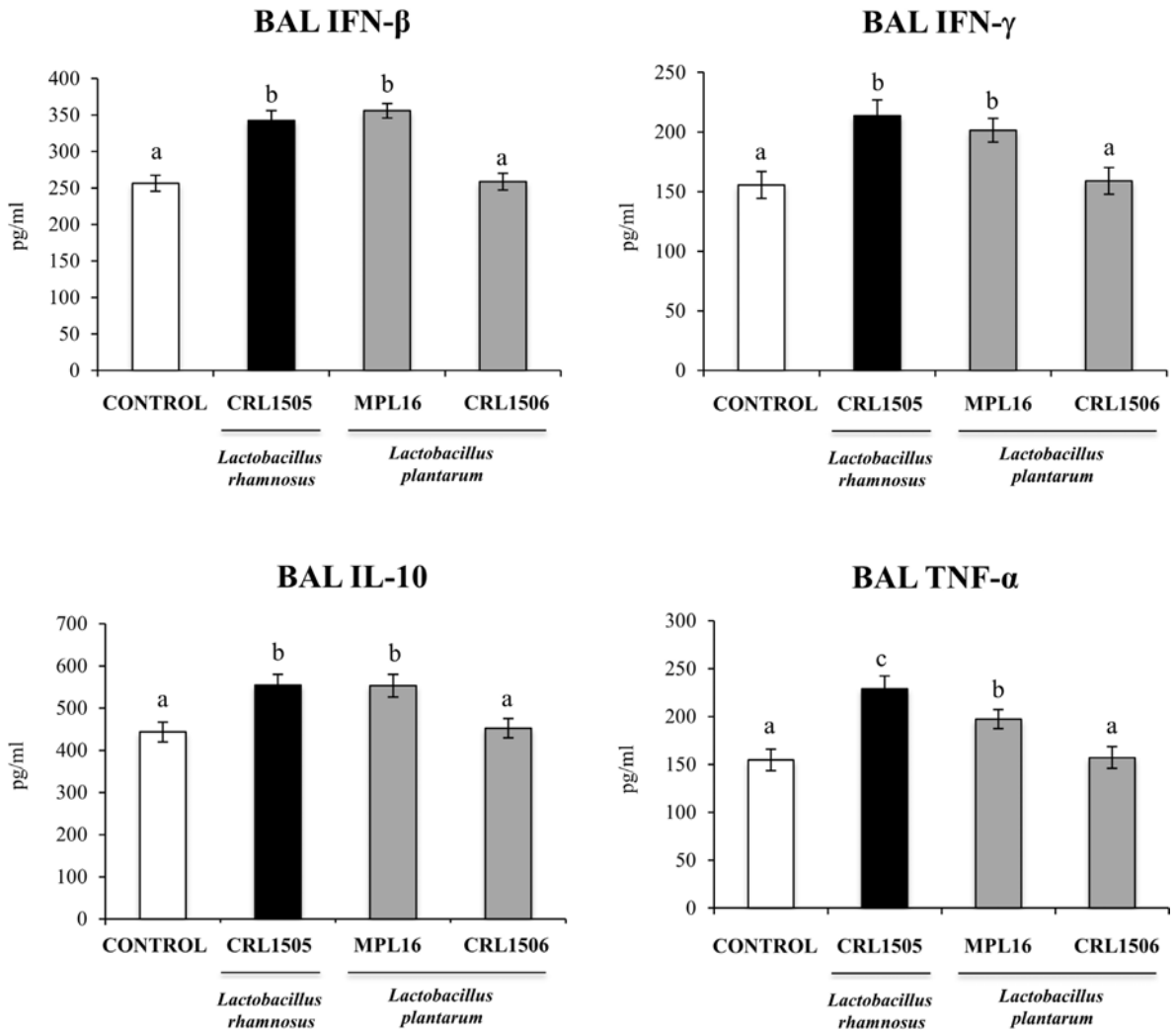


**FIGURE 11 |** Levels of bronchoalveolar lavage (BAL) interferons (IFN-β and IFN-γ), TNF-α, and interleukin 10 (IL-10) in mice orally treated with *Lactobacillus rhamnosus* CRL1505, *Lactobacillus plantarum* CRL1506, or *L. plantarum* MPL16 ($10^8$ cells/mouse per day for five consecutive days) and then challenged by the nasal route with RSV. Mice with no lactobacilli treatment and infected with RSV were used as controls. Immune markers were evaluated on day 2 after viral infection. The results represent data from three independent experiments ($n = 6$ per group). Letters indicate significant differences ($P < 0.05$), a < b < c.

lymphocytes (IELs) and promote epithelial destruction through the RAE1–NKG2D interaction (**Supplementary Figure S5**) (38). We reported previously that *L. rhamnosus* CRL1505 is able to significantly reduce the expression of *IL-15* and *RAE1* in poly(I:C)-challenged PIE cells (16) and to reduce the levels of intestinal TNF-α and IL-15 and diminish the gut damage mediated by $CD3^+NK1.1^+CD8\alpha\alpha^+$ IELs in mice after TLR3 activation (8). Here, we found that *L. plantarum* MPL16 is able to modulate the cytokine profile expression triggered by TLR3 activation in PIE cells as well as in mice intestinal mucosa, in a way similar to that observed for the CRL1505 strain. Then, it is tempting to speculate that *L. plantarum* MPL16 would have the ability to beneficially regulate intestinal inflammation in the context of TLR3 activation; however, more detailed studies using viral challenges are necessary to demonstrate this effect.

Our results allow us to speculate that *L. plantarum* MPL16 would be capable to modulate IECs innate immune response, improve the resistance to rotavirus infection, and reduce the severity of inflammatory-mediated damage, as we have previously demonstrated *in vitro* (16, 20), *in vivo* (8), and in clinical trials (2, 29) for the CRL1505 strain.

We also demonstrated here that orally administered *L. plantarum* MPL16 is able to differentially modulate the respiratory antiviral immune response. We reported previously that the improvement of IFN-β production by $CD11c^+SiglecF^+$ alveolar macrophages and IFN-γ by $CD3^+CD4^+$ T cells is related to the ability of immunobiotic treatments to enhance resistance to respiratory virus (39, 40), in line with studies demonstrating that these immune cell populations are the main producer of IFNs during pulmonary viral infections (36, 37). The increased levels of respiratory IFN-γ and IFN-β found in *L. plantarum*

MPL16–treated mice correlated with the improved resistance of mice to RSV infection. On the other hand, we have extensively used a mice experimental model of lung inflammation based on the nasal administration of poly(I:C) in order to mimic the respiratory innate antiviral immune response triggered by RSV and to evaluate the beneficial effects of immunobiotic bacteria (7, 9, 10, 39, 40). The respiratory priming with the TLR3 agonist induces a marked inflammatory damage characterized by impaired alveolar–capillary barrier function and epithelial cell death as well as increased levels of TNF-α, IL-6, IL-8, and MCP-1. Prominent improvements of the IL-8, MIP-1, RANTES, MCP-1, TNF-α, and IL-6 have been reported in both experimentally RSV-infected mice and naturally RSV-infected children (41). The increase in the respiratory levels of those inflammatory factors, especially TNF-α, contributes to clearance of the virus during the early stages of RSV infection; however, their continued production exacerbates lung injuries during the late stages of infection (41, 42). Then, the appropriate regulation of the respiratory immune response is also essential for the protection of RSV-infected hosts. In this regard, it was demonstrated that IL-10 has a crucial role in regulating the severity of RSV infection (42, 43). The deficiency of IL-10 does not affect RSV load in lungs, but significantly enhances the inflammatory cells influx into the lung, promotes lung damage, and increases weight loss of infected mice (42, 43). The results of this work demonstrated that orally administered *L. plantarum* MPL16 is able to reduce the levels of inflammatory factors, increase IL-10, and significantly diminish the markers of lung tissue damage after the nasal administration of poly(I:C). Moreover, we also demonstrated here that orally administered *L. plantarum* MPL16 significantly reduced the respiratory injury markers after RSV challenge and differentially modulated the levels of respiratory proinflammatory and anti-inflammatory cytokines induced by the viral infection. Those effects were similar to the previously described for the CRL1505 strain (**Supplementary Figure S9**) (7, 9, 10, 39).

The results of this work confirm that new immunobiotics strains with the ability of stimulating both local and distal antiviral immune responses when orally administered can be efficiently selected by evaluating the expression of appropriate biomarkers of the transcriptomic profile of poly(I:C)-challenged PIE cells. The comparison of the transcriptomic patterns of differentially modulated genes in PIE cells treated with different lactobacilli allowed us to select the MPL16 strain that clustered together with the immunobiotic strain *L. rhamnosus* CRL1505, which has been proved to differentially modulate the intestinal and the respiratory antiviral responses and protect against enteric and respiratory viruses (2, 7, 9, 10). The *in vivo* studies performed here conclusively demonstrated that *L. plantarum* MPL16 modulated the profiles of intestinal, serum, and respiratory cytokines; reduced the inflammatory damage triggered by TLR3 activation in both the intestinal and respiratory mucosa; and improved the resistance to RSV infection. The immunological changes induced by *L. plantarum* MPL16 were not different from those previously reported for the CRL1505 strain. Further mechanistic studies evaluating comparatively the effects of CRL1505 and MPL16 strains in different immune cell populations such as DCs and macrophages, as well as more detailed molecular and genomic characterization of both lactobacilli strains, could contribute significantly to the understanding of the molecular mechanisms involved in the ability of immunobiotics to stimulate distant mucosal sites such as the respiratory tract.

Of note, the biotechnological properties of the two strains are different. Whereas *L. rhamnosus* CRL1505 has been used mainly in the development of dairy functional products (2, 44), the MPL16 strain has shown a remarkable ability to growth and ferment wakame (*Undaria pinnatifida*) that is the most popular and economically important edible brown algae in Asian countries (24, 45). Then, the different biotechnological properties of *L. plantarum* MPL16 could potentiate the development of non-dairy functional foods or feeds with the ability to improve antiviral immunity in the intestine and the respiratory tract.

## DATA AVAILABILITY STATEMENT

The datasets generated for this study are available on request to the corresponding author.

## ETHICS STATEMENT

The animal study was reviewed and approved by the Ethical Committee of Animal Care CERELA-CONICET, Tucuman, Argentina.

## AUTHOR CONTRIBUTIONS

JV and HK designed the study and manuscript writing. LA, VG-C, YI, and MI did the laboratory work. LA, MI, and YS did the statistical analysis. AG-C, HA, HT, JV, and HK contributed to data analysis and interpretation. All authors read and approved the manuscript.

## FUNDING

This study was supported by ANPCyT–FONCyT Grant PICT-2016-0410 to JV, Grant-in-Aid for Scientific Research (A) (19H00965), and Open Partnership Joint Projects of JSPS Bilateral Joint Research Projects from the Japan Society for the Promotion of Science (JSPS) to HK. This research was also supported by grants from the project of NARO Bio-oriented Technology Research Advancement Institution (research program on the development of innovative technology, No. 01002A) to HK and JSPS Core-to-Core Program, A. Advanced Research Networks entitled Establishment of international agricultural immunology research-core for a quantum improvement in food safety. This study was also supported by grants for Scientific Research on Innovative Areas from the Ministry of Education, Culture, Science, Sports, and Technology (MEXT) of Japan (16H06429, 16K21723, and 16H06435) to HT.

## SUPPLEMENTARY MATERIAL

The Supplementary Material for this article can be found online at: https://www.frontiersin.org/articles/10.3389/fimmu.2020.00543/full#supplementary-material

**FIGURE S1 |** Expression of interferon (*IFN*)-α, and antiviral factors (*TLR3, RIG-1* and *OAS1*) genes in porcine intestinal epithelial (PIE) cells treated with *Lactobacillus rhamnosus* CRL1505, *L. rhamnosus* IBL027, *L. rhamnosus* CRL576, *Lactobacillus plantarum*C RL1506, *L. plantarum* MPL16, or *L. plantarum* CRL681 and challenged with the viral molecular associated pattern poly(I:C), analyzed by qPCR. PIE cells with no lactobacilli treatment and stimulated with poly(I:C) were used as controls. The results represent data from three independent experiments. Letters indicate significant differences ($P < 0.05$), a < b < c.

**FIGURE S2 |** Expression of genes involved in prostaglandins biosynthesis (*PTGS2, PLA2G4A, PTGER4* and *PTGES*) in porcine intestinal epithelial (PIE) cells treated with *Lactobacillus rhamnosus* CRL1505, *L. rhamnosus* IBL027, *L. rhamnosus* CRL576, *Lactobacillus plantarum* CRL1506, *L. plantarum* MPL16, or *L. plantarum* CRL681 and challenged with the viral molecular associated pattern poly(I:C), analyzed by qPCR. PIE cells with no lactobacilli treatment and stimulated with poly(I:C) were used as controls. The results represent data from three independent experiments. Letters indicate significant differences ($P < 0.05$), a < b < c.

**FIGURE S3 |** Global overview of the signaling pathways and immune genes differentially regulated in PIE cells treated with *L. rhamnosus* CRL1505 or *L. plantarum* MPL16 and challenged with poly(I:C). Detailed immunomodulatory mechanisms were previously studied for *L. rhamnosus* CRL1505 (16, 20).

**FIGURE S4 |** Levels of intestinal interferons (IFN-β and IFN-γ), proinflammatory cytokines (TNF-α and IL-6) and IL-10 in mice orally treated with *Lactobacillus rhamnosus* CRL1505, *L. rhamnosus* IBL027, *L. rhamnosus* CRL576, *Lactobacillus plantarum* CRL1506, *L. plantarum* MPL16, or *L. plantarum* CRL681 ($10^8$ cells/mouse/day for five consecutive days). Mice with no lactobacilli treatment were used as controls. Immune factors were evaluated on day 6. The results represent data from three independent experiments ($n = 6$ per group). Letters indicate significant differences ($P < 0.05$), a < b < c.

**FIGURE S5 |** Global overview of the effect of *L. rhamnosus* CRL1505 and *L. plantarum* MPL16 on the intestinal inflammatory injury induced by poly(I:C) and mediated by the activation of $CD3^+NK1.1^+CD8\alpha\alpha^+$ intraepithelial lymphocytes (IELs) that promote epithelial destruction through the RAE1–NKG2D interaction. Detailed immunomodulatory mechanisms were previously studied for *L. rhamnosus* CRL1505 (8).

**FIGURE S6 |** Levels of bronco-alveolar lavages (BAL) interferons (IFN-β and IFN-γ), TNF-α and IL-10 in mice orally treated with *Lactobacillus rhamnosus* CRL1505, *L. rhamnosus* IBL027, *L. rhamnosus* CRL576, *Lactobacillus plantarum* CRL1506, *L. plantarum* MPL16, or *L. plantarum* CRL681 ($10^8$ cells/mouse/day for five consecutive days). Mice with no lactobacilli treatment were used as controls. Immune factors were evaluated on day 6. The results represent data from three independent experiments ($n = 6$ per group). Letters indicate significant differences ($P < 0.05$), a < b < c.

**FIGURE S7 |** Levels of serum interferons (IFN-β and IFN-γ), TNF-α and IL-10 in mice orally treated with *Lactobacillus rhamnosus* CRL1505, *L. rhamnosus* IBL027, *L. rhamnosus* CRL576, *Lactobacillus plantarum* CRL1506, *L. plantarum* MPL16, or *L. plantarum* CRL681 ($10^8$ cells/mouse/day for five consecutive days). Mice with no lactobacilli treatment were used as controls. Immune factors were evaluated on day 6. The results represent data from three independent experiments ($n = 6$ per group). Letters indicate significant differences ($P < 0.05$), a < b < c.

**FIGURE S8 |** Levels of serum interferons (IFN-β and IFN-γ), TNF-α and IL-10 in mice orally treated with *Lactobacillus rhamnosus* CRL1505, *L. rhamnosus* IBL027, *L. rhamnosus* CRL576, *Lactobacillus plantarum* CRL1506, *L. plantarum* MPL16, or *L. plantarum* CRL681 ($10^8$ cells/mouse/day for five consecutive days), and then challenged by the nasal route with 250 μg of the viral molecular associated pattern poly(I:C) for three consecutive days. Mice with no lactobacilli treatment and challenged with poly(I:C) were used as controls. Serum immune factors were evaluated on day 2 after the last poly(:C) administration. The results represent data from three independent experiments ($n = 6$ per group). Letters indicate significant differences ($P < 0.05$), a < b < c.

**FIGURE S9 |** Global overview of the effect of *L. rhamnosus* CRL1505 and *L. plantarum* MPL16 on the respiratory innate immune response triggered by poly(I:C). Detailed immunomodulatory mechanisms were previously studied for *L. rhamnosus* CRL1505 (7, 9).

## REFERENCES


1. WHO/UNICEF. *Ending Preventable Deaths from Pneumonia and Diarrhoea by 2025*. New York, NY: UNICEF. (2013). doi: ISBN978-92-415-0523-9
2. Villena J, Salva S, Núñez M, Corzo J, Tolaba R, Faedda J, et al. Probiotics for everyone! The novel immunobiotic *Lactobacillus rhamnosus* CRL1505 and the beginning of social probiotic programs in Argentina. *Int J Biotechnol Wellness Ind*. (2012) 1:189–98. doi: 10.6000/1927-3037/2012.01.03.05
3. Kitazawa H, Villena J. Modulation of respiratory TLR3-anti-viral response by probiotic microorganisms: lessons learned from *Lactobacillus rhamnosus* CRL1505. *Front Immunol*. (2014) 5:201. doi: 10.3389/fimmu.2014.00201
4. Villena J, Vizoso-Pinto MG, Kitazawa H. Intestinal innate antiviral immunity and immunobiotics: beneficial effects against Rotavirus infection. *Front Immunol*. (2016) 7:563. doi: 10.3389/fimmu.2016.00563
5. Villena J, Oliveira MLS, Ferreira PCD, Salva S, Alvarez S. Lactic acid bacteria in the prevention of pneumococcal respiratory infection: future opportunities and challenges. *Int Immunopharmacol*. (2011) 11:1633–45. doi: 10.1016/j.intimp.2011.06.004
6. Zelaya H, Alvarez S, Kitazawa H, Villena J. Respiratory antiviral immunity and immunobiotics: beneficial effects on inflammation-coagulation interaction during influenza virus infection. *Front Immunol*. (2016) 7:633. doi: 10.3389/fimmu.2016.00633
7. Villena J, Chiba E, Tomosada Y, Salva S, Marranzino G, Kitazawa H, et al. Orally administered *Lactobacillus rhamnosus* modulates the respiratory immune response triggered by the viral pathogen-associated molecular pattern poly(I:C). *BMC Immunol*. (2012) 13:53. doi: 10.1186/1471-2172-13-53
8. Tada A, Zelaya H, Clua P, Salva S, Alvarez S, Kitazawa H, et al. Immunobiotic *Lactobacillus* strains reduce small intestinal injury induced by intraepithelial lymphocytes after Toll-like receptor 3 activation. *Inflamm Res*. (2016) 65:771–83. doi: 10.1007/s00011-016-0957-7
9. Chiba E, Tomosada Y, Vizoso-Pinto MG, Salva S, Takahashi T, Tsukida K, et al. Immunobiotic *Lactobacillus rhamnosus* improves resistance of infant mice against respiratory syncytial virus infection. *Int Immunopharmacol*. (2013) 17:373–82. doi: 10.1016/j.intimp.2013.06.024
10. Zelaya H, Tsukida K, Chiba E, Marranzino G, Alvarez S, Kitazawa H, et al. Immunobiotic *Lactobacilli* reduce viral-associated pulmonary damage through the modulation of inflammation-coagulation interactions. *Int Immunopharmacol*. (2014) 19:161–73. doi: 10.1016/j.intimp.2013.12.020
11. Parashar UD, Gibson CJ, Bresee JS, Glass RI. Rotavirus and severe childhood diarrhea. *Emerg Infect Dis*. (2006) 12:304–6. doi: 10.3201/eid1202.050006
12. Greenberg HB, Estes MK. Rotaviruses: from pathogenesis to vaccination. *Gastroenterology*. (2009) 136:1939–51. doi: 10.1053/j.gastro.2009.02.076
13. Villena J, Kitazawa H. Modulation of intestinal TLR4-inflammatory signaling pathways by probiotic microorganisms: lessons learned from *Lactobacillus jensenii* TL2937. *Front Immunol*. (2014) 4:512. doi: 10.3389/fimmu.2013.00512
14. Hosoya S, Villena J, Shimazu T, Tohno M, Fujie H, Chiba E, et al. Immunobiotic lactic acid bacteria beneficially regulate immune response triggered by poly(I:C) in porcine intestinal epithelial cells. *Vet Res*. (2011) 42:111. doi: 10.1186/1297-9716-42-111
15. Ishizuka T, Kanmani P, Kobayashi H, Miyazaki A, Soma J, Suda Y, et al. Immunobiotic bifidobacteria strains modulate rotavirus immune response in

porcine intestinal epitheliocytes via pattern recognition receptor signaling. *PLoS One*. (2016) 11:e0152416. doi: 10.1371/journal.pone.0152416
16. Albarracin L, Kobayashi H, Iida H, Sato N, Nochi T, Aso H, et al. Transcriptomic analysis of the innate antiviral immune response in porcine intestinal epithelial cells: influence of immunobiotic *Lactobacilli*. *Front Immunol*. (2017) 8:57. doi: 10.3389/fimmu.2017.00057
17. Moue M, Tohno M, Shimazu T, Kido T, Aso H, Saito T, et al. Toll-like receptor 4 and cytokine expression involved in functional immune response in an originally established porcine intestinal epitheliocyte cell line. *Biochim Biophys Acta Gen Subj*. (2008) 1780:134–44. doi: 10.1016/j.bbagen.2007.11.006
18. Shimazu T, Villena J, Tohno M, Fujie H, Hosoya S, Shimosato T, et al. Immunobiotic *Lactobacillus jensenii* elicits anti-inflammatory activity in porcine intestinal epithelial cells by modulating negative regulators of the Toll-like receptor signaling pathway. *Infect Immun*. (2012) 80:276–88. doi: 10.1128/IAI.05729-11
19. Tomosada Y, Villena J, Murata K, Chiba E, Shimazu T, Aso H, et al. Immunoregulatory effect of bifidobacteria strains in porcine intestinal epithelial cells through modulation of ubiquitin-editing enzyme A20 expression. *PLoS One*. (2013) 8:e59259. doi: 10.1371/journal.pone.0059259
20. Villena J, Chiba E, Vizoso-Pinto M, Tomosada Y, Takahashi T, Ishizuka T, et al. Immunobiotic *Lactobacillus rhamnosus* strains differentially modulate antiviral immune response in porcine intestinal epithelial and antigen presenting cells. *BMC Microbiol*. (2014) 14:126. doi: 10.1186/1471-2180-14-126
21. Kobayashi H, Albarracin L, Sato N, Kanmani P, Kober AKMH, Ikeda-Ohtsubo W, et al. Modulation of porcine intestinal epitheliocytes immunetranscriptome response by *Lactobacillus jensenii* TL2937. *Benef Microbes*. (2016) 7:769–82. doi: 10.3920/BM2016.0095
22. Macpherson C, Audy J, Mathieu O, Tompkins TA. Multistrain probiotic modulation of intestinal epithelial cells' immune response to a double-stranded RNA ligand, poly(i·c). *Appl Environ Microbiol*. (2014) 80:1692–700. doi: 10.1128/AEM.03411-13
23. Bagchi P, Nandi S, Chattopadhyay S, Bhowmick R, Halder UC, Nayak MK, et al. Identification of common human host genes involved in pathogenesis of different rotavirus strains: an attempt to recognize probable antiviral targets. *Virus Res*. (2012) 169:144–53. doi: 10.1016/j.virusres.2012.07.021
24. Masumizu Y, Zhou B, Kober AKMH, Islam MA, Iida H, Ikeda-Ohtsubo W, et al. Isolation and immunocharacterization of *Lactobacillus salivarius* from the Intestine of Wakame-Fed pigs to develop novel "Immunosynbiotics". *Microorganisms*. (2019) 7:167. doi: 10.3390/microorganisms7060167
25. Arce LP, Raya Tonetti MF, Raimondo MP, Müller MF, Salva S, Álvarez S, et al. Oral vaccination with Hepatitis E virus capsid protein and immunobiotic bacterium-like particles induce intestinal and systemic immunity in mice. *Probiotics Antimicrob Proteins*. (2019):doi: 10.1007/s12602-019-09598-7
26. Bardach A, Ciapponi A, Garcia-Marti S, Glujovsky D, Mazzoni A, Fayad A, et al. Epidemiology of acute otitis media in children of Latin America and the Caribbean: a systematic review and meta-analysis. *Int J Pediatr Otorhinolaryngol*. (2011) 75:1062–70. doi: 10.1016/j.ijporl.2011.05.014
27. Edmond K, Scott S, Korczak V, Ward C, Sanderson C, Theodoratou E, et al. Long term sequelae from childhood pneumonia; systematic review and meta-analysis. *PLoS One*. (2012) 7:e31239. doi: 10.1371/journal.pone.0031239
28. Gentile A, Bardach A, Ciapponi A, Garcia-Marti S, Aruj P, Glujovsky D, et al. Epidemiology of community-acquired pneumonia in children of Latin America and the Caribbean: a systematic review and meta-analysis. *Int J Infect Dis*. (2012) 16:e5–15. doi: 10.1016/j.ijid.2011.09.013
29. Bortz G, Thomas H. Biotechnologies for inclusive development: scaling up, knowledge intensity and empowerment. (the case of the probiotic yoghurt 'Yogurito' in Argentina). *Innov Dev*. (2017) 7:37–61. doi: 10.1080/2157930X.2017.1281206
30. Sen A, Rothenberg ME, Mukherjee G, Feng N, Kalisky T, Nair N, et al. Innate immune response to homologous rotavirus infection in the small intestinal villous epithelium at single-cell resolution. *Proc Natl Acad Sci USA*. (2012) 109:20667–72. doi: 10.1073/pnas.1212188109
31. Hoffmann HH, Schneider WM, Rice CM. Interferons and viruses: an evolutionary arms race of molecular interactions. *Trends Immunol*. (2015) 36:124–38. doi: 10.1016/j.it.2015.01.004
32. Bass DM. Interferon gamma and interleukin 1, but not interferon alfa, inhibit rotavirus entry into human intestinal cell lines. *Gastroenterology*. (1997) 113:81–9. doi: 10.1016/S0016-5085(97)70083-0
33. Hakim MS, Ding S, Chen S, Yin Y, Su J, van der Woude CJ, et al. TNF-α exerts potent anti-rotavirus effects via the activation of classical NF-κB pathway. *Virus Res*. (2018) 253:28–37. doi: 10.1016/j.virusres.2018.05.022
34. Gandhi GR, Santos VS, Denadai M, da Silva Calisto VK, de Souza Siqueira Quintans J, de Oliveira e Silva AM, et al. Cytokines in the management of rotavirus infection: a systematic review of in vivo studies. *Cytokine*. (2017) 96:152–60. doi: 10.1016/j.cyto.2017.04.013
35. Broggi A, Tan Y, Granucci F, Zanoni I. IFN-λ suppresses intestinal inflammation by non-translational regulation of neutrophil function. *Nat Immunol*. (2017) 18:1084–93. doi: 10.1038/ni.3821
36. Zhou R, Wei H, Sun R, Tian Z. Recognition of double-stranded RNA by TLR3 induces severe small intestinal injury in mice. *J Immunol*. (2007) 178:4548–56. doi: 10.4049/jimmunol.178.7.4548
37. Araya RE, Jury J, Bondar C, Verdu EF, Chirdo FG. Intraluminal administration of Poly I:C causes an enteropathy that is exacerbated by administration of oral dietary antigen. *PLoS One*. (2014) 9:e99236. doi: 10.1371/journal.pone.0099236
38. Zhou R, Wei H, Sun R, Zhang J, Tian Z. NKG2D recognition mediates Toll-like receptor 3 signaling-induced breakdown of epithelial homeostasis in the small intestines of mice. *Proc Natl Acad Sci USA*. (2007) 104:7512–5. doi: 10.1073/pnas.0700822104
39. Clua P, Kanmani P, Zelaya H, Tada A, Humayun Kober AKM, Salva S, et al. Peptidoglycan from immunobiotic *Lactobacillus rhamnosus* improves resistance of infant Mice to respiratory syncytial viral infection and secondary pneumococcal pneumonia. *Front Immunol*. (2017) 8:948. doi: 10.3389/fimmu.2017.00948
40. Kanmani P, Clua P, Vizoso-Pinto MG, Rodriguez C, Alvarez S, Melnikov V, et al. Respiratory commensal bacteria *Corynebacterium pseudodiphtheriticum* improves resistance of infant mice to respiratory syncytial virus and *Streptococcus pneumoniae* superinfection. *Front Microbiol*. (2017) 8:1613. doi: 10.3389/fmicb.2017.01613
41. McNamara PS, Smyth RL. The pathogenesis of respiratory syncytial virus disease in childhood. *Br Med Bull*. (2002) 61:13–28. doi: 10.1093/bmb/61.1.13
42. Sun J, Cardani A, Sharma AK, Laubach VE, Jack RS, Müller W, et al. Autocrine regulation of pulmonary inflammation by effector T-cell derived IL-10 during infection with respiratory syncytial virus. *PLoS Pathog*. (2011) 7:e1002173. doi: 10.1371/journal.ppat.1002173
43. Loebbermann J, Schnoeller C, Thornton H, Durant L, Sweeney NP, Schuijs M, et al. Openshaw PJ. IL-10 regulates viral lung immunopathology during acute respiratory syncytial virus infection in mice. *PLoS One*. (2012) 7:e32371. doi: 10.1371/journal.pone.0032371
44. Salva S, Nuñez M, Villena J, Ramón A, Font G, Alvarez S. Development of a fermented goats' milk containing *Lactobacillus rhamnosus*: in vivo study of health benefits. *J Sci Food Agric*. (2011) 91:2355–62. doi: 10.1002/jsfa.4467
45. Villena J, Saavedra L, Hebert EM, Suda Y, Masumizu Y, Albarracin L, et al. Draft genome sequence of *Lactobacillus plantarum* MPL16, a wakame-utilizing immunobiotic strain isolated from swine feces. *Genome Announc*. (2017) 5:e00006–17. doi: 10.1128/genomeA.00006-17

**Conflict of Interest:** The authors declare that the research was conducted in the absence of any commercial or financial relationships that could be construed as a potential conflict of interest.

frontiers in Immunology

ORIGINAL RESEARCH
published: 09 April 2020
doi: 10.3389/fimmu.2020.00571

# Lipoteichoic Acid Is Involved in the Ability of the Immunobiotic Strain *Lactobacillus plantarum* CRL1506 to Modulate the Intestinal Antiviral Innate Immunity Triggered by TLR3 Activation

*Hiroya Mizuno[1†], Lorena Arce[2†], Kae Tomotsune[1,3], Leonardo Albarracin[1,4], Ryutaro Funabashi[1,3], Daniela Vera[2,5], Md. Aminul Islam[1,6], Maria Guadalupe Vizoso-Pinto[2,5], Hideki Takahashi[7], Yasuko Sasaki[8], Haruki Kitazawa[1,3]* and Julio Villena[1,4]**

[1] Food and Feed Immunology Group, Laboratory of Animal Products Chemistry, Graduate School of Agricultural Science, Tohoku University, Sendai, Japan, [2] Infection Biology Laboratory, Instituto Superior de Investigaciones Biológicas (INSIBIO), CONICET-UNT, Tucumán, Argentina, [3] Livestock Immunology Unit, International Education and Research Center for Food Agricultural Immunology, Graduate School of Agricultural Science, Tohoku University, Sendai, Japan, [4] Laboratory of Immunobiotechnology, Reference Centre for Lactobacilli (CERELA-CONICET), Tucuman, Argentina, [5] Laboratorio de Ciencias Básicas Or. Genética, Facultad de Medicina de la Universidad Nacional de Tucuman, Tucumán, Argentina, [6] Department of Medicine, Faculty of Veterinary Science, Bangladesh Agricultural University, Mymensingh, Bangladesh, [7] Plant Immunology Unit, International Education and Research Center for Food Agricultural Immunology, Graduate School of Agricultural Science, Tohoku University, Sendai, Japan, [8] Graduate School of Agriculture, Meiji University, Kawasaki, Japan

Studies have demonstrated that lipoteichoic acid (LTA) is involved in the immunomodulatory properties of some immunobiotic lactobacilli. The aim of this work was to evaluate whether LTA contributes to the capacity of *Lactobacillus plantarum* CRL1506 in modulating the intestinal innate antiviral immune response. A D-alanyl-lipoteichoic acid biosynthesis protein (*dltD*) knockout CRL1506 strain (*L. plantarum* Δ*dltD*) was obtained, and its ability to modulate Toll-like receptor (TLR)-3-mediated immune response was evaluated *in vitro* in porcine intestinal epithelial (PIE) cells and *in vivo* in Balb/c mice. Wild-type (WT) CRL1506 (*L. plantarum* WT) was used as positive control. The challenge of PIE cells with the TLR3 agonist poly(I:C) significantly increased interferon (IFN)-β, interleukin (IL)-6, and monocyte chemoattractant protein (MCP)-1 expressions. PIE cells pretreated with *L. plantarum* Δ*dltD* or *L. plantarum* WT showed higher levels of IFN-β while only *L. plantarum* WT significantly reduced the expression of IL-6 and MCP-1 when compared with poly(I:C)-treated control cells. The oral administration of *L. plantarum* WT to mice prior the intraperitoneal injection of poly(I:C) significantly increased IFN-β and IL-10 and reduced intraepithelial lymphocytes ($CD3^+NK1.1^+CD8\alpha\alpha^+$) and pro-inflammatory mediators (TNF-α, IL-6, and IL-15) in the intestinal mucosa. Similar to the WT strain, *L. plantarum* Δ*dltD*-treated mice showed enhanced levels of IFN-β after poly(I:C) challenge. However, treatment of mice with

OPEN ACCESS

**Edited by:**
*Caroline Elizabeth Childs, University of Southampton, United Kingdom*

**Reviewed by:**
*Marjolein Meijerink, Risk Analysis for Products in Development (TNO), Netherlands*
*Lei Shi, Georgia State University, United States*

***Correspondence:**
*Haruki Kitazawa*
*haruki.kitazawa.c7@tohoku.ac.jp*
*Julio Villena*
*jcvillena@cerela.org.ar*

*† These authors have contributed equally to this work*

**Specialty section:**
*This article was submitted to Nutritional Immunology, a section of the journal Frontiers in Immunology*

**Received:** *08 December 2019*
**Accepted:** *12 March 2020*
**Published:** *09 April 2020*

**Citation:**
*Mizuno H, Arce L, Tomotsune K, Albarracin L, Funabashi R, Vera D, Islam MA, Vizoso-Pinto MG, Takahashi H, Sasaki Y, Kitazawa H and Villena J (2020) Lipoteichoic Acid Is Involved in the Ability of the Immunobiotic Strain Lactobacillus plantarum CRL1506 to Modulate the Intestinal Antiviral Innate Immunity Triggered by TLR3 Activation. Front. Immunol. 11:571. doi: 10.3389/fimmu.2020.00571*

*L. plantarum* Δ*dltD* was not able to increase IL-10 or reduce $CD3^+NK1.1^+CD8\alpha\alpha^+$ cells, TNF-α, IL-6, or IL-15 in the intestine. These results indicate that LTA would be a key molecule in the anti-inflammatory effect induced by the CRL1506 strain in the context of TLR3-mediated inflammation.

**Keywords: immunobiotic, *D-alanyl-lipoteichoic acid biosynthesis protein* mutant, *Lactobacillus plantarum* CRL1506, intestinal immunity, lipoteichoic acid**

## INTRODUCTION

One of the fundamental problems of the world related to nutrition is the immunosuppression associated with malnutrition (1, 2). Undernutrition is one of the factors that contribute most to the global burden of disease, with increasing numbers affecting the most vulnerable populations in developing countries (2). More than a third of child deaths worldwide are attributed to malnutrition and its profound impact on the host resistance to infections. In this regard, diarrhea remains the leading cause of death of children, particularly in those with severe malnutrition (3). Although in recent years it has been possible to reduce infant mortality and morbidity resulting from rotavirus gastroenteritis, such infection is still a persistent problem worldwide and is one of the most common causes of hospitalization and mortality in children. Globally, at least 200,000 children under 5 years of age die of diarrhea every year due to the severe dehydration and electrolyte disorders caused by rotavirus infection (4). The majority of rotavirus-related deaths (>80%) are found in low-income countries, where there is a high prevalence of child malnutrition and limited access to medical care (5).

The World Health Organization has proposed a cohesive approach to end preventable diarrhea deaths in children (3). The plan proposes interventions to create healthy environments, promotes practices to protect children from infectious diseases, and ensures that all children have access to appropriate preventive and treatment measures. The document emphasizes the importance of healthy food and vaccination for the prevention of intestinal infections in children. In this regard, various clinical trials and animal model studies have demonstrated the ability of probiotic lactic acid bacteria (LAB) with immunomodulatory activities, also known as immunobiotics, to improve the resistance to intestinal viral infections (6–8). Although great advances have been made in the use of immunobiotics for the development of immunomodulatory functional foods or as adjuvants in experimental mucosal vaccines (6–8), deeper studies are still necessary to achieve a better understanding of their interaction with the immune system. Deeper knowledge of the cellular and molecular interactions of immunobiotics with host immune and non-immune cells could help in the selection of the most efficient strains and lay the scientific basis for their safe use, in particular in high-risk populations such as malnourished children.

Previous *in vitro* transcriptomic studies showed that *Lactobacillus plantarum* CRL1506 is able to modulate the expression of type I interferons (IFNs), antiviral factors, cytokines, chemokines, and adhesion molecules in porcine intestinal epithelial (PIE) cells challenged with the Toll-like receptor (TLR)-3 ligand poly(I:C) (9). In addition, studies in porcine antigen-presenting cells isolated from Peyer's patches demonstrated that the CRL1506 strain differentially modulated the expression of IFN-γ, interleukin (IL)-1β, IL-12, IL-6, and tumor necrosis factor (TNF)-α (10). Moreover, *L. plantarum* CRL1506 was able to activate porcine $CD172a^+CD11R1^{high}$ dendritic cells (DCs) and $CD172a^+CD11R1^-$ macrophages as demonstrated by the enhanced levels of the major histocompatibility complex (MHC)-II and co-stimulatory molecules CD80/86 (10). The patterns of IFNs, cytokines, and chemokines induced by *L. plantarum* CRL1506 in resident intestinal immune and non-immune cells allow us to predict an improved recruitment and activation of immune cells to the gut mucosa, which could beneficially influence the elimination of the virus. On the other hand, taking into consideration that the deregulated activation of immune cells and/or their excessive recruitment into the infected tissue could contribute to the local cellular damage in the context of viral infection, we also evaluated the ability of *L. plantarum* CRL1506 to protect against the TLR3-mediated intestinal inflammatory alterations. Our *in vivo* studies in mice demonstrated that orally administered CRL1506 strain, prior to the intraperitoneal challenge of animals with poly(I:C), significantly reduced the severity of intestinal damage triggered by TLR3 activation. The beneficial effect of the immunobiotic strain was related to its capacity of modulating the expression of IL-15 and retinoic acid early inducible-1 (RAE1) in epithelial cells and the activation of $CD3^+NK1.1^+CD8\alpha\alpha^+$ intraepithelial lymphocytes (IELs) (11).

In order to gain deeper knowledge of the bacterial molecules involved in the beneficial effects of *L. plantarum* CRL1506, in this work, we aimed to evaluate whether lipoteichoic acid (LTA) contributes to the capacity of the immunobiotic strain of modulating the intestinal innate antiviral immune response. A D-alanyl-lipoteichoic acid biosynthesis protein (*dltD*) knockout CRL1506 strain (*L. plantarum* Δ*dltD*) was obtained, and its ability to modulate TLR3-mediated immune response was evaluated *in vitro* and *in vivo*. Similar to the wild-type (WT) strain, the mutant *L. plantarum* Δ*dltD* was able to differentially modulate IFN-γ and IFN-β in response to poly(I:C) challenge *in vitro* and *in vivo*. However, *L. plantarum* Δ*dltD* was not able to increase IL-10 or reduce the inflammatory damage mediated by $CD3^+NK1.1^+CD8\alpha\alpha^+$ cells and IL-15 in the intestinal mucosa. The results of this work indicate that LTA would be a key molecule in the anti-inflammatory effect induced by *L. plantarum* CRL1506 in the context of TLR3-mediated inflammation.

# MATERIALS AND METHODS

## Microorganisms

*Lactobacillus plantarum* CRL1506 was obtained from the Reference Centre for Lactobacilli (CERELA CONICET) Culture Collection (Tucuman, Argentina). Cultures were kept freeze-dried and then rehydrated using the following medium: tryptone, 10.0 g; meat extract, 5.0 g; peptone, 15.0 g; and distilled water, 1 L, pH 7. Bacteria were cultured for 12 h at 37°C (final log phase) in Man–Rogosa–Sharpe broth (MRS, Oxoid, Cambridge, United Kingdom).

The mutant *D-alanyl-lipoteichoic acid biosynthesis protein* knockout *L. plantarum* CRL1506 strain (*L. plantarum* Δ*dltD*) was obtained according to the method described by Yamauchi et al. (12). Briefly, the *dltD* gene was obtained by PCR using primers No. 65 and No. 66 (**Table 1** and **Figure 1**). By using this gene fragment as a template, the 27-bp in-frame deletion of *dltD* was obtained by PCR using primers No.67 and No. 98, followed by primers No. 99 and No. 100. These fragments were combined by overlap PCR using No. 67 and No. 100 (**Table 1** and **Figure 1**). This fragment was digested by *Sac*I and *Kpn*I and then inserted into pSG$^+$E2 (thermo-sensitive replicon) that was obtained from the Food Research and Development Center, Meiji Dairies Corporation (Tokyo, Japan), by DNA Ligation Kit Ver1 (Takara Bio Inc., Japan) to generate the pSG$^+$dD plasmid. The construction of this vector was performed in *Lactococcus lactis* IL1403 (kindly given by the Food Research and Development Center, Meiji Dairies Corporation, Tokyo, Japan). The pSG$^+$dD was electroporated into *L. plantarum* CRL1506 according to the method described by De Keersmaecker et al. (13). A double crossover event was performed according to the method described by Biswas et al. (14) in order to obtain a Δ*dltD L. plantarum* CRL1506 strain. The 27-bp deletion in the *dltD* gene of CRL1506 mutant was confirmed by sequencing.

Scanning electron microscope (SEM) was used to analyze the bacterial surfaces of WT *L. plantarum* CRL1506 (*L. plantarum* WT) and *L. plantarum* Δ*dltD*. For this purpose, the bacteria were cultured for 16 h at 37°C in MRS broth and then centrifuged (6,000 × *g* for 5 min at 5°C), and the pellets were diluted 10-fold with phosphate buffered saline (PBS). Samples were dropped into membrane filter polycarbonate of 0.2 μm × 13 mm (ADVANTEC), and the bacterial cells were placed on the filter using suction filtration. These filters were allowed to stand in 2% glutaraldehyde for 1 h at room temperature to fix the cells. The samples were observed by SEM.

Western blot analysis and high-performance liquid chromatography (HPLC) were performed to analyze LTA in *L. plantarum* WT and *L. plantarum* Δ*dltD*. The collection of cell walls was performed according to the method described by Hirose et al. (15). The overnight cultures of WT and Δ*dltD* in MRS medium were added to fresh MRS medium and cultured at 37°C for 5 h (middle of log phase). The cultures were centrifuged at 6,000 × *g* for 5 min. PBS wash was performed twice, and the pellets were resuspended by PBS. Then, bacterial cells were disrupted by Micro Smash$^{TM}$ MS-100R (Tomy Seiko Co., Ltd., Japan) (4,500 rpm for 3 min on ice). The recovered liquid was centrifuged at 5,000 rpm for 20 min at 4°C, and the supernatant was centrifuged again at 40,000 rpm for 20 min at 4°C. These pellets were freeze dried. For Western blot analysis, anti-LTA antibody (Ab), Mouse Lipoteichoic Acid Monoclonal Antibody (GeneTex, Inc., United States) was used as primary Ab (1:500) for 16 h at 4°C and Alkaline Phosphatase AffiniPure Goat Anti-Mouse IgG (H + L) (Jackson ImmunoResearch Laboratories, Inc., United States) was used as secondary Ab (1:20,000) for 1 h at room temperature. The ECF reaction was performed for 5 min by using ECF Substrate for Western blotting (GE HealthCare, Inc., United States). For HPLC, acid hydrolysis of the samples was performed by the method described Hirose et al. (15). The samples were diluted in 6N hydrochloric acid (HCl) at 100°C for 15 h and were neutralized, added to equal volume of 75% (vol/vol) EtOH. These samples were loaded to HPLC in order to measure the concentration of alanine, glutamic acid, and diaminopimelic acid.

**TABLE 1 |** Sequence of the primers used in this study.

| Primer number | Sequence |
|---|---|
| No. 65 | GGACGTTAACCTGTTTGATGAAGGA |
| No. 66 | CCATCCTTTGCTTGATAGTGTAACTCTAC |
| No. 67 | ACACGGTACCGGGTTCCGTCCAACTTTTATTGGAA |
| No. 98 | CATCATCCAGCGCCTCGTTGGCTGACAAGG |
| No. 99 | CCTTGTCAGCCAACGAGGCGCTGGATGATG |
| No. 100 | CACAGAGCTCGCCCGCAATTCCAAAACGTG |
| No. 129 | GATGCATTGGATCAAATCGTG |

## Porcine Intestinal Epithelial Cells

The PIE cell line was originally derived from intestinal epithelia isolated from an unsuckled neonatal swine (16). PIE cells are intestinal non-transformed cultured cells that assume a monolayer with a cobblestone and epithelial-like morphology and with close contact between cells during culture (16–18). PIE cells were maintained in Dulbecco's modified Eagle's medium (DMEM) (Invitrogen Corporation, Carlsbad, CA) supplemented with 10% fetal calf serum (FCS), 100 mg/mL streptomycin and 100 U/mL penicillin at 37°C in an atmosphere of 5% $CO_2$ (9, 10, 18, 19).

## Immunomodulatory Effect of Lactobacilli in Porcine Intestinal Epithelial Cells

The study of the immunomodulatory capacity of *L. plantarum* WT and *L. plantarum* Δ*dltD* was performed in PIE cells as described previously (9, 10). PIE cells were seeded at 3 × $10^4$ cells per well in 12-well type I collagen-coated plates (Sumitomo Bakelite Co., Tokyo, Japan) and cultured for 3 days. After changing medium, lactobacilli (5 × $10^8$ cells/ml) were added, and 48 h later, each well was washed vigorously with medium at least three times to eliminate all stimulants. Then, cells were stimulated with poly(I:C) (60 μg/ml) for 12 h for RT-PCR studies.

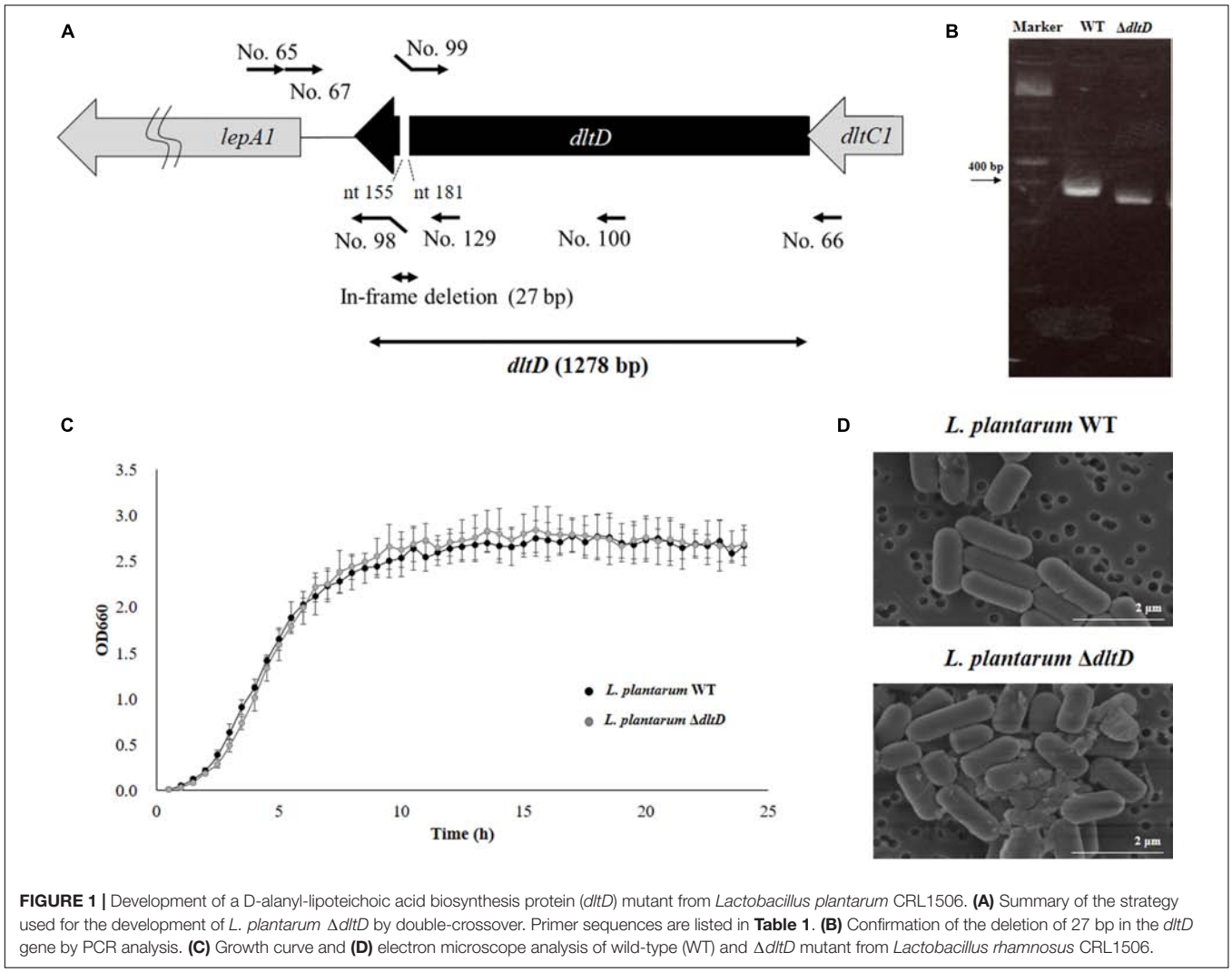


**FIGURE 1 |** Development of a D-alanyl-lipoteichoic acid biosynthesis protein (*dltD*) mutant from *Lactobacillus plantarum* CRL1506. **(A)** Summary of the strategy used for the development of *L. plantarum* Δ*dltD* by double-crossover. Primer sequences are listed in **Table 1**. **(B)** Confirmation of the deletion of 27 bp in the *dltD* gene by PCR analysis. **(C)** Growth curve and **(D)** electron microscope analysis of wild-type (WT) and Δ*dltD* mutant from *Lactobacillus rhamnosus* CRL1506.

## Quantitative Expression Analysis by Two-Step Real-Time Quantitative PCR

Two-step real-time quantitative PCR (qPCR) was performed to characterize the expression of selected genes in PIE cells as described previously (9). TRIzol reagent (Invitrogen) was used for total RNA isolation from each PIE cell sample, and Quantitect reverse transcription (RT) kit (Qiagen, Tokyo, Japan) was used for the synthesis of all cDNAs according to the manufacturer's recommendations. qPCR was carried out using a 7300 real-time PCR system (Applied Biosystems, Warrington, United Kingdom) and the Platinum SYBR green qPCR SuperMix uracil-DNA glycosylase (UDG) with 6-carboxyl-X-rhodamine (ROX) (Invitrogen). The primers used in this study were described before (9, 10, 20). The PCR cycling conditions were 2 min at 50°C, followed by 2 min at 95°C, and then 40 cycles of 15 s at 95°C, 30 s at 60°C, and 30 s at 72°C. The reaction mixtures contained 5 μl of sample cDNA and 15 μl of master mix, which included the sense and antisense primers. According to the minimum information for publication of quantitative real-time PCR experiments guidelines, β-actin was used as a housekeeping gene because of its high stability across porcine various tissues (17, 20, 21). Expression of β-actin was used to normalize cDNA levels for differences in total cDNA levels in the samples.

## Animals, Feeding Procedures, and Poly(I:C) Challenge

Male 6-week-old BALB/c mice were obtained from the closed colony kept at CERELA-CONICET (Tucuman, Argentina). Animals were housed in individual plastic cages in a controlled atmosphere (22°C ± 2°C temperature, 55% ± 2% humidity) with a 12-h light/dark cycle. *L. plantarum* WT and *L. plantarum* Δ*dltD* were orally administered to different groups of mice for five consecutive days at a dose of $10^8$ cells/mouse/day in a controlled volume of the drinking water supplemented with non-fat milk (10%) to ensure the complete consumption of the viable bacteria (22, 23). The treated groups and the untreated control mice were fed a conventional balanced diet *ad libitum*. Mice were challenged by the intraperitoneal route with 100 μl of PBS containing 30 μg poly(I:C) according to our previous publication (11). Biochemical markers of injury as well as intestinal cytokine concentrations

were evaluated 2 days after poly(I:C) administration as described below. All experiments were carried out in compliance with the Guide for Care and Use of Laboratory Animals and approved by the Ethical Committee of Animal Care at CERELA, Argentina (protocol number BIOT-CRL/14) (11).

## Biochemical Markers of Injury

Lactate dehydrogenase (LDH) and aspartate aminotransferase (AST) activities were determined in the serum to evaluate general toxicity of poly(I:C) in mice challenged by the intraperitoneal injection. Blood samples were obtained through cardiac puncture under anesthesia. LDH and AST activities, expressed as units per liter of serum, were determined by measuring the formation of the reduced form of nicotinamide adenine dinucleotide (NAD) using the Wiener reagents and procedures (Wiener Lab, Buenos Aires, Argentina) (11).

## Cytokine Concentrations

Serum samples were obtained as described before. Intestinal fluid samples were obtained according to our previous publication (11). Briefly, the small intestine was flushed with 5 ml of PBS and the fluid was centrifuged (10,000? × *g*, 4°C 10?min) to separate particulate material. The supernatant was kept frozen until use.

Tumor necrosis factor (TNF)-α, IL-6, IL-10, IL-15, IFN-β, and IFN-γ concentrations in serum and intestinal fluid samples were measured with commercially available enzyme-linked immunosorbent assay (ELISA) technique kits following the manufacturer's recommendations (R&D Systems, MN, United States).

## Total and Differential Blood Leukocyte Counts

The total number of leukocytes was determined with a hemocytometer. Differential cell counts were performed by counting 200 cells in blood smears stained with May Grünwald Giemsa stain using a light microscope (1,000×), and absolute cell numbers were calculated (24).

## Intestinal Intraepithelial Lymphocytes

Intraepithelial lymphocytes were isolated according to our previous publication (11). Briefly, Peyer's patches were excised; the small intestine was opened longitudinally and cut into 5-mm-long pieces. Samples were washed twice in PBS containing 150 μg/ml streptomycin and 120 U/ml penicillin. The pieces were then stirred at 37°C in prewarmed RPMI 1640 containing 150 μg/ml streptomycin, 120 U/ml penicillin, and 5% FCS for 30 min, followed by vigorous shaking for 40 s. This process was repeated, and the supernatants were passed through a small cotton-glass wool column to remove cell debris and were then separated on a Percoll density gradient (Amersham Biosciences). A discontinuous density gradient (40% and 70%) was used. The cells that layered between the 40% and 70% fractions were collected as IELs. These IELs contained >90% $CD3^+$ cells, as determined by fluorescence-activated cell sorting (FACS) analysis.

Cellular phenotypes in IEL populations were analyzed by flow cytometry using fluorescein isothiocyanate (FITC)-conjugated anti-CD3 and phycoerythrin (PE)-conjugated anti-NK1.1 (PK136) and anti-CD8α (CTCD8b) (R&D Systems). Anti-NKG2D (CX5) was purchased from eBioscience (San Diego, CA, United States). To prevent non-specific binding, respective isotype Abs were used as controls. Images of labeled cells were acquired on a BD FACSCalibur™ flow cytometer (BD Biosciences) and analyzed with FlowJo software (TreeStar).

## Statistical Analysis

Experiments were performed in triplicate, and results were expressed as mean ± standard deviation (SD). After verification of the normal distribution of data, two-way ANOVA was used. Tukey's test (for pairwise comparisons of the means) was used to test for differences between the groups. Differences were considered significant at $P < 0.05$ or $P < 0.01$.

# RESULTS

## Development of *L. plantarum* Δ*dltD*

*Lactobacillus plantarum* Δ*dltD* was produced by double-crossover (**Figure 1A**), and the deletion of 27-bp in the *dltD* gene was confirmed by PCR analysis (**Figure 1B**) and sequencing (data not shown). It has been reported that LTA mutations in lactobacilli can lead to modifications on growth, cell wall organization, cell morphology, or cell division. The Δ*dltD* mutant from *Lactobacillus rhamnosus* GG had defects in septum formation and an increased cell length (25), while the Δ*dltD* mutant from *L. plantarum* WCFS1 showed increased autolysis, defects in cell separation, and enhanced cell length (26). Then, the ability of the mutant strain *L. plantarum* Δ*dltD* to grow in MRS medium as well as its surface and shape characteristics were evaluated by comparing it with the WT *L. plantarum* CRL1506. As shown in **Figures 1C,D**, the deletion of 27 bp in the *dltD* gene did not affect the ability of *L. plantarum* Δ*dltD* to grow neither altered its shape or surface characteristics when compared to *L. plantarum* WT. Those results are in line with the findings of (27) that showed that the Δ*dltD* mutant from *L. acidophilus* NCFM had no growth or morphological defects.

In addition, LTA in WT and Δ*dltD* strains was analyzed by Western blot and HPLC. A reduction in LTA content (**Figure 2A**) as well as a decrease in the Ala/Glu ratio (**Figure 2B**) were found in *L. plantarum* Δ*dltD* when compared with the WT strain.

## Effect of *L. plantarum* Δ*dltD* in Toll-Like Receptor 3-Challenged Porcine Intestinal Epithelial Cells

In order to evaluate whether the alteration of the LTA in *L. plantarum* CRL1506 induced modifications on its immunomodulatory activities, we first studied *in vitro* its ability to functionally modulate immune factor expression in PIE cells after the activation of TLR3. For this purpose, PIE cells were treated with *L. plantarum* Δ*dltD* or *L. plantarum* WT and then challenged with the TLR3 agonist poly(I:C). The expressions of

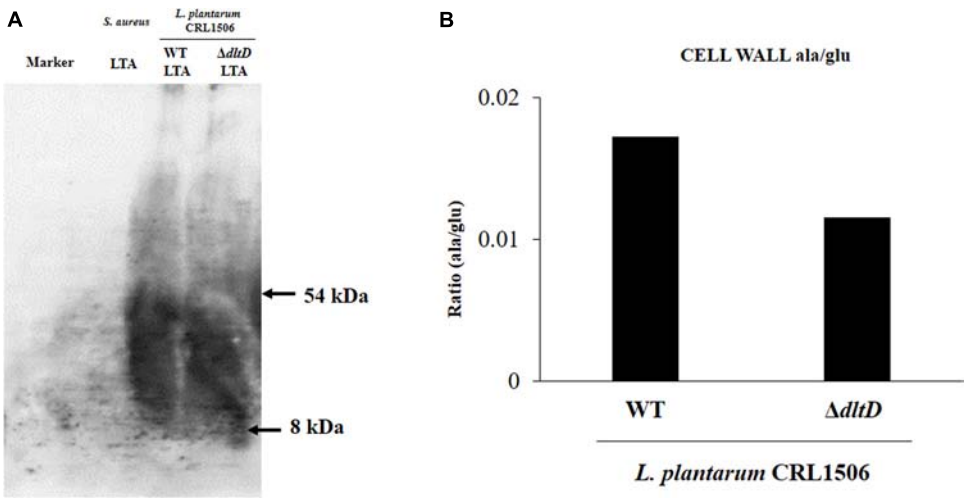


**FIGURE 2 |** Development of a D-alanyl-lipoteichoic acid biosynthesis protein (*dltD*) mutant from *Lactobacillus plantarum* CRL1506. Analysis of lipoteichoic acid (LTA) by **(A)** Western blot and **(B)** high-performance liquid chromatography (HPLC) (Ala/Glu ratio) in wild-type (WT) and Δ*dltD* mutant from *Lactobacillus rhamnosus* CRL1506.

*IFN*-β, *IL-6*, and *CCL2* were evaluated by qPCR (**Figure 3**). As it was described previously (9, 10), the treatment of PIE cells with *L. plantarum* WT significantly increased the expression of IFN-β, while a decrease in the mRNA levels of *IL-6* and *CCL2* was observed. No differences between Δ*dltD* and WT strains were found when the expression of *IFN*-β was compared. However, the expression of both *IL-6* and *CCL2* were significantly higher in Δ*dltD*-treated PIE cells when compared to those stimulated with *L. plantarum* WT (**Figure 3**).

## Effect of *L. plantarum*Δ*dltD* in Toll-Like Receptor 3-Induced Inflammatory Damage in Mice

Taking into consideration that the *in vitro* studies suggested that the alteration of LTA in *L. plantarum* CRL1506 would also alter its anti-inflammatory properties, we next aimed to evaluate whether *L. plantarum*Δ*dltD* was able to modulate the intestinal inflammatory response and protect against the damage induced by TLR3 activation by using an *in vivo* model. Then, different groups of mice were fed *L. plantarum*Δ*dltD* or *L. plantarum* WT and then challenged with the TLR3 agonist poly(I:C) as described in *Materials and Methods*. We evaluated body weight loss and the biochemical markers LDH and AST in serum to study the general health status of mice after poly(I:C) administration (**Figure 4**). As it was reported previously (11), poly(I:C) challenge significantly decreased the body weight gain and increased the levels of serum LDH and AST. Mice treated with *L. plantarum* WT showed reduced levels of injury biochemical markers and improved body weight gain when compared to control mice (**Figure 4**). On the other hand, mice treated with *L. plantarum*Δ*dltD* showed levels of serum LDH that were not different from those observed in the control group. In addition, the mutant strain was able to reduce the alteration of body weight gain and the levels of serum AST, but its effect was significantly lower when compared to *L. plantarum* WT (**Figure 4**).

Total and differential blood leukocyte counts were also evaluated to study the systemic inflammatory response. Challenge with poly(I:C) significantly increased the number of leukocytes and neutrophils in blood. However, the numbers of neutrophils were lower in *L. plantarum* WT-treated mice when compared to the *L. plantarum*Δ*dltD* and control groups (**Figure 5**).

## Effect of *L. plantarum*Δ*dltD* on the Innate Immune Response Induced by Toll-Like Receptor 3

The intraperitoneal administration of poly(I:C) significantly increased the levels of pro-inflammatory cytokines in the intestine (**Figure 6**) and serum (**Figure 7**). Both *L. plantarum*Δ*dltD* and *L. plantarum* WT were able to improve the production of the antiviral factors IFN-β and IFN-γ in the intestine and serum when compared to control mice and with no differences between lactobacilli. As reported previously (11), *L. plantarum* WT significantly reduced the concentrations of TNF-α, IL-6, and IL-15 in intestinal fluid (**Figure 6**) and serum (**Figure 7**). *L. plantarum*Δ*dltD* was as effective as the WT strain to diminish the concentrations of serum TNF-α (**Figure 7**). In addition, *L. plantarum*Δ*dltD* was able to reduce the levels of intestinal IL-15, but it was not efficient as the WT strain (**Figure 6**). The levels of intestinal TNF-α and IL-6 (**Figure 6**) as well as serum IL-6 and IL-15 (**Figure 7**) in Δ*dltD*-treated mice were not different from controls.

Only *L. plantarum* WT treatment was able to significantly increase the levels of intestinal and serum IL-10, while the concentrations of this regulatory cytokine in *L. plantarum*Δ*dltD*-treated mice were not different from controls (**Figures 6**, 7).

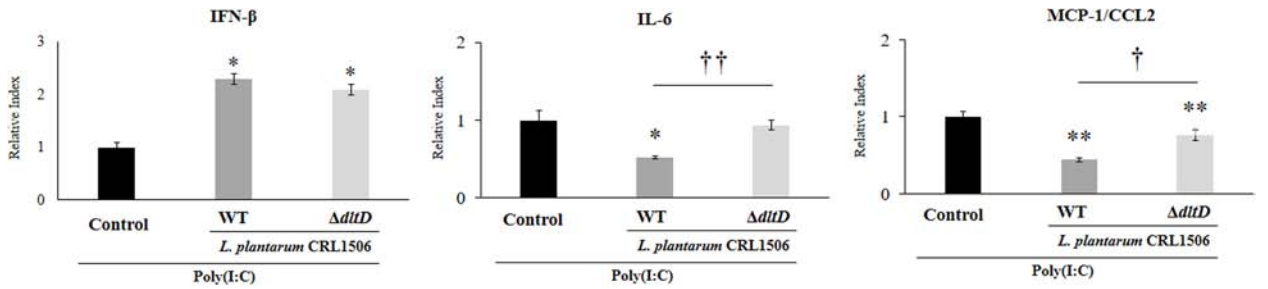


**FIGURE 3 |** Effect of a D-alanyl-lipoteichoic acid biosynthesis protein (*dltD*) mutant from *Lactobacillus plantarum* CRL1506 on innate antiviral immune response triggered by Toll-like receptor 3 (TLR3) activation in porcine intestinal epithelial (PIE) cells. Expression of interferon (*IFN*)-β, interleukin (*IL*)-*6*, and monocyte chemoattractant protein (*MCP*)-*1/CCL2* genes in PIE cells treated with wild-type (WT) or Δ*dltD* mutant from *Lactobacillus rhamnosus* CRL1506 and challenged with the viral molecular associated pattern poly(I:C). PIE cells with no lactobacilli treatment and stimulated with poly(I:C) were used as controls. The results represent data from three independent experiments. Significant differences when compared to the control group: $^{*}P < 0.05$, $^{**}P < 0.01$. Significant differences when compared to the indicated group: $^{\dagger}P < 0.05$, $^{\dagger\dagger}P < 0.01$.

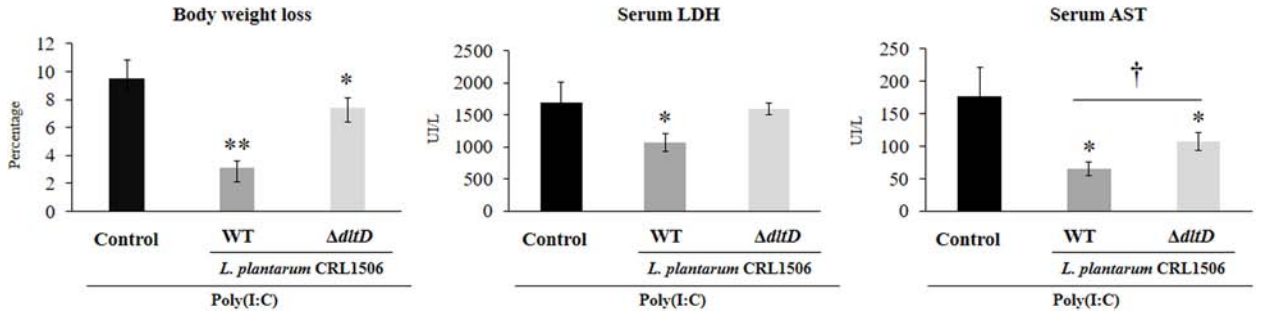


**FIGURE 4 |** Effect of a D-alanyl-lipoteichoic acid biosynthesis protein (*dltD*) mutant from *Lactobacillus plantarum* CRL1506 on the inflammatory damage induced by Toll-like receptor 3 (TLR3) activation in mice intestine. Body weight loss and serum biochemical markers lactate dehydrogenase (LDH) and aspartate aminotransferase (AST) in mice orally treated with wild-type (WT) or Δ*dltD* mutant from *L. rhamnosus* CRL1506 and challenged with an intraperitoneal injection of the viral molecular associated pattern poly(I:C). Mice with no lactobacilli treatment and challenged with poly(I:C) were used as controls. The results represent data from three independent experiments. Significant differences when compared to the control group: $^{*}P < 0.05$, $^{**}P < 0.01$. Significant differences when compared to the indicated group: $^{\dagger}P < 0.05$.

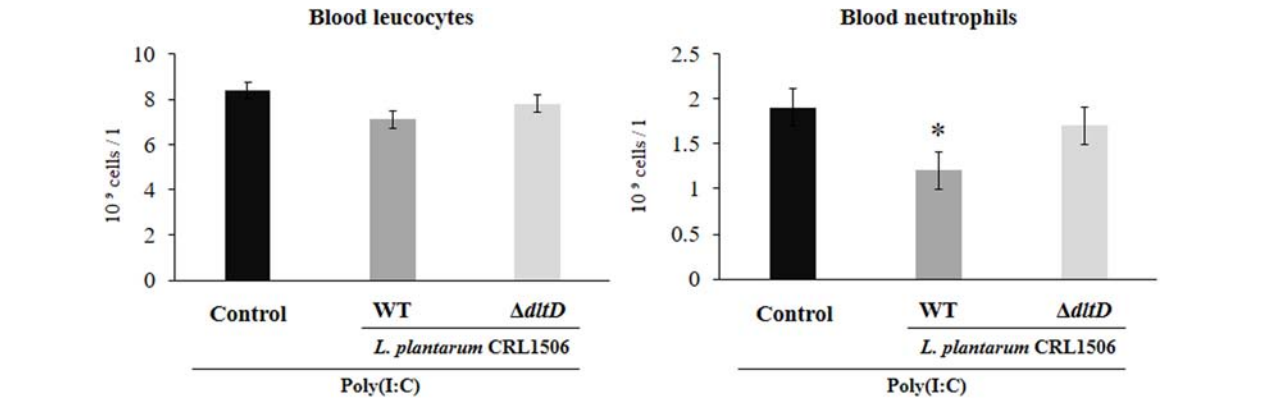


**FIGURE 5 |** Effect of a D-alanyl-lipoteichoic acid biosynthesis protein (*dltD*) mutant from *Lactobacillus plantarum* CRL1506 on the inflammatory response induced by Toll-like receptor 3 (TLR3) activation in mice intestine. Blood leukocyte and neutrophil counts in mice orally treated with wild-type (WT) or Δ*dltD* mutant from *Lactobacillus rhamnosus* CRL1506 and challenged with an intraperitoneal injection of the viral molecular associated pattern poly(I:C). Mice with no lactobacilli treatment and challenged with poly(I:C) were used as controls. The results represent data from three independent experiments. Significant differences when compared to the control group: $^{*}P < 0.05$.

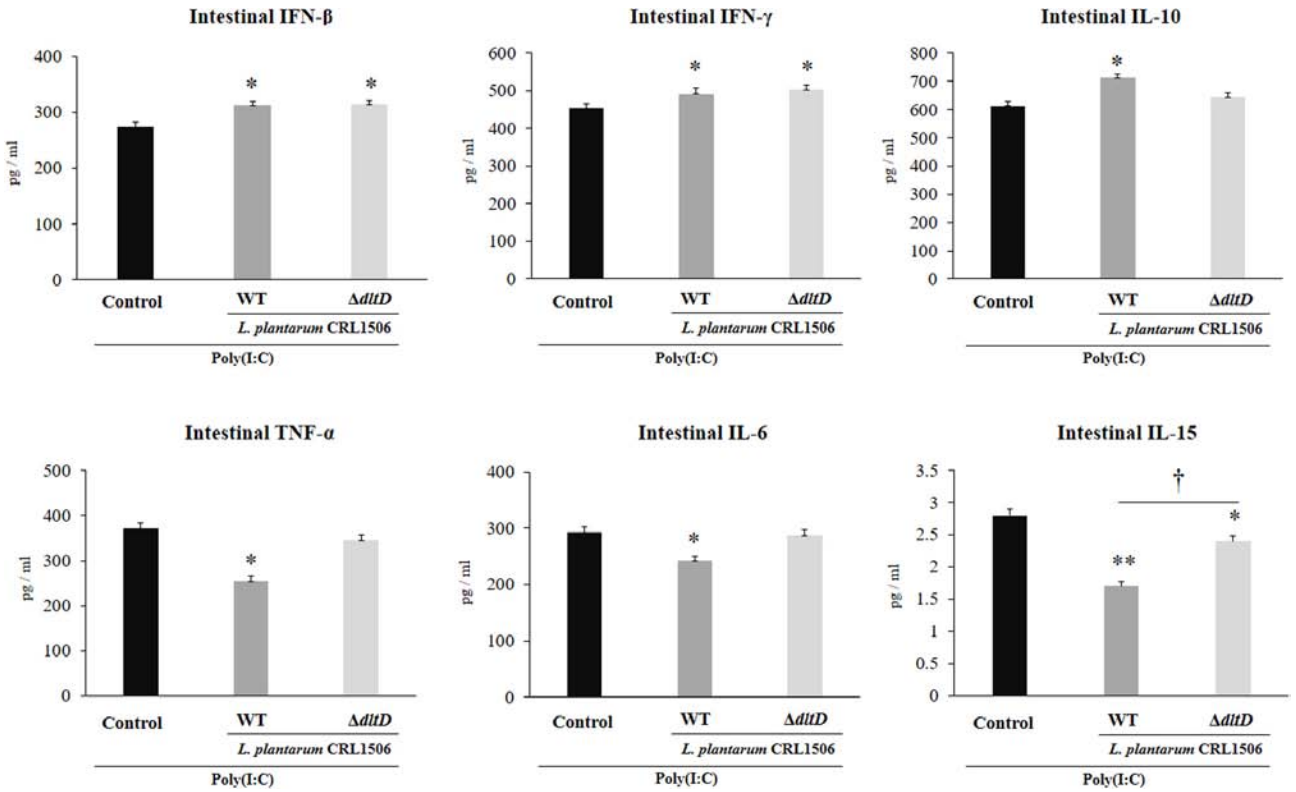


**FIGURE 6 |** Effect of a D-alanyl-lipoteichoic acid biosynthesis protein (*dltD*) mutant from *Lactobacillus plantarum* CRL1506 on the innate antiviral immune response triggered by Toll-like receptor 3 (TLR3) activation in mice intestine. Levels of intestinal interferon (IFN)-β, IFN-γ, interleukin (IL)-10, tumor necrosis factor (TNF)-α, IL-6, and IL-15 in mice orally treated with wild-type (WT) or Δ*dltD* mutant from *Lactobacillus rhamnosus* CRL1506 and challenged with an intraperitoneal injection of the viral molecular associated pattern poly(I:C). Mice with no lactobacilli treatment and challenged with poly(I:C) were used as controls. The results represent data from three independent experiments. Significant differences when compared to the control group: $^{*}P < 0.05$, $^{**}P < 0.01$. Significant differences when compared to the indicated group: $^{\dagger}P < 0.05$.

Finally, we assessed the changes in the populations of intestinal IELs in mice challenged with the TLR3 agonist poly(I:C). For this purpose, we studied variations in $CD3^{+}NK1.1^{+}$ and $CD3^{+}CD8\alpha\alpha^{+}$ populations as well as NKG2D expression within IELs by flow cytometry. Poly(I:C) administration induced an increase in all these three parameters evaluated (**Figure 8**). *L. plantarum* WT-treated mice showed significantly decreased numbers of intestinal $CD3^{+}NK1.1^{+}$ and $CD3^{+}CD8\alpha\alpha^{+}$ cells and NKG2D expression when compared to controls. On the contrary, the treatment of mice with *L. plantarum*Δ*dltD* was not able to reduce the numbers of $CD3^{+}CD8\alpha\alpha^{+}$ cells (**Figure 8**). The Δ*dltD* strain reduced the numbers of $CD3^{+}NK1.1^{+}$ cells and the expression of NKG2D, but those parameters were significantly higher than those observed in WT-treated mice (**Figure 8**). We also evaluated the expression of the NKG2D ligand RAE1 by qPCR. TLR3 activation increased the expression of RAE1 in all the experimental groups (**Figure 8**). Both *L. plantarum*Δ*dltD* and *L. plantarum* WT were able to reduce RAE1 expression in the intestinal tissue of mice; however, the levels of expression in WT-treated mice were significantly lower than those observed in Δ*dltD*-treated animals (**Figure 8**).

## DISCUSSION

Research from the last decade investigating the immunobiotic effector molecules has demonstrated that each individual immunobiotic strain has a characteristic set of molecules, which are responsible of its interaction with the host's immune receptors (28–30). Surface molecules of immunobiotic microorganisms, including exopolysaccharides, cell wall peptidoglycan, and LTA, have been frequently associated with their immunomodulatory effects (28, 29, 31, 32). In this regard, several reports have emphasized the importance of LTA in the immunomodulatory properties of some probiotic lactobacilli.

A Δ*dltD* mutant from *L. plantarum* WCFS1, affected in the LTA biosynthesis pathway, was found to incorporate much less D-Ala in its LTA than the WT strain (33). The D-Ala content defect in the LTA significantly altered the immunomodulatory ability of the Δ*dltD* mutant from WCFS1 strain. The mutant showed a higher anti-inflammatory activity when compared to the parental strain in both *in vitro* and *in vivo* studies. The Δ*dltD* mutant from *L. plantarum* WCFS1 was more efficient than the WT strain to improve IL-10 production and reduce TNF-α, IL-12, and IFN-γ in human PBMCs and monocytes.

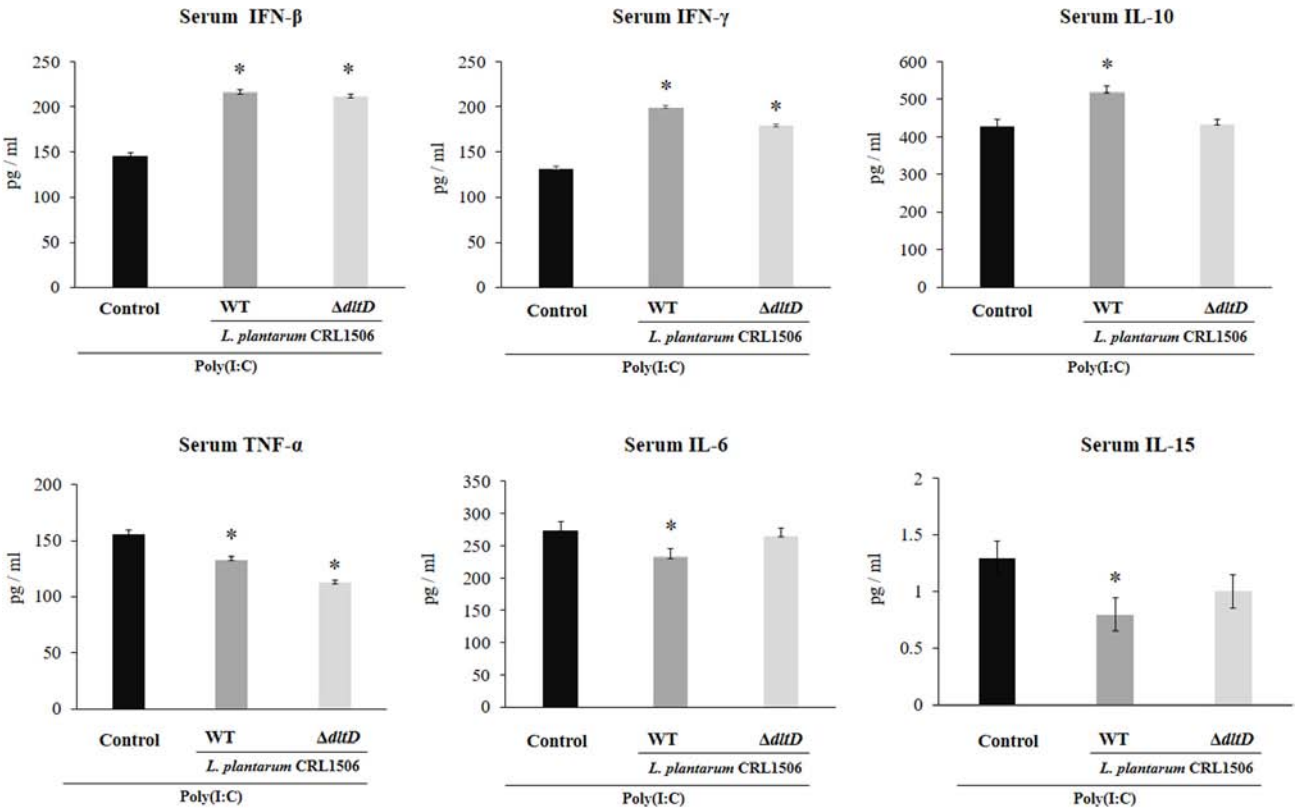


**FIGURE 7 |** Effect of a D-alanyl-lipoteichoic acid biosynthesis protein (*dltD*) mutant from *Lactobacillus plantarum* CRL1506 on the innate antiviral immune response triggered by Toll-like receptor 3 (TLR3) activation in mice intestine. Levels of serum interferon (IFN)-β, IFN-γ, interleukin (IL)-10, tumor necrosis factor (TNF)-α, IL-6, and IL-15 in mice orally treated with wild-type (WT) or Δ*dltD* mutant from *Lactobacillus rhamnosus* CRL1506 and challenged with an intraperitoneal injection of the viral molecular associated pattern poly(I:C). Mice with no lactobacilli treatment and challenged with poly(I:C) were used as controls. The results represent data from three independent experiments. Significant differences when compared to the control group: $^*P < 0.05$.

In addition, the treatment of mice with the Δ*dltD* mutant from *L. plantarum* WCFS1 significantly reduced the percentage of mice displaying diarrhea after trinitrobenzene sulfonic acid (TNBS) administration when compared with animals receiving the *L. plantarum* WT strain (33). Other reports provided similar results for *L. acidophilus* NCFM (27) and *L. rhamnosus* GG (34) in which LTA mutant strains improved the production of anti-inflammatory cytokines in immune cells and reduced the severity of dextran sulfate sodium (DSS)-induced colitis in mice. Those results indicated that LTA from some lactobacilli strains have immune stimulatory effects. In line with this assumption, it was demonstrated that LTA from *L. fermentum* YIT0159 and *L. casei* YIT9029 induces TNF-α expression in macrophages (35).

In contrast to the pro-inflammatory properties of lactobacilli LTA, others works reported that those molecules have anti-inflammatory activities in some *Lactobacillus* strains. The LTA from *L. plantarum* K8 was a weaker inducer of nitric oxide (NO) and TNF-α in macrophages when compared with the LTA from *Bacillus subtilis* or *Staphylococcus aureus* (36). The LTA from the K8 strain was able to act as an antagonist in the induction of TNF-α by monocytes challenged with lipopolysaccharide (LPS) (37), peptidoglycan of *Shigella flexneri* (38), or LTA from *S. aureus* (39). Moreover, the purified LTA from *L. plantarum* K8 differentially modulated the response of human keratinocytes to the stimulation with TNF-α or IFN-γ (40). LTA-treated keratinocytes had a significantly reduced activation of TNF-α/p65/p38 and IFN-γ/STAT1/2/JAK2 pathways with a subsequent reduced expression of inflammatory factors such as the complement protein C3. It was also described that the LTA from *L. plantarum* K8 had the ability to regulate the TLR2-triggered inflammatory response in intestinal epithelial cells (IECs). Caco-2 cells treated with *L. plantarum* K8 LTA and then challenged with the TLR2 agonist Pam2CSK4 showed significantly lower expression of IL-8 when compared to control cells (41). *In vivo* studies also support the anti-inflammatory activities of LTA from lactobacilli. *L. casei* BL23 had been shown to exert beneficial effects in the DSS-induced murine model of ulcerative colitis, and it was reported that the Δ*dltD* mutant from the BL23 strain was unable to protect against the inflammatory damage induced by DSS (42).

These contrasting results could be explained by the chemical and structural differences of LTA molecules. Chemical and

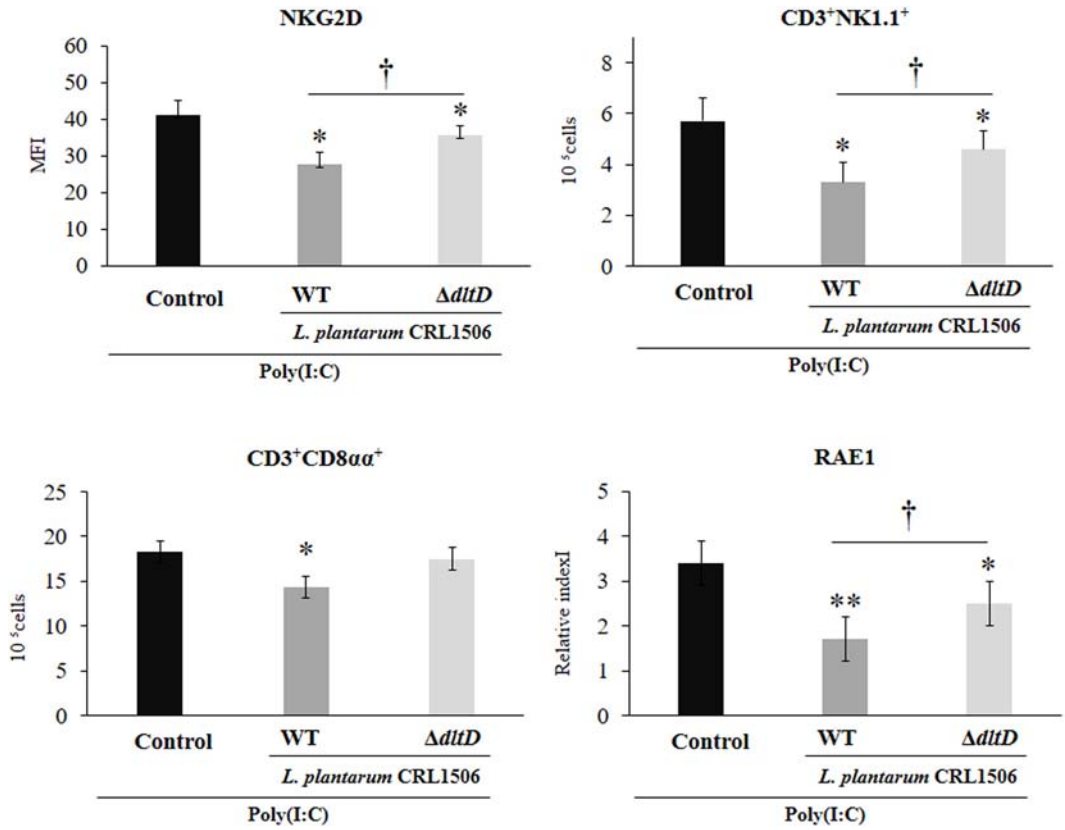


**FIGURE 8 |** Effect of a D-alanyl-lipoteichoic acid biosynthesis protein (*dltD*) mutant from *Lactobacillus plantarum* CRL1506 on the innate antiviral immune response triggered by Toll-like receptor 3 (TLR3) activation in mice intestine. Numbers of $CD3^+NK1.1^+$ and $CD3^+CD8\alpha\alpha^+$ intraepithelial lymphocytes (IELs), expression of NKG2D on IELs, and expression of intestinal *RAE1* gene in mice orally treated with wild-type (WT) or Δ*dltD* mutant from *Lactobacillus rhamnosus* CRL1506 and challenged with an intraperitoneal injection of the viral molecular associated pattern poly(I:C). Mice with no lactobacilli treatment and challenged with poly(I:C) were used as controls. The results represent data from three independent experiments. Significant differences when compared to the control group: $^*P < 0.05$, $^{**}P < 0.01$. Significant differences when compared to the indicated group: $^\dagger P < 0.05$.

molecular studies of LTA highlighted the variety in their structure by means of the number of acyl chains and the degree of saturation in the lipid chain as well as the D-ala or sugars substitutions on the Gro-P chains (43) that could explain their differential immunomodulatory effects. In addition, it should be considered that the immunomodulatory activities of LTA derived from lactobacilli have been studied in different contexts of cytokine- or bacteria-induced inflammatory responses, adding additional complexity to the interpretations. Of note, the potential beneficial effect of LTA from lactobacilli in the context of viral infection or viral pattern recognition receptors-mediated inflammation has not been explored in depth.

In an interesting study performed by Kim et al. (44), it was demonstrated that the LTA isolated from *L. plantarum* K8 was able to regulate mitogen-activated protein kinase (MAPK) phosphorylation and nuclear factor (NF)-κB activation and reduce IL-8 production in IPEC-J2 cells in response to the challenge with the TLR3 agonist poly(I:C). The work also demonstrated that LTA isolated from other lactobacilli strains including *L. delbrueckii*, *L. sakei*, and *L. rhamnosus* GG did not have the ability to differentially modulate IL-8 secretion in poly(I:C)-challenged IECs. Moreover, comparative studies evaluating the immunomodulatory potential of naive LTA and dealanylated LTA from *L. plantarum* K8 clearly showed that the dealanylated LTA failed to inhibit IL-8 secretion in IECs after the activation of TLR3. In line with these previous results, we demonstrated in this work that the LTA is involved in the ability of the immunobiotic strain *L. plantarum* CRL1506 to reduce the expression of pro-inflammatory factors in IECs challenged with poly(I:C). Previously, we demonstrated that PIE cells are able to upregulate the expression of several inflammatory factors including *TNF*-α, *IL-6* (9, 10), *IL-1*β, *IL-15*, and the chemokines *CCL4*, *CXCL2*, *CXCL5*, *CCL8*, *CXCL10*, and *CCL5* (9) in response to poly(I:C) challenge. We also reported that PIE cells treated with *L. plantarum* CRL1506 prior to TLR3 activation had a reduced expression of inflammatory cytokines and chemokines (9, 10). Here, by using the expression of *IL-6* and *CCL2* as markers of inflammation, we demonstrated that the alteration in the incorporation of D-ala in the LTA molecule of *L. plantarum* CRL1506 significantly diminished the ability of the immunobiotic strain to modulate inflammatory factor expression.

Moreover, this work is the first in demonstrating in an *in vivo* model the role of LTA from an immunobiotic strain in the beneficial modulation of the intestinal innate antiviral immune response triggered by TLR3 activation. We demonstrated previously that *L. plantarum* CRL1506 reduced the TLR3-induced small intestinal injury in mice by regulating the production of pro-inflammatory cytokines and the interaction of IECs with IELs (11) (**Figure 9**). Cell–cell interaction between IECs and IELs is essential as a first line of defense against viruses (45–47). In the context of viral infection, the cell death program of IECs is regulated by their upregulation in the expression of IL-15, which is a cytokine capable of stimulating the activation of $CD3^+NK1.1^+$ IELs and inducing perforin-mediated killing of virus-infected epithelial cells (46). The activation of TLR3 in the intestinal tract of mice enhances the expression of RAE1 in IECs, allowing their destruction by interacting with NKG2D expressed on $CD3^+NK1.1^+$ IELs (48). This mechanism of small intestinal injury that induces villous atrophy and mucosal erosion (49) is particularly relevant for rotavirus infection since it was reported that treatment of mice with poly(I:C) or purified dsRNA from rotavirus increased intestinal injury in a $CD8\alpha\alpha^+NKG2D^+$- and RAE1-dependent manner (48, 49). In fact, blockade of RAE1-NKG2D interaction avoids the cytotoxic effect of IELs on IECs and prevents acute small intestinal injury in mice challenged with rotavirus genomic dsRNA (48). Of interest, the oral administration of *L. plantarum* CRL1506 to mice prior the intraperitoneal challenge with poly(I:C) significantly reduced the inflammatory-mediated intestinal tissue damage through the downregulation of TNF-α, IL-1β, and IL-8, particularly IL-15 and RAE1, and the reduction of the numbers and activation ($NKG2D^+$ expression) of $CD3^+NK1.1^+CD8\alpha\alpha^+$ cells (11). Here, we observed that *L. plantarum*Δ*dltD* had a reduced capacity for the protection of mice against the TLR3-mediated inflammatory damage as demonstrated by the analysis of body weight loss and serum markers of damage. Moreover, we observed that the Δ*dltD* mutant from *L. plantarum* CRL1506 was inefficient for reducing the expression of IL-15 and RAE1 in IECs or the expression of NKG2D in IELs (**Figure 9**), indicating that the LTA from this immunobiotic strain is the main molecule involved in their ability to regulate IL-15/RAE1/NKG2D death pathway.

It was reported that the expression of NKG2D ligands such as RAE1 on IECs is strongly modulated by the intestinal microbiota.

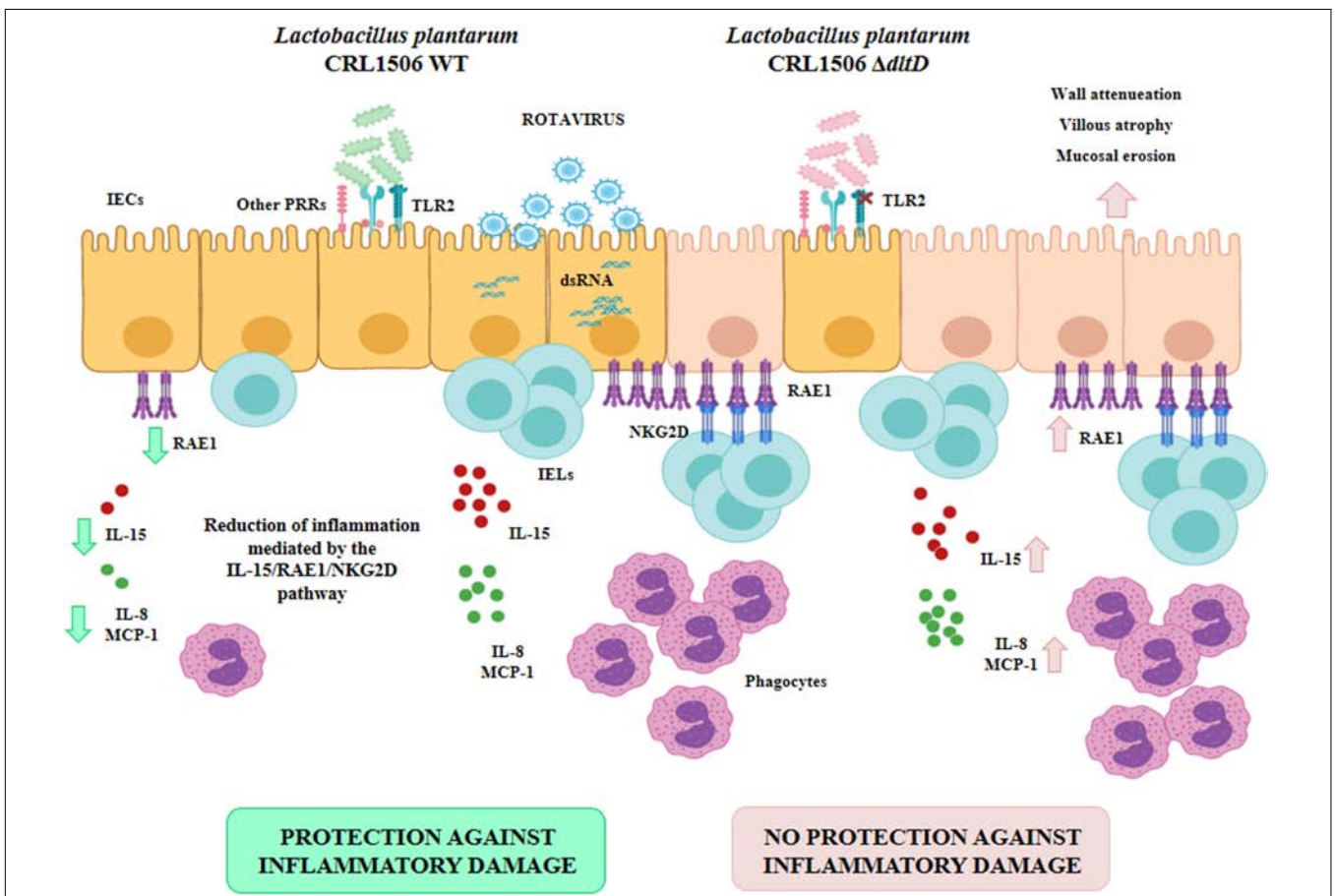


**FIGURE 9 |** Role of lipoteichoic acid in the beneficial effects *Lactobacillus plantarum* CRL1506 on the innate antiviral immune response triggered by Toll-like receptor 3 (TLR3) activation in the intestine.

Studies in germ-free mice and ampicillin-treated mice lacking gut commensal microbiota demonstrated that the absence of microbial stimuli significantly upregulates the expression of NKG2D ligands in IECs (50). Then, taking into consideration the results of this work, it is tempting to speculate that LTA would be at least one of the molecules used by the gut microbiota to regulate the innate antiviral immune response in the intestinal tract. In support of this assumption, it was shown that gut commensal bacteria help in the establishment of a regulatory milieu in the intestinal mucosa by increasing the expression of IL-10 and TGF-β, which diminish the expression of NKG2D ligands on the surface of IECs (51, 52). Of note, *L. plantarum* CRL1506 is able to improve the intestinal levels of IL-10 in poly(I:C)-challenged mice, while the Δ*dltD* mutant from CRL1506 strain was inefficient for inducing this effect. The molecular mechanisms and specific importance of LTA from microbiota and immunobiotic strains in the protection against viral inflammatory-mediated intestinal damage require further research.

Interestingly, although the *L. plantarum* CRL1506 Δ*dltD* was less efficient in regulating the TLR3-mediated inflammatory response in both *in vitro* and *in vivo* experiments, the mutant strain was as efficient as the WT to improve the levels of IFN-β in the intestine. It was reported that the LTA of probiotic bacteria mediates its immunomodulatory activities in a TLR2-dependent manner (33, 37, 39). Our previous studies evaluating the interaction of *L. plantarum* CRL1506 with IECs demonstrated that TLR2 is involved in the ability of the strain to differentially modulate cytokines in response to TLR3 activation (10). The use of anti-TLR2 Abs inhibited the ability of the CRL1506 strain to modulate *TNF*-α and *IL-6* transcripts in PIE cells. However, when blocking anti-TLR2 Abs were used to evaluate the influence of *L. plantarum* CRL1506 on the production of IFN-β in PIE cells, it was evident that this receptor was not involved in the modulation of this antiviral factor (10). Those previous findings and the results presented here indicate that TLR2 should be linked to the effect of biologically active LTA on IECs, but that other host receptors and microbial molecules might also be involved in *L. plantarum* CRL1506 recognition by the intestinal epithelium, and in its beneficial influence on intestinal innate antiviral immune response. In addition, our results demonstrated that *L. plantarum* CRL1506 Δ*dltD* was as effective as the WT to reduce the serum levels of AST and TNF-α and improve serum IFN-γ in poly(I:C)-challenged mice. It have been proposed that the systemic effects of orally administered probiotics are mediated mainly by the interaction of these beneficial microbes with innate immune cells such as macrophages. In the analyses of the profiles of cytokines induced by probiotic lactobacilli, it was observed that changes in serum cytokines reflected their production by intestinal and peritoneal macrophages (53, 54). Therefore, it is tempting to speculate that both Δ*dltD* and WT strains from *L. plantarum* CRL1506 would have the same capacity to modulate macrophage activity and that the TRL2-LTA interaction would not be involved in such modulation. More detailed experiments evaluating the interaction of both Δ*dltD* and WT strains with macrophages would be of great importance to improve our understanding of the role of LTA in the immunomodulatory activity of *L. plantarum* CRL1506.

In conclusion, although further studies are needed to elucidate all the active bacterial components responsible for the immunomodulatory capacities of *L. plantarum* CRL1506, the results of this work indicate that LTA is an important molecule involved in the immunobiotic effects induced by this strain in the intestinal innate antiviral immune response triggered by TLR3 activation. In line with previous studies (27, 33, 34), our results also indicate that the use of immunobiotic mutants carrying directed mutations could help to improve the understanding of the molecular interactions of immunobiotics with the host immune system and how that interaction beneficially modulates the innate antiviral immune response. This study is an important step toward insights in the mode of action of immunobiotics and their influence in the protection against viral-mediated inflammation.

## DATA AVAILABILITY STATEMENT

The datasets generated for this study are available on request to the corresponding author.

## ETHICS STATEMENT

The animal study was reviewed and approved by the Ethical Committee of Animal Care at CERELA, Argentina.

## AUTHOR CONTRIBUTIONS

JV, YS, and HK designed the study. JV and HK contributed to the manuscript writing. HM, LoA, KT, LeA, and RF did the laboratory work. MI and LeA did the statistical analysis. MV-P, HT, YS, HK, and JV contributed to the data analysis and interpretation. All authors read and approved the manuscript.

## FUNDING

This study was supported by ANPCyT–FONCyT Grant PICT-2016-0410 to JV. This study was supported by a Grant-in-Aid for Scientific Research (A) (19H00965) and Open Partnership Joint Projects of JSPS Bilateral Joint Research Projects from the Japan Society for the Promotion of Science (JSPS) to HK. This research was supported by grants from the project of NARO Bio-oriented Technology Research Advancement Institution (research program on the development of innovative technology, No. 01002A) to HK. This work was also supported by JSPS Core-to-Core Program, A. Advanced Research Networks entitled Establishment of international agricultural immunology research-core for a quantum improvement in food safety. This study was also supported by grants for Scientific Research on Innovative Areas from the Ministry of Education, Culture, Science, Sports, and Technology (MEXT) of Japan (16H06429, 16K21723, and 16H06435) to HT.

## REFERENCES


1. de Heredia FP, Gómez-Martínez S, Marcos A. Obesity, inflammation and the immune system. *Proc Nutr Soc*. (2012) 71:332–8. doi: 10.1017/s0029665112000092
2. Rytter MJH, Kolte L, Briend A, Friis H, Christensen VB. The immune system in children with malnutrition – a systematic review. *PLoS One*. (2014) 9:e105017. doi: 10.1371/journal.pone.0105017
3. WHO/UNICEF *Ending Preventable Deaths from Pneumonia and Diarrhoea by 2025*. New York, NY: UNICEF. (2013).
4. Tate JE, Burton AH, Boschi-Pinto C, Parashar UD, Agocs M, Serhan F, et al. Global, regional, and national estimates of rotavirus mortality in children <5 years of age, 2000-2013. *Clin Infect Dis*. (2016) 62(Suppl. 2):S96–105. doi: 10.1093/cid/civ1013
5. Lin C-L, Chen S-C, Liu S-Y, Chen K-T. Disease caused by *Rotavirus* infection. *Open Virol J*. (2014) 8:14–9. doi: 10.2174/1874357901408010014
6. Kitazawa H, Villena J. Modulation of respiratory TLR3-anti-viral response by probiotic microorganisms: lessons learned from *Lactobacillus rhamnosus* CRL1505. *Front Immunol*. (2014) 5:201. doi: 10.3389/fimmu.2014.00201
7. Villena J, Vizoso-Pinto MG, Kitazawa H. Intestinal innate antiviral immunity and immunobiotics: beneficial effects against *Rotavirus* infection. *Front Immunol*. (2016) 7:563. doi: 10.3389/fimmu.2016.00563
8. Villena J, Aso H, Rutten VPMG, Takahashi H, van Eden W, Kitazawa H. Immunobiotics for the bovine host: their interaction with intestinal epithelial cells and their effect on antiviral immunity. *Front Immunol*. (2018) 9:326. doi: 10.3389/fimmu.2018.00326
9. Albarracin L, Kobayashi H, Iida H, Sato N, Nochi T, Aso H, et al. Transcriptomic analysis of the innate antiviral immune response in porcine intestinal epithelial cells: influence of immunobiotic *Lactobacilli*. *Front Immunol*. (2017) 8:57. doi: 10.3389/fimmu.2017.00057
10. Villena J, Chiba E, Vizoso-Pinto M, Tomosada Y, Takahashi T, Ishizuka T, et al. Immunobiotic *Lactobacillus rhamnosus* strains differentially modulate antiviral immune response in porcine intestinal epithelial and antigen presenting cells. *BMC Microbiol*. (2014) 14:126. doi: 10.1186/1471-2180-14-126
11. Tada A, Zelaya H, Clua P, Salva S, Alvarez S, Kitazawa H, et al. Immunobiotic *Lactobacillus* strains reduce small intestinal injury induced by intraepithelial lymphocytes after Toll-like receptor 3 activation. *Inflamm Res*. (2016) 65:771–83. doi: 10.1007/s00011-016-0957-7
12. Yamauchi R, Maguin E, Horiuchi H, Hosokawa M, Sasaki Y. The critical role of urease in yogurt fermentation with various combinations of *Streptococcus thermophilus* and *Lactobacillus delbrueckii* ssp. bulgaricus. *J Dairy Sci*. (2019) 102:1033–43. doi: 10.3168/jds.2018-15192
13. De Keersmaecker SCJ, Braeken K, Verhoeven TLA, Vélez MP, Lebeer S, Vanderleyden J, et al. Flow cytometric testing of green fluorescent protein-tagged lactobacillus rhamnosus GG for response to defensins. *Appl Environ Microbiol*. (2006) 72:4923–30. doi: 10.1128/AEM.02605-05
14. Biswas EE, Chen PH, Biswas SB. DNA helicase associated with DNA polymerase α: isolation by a modified immunoaffinity chromatography. *Biochemistry*. (1993) 32:13393–8. doi: 10.1021/bi00212a003
15. Hirose Y, Murosaki S, Fujiki T, Yamamoto Y, Yoshikai Y, Yamashita M. Lipoteichoic acids on *Lactobacillus plantarum* cell surfaces correlate with induction of interleukin-12p40 production. *Microbiol Immunol*. (2010) 54:143–51. doi: 10.1111/j.1348-0421.2009.00189.x
16. Moue M, Tohno M, Shimazu T, Kido T, Aso H, Saito T, et al. Toll-like receptor 4 and cytokine expression involved in functional immune response in an originally established porcine intestinal epitheliocyte cell line. *Biochim Biophys Acta Gen Subj*. (2008) 1780:134–44. doi: 10.1016/j.bbagen.2007.11.006
17. Hosoya S, Villena J, Shimazu T, Tohno M, Fujie H, Chiba E, et al. Immunobiotic lactic acid bacteria beneficially regulate immune response triggered by poly(I:C) in porcine intestinal epithelial cells. *Vet Res*. (2011) 42:111. doi: 10.1186/1297-9716-42-111
18. Shimazu T, Villena J, Tohno M, Fujie H, Hosoya S, Shimosato T, et al. Immunobiotic *Lactobacillus jensenii* elicits anti-inflammatory activity in porcine intestinal epithelial cells by modulating negative regulators of the Toll-like receptor signaling pathway. *Infect Immun*. (2012) 80:276–88. doi: 10.1128/IAI.05729-11
19. Tomosada Y, Villena J, Murata K, Chiba E, Shimazu T, Aso H, et al. Immunoregulatory effect of bifidobacteria strains in porcine intestinal epithelial cells through modulation of ubiquitin-editing enzyme A20 expression. *PLoS One*. (2013) 8:e59259. doi: 10.1371/journal.pone.0059259
20. Kobayashi H, Albarracin L, Sato N, Kanmani P, Kober AKMH, Ikeda-Ohtsubo W, et al. Modulation of porcine intestinal epitheliocytes immunetranscriptome response by *Lactobacillus jensenii* TL2937. *Benef Microbes*. (2016) 7:769–82. doi: 10.3920/BM2016.0095
21. Ishizuka T, Kanmani P, Kobayashi H, Miyazaki A, Soma J, Suda Y, et al. Immunobiotic *Bifidobacteria* strains modulate *Rotavirus* immune response in porcine intestinal epitheliocytes via pattern recognition receptor signaling. *PLoS One*. (2016) 11:e0152416. doi: 10.1371/journal.pone.0152416
22. Bagchi P, Nandi S, Chattopadhyay S, Bhowmick R, Halder UC, Nayak MK, et al. Identification of common human host genes involved in pathogenesis of different rotavirus strains: an attempt to recognize probable antiviral targets. *Virus Res*. (2012) 169:144–53. doi: 10.1016/j.virusres.2012.07.021
23. Macpherson C, Audy J, Mathieu O, Tompkins TA. Multistrain probiotic modulation of intestinal epithelial cells' immune response to a double-stranded RNA ligand, poly(i·c). *Appl Environ Microbiol*. (2014) 80:1692–700. doi: 10.1128/AEM.03411-13
24. Villena J, Chiba E, Tomosada Y, Salva S, Marranzino G, Kitazawa H, et al. Orally administered *Lactobacillus rhamnosus* modulates the respiratory immune response triggered by the viral pathogen-associated molecular pattern poly(I:C). *BMC Immunol*. (2012) 13:53. doi: 10.1186/1471-2172-13-53
25. Vélez MP, Verhoeven TLA, Draing C, Von Aulock S, Pfitzenmaier M, Geyer A, et al. Functional analysis of D-alanylation of lipoteichoic acid in the probiotic strain *Lactobacillus rhamnosus* GG. *Appl Environ Microbiol*. (2007) 73:3595–604. doi: 10.1128/AEM.02083-06
26. Palumbo E, Deghorain M, Cocconcelli PS, Kleerebezem M, Geyer A, Hartung T, et al. D-alanyl ester depletion of teichoic acids in *Lactobacillus plantarum* results in a major modification of lipoteichoic acid composition and cell wall perforations at the septum mediated by the Acm2 autolysin. *J Bacteriol*. (2006) 188:3709–15. doi: 10.1128/JB.188.10.3709-3715.2006
27. Mohamadzadeh M, Pfeiler EA, Brown JB, Zadeh M, Gramarossa M, Managlia E, et al. Regulation of induced colonic inflammation by *Lactobacillus acidophilus* deficient in lipoteichoic acid. *Proc Natl Acad Sci USA*. (2011) 108(Suppl. 1):4623–30. doi: 10.1073/pnas.1005066107
28. Bron PA, Tomita S, Mercenier A, Kleerebezem M. Cell surface-associated compounds of probiotic lactobacilli sustain the strain-specificity dogma. *Curr Opin Microbiol*. (2013) 16:262–9. doi: 10.1016/j.mib.2013.06.001
29. Lee IC, Tomita S, Kleerebezem M, Bron PA. The quest for probiotic effector molecules – unraveling strain specificity at the molecular level. *Pharmacol Res*. (2013) 69:61–74. doi: 10.1016/j.phrs.2012.09.010
30. Lebeer S, Bron PA, Marco ML, Van Pijkeren JP, O'Connell Motherway M, Hill C, et al. Identification of probiotic effector molecules: present state and future perspectives. *Curr Opin Biotechnol*. (2018) 49:217–23. doi: 10.1016/j.copbio.2017.10.007
31. Clua P, Kanmani P, Zelaya H, Tada A, Humayun Kober AKM, Salva S, et al. Peptidoglycan from immunobiotic *Lactobacillus rhamnosus* improves resistance of infant Mice to respiratory syncytial viral infection and secondary pneumococcal pneumonia. *Front Immunol*. (2017) 8:948. doi: 10.3389/fimmu.2017.00948
32. Kanmani P, Albarracin L, Kobayashi H, Hebert EM, Saavedra L, Komatsu R, et al. Genomic characterization of *Lactobacillus delbrueckii* TUA4408L and evaluation of the antiviral activities of its extracellular Polysaccharides in porcine intestinal epithelial cells. *Front Immunol*. (2018) 9:2178. doi: 10.3389/fimmu.2018.02178
33. Grangette C, Nutten S, Palumbo E, Morath S, Hermann C, Dewulf J, et al. Enhanced antiinflammatory capacity of a *Lactobacillus plantarum* mutant synthesizing modified teichoic acids. *Proc Natl Acad Sci USA*. (2005) 102:10321–6. doi: 10.1073/pnas.0504084102
34. Claes IJJ, Lebeer S, Shen C, Verhoeven TLA, Dilissen E, De Hertogh G, et al. Impact of lipoteichoic acid modification on the performance of the probiotic

*Lactobacillus rhamnosus* GG in experimental colitis. *Clin Exp Immunol*. (2010) 162:306–14. doi: 10.1111/j.1365-2249.2010.04228.x
35. Matsuguchi T, Takagi A, Matsuzaki T, Nagaoka M, Ishikawa K, Yokokura T, et al. Lipoteichoic acids from *Lactobacillus* strains elicit strong tumor necrosis factor alpha-inducing activities in macrophages through toll-like receptor 2. *Clin Diagn Lab Immunol*. (2003) 10:259–66. doi: 10.1128/CDLI.10.2.259-266.2003
36. Ryu YH, Baik JE, Yang JS, Kang SS, Im J, Yun CH, et al. Differential immunostimulatory effects of Gram-positive bacteria due to their lipoteichoic acids. *Int Immunopharmacol*. (2009) 9:127–33. doi: 10.1016/j.intimp.2008.10.014
37. Kim HG, Lee SY, Kim NR, Ko MY, Lee JM, Yi TH, et al. Inhibitory effects of *Lactobacillus plantarum* lipoteichoic acid. (LTA) on Staphylococcus aureus LTA-induced tumor necrosis factor-alpha production. *J Microbiol Biotechnol*. (2008) 18:1191–6.
38. Kim HG, Lee SY, Kim NR, Lee HY, Ko MY, Jung BJ, et al. *Lactobacillus plantarum* lipoteichoic acid down-regulated *Shigella flexneri* peptidoglycan-induced inflammation. *Mol Immunol*. (2011) 48:382–91. doi: 10.1016/j.molimm.2010.07.011
39. Kim HG, Kim N-R, Gim MG, Lee JM, Lee SY, Ko MY, et al. Lipoteichoic acid isolated from *Lactobacillus plantarum* inhibits lipopolysaccharide-induced TNF-α production in THP-1 cells and endotoxin shock in mice. *J Immunol*. (2008) 180:2553–61. doi: 10.4049/jimmunol.180.4.2553
40. Jeon B, Kim HR, Kim H, Chung DK. In vitro and in vivo downregulation of C3 by lipoteichoic acid isolated from *Lactobacillus plantarum* K8 suppressed cytokine-mediated complement system activation. *FEMS Microbiol Lett*. (2016) 363:fnw140. doi: 10.1093/femsle/fnw140
41. Noh SY, Kang SS, Yun CH, Han SH. Lipoteichoic acid from *Lactobacillus plantarum* inhibits Pam2CSK4-induced IL-8 production in human intestinal epithelial cells. *Mol Immunol*. (2015) 64:183–9. doi: 10.1016/j.molimm.2014.11.014
42. Lee B, Yin X, Griffey SM, Marco ML. Attenuation of colitis by *Lactobacillus casei* BL23 is dependent on the dairy delivery matrix. *Appl Environ Microbiol*. (2015) 81:6425–35. doi: 10.1128/AEM.01360-15
43. Lebeer S, Claes IJJ, Vanderleyden J. Anti-inflammatory potential of probiotics: Lipoteichoic acid makes a difference. *Trends Microbiol*. (2012) 20:5–10. doi: 10.1016/j.tim.2011.09.004
44. Kim KW, Kang SS, Woo SJ, Park OJ, Ahn KB, Song KD, et al. Lipoteichoic acid of probiotic Lactobacillus plantarum attenuates poly I: C-induced IL-8 production in porcine intestinal epithelial cells. *Front Microbiol*. (2017) 8:1827. doi: 10.3389/fmicb.2017.01827
45. Ebert EC. Interleukin 15 is a potent stimulant of intraepithelial lymphocytes. *Gastroenterology*. (1998) 115:1439–45. doi: 10.1016/S0016-5085(98)70022-8
46. Kinoshita N, Hiroi T, Ohta N, Fukuyama S, Park EJ, Kiyono H. Autocrine IL-15 mediates intestinal epithelial cell death via the activation of neighboring intraepithelial NK cells. *J Immunol*. (2002) 169:6187–92. doi: 10.4049/jimmunol.169.11.6187
47. Trembath AP, Markiewicz MA. More than decoration: roles for natural killer group 2 member D ligand expression by immune cells. *Front Immunol*. (2018) 9:231. doi: 10.3389/fimmu.2018.00231
48. Zhou R, Wei H, Sun R, Zhang J, Tian Z. NKG2D recognition mediates Toll-like receptor 3 signaling-induced breakdown of epithelial homeostasis in the small intestines of mice. *Proc Natl Acad Sci USA*. (2007) 104:7512–5. doi: 10.1073/pnas.0700822104
49. Zhou R, Wei H, Sun R, Tian Z. Recognition of double-stranded RNA by TLR3 induces severe small intestinal injury in mice. *J Immunol*. (2007) 178:4548–56. doi: 10.4049/jimmunol.178.7.4548
50. Hansen CHF, Holm TL, Krych L, Andresen L, Nielsen DS, Rune I, et al. Gut microbiota regulates NKG2D ligand expression on intestinal epithelial cells. *Eur J Immunol*. (2013) 43:447–57. doi: 10.1002/eji.201242462
51. Serrano AE, Menares-Castillo E, Garrido-Tapia M, Ribeiro CH, Hernández CJ, Mendoza-Naranjo A, et al. Interleukin 10 decreases MICA expression on melanoma cell surface. *Immunol Cell Biol*. (2011) 89:447–57. doi: 10.1038/icb.2010.100
52. Kühn R, Löhler J, Rennick D, Rajewsky K, Müller W. Interleukin-10-deficient mice develop chronic enterocolitis. *Cell*. (1993) 75:263–74. doi: 10.1016/0092-8674(93)80068-P
53. Galdeano CM, de Moreno de LeBlanc A, Vinderola G, Bonet ME, Perdigón G. Proposed model: mechanisms of immunomodulation induced by probiotic bacteria. *Clin Vaccine Immunol*. (2007) 14:485–92. doi: 10.1128/CVI.00406-06
54. Marranzino G, Villena J, Salva S, Alvarez S. Stimulation of macrophages by immunobiotic *Lactobacillus* strains: influence beyond the intestinal tract. *Microbiol Immunol*. (2012) 56:771–81. doi: 10.1111/j.1348-0421.2012.00495.x

**Conflict of Interest:** The authors declare that the research was conducted in the absence of any commercial or financial relationships that could be construed as a potential conflict of interest.

frontiers in Nutrition

ORIGINAL RESEARCH
published: 24 June 2020
doi: 10.3389/fnut.2020.00067

# Intestinal Microbiota and Immune Modulation in Zebrafish by Fucoidan From Okinawa Mozuku (*Cladosiphon okamuranus*)

*Wakako Ikeda-Ohtsubo*[1,2,3,4]*, *Adrià López Nadal*[1], *Edoardo Zaccaria*[2], *Masahiko Iha*[5], *Haruki Kitazawa*[3,4], *Michiel Kleerebezem*[2] and *Sylvia Brugman*[1,2]*

[1] Cell Biology and Immunology Group, Department of Animal Sciences, Wageningen University and Research, Wageningen, Netherlands, [2] Host-Microbe Interactomics Group, Department of Animal Sciences, Wageningen University and Research, Wageningen, Netherlands, [3] Laboratory of Animal Products Chemistry, Graduate School of Agricultural Science, Tohoku University, Sendai, Japan, [4] Livestock Immunology Unit, International Education and Research Center for Food Agricultural Immunology, Graduate School of Agricultural Science, Tohoku University, Sendai, Japan, [5] South Product Co., Ltd., Uruma, Japan

OPEN ACCESS

**Edited by:**
Jia Sun,
Jiangnan University, China

**Reviewed by:**
Hailong Song,
University of Pennsylvania, United States
Xi Ma,
China Agricultural University, China

***Correspondence:**
Wakako Ikeda-Ohtsubo
wakako.ohtsubo@tohoku.ac.jp
Sylvia Brugman
sylvia.brugman@wur.nl

**Specialty section:**
This article was submitted to Nutritional Immunology, a section of the journal Frontiers in Nutrition

**Received:** 20 December 2019
**Accepted:** 20 April 2020
**Published:** 24 June 2020

**Citation:**
Ikeda-Ohtsubo W, López Nadal A, Zaccaria E, Iha M, Kitazawa H, Kleerebezem M and Brugman S (2020) Intestinal Microbiota and Immune Modulation in Zebrafish by Fucoidan From Okinawa Mozuku (Cladosiphon okamuranus). Front. Nutr. 7:67. doi: 10.3389/fnut.2020.00067

Fucoidan represents fucose-rich sulfated polysaccharides derived from brown seaweeds, which exerts various biological activities applicable for functional foods and therapeutic agents. The objective of the present study was to investigate *in vivo* effects of fucoidan extracted from Okinawa mozuku (*Cladosiphon okamuranus*), common edible seaweed in Japan, on immune responses and microbiota composition in zebrafish. We treated larvae and adult zebrafish with Okinawa mozuku (OM) fucoidan by immersion (100 and 500 μg/mL, 3 days) and by feeding (3 weeks), respectively. The effect of OM fucoidan on immune responses in zebrafish larvae was evaluated by live imaging of neutrophils and macrophages as well as quantitative polymerase chain reaction of pro- and anti-inflammatory cytokine genes. Whole microbiota of zebrafish larvae and intestinal microbiota of adult zebrafish treated with OM fucoidan were analyzed by Illumina MiSeq pair-end sequencing of the V3–V4 region of 16S rRNA genes. Fucoidan treatment only slightly affected the composition of the larvae microbiota and the number of neutrophils and macrophages, while pro- and anti-inflammatory cytokine gene expression levels were upregulated in the larvae treated with 500 μg/mL OM fucoidan. In contrast, feeding of OM fucoidan clearly altered the intestinal microbiota composition of adult zebrafish, which was characterized by the emergence and predominance of multiple bacterial operational taxonomic units (OTUs) affiliated with Rhizobiaceae and Comamonadaceae at the expense of *E. coli*-related Enterobacteriaceae, the dominant OTUs throughout the studied samples. These changes were accompanied by decreased expression levels of pro-inflammatory cytokine *il1b* in the intestines of the adult zebrafish. Our current study provides the first insights into *in vivo* modulatory effects of fucoidan on microbiota and immune responses of unchallenged zebrafish, which underscores the potential of fucoidan to play a modulatory role in the diet–microbiota–host interplay.

**Keywords: fucoidan, immunomodulation, microbiota, seaweed polysaccharides, zebrafish**

## INTRODUCTION

Fucoidan represents polysaccharides consisting of α-(1→3) or α-(1→4) -linked L-fucose residues with sulfate substitutions, which occasionally contain acetate, glucuronic acid, and monosaccharides such as mannose and galactose (1). Fucoidan from different algal origins has been reported to exhibit unique properties such as antiinflammatory, antiallergic, antitumor, or antiviral effects (2, 3) and is therefore recognized as a prospective ingredient for functional foods and for therapeutic agents (3, 4). Although beneficial effects of fucoidan have been well-studied and described, daily intake of fucoidan from brown seaweed is still not common in Western countries. In Japan, daily seaweed consumption can exceed ∼5 g/day (5) and the brown seaweed *mozuku* represents one of the most common edible seaweeds, which is usually consumed raw. Okinawa mozuku (*Cladosiphon okamuranus*) is exclusively cultivated and used in the traditional cuisine on the Okinawan Islands in Japan, a region that is well-known for its high prevalence of centenarians and the general healthy states of its elderly population (6). Fucoidan extracted from Okinawa *mozuku* (OM fucoidan) has a simple structure with a backbone of α-(1→3) fucopyranose, substituted with sulfate and α-glucuronic acid at ∼50 and 17% of its residues, respectively (7). Similar to what has been shown for fucoidan derived from other origins, OM fucoidan has been reported to exert antitumor and antiviral effects. In a murine model, antitumor activity has been attributed to the fucoidan-mediated stimulation of macrophages and natural killer cells (8, 9), while antiviral activities seem to be more complex and may involve both host–virus and virus–fucoidan interactions. Previous studies have reported antiviral activities of OM fucoidan against human T-cell leukemia virus type 1 (HTLV-1) (10, 11), dengue virus type 2 (12), hepatitis C (13), Newcastle disease virus (DSV) in poultry (14, 15), and canine distemper virus (CDV) (16). Collectively, these studies support the high potential of OM fucoidan as a therapeutic agent in viral infections.

Meanwhile, effects of OM fucoidan on the intestinal microbiota remain poorly understood. Polysaccharides such as fucoidan have a potential to not only mechanistically interfere with host–microbiota interactions but also to serve as nutrition for bacteria constituting the microbiota (17, 18). Since no enzymes digesting fucoidan have been found in animal intestinal tracts, fucoidan can reach the lower intestinal tract intact and may confer beneficial effects on microbiota as prebiotics (19–21). Importantly, some studies have suggested that bioactivities of fucoidan may be attributable to its modulatory effects on gut microbiota. A recent study has shown that fucoidan from *Undaria pinnatifida* can affect host lipid metabolism by modulating the gut microbiota composition (22), which may also explain the effect of OM fucoidan to ameliorate dyslipidemia in rodents (23). Other studies have reported that fucoidan from sea cucumber (*Acaudina molpadioides*) and *hijiki* seaweed (*Sargassum fusiforme*) can relieve symptoms of diabetes by modulating gut microbiota (24, 25).

Considering possible interactions between microbiota and host immune responses, it is crucial to evaluate host immunity and microbiota simultaneously to elucidate the prebiotic potential OM fucoidan (18). Zebrafish offer an ideal *in vivo* model to investigate how fucoidan affects host immunity and microbiota under normal (unchallenged) conditions because of their compatibility with live visualization (26). Using a double-transgenic zebrafish model combined with next-generation sequencing of 16S rRNA genes, we have recently shown that microbiota modulation by antibiotics can significantly affect host inflammatory immune responses in zebrafish larvae immersed in saponin (27). In this study, we exploited this approach to investigate how OM fucoidan can affect immune response and microbiota composition of zebrafish larvae. We also investigated the effect of OM fucoidan on immune responses and intestinal microbiota of adult zebrafish, which were fed with OM fucoidan for 3 weeks.

## MATERIALS AND METHODS

### Ethics Statement

The present study was approved by the Dutch Committee on Animal Welfare and the Animal Welfare Body (IvD) of Wageningen University, The Netherlands. Furthermore, we adhere to our standard biosecurity and institutional safety procedures at Wageningen University and Research.

### Zebrafish and Fucoidan

Tg (mpeg1:mCherry/mpx:eGFPi$^{114}$) (28, 29) and wild-type zebrafish were maintained in Zebtec family tanks (Tecniplast, Buguggiate, Italy) under continuous flow-through at 28°C (14/10-h light/dark cycle) and fed daily with Tetramin Flakes (Tetra, Melle, Germany). For the experiments using zebrafish larvae, embryos were obtained from the adult transgenic zebrafish by natural spawning and raised with embryo medium (E3) water as described previously (27). OM fucoidan powder (>95% pure fucoidan) extracted from *C. okamuranus* as described previously (30) was provided by South Product Co., Ltd., Okinawa, Japan. The characteristics of this fucoidan were as follows: average molecular weight of 49.8 kDa, L-fucose content of 52.7%, uronic acid content of 18.0%, and sulfate ion content of 17.6%. The OM fucoidan powder was stored at room temperature until use. Fucoidan treatment of larvae and adult zebrafish was performed as follows: the zebrafish larvae (3 days post fertilization; dpf) were randomly distributed in six-well plates ($n$ = 8 fish/well) and kept in different concentrations (0, 100, and 500 μg/mL of E3 water) of OM fucoidan (immersion) until 6 dpf. Ten adult zebrafish were maintained in two separate tanks in a continuous flow and temperature-controlled (28°C) system and fed once daily with Tetramin Flakes (control group) or a combination of the flakes and OM fucoidan at the ratio of 1:1 (fucoidan group) over 3 weeks.

### *In vivo* Imaging of Neutrophils and Macrophages in Zebrafish Larvae

Tg (mpeg1:mCherry/mpx:eGFPi$^{114}$) zebrafish larvae were anesthetized with MS-222 (tricaine methane sulfonate) solution and embedded in 1% low melting point agarose (Thermo Fisher Scientific, Waltham, MA, USA), as previously described (27). Larvae were imaged as whole mounts with a Leica M205 FA

Fluorescence Stereo Microscope. Neutrophils and macrophages in the intestinal region of each specimen were quantified by counting the total number of cells per defined area using the cell counter plugin available in ImageJ® software (31).

## Relative Gene Expression by Quantitative Polymerase Chain Reaction

Zebrafish were euthanized with MS-222 and the whole larvae (five or six fish per 1.5-mL tube) were preserved in RNA later™ at −20°C. Adult zebrafish were anesthetized with MS-222 and intestines were isolated by dissection and were preserved in RNA later™ at −20°C. Total RNA was isolated from larvae or intestinal samples from adult zebrafish using the RNeasy® Micro Kit (QIAGEN, Venlo, The Netherlands) according to the manufacturer's instructions. After quantifying RNA by a NanoDrop 1000 Spectrophotometer (Thermo Fisher Scientific, Waltham, MA, USA), cDNA was generated from 1 μg of RNA using Superscript™ III First Strand Synthesis Systems (Invitrogen, Carlsbad, CA, USA) according to the manufacturer's instructions. The diluted cDNA corresponding to 125 ng of RNA was used as a template for each reaction of quantitative polymerase chain reaction (qPCR) using the ABsolute™ qPCR SYBR® Green Mix (Thermo Fisher Scientific, Waltham, MA, USA) as previously described (27). The sequences of the primer used in this study can be found in **Table S1**. The amplification data of each sample were normalized to the reference gene *elf1α* and calculated using the Pfaffl quantification method with efficiency correction (32), as described by Forlenza et al. (33). The statistical significance of differences between the control and fucoidan-treated groups was assessed by a one-way analysis of variance (ANOVA) test using R version 3.5.3 (34) where $<0.05$ was regarded as significant.

## 16S rRNA-Based Analyses of Zebrafish Microbiota

Zebrafish were euthanized with MS-222 and the whole larvae (four fish per 1.5-mL tube) were washed with sterilized phosphate-buffered saline and preserved at −20°C. Adult zebrafish were euthanized with MS-222 and the intestines were isolated by dissection. The intestinal contents were preserved in InhibitEX Buffer supplied in the QIAamp® DNA Fast Stool Mini Kit (QIAGEN, Venlo, The Netherlands) at −20°C. Total DNA was isolated from the whole larvae or intestines of adult zebrafish using the QIAamp® DNA Fast Stool Mini Kit according to the manufacturer's instructions. Pair-end sequencing was performed using Illumina MiSeq (BaseClear, Leiden, The Netherlands) using amplicons generated with the primer pair 341F−785R that target the V3–V4 variable region of the 16S rRNA gene of most bacteria (35). Raw Illumina sequencing reads were pair-ended, end-trimmed, filtered, and clustered into operational taxonomic units (OTUs) using the microbial genomic module 3.0 implemented in the CLC Bio Genomics Workbench v7.5.1 (Qiagen, Venlo, The Netherlands), 16S Microbiome Pipeline in the EZBioCloud web server (36), or the MICCA pipeline (37), for which OTU assignment was performed using the SILVA ribosomal RNA reference database [release 128, 97% similarity threshold, (38)], the EZBioCloud database (36), and the Ribosomal Database Project (RDP) classifier [version 2.11, 97% identity threshold, (39)], respectively. After confirming the reproducibility of the core microbiota composition of each sample, OTU tables in BIOM format generated by the CLC Bio Genomics Workbench was used for statistical analyses of the diversity and richness (alpha- and beta-diversity) implemented in MicrobiomeAnalyst© using the default filtering parameter settings (40). Significantly different taxa between control and fucoidan-treated group were identified by differential abundance (DESeq2) analysis by R version 3.5.3 (34) and by Linear Discriminant Analysis Effect Size (LEfSe) analysis implemented with EZBioCloud (36, 41).

## Statistical Analysis

The quantified data collected from the fluorescent *in vivo* imaging of the zebrafish larvae and qPCR was analyzed using Student's *t*-test assuming unequal variation as well as one-way analysis of variance (ANOVA) test using Microsoft Excel® and R version 3.5.3 (34), where $<0.05$ was regarded as significant. The indices of α-diversity and β-diversity for comparing compositional structure of microbiota of each larva and adult zebrafish group were calculated on a species-level summarization of the rarefied OTU tables generated as described in the preceding text. Chao1 and Abundance-based Coverage Estimator (ACE) as well as Shannon and Simpson indices were used to measure the species-level community richness and species level community evenness, respectively, and each index was calculated using the online module of Microbiomeanalyst© (40). The plots of β-diversity indicating dissimilarities between samples were produced by principal coordinates analyses (PCoA) calculated using the Bray–Curtis dissimilarity index implemented in Microbiomeanalyst© (40).

# RESULTS

## Effect of OM Fucoidan on Innate Immunity of Zebrafish Larvae

Zebrafish larvae (3−6 dpf) treated with OM fucoidan (0, 100, and 500 μg/mL of E3 water) by immersion showed normal development without visible signs of damage relative to untreated controls (data not shown). To investigate whether the treatment with OM fucoidan affected cellular immunity of zebrafish larvae, the numbers of neutrophils (mpx:GFP) and macrophages (mpeg1:mCherry) in the intestinal area of the control and the fucoidan-treated larvae were compared. There was no observable difference between the live-imaged control and the fucoidan-treated larvae (**Figure 1A**). The cell counts of neutrophils and macrophages in fucoidan-treated zebrafish larvae tended to be reduced compared to the control, but the difference was not significant ($P > 0.1$, **Figure 1B**).

Using the same experimental setup, we performed qPCR to measure the relative expression levels of selected genes representing host immune cell responses in the fucoidan (500 μg/mL) -treated zebrafish larvae and the untreated control. The relative gene expression levels of pro- (*il1b, tnfa*) and

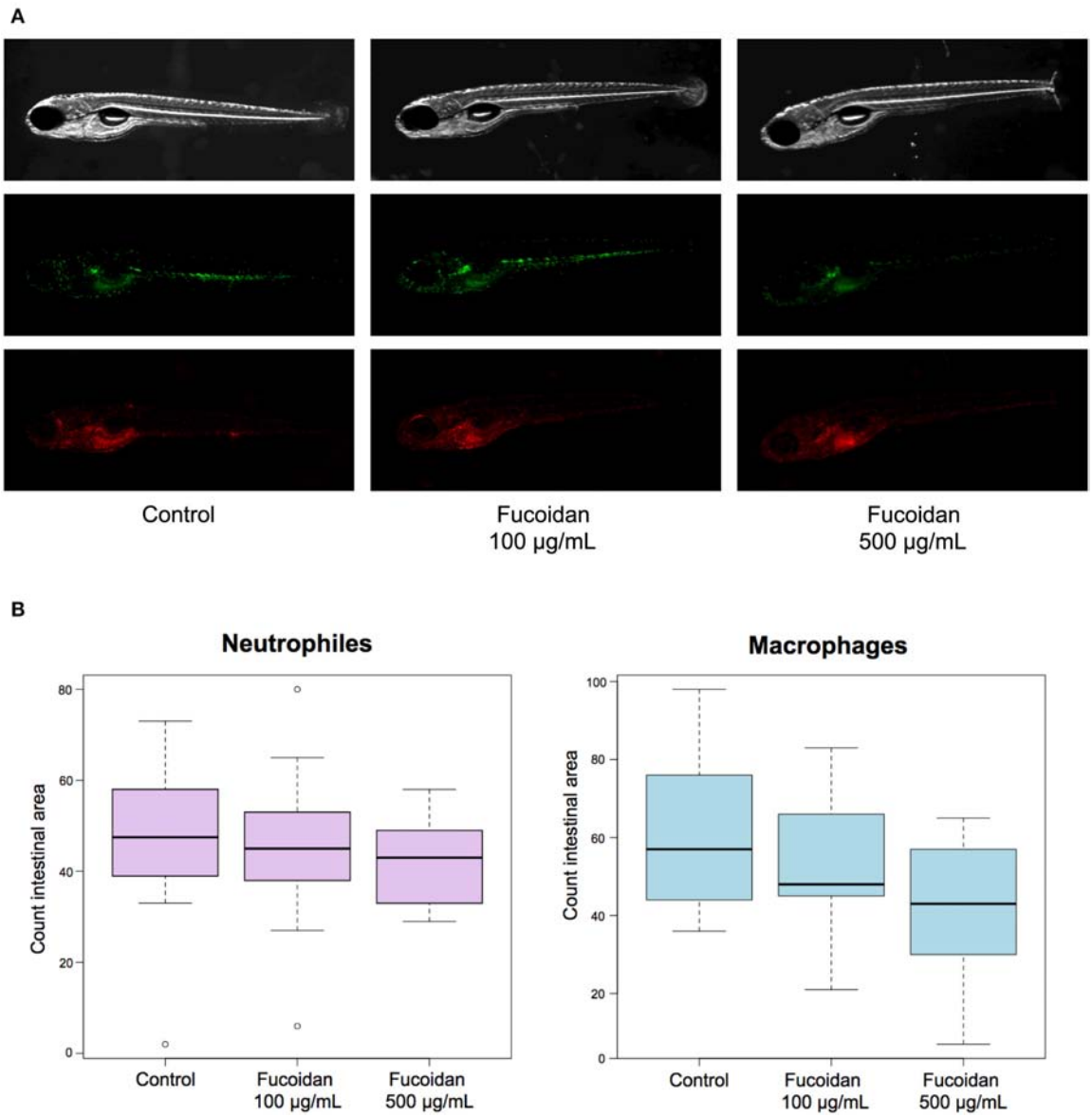


**FIGURE 1 |** Effect of OM fucoidan on lymphocyte recruitment to the intestinal region of zebrafish larvae. **(A)** Representative pictures of 6 dpf zebrafish larvae (mpeg:mCherry, mpx:GFP) displaying neutrophils (green) and macrophages (red). F100, the zebrafish larvae treated with 100 µg/mL OM fucoidan from 3 dpf for 3 days; F500, the zebrafish larvae treated with 500 µg/mL OM fucoidan from 3 dpf for 3 days. **(B)** Quantification of neutrophils and macrophages in the intestinal area of larval zebrafish. Control, no treatment ($n = 14$); F100, treated with 100 µg/mL ($n = 13$); F500, treated with 500 µg/mL ($n = 17$).

antiinflammatory (*il10*) cytokines as well as *mmp9* were moderately (1.7–2.2 fold) upregulated in the larvae treated with 500 µg/mL of fucoidan (**Figure 2A**). No significant difference was observed for *cxcl-8a* (**Figure 2A**) and gene transcripts for *il-17f*, *il-22*, and *tnfb* were not detected in our samples (data not shown).

Adult zebrafish fed with OM fucoidan for 3 weeks did not show visible changes in fitness and behavior compared to controls fed the Tetramin Flakes only (data not shown). Immune responses of the adult zebrafish intestines were examined by quantitative PCR using primers specific for *il1b*, *il-10*, *cxcl-8a*, *tnfa*, and *mmp9*. Overall, there was no significant difference between the fucoidan-fed zebrafish and the control, except for *il1b,* which was expressed at slightly decreased levels (0.63-fold) in the fucoidan-fed zebrafish compared to the control (**Figure 2B**).

## Effect of OM Fucoidan on Microbiota Diversity and Composition of Larval and Adult Zebrafish

The effects of OM fucoidan on diversity of larval and adult zebrafish microbiota were analyzed by 16S rRNA gene amplicon

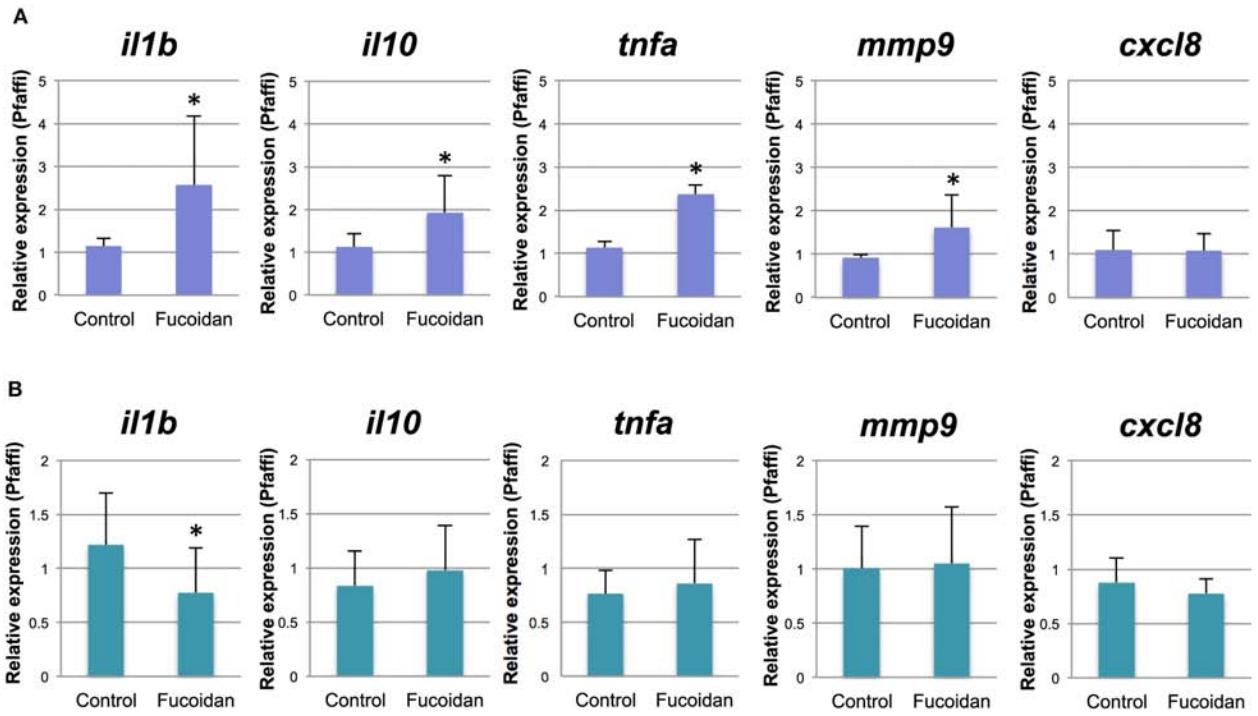


**FIGURE 2 |** Relative gene expression of immune genes of zebrafish treated with OM fucoidan. **(A)** Control, 6 dpf zebrafish larvae; Fucoidan, 6 dpf zebrafish larvae immersed in 500 μg/mL fucoidan from 3 dpf for 3 days. **(B)** Control, intestinal samples of adult zebrafish fed with standard fish meal for 3 weeks; Fucoidan, intestinal samples of adult zebrafish fed with OM fucoidan meal (Tetramin fish flakes: OM fucoidan = 1:1). The asterisk denotes significant differences from the control samples ($P < 0.05$, 1-way ANOVA).

sequencing. Whole-body DNA samples of pools of 6 dpf zebrafish larvae were obtained from the three groups ($n = 4$ per group; immersion in 0, 100, and 500 μg/mL of OM fucoidan in E3 water) and used for Illumina MiSeq sequencing of 16S rRNA genes. For adult zebrafish, intestinal DNA from each of the two groups ($n =$ 5 per group; control vs. OM-fucoidan fed) was used. A summary of the sequencing results is shown in **Table S2** and the rarefaction curves of all samples, except one sample (WO3, a control sample of zebrafish larvae), reached saturation (**Figure S1**).

In microbiota of zebrafish larvae, no significant differences were observed in the species richness (Chao1, $P = 0.47265$; ACE; $P = 0.74339$; **Figure 3A**) or the species evenness (Shannon, $P = 0.96621$; Simpson, $P = 0.96058$; **Figure 3B**) between the control and fucoidan-treated fish, regardless of the fucoidan concentrations. In intestinal microbiota of adult zebrafish, the species richness was also not affected (Chao1, $P = 0.88482$; ACE; $P = 0.90299$; **Figure 3C**), while the species evenness tended to be moderately increased in the fucoidan-fed zebrafish (Shannon, $P = 0.079088$; Simpson, $P = 0.078456$; **Figure 3D**). β-Diversity analyses showed no significant association between fucoidan treatment and microbiota composition of zebrafish larvae ($P <$ 0.49845; **Figure 3E**), which was in contrast to adult zebrafish, in which fucoidan-feeding was moderately associated with changes in the species composition of intestinal microbiota ($P < 0.023$, **Figure 3F**). Collectively, these results indicate that the treatments with OM fucoidan affected the diversity and composition of intestinal microbiota of adult zebrafish, but not the larvae zebrafish microbiota.

Taxonomic assignment of OTUs generated from each sample was performed using EzBioCloud database (https://www.ezbiocloud.net), which offers a high genus and species-level resolution (36). Consistent with our previous work (27), microbiota of zebrafish larvae was predominated (>95%) by Enterobacteriaceae (**Figure 4A**), which were affiliated with the *Escherichia coli* group (**Figure S2**, **Table S3**). Consistent with the diversity analyses (**Figure 3**), the relative abundance of each bacterial species and OTUs were similar between the larvae samples and did not reflect an effect of OM fucoidan (**Figure 4A**, **Figure S2**). In addition, DESeq2 and LEfSe analyses failed to identify significantly different taxa between the control and fucoidan-treated zebrafish larvae.

In contrast, a significant difference was observed in the intestinal microbiota between the control and fucoidan-fed adult zebrafish (**Figures 4B,C**, **Figure S3**). The class to species-level composition of intestinal microbiota of fucoidan-fed zebrafish was clearly different from the control (**Figure S3**), and this difference is characterized by the emergence and increase of relative abundance of several bacterial groups affiliated with Comamonadaceae and Rhizobiaceae (**Figure 4B**, **Figure S3**). At the genus and species level, these families were represented by unclassified genus of Comamonadaceae [AB076847, (42)] and the genus *Shinella granuli* group (Rhizobiaceae) (**Figure 4C**,

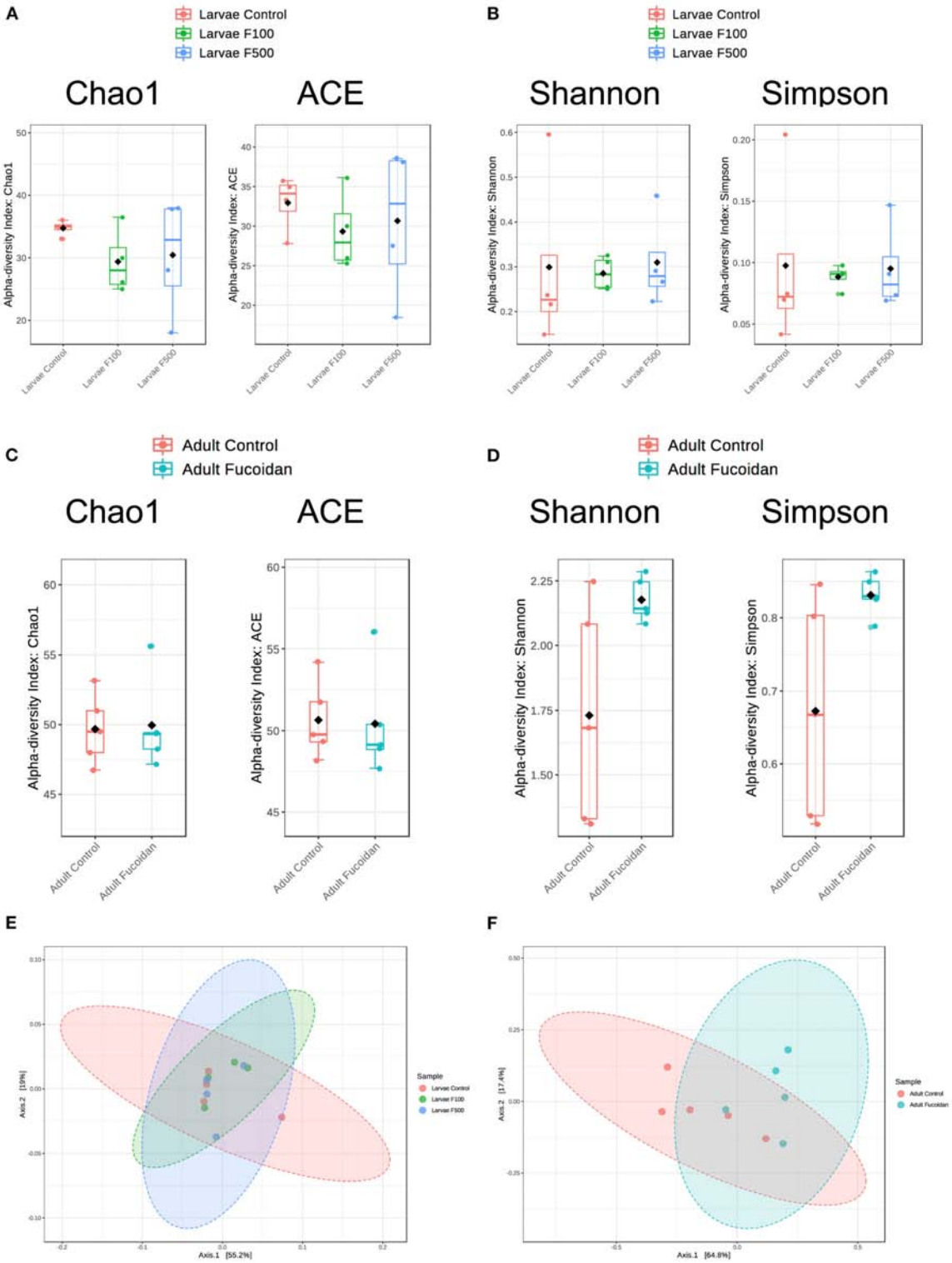


**FIGURE 3 |** Effect of OM fucoidan on the diversity of larvae zebrafish microbiota and adult zebrafish intestinal microbiota. Species-level community richness **(A,C)** and species level community evenness **(B,D)** were compared between larvae zebrafish samples (**A**, **B**, **E**; F100, the zebrafish larvae treated with 100 μg/mL OM fucoidan from 3 dpf for 3 days; F500, the zebrafish larvae treated with 500 μg/mL OM fucoidan from 3 dpf for 3 days) and adult zebrafish intestinal samples (**C**, **D**, **F**; Fucoidan [Tetramin fish flakes: OM fucoidan = 1:1] for 3 weeks). Beta-diversity of larval **(E)** and adult intestinal **(F)** microbiota compared by the principal coordinates analyses (PCoA) based on Bray–Curtis dissimilarity index.

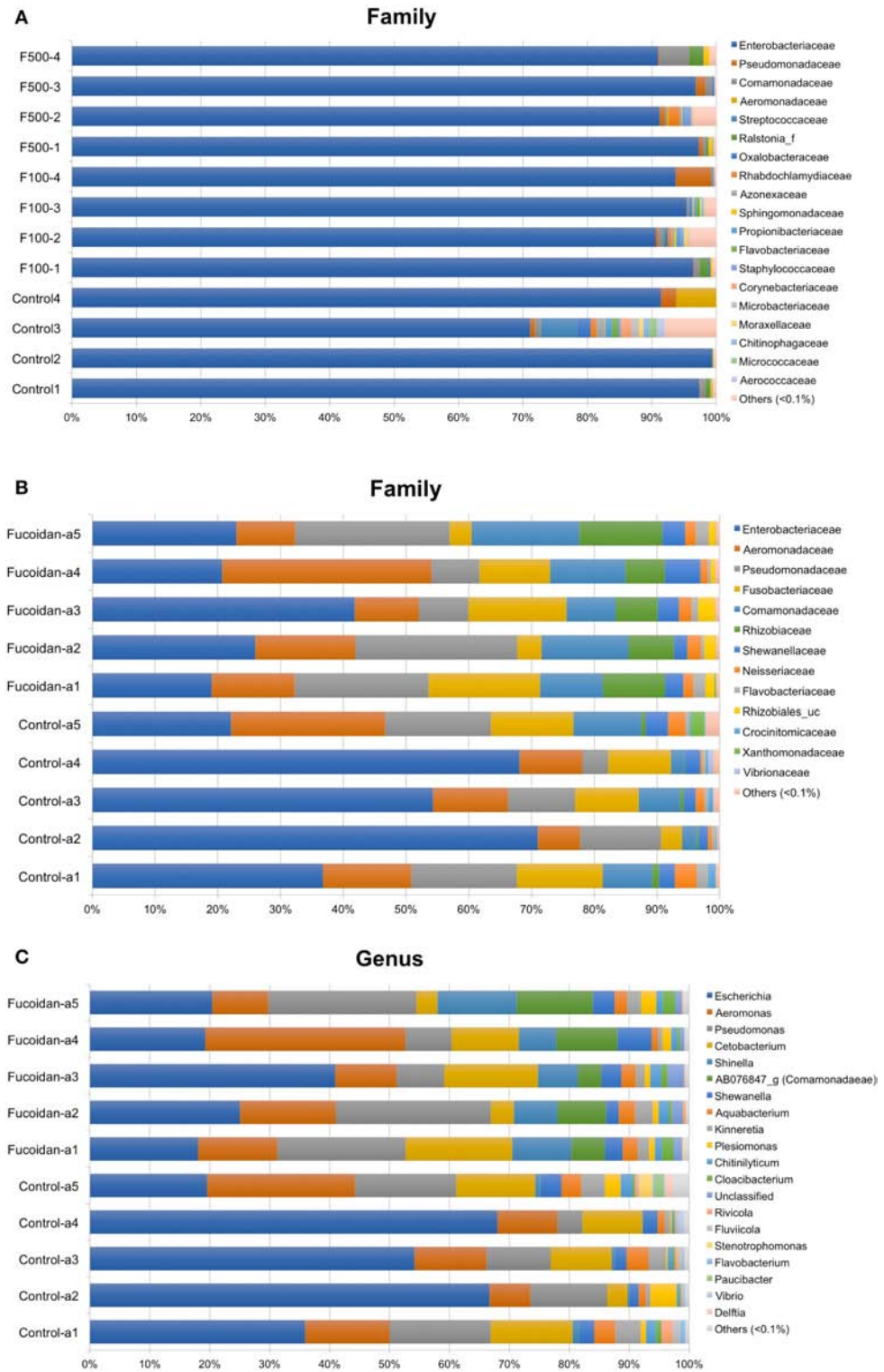


**FIGURE 4 |** Effects of OM fucoidan on the bacterial community structure of larvae zebrafish microbiota and adult zebrafish intestinal microbiota. **(A)** Composition of family-level bacterial groups in the larvae zebrafish microbiota (F100, the zebrafish larvae treated with 100 μg/mL OM fucoidan from 3 dpf for 3 days; F500, the zebrafish larvae treated with 500 μg/mL OM fucoidan from 3 dpf for 3 days.). **(B)** Composition of family-level bacterial groups in the adult zebrafish intestinal microbiota. **(C)** Composition of genus-level bacterial groups in adult zebrafish intestinal microbiota. **(B,C)** Fucoidan [Tetramin fish flakes: OM fucoidan = 1:1] for 3 weeks). The taxonomic assignment is based on the latest EZbioCloud database (36). Taxa representing <0.1% of the total community are not visualized.

**Figure S3**). The predominant families Comamonadaceae and Rhizobiaceae were also identified as the significantly different taxa represented in the fucoidan-fed zebrafish by the DESeq2 and LEfSe analyses (**Figures 5A,B**). Interestingly, both analyses revealed that the increase of Comamonadaceae and Rhizobiaceae were concomitant with the decrease of Enterobacteriaceae (**Figures 5A,B**, **Figure S3**). LEfSe analysis also found that unclassified groups of Rhizobiales and Betaproteobacteria were significantly associated with the fucoidan-feeding, while Flavobacteriia (phylum Bacteroides) were negatively affected (**Figure 5B**).

## DISCUSSION

Our current study showed that fucoidan derived from Japanese brown seaweed *C. okamuranus* has the potential to modulate the intestinal microbiota of adult zebrafish. The profound compositional change associated with the fucoidan-feeding in adult zebrafish can be characterized by the increased abundance of bacterial groups affiliated with Comamonadaceae and Rhizobiaceae and a decreased abundance of Enterobacteriaceae. Although non-pathogenic bacteria of the *E. coli* species have been proposed to confer a protective effect on zebrafish larvae via lipopolysaccharide (LPS) tolerance and acid production (43, 44), numerous studies have reported proinflammatory effects of Enterobacteriaceae in fish (45, 46). In addition, Enterobacteriaceae are thought to be responsible for the spread of antimicrobial resistance in aquatic environments (47). In this context, it is intriguing that the relative expression of *il1b*, a proinflammatory cytokine, was moderately downregulated in the fucoidan- fed adult zebrafish (**Figure 2B**), which suggests that OM fucoidan may have directly or indirectly suppressed the dominance of Enterobacteriaceae that can induce proinflammatory responses. This type of diet–microbiota–host interplay is likely to play a crucial role in pro- and antiinflammatory states in animal intestines [(48) for review], and it is therefore of great interest further investigate in future studies on the mechanism that OM fucoidan decreases the relative abundance of Enterobacteriaceae in the fish intestine with regard to how it may impact the health of the fish population.

While metabolic and physiological properties of the intestinal bacteria of adult zebrafish that responded to the fucoidan feeding are yet to be determined, the increase of Comamonadaceae and Rhizobiaceae suggests their involvement in the degradation of OM fucoidan. Interestingly, Comamonadaceae and Rhizobiaceae have been frequently found in a nitrogen removal process in wastewater treatment systems called solid-phase denitrification (49), where solid biodegradable polymers are used as carbon sources for denitrifying bacteria (50). This system is also applicable for nitrogen removal in aquaculture, where increased nitrate concentration poses negative effects on fish (51). Indeed, the unclassified Comamonadaceae [AB076847, (42)] and *Shinella* spp., the intestinal abundance of which increased in response to the fucoidan feeding of adult zebrafish in our current study, have been reported to belong to denitrifying bacteria possessing biodegrading abilities of diverse compounds including biopolymers and xenobiotics (42, 52, 53). Therefore, it seems plausible that OM fucoidan may serve as a carbon source for intestinal bacteria of adult zebrafish, and identification of the degradation pathways involved awaits further investigation

Although a large body of studies has documented that the host innate immunity plays significant roles for shaping microbiota and vice versa (26, 54), our current results imply that the compositional structure of microbiota is not strongly correlated to the expression patterns of host immune genes. Feeding of OM fucoidan for 3 weeks profoundly altered gut microbiota composition in adult zebrafish; however, the analysis of a selected set of immune genes only showed a slight reduction in the expression of *il1b*. In contrast, the exposure of zebrafish larvae to OM fucoidan resulted in changes in expression of immune genes (*il1b*, *il10*, *tnfa*, and *mmp9*) but did not affect the microbiota composition. These results might be partly explained by the timing and duration of the exposure. Since larval feeding starts in the immersion window, it is expected that the immune system of these developing larvae is responding to novel antigens that it is exposed to. In contrast, in adult fish, the immune system has fully developed and a proper homeostasis is reached at the mucosal surfaces such as the intestines (55). Furthermore, since we only evaluated the immune response in the intestines at 3 weeks after feeding, the initial immune modulatory effect of primary exposure to fucoidan might have been missed, while the microbiota had 3 weeks to adapt to the new substrate provided. Future studies will include multiple time points to address early vs. late immune modulatory effects at different time points in life (of fish).

Furthermore, as has been shown in a study by Burns et al. using innate immune-deficient Myd88 knockout zebrafish (56), the gut microbiota composition can be better explained by the interhost dispersal effect, i.e., transmission and sharing microbiota among hosts, than immune gene expression patterns. Also, Stagaman et al. have reported that the effects of adaptive immunity on microbiota composition can be overwhelmed by other factors derived from co-housing within the same tank (57). Our study also reflected this phenomenon, since all adult zebrafish fed with OM fucoidan showed the same compositional changes in the relative abundance of specific bacterial groups (**Figures 4B,C**, **Figure S3**). The interhost dispersal of Comamonadaceae and Rhizobiaceae among adult zebrafish associated with the fucoidan-feeding suggests that these specific bacterial groups are subject to filtering by local host environments. Further studies are warranted to determine whether the interhost dispersal and OM fucoidan reciprocally affected the microbial composition.

In contrast to previous studies reporting inhibitory effects of fucoidan on inflammatory responses of injury zebrafish models (58, 59), the influence of OM fucoidan treatments on the baseline zebrafish immune responses were rather mild in our current study. In addition, while a previous study has implied a high concentration of fucoidan may be cytotoxic (60), immersion of zebrafish larvae (3–6 dpf) in OM fucoidan at concentrations of 100 and 500 μg/mL did not affect their fitness. In previous studies using LPS-challenged zebrafish models (58, 59), the antiinflammation effects of fucoidan may be rather explained by the interference of LPS–host interaction rather than direct modulation of host immunity. Another interpretation of the less profound effect on the baseline immune response of zebrafish to

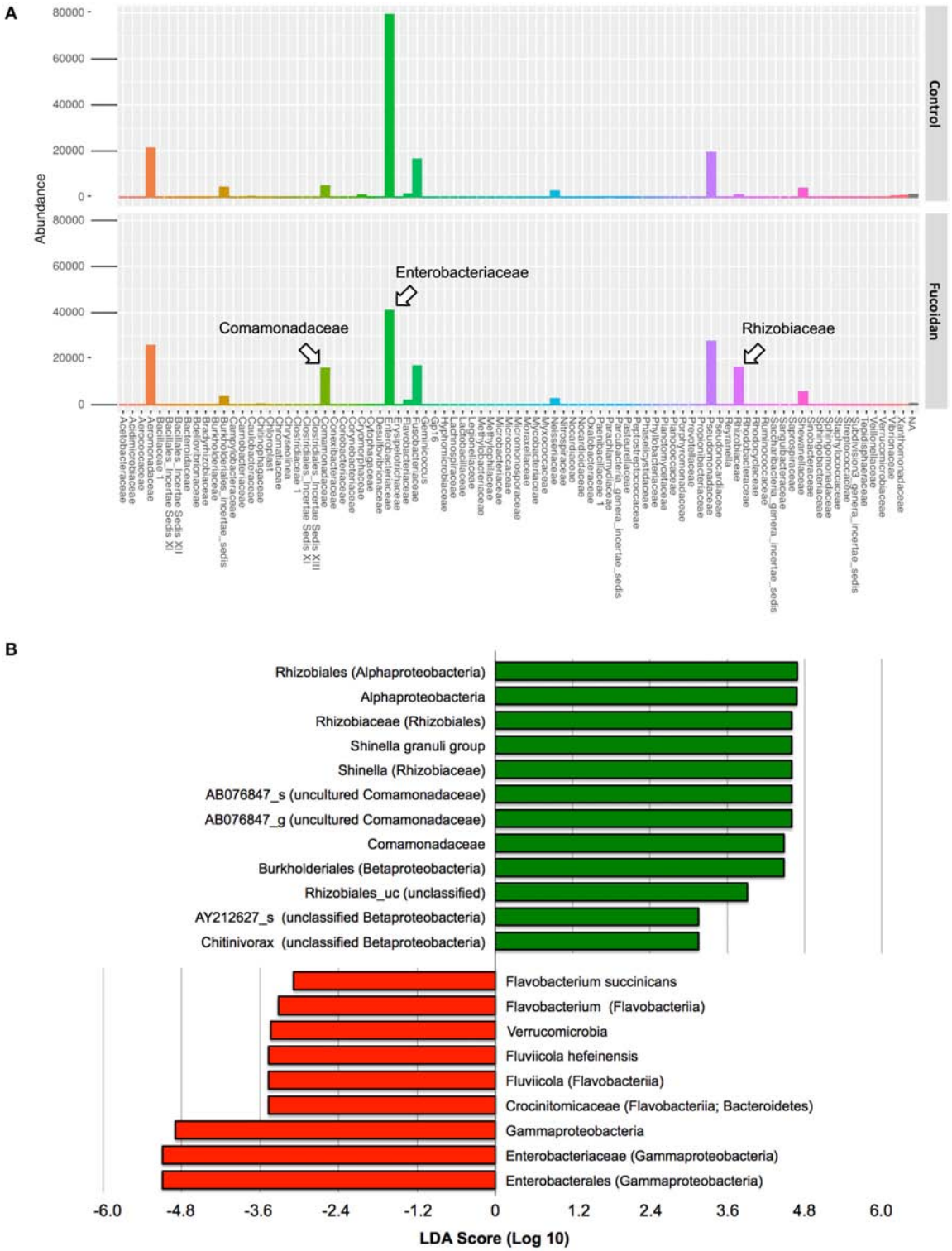


**FIGURE 5 |** Significantly different taxa in the adult zebrafish intestinal microbiota associated with the OM fucoidan treatment. **(A)** Differently abundant bacterial families between the intestinal microbiota of the control and OM fucoidan-fed adult zebrafish, identified by differential abundance analysis using DESeq2 in R. The taxonomy assignment of the OTU dataset used is based on the RDP classifier (version 2.11, 97% identity threshold, 39). **(B)** Specific bacterial groups positively (green)- and negatively (red)- associated with OM fucoidan treatment. Identification of the significantly different taxa and LDA score calculation were performed by Linear discriminant analysis effect size (LEfSe) tool implemented with EZBioCloud (36). The taxonomic assignment is based on the latest EZbioCloud database (36).

fucoidan is that zebrafish immunity may have evolved to become tolerant to the constituents of blown algae abundant in their original habitats (61).

Our current finding that OM fucoidan modulated the gut microbiota composition of zebrafish is in line with studies using rodents (22, 23). The improvement of diabetic symptoms attributed to the modulation of gut microbiota by fucoidan that have been shown in previous studies (24, 25) implies that fucoidan feeding and the subsequent alteration of intestinal microbiota may also affect metabolic properties of fish. Future studies toward a better understanding of the commonalities between intestinal microbial metabolism and host responses shared by fish and animals (62, 63) will help us to evaluate the potential of OM fucoidan as a new prebiotic in aquaculture (64).

## CONCLUSIONS

Treatment with OM fucoidan moderately modulated the relative expression of innate immune genes in larvae zebrafish, while no change in microbiota composition was observed. In adult zebrafish, feeding OM fucoidan increased the relative abundance of Comamonadaceae and Rhizobiaceae at the expense of Enterobacteriaceae, which was accompanied by a slight decrease of relative expression of a proinflammatory gene *il1b*, which suggests a potential of OM fucoidan to shift the microbial composition to an antiinflammatory state by selectively suppressing populations of bacteria that are associated with proinflammatory responses. To our knowledge, this is the first study to describe *in vivo* modulatory effects of fucoidan on microbiota and immune responses of unchallenged zebrafish.

## DATA AVAILABILITY STATEMENT

The raw sequence data files were deposited in the NCBI sequence read archive (SRA) database under BioProject number PRJNA597701 (SRA accession numbers listed in **Supplementary File** "data sheet 3.xlsx").

## ETHICS STATEMENT

The animal study was reviewed and approved by Dutch Committee on Animal Welfare (2017.W-0034) and the Animal Welfare Body (IvD) of the Wageningen University (Netherlands).

## AUTHOR CONTRIBUTIONS

WI-O, AL, MK, and SB designed the research. WI-O, AL, and SB conducted the experiments. WI-O, AL, EZ, MK, and SB analyzed the data. WI-O and SB wrote the article. MK and SB provided the funding. All authors critically reviewed the manuscript and approved the manuscript.

## FUNDING

This work was financially supported by the Japan Society for the Promotion of Science (JSPS) through JSPS Core-to-Core Program (Advanced Research Networks) entitled Establishment of International Agricultural Immunology Research-Core for a Quantum Improvement in Food Safety. WI-O was supported by WIAS (Wageningen Institute of Animal Sciences) fellowship (WIAS1807229) provided by Graduate School of Animal Science of Wageningen University and Research and Leading Young Researcher Overseas Visit Program of Tohoku University.

## SUPPLEMENTARY MATERIAL

The Supplementary Material for this article can be found online at: https://www.frontiersin.org/articles/10.3389/fnut.2020.00067/full#supplementary-material

## REFERENCES

1. Ale MT, Meyer AS. Fucoidans from brown seaweeds: an update on structures, extraction techniques and use of enzymes as tools for structural elucidation. *RSC Adv*. (2013) 3:8131–41. doi: 10.1039/C3RA23373A
2. Vo TS, Kim SK. Fucoidans as a natural bioactive ingredient for functional foods. *J Funct Foods*. (2012) 5:16–27. doi: 10.1016/j.jff.2012.08.007
3. Fitton JH, Stringer DS, Park AY, Karpiniec SN. Therapies from Fucoidan: new developments. *Mar Drugs*. (2019) 17:571. doi: 10.3390/md17100571
4. Chollet L, Sabboural P, Chauvierre C, Villemin JN, Letourneur D, Chaubet F. Fucoidans in nanomedicine. *Mar Drugs*. (2016) 14:145. doi: 10.3390/md14080145
5. Lange KW, Hauser J, Nakamura Y, Kanaya S. Dietary seaweeds and obesity. *Food Sci Hum Wellness*. (2015) 4:87–96. doi: 10.1016/j.fshw.2015.08.001
6. Willcox BJ, Willcox DC, Suzuki M. Demographic, phenotypic, and genetic characteristics of centenarians in Okinawa and Japan: part 1- centenarians in Okinawa. *Mech Ageing Dev*. (2017) 165:75–9. doi: 10.1016/j.mad.2016.11.001
7. Nagaoka M, Shibata H, Kimura-Tagaki I, Hashimoto S, Kimura K, Makino T, et al. Structural study of fucoidan from *Cladosiphon okamuranus* TOKIDA. *Glycoconj J*. (1999) 45:325–36. doi: 10.3177/jnsv.45.325
8. Takeda K, Tomimori K, Kimura R, Ishikawa C, Nowling TK, Mori N, et al. Anti-tumor activity of fucoidan is mediated by nitric oxide released from macrophages. *Int J Oncol*. (2012) 40:251–60. doi: 10.3892/ijo.2011.1168
9. Nagamine T, Kadena K, Tomori M, Nakajima K, Iha M. Activation of NK cells in male cancer survivors by fucoidan extracted from *Cladosiphon okamuranus*. *Mol Clin Oncol*. (2020) 12:81–8. doi: 10.3892/mco.2019.1943
10. Haneji K, Matsuda T, Tomita M, Kawakami H, Ohshiro K, Uchihara JN, et al. Fucoidan extracted from *Cladosiphon okamuranus* tokida induces apoptosis of human T-cell leukemia virus type 1-infected T-cell lines and primary adult T-cell leukemia cells. *Nutr Cancer*. (2005) 52:189–201. doi: 10.1207/s15327914nc5202_9
11. Araya N, Takahashi K, Sato T, Nakamura T, Sawa C, Hasegawa D, et al. Fucoidan therapy decreases the proviral load in patients with human t-lymphotropic virus type-1-associated neurological disease. *Antivir Ther*. (2011) 16:89–98. doi: 10.3851/IMP1699
12. Hidari KI, Takahashi N, Arihara M, Nagaoka M, Morita K, Suzuki T. Structure and anti-dengue virus activity of sulfated polysaccharide from a marine alga. *Biochem Biophys Res Commun*. (2008) 376:91–5. doi: 10.1016/j.bbrc.2008.08.100
13. Mori N, Nakasone K, Tomimori K, Ishikawa C. Beneficial effects of fucoidan in patients with chronic hepatitis c virus infection. *World J Gastroenterol*. (2012) 18:2225–30. doi: 10.3748/wjg.v18.i18.2225
14. Elizondo-Gonzalez R, Cruz-Suarez LE, Ricque-Marie D, Mendoza- Gamboa E, Rodriguez-Padilla C, Trejo-Avila LM. *In vitro* characterization of the antiviral activity of fucoidan from Cladosiphon okamuranus against newcastle disease virus. *Virol J*. (2012) 9:307. doi: 10.1186/1743-422X-9-307

15. Trejo-Avila LM, Elizondo-Gonzalez R, Rodriguez-Santillan P, Aguilar-Briseno JA, Ricque-Marie D, Rodriguez-Padilla C, et al. Innocuity and anti-Newcastle-virus-activity of *Cladosiphon okamuranus* fucoidan in chicken embryos. *Poult Sci*. (2016) 95:2795–802. doi: 10.3382/ps/pew201
16. Trejo-Avila LM, Morales-Martínez ML, Ricque-Marie D, Cruz-Suarez LE, Zapata-Benavides P, Morán-Santibañez K, et al. *In vitro* anti-canine distemper virus activity of fucoidan extracted from the brown alga *Cladosiphon okamuranus*. *Virus Dis*. (2014) 25:474–80. doi: 10.1007/s13337-014-0228-6
17. Shang Q, Jiang H, Cai C, Hao J, Li G, Yu G. Gut microbiota fermentation of marine polysaccharides and its effects on intestinal ecology: an overview. *Carbohydr Polym*. (2018) 179:173–85. doi: 10.1016/j.carbpol.2017.09.059
18. Ma N, Guo P, Zhang J, He T, Kim SW, Zhang G, et al. Nutrients mediate intestinal bacteria–mucosal immune crosstalk. *Front Immunol*. (2018) 9:5. doi: 10.3389/fimmu.2018.00005
19. Michel C, Lahaye M, Bonnet C, Mabeau S, Barry JL. *In vitro* fermentation by human faecal bacteria of total and purified dietary fibers from brown seaweeds. *Br J Nutr*. (1996) 75:263–80. doi: 10.1079/BJN19960129
20. de Jesus Raposo MF, de Morais AMMB, de Morais RMSC. Emergent sources of prebiotics: seaweeds and microalgae. *Mar Drugs*. (2016) 14:27. doi: 10.3390/md14020027
21. Brugman S, Ikeda-Ohtsubo W, Braber S, Folkerts G, Pieterse CMJ, Bakker PAHM. A comparative review on microbiota manipulation: lessons from fish, plants, livestock and human research. *Front Nutr*. (2018) 5:80. doi: 10.3389/fnut.2018.00080
22. Chen Q, Liu M, Zhang P, Fan S, Huang J, Yu S, et al. Fucoidan and galacto-oligosaccharides ameliorate high-fat diet-induced dyslipidemia in rats by modulating the gut microbiota and bile acid metabolism. *Nutrition*. (2019) 65:50–9. doi: 10.1016/j.nut.2019.03.001
23. Yokota T, Nomura K, Nagashima M, Kamimura N. Fucoidan alleviates high-fat diet-induced dyslipidemia and atherosclerosis in ApoE $^{shl}$ mice deficient in apolipoprotein E expression. *J Nutr Biochem*. (2016) 32:46–54. doi: 10.1016/j.jnutbio.2016.01.011
24. Hu S, Wang J, Wang J, Yang H, Yan X, Su L. Fucoidan from *Acaudina molpadioides* improves insulin resistance by altering gut microbiota dysfunction. *J Funct Foods*. (2019) 57:59–67. doi: 10.1016/j.jff.2019.03.033
25. Cheng Y, Luthuli S, Hou LF, Jiang HJ, Chen PC, Zhang X, et al. *Sargassum fusiforme* fucoidan modifies the gut microbiota during alleviation of streptozotocin-induced hyperglycemia in mice. *Int J Biol Macromol*. (2019) 131:1162–70. doi: 10.1016/j.ijbiomac.2019.04.040
26. López Nadal A, Ikeda-Ohtsubo W, Sipkema D, Peggs D, Mcgurk C, Forlenza M, et al. Feed, microbiota and gut immunity: using the zebrafish model to understand fish health. *Front Immunol*. (2020) 11:114. doi: 10.3389/fimmu.2020.00114
27. López Nadal A, Peggs D, Wiegertjes GF, Brugman S. Exposure to antibiotics affects saponin immersion-induced immune stimulation and shift in microbial composition in zebrafish larvae. *Front Microbiol*. (2018) 9:2588. doi: 10.3389/fmicb.2018.02588
28. Renshaw SA, Loynes CA, Trushell DM, Elworthy S, Ingham PW, Whyte MK. A transgenic zebrafish model of neutrophilic inflammation. *Blood*. (2006) 108:3976–8. doi: 10.1182/blood-2006-05-024075
29. Bernut A, Herrmann JL, Kissa K, Dubremetz JF, Gaillard JL, Lutfalla G, et al. *Mycobacterium* abscessus cording prevents phagocytosis and promotes abscess formation. *Proc Natl Acad Sci USA*. (2014) 111:E943–52. doi: 10.1073/pnas.1321390111
30. Nagamine T, Hayakawa K, Kusakabe T, Takada H, Nakazato K, Hisanaga E, et al. Inhibitory effect of fucoidan on Huh7 hepatoma cells through downregulation of CXCL12. *Nutr Cancer*. (2009) 61:340–7. doi: 10.1080/01635580802567133
31. Abràmoff MD, Magalhães PJ, Ram SJ. Image processing with ImageJ. *Biophotonics Int*. (2004) 11:36–42.
32. Pfaffl MW. A new mathematical model for relative quantification in real-time RT-PCR. *Nucleic Acids Res*. (2001) 29:e45. doi: 10.1093/nar/29.9.e45
33. Forlenza M, Kaiser T, Savelkoul HF, Wiegertjes GF. The use of real-time quantitative PCR for the analysis of cytokine mRNA levels. *Methods Mol Biol*. (2012) 820:7–23. doi: 10.1007/978-1-61779-439-1_2
34. R Core Team. R: a language and environment for statistical computing. *R Foundation for Statistical Computing*, Vienna. (2019) Available online at: https://www.R-project.org/ (accessed May 22, 2020).
35. Klindworth A, Pruesse E, Schweer T, Peplies J, Quast C, Horn M, et al. Evaluation of general 16S ribosomal RNA gene PCR primers for classical and next-generation sequencing-based diversity studies. *Nucleic Acids Res*. (2013) 41:e1. doi: 10.1093/nar/gks808
36. Yoon SH, Ha SM, Kwon S, Lim J, Kim Y, Seo H, et al. Introducing EzBioCloud: a taxonomically united database of 16S rRNA and whole genome assemblies. *Int J Syst Evol Microbiol*. (2017) 67:1613–7. doi: 10.1099/ijsem.0.001755
37. Albanese D, Fontana P, de Filippo C, Cavalieri D, Donati C. MICCA: a complete and accurate software for taxonomic profiling of metagenomic data. *Sci Rep*. (2015) 5:9743. doi: 10.1038/srep09743
38. Quast C, Pruesse E, Yilmaz P, Gerken J, Schweer T, Yarza P, et al. The SILVA ribosomal RNA gene database project: improved data processing and web-based tools. *Nucleic Acids Res*. (2013) 41:D590–6. doi: 10.1093/nar/gks1219
39. Wang Q, Garrity GM, Tiedje JM, Cole JR. Naive Bayesian classifier for rapid assignment of rRNA sequences into the new bacterial taxonomy. *Appl Environ Microbiol*. (2007) 73:5261–7. doi: 10.1128/AEM.00062-07
40. Dhariwal A, Chong J, Habib S, King IL, Agellon LB, Xia J. MicrobiomeAnalyst: a web-based tool for comprehensive statistical, visual and meta-analysis of microbiome data. *Nucleic Acids Res*. (2017) 45:W180–8. doi: 10.1093/nar/gkx295
41. Segata N, Izard J, Waldron L, Gevers D, Miropolsky L, Garrett WS, et al. Metagenomic biomarker discovery and explanation. *Genome Biol*. (2011) 12:R60. doi: 10.1186/gb-2011-12-6-r60
42. Khan ST, Horiba Y, Yamamoto M, Hiraishi A. Members of the family Comamonadaceae as primary poly (3-hydroxybutyrate-co-3-hydroxyvalerate) -degrading denitrifiers in activated sludge as revealed by a polyphasic approach. *Appl Environ Microbiol*. (2002) 68:3206–14. doi: 10.1128/AEM.68.7.3206-3214.2002
43. Novoa B, Figueras A. Zebrafish: model for the study of inflammation and the innate immune response to infectious diseases. *Adv Exp Med Biol*. (2012) 946:253–75. doi: 10.1007/978-1-4614-0106-3_15
44. Nag D, Breen P, Raychaudhuri S, Withey JH. Glucose metabolism by *Escherichia coli* inhibits *Vibrio cholerae* intestinal colonization of zebrafish. *Infect Immun*. (2018) 86:e00486–18. doi: 10.1128/IAI.00486-18
45. Swain P, Nayak SK, Nanda PK, Dash S. Biological effects of bacterial lipopolysaccharide (endotoxin) in fish: a review. *Fish Shellfish Immunol*. (2008) 25:191–201. doi: 10.1016/j.fsi.2008.04.009
46. Pressley M, Phelan P, Witten P, Mellon M, Kim C. Pathogenesis and inflammatory response to *Edwardsiella tarda* infection in the zebrafish. *Dev Comp Immunol*. (2005) 29:501–13. doi: 10.1016/j.dci.2004.10.007
47. Dib AL, Agabou A, Chahed A, Kurekci C, Moreno E, Espigares M, et al. Isolation, molecular characterization and antimicrobial resistance of enterobacteriaceae isolated from fish and seafood. *Food Control*. (2018) 88:54–60. doi: 10.1016/j.foodcont.2018.01.005
48. Makki K, Deehan EC, Walter J, Bäckhed F. The impact of dietary fiber on gut microbiota in host health and disease. *Cell Host Microbe*. (2018) 23:705–15. doi: 10.1016/j.chom.2018.05.012
49. Hiraishi A., Khan ST. Application of polyhydroxyalkanoates for denitrification in water and wastewater treatment. *Appl Microbiol Biotechnol*. (2003) 61:103–9. doi: 10.1007/s00253-002-1198-y
50. Chu L, Wang J. Denitrification performance and biofilm characteristics using biodegradable polymers PCL as carriers and carbon source. *Chemosphere*. (2013) 91:1310–6. doi: 10.1016/j.chemosphere.2013.02.064
51. Luo GZ, Hou ZW, Tian LQ, Tan HX. Comparison of nitrate removal efficiency and bacterial properties using PCL and PHBV polymers as a carbon source to treat aquaculture water. *Aquaculture Fish*. (2020) 5:92-8. doi: 10.1016/j.aaf.2019.04.002
52. Wu H, Shen J, Wu R, Sun X, Li J, Han W, et al. Biodegradation mechanism of 1H-1,2,4-triazole by a newly isolated strain *Shinella* sp. NJUST26. *Sci Rep*. (2016) 6:29675. doi: 10.1038/srep29675
53. Ntougias S, Melidis P, Navrozidou E, Tzegkas F. Diversity and efficiency of anthracene-degrading bacteria isolated from a denitrifying activated sludge system treating municipal wastewater. *Int Biodeterior Biodegradation*. (2015) 97:151– 8. doi: 10.1016/j.ibiod.2014.11.009

54. Hooper LV, Littman DR, Macpherson AJ. Interactions between the microbiota and the immune system. *Science*. (2012) 336:1268–73. doi: 10.1126/science.1223490
55. Brugman S. The zebrafish as a model to study intestinal inflammation. *Dev Comp Immunol*. (2016) 64:82–92. doi: 10.1016/j.dci.2016.02.020
56. Burns AR, Miller E, Agarwal M, Rolig AS, Milligan-Myhre K, Seredick S, et al. Interhost dispersal alters microbiome assembly and can overwhelm host innate immunity in an experimental zebrafish model. *Proc Natl Acad Sci*. (2017) 114:11181–6. doi: 10.1073/pnas.1702511114
57. Stagaman K, Burns AR, Guillemin K, Bohannan BJ. The role of adaptive immunity as an ecological filter on the gut microbiota in zebrafish. *ISME J*. (2017) 11:1630–9. doi: 10.1038/ismej.2017.28
58. Jeong JW, Hwang SJ, Han MH, Lee DS, Yoo JS, Choi IW, et al. Fucoidan inhibits lipopolysaccharide-induced inflammatory responses in RAW 264.7 macrophages and zebrafish larvae. *Mol Cell Toxicol*. (2017) 13:405–17. doi: 10.1007/s13273-017-0045-2
59. Lee SH, Ko CI, Jee Y, Jeong Y, Kim M, Kim JS. Anti-inflammatory effect of fucoidan extracted from Ecklonia cava in zebrafish model. *Carbohydr Polym*. (2013) 92:84–9. doi: 10.1016/j.carbpol.2012.09.066
60. Kim MH, Joo HG. Immunostimulatory effects of fucoidan on bone marrow-derived dendritic cells. *Immunol Lett*. (2008) 115:138–43. doi: 10.1016/j.imlet.2007.10.016
61. Spence R, Gerlach G, Lawrence C, Smith C. The behaviour and ecology of the zebrafish, *Danio rerio*. *Biol Rev Camb Philos Soc*. (2008) 83:13–34. doi: 10.1111/j.1469-185X.2007.00030.x
62. Ikeda-Ohtsubo W, Brugman S, Warden CH, Rebel JMJ, Folkerts G Pieterse CMJ. How can we define "optimal microbiota?": a comparative review of structure and functions of microbiota of animals, fish, and plants in agriculture. *Front Nutr*. (2018) 5:90. doi: 10.3389/fnut.2018.00113
63. Rawls JF, Mahowald MA, Ley RE, Gordon JI. Reciprocal gut microbiota transplants from zebrafish and mice to germ-free recipients reveal host habitat selection. *Cell*. (2006) 127:423–33. doi: 10.1016/j.cell.2006.08.043
64. Ringø E, Olsen RE, Gifstad TO, Dalmo RA, Amlund H, Hemre GI, et al. Prebiotics in aquaculture: a review. *Aquacult Nutr*. (2010) 169:117–36. doi: 10.1111/j.1365-2095.2009.00731.x

**Conflict of Interest:** MI is employed by the company South Product Co., Ltd.

The remaining authors declare that the research was conducted in the absence of any commercial or financial relationships that could be construed as a potential conflict of interest.

# Advantages of publishing in Frontiers

**OPEN ACCESS**
Articles are free to read for greatest visibility and readership

**FAST PUBLICATION**
Around 90 days from submission to decision

**HIGH QUALITY PEER-REVIEW**
Rigorous, collaborative, and constructive peer-review

**TRANSPARENT PEER-REVIEW**
Editors and reviewers acknowledged by name on published articles

**Frontiers**
Avenue du Tribunal-Fédéral 34
1005 Lausanne | Switzerland

**Visit us:** www.frontiersin.org
**Contact us:** info@frontiersin.org | +41 21 510 17 00

**REPRODUCIBILITY OF RESEARCH**
Support open data and methods to enhance research reproducibility

**DIGITAL PUBLISHING**
Articles designed for optimal readership across devices

**FOLLOW US**
@frontiersin

**IMPACT METRICS**
Advanced article metrics track visibility across digital media

**EXTENSIVE PROMOTION**
Marketing and promotion of impactful research

**LOOP RESEARCH NETWORK**
Our network increases your article's readership